LOUDSPEAKER HANDBOOK
SECOND EDITION

LOUDSPEAKER HANDBOOK
SECOND EDITION

by

John Eargle
JME Consulting Corporation

SPRINGER SCIENCE+BUSINESS MEDIA, LLC

Library of Congress Cataloging-in-Publication Data

Eargle, John.
Loudspeaker handbook / by John Eargle.--2nd ed.
p. cm.
Includes bibliographical references and index.
ISBN 978-1-4419-5390-2 ISBN 978-1-4757-5678-4 (eBook)
DOI 10.1007/978-1-4757-5678-4
1. Loudspeakers--Handbooks, manuals, etc. I. Title.

TK5983.E27 2003
621.382'84--dc22 2003058802

Printed on acid-free paper.

CONTENTS:

AUTHOR'S PREFACE:

The second edition of *The Loudspeaker Handbook* follows the same general outline as the first edition and has been augmented and updated in many areas of technology. Most notable here the developments in large-scale, programmable line arrays, distributed mode loudspeakers, and ultrasonic-based audio transduction. Additionally, the core chapters on low frequency systems, systems concepts, and horn systems have been expanded.

Much of the success of the first edition has been due to its accessibility both to loudspeaker engineers and to lay technicians working in the field – a point of view the author maintains in the present work. A full understanding of the underlying technology requires a fairly rigorous engineering background through the second year of professional study. At the same time, the generous use of graphs, with their intuitive thrust, will be useful to all readers.

Here are short descriptions of chapter content:

Chapter 1 deals with the basic electro-mechano-acoustical chain between input to the loudspeaker and its output, with emphasis on the governing equations and equivalent circuits.

Chapter 2 is a survey of cone and dome drivers, the stock-in-trade of the industry. They are discussed in term s of type, design, performance, and performance limits.

Chapter 3 deals with magnetics. Once a source of difficulty in loudspeaker design, magnetics today yields easily to modeling techniques.

Chapter 4 discusses low frequency (LF) system performance, primarily from the viewpoint of Thiele-Small parameters. We also discuss a wide variety of enclosure designs.

Chapter 5 deals with systems concepts. There is more diversity in this area than in any other aspect of loudspeaker design. Basic network types, baffle layout, and component matching are all discussed.

Chapter 6 discusses line and planar loudspeakers, including modern electronically steerable arrays.

Chapter 7 covers horns and compression drivers in detail. Horn systems are a mainstay of professional sound reinforcement and have been a key element in electroacoustics from the start.

Chapter 8 discusses the electronic interface, including matching loudspeaker and amplifier, series and parallel operation of amplifiers, aspects of multi-amplification, and line losses.

Chapter 9 deals with the performance shifts associated with heating as loudspeakers are driven to their maximum limits in high-level use. Techniques for minimizing these effects are discussed.

Chapters 10, 11, and 12 examine the application areas of recording and broadcast monitoring, sound reinforcement, and motion picture/video, respectively. Current practice in these disciplines is discussed in detail.

Chapter 13 covers loudspeaker measurements and modeling. A quiet revolution has taken place in the last two decades as measurement systems based on digital transform techniques have virtually replaced analog systems. Both methods are discussed, along with techniques for modeling loudspeaker performance.

Chapter 14 discusses loudspeaker specifications for professional applications. Data presentation is an important first step in this area. Current practice is reviewed.

Chapter 15 discusses stereo reproduction the home listening environment along with techniques for improvement of room acoustics.

Chapter 16 considers the wide variety of physical principles that have been used over the years for transduction in loudspeakers. Many of these are exotic and transitory, while others have reached a high level of maturity.

The author would like acknowledge the many persons at JBL and other companies of Harman International Industries for their direct help in gathering material for this book and for stimulating discussions over the years. Further recognition is given to numerous manufacturers who have provided illustrative material for the book. They are gratefully cited in the figure captions.

John Eargle,
July 2003

Symbols Used in this Book:

ω, $2\pi f$, angular frequency (rad/s)
λ, acoustical wavelength (m)
θ, independent variable, polar coordinates
ρ, dependent variable, polar coordinates
$\rho_0 c$, characteristic acoustical impedance of air
a, radius (m or mm)
A, ampere (SI base unit of electrical current)
AF, audio frequency
B, magnetic induction (gauss, G)
B, magnetic flux density (tesla, T)
$B_d H_d$, magnetic gap energy (erg)
B_r, remnant magnetic induction (gauss)
c, speed of sound (m/s)
C electrical capacitance (farad, F)
C, electrical charge, coulomb (A•s)
C, mechanical compliance (m/N)
C_{MS}, compliance, moving system
C_p, specific heat of a gas under constant pressure (calories/mol × °C)
C_V, specific heat of a gas under constant volume (calories/mol × °C)
DI, directivity index (dB)
e(t), time-varying voltage
f(t), time-varying force
H, magnetizing force field, oersted (Oe)
H_c, magnetic coercivity, oersted
HF, high frequency
i(t), time-varying current signal
i, instantaneous current (A)
J_X, Bessel function of order *x*
k, wave number ($2\pi/\lambda$, m^{-1})
kg, kilogram (SI base unit of mass)
L, electrical inductance (henry, H)
L, liter, unit of volume
l, length of wire in magnetic gap (m)
LF, low frequency

L_p, sound pressure level (re 20 μPa)
m, meter (SI base unit of length)
M, mass, kg (SI base unit of mass)
MAF, minimum audible sound field
MF, mid frequency
M_{MS}, mass, loudspeaker moving system
N, force, newton ($kg \cdot m/s^2$)
p(t), time varying pressure (N/s)
Q, quality factor; directivity factor (dimensionless)
r, radius of circle (m)
r, distance (m or mm)
R, electrical resistance (ohm, Ω)
R, mechanical resistance, damping (Ns/m, SI mechanical ohm)
R_A, radiation impedance (SI acoustical ohm)
R_E, voice coil resistance (Ω)
RF, radio frequency (Hz)
R_{MS}, resistance, moving system
s, second (SI base unit of time)
S_D, cone area (m^2)
T, tesla, unit of magnetic flux density
THD, total harmonic distortion (percent)
u, instantaneous velocity (m/s)
U(t), time varying air volume velocity (m^3/s)
UHF, ultra high frequency
W, power (watt)
W_A, acoustical power (watt)
x, displacement (m)
X, electrical reactance (ohm)
Z, electrical impedance (ohm)

Chapter 1:
ELECTROACOUSTICAL ENGINEERING FUNDAMENTALS: THE DYNAMIC LOUDSPEAKER

1 Introduction

In this chapter we will develop the basic electro-mechano-acoustical model of the dynamic cone loudspeaker, detailing how the device attains its flat power response passband and reference efficiency. We will also discuss the basic directional properties of cone loudspeakers under several conditions of baffling. A number of assumptions will be made based on the physics of the acoustic wave equation, drawing on primary references in the literature as needed. In the way of terminology, a loudspeaker mechanism is generically referred to as a *transducer* or as a *driver*. The term *loudspeaker* is all-embracing, referring both to drivers and complete systems.

The dynamic cone driver is based on work originally described by Siemens (1874). The seminal paper on the modern form the cone driver has taken is that of Rice and Kellogg (1925), in which the authors describe the specific roles of cone resonance and radiation resistance in attaining a wide frequency range of uniform power response. Over more than three quarters of a century since that time, the cone driver has seen countless variations and improvements, and yet remains clearly what it was at the outset. Needless to say, the cone driver and its close cousin, the dome driver, have occupied a central position in a vast complex of consumer inventions and applications that continues today.

1.1 A simple electrical series resonant circuit

Figure 1-1A shows a series electrical circuit with three passive elements and an active, time varying voltage generator, $e(t)$. The equation relating the impedance of the circuit, the current, $i(t)$, flowing through it, and the applied voltage is:

$$e(t) = i(t)(1/j\omega C + j\omega L + R) \qquad 1.1$$

J. Eargle, *Loudspeaker Handbook*

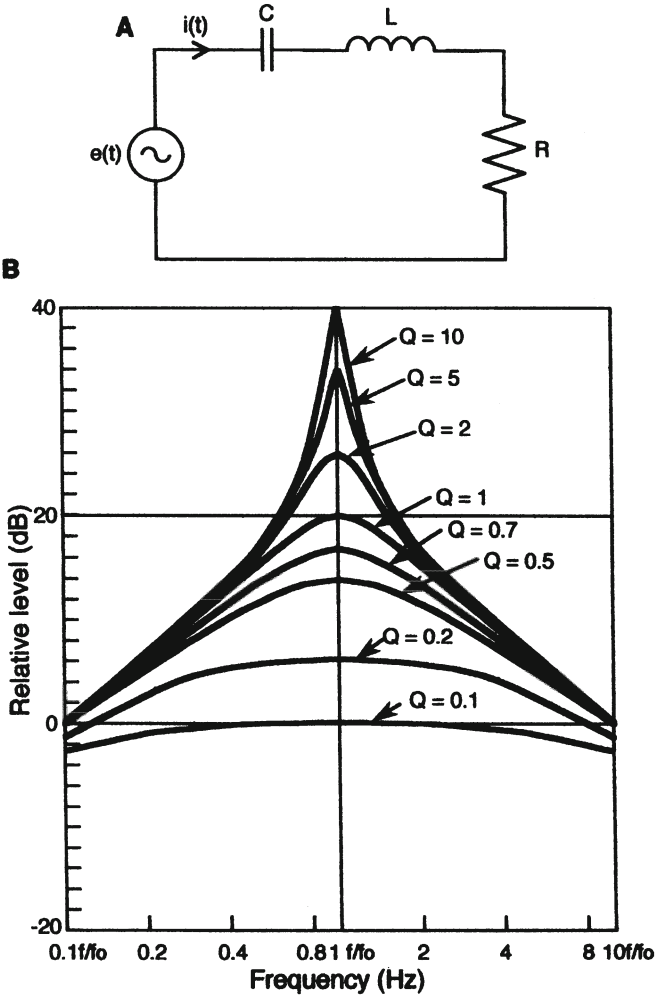

Figure 1-1. Example of electrical resonance. A series LCR (inductance, capacitance, resistance) circuit (A); family of resonance curves for different values of *Q* (B).

where: $\omega = 2\pi f$ (radians/sec)
j = square root of –1
C = capacitance (farads)
L = inductance (henrys)
R = resistance (ohms)

We can also define the resonance frequency, f_0, of the circuit:

$$f_0 = \frac{1}{2\pi}\sqrt{\frac{1}{LC}} \qquad 1.2$$

This is the driving frequency at which the reactive terms, $1/j\omega C$ and $j\omega L$, are equal and cancel each other, leaving only the resistive term in the right half of equation 1.1. At this frequency the current through the circuit will be maximum.

The capacitive and inductive elements are reactive; they store power but do not consume it; only the resistive element dissipates power, and that is given by:

$$W = \frac{[e(t)]^2}{R} = [i(t)]^2 R \qquad 1.3$$

If we plot the current flowing through the circuit as we vary the driving frequency of $e(t)$, we will get a curve resembling one of those shown in Figure 1-1B. The value of Q, the sharpness of the resonance curve, is given by:

$$Q = \omega_0 L/R \qquad 1.4$$

$\omega_0 L$ is the value of inductive reactance at the resonance frequency. If R is small relative to $\omega_0 L$ then the Q will be high, with a characteristic peak in the shape of the curve. If R is large, the shape of the curve will be smoother, as indicated by the lower values of Q in the set of curves.

We have shown electrical resonance in this example, and we will now move on to an example of mechanical resonance.

1.2 A simple mechanical resonant system

Figure 1-2A shows a mechanical arrangement in which a rigid platform, free to move vertically, is suspended on spring and damping (resistive) elements. The mass of the platform is shown as a lumped value, M, and the platform is constrained to being driven up and down by a force generator, $f(t)$.

If we vary the driving frequency of the force generator we will soon discover that the velocity, $u(t)$, of the platform will be maximum at some resonance frequency, f_0, and we will observe a family of resonance curves identical to those shown in Figure 1-1B.

The equation relating driving force, platform velocity, and mechanical impedance is:

$$f(t) = u(t)(1/j\omega C + j\omega M + R) \qquad 1.5$$

where:

C = mechanical compliance, meters per newton
M = mechanical mass, kilograms
R = mechanical resistance, newton-seconds per meter
f(t) = driving force, newtons
u(t) = platform velocity, m/sec

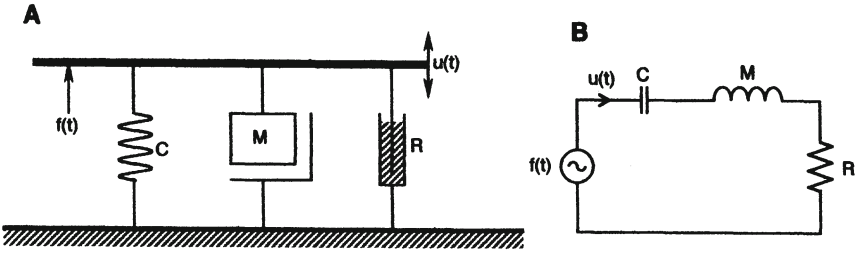

Figure 1-2. A mechanical resonant circuit (A); impedance analogy of mechanical circuit (B).

Both electrical and mechanical circuits are described by equations of the same form and are said to be equivalent. Mass is analogous to inductance, compliance to capacitance, and damping to resistance. Force is analogous to voltage, and velocity to current. Power dissipated in the damping element is:

$$W = [f(t)]^2/R = [u(t)]^2R \qquad 1.6$$

1.3 Impedance and mobility analogies

The mechanical analogy discussed here is called the *impedance analogy*. It is easy to understand because the related quantities are intuitively obvious. Below are listed these quantities in the electrical, mechanical, and acoustical domains:

Electrical	Mechanical	Acoustical
Voltage	Force (f)	Pressure (p)
Current	Velocity (u)	Volume velocity (U)
Inductance	Mass	Acoustical mass
Capacitance	Compliance	Acoustical compliance
Resistance	Resistance	Acoustical damping

However, from the viewpoint of constructing equivalent circuits, the so-called *mobility analogy* may be more useful to implement. Note the example in Figure 1-3. Here, the actual mechanical circuit we dealt with in Figure 1-2 is paired with its mobility analogy. The two are virtually of the same form, and herein lies the usefulness of the mobility analogy; the equivalent circuit can be drawn directly by inspection.

In order to do this, the roles have been switched in the mechanical and acoustical domains, as given below:

Electrical	Mechanical	Acoustical
Voltage	Velocity (u)	Volume velocity (U)
Current	Force (f)	Pressure (p)
Inductance	Compliance	Acoustical compliance
Capacitance	Mass	Acoustical inertance
Resistance	Responsiveness(r)	Acoustical responsiveness

The mobility equivalent circuit is known as the *dual* of the impedance equivalent circuit, and the governing equations are of the same form. As we proceed through the book you will see the value of the mobility analogy in the analysis of LF loudspeaker subsystems.

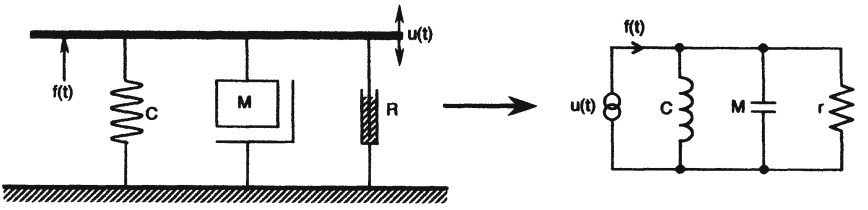

Figure 1-3. Illustration of mobility analogy of a mechanical circuit.

1.4 Combining electrical and mechanical domains

The laws of elementary magnetism provide a simple connection between the electrical and mechanical domains via the following equations:

$$f = Bli \qquad 1.7$$

$$e = Blu \qquad 1.8$$

where: B = magnetic field strength (T)
l = length of conductor in magnetic field (m)
f = force (N)
u = velocity (m/s)
i = current (A)
e = voltage (E)

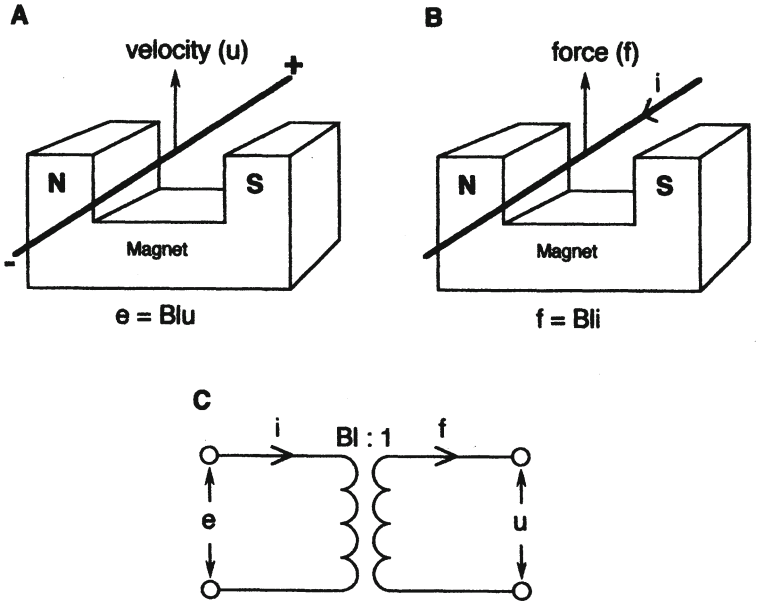

Figure 1-4. Magnetic relationships. A conductor moving in a magnetic field with velocity *u* will generate a voltage *e* across the conductor (A); a force *f* applied to a conductor in a magnetic field will produce a current *i* in the conductor (B); a transformer representation between electrical and mechanical domains that demonstrates e = Blu and f = Bli (C).

These relationships are shown in Figure 1-4A and *B*. Together, they form the basis for a simple transducer that allows us to convert voltage and current into mechanical force and velocity, as symbolized by the transformer shown at *C*. Any moving coil transducer is an example of this, from a tiny earphone to a large loudspeaker.

The product of voltage and current is electrical power, and the product of force and velocity is mechanical power – both the same quantities in terms of their units. We can now construct an electrical driving system for our prototype mechanical circuit, and this is shown in Figure 1-5A. The equivalent electrical circuit is shown at *B*. This transducer is capable of transforming electrical power into mechanical power. It can be used for shaking things, or even for canceling vibrations. But as yet it cannot make sound.

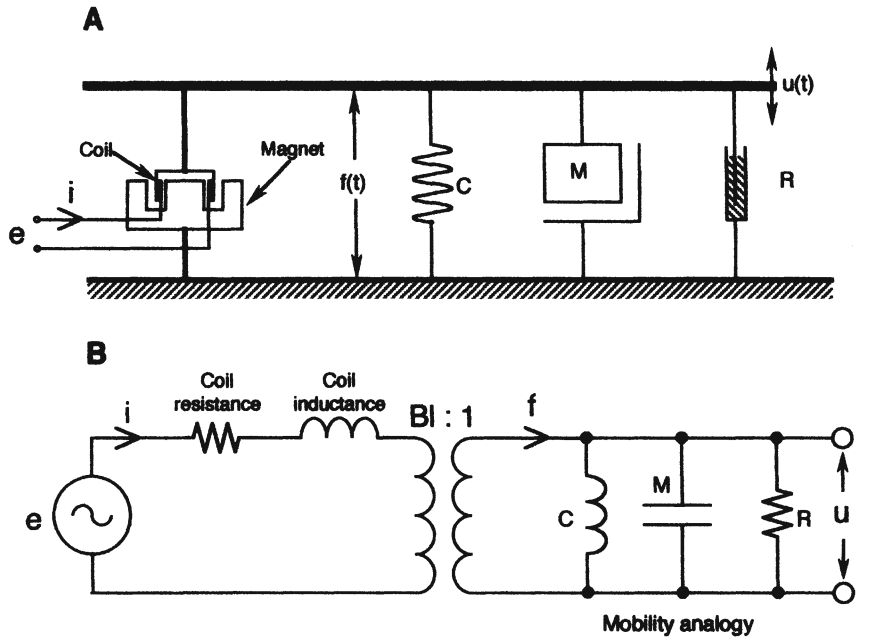

Figure 1-5. A simple electromechanical transducer. mechanical ciruit (A); electrical equivalent circuit using mobility analogy on the mechanical side (B).

1.5 Combining the mechanical and acoustical domains

In order to produce sound, a vibrating object or surface must have sufficient expanse or area. The size of a piano sounding board, the size of a bass viol or the bell of a tuba are all examples of this. For very low frequencies, a vibrating surface may do little more than move air back and forth. At these low frequencies the surface and its associated air load present essentially a mass reactance to the moving system, and no power can be radiated. The air mass associated with the cone is given by:

$$M_{air} = 8a^3\rho_0/c \qquad 1.9$$

where a is the radius of the piston in meters, c is the speed of sound (344 m/s), and ρ_0 is the density of air (1.18 kg/m^3).

As the frequency of motion increases, sound begins to be radiated, as determined by *radiation impedance*. The nature of radiation impedance is fairly complex, and our discussion of it in this book is necessarily limited. Basically, it consists of two terms, the *reactance* of the air mass adjacent to the surface and the *resistance* term associated with the radiation of sound from the surface.

The resistive *(R)* and reactive *(X)* components of radiation impedance *(Z)* for a circular piston in a large baffle are shown in Figure 1-6, where $\rho_0 c$ is the specific acoustical impedance (415 Pa•s/m), a is the radius of the piston (meter), and k is equal to $2\pi/\lambda$, where λ is the radiated wavelength (meter). The useful part of the impedance is the radiation resistance portion.

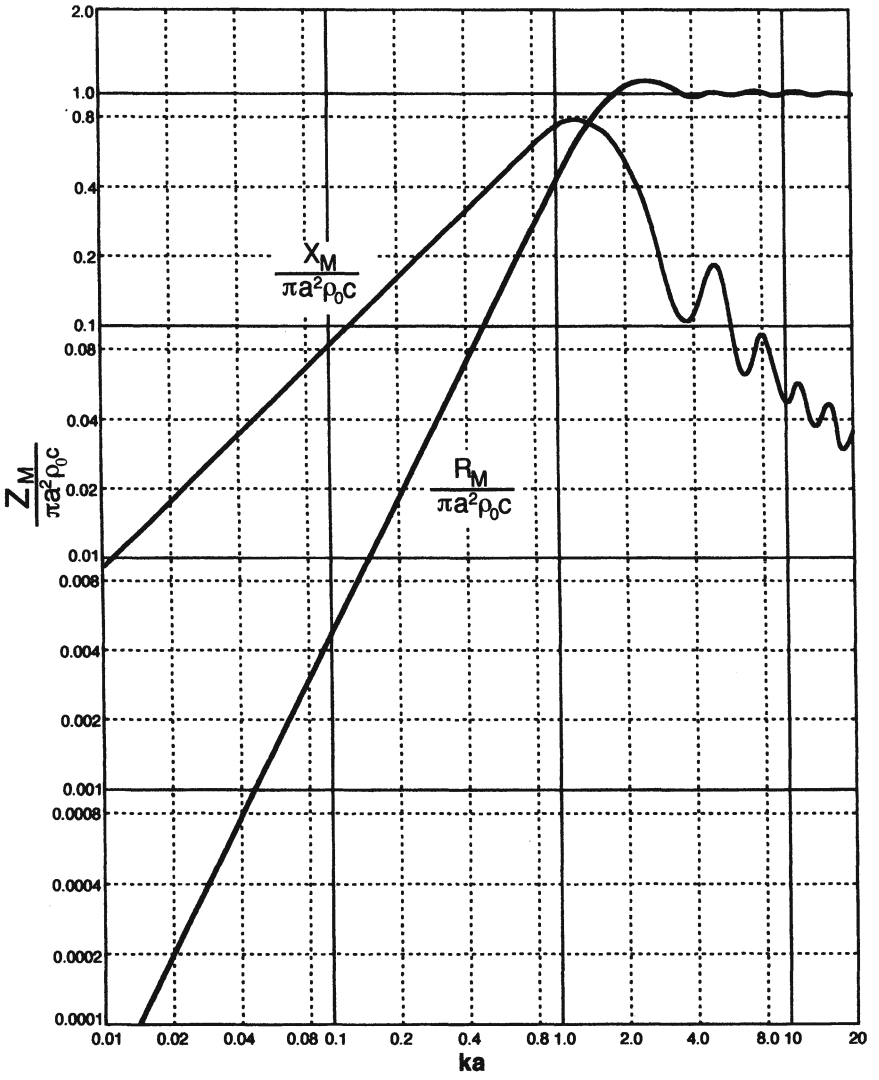

Figure 1-6. Resistive and reactive components of radiation impedance for a piston mounted in a large baffle. Ripples in response above ka = 2 are due to interference effects when wavelengths are small compared to the piston diameter.

We may think of *ka* as circumference of the piston divided by the wavelength. Note that the radiation resistance falls off below ka = 2 at a rate proportional to the square of frequency. This is equivalent to a low frequency rolloff of 12 dB per octave for constant displacement of the piston, or 6 dB per octave for constant velocity. As we can see in Figure 1-6, the radiation resistance, R_A, in the region below ka = 1, is proportional to the square of frequency; that is, doubling the frequency in that range will produce a 4-times increase in R_A. We can then say that:

$$R_A \propto f^2 \qquad 1.10$$

Recall from equation 1.6 that:

$$\text{Power} = [u(t)]^2 R$$

From Figure 1-7 we observe the mechanical resonance curve and note that in the mass controlled region above f_0:

$$u(t) \propto 1/f \qquad 1.11$$

and therefore:

$$[u(t)]^2 \propto 1/f^2 \qquad 1.12$$

Since:

$$W_A \propto R_A[u(t)]^2$$

we can substitute terms and get:

$$\text{Power} \propto f^2 \times 1/f^2 = 1 \text{ (constant)} \qquad 1.13$$

Thus, the radiated power from the cone will be constant over the frequency region between f_0 and a *ka* value of about 1.5 to 2.

The final electro-mechano-acoustical system, now drawn in the mechanical form of a loudspeaker, is shown as in Figure 1-7A. Note that we have now lumped the system moving mass into the cone, with elements of compliance (C_{MS}) and damping (R_{MS}) now associated with the system suspension. The cone mass (plus its associated air mass) is indicated as M_{MS} and the cone area as S_D. (The subscript *MS* indicates "moving system".)

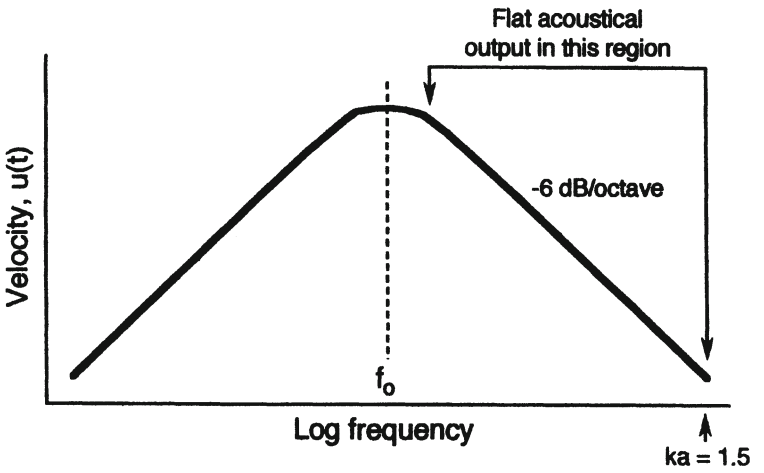

Figure 1-7. Resonance curve of mechano-acoustical moving system. Uniform acoustical output can be obtained above f_o.

The radiation impedance terms are shown as M_A and R_A. They are related to the mechanical circuit through the transformation ratio of *1:S*, where *S* is the area of the cone.

The response is as shown at B for a number of values of Q, as indicated in the figure. These values of Q are related to those shown in Figure 1-1B, with their values of $\omega L/R$ when all acoustical and mechanical values have been transformed to the electrical domain.

The final equivalent circuit is shown at C, with the mechanical and acoustical elements shown in the mobility analogy. The terms used in the equivalent circuit are known as the *electromechanical parameters*.

1.5.1 Loudspeaker efficiency and sensitivity

For typical loudspeakers intended for low frequency application, the range between f_0 and ka = 2 may be about a decade (a ten-to-one frequency range), or slightly more. The frequency range of flat output for a loudspeaker placed in a large baffle is often called the *piston band* of the loudspeaker, and we can easily calculate the efficiency of the device in this range, as measured on one side of a large baffle. This is the so-called *half-space efficiency*.

Efficiency is the measure of the acoustical power output divided by the electrical power input to the loudspeaker. At any given frequency in the

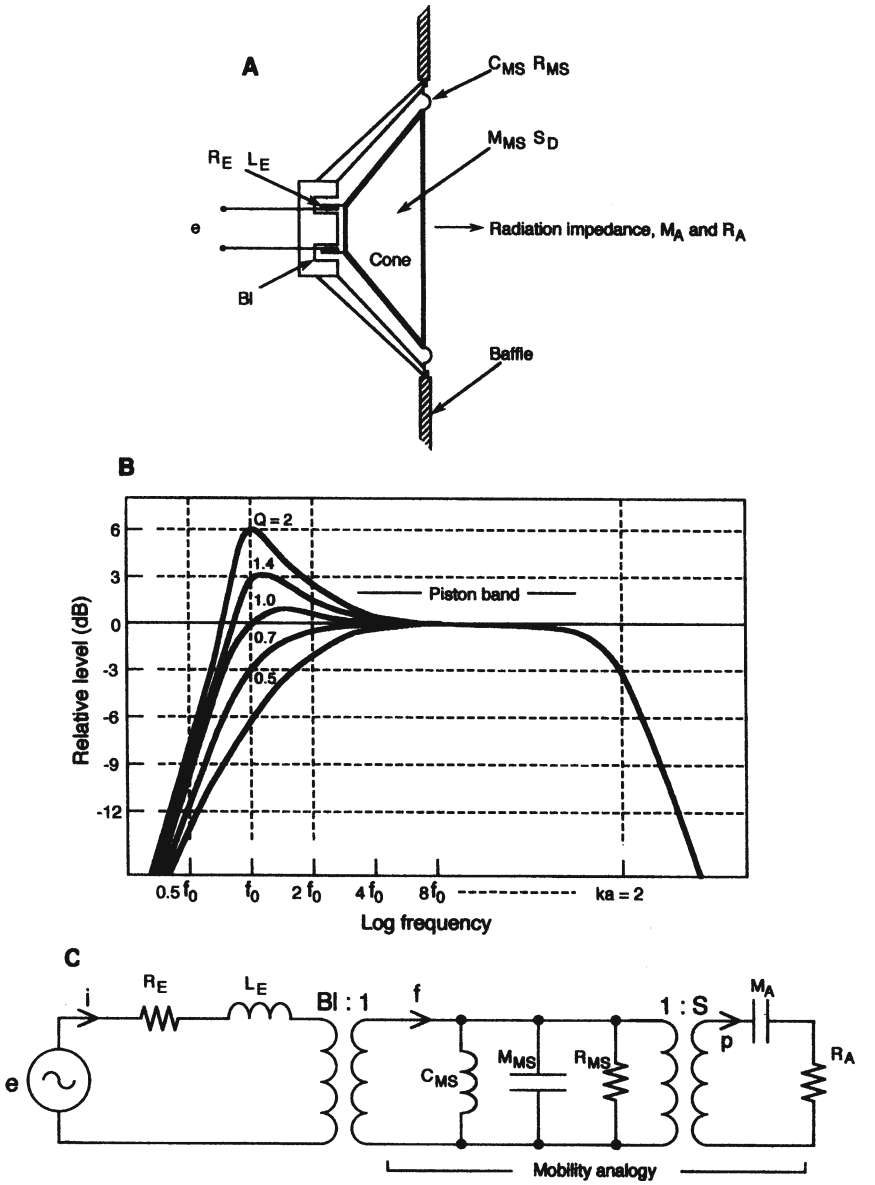

Figure 1-8. The loudspeaker driver: a simple electro-mechano-acoustical transducer. Physical view (A); typical ranges of response (B); equivalent electrical circuit with mobility analogy in mechanical and acoustical portions.

piston band, the overall efficiency is the product of the electrical-to-mechanical and mechanical-to-acoustical conversion efficiencies. As we have seen, the balance between these quantities is not constant with frequency, but their product is. In the frequency range in which the motion of the cone is mass

controlled, and in which the directivity of the loudspeaker is uniform, Small (1972) gives the conversion efficiency, η_0, of the loudspeaker as:

$$\eta_0 = [\rho_0(Bl)^2 S_D^2]/[2\pi c R_E M_{MS}^2] \qquad 1.14$$

where:

B = magnetic flux density, tesla
l = length of voice coil, meter
ρ_0 = density of air (1.18 kg per cubic meter)
R_E = voice coil resistance, ohm
M_{MS} = total moving mass, kilogram
S_D = area of diaphragm, square meter

As an example, let us consider the JBL model 2226H driver. The relevant parameters are given as:

Bl = 19.2 tesla-meter
$R_E = 5\ \Omega$
$M_{MS} = 0.096$ kg
$S_D = 0.088$ meter squared

Calculating:

$$\eta_0 = [1.18(368.6)(7.74)\text{x}10^{-3}]/[2166.6(5)9.2\text{x}10^{-3}]$$

$\eta_0 = 0.0338$, or about 3.4%

The measured efficiency of the driver is 3.3%, so the agreement is excellent.

If we know the efficiency of a driver we can determine its *sensitivity*. Sensitivity is normally stated as the sound pressure level measured at a distance of 1 meter on-axis with a power input of one watt to the driver, with the driver mounted in a large baffle so that it radiates essentially into "half-space".

From physical acoustics we have the following equation for determining the sound pressure level (dB) at a distance *r* from a sound source in a free field radiating power *W* (Beranek, 1954, p. 314):

$$\text{dB } L_p = 10 \log W + 10 \log \rho_0 c + 94 + 10 \log (1/4\pi r^2) \qquad 1.15$$

where *r* is the distance from the source in meters.

With one electrical watt applied to the JBL 2226H transducer, we know that the output power will be 0.033 watts. With *r* taken as 1 meter:

$$dB\ L_p = 10 \log (0.033) + 10 \log (1.18 \times 345) + 94 + 10 \log (0.08)$$

$$= -14.8 + 26.1 + 94 - 11 = 94.3\ dB$$

If the power is radiated into half-space, then the pressure will be 3 dB greater, giving a total of 97.3 dB. The published sensitivity value for the 2226H is 97 dB, so the agreement is excellent.

We can construct a simple table for converting efficiency directly into 1-watt, 1 meter piston band sensitivity ratings:

Half-space efficiency:	1-watt, 1-meter piston band sensitivity:
25%	106
20	105
16	104
12.5	103
10	102
8	101
6.3	100
5	99
4	98
3.15	97
2.5	96
2	95
1.6	94
1.25	93
1	92

1.6 Directional characteristics

We have almost finished our model. Our final step is to consider the directionality of the radiating surface and how it might extend the useful frequency range of a loudspeaker. A circular piston mounted in a large wall will exhibit a radiation pattern that is highly dependent on frequency and the angle of observation. for an observer on axis at some distance from the piston, radiation from all portions of the piston will arrive virtually at the same time, and the response will be maximum for all frequencies. For an off-axis position, radiation from some portions of the piston will arrive later than others, and

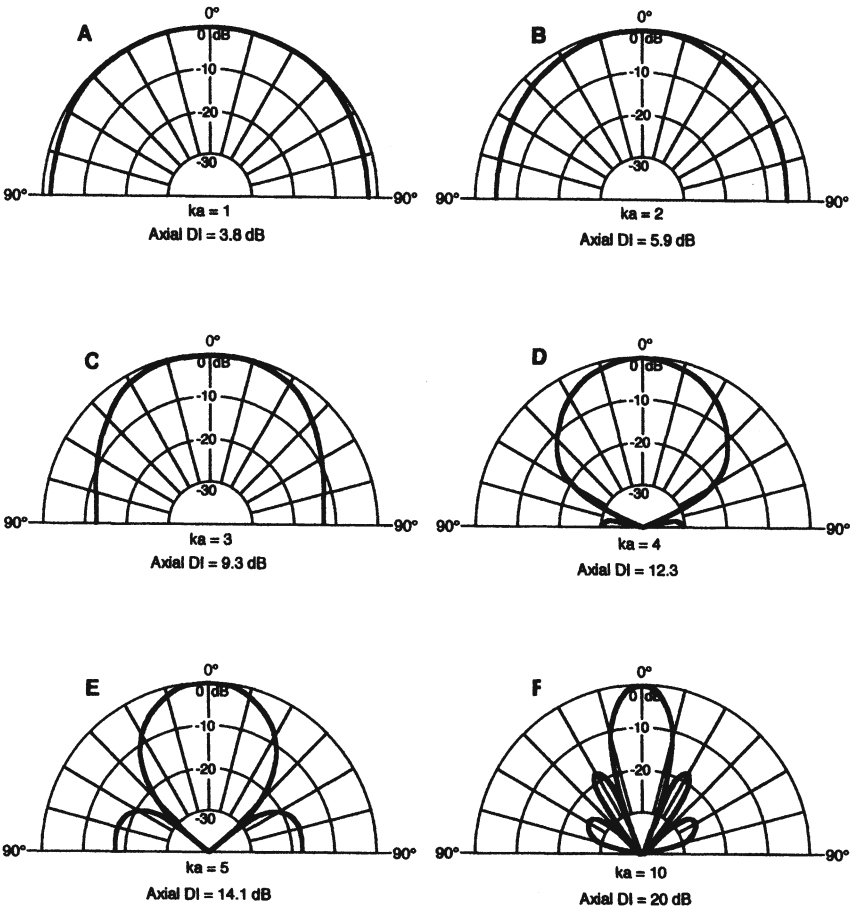

Figure 1-9. Directional (polar) response of a piston mounted in a large baffle. (Data after Beranek, 1954)

the response will be less than that observed on axis, especially at higher frequencies (shorter wavelengths). This is intuitively obvious, and the effects are shown in Figure 1-9.

Polar plots for a wall mounted piston are shown in Figure 1-9. For wavelengths that are long with respect to piston radius, the directionality will be virtually uniform. For shorter wavelengths, it will become progressively more directional on axis. The scale factor here is the quantity *ka*, where:

k = wave number, $2\pi/\lambda$
a = radius of the piston (m)

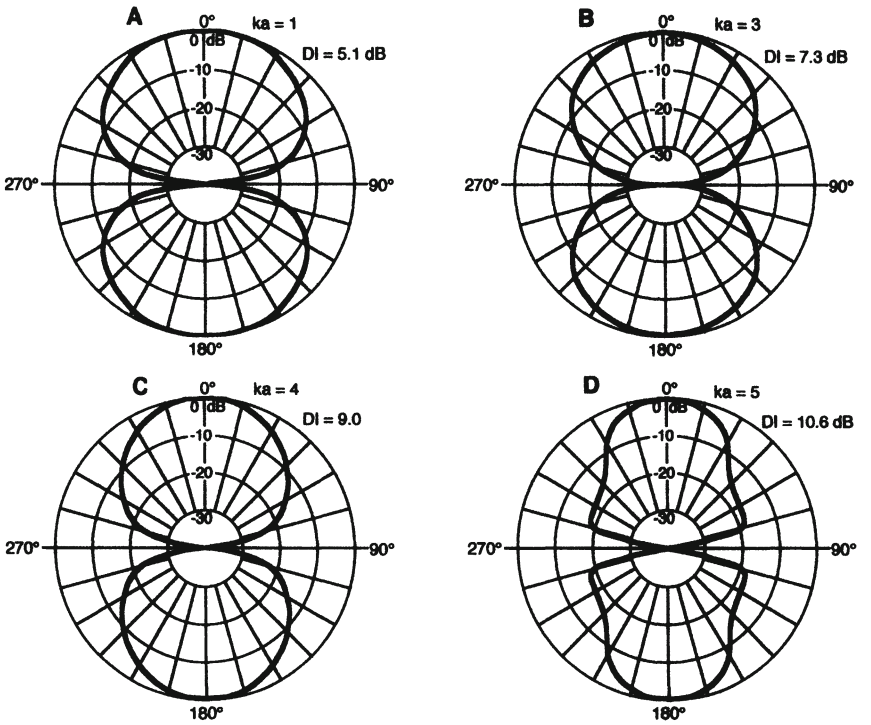

Figure 1-10. Directional (polar) response of an unbaffled piston. (Data after Beranek 1954)

The directional function, $\Gamma(\alpha)$, is given by:

$$\Gamma(\alpha) = 2J_1(ka \sin \alpha)/ka \sin \alpha \qquad 1.16$$

where:

J_1 represents a Bessel function of the first order
a = radius of piston (meter)
$k = 2\pi/\lambda$
α = off-axis measurement angle

As a convenient rule, recall that *ka* equals circumference divided by wavelength. For values of *ka* of 1 or less, we can assume that the radiation is uniform over the solid angle in front of the large wall. For values of *ka* of 3 and greater, the piston takes on progressively more pronounced directivity.

Directionality for an unbaffled piston (a dipole) is shown in Figure 1-10 and for a piston mounted at the end of a long tube at Figure 1-11.

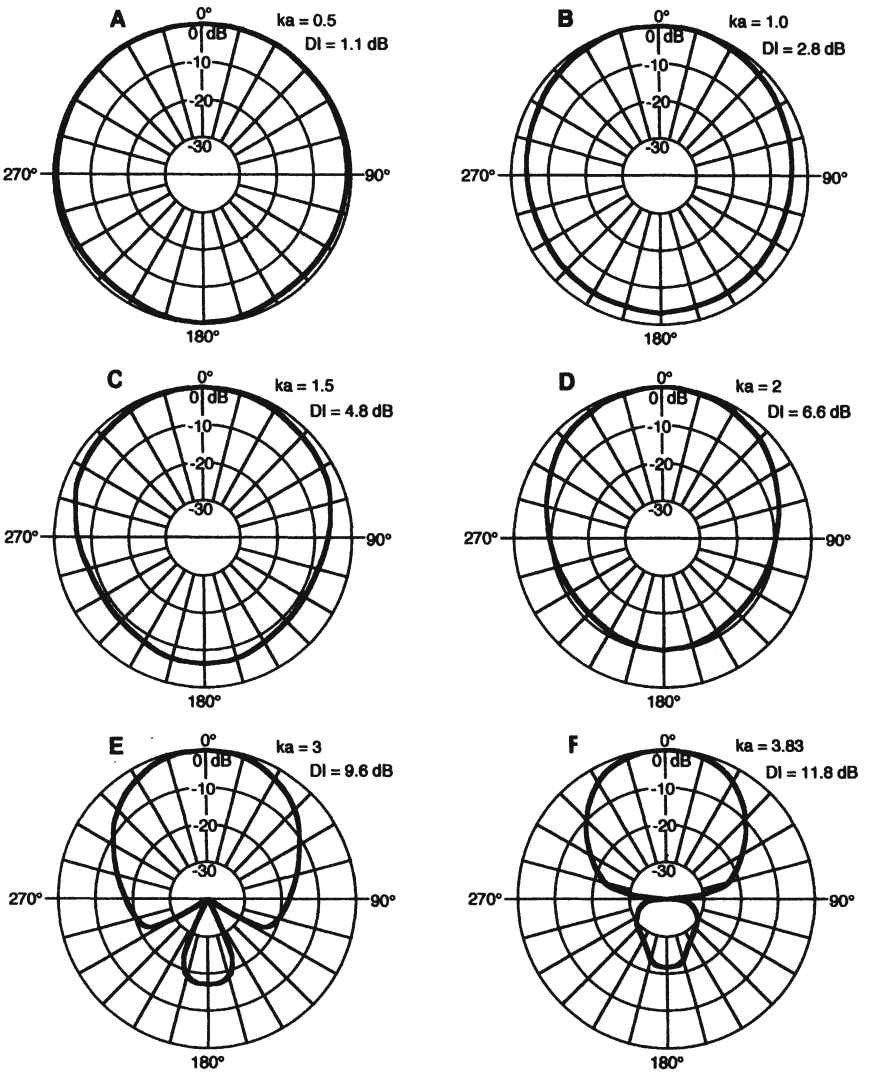

Figure 1-11. Directional response of a piston mounted in the end of a long tube. (Data after Beranek 1954)

A convenient way to quantify the on-axis directional response of a loudspeaker is by *directivity index* (DI). DI is the ratio in dB of sound pressure radiated along the preferential axis of a device, as compared to the sound pressure at the same measuring point if all power from the device were radiated omnidirectionally. A graphical definition of DI is given in Figure 1-12.

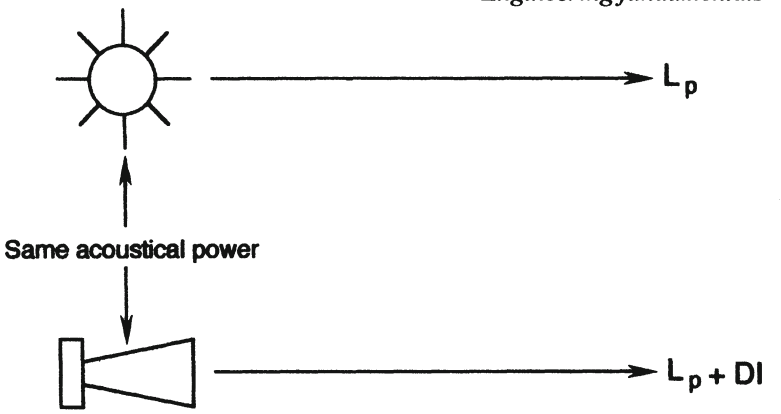

Figure 1-12. A graphical definition of directivity index (DI).

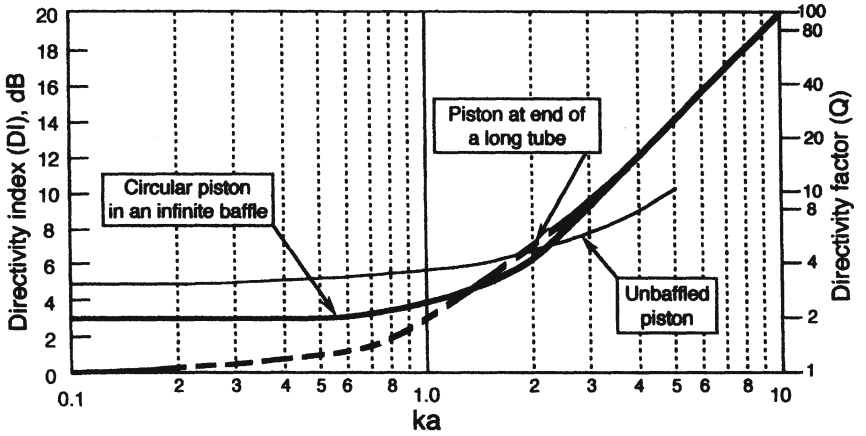

Figure 1-13. On-axis directivity of a piston in a large baffle, at the end of a long tube, and in free space. (Data after Beranek 1954)

1.6.1 The final model

As we have seen, the range of flat power response for our driver model extends from the fundamental resonance, f_0, up to about ka = 2, the frequency at which the power response begins to roll off. In practice, we can use a loudspeaker above that point, taking advantage of the on-axis increase in output due to directional effects. As a rule, we can just about double the upper usable frequency, allowing it to attain a DI of about 10 dB, corresponding to ka = 3. This corresponds roughly to a 380 mm (15") loudspeaker maintaining a reasonably flat on-axis response to approximately 1 kHz.

Figure 1-13 summarizes the data given in Figures 1-9, 1-10 and 1-11 in terms of on-axis directivity index as a function of *ka*.

1.7 Cone excursion, power, and pressure relationships in graphical form

Figure 1-14 shows the relationship of power output from a piston on one side of a large baffle as a function of amplitude, piston radius, and driving frequency. The governing equation is:

$$W_A = \frac{[x_{peak}(f^2a^2)]^2}{2.32 \times 10^{17}} \qquad 1.17$$

where W_A is the radiated power, x is the peak amplitude of motion (mm), f is the driving frequency, and a is the piston radius (mm).

Figure 1-15 shows the sound pressure level produced by a piston in a large baffle as a function of radiated power and distance. The governing equation is:

$$L_p = 112 + 10 \log W_A - 20 \log r \text{ (dB)} \qquad 1.18$$

where W_A is the radiated power and r is the distance (meter).

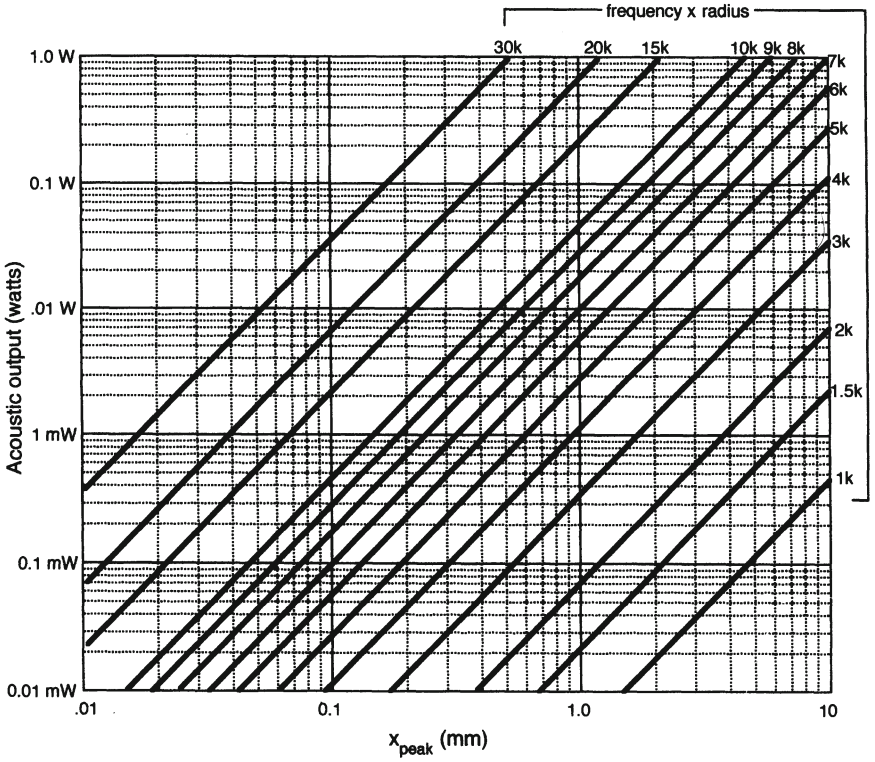

Figure 1-14. Acoustical power output on one side of a piston mounted in a large baffle, as a function of piston amplitude, radius, and frequency.

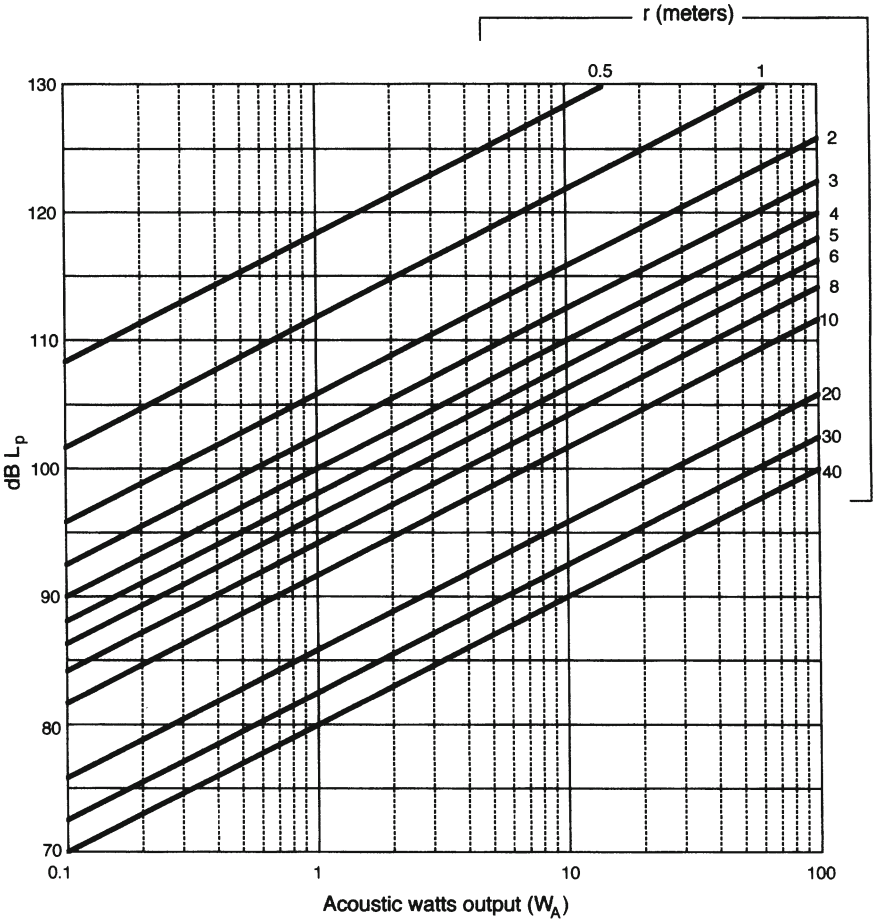

Figure 1-15. Sound pressure level produced by a piston in a large baffle as a function of radiated power and distance.

BIBLIOGRAPHY AND REFERENCES:

Beranek, L., *Acoustics*, John Wiley and Sons, New York (1954). (Reprinted 1993 by American Institute of Physics, Woodbury, NY)

Borwick, J., *Loudspeaker and Headphone Handbook*, Butterworths, London (1988).

Colloms, M., *High Performance Loudspeakers, Fourth Edition*, John Wiley & Sons, New York (1991).

Eargle, J., *Electroacoustical Reference Data*, Kluwer Academic Publishers, Boston (1994).

Hunt, F., Electroacoustics: *The Analysis of Transduction and its Historical Background*, Acoustical Society of America, New York (1982).

Kinsler, L., et al., *Fundamentals of Acoustics*, third edition, John Wiley & Sons, New York (1982).

Massa, F., *Acoustical Design Charts*, The Blakiston Company, Philadelphia (1942).

Olson, H., *Acoustical Engineering*, D. Van Nostrand, New York (1957).

Rice, C., and Kellogg, E., "Notes on the Development of a New Type of Hornless Loudspeaker," *Transactions, AIEE*, volume 44, pp. 461-475 (1925).

Sakamoto, N., *Loudspeakers and Loudspeaker Systems*, Nikankogyu Shimbun, Tokyo (1967). In Japanese.

Siemens, E., U. S. Patent 149,797, issued 14 April 1874.

Small, R., "Direct Radiator Loudspeaker System Analysis," *J. Audio Engineering Society*, volume 20, number 5 (1972).

Chapter 2:
STRUCTURAL DETAILS OF CONE AND DOME DRIVERS

2 Introduction

Cone and dome drivers form the backbone of loudspeaker system design, primarily because of their ease and economy of manufacture and their high level of performance. In this chapter we will examine these factors in detail, as well as discuss many variations on the basic design theme. Mechanical performance limits and distortion will also be addressed.

2.1 Mechanical construction details of the cone driver

Figure 2-1A shows a section view of a 380 mm (15 in) cone driver with the main parts labeled. We will use this view as a guide in discussing the design and construction of the driver. A cutaway view of a cone-voice coil assembly for this driver is shown at *B*.

2.1.1 The frame

The frame, sometimes referred to as "basket," is the ribbed conical structure that holds the driver together. Professional drivers use frames made of die-cast aluminum, while many lower cost frames are made of stamped metal or injection molded plastic. The advantages of the die-cast structure are dimensional accuracy and relative freedom from warping when installed in an enclosure. However, where the magnetic gap dimensions are fairly large, a stamped frame design may have a clear economic advantage.

While there would seem to be little to comment on regarding frame design, it is worth mentioning that considerable engineering effort has been expended over the years in reducing the metal content in frames while maintaining structural integrity. Thin wall castings preserve mechanical strength in a manner similar to stamped automotive body parts. Heat sinking fins and flat surfaces for mounting transformers and/or terminals are among the details that are often designed into frames.

J. Eargle, *Loudspeaker Handbook*

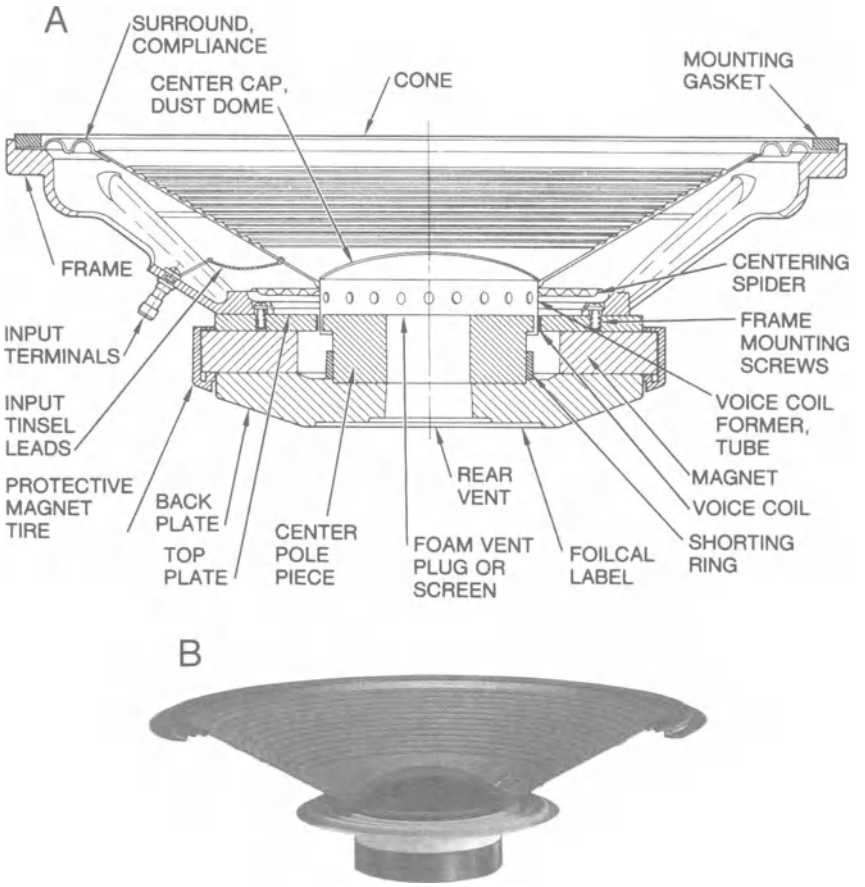

Figure 2-1. Section view of a professional grade 380 mm (15") diameter LF driver (A); cutaway view of a typical cone-voice coil assembly (B). (Data courtesy JBL)

2.1.2 The magnetic motor structure

Chapter 3 will deal with the engineering specifics of magnetics; here we will consider only the mechanical nature of the magnetic structure and its basic function of providing a uniform magnetic field for the voice coil. In the days before high energy permanent magnet materials, driver magnets were electrically energized with direct current (dc) flowing through the windings of a field coil. Today, permanent magnets are universally used.

Three types of common magnetic motor structures are shown in Figure 2-2. The Alnico V (aluminum-nickel-cobalt) version shown at *A* was in common use from the period after World War II until the mid-seventies, when cobalt

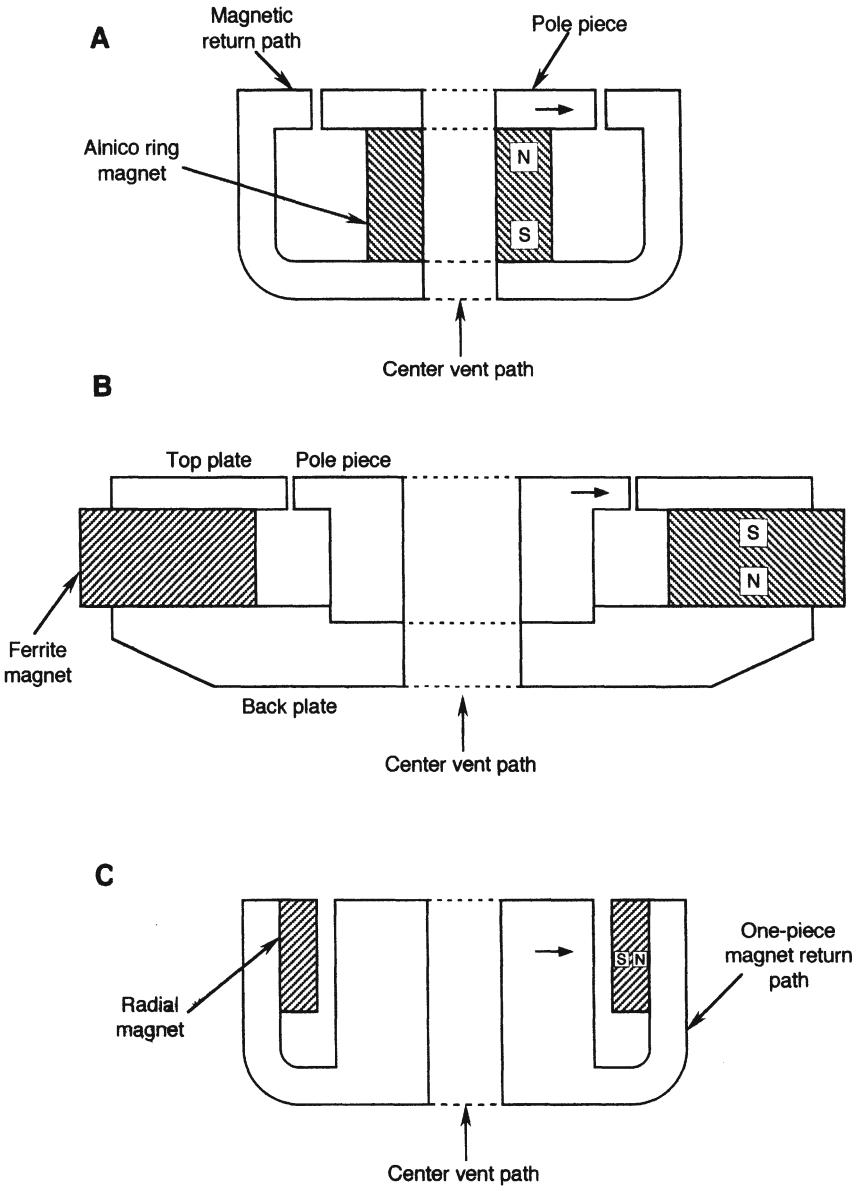

Figure 2-2. Typical magnetic structures. Alnico ring magnet structure (A); ferrite magnet structure (B); high-energy magnet material with polarization along the radius of the structure.

became a very expensive commodity. A typical ferrite, or ceramic, magnet structure is shown at *B*, and is by far the most common structure today. The structure shown at *C* illustrates the use of high energy, radially charged small magnets made of rare earth materials such as samarium and neodymium.

The flux is concentrated in the magnetic gap, but there will always a certain amount of so-called *fringe flux* extending above and below the gap. Any flux extending around the magnetic structure as a whole is referred to as *stray*, or leakage, flux, and care is taken in design to minimize it.

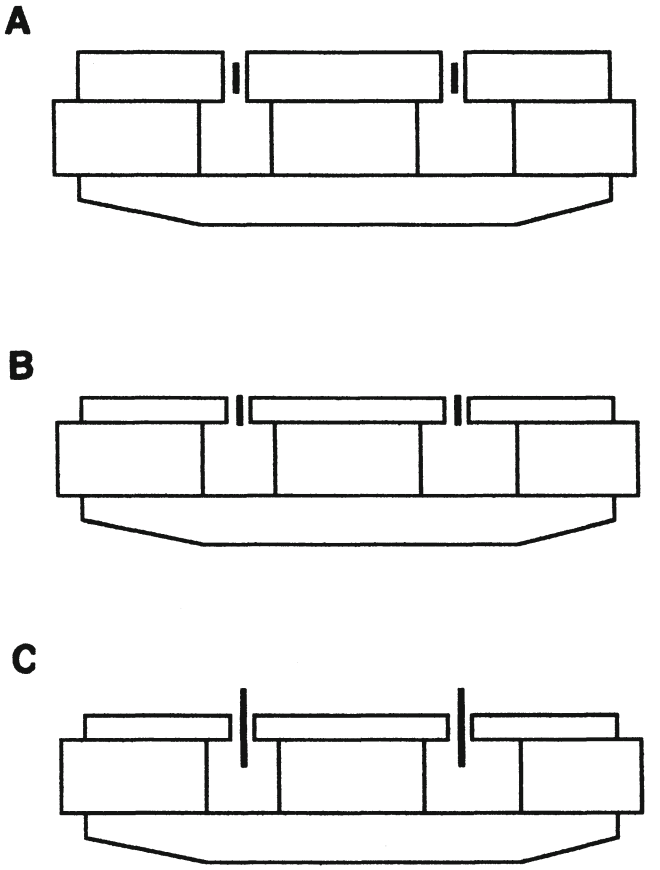

Figure 2-3. Voice coil and top plate topology. Underhanging voice coil (A); voice coil and top plate of equal length (B); overhanging voice coil (C)

Figure 2-3 shows the voice coil-top plate topologies available to the transducer engineer. The underhanging voice coil, shown at *A*, lies completely within the axial range of uniform magnetic flux density. Such a structure is expensive, due to the metal and magnet requirements, but it completely engages a short voice coil over its normal travel and is often used in high linearity drivers of moderate to high efficiency.

The form shown at *B* concentrates all of the flux in the coil at its rest position. It is evident that even moderate excursions of the voice coil will result in some loss of total flux engaging the voice coil, thus producing distortion. This design is common in very high efficiency drivers used for musical instrument amplification, where some degree of distortion may indeed be sonically beneficial.

The overhanging design shown at *C* provides constant flux engaging a portion of the voice coil over a fairly large excursion range. The compromise here is that a large percentage of the voice coil lies entirely outside the flux field at all times, causing a relatively low $(Bl)^2/R_E$ ratio. This design approach may be applicable for drivers intended for high linearity, but with relatively low efficiency.

The design shown in Figure 2-4 combines elements of the over- and underhanging approaches shown in Figure 2-3. The undercut pole piece is extended above and below the top plate and thus spreads the magnetic flux over a larger axial range. This design is also beneficial in that it provides an effective heat sinking surface adjacent to the voice coil over a large excursion range.

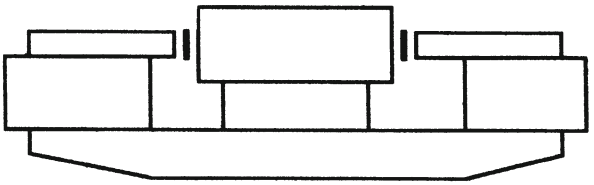

Figure 2-4. Detail of extended pole piece.

The motor design shown in Figure 2-5 uses a single high-energy magnet to create a pair of reversely polarized gaps in a series magnetic circuit. A dual voice coil structure with reversely wound coils is used. The push-pull arrangement reduces second harmonic distortion and produces a uniform magnetic field over a fairly large axial range. Other advantages are that the magnetic field of the motor is effectively contained, producing little stray flux, and that relatively little iron is used in the overall structure. The requirement for two magnetic gaps in series calls for high energy magnetic material and relatively small diameter voice coils in order to achieve high flux densities in each active gap. In most designs using this topology the voice coils are wired in series.

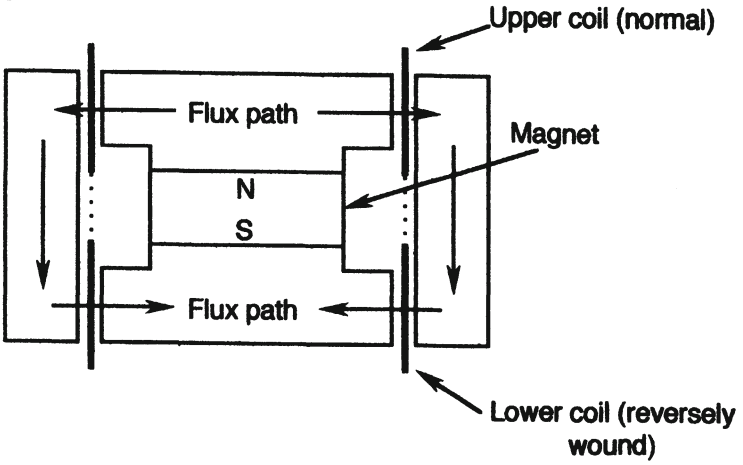

Figure 2-5. Dual gap, with reverse flux paths and reversely wound dual voice coils.

In some early stereo systems, dual voice coils, wound on the same former, were used for combining stereo low frequency signals in a single driver for systems with a common bass unit. In this application, it is desirable for the coupling between the two windings to be minimal so that amplifier stability does not become a problem.

2.2 The moving system

The driver moving system consists of five elements: the cone, voice coil assembly, outer suspension (surround), inner suspension (spider), and dust dome, as shown in Figure 2-1. The purpose of the two suspensions is to ensure that the motion of the cone assembly is basically constrained to the axial dimension, with minimal radial and rocking motions. Each of these elements has a profound effect on the response of the driver, and we will discuss each in detail.

2.2.1 The cone

The cone is the part of the driver that radiates sound and is the approximation of the ideal piston we discussed in the previous chapter. For operation in the driver's piston band at moderate driving levels, a simple cone made of a light, rigid material does very well. But for large excursions over a wide frequency range there are other considerations.

At high excursions the cone has a tendency to break up, producing erratic response and distortion. At the same time, high frequency response of any

magnitude of cone motion brings into play complex vibrational modes. The cone profile and material are critical factors in controlling these effects.

Section views of several cone profiles are shown in Figure 2-6. A shallow cone with annular ribs is shown at *A*. The purpose of the ribs is to add stiffness to the cone with minimal addition of mass. This promotes good pistonic action with extended high frequency response. A deep cone is shown at *B*. In general, a deep cone has greater rigidity than a shallow one, all else being equal, and we find them used in robust designs intended for high level applications. The on-axis high frequency response of the deep cone may be compromised to some extent due to the fact that the rear portion of the cone (the apex) is displaced from the edge of the cone by an amount that will cause a cancellation in response on-axis when the front-to-back distance is equal to a half wavelength. A shallower cone raises the frequency at which this cancellation will take place.

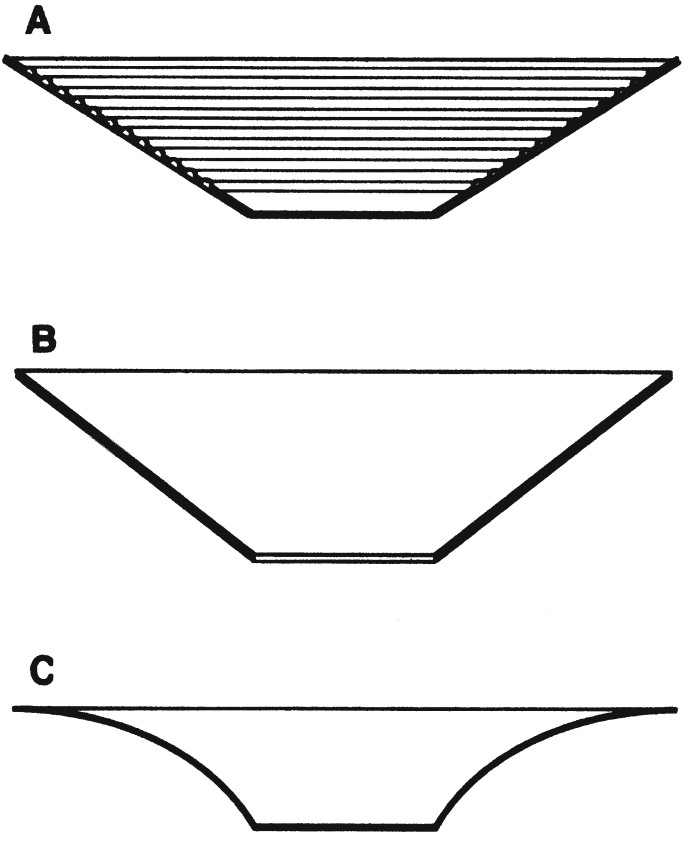

Figure 2-6. Typical cone profiles in section view. Ribbed cone (A); straight sided cone (B); "curvilinear" cone (C).

The so-called *curvilinear* cone profile shown in Figure 2-6C is often used in light weight moving systems where efficiency and extended output at high frequencies are the chief considerations. The shape of the cone actually promotes decoupling from the voice coil at high frequencies, increasing the driver's output while maintaining a fairly smooth response on axis. The original JBL 380 mm diameter D-130 from the late 1940s was the first design of this type to attain wide professional acceptance, and the approach is still favored in drivers used with electronically amplified instruments.

Figure 2-7 shows typical "bell modes" that a cone may exhibit at high frequencies; these can often be identified as such in the on-axis response of drivers when driven at any level. The figures represent a "snapshot" of a cone, as seen from the front, with the plus and minus signs indicating instantaneous outward and inward motions of the cone.

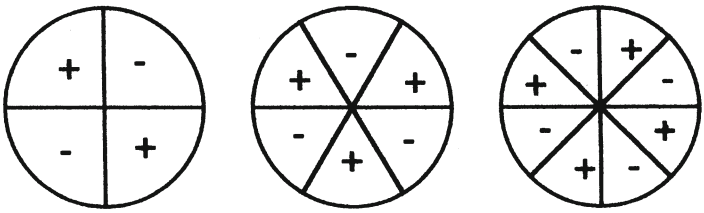

Figure 2-7. Representation of "bell modes" of vibration.

The on-axis data shown in Figure 2-8 shows the effects of cone breakup for three drivers, each designed for a specific application. The JBL 2220 has a light curvilinear cone, and its mid-band sensitivity of 101 dB, 1 watt at 1 meter, indicates a piston band efficiency of about 8%. Note that the response extends well beyond 2 kHz with relative freedom of sharp peaks and dips. The JBL 2225 driver is designed for general sound reinforcement applications and has a piston band efficiency of about 3.5%. The pronounced peak in cone breakup at about 4 kHz is well outside the normal bandpass of the driver. The JBL 2235 is designed for use in studio monitor loudspeakers and has a piston band efficiency of 1.3%. Although there are a number of ripples in the pattern of breakup modes, they are fairly small and diminish quickly above 2 kHz.

The response of a typical 125 mm (5 in) midrange driver is shown in Figure 2-9. Note the similar pattern of breakup, in this case transposed upward in frequency by the inverse of the relative dimensions of the drivers.

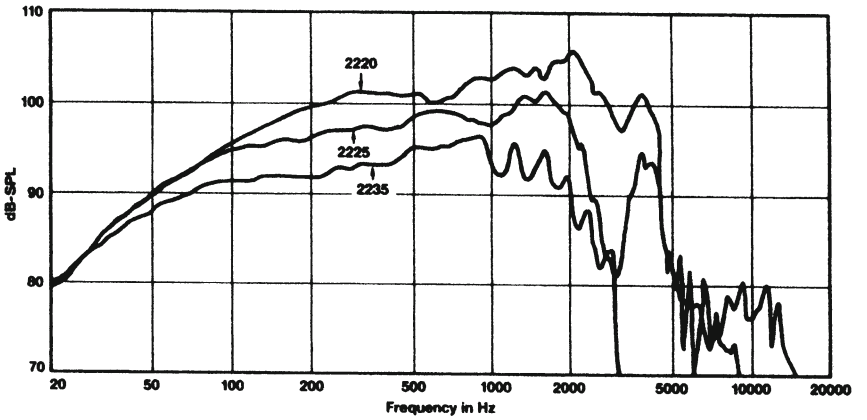

Figure 2-8. On-axis response of JBL 2220, 2225, and 2235 LF drivers (Data courtesy JBL)

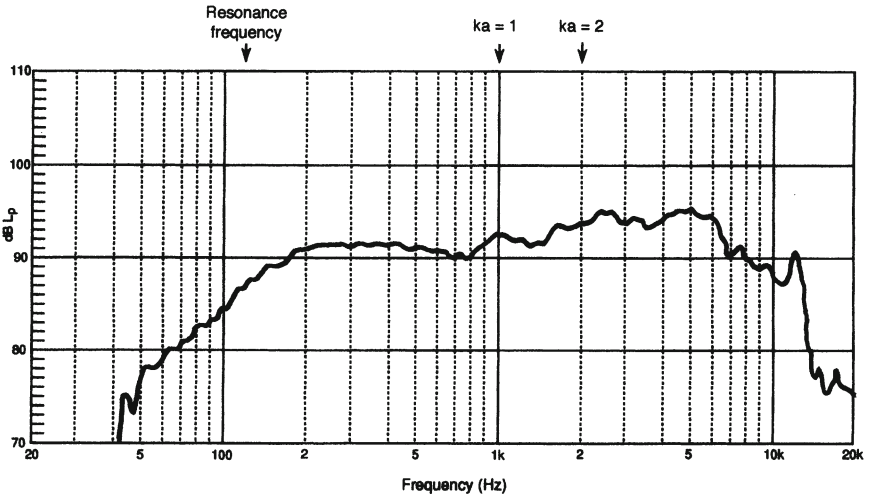

Figure 2-9. On-axis response of JBL model LE-5 midrange driver. (Data courtesy JBL)

2.2.2 Cone materials

Cone materials include paper (cut and seamed), paper pulp (molded or felted to fit), plastic, metal, and all types of composites. The most generally used material is felted paper pulp made by drawing a fibrous slurry through a fine screen in the shape of the desired cone. The cones are then cured, dried, and trimmed to fit. Molded plastic materials are also in wide use and have the virtues of being more consistent, batch to batch, than the felted variety.

The desirable mechanical characteristics of a cone are rigidity and high damping (internal loss). These characteristics are normally opposed to one another in that anything that improves one will generally work to the detriment of the other. The necessity of rigidity is clear; the high excursions that drivers exhibit at low frequencies demand that the cone have sufficient strength not to buckle or deform under the forces imparted to it.

The need for internal damping in the cone is illustrated in Figure 2-10. At sufficiently high frequencies, the cone does not act as a single unit; rather, it acts as a mechanical transmission line with distributed mass, resistance, and compliance, providing a medium for mechanical waves to travel outward as shown. If these waves (shown highly exaggerated) reach the edge of the cone with little attenuation, they will reflect back to the cone apex, creating a pattern of peaks and dips in response.

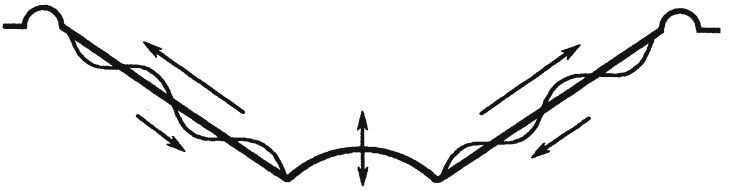

Figure 2-10. Representation of traveling waves in a cone.

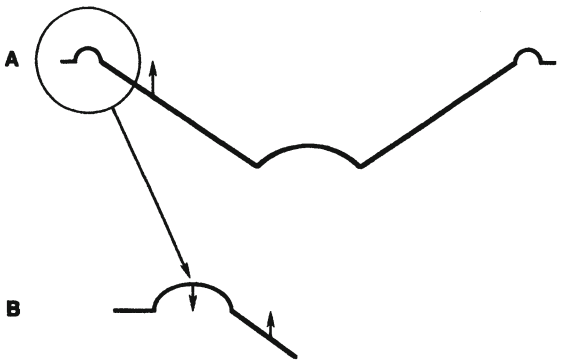

Figure 2-11. Representation of a surround resonance mode in antiphase with cone.

The cure for this problem lies in a combination of damping in the cone itself as well as attention to damping in the outer surround so that it will act, insofar as possible, as a matched impedance load. Figure 2-11 illustrates a typical problem that can occur when a resonance in the surround is driven by an unattenuated signal from the cone. Here, the center section of the surround

is vibrating in antiphase to the cone, creating what is commonly called a "surround dip" in response.

As an example of how well the compromise can be made, we show the on-axis response of the JBL LE-14 driver in Figure 2-12. This driver has a felted cone treated on both sides with a controlled amount of damping material known as *Aquaplas*™. The surround is a half-roll of polyurethane foam that provides an excellent termination for the traveling wave in the cone. Note that the on-axis rolloff in the 1-to-2 kHz range is very smooth, with a minimum of peaks and dips.

Plastic cones are attractive in that the desired attributes of stiffness and damping can be uniformly maintained in production. Additionally, the material is not affected by environmental humidity, as is paper or other felted products.

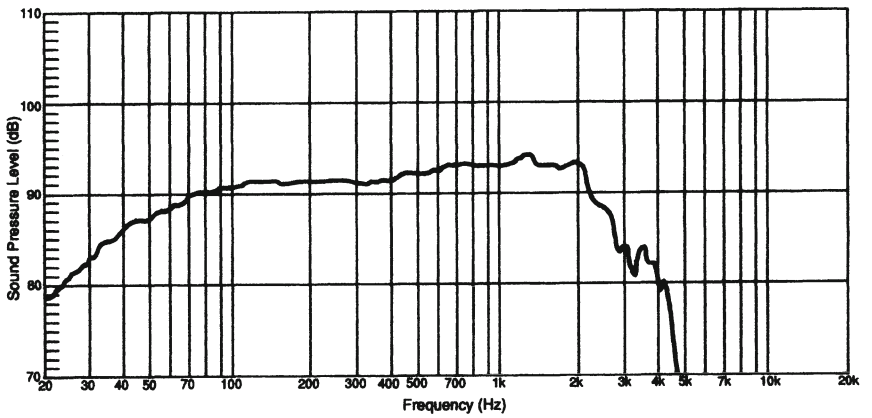

Figure 2-12. On-axis response of JBL model LE-14 LF driver. (Courtesy JBL)

2.2.3 The outer suspension (surround)

Figure 2-13 shows a variety of surround details in common use. The half-roll form shown at *A* is usually made of polyurethane foam or Neoprene, a type of synthetic rubber. The design offers high compliance and long axial travel, but the price paid for this is diminished radial stability. The form shown at *B* is a double half-roll, normally made of treated cloth. The design is very rugged and can be treated so that it is fairly stiff and well damped, making it a good choice for drivers intended for music and sound reinforcement.

A common form of mechanical distortion in surrounds is known as *hoop stress*. Imagine that the half roll surround shown in Figure 2-13A was made of

a non-warping material, such as treated cloth. Then we could view the surround as composed of a number of concentric circular elements, or hoops. Now, as we attempt to move the cone in an axial direction, some of the hoop elements are constrained to move inward or outward and thus take on a smaller or larger diameter. This of course cannot happen, and instead the surround will tend to wrinkle. In cones of this sort you may often hear a "crinkling" sound when the driver is driven to high excursions at very low frequencies. Materials that can warp, such as synthetic rubber or various foams, will actually deform to eliminate hoop stresses — but this can result in slightly less radial stability in the surround.

The multiple roll, or accordion roll, form shown at *C* offers high excursion capability, but with some tendency for resonances. Olson et al. (1954) present the data shown in Figure 2-14. Here, the nature of the suspension motions are clearly indicated, and the addition of a rubber damping ring to the suspension smooths the response dip, as shown.

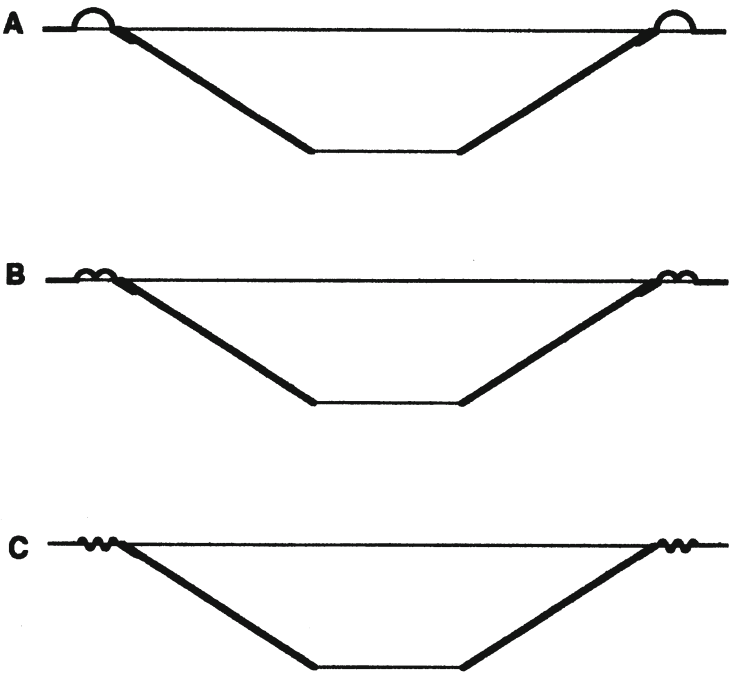

Figure 2-13. Various surrounds in section view. Half-roll surround (A); double half-roll surround (B); "accordion" surround (C).

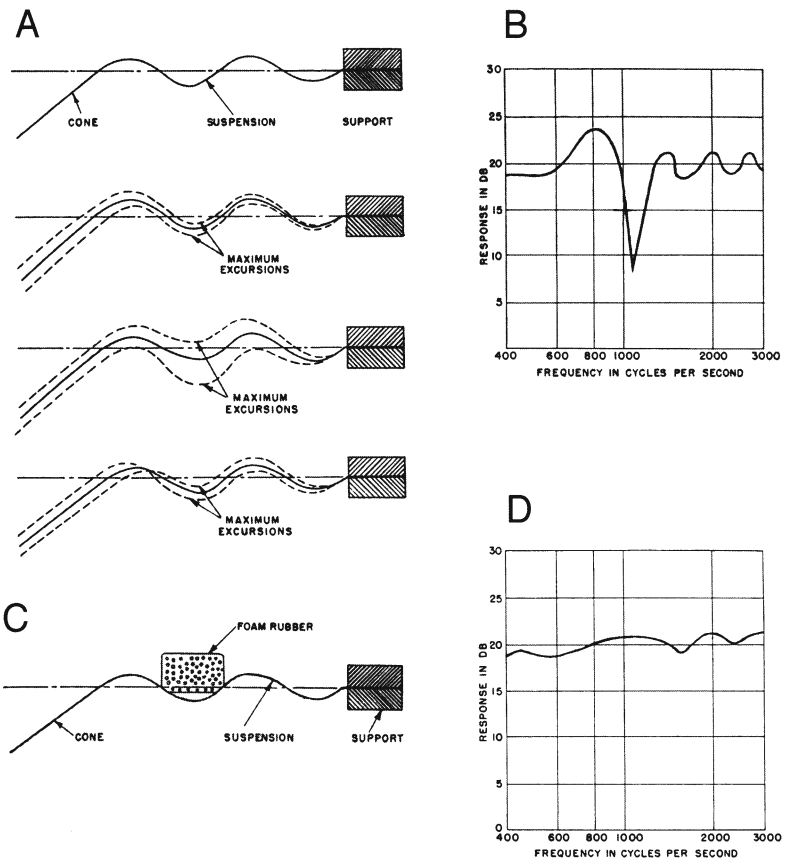

Figure 2-14. Surround resonance modes. Surround and cone motion (A); dip in response caused by effect shown at *A* (B); surround treatment to reduce motion (C); improvement in response (D).
(Data courtesy Journal of the AES)

2.2.4 The inner suspension

Often called the "spider," the inner suspension is connected to the voice coil former, and its outer edge is bonded to the frame. The original designs, many years ago, had legs that were bonded to the frame, hence the familiar name.

Figure 2-15 shows a profile views of a typical spiders. The form shown at *A* is a flat spider, and the form shown at *B* is a cup spider. The material normally used is a fairly open weave cloth impregnated with phenolic resin and formed under heat. The multiple rolls afford excellent opportunities for

spurious resonances at high drive levels, just as we have observed in the outer suspension.

Some manufacturers, notably Gauss, have made use of a double spider arrangement in LF driver design, as shown in Figure 2-15C, for added stability during high excursion operation.

In some driver designs, the spider must be porous in order to provide venting of the volume of air captured behind it. It is clear from the section view shown in Figure 2-1 that venting in that particular design is through a center hole at the back of the magnet structure. However, many magnet structures are not open to the rear, and venting must take place through the spider or through a porous section in the dust dome.

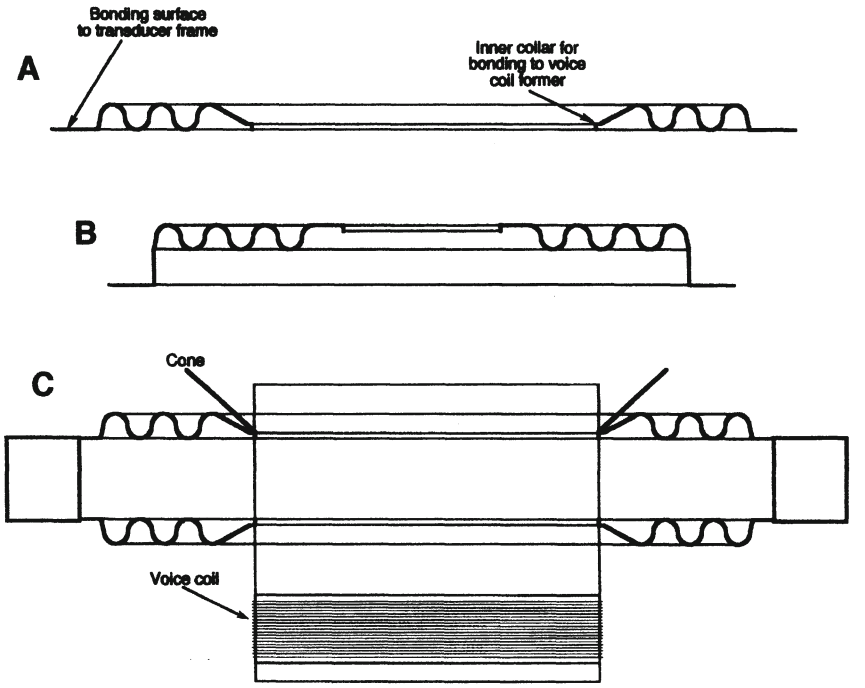

Figure 2-15. Section views of the spider. Flat type (A); cup type (B); view of dual spider assembly (C).

2.2.5 The voice coil

Figure 2-16A shows a view of a voice coil that has been directly wound onto the former. A section view is shown at *B*. The design shown here is made of flat (ribbon) aluminum wire milled specifically for this purpose. The return of the bottom lead on the inside of the former can be seen in the drawing. Both leads exit at the top of the coil and, after the coil assembly has been glued to the cone, they are dressed on the front of the cone to a set of eyelets near the apex of the cone. From here, they are connected by loops of tinsel lead on the back side of the cone to a set of terminals on the frame. Refer again to Figure 2-1B for a photograph showing the actual positioning of the voice coil assembly to the cone assembly.

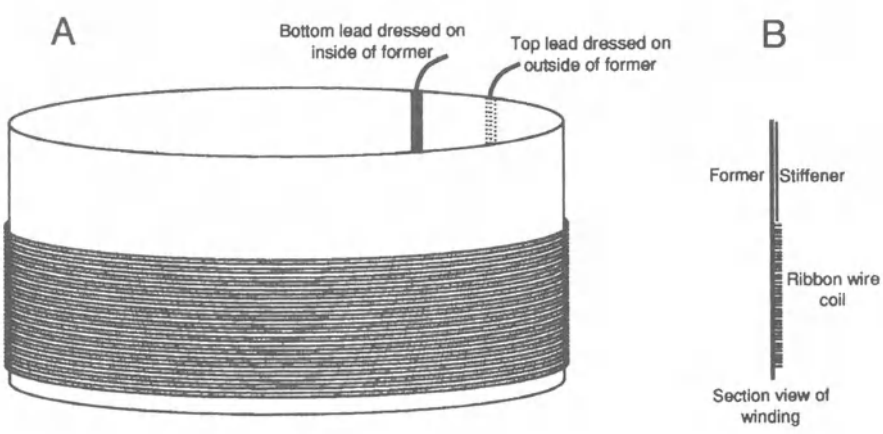

Figure 2-16. An assembled voice coil (A); section view of winding (B).

In drivers intended for professional applications, ribbon wire has several distinct advantages over round wire:

1. *Greater packing density.* Theoretically, the "dead" space between adjacent windings is minimal, providing about a 27% improvement over round wire, providing minimum R_E for the wire volume occupied.

2. *Slightly increased rigidity.* The tight bonding between adjacent layers of the coil provides an integral structure that resists warping.

3. *Impedance adjustment.* This is a very significant advantage of ribbon wire, as shown in Figure 2-17. It is possible, by adjusting the ribbon thickness

appropriately, to operate a driver at a new design impedance with no change in the $(Bl)^2/R_E$ ratio.

The $(Bl)^2/R_E$ ratio is the electromechanical coupling coefficient of a driver between electrical and mechanical domains. It has the dimensions of N^2/W (newtons squared per watt), and as such is independent of the design impedance of the driver. It is also dimensionally equivalent to R_M, the mechanical resistance, or damping, in SI mechanical ohms. It is equivalent to the mechanical cone damping sensed when the cone of a driver is deflected with the voice coil terminals short-circuited.

In Figure 2-17*A*, assume that we have a voice coil at a design impedance of, say, 8 ohms. We wish now to design a new coil that presents a 16 ohm impedance. To do this, we mill the wire so that it has 0.7 the previous thickness, as shown at *B*. It is clear that the total length of wire in the voice coil will now be 1.4 times as at *A*. The new R_E will be twice what it was at *A*, because of the added length and reduced cross-section, and the new value of *Bl* will be 1.4 times greater. However, $(Bl)^2$ will have increased by a factor of 2, so we will maintain the same $(Bl)^2/R_E$ ratio as before.

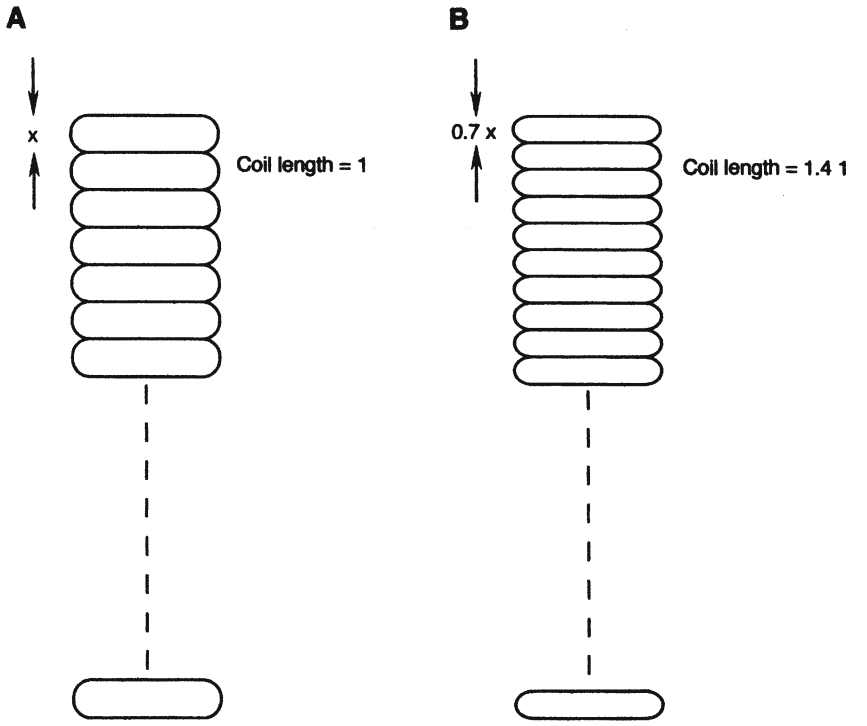

Figure 2-17. Voice coil impedances. Section view showing flat wire profile for normal impedance (A); view showing profile for 2-times impedance (B).

Voice coils are invariably made of aluminum or copper wire. The resistivity of aluminum is about 1.6 times that of copper, but its advantage lies in its lower mass, which is less than one-third that of copper.

Typical impedance curves for 8 and 16 ohm versions of the same driver are shown in Figure 2-18. In both cases the driver was mounted in a 280 liter (10 cu ft) sealed enclosure. The rise in impedance at the fundamental system resonance, as modified by the enclosure volume, is apparent and is a reflection of the mechanical resonance through the *Bl* coupling coefficient into the electrical domain. The rise in impedance at higher frequencies is primarily due to the inductance of the voice coil, L_E. It is the dominant element in the driver's impedance above about 1 kHz.

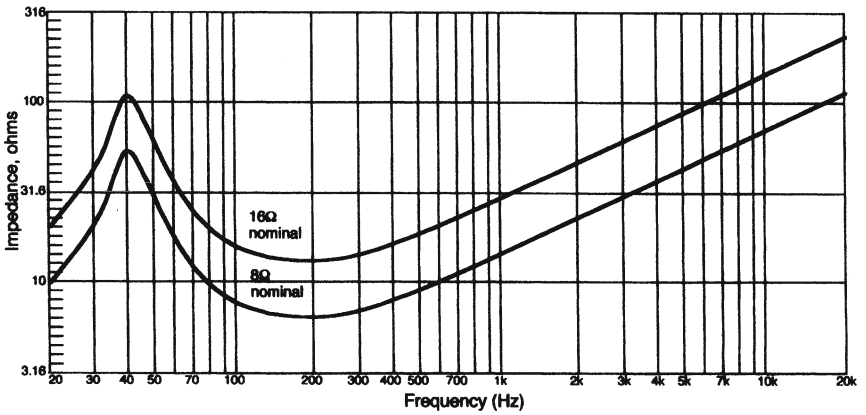

Figure 2-18. Typical impedance curves for 8 and 16-ohm versions of the same LF driver. Impedance shown on logarithmic scale.

The minimum value of impedance in the region just above the impedance peak is where all reactive terms have cancelled each other, and we are left only with resistive terms: voice coil resistance, mechanical loss terms reflected through to the electrical domain, and of course the radiation load itself.

The effect of voice coil inductance can be partially reduced by plating a highly conductive copper or silver ring on the pole piece in the vicinity of the voice coil. In this application, the plated ring acts as a shorted turn secondary winding of a transformer and swamps out the effect of the inductance. This is commonly done in any large driver that is designed for both mid and high frequency response.

In general, maximum driver efficiency is attained when the mass of the voice coil is equal to the mass of the cone and its associated air load, with both sets of masses designed to be as low as possible. The actual ratio of the two mass terms will vary over the operating frequency range. For example, at LF the air mass will dominate, while at HF, due primarily to the decoupling of the cone, the voice coil mass may dominate. For a loudspeaker with extended HF response, an aluminum voice coil would be advantageous, since its lower mass would materially improve HF response. On the other hand, a driver intended for delivering large amounts of power at low frequencies will benefit from a copper voice coil, since it would provide greater electromechanical coupling.

2.2.6 The dust dome

Almost an afterthought, the dust dome is a spherical section, normally made of molded paper or drawn aluminum, that is glued to the top of the voice coil former as the driver reaches the end of the assembly line. Its primary purpose is to keep debris from entering the magnetic gap, but it also functions to stiffen the moving system to some degree.

Over the years, numerous "full-range" drivers have been designed with aluminum domes that take advantage of the decoupling of the relatively massive cone from the voice coil at high frequencies. On-axis response can be maintained to fairly high frequencies, purely through the direct mechanical coupling of the voice coil to the aluminum dome.

2.3 Variations on the cone driver

In its more than three-quarters of a century of existence, the cone driver has seen a vast number of modifications and changes, and in this section we will describe some the more interesting of these.

2.3.1 The decoupled cone

As we have stated, in all cone drivers there is a certain amount of decoupling of the voice coil and cone at high frequencies. One of the earliest efforts to make use of this was the Duo-Cone design of the Altec-Lansing Company, shown in Figure 2-19. The cone (A) was divided about midway, providing it with an added suspension element and damping for that element. The assumption was that, at low frequencies, the entire cone moved as a unit,

while at higher frequencies only the inner, smaller, cone was moving. The theoretical mobility equivalent circuit of the moving system is shown at *B*. In many aspects, such a design as this tended to elevate loudspeaker driver manufacturing to the high art of making a violin! Fine in concept, but very difficult to control on the production line because of spurious resonances.

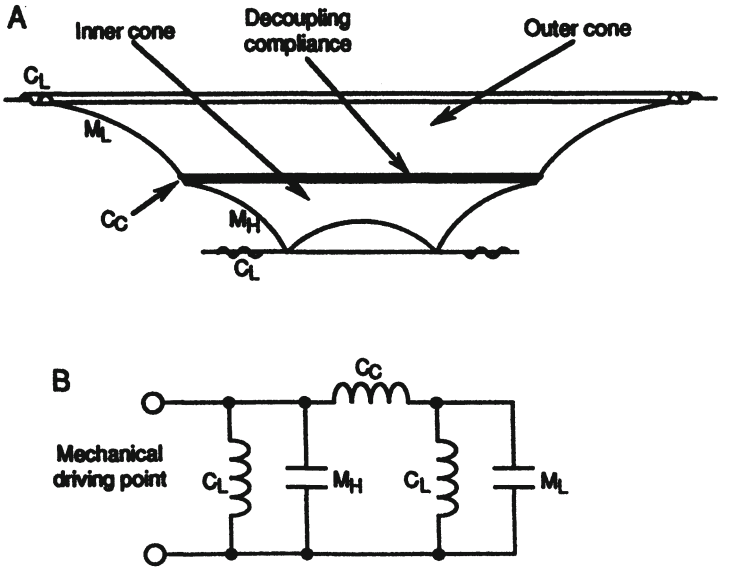

Figure 2-19. Section view of the Altec-Lansing Duo-Cone profile (A); mobility equivalent circuit for system (B).

2.3.2 The "whizzer" cone

To take full advantage of the decoupled voice coil, a free-edged whizzer cone can be attached to the voice coil former, providing a highly resonant acoustical termination for direct radiation of very high frequencies, as shown in Figure 2-20. Whizzers are widely used today in low priced loudspeaker systems and actually perform better than one would suspect. Again, there is considerable response variation from unit to unit.

2.3.3 The JBL LE-8

The venerable LE-8 dates from the late 1950s. This remarkable 200 mm (8-inch) diameter driver has a light cone, treated with Aquaplas for damping. The top plate is thick and accommodates an underhanging voice coil for good linearity. The 50 mm (2 inch) aluminum dust dome is carefully damped on the underside to control its response. Figure 2-21A shows a cutaway view of the

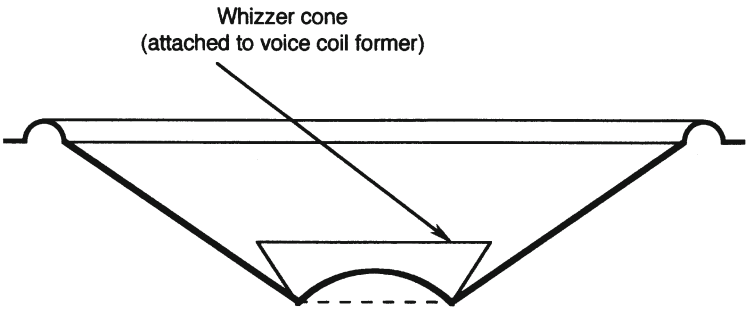

Figure 2-20. Section view showing "whizzer" HF cone attached to LF cone.

A

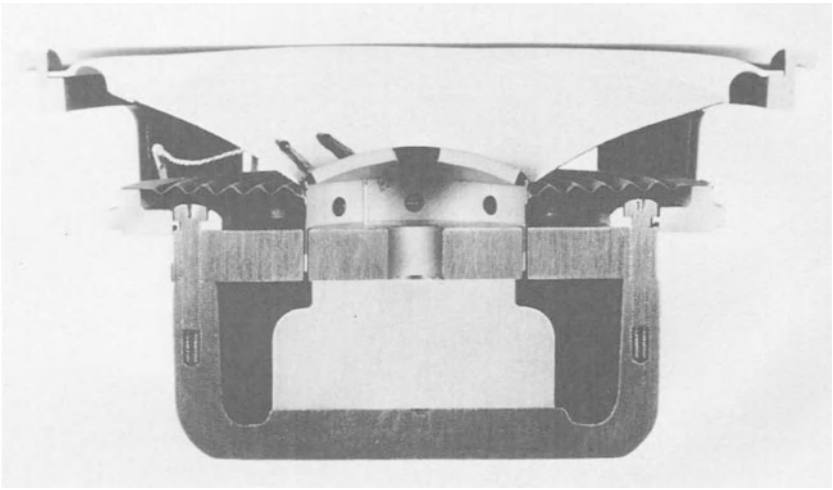

B

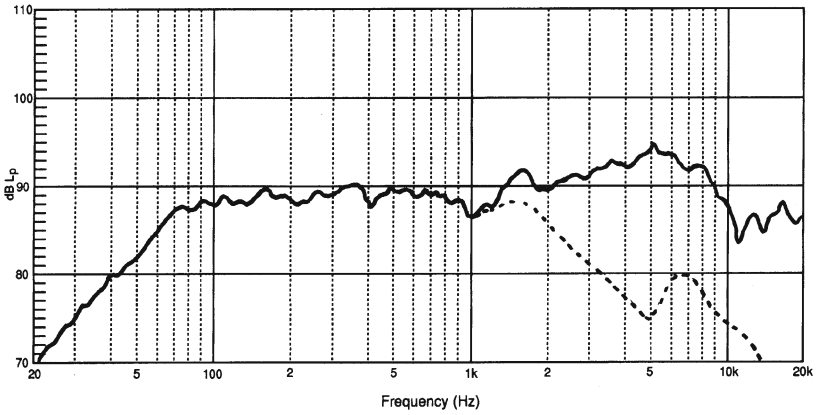

Figure 2-21. The JBL model LE-8 full range cone driver. Photo (A); typical on-axis response (solid curve); dashed curve indicates typical 45° off-axis response (B). (Data courtesy JBL)

LE-8, and typical response is shown at *B*. The LE-8 once was very popular as a close-in monitor loudspeaker, where its axial response predominates over its power response, which falls off rapidly at high frequencies. For controlled response beyond 10 kHz, the LE-8 required a great deal of on-line manufacturing process control.

2.3.4 Dual magnetic gap designs

The idea of combining two or more transducers on one chassis has always been attractive, and there are numerous successful designs attesting to this. None has been as elegant as the British Tannoy Dual-Concentric loudspeaker, which uses a single magnet with two parallel gaps, one for the low frequency section and the other for the horn loaded high frequency section. A section view of the magnetic structure is shown in Figure 2-22.

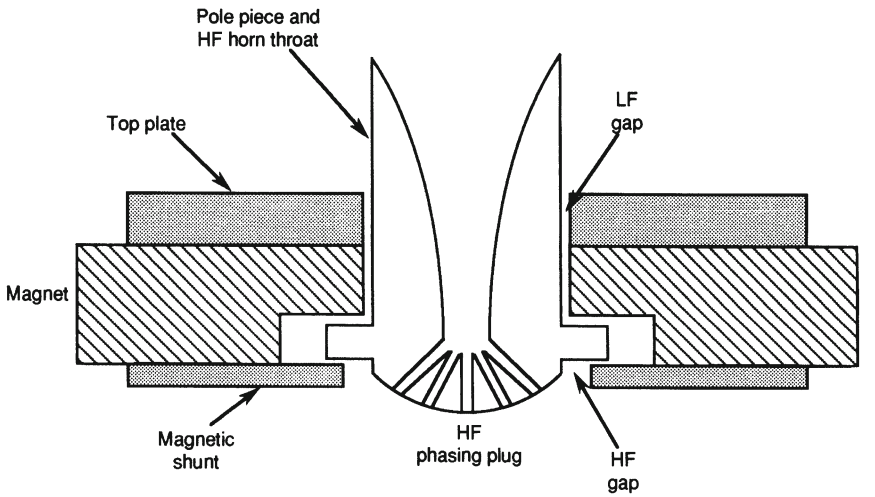

Figure 2-22. Section view of the Tannoy Dual-Concentric loudspeaker magnetic structure.

2.4 HF dome drivers

It is very difficult to make a small cone high frequency driver with double suspensions because of size limitations, and the simple dome driver has become the standard here. The major structural difference between the cone and dome is that the dome has only a single suspension. The dome resembles a very small cone loudspeaker with its cone removed, leaving only the inner suspension, voice coil, and the dust dome operative.

Figure 2-23 shows a section view of a typical 25-mm (1 in) high frequency dome. There is normally a metal mesh screen on the front to protect the dome. Typical materials used for the dome construction include metals such as aluminum, titanium, and beryllium. Soft domes are made of thin molded cloth material that has been sized and "doped" with a viscous damping compound.

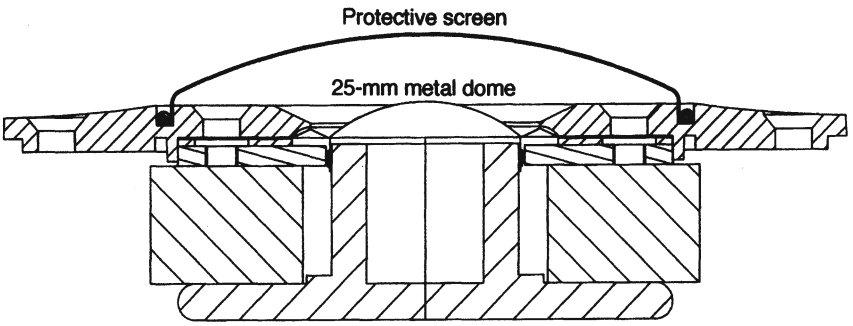

Figure 2-23. Section view of a typical dome HF driver. (Data courtesy JBL)

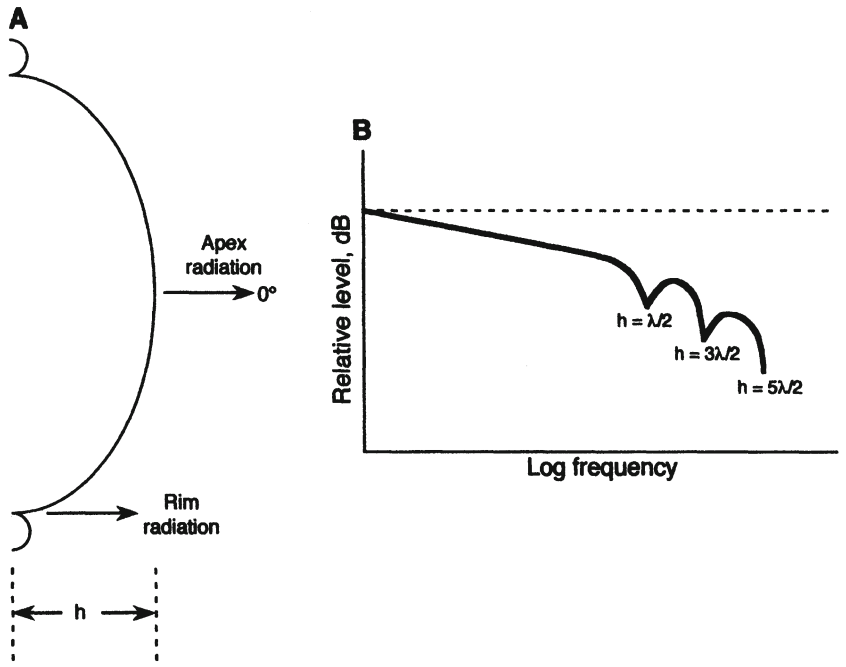

Figure 2-24. On-axis HF losses in a dome transducer.

Although the metal dome is a sector of a sphere, the radiation from the dome is not that of a pulsating sphere. Rather, it moves as a unit and will exhibit a pattern of high frequency dips in on-axis response as portions of it propagate in-phase and anti-phase with each other. This is shown in Figure 2-24. For example, a dome with height of *h* meters will show a dip in response at the frequency whose wavelength is equal to *h/2*. For a dome high frequency device with a height of 10 mm (0.4 in):

$$f = 345/[2(10) \times 10^{-3}] = 17.25 \text{ kHz} \qquad 2.1$$

While such a response dip is normally located at the upper end of the device's bandpass, it is worth noting that the phase shift is a gradual one and may be noticeable in the 5 to 6 kHz range.

The typical soft dome acts as a unit at lower frequencies; however, at progressively higher frequencies, the mass of the dome gradually decouples so that at the highest frequencies the radiation is primarily from the voice coil itself. It in effect becomes a ring radiator at the highest frequencies.

Because of the decoupling, the radiating mass is small at high frequencies, and the output power can be maintained fairly flat. The high internal damping in the moving system tends to flatten the overall response, freeing it of prominent peaks and dips. The basic shortcoming of the typical soft dome is its fairly modest power rating. Well designed metal and soft dome high frequency devices normally exhibit flat on-axis response out to 20 kHz, or slightly beyond that frequency.

2.5 MF dome drivers

Figure 2-25 shows a section view of a highly regarded midrange dome driver manufactured by ATC Loudspeaker Technology Ltd. in the UK. The voice coil has a diameter of 75 mm (3 in.), and the dome is made of treated cloth. Sensitivity of this driver is 94 dB, 1 watt at 1 meter, and the program power rating is 150 watts. The normal operating bandwidth is from 380 Hz to 3.8 kHz, and peak levels of 115 dB L_p can be produced at a distance of 1 meter. Such drivers as these are widely used in medium to high level monitoring applications as an alternative to horn systems.

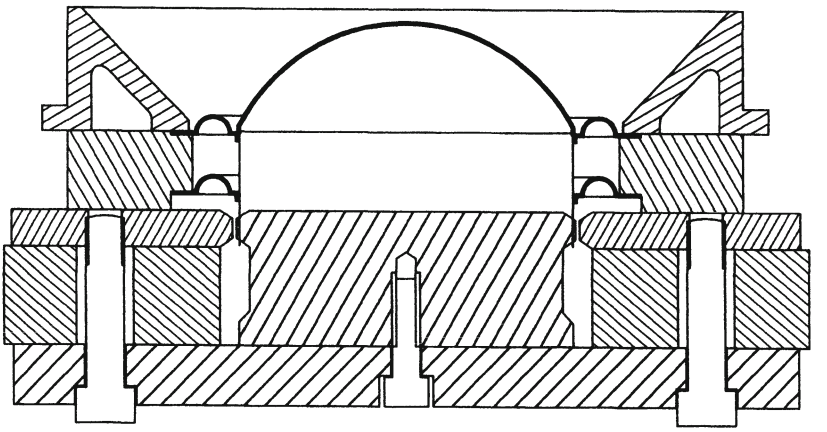

Figure 2-25. Section view of a midrange dome driver. (Data courtesy ATC Loudspeaker Technology, Ltd.)

2.6 Distortion in cone and dome drivers

In general, the very low mechanical driving point mechanical impedance of the voice coil and motor system will swamp out many small nonlinearities in the suspension elements of a driver. In a well designed driver, it is only at high excursions where suspension nonlinearities become significant.

Another source of distortion in the driver may come as a result of nonuniform magnetic flux surrounding the voice coil as it makes its excursions. Yet another form of distortion is due to the particular interaction of voice coil current with the static flux field provided by the magnet itself. We will examine some of these effects.

2.6.1 Mechanical nonlinearities

The nominal power rating of a driver is based on long-term effects of heating as well as the effects of excessive displacement at lower driving frequencies. Many 380 mm (15 in) drivers intended for heavy duty professional applications may have a nominal power rating of 600 watts, implying that the device can withstand continuous power input of that amount with a given input spectrum.

The JBL model 2226H driver, whose response is shown in Figure 2-26, is rated at 600 watts with a shaped pink noise signal covering the frequency decade from 50 to 500 Hz. The noise signal is limited to a 6 dB crest factor. Normal operation of the driver is in the range perhaps 10 dB lower than full

rating (one-tenth rated power), so it is customary for the manufacturer to publish the 60-watt distortion data for such a driver.

Generally, second and third harmonic components are dominant in the driver's distortion signature. Higher harmonic components are usually indicative of some gross defect, such as a rubbing voice coil or rattle. In data presentation it is customary to raise the distortion components 20 or 30 dB, as the case may be, so that they can be read on the same graph as the fundamental.

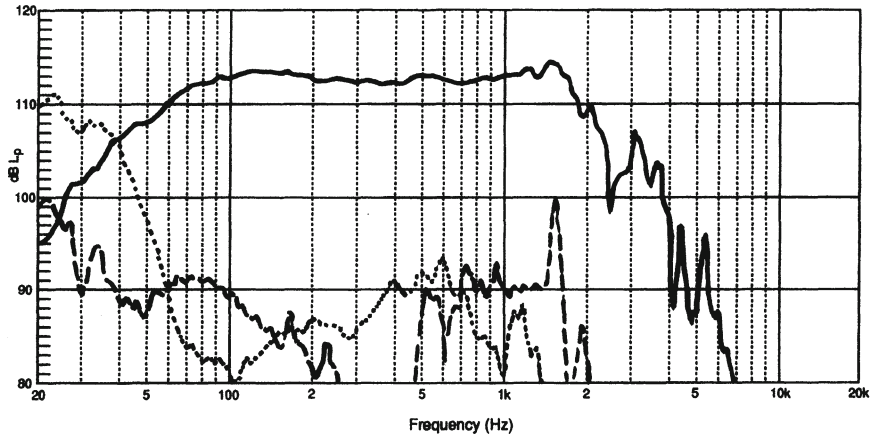

Figure 2-26. On-axis response of JBL model 2226 LF driver, with 2nd (dashed curve) and 3rd (dotted curve) harmonic distortion. Distortion raised 20 dB. (Data courtesy JBL)

In the case of the JBL 2226H we can see that the reference fundamental output in the piston band is about 113 dB Lp, as measured at one meter. Over the range from 60 Hz to about 600 Hz, the levels of second and third harmonics are about 40 dB below the fundamental (recall the 20-dB offset in the graph), and this corresponds to distortion values for each harmonic of about 1%. At low frequencies the third harmonic dominates, due to the nonlinearity of both inner and outer suspensions at their excursion limits, as well as the loss of *Bl* product at excursion extremes. Above 1 kHz, a second harmonic peak of -33 dB appears and is associated with breakup modes of the cone.

The distortion generated by a 25 mm (1 in) titanium dome device is shown in Figure 2-27. Again, the curves are run at one-tenth the nominal power rating of the device. Below about 5 kHz the distortion is due largely to suspension nonlinearity. Above 6 kHz the distortion is largely a result of breakup modes in the diaphragm.

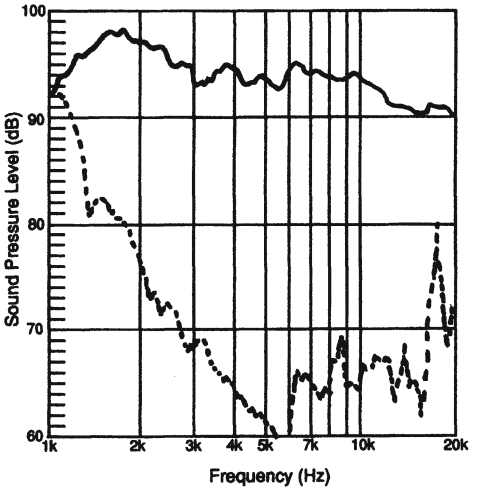

Figure 2-27. On-axis response of a 25-mm (1 in) titanium dome HF driver at one-tenth rated power. (Data courtesy JBL)

Another form of distortion found in some low frequency drivers is called *dynamic offset*. This is a tendency for the cone to execute a mechanical offset out of the gap during high level low frequency signals. This static displacement can be either in or out of the driver. While the actual cause of the effect is rather complex, it can be roughly described as follows. During high excursions there may be a lowering of *Bl* product as the voice coil leaves the gap, during which times the motional impedance of the driver drops. When this happens the driver will draw more current from the amplifier. Since the driver's mechanical elements are never quite symmetrical, there will be a tendency for the cone to pull to one side or the other during such heavy drive signals. The general cure for dynamic offset is to use inner suspensions whose stress-strain curve is matched to the loss of *Bl* product, thereby offering more resistance to cone displacement as the voice coil moves out of the gap.

Another type of distortion sometimes found in drivers is *subharmonic generation*. This normally happens in very light weight cones or domes when they are driven at very high levels. Portions of the cone or dome will execute alternate in-and-out motions as they are excited by driving frequencies an octave higher. While these effects are quite audible on sine wave test signals, they are rarely audible on program material. The cure for subharmonic generation is the use of stiffer cone and dome materials.

Rocking modes of cone or dome vibration may become apparent at high drive levels at specific frequencies. During such times the acoustical output

usually drops, and the voice coil may have a tendency to rub against the top plate or pole piece. Extended operation under these conditions may lead to failure of the voice coil. In some rare cases, the condition is influenced by standing wave patterns in the loudspeaker enclosure, where the acoustical loading may vary from one portion of the cone to the next.

2.6.2 Distortion due to magnetic nonlinearities

Example of the distortion generated by magnetic flux modulation are shown in Figure 2-28. The same moving system was used in making this set of measurements; only the magnetic structures were changed. The data shown at *A* is for an earlier design Alnico V magnet structure. The distortion is about 1% over the range from 100 Hz to 1 kHz. The data shown at *B* is for a

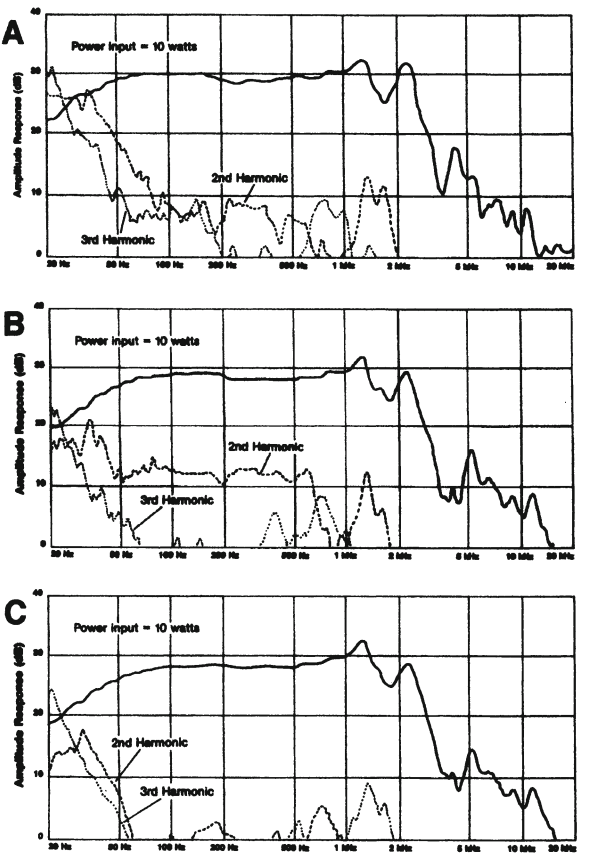

Figure 2-28. Effect of magnetic structure on harmonic distortion. same moving system mounted in Alnico V structure (A); ferrite structure (B); and Symmetrical Field Geometry structure (C). Distortion +20 dB. (Data courtesy JBL)

conventional ferrite magnet structure, showing a moderate amount of second harmonic distortion in the midrange resulting from flux modulation.

The data shown at *C* illustrates a ferrite structure that has been fitted with a flux stabilizing ring as well as further changes in the pole piece geometry . Note that the distortion has been reduced to well below 1% in the range from 100 Hz to 1 kHz. The specific means by which the flux stabilizing ring works will be discussed in the following chapter dealing with magnetic systems.

BIBLIOGRAPHY AND REFERENCES:

Beranek, L., *Acoustics*, McGraw-Hill, New York (1954).

Borwick, J.,ed., *Loudspeaker and Headphone Handbook*, Butterworths, London (1988).

Colloms, M., *High Performance Loudspeakers*, 4th edition, John Wiley & Sons, New York (1991).

Henricksen, C., "Loudspeakers, Enclosures, and Headphones," Chapter 14 from *Handbook for Sound Engineers*, G. Ballou, ed. Sams & Company, Indianapolis (1987).

Jordan, E., *Loudspeakers*, Focal Press, London (1963).

McLachlan, N., *Loudspeakers*, Dover Publications, New York (1960).

Olson, H., *Acoustical Engineering*, D. Van Nostrand, New York (1957).

Olson, H., et al., "Recent Developments in Direct Radiator High Fidelity Loudspeakers," *J. Audio Engineering Society*, vol. 2, number 4 (1954).

Sakamoto, N., *Loudspeakers and Loudspeaker Systems*, (in Japanese), Nikankogyo Shimbun, Tokyo (1967).

Various, "Loudspeakers," Volumes 1 through 4, anthologies of papers from the pages of the Journal of the Audio Engineering Society, New York (1978, 1984, and 1995); editors: R. Cooke and M. Gander.

———, "Choosing JBL Low-Frequency Transducers," Technical Note, Volume 1, Number 3, JBL Incorporated, Northridge, CA (1983).

Chapter 3:
PRINCIPLES OF MAGNETICS

3 Introduction

In this chapter we will cover basic magnetic theory, including an overview of the steps involved in designing a typical magnet structure for a cone driver. We will also discuss aspects of various magnetic materials and examine some of the fundamental nonlinearities present in the magnetic motor structure.

3.1 Fundamentals

We can create a magnetizing field by passing direct current through a coil of wire. In the cgs (centimeter-gram-second) system of units the magnetizing force field, *H*, is given in *oersteds*, and the resulting magnetic induction, *B*, is given in *gauss*. The *H* field is proportional to the current and the number of turns in the coil. If we measure the *H* and *B* fields as they exist in air (no magnetic sample present in the coil), then the numerical values of *H* and *B* will, by definition, be equal. This simple fact is why a great deal of magnetic system design takes place in the *cgs* system of units rather than in *SI* (or *mks*) units.

If we now place a ferromagnetic sample in the coil the situation will change dramatically, as shown in Figure 3-1. If the sample is unmagnetized to begin with, we start at position *1* in the diagram. As we increase the magnetizing field, the induction in the sample will follow the curved path up to position *2*, where the induction or *B* field will level off as it reaches saturation.

If we then reduce the *H* field back to zero we will observe that the *B* field is only reduced to some value at position *3*, known as B_r, or the *remanant* induction. Our sample is now permanently magnetized. Now, if we reverse the flow of current in the coil and increase it, we will eventually reduce the

J. Eargle, *Loudspeaker Handbook*

magnetic induction in the sample to zero at position *4* in the graph. The value of the *H* field that will cause this is know as H_c, the coercivity of the magnetic sample.

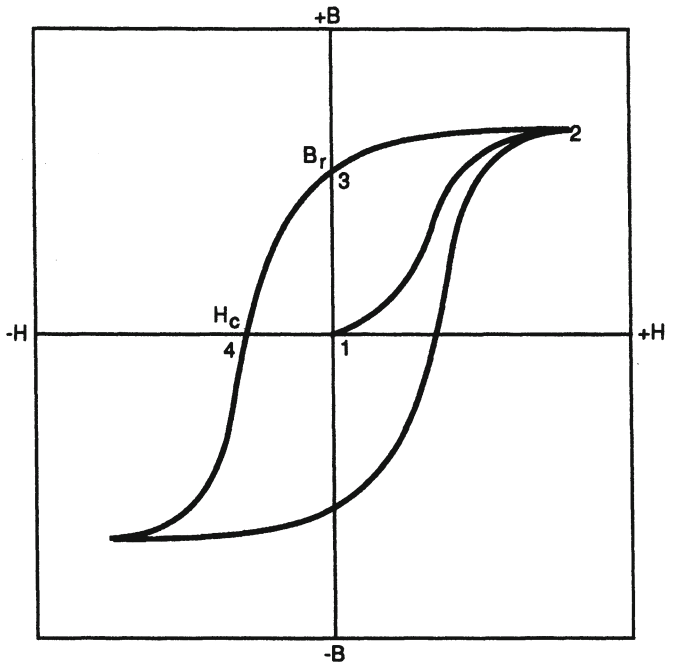

Figure 3-1. Hysteresis curve for a sample of ferromagnetic material.

3.1.1 Hysteresis

We can continue the process, remagnetizing the sample in the opposite direction, and then demagnetizing it again. The curve that this process outlines is known as a *hysteresis* curve (from the Greek meaning *to lag*).

The second quadrant of the graph (upper left portion) is known as the demagnetizing quadrant, and it is the behavior of magnetic materials in this portion of the graph that will be of greatest interest to us. In Figure 3-2 we will look at several magnetic samples only in the second quadrant, carefully observing their values of B_r and H_c. Curve 1 is for Alnico V material, a common magnetic material widely used from the 1940s to about the mid-1970s, when chronic cobalt shortages forced the loudspeaker industry to find other solutions. The high value of B_r indicates that the material can create high values of flux in a driver, but the low value of H_c indicates that it is relatively easy to demagnetize.

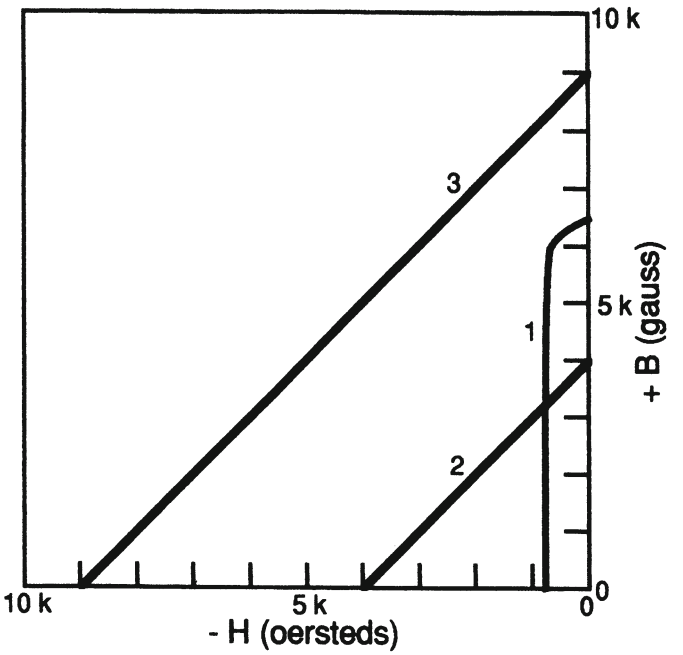

Figure 3-2. Demagnetizing curves for Alnico V (1); typical ferrite (2); and neodymium material (3).

Curve 2 is typical of many ferrite (or ceramic) materials. Such magnet materials are made of various ferrite (Fe_2O_3) combinations with other oxides and are generally far less costly than Alnico V.

As can be seen in the figure, the low value of remanance, B_r, indicates that a large contact surface area will be required to generate a high flux level in the gap. The high value of H_c indicates that the ferrite magnet is relatively difficult to demagnetize.

Curve 3 is typical of magnets such as the neodymium-iron-boron type that have very high energy for their size and weight. They combine the best properties of both Alnico V and ferrite, exhibiting both high values of B_r and H_c.

3.1.2 Constructing the load line

In designing a magnet structure the transducer engineer targets a specific flux density and the geometry of the magnetic gap over which that flux value is to exist. The next step is normally to specify the minimum amount of magnet and iron material that will satisfy these requirements. Figure 3-3A shows the

second quadrant for a typical sample of Alnico V, and Figure 3-3B shows the associated external energy, B_dH_d, associated with it.

When an air gap is placed in the magnetic circuit, magnetic flux passes across the gap, and we are in effect partially demagnetizing the magnet by forcing the flux across a high-reluctance path. The load line helps the engineer to get the most efficiency from the magnet by maximizing the energy product, B_dH_d.

The engineer then draws a horizontal line left from the B_r point and a vertical line upward from the H_c point. The load line is then drawn from the origin (lower right corner of the graph) to the intersection of these two lines, as shown. The intersection of the load line and the demagnetization curve is the target operating point of the system. In Figure 3-3B, we have plotted the product of B and H for all the values in the second quadrant, and a horizontal line drawn from the operating point will intersect the B_dH_d curve at its maximum value. The slope of the load line, B_d/H_d, is known as the *permeance* of the magnet.

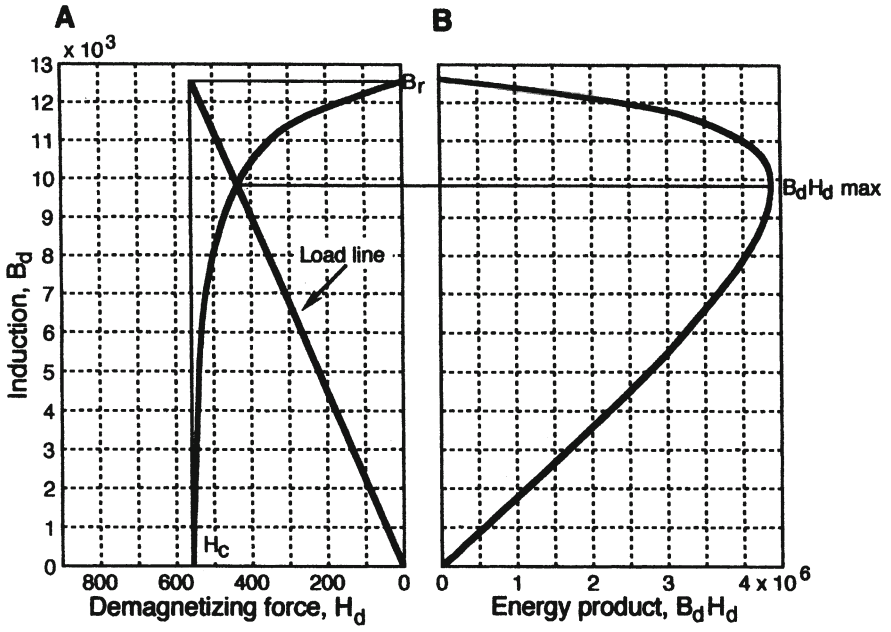

Figure 3-3. Construction of the load line. Demagnetization curve for Alnico V showing load line (A); energy product curve for Alnico V (B).

The magnetic material requirements will be minimized when the *BH* product is maximized, but for various reasons the engineer may not choose to operate the system at this point. For example, a steeper load line slope will result in an operating point closer on the demagnetization curve to the value of B_r and operating the system at this new point will make it more immune to demagnetization effects. This will require a larger magnet, but the choice may be a good one, depending on the intended use of the driver.

3.2 Details of the magnetic circuit

The magnetic circuit, commonly called the motor structure, is composed of iron and magnetic material and was discussed in detail in the previous chapter. We may view the relationship between flux and magnetomotive force as an equivalent to Ohm's law for a simple series electrical circuit, where flux (ϕ) is analogous to current, magnetomotive force (M) is analogous to voltage, and magnetic reluctance (R) is analogous to resistance. Thus:

$$\phi = M/R \qquad 3.1$$

In order to get the required flux densities in the gap of a transducer, we need an iron material with low enough reluctance and proper gap geometry to concentrate the flux where it is needed. The iron commonly used in the structure is what is called *mild steel*; it is low in carbon and easily worked. Figure 3-4 shows the H field requirements for various amounts of induction for some metals used in magnetic structures. A mild steel material such as EN1A can produce gap flux density up to 1.7 tesla, which should take care of most transducer requirements. However, for gap requirements in excess of 2 tesla, as in some compression drivers, a material called Permendur may be needed.

3.3 Linearity issues

In Chapter 2 we described distortion effects that were caused by nonlinear flux distribution in the gap and by loss of flux during high excursions, both of which can usually be improved through attention to geometry in design. There are other effects involving the voice coil and magnet structure that are not so easily solved, as discussed by Buck (1994):

Flux modulation: This occurs when the magnet is alternately over-magnetized and reversely magnetized by the cyclic signal current in the voice coil itself. This effectively amounts to a shifting of the instantaneous operating point up

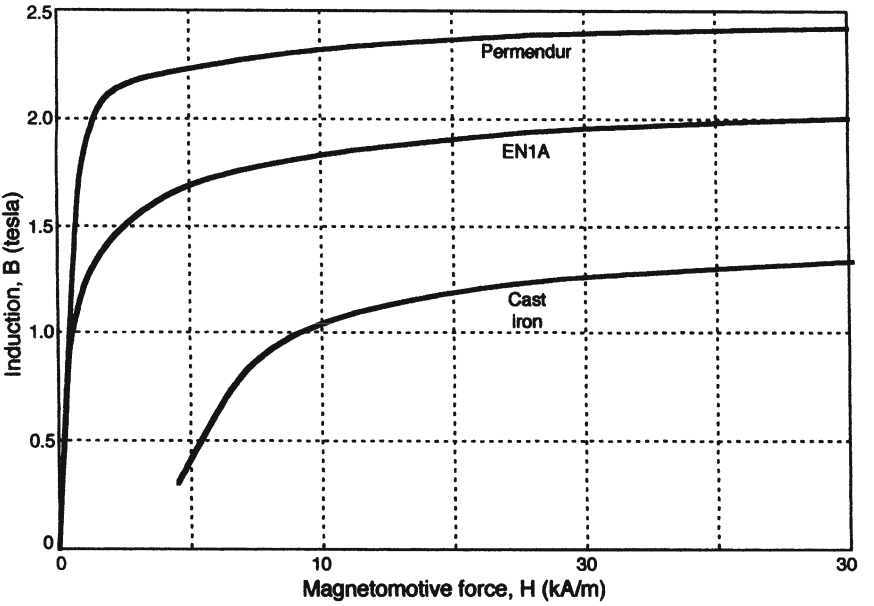

Figure 3-4. Induction curves for three iron materials used in magnet structure design.

and down along the demagnetization curve. It is minimal when the demagnetization curve is itself fairly flat, as in the upper portion of a typical Alnico V demagnetization curve.

However, in the case of a ferrite magnet, with its high-sloped demagnetization curve, no such solution is available. When cobalt became too expensive during the 1970s, many manufacturers were forced to develop new ferrite motor structures. Some added a large conductive aluminum ring at the base of the pole piece. Through transformer action, the voice coil signals induced into the magnet structure will set up a counter current in the aluminum ring. The ring, a single turn with a cross-section area of about one square centimeter, has an extremely low resistance; consequently, there is substantial current flow through the ring at high signal levels. As in all induction phenomena, the action of the induced current is to counter the effect that produced it in the first place; thus the tendency for flux modulation is greatly reduced at a price about 1 dB of overall magnetic efficiency. A section view of a motor structure with flux stabilizing ring is shown in Figure 3-5.

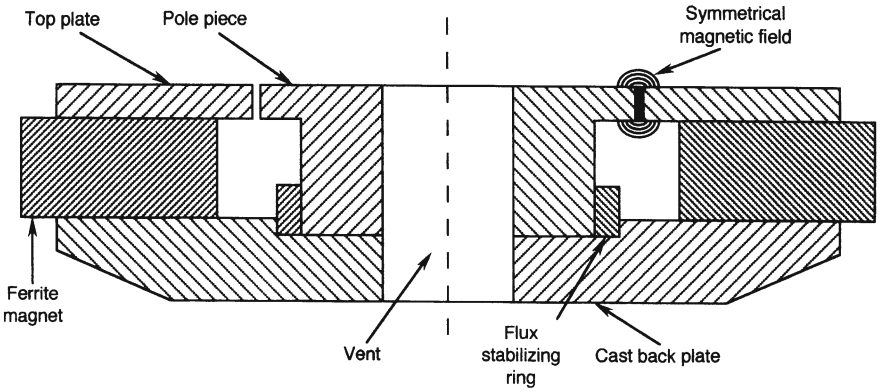

Figure 3-5. Section view of a magnetic structure using an aluminum flux stabilizing ring.

Interaction between voice coil and pole piece: The effect here is that the solenoid action of the energized voice coil magnetically attracts the iron in the pole piece, regardless of the polarity of the signal. This amounts to signal rectification and produces low-level second harmonic components whose value depends on the *Bl* product of the driver.

Modulation of voice coil inductance: The in-and-out motion of the voice coil over the pole piece varies the amount of iron that is instantaneously inclosed by the voice coil. Since the voice coil acts as an iron core inductor, the instantaneous inductance of the voice coil changes. The cure for this problem is to plate a silver or copper ring on the pole tip, or affix a copper sleeve to it. This acts as a shorted turn transformer secondary, reducing the inductance so that its modulation is minimized.

Eddy currents in the top plate and pole piece: Current in the voice coil will cause small, local loops of current to flow in the iron adjacent to the voice coil, primarily causing heat and loss of efficiency. It is minimized through the use of shorting rings on the pole piece, which, as we have discussed, have other advantages as well.

3.4 Temperature rise and demagnetization

With continued operation at high power input, all drivers will increase in temperature as heat develops in the voice coil and is transmitted to the surrounding parts. When magnets increase in temperature there is a loss of

magnetomotive force, and this decreases the B field flux in the gap. To a large extent this is a temporary effect; when the temperature returns to normal the full flux is restored. However, Alnico is far more prone to permanent demagnetization than either ferrite (ceramic) or neodymium based materials, so care must be taken in routine operation to avoid this.

During the heating cycle the sensitivity of the driver is diminished as a result of two effects: the loss of Bl product and the increase in the resistance of the voice coil, R_E. As a result the $(Bl)^2/R_E$ value is diminished, and there is a considerable drop in the power output of the driver for a fixed input power. As a rule, the effects of voice coil heating are much greater than flux losses in reducing loudspeaker output.

Figure 3-6 shows the degree of loss to be expected for three magnet materials as a function of temperature rise. This data, measured by Button (1992), shows that the percentage flux loss is approximately linear with regard to temperature. The examples measured here were magnetic structures in which the H_dB_d product was maximized.

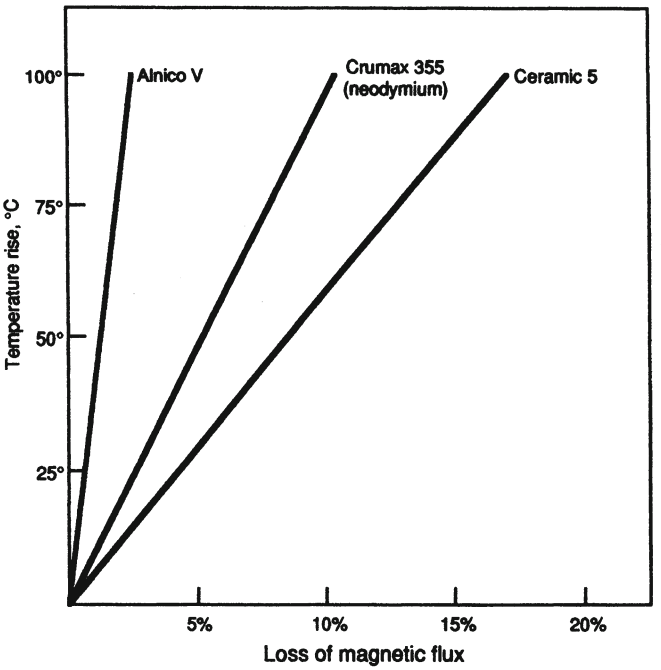

Figure 3-6. Loss of magnetic flux as a function of temperature for three magnetic materials.

3.5 Modeling of magnetic phenomena

Not too many years ago, the design of magnetic structures was a complicated process, with a good bit of cut-and-try engineering. Today, *finite element analysis* (*FEA*) allows the design engineer to model the radial cross-section of a magnet structure with specified magnet and iron materials and quickly get an accurate estimate of the final gap flux density. The effects of topology and shape can easily be seen. Figure 3-7 shows an example of such modeling (Bie, 1992). In this computer analysis, the distance between flux lines is inversely proportional to flux density, with density being the greatest through the gap region. Note also that most of the flux is contained within the structure, with only a few lines of flux (known as leakage flux) completing their return

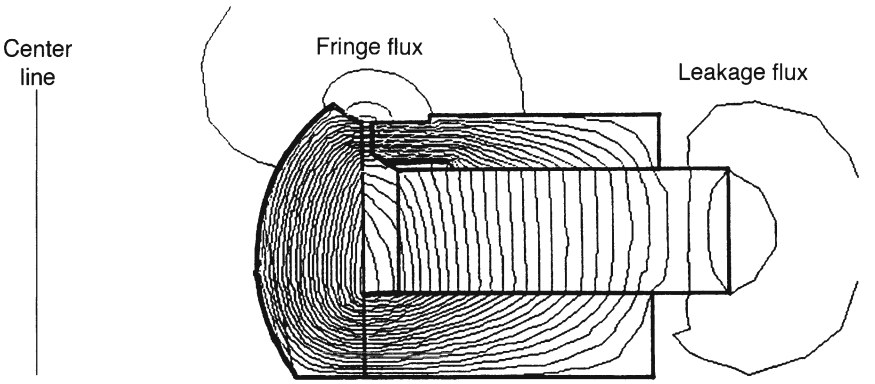

Figure 3-7. Half-section view of a magnetic structure for a compression driver. Magnet is the rectangular element in the middle, with top plate above. Back plate is at bottom, and pole piece is at left. Flux lines modeled via a finite element analysis program.

paths outside the structure. The flux paths that occur just outside the gap are known as *fringe flux*.

3.6 Magnetic shielding

Loudspeaker systems intended for application adjacent to video monitors must be magnetically shielded in order to minimize color aberrations on the the video screen. There are several design techniques here. A bucking magnet may be attached to the back of the basic structure. In the far field, the overall stray magnetic flux will be reduced considerably, with the possible cost of 1 dB or so in loudspeaker piston band performance. Figure 3-8 shows a view of a generic approach to minimizing the stray flux field around a ferrite magnetic

structure. An external, reversely polarized magnet is place close to the primary magnet, and a drawn *mu metal* cup is placed around the entire magnetic structure. Mu-metal (an alloy of iron, copper, and nickel) is known for its high magnetic permeability and low hysteresis losses; it acts as an additional magnetic shield.

Magnetic structures that incorporate their magnets internally may not need further modification in order to achieve adequate shielding. For many computer terminals, neodymium magnets, inherently small and already internal to the overall magnetic structure, provide excellent shielded performance in small loudspeakers.

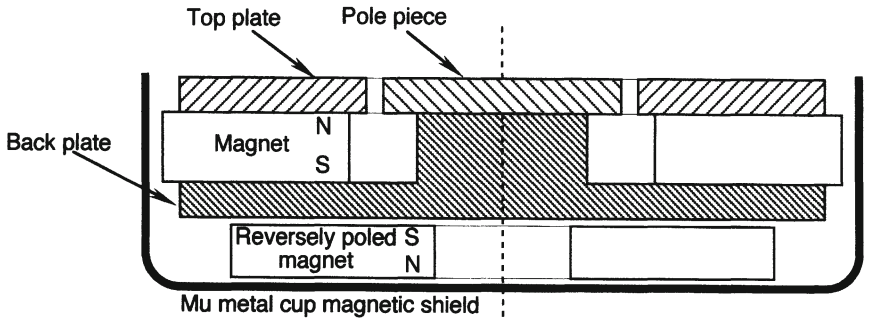

Figure 3-8. Details of magnetic shielding of a ferrite motor structure.

BIBLIOGRAPHY AND REFERENCES:

Ballou, G., ed., *Handbook for Sound Engineers,* Sams, Indianapolis (1987).

Bie, D., "Design and Theory of a New Midrange Horn Driver," presented at 93rd AES Convention, October 1992, preprint number 3429.

Buck, M., "How Woofers Work Magnetically," *Sound and Video Contractor,* volume 12, number 4 (20 August 1994).

Button, D., "Heat Dissipation and Power Compression in Loudspeakers," *J. Audio Engineering Society,* vol. 40. no. 1/2 (1992).

Borwick, J., ed., *Loudspeaker and Headphone Handbook,* Butterworth's, London (2001).

Collums, M., *High Performance Loudspeaker*s (4th ed.), Wiley, New York (1991).

Cooke, R., ed., *Loudspeakers Anthology*, Vols. 1 and 2, Audio Engineering Society, New York (1978 and 1984).

Gander, M., ed., *Loudspeakers Anthology*, Vols. 3 and 4, Audio Engineering Society, New York (1995).

Olson, H., *Acoustical Engineering*, D. Van Nostrand, New York (1957).

Pender, H., and McIlwain, K., *Electrical Engineers' Handbook*, John Wiley and Sons, New York (1950).

Sakamoto, N., *Loudspeakers and Loudspeaker Systems*, Nikankogyu Shimbun, Tokyo (1967) in Japanese.

Chapter 4:
LOW FREQUENCY SYSTEMS AND ENCLOSURES

4 Introduction

The vast majority of loudspeaker systems sold today make use of sealed or simple ported low frequency enclosures. The primary purpose of the enclosure is to act as a baffle, preventing back radiation of the driver from directly cancelling the front radiation. The enclosure may be sealed, in which case there is no interaction between the front and back of the driver; or it may be ported, in which case there may be significant beneficial interaction between front and back. (By way of terminology, ported systems are also referred to as *phase inverting* and *bass reflex* systems.)

In this chapter we will analyze a variety of LF enclosure types and methods, primarily by use of the Thiele-Small parameters. We will also discuss briefly some of the more unusual enclosure and baffle designs that have been used over the years.

4.1 An introduction to Thiele-Small parameters

From the earliest days of loudspeaker design to the early seventies, engineers made use of the basic electromechanical parameters of drivers in systems engineering. There was no simple methodology for arriving at a given set of performance goals, and the design process itself was often an informed cut-and-try procedure.

Since the early seventies the synthesis of sealed and ported low frequency systems has been carried out using the Thiele-Small (T-S) parameters. The work of Thiele, Small, and Benson is widely published, and the references given at the end of this chapter will be useful, along with references to the equally important work of Locanthi and Novak.

T-S parameters are routinely measured and published by driver manufacturers and provide a relatively simple method of synthesizing the

J. Eargle, *Loudspeaker Handbook*

high-pass filter nature of loudspeaker driver performance at low frequencies. Essentially, the approach is based on electrical filter theory, and as such adapts many of the techniques used in that field to loudspeaker design. Much of the terminology used in the analysis is taken directly from that of filter design.

The T-S parameters are defined as follows:

f_S, free air resonance frequency of the driver's moving system.
V_{AS}, equivalent volume of air that has a compliance equal to that of the driver's moving system. It is equal to $\rho c^2 C_{AS}$, where C_{AS} is the acoustic compliance of the driver's suspension. Stated differently, it is the volume of air in a sealed enclosure that will raise the resonance frequency of the driver to a value of 1.4 times its free air value.
Q_{MS}, ratio of the driver's electrical equivalent frictional resistance to the reflected motional reactance at f_S.
Q_{ES}, ratio of the voice coil dc resistance to the reflected motional reactance at f_S.
Q_{TS}, parallel combination of the two Q values, equal to: $(Q_{MS}Q_{ES})/(Q_{MS} + Q_{ES})$.
R_E, voice coil dc resistance.
S_D, area of the radiating portion of the driver.
X_{MAX}, peak displacement capability of the moving system measured in one direction. It is commonly defined as the 10% harmonic distortion limit of the moving system.
V_D, maximum volume displacement of the cone in one direction. It is the product of X_{MAX} and S_D.
L_E, inductance of the voice coil.
P_E, nominal power rating of the driver, based on thermal (heating) limitations.
η_0, half-space reference efficiency, equal to $(4\pi^2/c^3)(f_S^3 V_{AS}/Q_{ES})$.

For V_{AS} given in liters (L), the above equation reduces to:

$$\eta_0 = (9.6 \times 10^{-10}) f_S^3 V_{AS}/Q_{ES}$$

and for V_{AS} given in cubic feet it reduces to:

$$\eta_0 = (2.7 \times 10^{-8}) f_S^3 V_{AS}/Q_{ES}$$

In addition to the basic parameters, there are some additional quantities that appear in T-S analysis:

V_B, volume of the "box" or enclosure.
Q_{TC}, Q of a sealed enclosure.
f_C, sealed enclosure resonance frequency with driver in place.
α, compliance ratio: ratio of driver compliance to that of the enclosure.

From these parameters Thiele and Small derived functions that give the LF system complex response (amplitude and phase) when the enclosure volume and enclosure tuning frequency are given. They also derived functions for system impedance, cone excursion, and group delay. Measurement of the T-S parameters is discussed by Small (1972).

Today there are numerous personal computer programs available for directly plotting system performance using the parameters, and we recommend that all readers familiarize themselves with one or more of these programs. As a matter of filter terminology, we refer to *alignments* of system performance when using T-S parameters. What we are aligning is of course the driver and the enclosure, both with their own resonance frequencies in a coupled system. Modeling of the system's response functions assumes that the enclosure is mounted in a large wall (a so-called 2π, or half-space, boundary condition). Regarding units, users in the U. S. normally use inches and cubic feet for linear and volume measurement, while elsewhere SI dimensions are generally used. Any PC program you will encounter will have the capability of using either set, with all adjustments and conversions made within the program itself.

There is a continuous range of alignments possible with any driver and enclosure, but Thiele and Small have labeled certain of the possible alignments by a convenient shorthand notation; for example, *B4* stands for Butterworth, fourth order, while *B2* stands for a second-order Butterworth alignment. The term *Butterworth* indicates the maximally flat pass-band, ripple-free cutoff response of the alignment which is a characteristic of a Butterworth electrical filter. The terms *fourth order* and *second order* indicate 24-dB/octave and 12-dB/octave rolloff rolloffs, respectively, each "order" contributing 6 dB to the total LF rolloff. Another common filter type referred to is the *Chebyshev*, with equal "ripple" in the pass-band response.

The serious loudspeaker engineer will want to study the T-S parameters and their synthesis techniques in detail. Many others will be quite content to master one of the many available PC design programs, since these will lead to

excellent designs with a minimum of cut-and-try procedures. Many programs include additional modules for enclosure design, baffle details, and network synthesis.

4.2 Sealed LF system analysis

The sealed enclosure is relatively simple to analyze, since the restoring force provided by the enclosed air acts directly in parallel with the mechanical restoring force of the low frequency driver's suspension elements. Normally, it can be assumed that a small amount of damping material at the enclosure inner boundaries will have a relatively small effect on the alignment. In addition to damping possible standing waves in the enclosure, the use of this material in greater quantity has an added effect in making the enclosed volume behave as though it were physically larger than it actually is. We will discuss this in section 4.3.1.

Another concern with the "air spring" provided by a sealed enclosure is its linearity (Avedon 1960). For high air volume displacements the restoring force of the enclosure can become non-linear; normally, for volume changes no greater than about ±5%, this non-linearity may be neglected.

The upper panel of Figure 4-1 shows the simulated signal output (A) and cone excursion (B) of a JBL 2240 driver mounted in a sealed enclosure with a volume of 85 L (3 ft^3). In an enclosure of this size, the system response rolls off below 100 Hz at a rate approaching 12 dB per octave. Note that the excursion (scale at right) increases markedly below 200 Hz, eventually leveling off at very low frequencies just below the driver's X_{MAX} excursion limit. In this regard, sealed systems are "self protecting" at high drive levels at very low frequencies. The response is simulated for rated power input and is given in dB L_p at a measuring distance of one meter, as shown on the left vertical scale.

In the lower panel of Figure 4-1 we show the impedance (C), group delay (E), and phase response (D) of this system. The free air resonance frequency of the driver is 30 Hz. When mounted in a relatively small box, as in this example, the compliance of the air spring dominates, raising the resonance, as shown by the impedance curve, to just below 80 Hz. The impedance curve shown at *C* represents the *modulus* of the impedance in ohms. The phase angle, measured in degrees, represents the deviation in driver output phase response relative to the input signal.

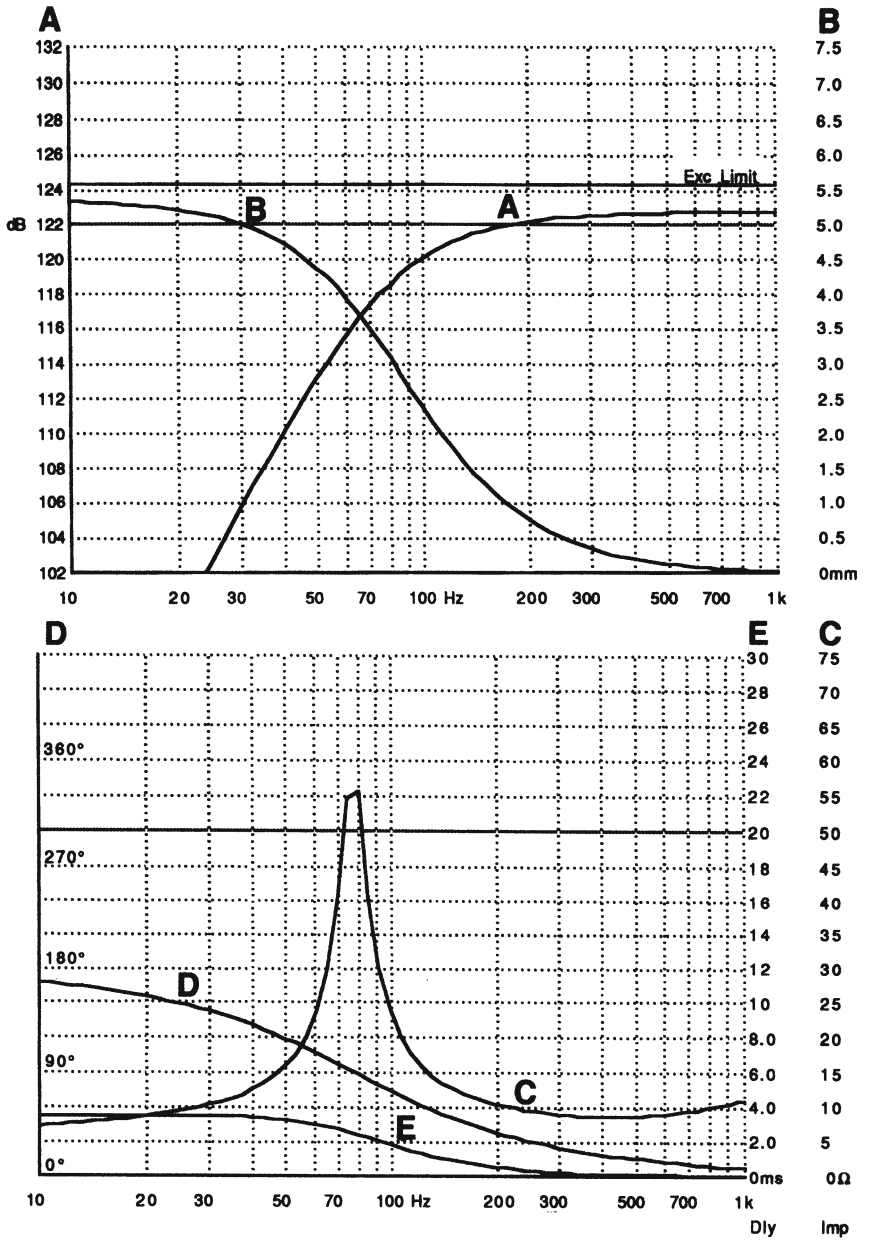

Figure 4-1. Response of a driver in a sealed enclosure. Output amplitude (A); cone displacement at rated power (B); impedance (C); phase response (D); group delay (E).

Group delay is another way of viewing this, in terms of actual output signal delay. It is equal to $-d\phi/d\omega$, where ϕ is the phase angle and ω is the angular frequency, $2\pi f$. Group delay is measured in milliseconds.

Figure 4-2 shows the effect of varying the volume of a sealed LF system, while keeping all other parameters constant. Here, we have shown the simulated response of a JBL model 128H driver mounted in enclosure volumes of 7, 14, 28, 56, 112, and 224 L (0.25, 0.5, 1, 2, 4, and 8 ft^3). The response is peaked when the volume is small, progressively becoming smoother, and finally more rolled off at low frequencies as the volume is increased. For this particular driver, note that there is little to be gained in LF response by increasing the volume beyond 56 L (2 ft^3). The system simulations are for rated power input measured at a distance of 1 meter.

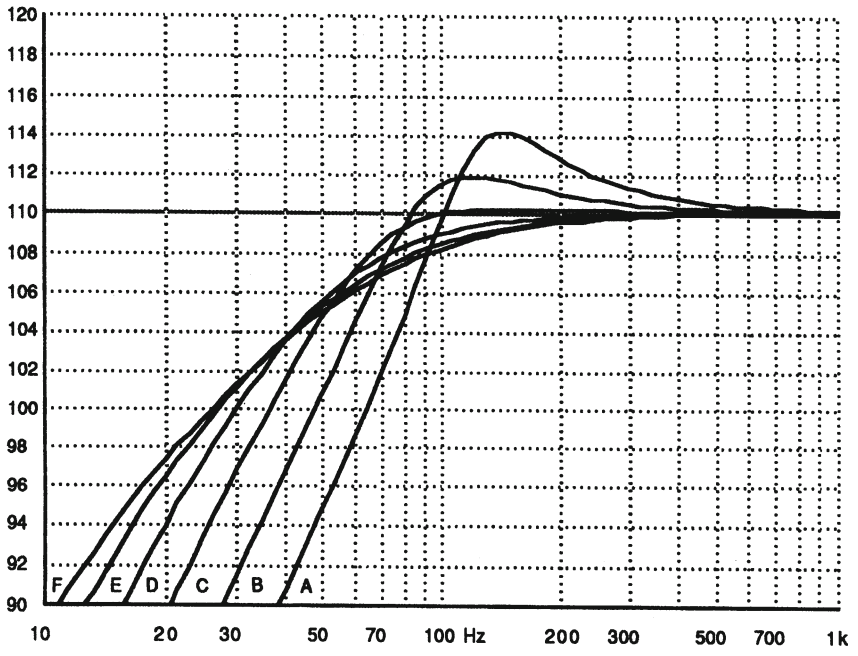

Figure 4-2. Variation in output as a function of enclosure volume: 7 L (A); 14 L (B); 28 L (C); 56 L (D); 112 L (E); 224 L (F).

Figure 4-3 shows a family of curves in which the value of Q_{TS} is the only variable. This is roughly equivalent to inversely varying the *Bl* product of the driver. Reducing *Bl* (increasing Q_{TS}) diminishes the piston band sensitivity of

the system, while allowing the response at system resonance to peak progressively higher, relative to the piston band value. The driver modeled here is the JBL 128H in a 56 liter enclosure, with values of Q_{TS} set at 0.24, 0.4 and 0.8, Again, the system simulations are for rated power input measured at a distance of 1 meter.

Figures 4-2 and 4-3 point out the value of the T-S parameters in analyzing system performance and determining the nature of trade-offs in the design process. Figure 4-4 presents graphical data developed by Small (1972) relating the maximum efficiency of a sealed system as a function of enclosure volume and the nominal cutoff frequency (-3 dB point), f_3. A *C2* (Chebyshev second order) type of alignment is assumed here, with its characteristic system Q of unity.

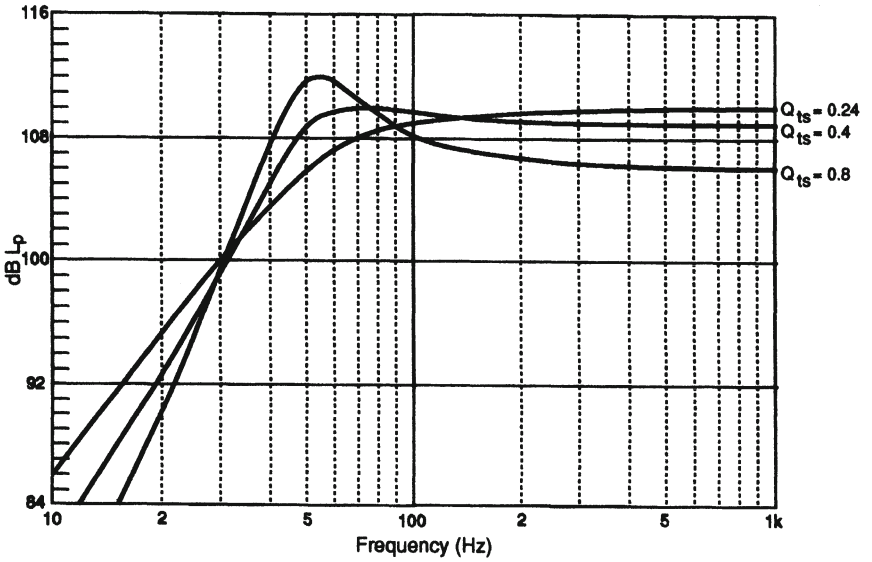

Figure 4-3. Variation in output as a function of Q_{TS}.

Figure 4-5 shows the impulse response of sealed systems for varying values of Q_{TS} at system resonance. Note that the undershoot of the impulse signal is minimal for values of 0.50 or lower.

In sealed system design, the *tuning ratio* (*a*) is often used to denote the ratio of driver compliance to enclosure compliance. When the value of *a* is less than unity, the driver's compliance dominates, and when higher than unity the enclosure compliance is dominant. When the ratio is about 4 or higher, the design is generally referred to as an *acoustic suspension,* or *air suspension,* system.

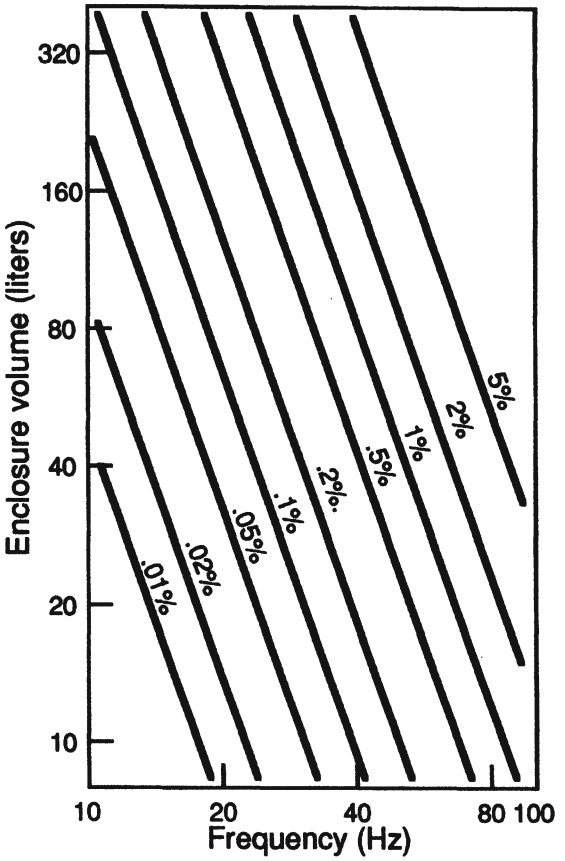

Figure 4-4. Maximum efficiency of a sealed system as a function of f_3 and enclosure volume. (Data after Small)

4.2.1 Effect of acoustical damping material in the enclosure

In the frequency range where internal enclosure dimensions are equal to one or more wavelengths, standing waves may exist in the enclosure. Placing absorptive material on the inner walls of the enclosure will damp these out to some extent, resulting in smoother response. At low frequencies (long wavelengths), damping material may have other beneficial effects that derive from certain thermodynamic action. Normal acoustical processes are *adiabatic*. This implies that there is a rise and fall in the instantaneous temperature of the the air as it undergoes compressions and rarefactions in pressure.

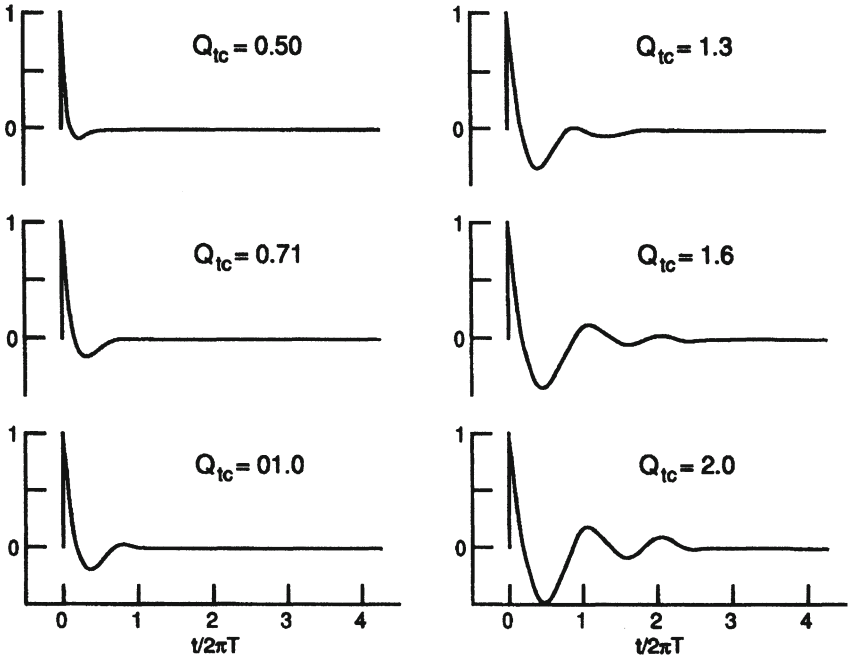

Figure 4-5. Impulse response of a sealed system as a function of Q_{TC}. (Data after Small)

If an enclosure is filled with damping material, the thermodynamic process tends to become *isothermal*. The temperature remains relatively constant as heat is transferred to the damping material on the compression cycle, reversing itself during the rarefaction cycle. Under these conditions, the velocity of sound decreases, and this has the effect of increasing the volume of the enclosure by a significant factor. Previously, it was assumed that the maximum possible increase in effective volume was in the range of 1.4, or 40%, but Leach (1989) has provided a more accurate analysis indicating that the maximum ratio is closer to 1.31. In normal practice most loudspeaker engineers observe an increase of perhaps 1.2 in the apparent size increase.

The Acoustic Research AR-1, which was introduced in 1954, was the first commercially successful wide range "bookshelf" system to make use of optimum "stuffing" a sealed enclosure with material. It virtually revolutionized home high fidelity expectations during an era in which "bigger is better" was the motto of the industry. The AR-1 had external dimensions of approximately 13.5 x 21.5 x 11 inches, and the LF driver was nominally 12 inches in diameter. The dots in Figure 4-6 show the measured half-space LF response of the system (Villchur, 1957) along with a T-S simulation of the system using parameters

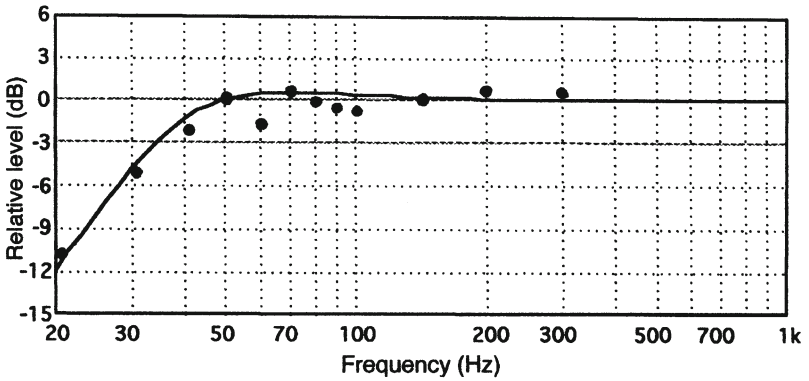

Figure 4-6. Response of the Acoustic Research AR1-W LF system. Dots indicate measured data. T-S parameters were estimated as: f_S = 15 Hz; Q_{TS} = 0.32; V_{AS} = 250 L; sensitivity (1-W at 1-m) = 86 dB L_P; enclosure volume = 39 L (1.4 cubic feet). Piston band efficiency is approximately 0.25%.

estimated from the measured response. In the light of later analysis, it is interesting to see how keen intuition, working some twenty years earlier than Thiele and Small, arrived at one of the "classical" sealed enclosure alignments.

To optimize these effects, the damping material should be chosen for relatively low mass and relatively high specific heat. The amount of material is usually determined empirically; too much material, tightly packed, will of course diminish the effective volume in the enclosure. If the material is placed too close to the cone, viscous losses may be significant, since the air volume velocity will be at its greatest close to the cone.

As a practical matter, many engineers feel that the isothermal volume increase of normal amounts of damping material is roughly equal to the internal volume displaced by the driver and internal bracing in the construction of the enclosure, and they may make their initial volume calculations accordingly. In any event, the effect, to whatever degree, will manifest itself early enough in the design process to be accounted for.

4.2.2 Use of Freon gas-filled enclosures

Czerwinski (1978) describes the use of a plastic bag of Freon refrigerant gas functioning as the basic element of compliance in an enclosure. The gas reduces the value of C_p/C_v from 1.4 for air to a value of 1.12. C_p and C_v represent,

respectively, the specific heats of a gas under constant pressure and constant volume conditions.

The reduction of the ratio to 1.12 for Freon 114 gas has the overall effect of increasing the enclosure compliance, making it possible to design a somewhat smaller enclosure for a given tuning frequency. The technique was used by the Cerwin-Vega company during the 1970s and 1980s. Further discussion of this subject is in the domain of thermodynamics and heat transfer, and most readers need not pursue the topic beyond this point.

4.3 Ported LF system analysis

A ported enclosure provides a path to the outside of the enclosure, as shown in Figure 4-7A. The volume of air in the enclosure acts as an acoustical compliance, or spring, while the air in the port behaves as an acoustical mass. Sound radiates from both cone and port.

The equivalent mobility electrical circuit is shown in Figure 4-7B, with all values reflected to the electrical input side. The acoustical output of the system is the sum of volume velocities, represented by i_t and i_e, which are the outputs of the transducer and port, respectively. In terms of acoustical output, the picture is as shown in Figure 4-7C. The enclosure and its port are normally tuned to a frequency in the 20 to 45 Hz range, representing the lower range of target system response. At the tuning frequency the cone excursion is minimized and the volume velocity through the port takes on its maximum value, producing the bulk of the output power. The primary benefit here is that mechanical distortion in the driver is lowered because of minimized cone excursion. A secondary benefit is that it is possible, with the correct driver choice, to design a LF system that can deliver substantial output power at low frequencies with reduced enclosure volume, relative to a sealed system.

The price paid for this extra measure of performance is a low frequency rolloff of 24 dB per octave below system resonance and the possible requirement for electrical high-pass filtering of the driving signal below resonance to avoid over-excursion of the driver at sub-sonic frequencies. A well thought out alignment not only achieves the desired system response, but also takes into account system requirements in terms of both thermal and displacement overload.

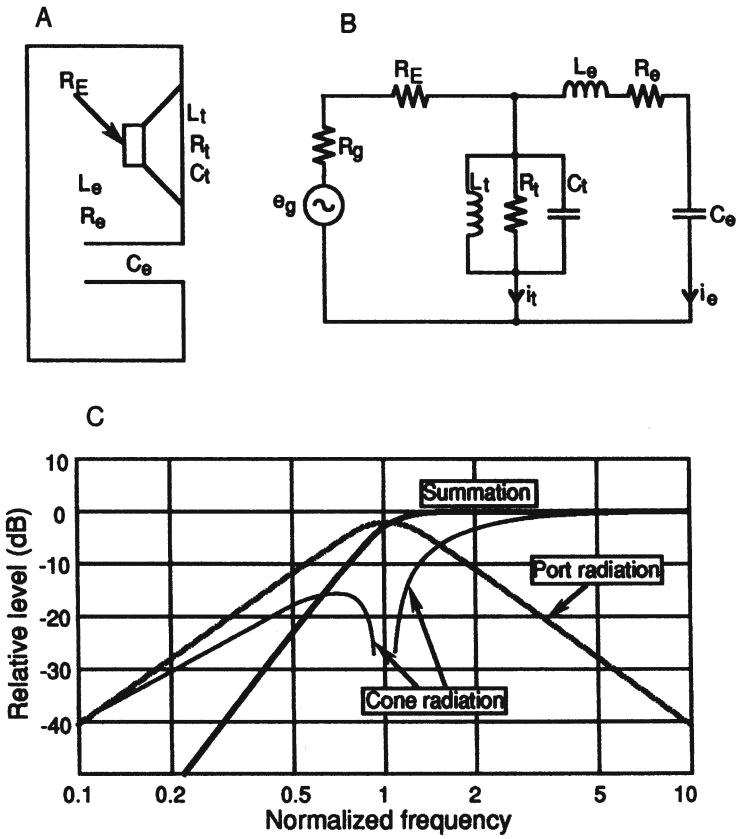

Figure 4-7. Ported systems. Section view (A); equivalent mobility circuit (B); Relative outputs from cone and port (C).

The upper panel of Figure 4-8 shows the total pressure output (A) and cone excursion (B) in a ported system. In this example, the JBL 2235H driver is mounted in a 140 L (5 cubic foot) enclosure tuned to 30 Hz. The response is 3 dB down at 35 Hz, and it will be necessary to limit the signal to the system below about 25 Hz if excessive cone excursion is to be minimized. The system simulation is for rated power input to the driver, measured at a distance of 1 meter.

The lower panel of Figure 4-8 shows the impedance (C), phase response (D), and group delay (E) of this system. Note that there are two peaks in the impedance response; the minimum value of impedance between these two peaks takes place at the enclosure resonance frequency. Phase response approaches 360 degrees at very low frequencies, while group delay is at a maximum (about 16 msec) at the impedance minimum. The impedance and

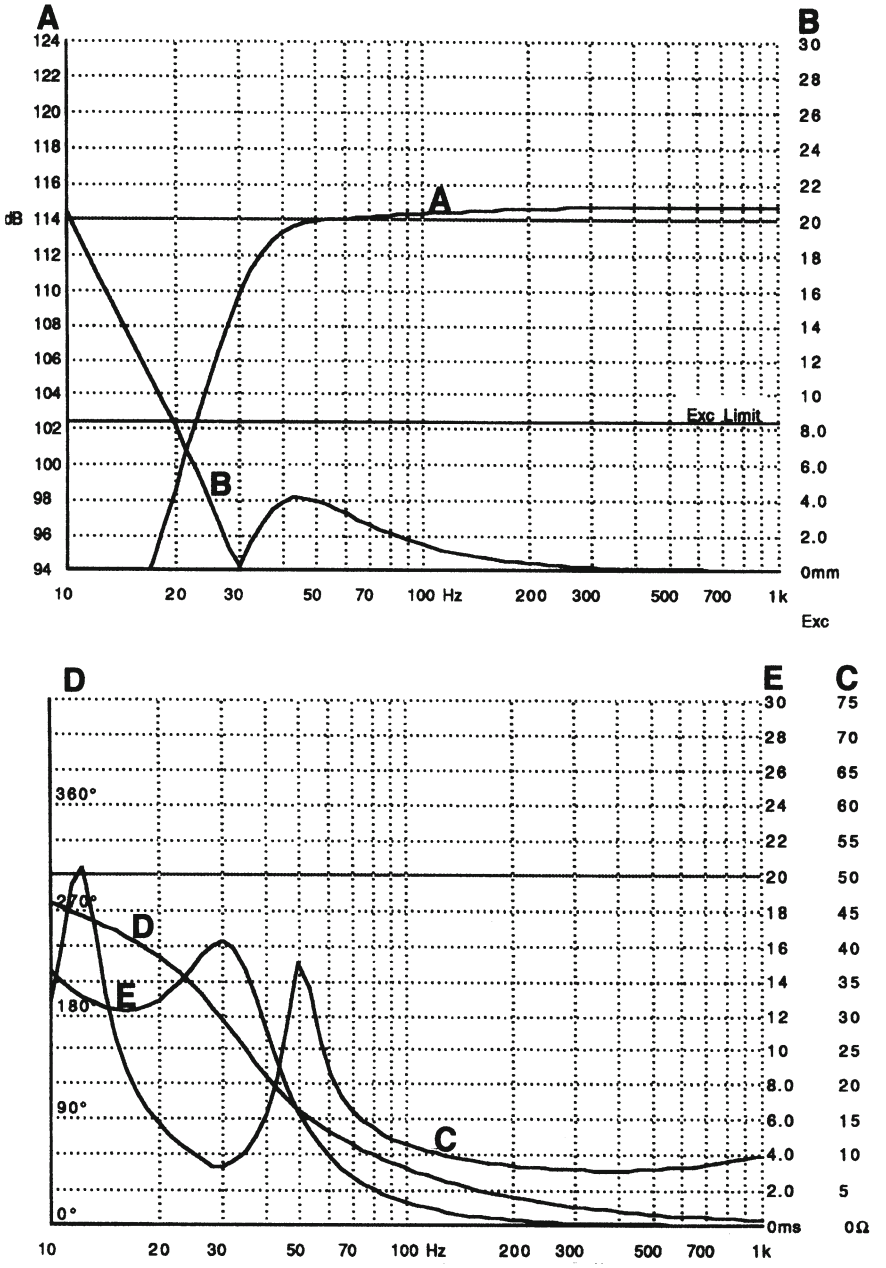

Figure 4-8. Response of a driver in a ported system. Output amplitude (A); cone displacement at rated power (B); impedance (C); phase response (D); group delay (E).

group delay scales are along the right axis of the the graph, and the phase angle is along the left axis.

Both sealed and ported systems have their partisans. Devotees of ported systems point out the increased LF capability for a given enclosure size, while the the devotees of sealed systems point out the more gentle LF rolloff afforded by those systems.

Ported systems involve both driver and enclosure resonances, and they present group delay and phase shift variations in the LF cutoff region in excess of that of sealed enclosures. In this regard, it is interesting to compare the data of Figures 4-5 and 4-14. In general it is felt that the transient time domain behavior of ported systems at low frequencies is small when compared to the time domain nature of both music and the listening environment in the same frequency range, and may thus be ignored. Figure 4-9 shows a useful enclosure tuning chart developed by Small.

4.4 Some useful alignments

One of the earliest benefits of the Thiele and Small analytical approach was that it allowed the loudspeaker industry to concentrate on those drivers that provided useful alignments and design them better. Today there are drivers that readily adapt to their target alignments nicely, and one rarely has to go in search of the elusive "right" driver.

Figure 4-10 shows target *B2* and *C2* alignments. The *B2* alignment is maximally flat and has no ripple in the pass-band. In this example (Small 1973), f_S = 19 Hz, Q_{TS} = 0.32, and V_{AS} = 540 L (19 ft^3). Small presents the following table for determining the effect of the compliance ratio *a* on enclosure volume, system resonance, and f_3 for this example:

Table 4-1. Effect of compliance ratio on enclosure volume, tuning, and -3-dB frequency:

a:	f_C:	Q_{TC}:	f_3:	$V_{box}(L)$
4	42.5	0.72	42	135
6	50.3	0.85	44	90
9	60.0	1.01	47	60
12	68.6	1.15	50	45

The *C2* alignment has a Q_{TC} of unity, which results in a slight overshoot in response in the region of f_3.

One of the most useful fourth order alignments is the *B4*. Thiele (1971) states that this alignment is maximally flat at low frequencies when the Q_{TS} of the driver is 0.383. In the example shown here, a hypothetical driver with f_S = 20 Hz, V_{AS} = 815 L (29 cu ft), and the requisite Q_{TS}. The tuning and volume ratios for the enclosure and f_3 are as given by Thiele in Table 4.2, item 1.

Table 4.2 Tuning and volume ratios for fourth-order alignments:

	Type	f_3/f_S	f_3/f_{encl}	V_{AS}/V_{ENC}	Q_{Ts}
1.	B4	1.00	1.00	1.414	0.383
2.	C4	.641	0.847	0.559	0.518

Note that for the *B4* alignment, the enclosure tuning frequency is set equal to f_S and that the ratio of V_{AS} to enclosure volume is 1.414. Using these values gives the simulated response shown in Figure 4-11A.

This example points out very clearly the advantages of T-S analysis and drivers that have been engineered for specific alignments. The extended LF response exhibited here (-3 dB at 23 Hz) would be difficult to achieve with most high-powered professional LF drivers designed for high piston band sensitivity, with their lower values of Q_{TS}. T-S analysis has shown that a less efficient (and less expensive) driver may actually perform better in the LF range.

Continuing in the same vein, the Chebyshev fourth-order (*C4*) alignment provides further LF extension, using an even lower efficiency driver with Q_{TS} = .518. Tuning and volume ratios are given as item 2 in Table 4.2, and the response is shown in Figure 4-11B. The upper curve assumes that the enclosure has negligible losses; more likely, we would see the response shown in the lower curve in modeling this alignment with a typically "lossy" enclosure. In either case, the LF extension down to about 0.707 of the driver's resonance is exemplary. Such a system would require very careful monitoring of its input signal in the subsonic range.

Another useful alignment is the so-called *B6* (Butterworth type, sixth-order), first discussed by Thiele (1971) and later by Keele (1975). In this alignment, a ported system is first designed to exhibit flat response (*B4* alignment). The enclosure tuning is then reduced by a factor 0.707 to produce an overdamped low frequency response, and is subsequently equalized for

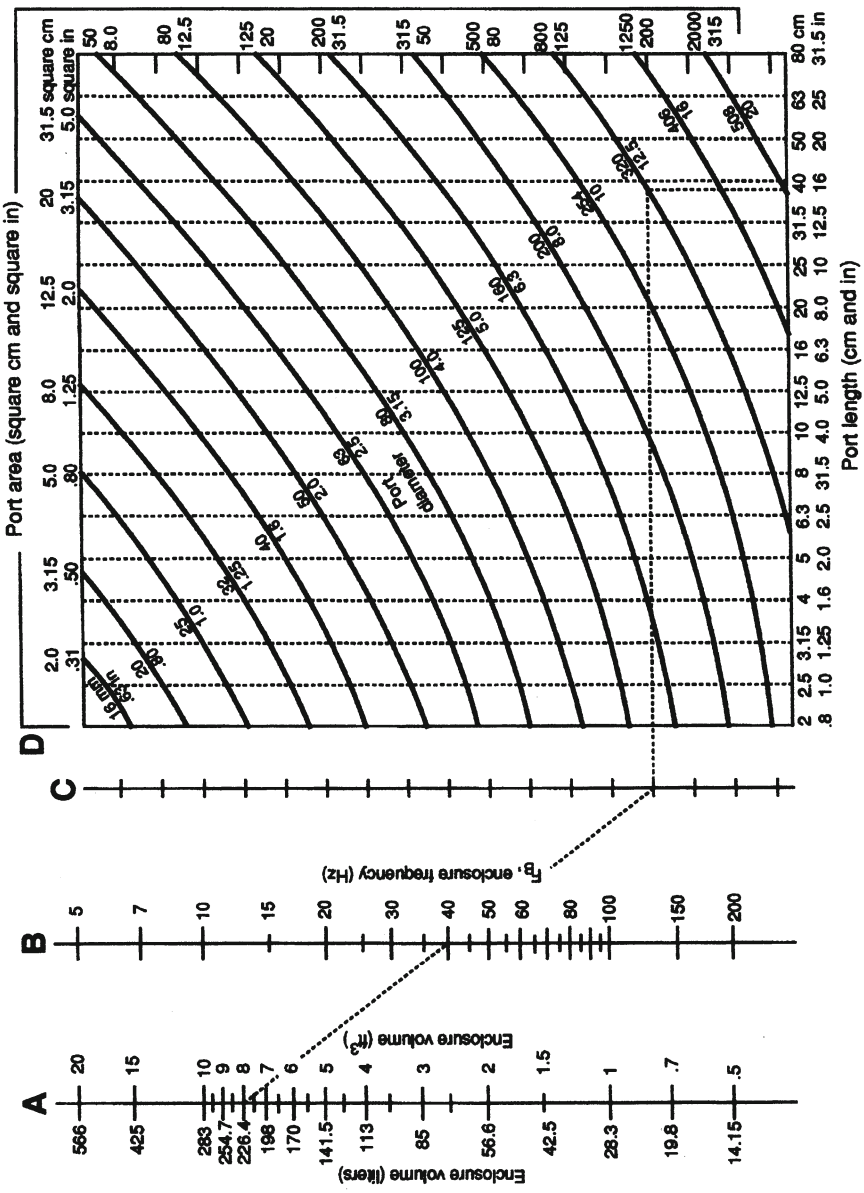

Figure 4-9. Enclosure tuning chart for determining port dimensions.

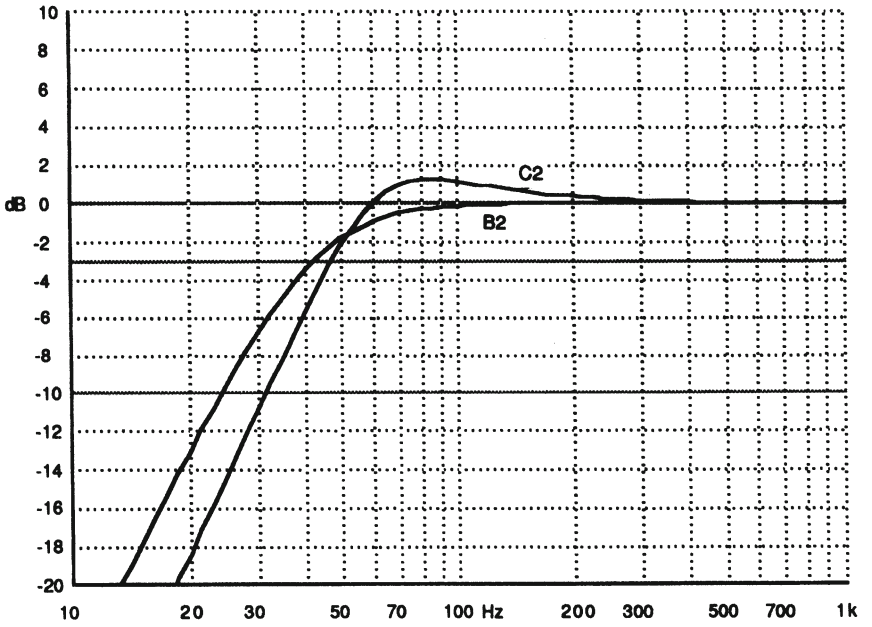

Figure 4-10. Sealed system B2 and C2 alignments. B2 enclosure volume 137 L.

flat acoustical output in the LF region by using a 6-dB electrical boost with a Q of 2. If carefully done, the design exhibits smooth response over its pass-band and maintains good immunity to displacement overload at full thermal rating. Figure 4-12 shows the rolled off natural response, the electrical filter response, and the net response of the system.

Electro-Voice has designed a number of LF systems that make use of what they term a "step-down" mode. Normally, the system is of the *B4* type; it can be converted to a *B6* alignment by lowering the port tuning with an appropriate cover blocking a portion of the port and electrically equalizing the system accordingly. A step-down kit provides these elements.

Figure 4-13 shows the relation between enclosure volume, f_3, and system efficiency that can be realized with ported systems. Figure 4-14 shows the response of two fourth-order alignments to an impulse signal. It is instructive to compare these two figures with the corresponding ones for sealed systems, Figures 4-4 and 4-5.

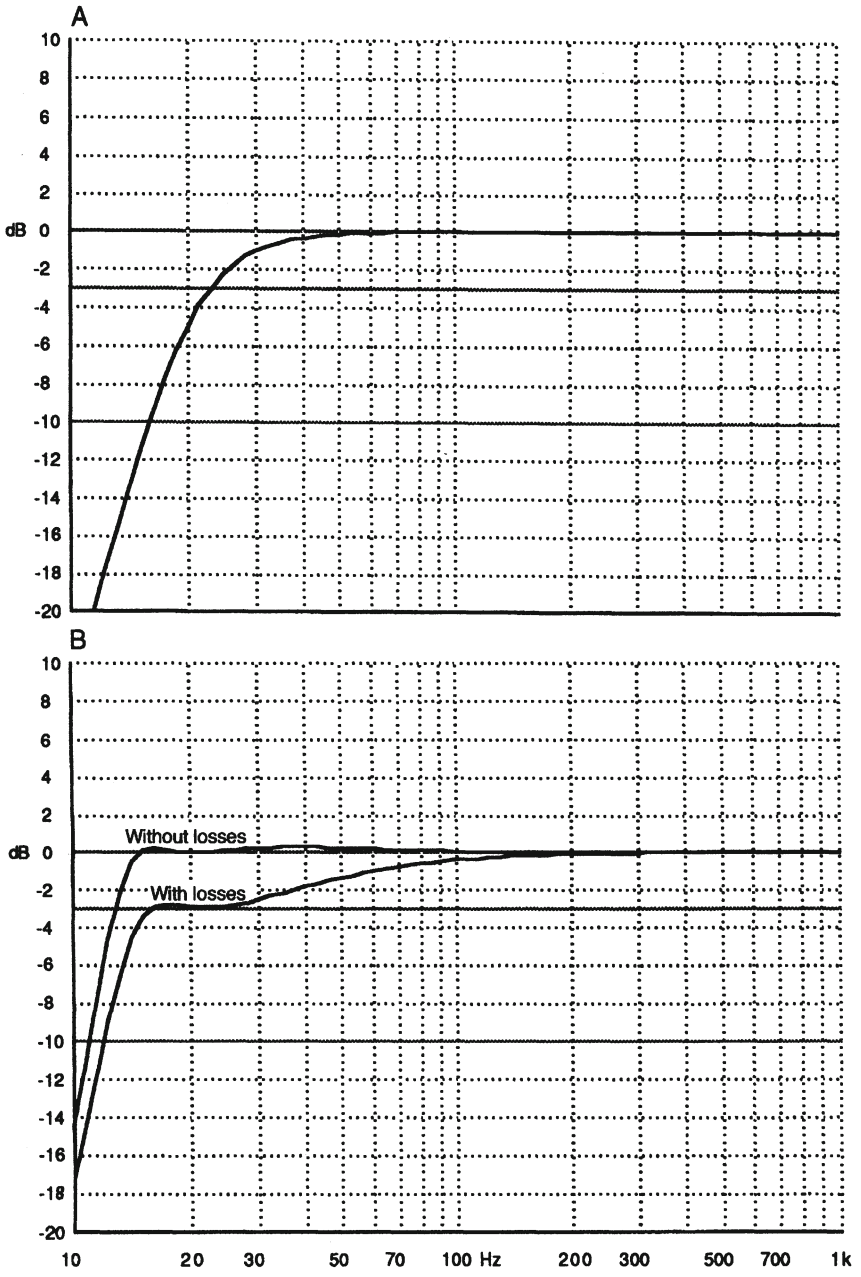

Figure 4-11. Ported system alignments. B4 alignment (A); C4 alignment with and without enclosure losses.

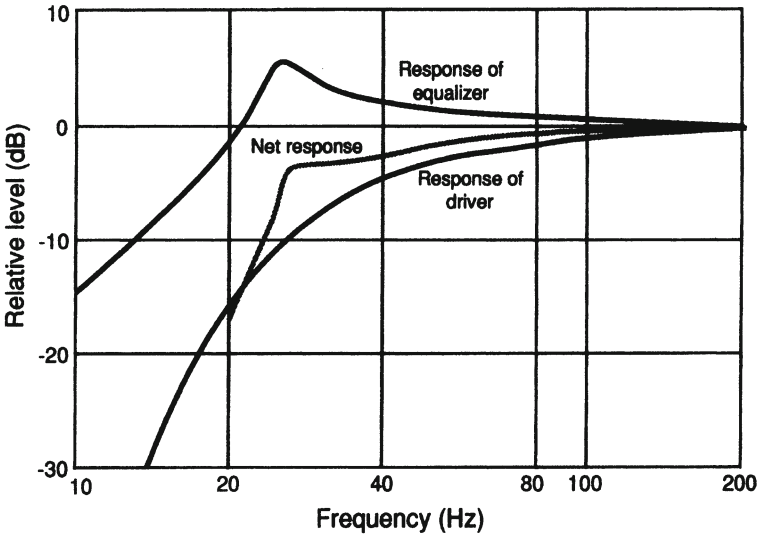

Figure 4-12. The B6 alignment.

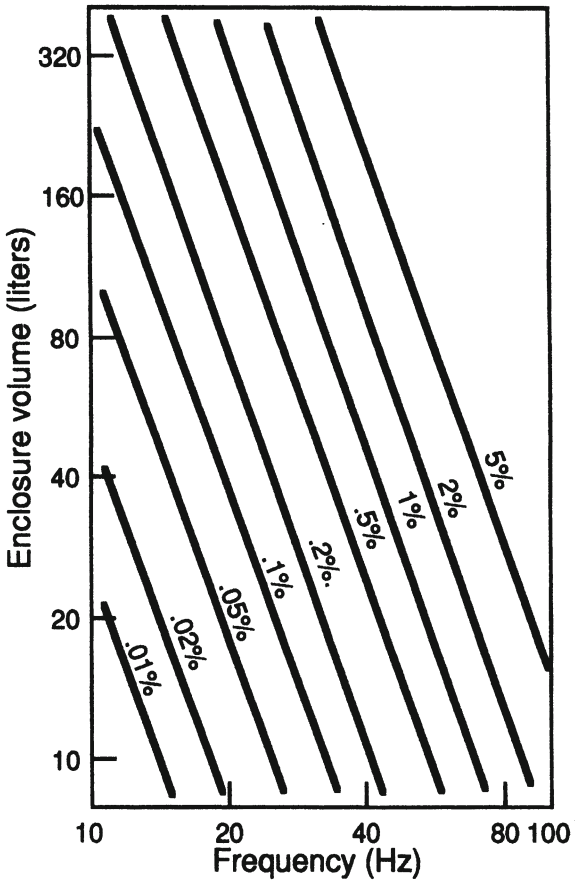

Figure 4-13. Maximum efficiency of a ported system as a function of f_3 and enclosure volume. (Data after Small)

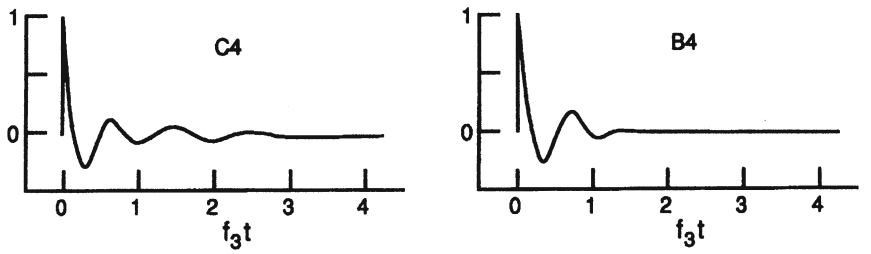

Figure 4-14. Typical impulse response of C4 and B4 ported alignments. (Data after Small)

4.5 Port turbulence under high drive conditions

At the port tuning frequency of a vented enclosure there may be considerable air volume velocity in the port tube at high operating levels. Proper port operation depends on non-turbulent air motion in and out of the port, and at high air particle velocities, turbulence may create noise and reduce the efficiency of port action.

A simple cylindrical port, as shown at (1) in Figure 4-15A, works very well when the port is large enough in diameter so that air particle velocity is small. However, at higher velocities, the abrupt transitions at each end of the port tube may cause noise as well as disruption of the port air mass, which is essential to the proper operation of the port. Years ago, designers found that simple rounding of the port's boundaries, as shown at (2), alleviated many of these problems. In recent years, the trend toward smaller subwoofer enclosures for consumer use has placed a premium on smaller diameter ports and consequently focused attention on the precise nature of port tube tapering. The profile shown at (3), is typical of what many manufacturers are now using; however, the precise mathematical descriptions of the contour shapes are widely discussed, and in some cases the subject of patents.

Figure 4-15B shows a comparison in port performance with a high-powered subwoofer system using both cylindrical and contoured ports. In this example, a large enclosure of 56 L (ft^3) tuned to 30 Hz is driven by two 300 mm (12 in) units at a frequency of 25 Hz. Zero dB along the horizontal axis represents a power input of 0.44 watts into the system, and the vertical axis represents the relative output of the system using each of the two porting methods indicated. In each case, the measurement microphone is placed parallel to the baffle approximately at the center of the port tube. Note that the difference in maximum output from the two ports is in the range of 8 dB, just before the

level at the radiused port exhibits a 3-dB drop from its maximum output value. Significant recent references in this area are Button and Salvatti (2002), Vanderkooy (1997-8), Roozen, et al. (1998), and Bose Corporation (U. S. Patent 5,714,573)

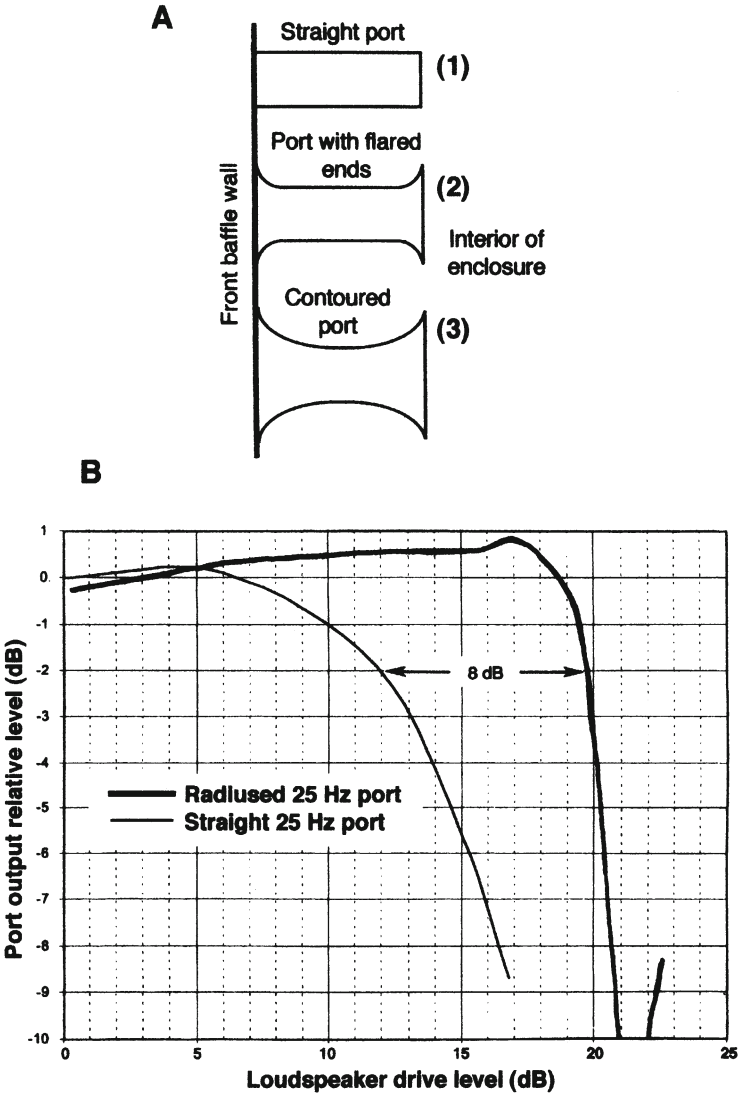

Figure 4-15. Port turbulence. Port profiles (A); system output capability with straight and contoured port tubes (B).

4.6 The passive radiator

Figure 4-16A shows a section view of a low frequency system with a passive radiator (*drone cone* and *auxiliary bass radiator* are other terms for the passive radiator). The passive radiator (*PR*) resembles a cone driver without a motor; it is effectively a mass with related compliance and mechanical damping used in place of a port. The PR is normally chosen to be of the same diameter as the active driver. As shown in Figure 4-16B, the simplified mobility circuit shows the compliance of the PR in parallel with its mass. It is the added compliance that sets the system apart from the standard ported system, and if the compliance is made large enough, the behavior of the system over the useful audio passband is very close to that of a conventional ported system (Small 1974).

The benefit of a PR is primarily the reduction of port air turbulence and a slight reduction of enclosure size for a given LF response limit. On the debit side, the PR normally suffers from the nonlinearity of its suspension elements at high excursions and can contribute to distortion at high levels. Once in vogue, the passive radiator is now rarely used as a substitute for a properly designed ported system.

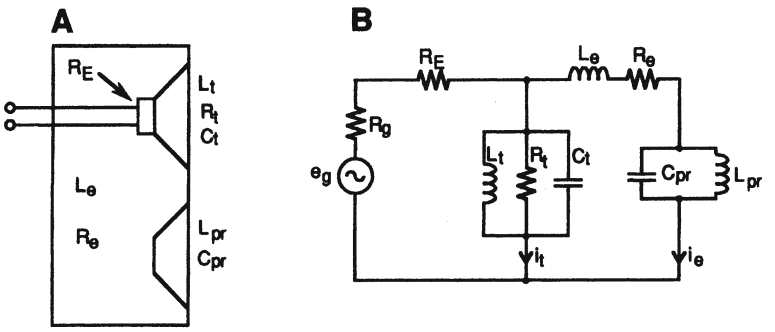

Figure 4-16. The passive radiator. Section view of system (A); mobility equivalent circuit (B).

4.7 Transmission line systems

Interest in transmission line systems dates back to the acoustical labyrinth system described by Olney (1936). There are several types of enclosures that qualify for the term *transmission line*. Basically, these are enclosures that are long enough in one internal dimension to accommodate at least one-quarter

wavelength at the lowest design frequency of the system. The path is usually folded and lined with damping material, as shown in Figure 4-17A. The system is normally open at the end of the transmission line, but when considerable damping material is employed there is little radiation from the end of the line. In this case the system may perform very much like a large well damped sealed enclosure.

The effect of the damping material is to make the transmission line "lossy" so that reflections from the end of the line back toward the driving source are attenuated. With moderate amounts of damping material, as shown at *B*, there may be significant LF response from the end of the line extending down to the frequency whose half-wavelength is approximately equal to the transmission line length (Olson 1957).

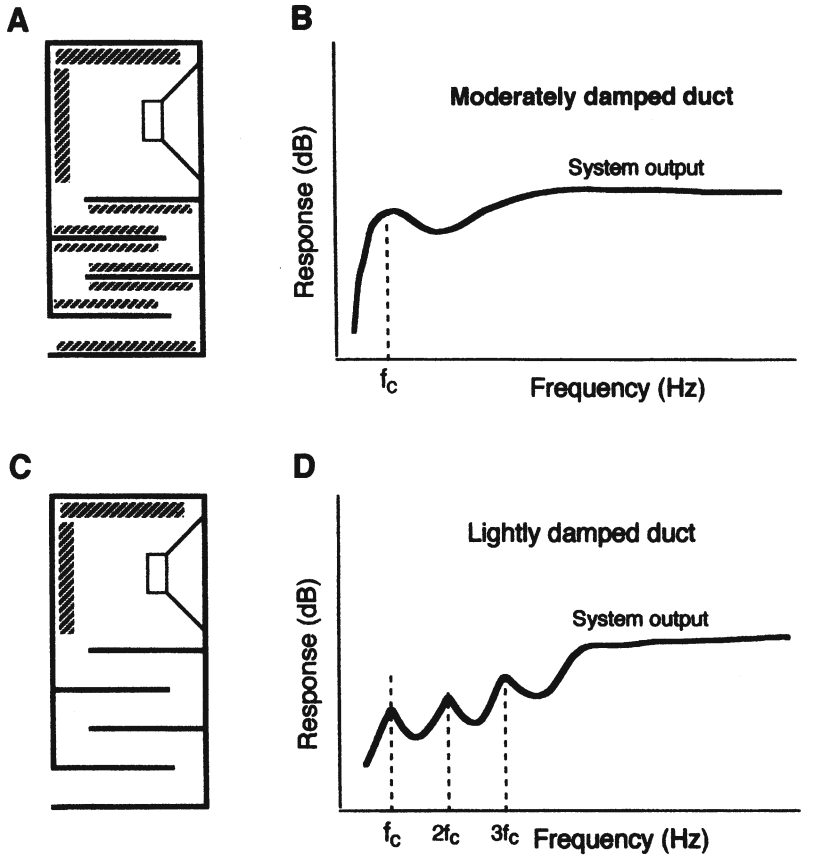

Figure 4-17. Transmission line systems. Section view of damped half-wavelength system (A); nominal response of system shown at *A* (B); section view of lightly damped half-wavelength system (C); nominal response of system shown at *C* (D).

If the transmission line has little damping, as shown in Figure 4-17C, the system's output will show typical harmonically related peaks and dips in response, somewhat characteristic of an organ pipe. For a frequency, f_c, whose half wavelength is equal to the transmission path length, the response will be as shown. Note that there are harmonic intervals ($2f_c$, $3f_c$, and so forth) appearing as lesser peaks in response. This approach has been used in very small loudspeaker systems to maximize LF output, often at the expense of smoothness of overall response. Augspurger (1999) provides excellent modern analyses of transmission line systems using T-S parameters, which are essential reading for anyone interested in these designs.

Details of the Jensen *Transflex* system are shown in Figure 4-18. Departing somewhat from the traditional transmission line design, this system is described as a "bass reflex transmission line system" (Jensen, 1952). Here, the transmission line is one-quarter wavelength long at approximately 37 Hz, and there is a null at this frequency. In the range between 40 and 80 Hz the output is maximum and is fairly uniform. Such systems were once installed under living room floors, where building structural elements could be used as basic parts of the enclosure. Such systems were often made fairly long, affording about one-octave's worth of LF response. A detailed analysis of this design is given by Tappan (1959).

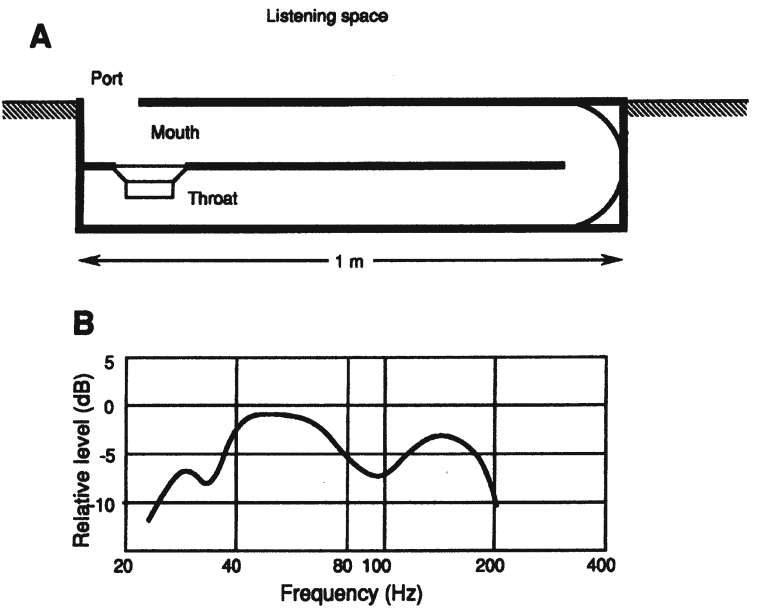

Figure 4-18. Section view of Jensen Transflex transmission line system (A); typical response (B). (Data after Tappan)

4.8 Dipole LF systems

A dipole produces a *pressure gradient*, or difference, between front and back radiating surfaces and can be represented by a cone driver open equally on both front and back sides to the environment. A characteristic of the dipole is that front and back radiation patterns are equal but in antiphase. When mounted on a large flat baffle the output of the dipole at LF can be significant, and one performance advantage of this is the fairly high directivity index that the dipole radiator maintains along its principal axis at LF, as compared with normal ported or sealed system. (Refer to Figure 1-10 for views of the radiation patterns of a dipole.)

Many users of electrostatic and planar magnetic drive systems prefer to use LF dipoles in a subwoofer role with their main systems, inasmuch as room loading characteristics will be virtually the same if the LF dipoles are positioned at the same locations in the listening room.

Figure 4-19A and *B* show front and side views of a driver mounted on a flat baffle. The effect of baffle size is shown at *C* and *D*, where the circumference is that of the baffle itself. When the driver is mounted on a very small baffle, the LF response on axis falls off at 6 dB/octave. When a large baffle is used, extended flat response on axis can be achieved down to the frequency whose wavelength is approximately equal to the baffle perimeter. In a practical design, response should be maintained flat down to the normal resonance of the driver, as shown at *D*.

It is customary in dipole designs such as this to mount the driver somewhat off-center, as shown. The actual position is often determined empirically, and the purpose is to distribute the distances from the driver to the baffle edges in order to randomize the effect on amplitude response due to reflections from the abrupt boundary edges.

The size requirement of the baffle can be alleviated by mounting the driver on a septum placed mid-way in a box open at both front and back. This is an approach that is useful only at low frequencies, where the effect of box resonances will be minimal.

A related dipole design is the Altec *Extenda-Voice* system shown in Figure 4-20. As shown at *A*, the back of the driver looks into an acoustical phase shift network that causes a delay of the rear signal at LF, resulting in reduced system

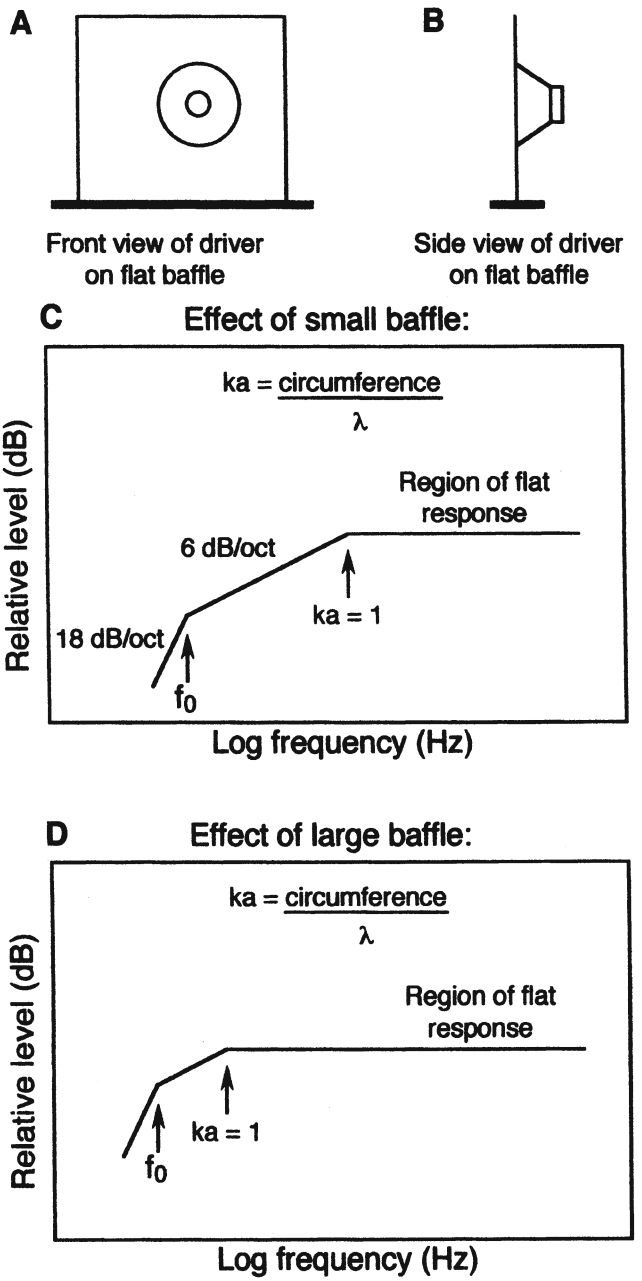

Figure 4-19. Dipole LF system. Front view (A); side view (B); nominal response on small baffle (C); nominal response on large baffle (D).

output along the 135° off-axis angle. An approximate physical circuit is shown at *B*. These high directivity systems have been used as LF components in vertical line arrays for speech reinforcement in reverberant spaces, and it is necessary to boost the LF response electrically to compensate for the fairly short gradient distance. The acousto-mechanical analysis of the system is virtually the same as that for a single diaphragm dynamic hypercardioid microphone. Directional response is shown at *C*.

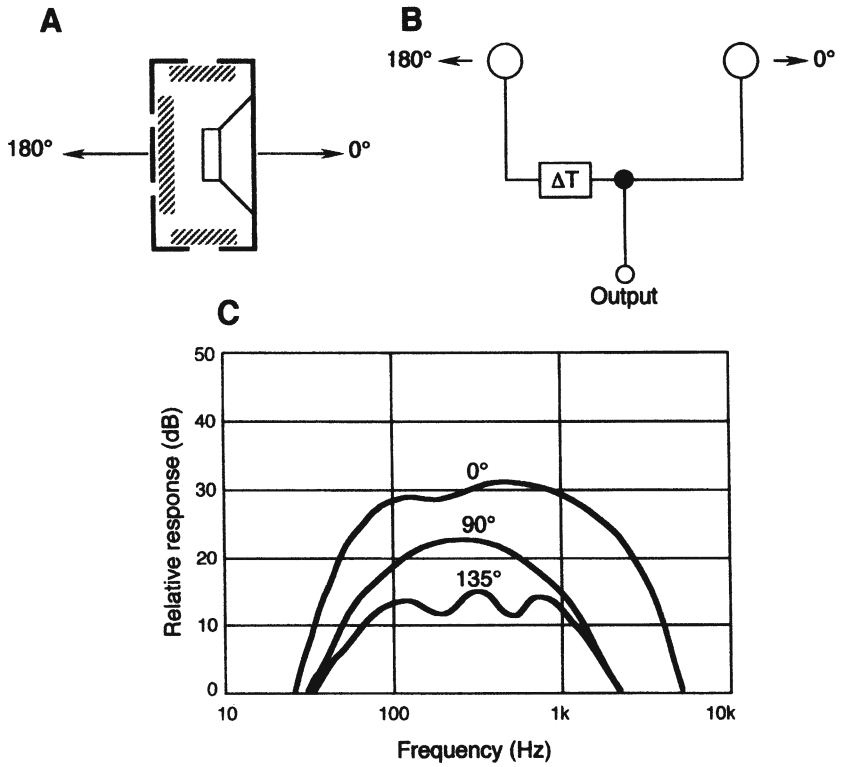

Figure 4-20. Altec "Extenda-Voice" gradient system. Section view (A); physical circuit (B); nominal directional response of unequalized system (C). (Data after Altec)

4.9 Multi-chamber LF bandpass systems

In normal ported enclosures there is useful output from both cone and port. The LF limit of the system is governed by the driver-enclosure alignment, while the HF limit of the system is governed by the diameter of the exposed driver and related values of *ka*, dependent on cone diameter.

In multi-chamber LF systems, the driver is physically placed between two of the chambers. Two or more chambers may be used, and both low and high pass limits of the system are governed largely by tunings of the enclosures. The advantages of these systems are bandpass response without the need for electrical equalization and, in some cases, lower overall system volume for their bandpass and output capabilities. On the debit side, these systems are physically complex and are relatively susceptible to boundary (mounting) conditions. The analogous circuits shown in the following three figures use the impedance anlogy for the electrical input section; the mechanical and acoustical sections use the mobility analogy.

The form shown in Figure 4-21A consists of a driver in a sealed chamber. A second chamber is placed in series with the driver and is ported to the outside. The equivalent circuit is shown at *B*, and the nominal response is shown at *C*. In this design, f_1, the lower cutoff frequency, is determined primarily by the inner chamber, while f_2, the upper cutoff frequency, is determined by the outer chamber. This design is in the public domain.

The form shown in Figure 4-22A consists of a second ported chamber in series with both the cone and port outputs of the normally ported inner enclosure. The equivalent circuit is shown at *B*, and nominal response is shown at *C*. This design, at least in the United States, is covered by patents held by Teledyne and Bose Corporations, with distinctions based on relative volumes of the chambers and and their tuning ratios.

The form shown in Figure 4-23A consists of parallel tuned chambers on both sides of a driver. The equivalent circuit is shown at *B*, and nominal response is shown at *C*. In the United States, this design is covered by a patent held by the Bose Corporation. Elsewhere, prior art, most notably a French patent issued to d'Alton in 1937, governs.

In all of these designs the ratio of f_1 and f_2 are critical in the proper functioning of the systems. If these frequencies are too closely spaced, the system is apt to coalesce into a single resonance; if the two frequencies are too far apart, the ideal bandpass response is compromised.

As a final comment on multi-chamber bandpass systems, we can state that the number of possible combinations of multiple chambers, drivers, and connecting tubes is well nigh unlimited. The ones shown here are the most practical and useful.

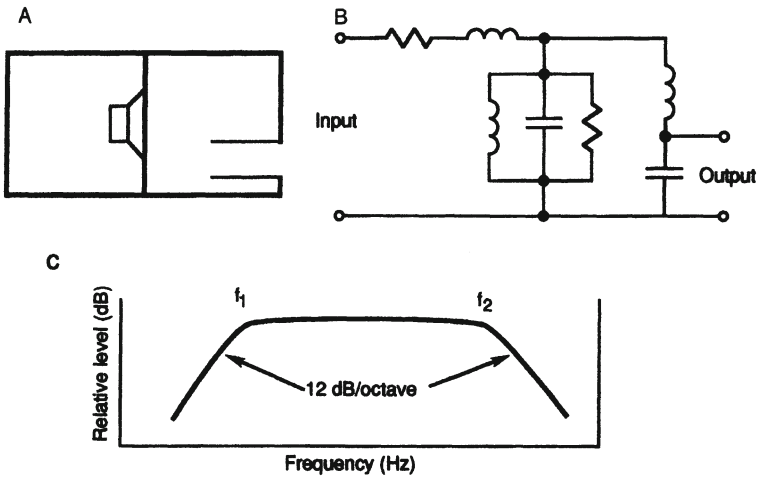

Figure 4-21. Bandpass systems: sealed-series operation. Section view (A); equivalent circuit (B); target response (C).

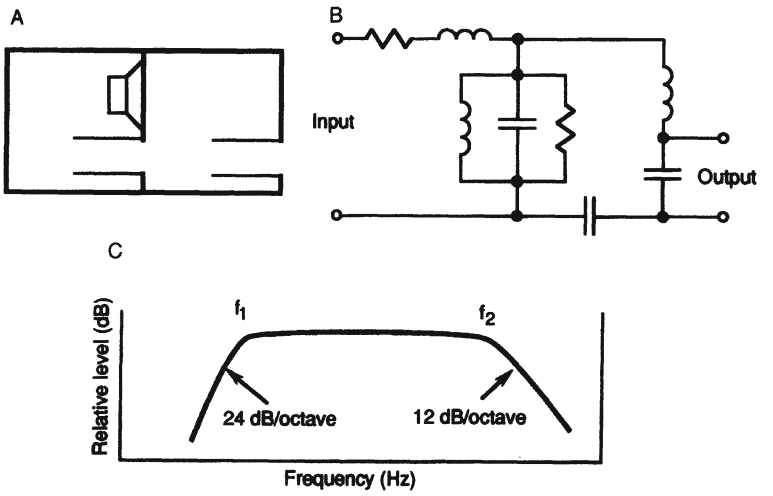

Figure 4-22. Bandpass systems: ported-series operation. Section view (A); equivalent circuit (B); target response (C).

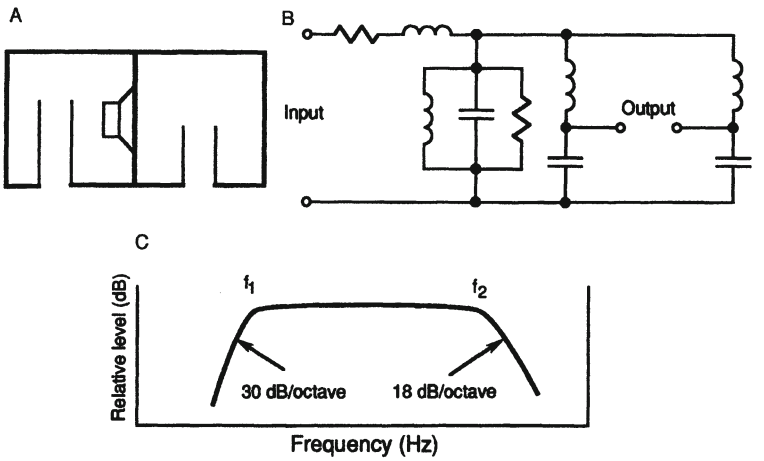

Figure 4-23. Bandpass systems: parallel operation: Section view (A); equivalent circuit (B); target response (C).

4.10 The acoustic lever

Modern bandpass LF systems have reached a high degree of sophistication and engineering refinement. Using only enclosed volumes, interconnecting ports and drivers, these systems, when well executed, produce high output over a defined LF passband. Essentially, the improvements in response come from the beneficial use of controlled resonances through maximizing the system's bandwidth-efficiency product commensurate with the total volume occupied by the system. The *acoustic lever* is a relatively new element in such system synthesis.

Geddes (1999) describes the acoustic lever, which is a variation of the passive radiator. An application is shown in Figure 4-24. Note that there are three chambers. The two at the right have PRs, and the PR facing the outside has greater cone area than the inner one. The two PRs are joined by a rigid connecting rod, and the entire coupled assembly is referred to as an acoustic lever.

Geddes describes a number of applications, and that shown in Figure 4-24 is one of the simplest. Intuitively, we can see that the driver imparts a linear velocity to PR1, which directly couples it to PR2. The volume velocity of PR1 will be translated into a higher volume velocity at PR2, proportional to the ratio of the two PR cone areas. This will be reflected back as an increased mechanical impedance as seen by the driver.

The approach enables a smaller driver to be used, and, as long as it has the requisite $(Bl)^2/R_E$, the area transformation ratio of the acoustic level will, in a sense, enable the smaller driver to perform as though it had a larger cone. The back air chamber, *V1*, can also be made smaller to accommodate the smaller driver. Thus, there are two cost-performance attributes that can be satisfied at once. The methodology is not simple, and interested engineers will want to study the cited article in detail.

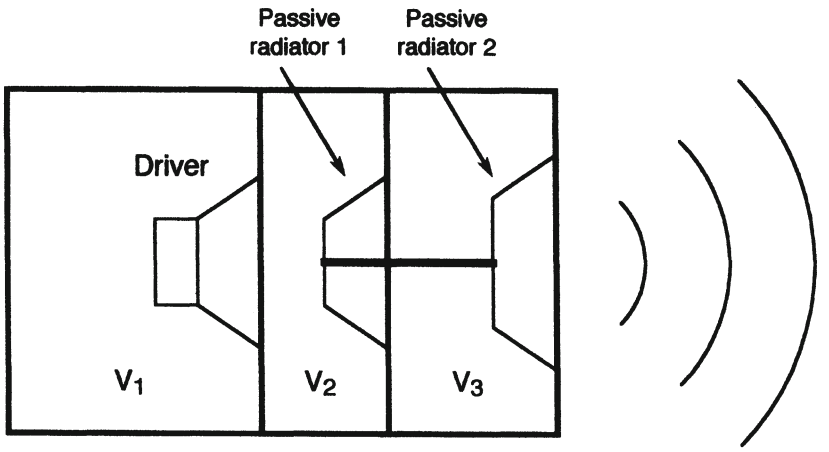

Figure 4-24. The acoustic lever.

4.11 Transducers in acoustical series and in parallel

4.11.1 Parallel operation and mutual coupling

It is common in many applications to mount two or more LF drivers adjacent to each other on the same baffle and drive them in electrical parallel. At the same time, the drivers are acting acoustically in parallel. Figure 4-25A shows a front view of a LF system consisting of two 380 mm (15 in) drivers mounted in a 225 L enclosure tuned to 40 Hz. The curves shown in Figure 4-25B show the relative power response of this system, as compared to that of a single driver mounted in a 112 liter enclosure tuned to 40 Hz. In the case of the single driver, one watt of power has been applied; in the case of the dual drivers, one-half watt of power has been applied to each driver.

Note that the response of the dual driver system is three dB greater than the single unit, both with the same overall electrical power input. This increase

is caused by the fact that the two closely coupled drivers behave essentially like a single "new" driver with twice the cone area, twice the V_{AS}, and the same f_S and Q_{ES}. These factors will result in a doubling of efficiency, but the overall LF alignment will remain essentially the same. The HF rolloff commencing at ka = 2 will be shifted downward by a factor of 0.7 in frequency, since the effective perimeter of the radiating surface has been increased by a factor of about 1.4. The term *mutual coupling* is often used to describe this effect. It is further obvious that the dual driver system can handle twice the electrical input power than the single unit. Therefore, there is a net 6 dB greater output capability with the dual unit as opposed to the single unit.

The property of mutual coupling extends to multiple drivers well beyond the two shown here, but with each doubling of the number of closely clustered drivers the 0.7 factor in LF system bandwidth must be applied. In practice it is possible to attain a maximum efficiency no greater than 25% for large LF arrays.

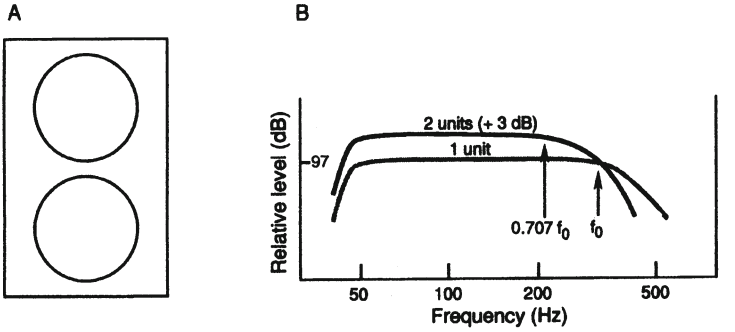

Figure 4-25. LF drivers in acoustical parallel. System front view (A); response, as compared to a single driver (B). Response shown for input of one watt at one meter.

4.11.2 Series operation

The arrangement shown in Figure 4-26 places a pair of drivers one behind the other with a small enclosed air space between them. The basic intent in this design is that the rear driver will move "out of the way" of the front driver, allowing the latter to look into what is effectively a larger enclosure volume. The pair are normally driven electrically in parallel, but they are acting acoustically in series. Colloms (1991) describes the combination as acting like a single driver having twice the moving mass, half the compliance, and half the impedance of the single driver. For a given voltage input, it will absorb twice the power of the single unit, and in a sealed enclosure, the air spring will

be the dominant restoring force. The net result of this will be a reduction of the system resonance to 0.7 that of the single driver in the same size enclosure, along with an increase in power handling and linearity. The design approach is commonly known as *Isobarik*, a trade name of Linn Products.

Olson (1957) presents a detailed analytical description of the series driver arrangement, essentially showing that LF response is extended to about 0.7 the cutoff frequency of a single driver mounted in an enclosure of the same volume.

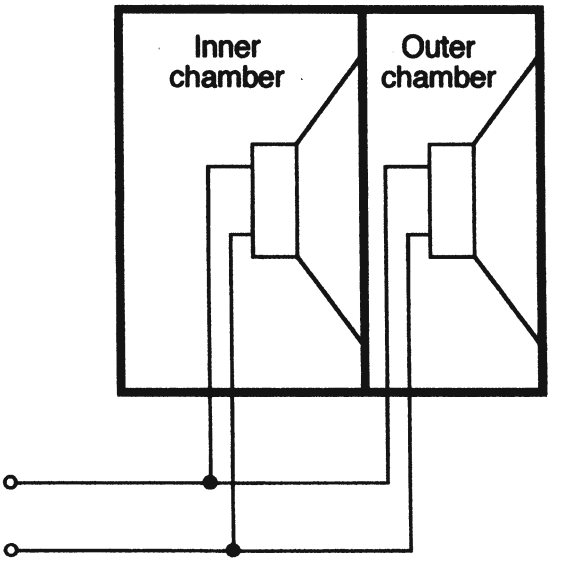

Figure 4-26. LF drivers in acoustical series.

4.12 Slot loading of LF drivers

The term *slot loading* covers a wide variety of designs. Many of these originated during the first flowering of high fidelity during the 1950s and 1960s – an era of grass-roots experimentation and a great deal of home construction of loudspeaker systems. The basic premise of slot loading is that the additional damping and mass afforded by the technique can be added to a driver to extend its LF response, as well as possibly smooth out response variations. The idea was probably a reasonable one at the time, since there were relatively few available drivers specifically engineered for extended response in medium to small-size enclosures. One notable design from that era was the R-J enclosure, shown in Figure 4-27A. Here, the LF back path from the cone is fed in parallel with the front path. The slot-loading portion of the design takes place between the inner and outer (front) baffle.

Today, slot loading is used in a number of subwoofer designs with downward-facing cones, as shown in Figure 4-27B. There is an advantage here in using a cone with a fairly high free-air resonance in that it will exhibit less gravitational sag than a cone with a lower resonance frequency. The degree of cone sag (Olson, 1957) can be computed as:

$$x(mm) = 247/f^2 \qquad 4.1$$

Thus, a driver with a free-air cone resonance of 50 Hz will exhibit a gravitational sag of about 0.1 mm, while a cone with a free-air resonance of 30 Hz will exhibit a sag of about 0.3 mm.

Because of the added mechanical mass and resistive loading on the driver, only those drivers with fairly high values of $(Bl)^2/R_E$ are recommended for use in slot loaded systems.

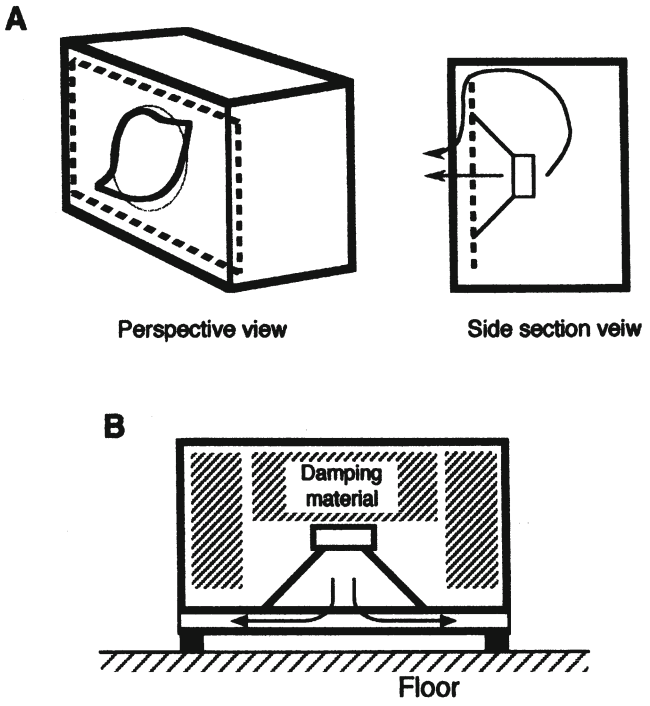

Figure 4-27. Slot-loading of LF drivers. The R-J enclosure (A); downward-firing subwoofer (B).

4.13 Subwoofers

While any system designed for LF bandpass operation may be referred to as a subwoofer, the term is taking on the added qualifications of small size with maximized output capability. The home theater marketplace has put a premium on small subwoofers, which are often used in conjunction with five-channel satellite loudspeakers. Many of these systems, known collectively as "5.1" systems, employ small satellites with their internal LF units no larger than 150 mm or 200 mm (6 in or 8 in) which have been equalized for response down to about 100 Hz. A single subwoofer is then used to provide summed response below about 100 Hz. (This is the "point-one" value in the designation "five-point-one.") In mass produced systems, the subwoofers themselves are often self-powered, including on-board displacement limiting and the necessary equalization to produce uniform response down to about 40 Hz.

Given the many recent improvements in cone driver design, amplifier topology, and signal processing, there are notable subwoofer designs that have raised expectations among demanding consumers and professional users alike. These systems are often capable of response down to the 25-30 Hz region.

The Sunfire subwoofer products, designed by noted engineer Robert Carver, very likely take the prize for maximum usable LF output from the smallest volume. The basic design topology is shown in Figure 4-28. A long-throw LF driver with a very high $(Bl)^2/R_E$ product is mounted in a relatively small enclosure with a passive radiator. Resonance frequencies for both the driver and PR are nominally in the 25-to-35 Hz range, and the excursion capabilities of both units are considerable. Because of the staggering of resonances, the driver and PR do not exhibit antiphase performance until well below 20 Hz. The driving electronics include frequency-dependent limiting, equalization, and an amplifier output section that can swamp out the extremely high back EMF of the driver.

The resultant response is remarkably flat to below 30 Hz at levels that can accommodate normal listening requirements in a midsize to large living room. Distortion levels are marginally high, due primarily to the nonlinearity of the small air spring volume, but these are generally well masked by normal program requirements.

A problem sometimes noticed with small high-powered subwoofers at high drive levels is the tendency for them to migrate along the floor as the drivers create inertial forces internally, exceeding the force required to move the entire system along the floor. This is known as loss of *inertial ground*, and can be corrected by anchoring the system to the floor one way or another. The easiest method is to stack fairly massive concrete blocks on top of the systems.

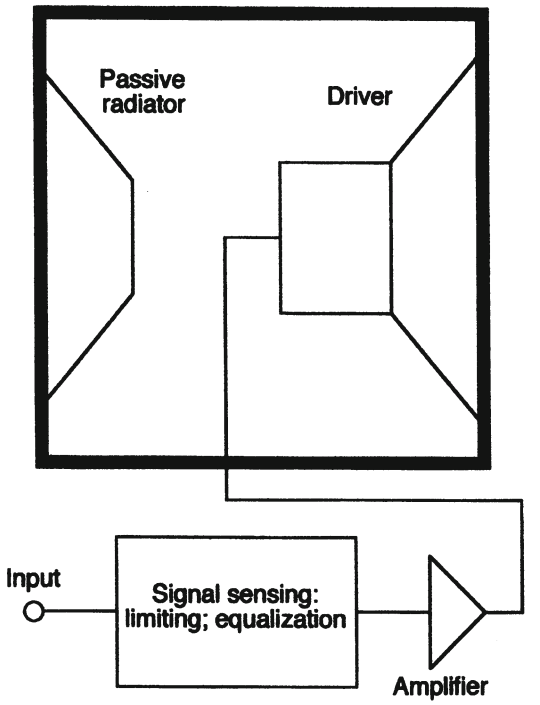

Figure 4-28. Typical small subwoofer with high output capability.

Bag End Loudspeakers takes advantage of the preference of many listeners for the smooth LF rolloff of sealed systems. When designed around long-throw drivers, suitably equalized and signal-limited, arrays of such systems can provide output capability limited only by the available hardware. The basic scheme is shown in Figure 4-29A, and the equalization process is shown at *B*. An important limitation to remember is that, for flat LF output, the cone excursion requirements in sealed systems *quadruple* for each halving of frequency. Thus, a system such as this must be self-monitoring under all drive conditions. These products are used in numerous professional postproduction operations as well as in large-scale music reinforcement.

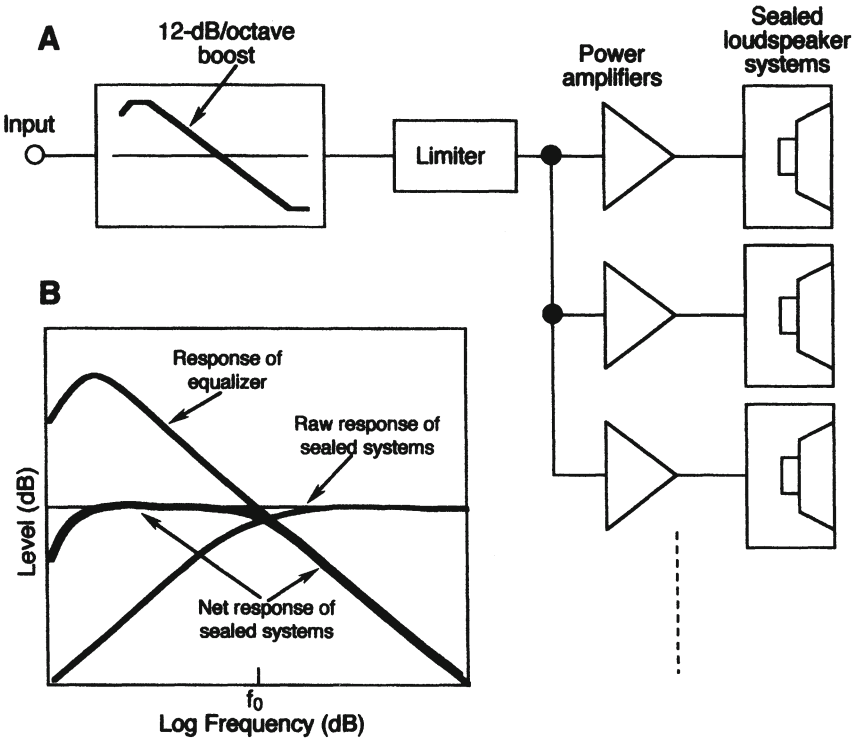

Figure 4-29. Sealed subwoofers with equalization for flat response. Electrical circuit (A); equalization scheme (B).

4.14 Directional properties of dual LF drivers mounted vertically

In many applications, LF units are operated in pairs arrayed vertically, so that maximum directivity will be in the vertical plane with normal wide dispersion in the horizontal plane. The nominal –6 dB beamwidth and DI of three sizes of dual LF systems are shown.

Figure 4-30 shows beamwidth and directivity data for a double stack of 250 mm (10 in) diameter drivers; Figure 4-31 shows similar data for 300 mm (12 in) drivers, and Figure 4-32 shows similar data for 380 mm (15 in) drivers, all mounted in vertical pairs.

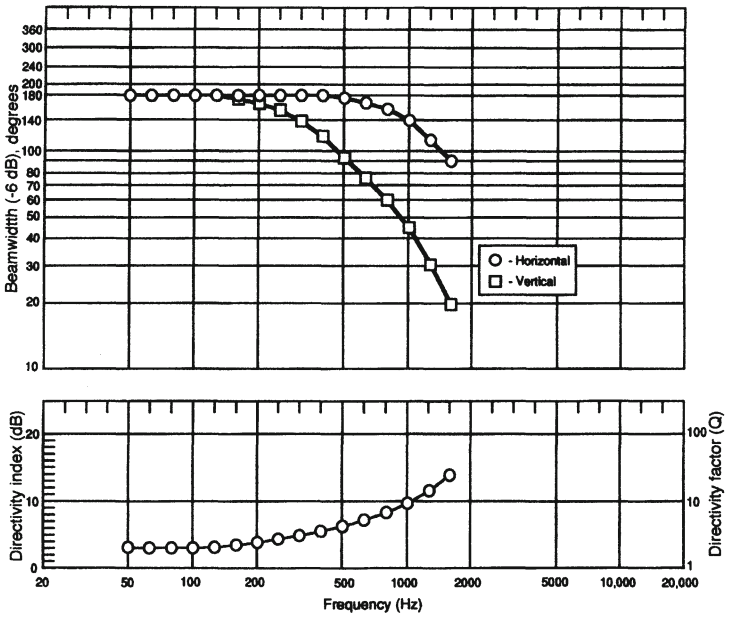

Figure 4-30. Directional properties of dual LF driver vertical array: 250 mm (10") drivers.

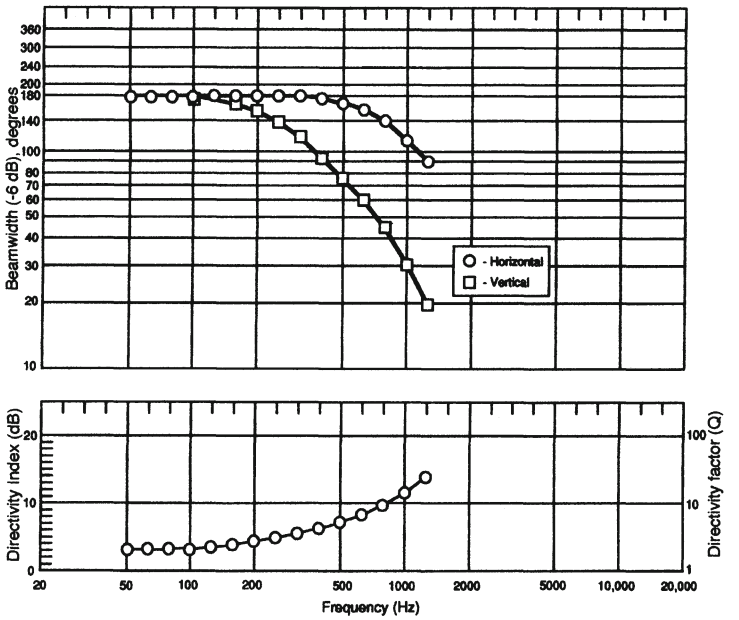

Figure 4-31. Directional properties of dual LF driver vertical array: 300 mm (12") drivers.

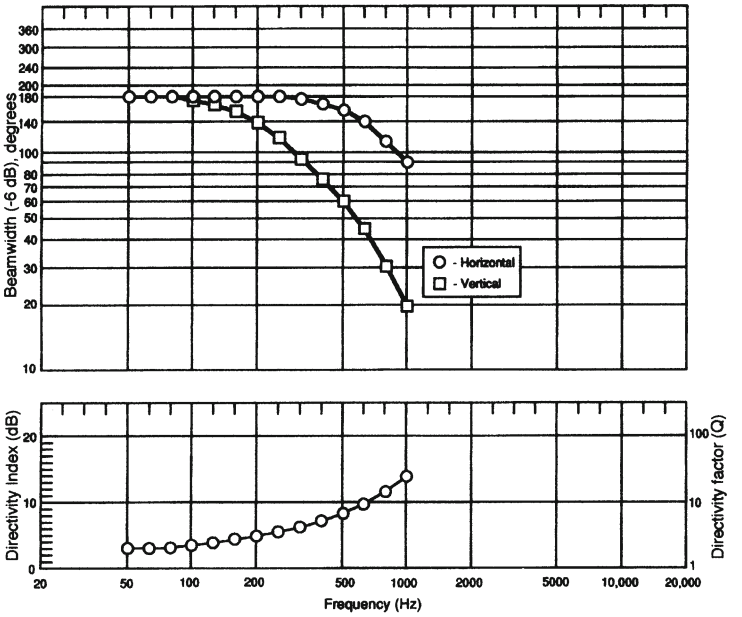

Figure 4-32. Directional properties of dual LF driver vertical array: 380 mm (15") drivers.

4.15 Alignment shifts

Large arrays of subwoofers, such as may be used in high level music reinforcement or in motion picture theaters, will exhibit a shift in alignment, as shown in Figure 4-33. Here, the shift in the impedance null at enclosure resonance is observed with one, two, and four ported LF systems. Measurements were made with the systems placed on an extended ground plane outdoors.

The progressive shift of the impedance null from 31 Hz, downward to 29 and 27 Hz, indicates a trend that, if extended much beyond the point shown, could compromise system performance. The downward shift may make the combined system of LF units susceptible to displacement overload in the octave above enclosure resonance and should be carefully monitored in this regard. In extreme cases it may be necessary to realign the LF systems, taking these shifts into consideration.

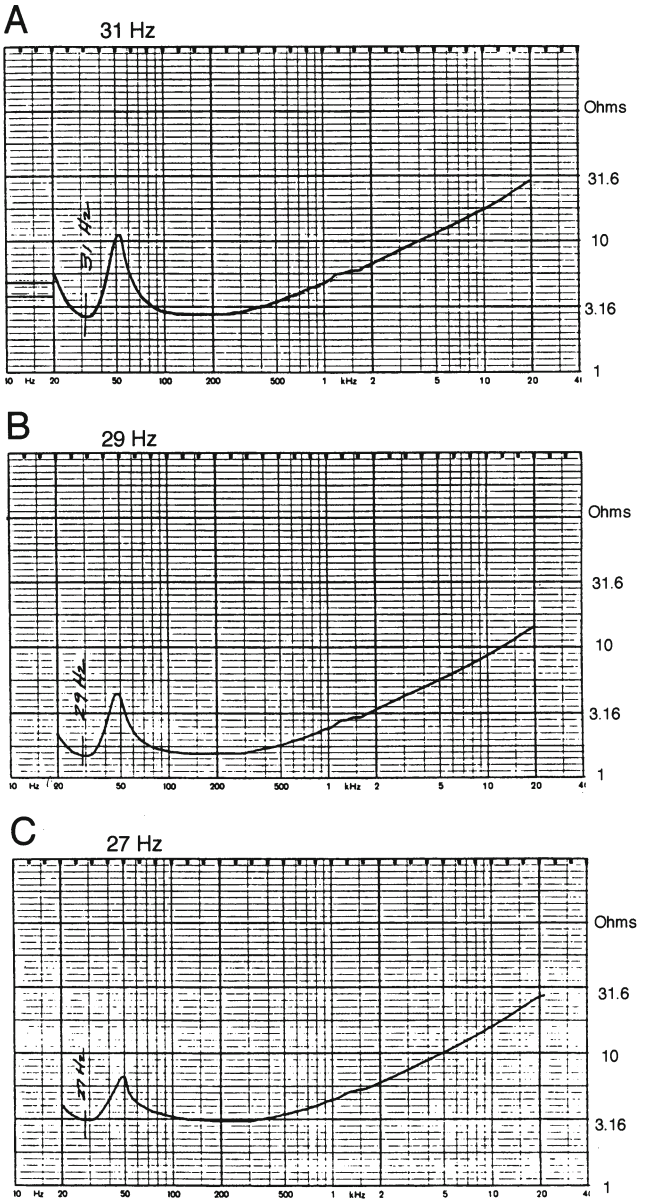

Figure 4-33. Alignment shifts in multiple LF system operation. (Data courtesy *Audio Engineering Society*, Gander and Eargle, 1990)

BIBLIOGRAPHY AND REFERENCES:

Augspurger, G., "Theory, Ingenuity, and Wishful Wizardry in Loudspeaker Design — a Half-Century of Progress?" *J. Acoustical Society of America*, volume 77, number 4 (1985).

Augspurger, G., "Loudspeakers on Damped Pipes, Part 1: Modeling and Testing; Part 2: Behavior." Presented at the 108th Audio Engineering Society Convention, preprint number 5011 (Los Angeles, 1999).

Avedon, R., "More on the Air Spring and the Ultra-Compact Loudspeaker," *Audio Magazine*, June (1960).

Beranek, L., *Acoustics*, McGraw-Hill, New York (1954), reprinted by ASA, 1993.

Borwick,J., (editor), *Loudspeaker and Headphone Handbook*, 3rd edition; Focal Press, Boston (2001).

Czerwinski, E., U. S. Patent 4,101,736 (1978).

Colloms, M., *High Performance Loudspeakers*, fourth edition, John Wiley & Sons, New York (1991).

Engebretson, M., "Low-Frequency Sound Reproduction," *J. Audio Engineering Society*, volume 32, number 5 (1984).

Gander, M., and Eargle, J., "Measurement and Estimation of Large Loudspeaker Array Performance," *J. Audio Engineering Society*, volume 38, number 4 (1990).

Geddes, E., "An Introduction to Band-Pass Loudspeaker Systems," *J. Audio Engineering Society*, volume 37, number 5 (1989).

Geddes, E., *Audio Transducers*, (ISBN 0-9722085-0-X), 2002.

Jensen Manufacturing Company, Technical Bulletin number 4, "The Reproducer of the Future" (December 1952)

Keele, D., "A New Set of Sixth-order Vented-Box Loudspeaker System Alignments," *J. Audio Engineering Society*, volume 23, number 5 (1975).

Leach, M., "Electroacoustic-Analogous Circuit Models for Filled Enclosures," *J. Audio Engineering Society*, volume 37, number 7/8 (1989).

Locanthi, B., "Application of Electric Circuit Analogies to Loudspeaker Design Problems," *J. Audio Engineering Society*, volume 19, number 9 (1971).

Novak, J., "Performance of Enclosures for Low-Resonance High-Compliance Loudspeakers, *J. Audio Engineering Society*, volume 7, number 1 (1959).

Olney, B., "A Method of Eliminating Cavity Resonance, Extending Low Frequency Response and Increasing Acoustic Damping in Cabinet Type Loudspeakers," *J. Acoustical Society of America*, volume 8, number 2 (October 1936).

Olson, H., *Acoustical Engineering*, D. Van Nostrand, New York (1957), reprinted by Professional Acoustical Journals, 1991.

Small, R., "Direct Radiator Loudspeaker System Analysis and Synthesis (parts 1 and 2)" *J. Audio Engineering Society*, volume 20, number 5 and volume 21, number 1 (1972 and 1973).

Small, R., "Passive-Radiator Loudspeaker Systems Part I: Analysis," *J. Audio Engineering Society*, volume 22, number 8 (1974).

Tappan, P., "Analysis of a Low-Frequency Loudspeaker System," *J. Audio Engineering Society*, volume 7, number 1 (1959).

Thiele, N., "Loudspeakers in Vented Boxes, Parts I and II," *J. Audio Engineering Society*, volume 19, numbers 5 and 6 (1971).

Various, *Loudspeakers, anthologies, volumes 1 and 2*, papers taken from the pages of the Journal of the Audio Engineering Society, 1953 to 1983, New York (1978 and 1984).

Villchur, E., "Problems of Bass Reproduction in Loudspeakers," *J. Audio Engineering Society*, volume 5, number 3 (1957).

Chapter 5:
DIVIDING NETWORKS AND SYSTEMS CONCEPTS

5 Introduction

Loudspeaker engineers may generally agree on what is or is not a good loudspeaker, but they may argue at length on the relative importance of the attributes that define a good loudspeaker. Often, the refinement of one performance attribute comes at the expense of another, and there are economic trade-offs in the world of commerce. There are many design variables that must be dealt with, and in this chapter we will cover systems concepts, details of dividing network topology and design, off-axis lobing, or interference, problems, baffle layout and enclosure edge treatment.

We also stress that there are three loudspeaker attributes that are difficult to reconcile: enclosure size (smaller is better), bandwidth (extended low frequency response is better), and efficiency (higher is better). This has often been referred to as the "eternal triangle" of loudspeaker design. Any improvement in one of these attributes always comes at the expense of the other two, and the design of commercial loudspeaker systems involves continuous tradeoffs among these attributes.

5.1 Basic dividing networks

The function of a frequency dividing network is to channel the audio spectrum into two or more bands so that the system drivers receive their intended signals. The necessity for this is the fact that a loudspeaker system is a collection of bandpass devices, each requiring its share, and only its share, of the input spectrum. Additionally, it is imperative to keep low frequency signals from reaching high frequency drivers and possibly damaging them.

J. Eargle, *Loudspeaker Handbook*

Networks are primarily defined in terms of their nominal rolloff slopes. As discussed in the previous chapter, the *order* of a network slope defines the number of reactive elements contributing to the rolloff, each element producing a slope of 6 dB/octave. Thus, a first-order network produces a 6 dB/octave slope, while a fourth-order network will produce a 24 dB/octave slope. The term *pole* is often used to describe the network action that contributes a 6 dB/octave rolloff. As we will see, the natural acoustic rolloff off a given driver may function as an added *acoustical pole*, in additional to the network's electrical poles.

Figure 5-1 shows design data for first and second order two-way networks in both parallel and series form. The first-order networks are shown at *A* and *B*, and both make use of the same circuit values for a given crossover frequency. The parallel form is used more often, but an advantage of the series form is that the network slopes in the region of crossover are very nearly second-order, becoming first order at frequencies removed from the crossover point.

Second-order networks are shown at *C* and *D*, with their circuit values expressed in terms of L_1 and C_1. Note that the circuit values are not the same for parallel and series forms.

In using the network types described in Figures 5-1, it is essential that the design load impedances closely match the actual impedance values of their respective drivers at the selected crossover frequencies. All target values should be constructed and measured to ensure that they are correct.

A 3-way parallel second order network is shown in Figure 5-1E. Here, the MF section is bandpass, composed of both LF and HF sections. Circuit values are obtained using the data given in Figure 5-1C and *D*.

5.1.1 Vector relationships in networks

Figure 5-2A shows the vector relationship at crossover between high and low-pass sections for a first-order network. Note that the amplitude of both high and low signals at crossover is 0.7 and that both are displaced ±45°. The on-axis summation is unity at a phase angle of zero, and the power response, proportional to $(0.7^2 + 0.7^2)^{0.5}$, is likewise unity. These are both desirable attributes, but the chief problem with first-order networks is that the out-of-band signals may not be sufficiently attenuated for proper component protection, depending on the system's application.

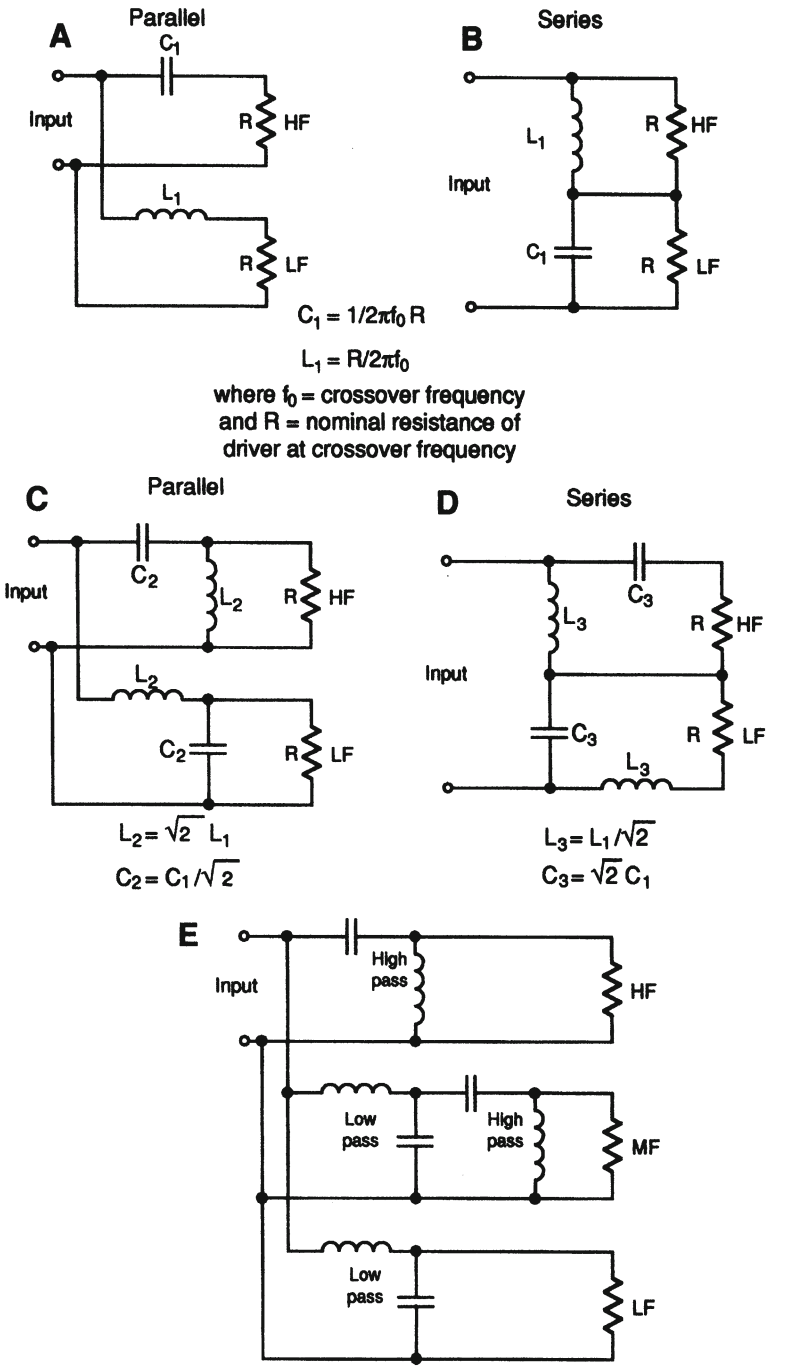

Figure 5-1. Basic network circuits. First-order parallel (A); first-order series (B); second-order parallel (C); second-order series (D); second-order parallel three-way (E).

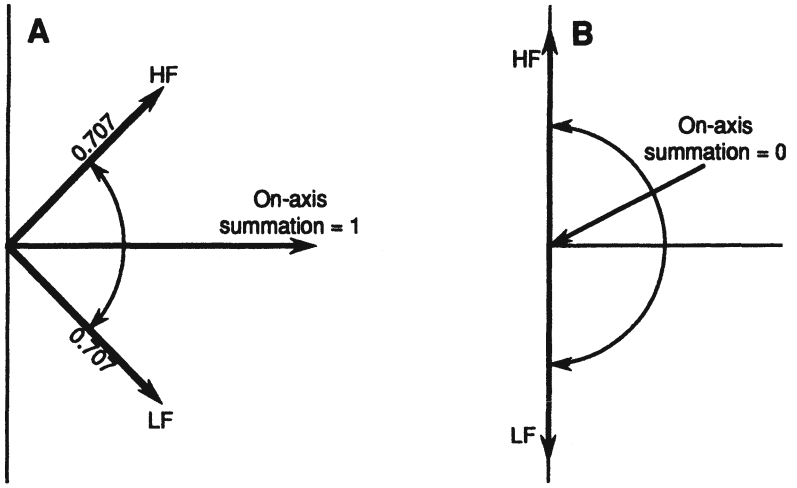

Figure 5-2. Vector relationships at the crossover frequency. First-order (A); second-order (B).

Second-order vector relationships are shown in Figure 5-2B. Here, the two signals are each shifted 90° for a total of 180°. In this case it is necessary for one of the two outputs of the network to be reversed in polarity so that the signals will add at the crossover frequency.

5.1.2 Higher-order networks

Third order networks are often used in professional applications, where considerable out of band attenuation is necessary because of the high powers that may be involved. A typical circuit is shown in Figure 5-3A, and the normal vector relationships are as shown at *B*. If the HF output of the network is inverted the system phase response will change, as shown at *C*.

The so-called Linkwitz-Riley network is of fourth-order and is normally designed so that both HF and LF outputs are 0.5 amplitude (–6 dB) at the crossover frequency. Both sections are rotated 180° at crossover and will of course add to produce unity output on axis, as shown at Figure 5-4A. Power response will dip 3 dB at crossover, however, as shown at *B*. The advantages of the design is that out-of-band signals are greatly attenuated and that lobing effects between adjacent drivers will take place over a very small frequency interval.

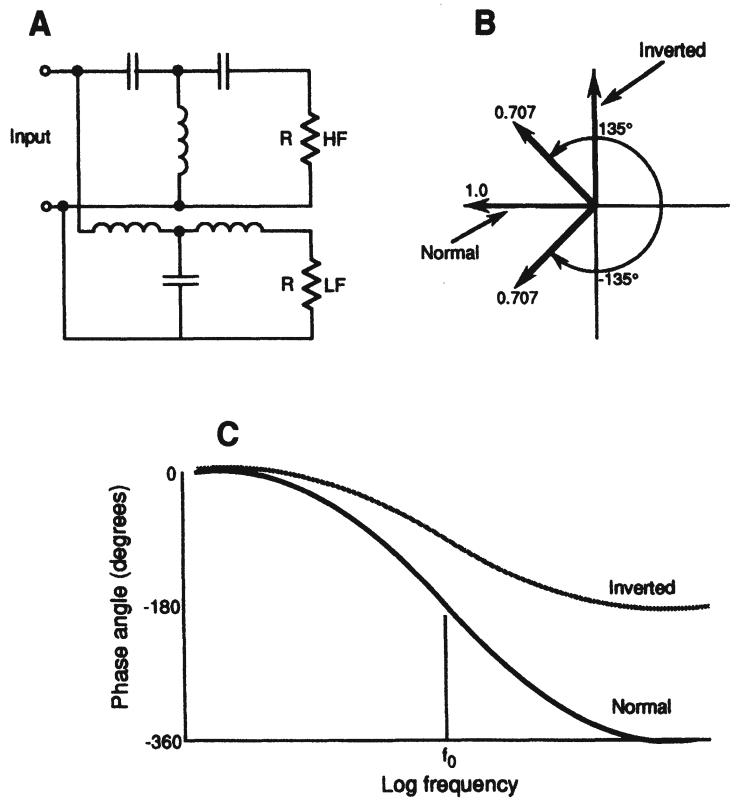

Figure 5-3. Third-order network design. Parallel circuit (A); vector relationships (B); phase response, normal and inverted (C).

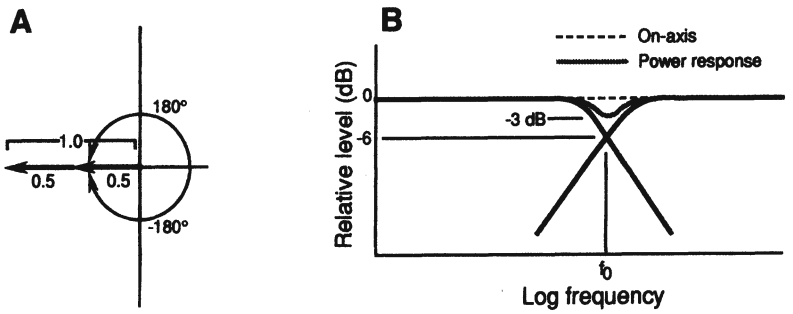

Figure 5-4. Fourth-order design (Linkwitz-Riley). Vector relationship at crossover (A); system response (B).

The network circuits we have discussed thus far can be combined to provide three- and four-way designs, as required. However, parallel networks may easier to work with in the design of 3-way or higher systems.

5.1.3 Conjugate networks, level adjustment, and bypass elements

Conjugate networks can be used to compensate for the effects of resonance in drivers as well as the impedance rise at HF due to driver inductance. Examples of this are shown in Figure 5-5. The basic driver is shown at *A* and its impedance at *B*. The addition of a conjugate impedance network (shown at *C*) will swamp out the impedance, as shown at *D*. Further addition of an inductance compensating network (shown at *E*) will further flatten the impedance curve, as shown at *F*. (The inductance compensating network added at *E* is often referred to as a Zobel network.)

When a driver has been compensated as shown in Figure 5-5 it may effectively be treated as a resistance, and network values calculated in a straightforward manner. The resulting crossover slopes will be well behaved, since there will be very little reactive loading on the dividing network. The calculation of circuit values for impedance compensation is provided by a number of the system design programs that are available.

For the voice coil inductance compensating network, the value of capacitance, in farads, is given by:

$$C = L/(Z)^2 \qquad 5.1$$

where *L* is the voice coil inductance, in henrys, and *Z* is the nominal impedance of the driver. The value of *R* in the inductance compensating network is the design impedance of the driver.

The resonance compensating network component values are given by:

$$L = Q_t R/2\pi f_0 \qquad 5.2$$

where Q_t is the system Q at resonance, *R* is the nominal impedance of the driver, and f_0 is the resonance frequency. *L* is given in henrys.

$$C = 1/L(2\pi f_0)^2 \qquad 5.3$$

where *C* is given in farads and *L* in henrys.

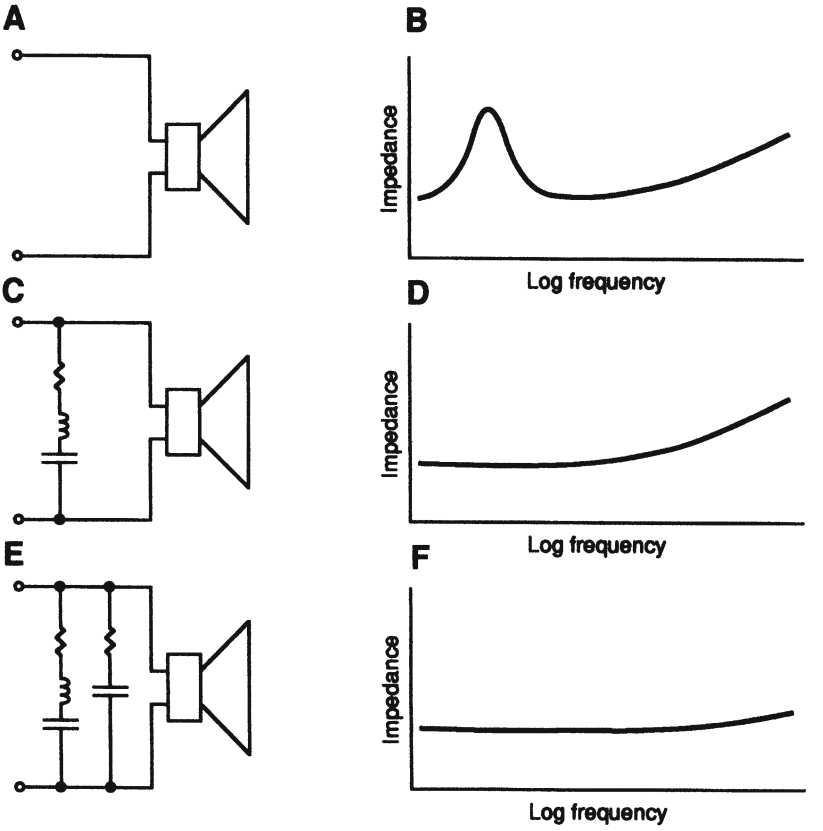

Figure 5-5. Use of conjugate networks. Cone driver and impedance (A and B); effect of impedance conjugate network (C and D); effect of both inductance and impedance conjugate networks (E and F).

Figure 5-6A shows a fixed L-pad, which can be used to adjust downward the drive level to a given component. A variable version is shown at *B*, and such controls as these are often accessible on the baffle of a loudspeaker system as a user adjustment. The chart shown in Table 5.1 gives L-pad values for a number of loss settings for both 4 and 8-ohm applications.

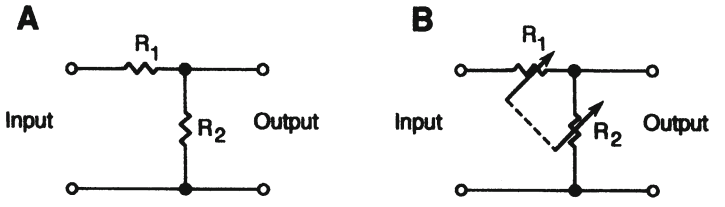

Figure 5-6. Loss pads. Fixed (A); variable (B).

Table 5.1. L-pad values for 4 and 8-ohm applications

	4-ohm		8-ohm	
dB Loss	R_1	R_2	R_1	R_2
0.5	0.2	67	0.4	135
1.0	0.4	33	0.8	65.5
2.0	0.8	15	1.6	31.0
3.0	1.2	9.8	2.4	19.4
4.0	1.5	6.8	3.0	13.7
5.0	1.7	5.1	3.5	10.3
6.0	2.0	4.0	4.0	8.0
7.0	2.3	3.3	4.5	6.5
8.0	2.4	2.7	4.8	5.3
9.0	2.5	2.2	5.1	4.4
10.0	2.7	1.9	5.5	3.7

A bypass network may be shunted across a series pad element in order to equalize the following driver. For example, the capacitive shunt shown in Figure 5-7A can be used to provide unattenuated drive to the following driver above a frequency approximately equal to:

$$f = 1/(2\pi RC) \qquad 5.4$$

The resonant shunt shown at *B* can be used to add a HF peak to the response of the following element.

5.2 Upper useful frequency limits for drivers

As we have discussed earlier, cone type loudspeakers begin to roll off in power response at values of *ka* of 2 and higher. However, due to the accompanying increase in their on-axis directivity index, it is possible to use these drivers at values higher than ka = 2. Table 5.2 presents upper useful frequency limits, based on DI values of 6 and 10 dB. As a general rule, using a cone driver higher than a DI of 10 is considered a bit risky, in that manufacturing tolerances at high frequencies may come into play, and unit-to-unit consistency may be questioned.

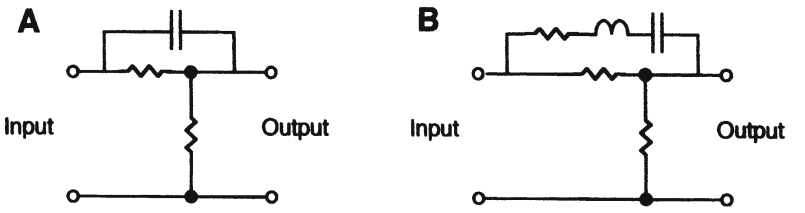

Figure 5-7. Bypass networks. A capacitive bypass provides unattenuated HF response (A); a resonant bypass provides a HF response peak (B).

Table 5.2 Useful upper frequency limits for cone drivers

Diameter, mm (inches):	ka = 2 (DI = 6 dB):	DI = 10 dB:
460 mm (18")	547 Hz	820 Hz
380 mm (15")	673	1010
300 mm (12")	875	1313
250 mm (10")	1100	1650
200 mm (8")	1460	2190

5.3 Some notes on network component quality

High quality network components should be used whenever possible, and careful note should be taken of working voltages so that the components will not be stressed in normal use. Inductances in particular need to be made of fairly large gauge wire so that their associated resistance can be minimized. Iron core inductors may be used, but only if effects of core saturation, and the consequent shift in inductance, are minimal and accounted for in the design calculations. Powdered core inductors are less prone to inductance shifts.

When higher sensitivity drivers are padded down to match lower sensitivity drivers, the padding resistors may dissipate a good bit of heat when the system is heavily driven. Choose the sizes carefully. In particular, watch the gauge of rotary L-pads that are often used for user adjustable driver levels on many systems.

Many of the capacitors used in dividing networks are fairly large and may handle substantial working voltages. Non-polarized electrolytic types may be used in shunt network paths, but only the highest quality components should be specified for primary signal paths.

5.4 Stock networks and autotransformers

For medium-power professional applications where there may be mixing and matching of separate HF and LF systems, stock networks are often used. Figure 5-8A shows a photograph of typical examples. A stock network schematic is shown at *B* and typical response curves are shown at *C*. The basic design is as a second-order network with variable HF output so that the HF driver sensitivity (normally a horn system) can be properly matched to the LF section. A switch allows HF power response boost equalization to be introduced into the HF output, with typical curves shown at *D*. This technique was discussed in Section 5.1

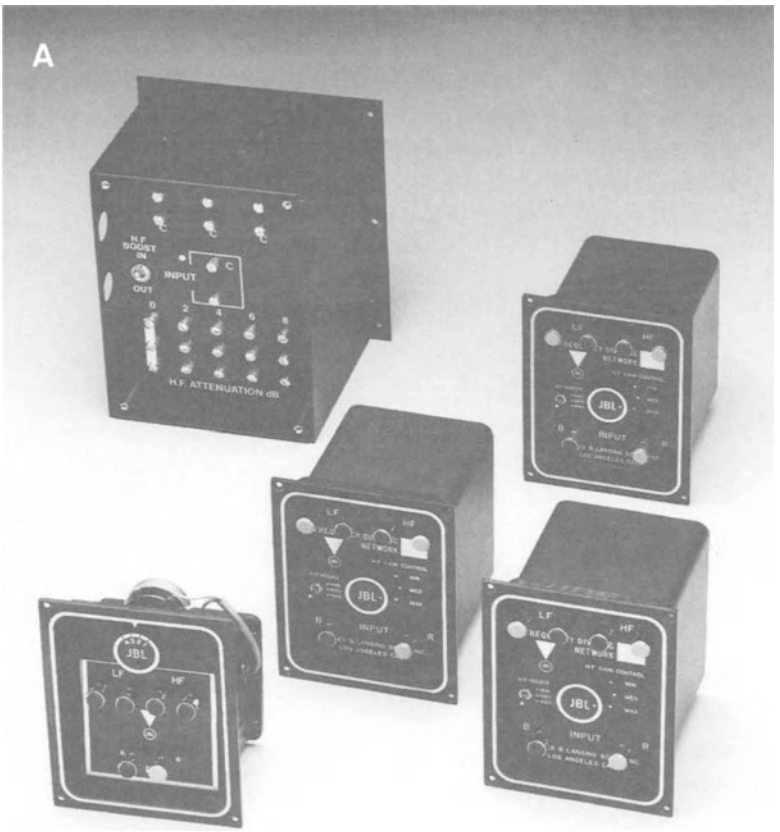

Figure 5-8. Stock networks. Photo of group (A); typical circuit diagram (B); normal response range (C); response with HF power response compensation (D). (Photo courtesy JBL)

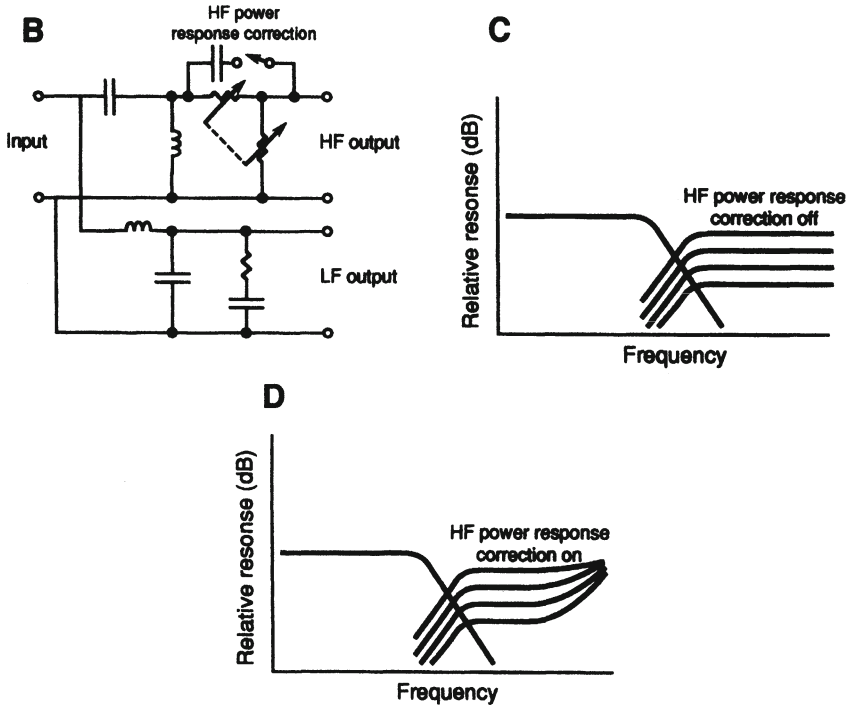

Figure 5-8. Continued.

Such networks are normally designed as a "best fit" for a number of applications and may not represent an ideal crossover solution to any one of them.

Details of the autotransformer (also known as autoformer) are shown in Figure 5-9A. This single winding version of the transformer can be used to adjust impedances and drive levels in a network as shown. In the application shown at *B*, a 4-ohm load is transformed so that it appears as a 16-ohm load. When a load impedance is transformed to a higher value, it will absorb less power. Accordingly, the autoformer is often used to adjust drive levels at the output of passive network designs.

5.5 Case studies

We present two examples of network design based on the specific requirements at hand. The various techniques we have so far discussed will be used. The 2-way example illustrates the problems encountered in coupling a 380 mm LF driver with a medium format uniform coverage horn/compression driver. The 4-way example combines a powered subwoofer with a 3-way cone-dome system intended for high-end consumer use.

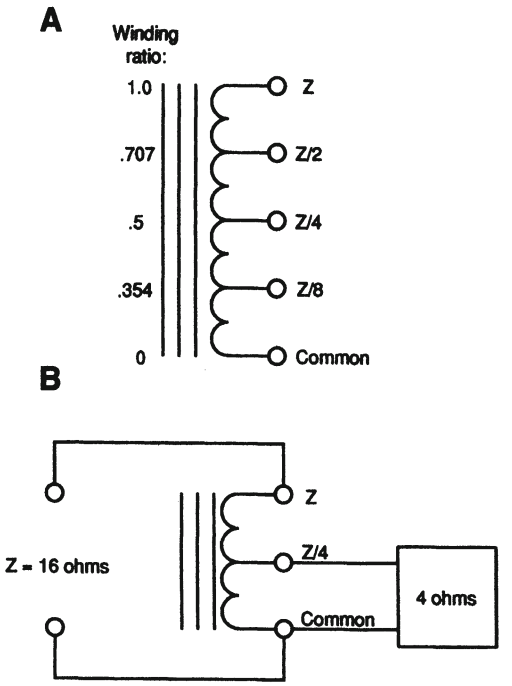

Figure 5-9. The autotransformer. Circuit (A); typical application (B).

5.5.1 A 2-way monitor system combining cone and horn elements

Cone and horn elements normally differ in sensitivity by about 12 to 14 dB, and the JBL 4430 monitor system is an example of how the match between components is made. A nominal crossover frequency of 1 kHz was chosen for this system. Figure 5-10 shows a side view of the basic monitor design, in which the HF horn is located directly above the LF driver.

Figure 5-11 shows the use of both electrical and acoustical poles in establishing a fourth-order rolloff for the LF section. The nominal sensitivity of the LF section is 90 dB L_p, 1 W at 1 m.

The HF section likewise makes use of both electrical and acoustical poles and is shown in Figure 5-12. It has a mid-band sensitivity of 114 dB LP, and the effect of the network padding, plus shunt HF boost, is shown in Figure 5-13. The complete network design is shown in Figure 5-14. Included here are many of the design elements we have previously discussed.

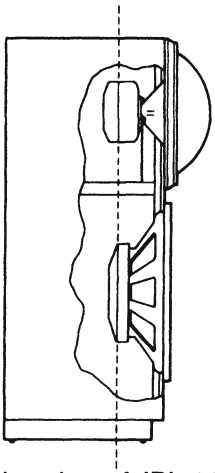

Figure 5-10. Side section view of JBL 4430 monitor loudspeaker.

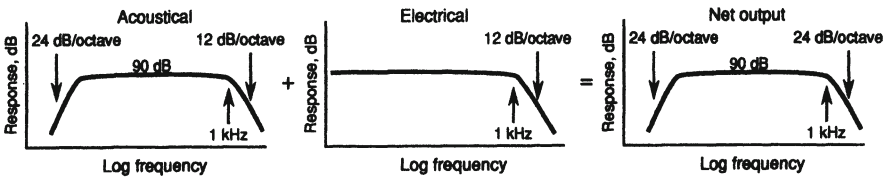

Figure 5-11. Combining acoustical and electrical poles at LF.

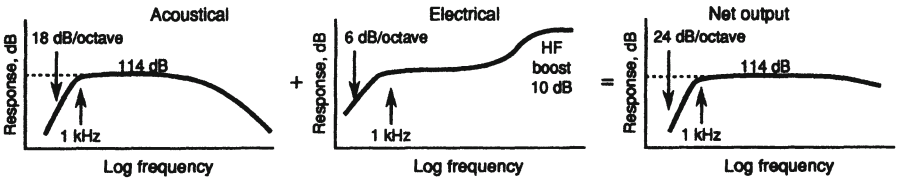

Figure 5-12. Combining acoustical and electrical poles at HF.

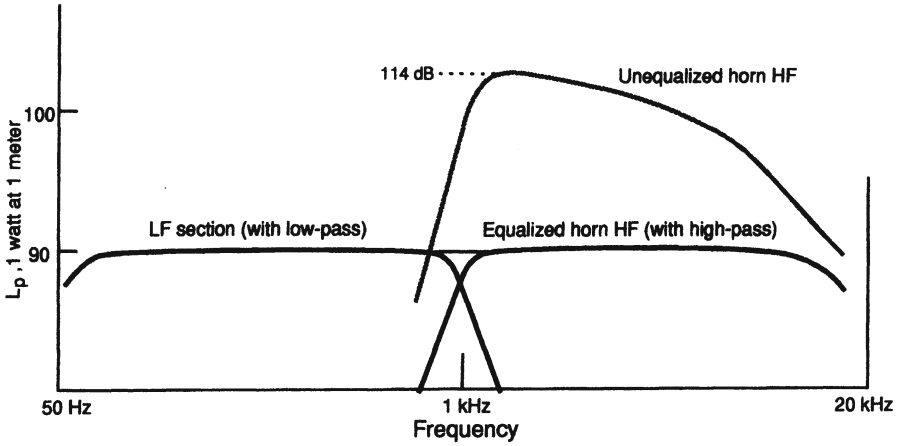

Figure 5-13. Equalizing the HF power response and level to match the LF response.

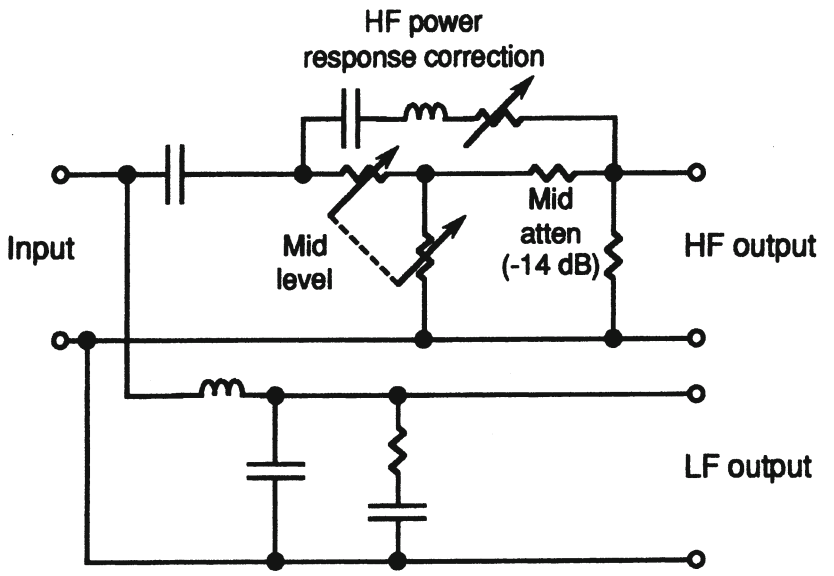

Figure 5-14. Dividing network for JBL 4430 monitor system.

5.5.2 A 4-way high-end consumer system

The Infinity Systems Prelude model is shown in Figure 5-15. It is a multi-element column array placed above a subwoofer (there is an option for powering the subwoofer independently of the rest of the system). The elements in the array are all fed by the detailed passive dividing network shown in Figure 5-16. This network deals only with the 3-way column portion of the system. Significant network functions are labeled, and you will note that impedance compensation is used on all sets of drivers. There is also an overall impedance compensating network at the input which fixes the passive array impedance at 4 ohms ±1 ohm over the entire frequency range.

Figure 5-17 shows the individual contribution from each section of the system, along with the overall summation of on-axis response. The impedance is shown at the bottom of the graph. Note that both electrical and acoustical poles are used in achieving the sharp bandpass nature of the network.

Figure 5-15. Photo of Infinity Systems Prelude system. (Photo courtesy Infinity Systems)

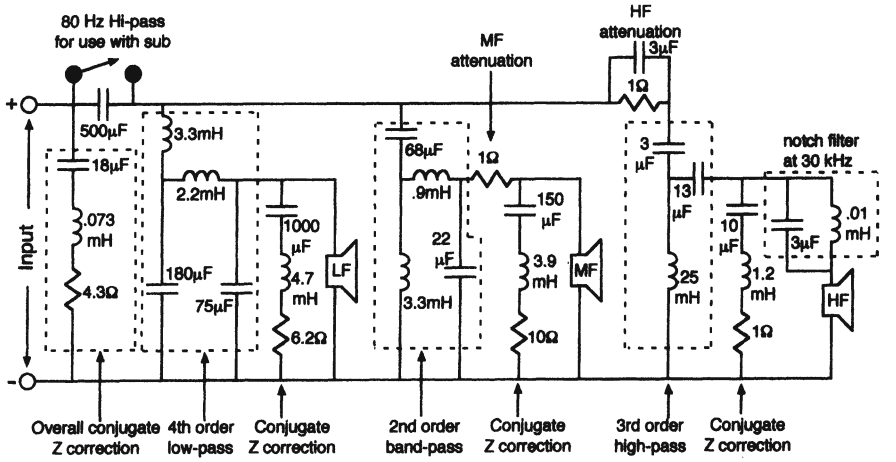

Figure 5-16. Network for upper three system sections. (Data courtesy Allan Devantier and Infinity systems)

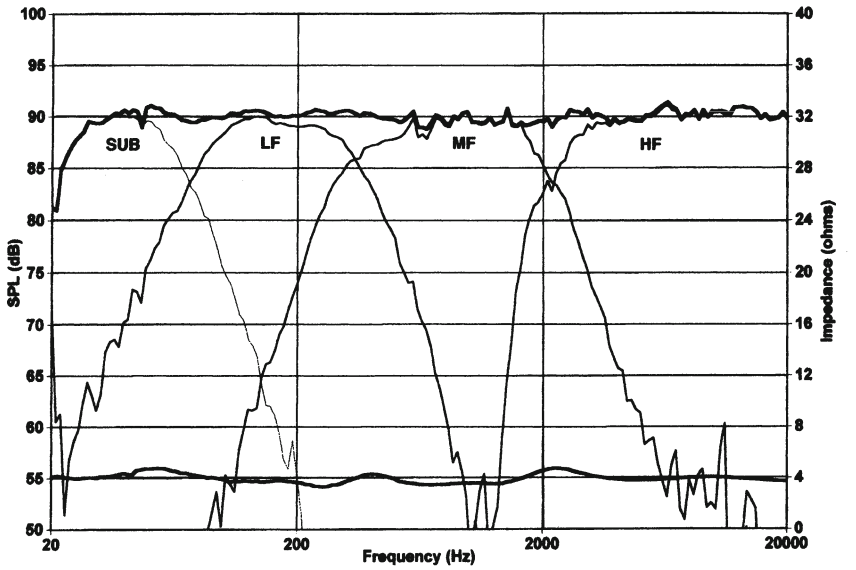

Figure 5-17. System on-axis response and individual contributions. Modulus of impedance is shown at bottom of graph. (Data courtesy Allan Devantier)

5.6 Off-axis lobing effects

While the response of combined HF and LF radiators can be made quite flat on-axis, the response observed off-axis in the plane of the two drivers may exhibit lobing errors – departures from smooth response. The less lobing error a system exhibits, the less critical the listening angle will be; the greater the lobing error, the more restricted the listening angle will be.

In the following examples of lobing error, we are assuming that the HF and LF components are vertically mounted in an enclosure and that the effective distance between them is 40 cm (16 inches). A crossover frequency of 1 kHz is assumed.

The basic system configuration is shown in Figure 5-18A. Lobing response for second-order, normal connection, is shown at *B*, and lobing response for reversed connection is shown at *C*. Both sets of curves are for a signal at 1 kHz.

Figure 5-19A shows the response of the second-order system half an octave above crossover, while the response half an octave below crossover is shown at *B*.

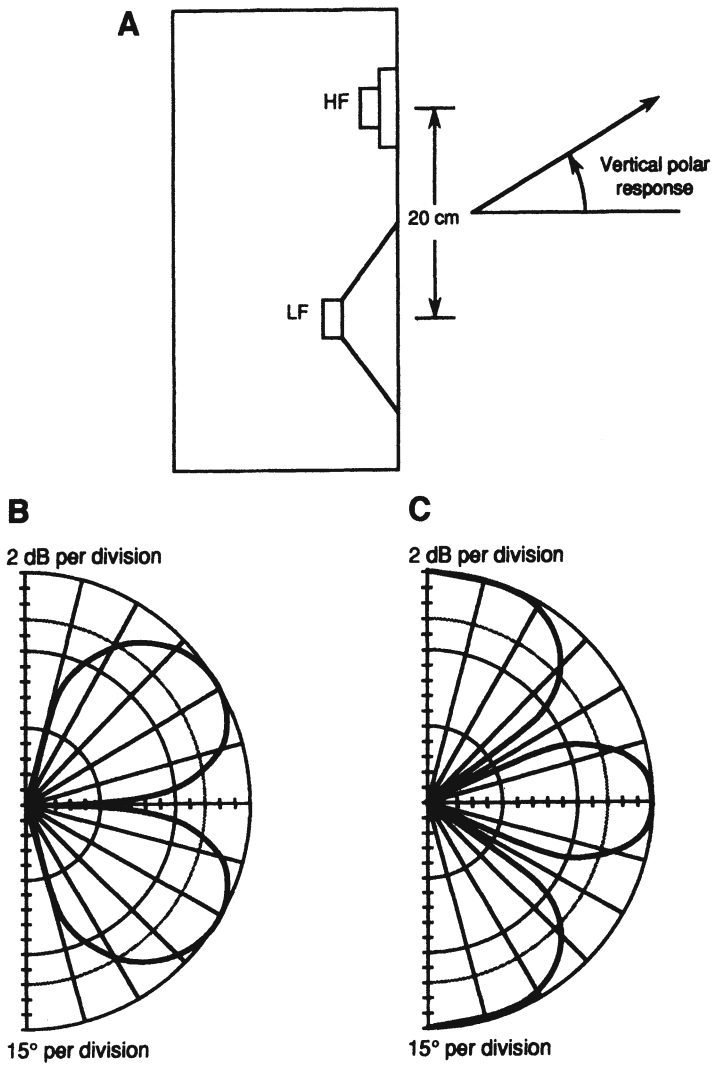

Figure 5-18. Lobing effects. Side section view of test system (A); lobing response, second-order, normal connection (B); lobing response, second-order, reversed connection (C).

Figure 5-20A shows the lobing response of a third-order system with reverse connection; response half an octave above crossover is shown at *B*, and half an octave below crossover is shown at *C*.

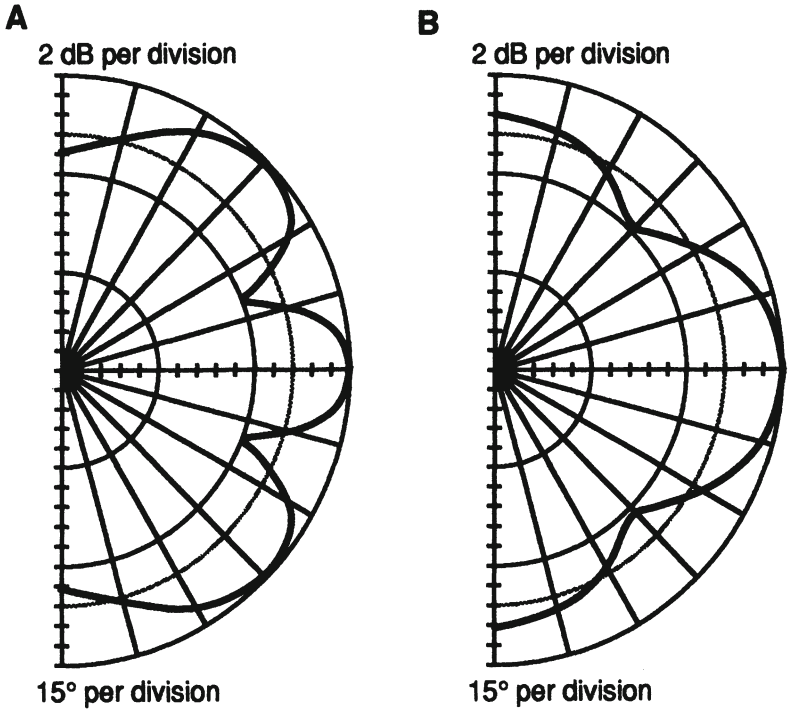

Figure 5-19. Second-order system; half-octave above crossover (A); half-octave below crossover (B).

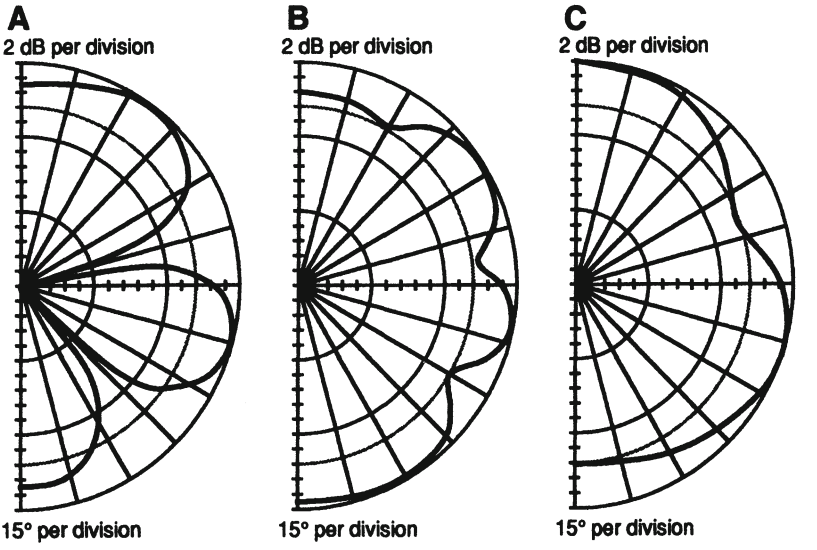

Figure 5-20. Third-order system, reverse connection (A); third-order, half-octave above crossover (B); half-octave below crossover (C).

Figure 5-21A shows lobing response of a fourth-order system on-axis; response half an octave above crossover is shown at *B*, and half an octave below crossover is shown at *C*.

The main observation to be made here is that lobing errors are minimized when the wavelength at the crossover frequency is large relative to the spacing of adjacent HF and LF drivers. A concern for this normally leads loudspeaker engineers to specify very small distances between elements whenever possible. A secondary observation is that great care, and expense, go into a loudspeaker system that preserves uniform polar response in the driver plane in the crossover range.

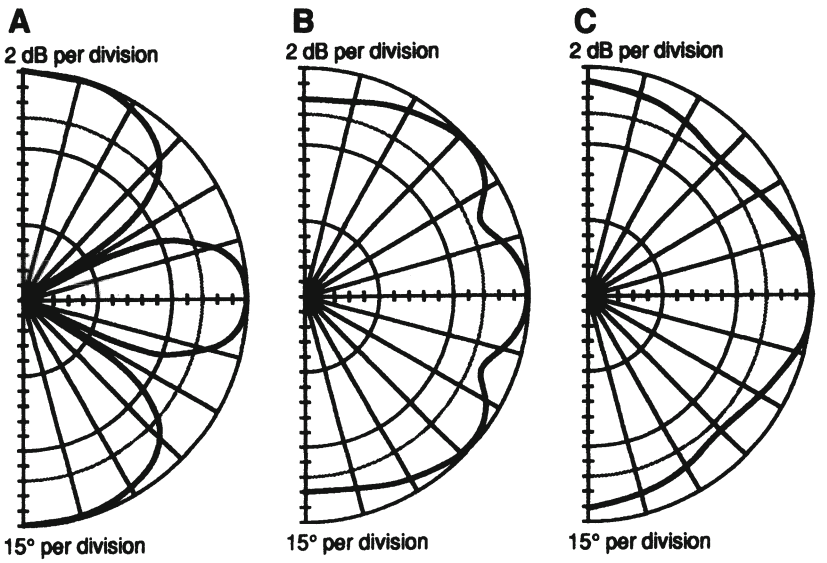

Figure 5-21. Fourth-order, on-axis (A); half-octave above crossover (B); half-octave below crossover (C).

5.7 Baffle component layout and edge details

Figure 5-22 shows a variety of front views of typical baffle layouts. A symmetrical vertical array is shown at *A*. This is typical of most loudspeakers on the market today in that the design does not require separate left and right models. Due to cost constraints, most rectangular enclosures are made with no rounding of their edges, and this aggravates certain boundary conditions.

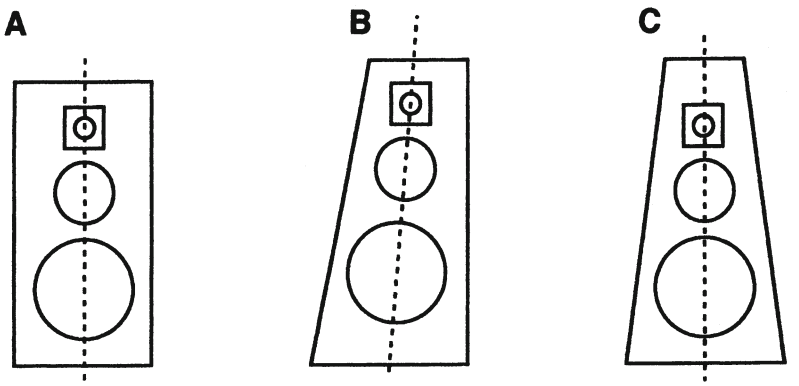

Figure 5-22. Some typical baffle details. Rectangular enclosure (A); trapezoidal enclosure (B); truncated pyramidal enclosure (C).

The design shown at *B* does not have left-right symmetry, and it is necessary for separate left and right models to be offered as a pair.

The design shown at *C* combines these virtues. It has lateral symmetry and also provides a graduated set of boundary details for the mid and HF transducers. The designs shown at *B* and *C* are often made with rounded or tapered edge details, thus providing further "softening" of boundaries for smoother response.

The worst case here is when a transducer is placed on a baffle so that its distances from the nearest boundaries are equal. The acoustical transmission line path from driver to the multiple edges will produce an impedance discontinuity that will reflect back to the driver, producing an irregularity in response. Distributing these distances, as shown in Figure 5-22*B* and *C* will minimize the effect.

Figure 5-23 shows some baffle details. The square detail of the typical rectangular enclosure is shown at *A* in horizontal section view. A strong reflection back to the driver results. Rounding the edge, as shown at *B* minimizes this. Placing damping material at the edge, as shown at *C*, creates a lossy transmission line boundary and also minimizes reflections. Serrated edges are often used adjacent to the driver to maximize this effect.

The slight recessing of a high frequency element, as shown at *D*, is often effective in narrowing the response of the driver in its lower frequency range, and this makes for a smoother transition with the MF driver.

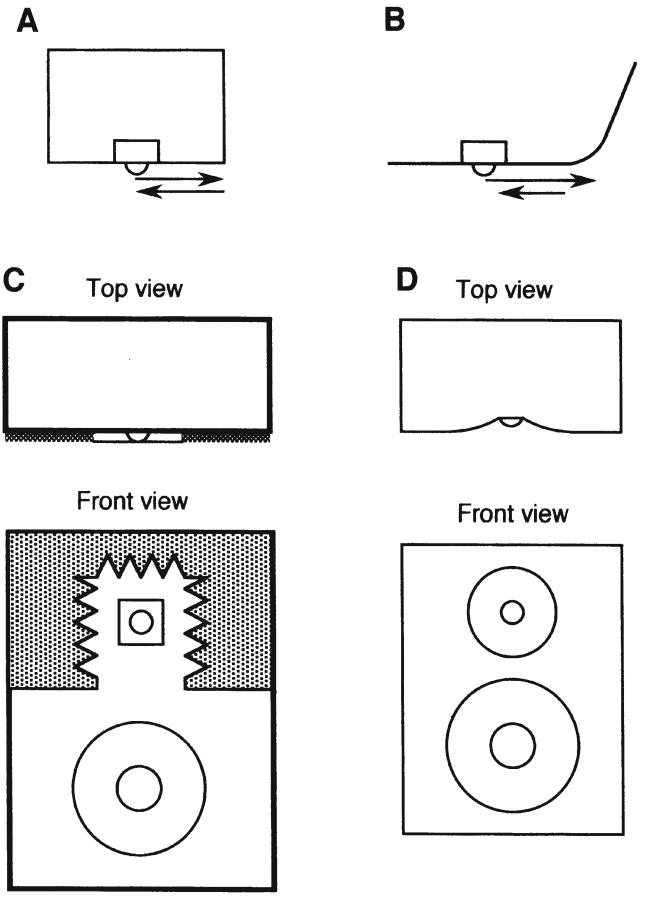

Figure 5-23. Reducing edge reflections. Rectangular, horizontal section view (A); horizontal section view, rounded edge (B); use of damping material as a surface treatment (C); driver mounting in concave recess (D).

The shape of the baffle and enclosure have a profound effect on the response of drivers, as shown in Figure 5-24. In these graphs, a small loudspeaker is mounted as shown in the various baffles. The main observations here are the transitions between the 4π and 2π boundary conditions (showing a 6 dB step from low to high frequencies) and the patterns of peaks and dips produced by the various edge details. The data presented here can be scaled as required from the dimensions given.

It is apparent that the spherical enclosure and the truncated pyramidal enclosure offer the smoothest overall response, and this accounts for their general popularity in contemporary enclosure design.

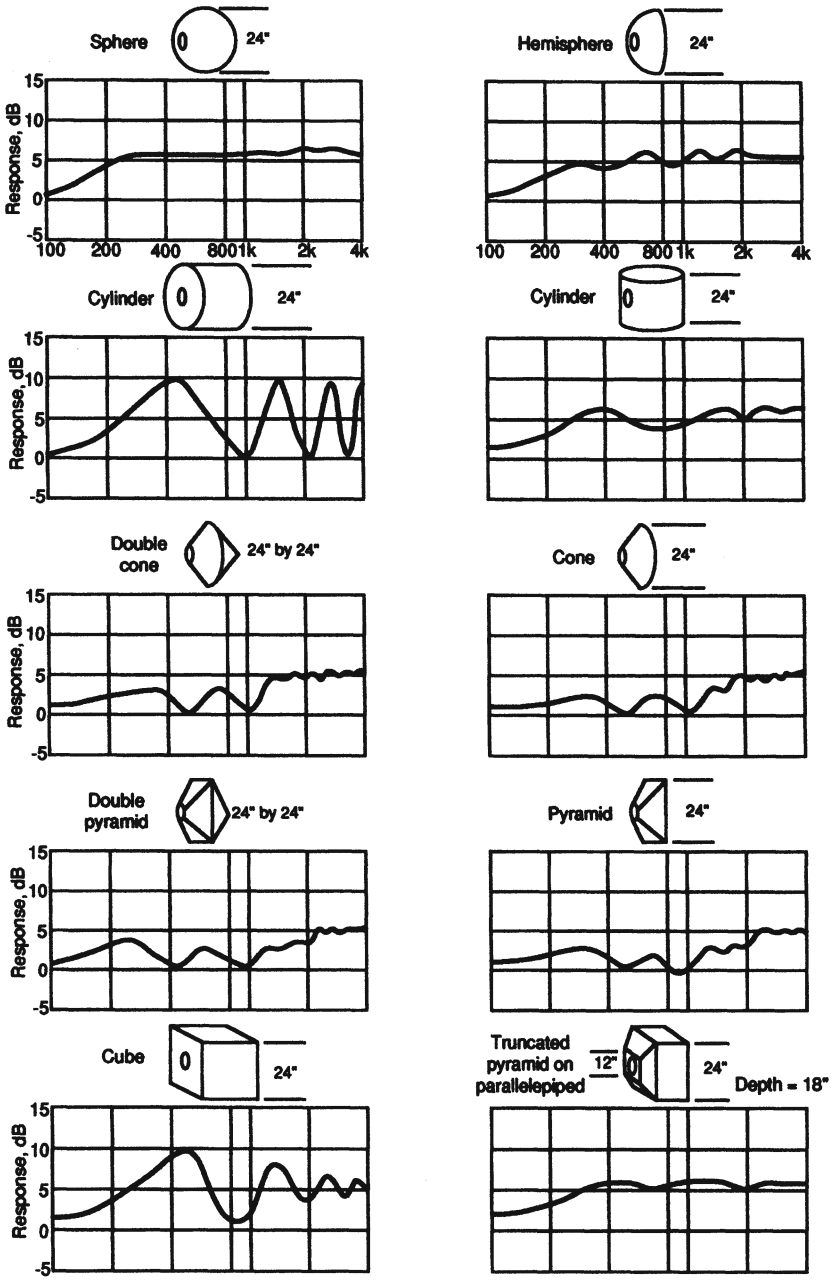

Figure 5-24. Diffraction effects of ten different objects. The response curves are for small drivers located as shown on each object. (Olson, 1957)

Figure 5-25 shows side views of systems consisting of individual enclosures for each transducer (*A*) and stepped baffle details (*B*). Both techniques are useful in determining the precise location for ideal listening. The stepped baffle approach is usually the more economical of the two.

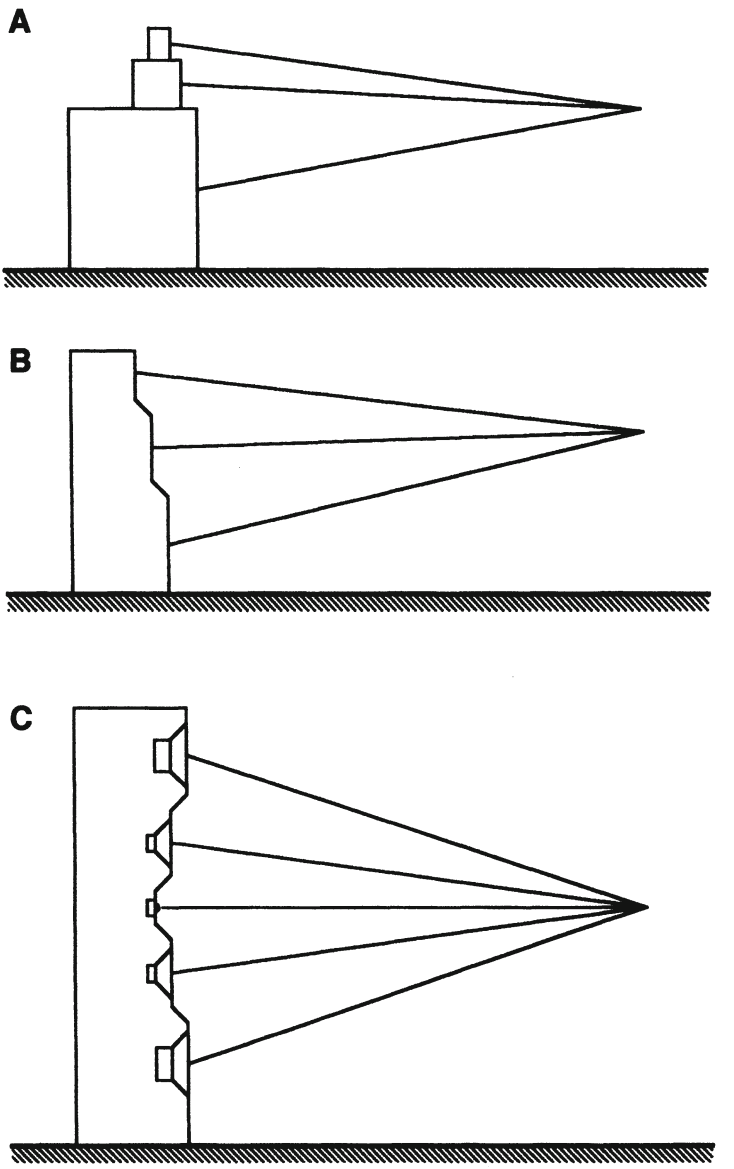

Figure 5-25. Driver displacement, fore and aft. Separate enclosures (A); stepped baffle (B); d'Appolito array (C).

The array shown at *C* is often referred to as the d'Appolito array. The design is quite popular and has an advantage of creating subjective sources for the various band-pass sections that seem to originate from the vertical center point of the array. It is clear that vertical positioning of the listener is quite critical.

5.8 Time domain response of loudspeakers

Because of the variety of dividing networks, their specific time domain response, and above all the fore-aft relation between drivers, the overall time domain performance of a loudspeaker system is apt to be anything but uniform over its bandwidth. The steps necessary to provide ideal response may not be absolutely necessary in terms of general audibility, as suggested by the Blauert and Laws criteria (1978), shown in Figure 5-26. In deriving this data, Blauert and Laws carefully conditioned listening panels to the effects of group delay variations on octave centers over the audio range, and it is generally felt today that the group delay of a loudspeaker system that falls within the envelope will not be audible as such when compared with a system that has no group delay anomalies.

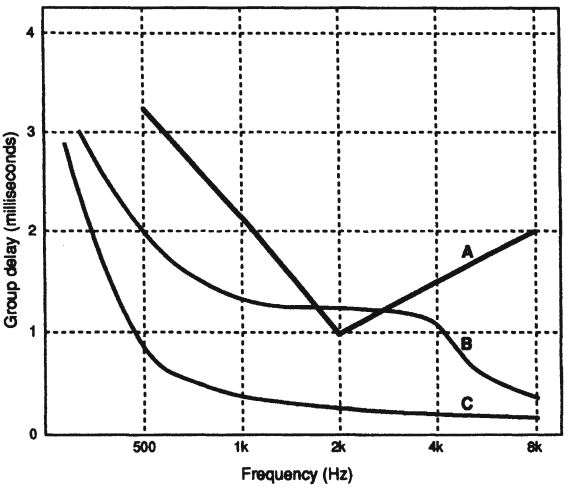

Figure 5-26. Blauert & Laws criteria for audibility of group delay variations in electroacoustic systems.

Loudspeakers with long MF horns are marginal offenders here, unless their response has been delay compensated, usually via digital processing. Older full-range horn systems, with their long LF sections, are also potential offenders unless similar measures have been taken.

5.9 Loudspeaker dispersion and power response

The data shown Figure 5-27 is based on a measurement technique developed by Toole (1986) at the National Research Council in Canada and subsequently at Harman International in Los Angeles. Multiple measurements of the system are made at 5-degree intervals in both horizontal and vertical planes. The data is weighted and presented as a set of response curves versus frequency. The data shown at *A* is for an excellent system, while that shown at *B* is for a marginal design.

Curve 1 is the on-axis response of the system. Curve 2 is the spatially averaged response over a range of ±30° horizontally and ±15° vertically, giving a realistic view of average response over the normal listening solid angle. Curve 3 is proportional to the first reflection sound power in a typical listening room.

Curve 4 is proportional to the total radiated sound power (power response) in a typical room. Curve 5 is the system directivity index, and Curve 6 is the directivity index based on first room reflections.

Consistently, over years of double-blind testing with subjects from virtually all parts of the world, listeners have rated systems with flat on-axis response and uniform power response as superior to those with response anomalies. Given that the audio industry uses electronics and microphones with virtually flat response, it should come as no surprise that loudspeakers designed similarly will sound better than those that are not.

For the neophyte, as well as experienced loudspeaker engineer, we recommend the excellent design analyses of Dickason (1994). The author clearly presents the complex design processes that are involved, even with the simplest 2-way system. The role of the computer is emphasized, both in modeling and in measuring systems. Likewise, Fincham's excellent chapter on multiple driver loudspeakers in Borwick (2001) is recommended for its thoroughness and technical detail.

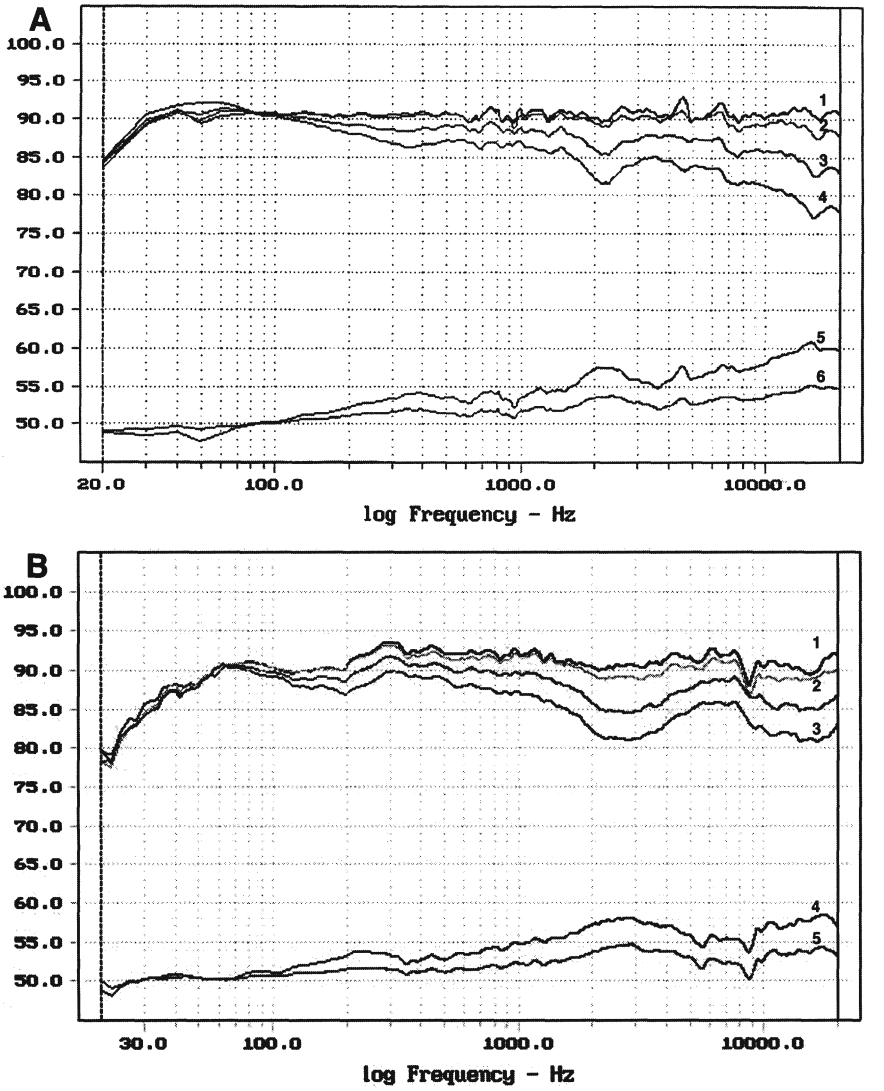

Figure 5-27. Loudspeaker dispersion and power response. An "excellent" system (A); a "good" system (B).

BIBLIOGRAPHY AND REFERENCES:

Ballou, G., ed., *Handbook for Sound Engineers*, H. Sams, Indianapolis (1987).

Beranek, L., *Acoustics*, McGraw-Hill, New York (1954).

Blauert, J. and Laws, P., "Group delay distortion in electroacoustical systems," *Journal, Acoustical Society of America*, volume 63, number 5 (1978).

Borwick, J., *Loudspeaker and Headphone Handbook*, Focal Press, Boston (2001).

Collums, M., *High Performance Loudspeakers*, John Wiley & Sons, New York (1991).

Dickason, V., *Loudspeaker Recipes, Book 1*, Audio Amateur Press, Peterborough, NH (1994).

Jordan, E., *Loudspeakers*, Focal Press, London (1963).

Olson, H., *Acoustical Engineering*, D. Van Nostrand, New York (1957).

Toole, F., "Loudspeaker measurements and their relationship to listener preferences," *Journal, Audio Engineering Society*, volume 34, numbers 4 and 5 (1986).

Various, *Loudspeakers, Volumes 1 through 4.* Anthologies of articles from the Journal of the Audio Engineering Society, New York, (1978, 1984 and 1996).

Chapter 6:
IN-LINE, PLANAR LOUDSPEAKERS, AND ARRAYS

6 Introduction

While the vast majority of loudspeaker systems are designed around cone or dome transducers, in-line and planar loudspeaker arrays have always occupied a special niche in the high-end consumer market. The electrostatic loudspeaker (ESL) has been highly regarded, and in recent decades has made important strides in sensitivity, power handling, and directional control. In much the same vein, its electromagnetic equivalent, with its printed circuit voice coil positioned on a large diaphragm, has gained adherents.

Linear arrays, often made up of a large number of small cones or domes, have been on the fringe of loudspeaker system design for some time, and they have now come of age. Electromagnetic ribbon systems have had a long history but have not enjoyed the popularity of ESL's.

While single cones and domes behave essentially as point sources, exhibiting a 6-dB fall-off in level for each doubling of distance from the driver when measured in a free field, line and plane arrays behave quite differently. At low frequencies (those whose wavelengths are equal to the array length or longer), the fall-off in level of a line array will be approximately as shown in Figure 6-1A.

If we excite such an array and observe its output level as a function of distance, we will note that the level falls off initially at 3 dB per doubling of distance. This will continue up to some distance A/π, where A is the length of the linear array. Beyond this point the falloff in level will begin to approximate that of a point source, with its characteristic 6-dB per doubling of distance.

J. Eargle, *Loudspeaker Handbook*

In a listening environment, a linear array that stretches from floor to ceiling will produce reflected images in both the floor and ceiling planes, effectively extending the array in the vertical plane. In this environment the 3-dB falloff per doubling of distance may be noticed throughout the listening space.

The attenuation with distance from a plane array is shown in Figure 6-1B. Here, there will be no attenuation until the distance A/π has been reached, at which point a 3-dB per doubling of distance falloff is noticed. This will continue until the distance B/π is reached, beyond which point the familiar 6 dB per doubling of distance will be noticed. In this representation, A is the smaller of the two dimensions of the plane.

Remember that these level relationships apply to low frequencies, those whose wavelengths are equal are greater than the array length. At higher frequencies, the situation may be considerably different, as we will discuss later in this chapter.

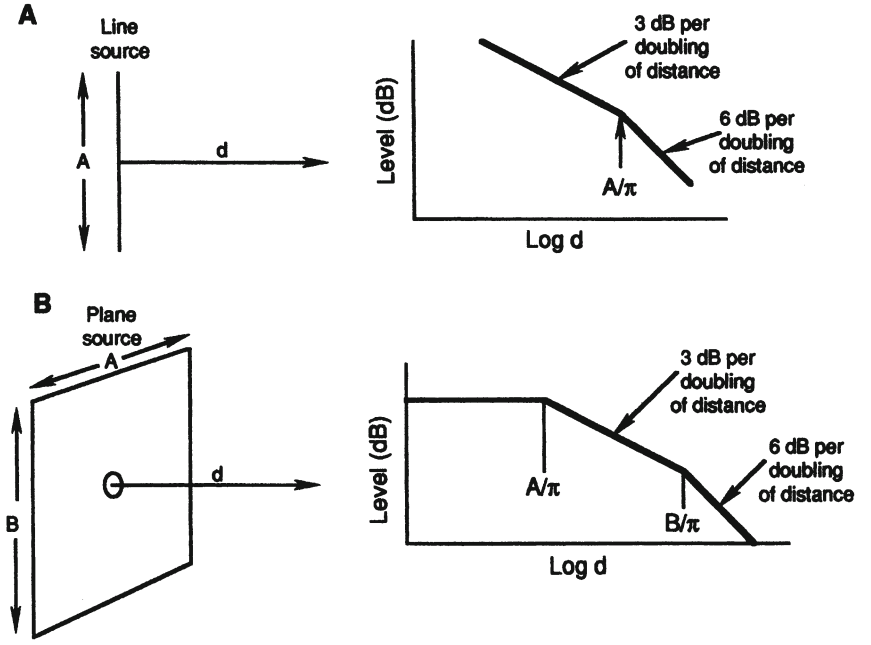

Figure 6-1. Attenuation of sound with distance from a line source (A) and a plane source (B). (Rathe, 1969)

Boundary conditions can alter things considerably. If one wall of a rectangular room is made into a plane loudspeaker array, images in the adjacent planes can create a very large effective plane radiating surface, with little attenuation throughout the listening space. This will create certain problems for stereophonic reproduction, however. In the data shown in Figure 6-1, the transitions between regimes are shown asymptotically; they are actually rather gradual as observed in the real world.

Much of the appeal of ESL's and their magnetic equivalents comes from their unique radiation properties as well as their generally low degrees of distortion at moderate drive levels. We begin our discussion with an analysis of the constant charge ESL design.

6.1 Analysis of the constant charge ESL

The analysis given here is based on the detailed descriptions given by Baxandall (1988) and Jordan (1963). Readers who wish to learn more about ESL's are encouraged to study these references.

The basic form of the push-pull ESL is as shown in section view in Figure 6-2A. A high dc polarizing voltage is applied to an inner, movable diaphragm, while ground potential is applied to the two outer fixed, perforated electrodes. Under quiescent (no signal) conditions, the inner diaphragm is suspended equidistant from the two electrodes. If a signal is impressed on the primary of the transformer so that the positive half of the signal appears on the left electrode, the condition shown at *B* will exist. Since like charges repel, the diaphragm will move to the right, as shown, until balanced by the mechanical restoring force of the diaphragm. Typical values of polarizing electrical fields may be in the range of 20 to 30 kV/cm; thus, for a typical model the actual polarizing voltage may be of the order of 2000 or 3000 volts.

The governing equation here is:

$$Q = CE = \text{Constant} \qquad 6.1$$

where Q is the total charge between the diaphragm and electrodes, C is the total capacitance in the system, and E is the applied voltage. Because of the high value of resistance in series with the diaphragm, the total charge on the plates will not change under normal signal conditions, once the

polarizing charging process has reached equilibrium. Therefore, C and E will both vary in inverse relationship in order for their product to be constant.

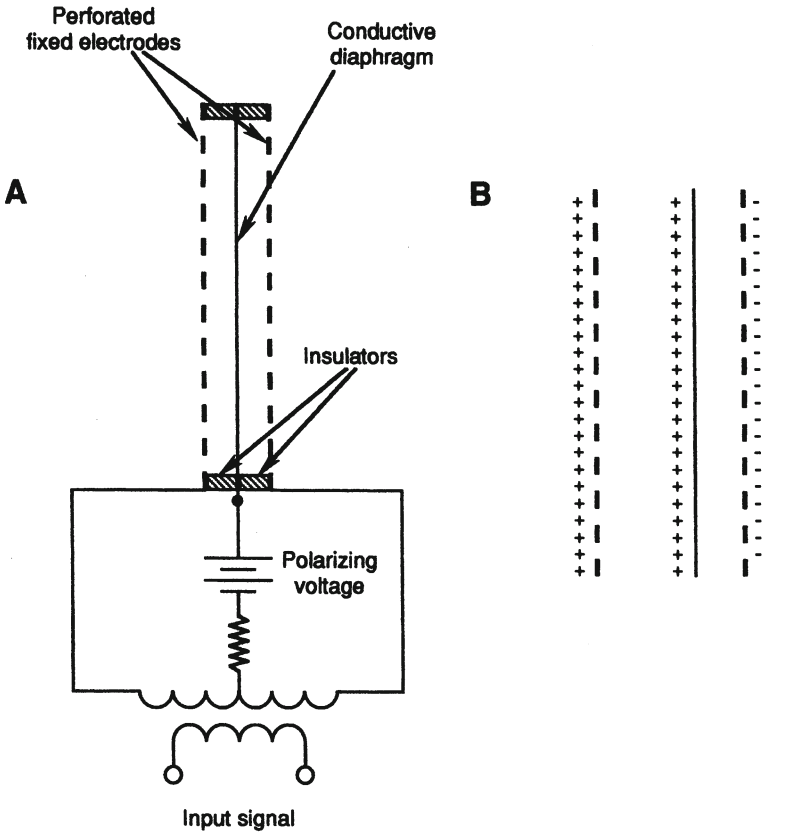

Figure 6-2. The push-pull electrostatic loudspeaker. Section view (A); movement of diaphragm for a positive-going signal on the left electrode.

Under these conditions:

$$Q = SE/4\pi d^2 \qquad 6.2$$

where S is the total area of the diaphragm on both sides (cm^2),
E is the polarizing voltage, and d is the distance from the diaphragm to one electrode (cm).

In the presence of a signal, e_{SIG}, the total force, F, generated then becomes:

$$F = (e_{SIG}ES/8\pi d^2)(1.11 \times 10^{-5}) \text{ dynes} \qquad 6.3$$

where E and e_{SIG} are in volts, d is in cm, and S is in cm^2. Force is thus directly proportional to the applied signal voltage. A perspective section view of a typical ESL panel is shown in Figure 6-3.

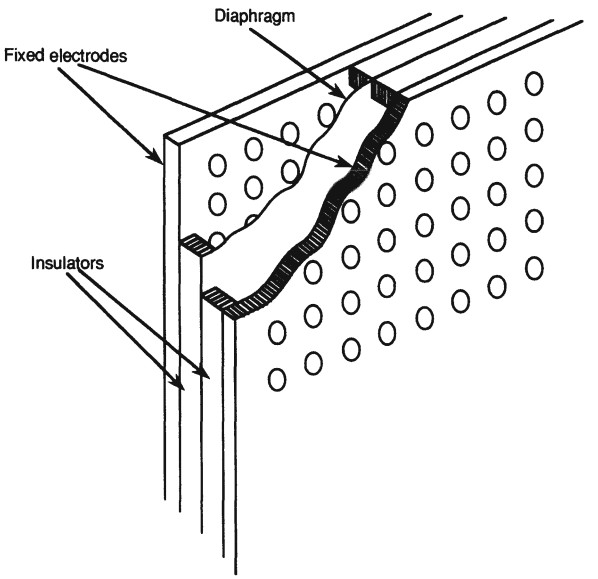

Figure 6-3. Perspective cut-away view of a push-pull electrostatic panel.

6.1.1 Frequency response and directivity

The upper frequency limit of an ESL is generally determined by the high current drawn from the amplifier. Since the loudspeaker load is very largely a capacitive reactance, the current demands and phase angle of the load can be excessive at high frequencies.

Low frequency displacement limits are generally set by the excursion capability of the diaphragm relative to the fixed electrodes. In terms of acoustical output, the natural LF rolloff of the dipole nature of the system will dominate at the lower frequencies. The larger the radiating area, the lower the useful frequency limit of the system will be.

A single large radiating surface will of course have very irregular HF directional control, as we have seen in polar data for pistons presented in Chapter 1. It is customary to construct the ESL as a 2- or 3-way system, with

the highest frequencies being radiated by a single, relatively narrow vertical strip placed between larger ones for the middle and lower frequencies. In this way, smooth horizontal polar response, with relative freedom from lobing, can be maintained over the normal horizontal listening angle.

A common misconception about ESL's is that their moving mass is extremely small; and therefore that their transient behavior can be exemplary. The fact of the matter is that there is an air layer directly associated with the diaphragm, as discussed in Chapter 1. Jordan (1963) estimates the per-unit area air mass to be about five times greater than the actual per-unit area mass of the diaphragm itself. There may also be a misconception that the diaphragm vibrates essentially with a single degree of freedom – that is, as a unit. The acousto-mechanical impedance of the diaphragm varies over its area, ranging from being clamped at the edges and relatively free to move in the middle. Portions of the diaphragm near the edges may be stiffness controlled at high frequencies, while other portions of the diaphragm may not.

There are a number of breakup modes that a rectangular diaphragm can execute, but these are normally damped by viscous air losses through the perforations in the fixed electrodes.

As with the cone driver, the ESL's frequency response depends entirely on its complex radiation impedance and its variation with frequency. Figure 6-4 shows the relative variation in velocity and power radiation per unit area for an ideal unbaffled piston, approximating the acoustical radiation of an ESL. Surface area is all-important with an ESL just as it is for a dynamic driver, and a doubling of radiating area will increase the radiated power by a factor of 4, or 6 dB, for a given frequency and excursion. The increase will be due to both mutual coupling and a doubling of volume velocity.

6.1.2 Maximum level capabilities

In addition to the matter of diaphragm displacement limits, there are electrical limits in level capability of an ESL due to dielectric breakdown between diaphragm and the fixed electrodes. In normal design, it is desirable that the polarizing voltage, plus the maximum intended signal voltage, be slightly less than the break-down voltage of air itself, so that some degree of safety margin can be held. All insulating materials, plus the coatings on the fixed electrodes should have dielectric constants appropriately high for this application.

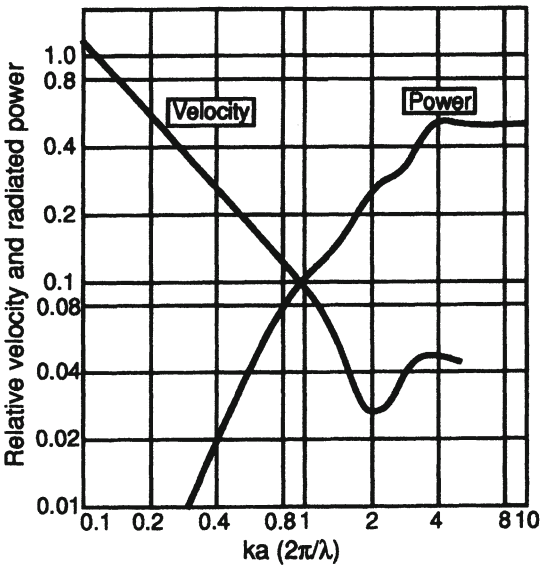

Figure 6-4. Relative values of velocity and radiated power for an unbaffled piston.

The maximum force per unit area that can be generated is:

$$F = (u^2/16\pi)(1.11 \times 10^{-5}) \text{ dynes/cm}^2 \qquad 6.4$$

where u is the maximum electrical field strength (volts/cm) before the onset of air ionization.

In terms of acoustical pressure output, Walker presents the following equation (see Baxandall, 1988):

$$P = i_{SIG} \times E/2\pi crd \qquad 6.5$$

where i_{SIG} is the input signal (amperes), E is the polarizing voltage, c is the velocity of sound (m/sec), r is the measuring distance (m), and d is the diaphragm-electrode spacing (m). P is given in pascals (N/m^2), and the measurement is assumed to be made in the far field.

6.1.3 Details of construction

In addition to the traditional flat form shown in Figure 6-3, other configurations for ESL's use curved or splayed panels for better control of dispersion. Figure 6-5A shows details of the early Janszen ESL array, which played an important role during the 1960s. Here, individual panels, approximately 6 inches on a side, were combined in the form required to achieve a desired radiation pattern.

The British Quad ESL has been noted for decades, and the current form, the Quad ESL-63 is shown in Figure 6-5B. This medium size floor standing system uses a set of six concentric, sequentially firing, radiating rings in order to achieve effective hemispherical radiation.

6.2 Electromagnetic planar loudspeakers

One of the earliest commercial electromagnetic line radiators was the Kelly ribbon tweeter, made in England. The design was essentially the same as a ribbon microphone scaled upward in size, and its performance was enhanced through the use of a small horn.

Planar loudspeakers extend this principle by making use of printed voice coil circuits on a sheet of tensioned light plastic, with appropriate layout of ferrite bar magnets arranged in a frame adjacent to the plastic sheet. Openings in the magnet frame provide sufficient egress of sound. Many topologies have been used, and the arrangement shown in Figure 6-6 is typical. The magnets used in these systems are similar in size and shape to the small magnets that are used in just about every home to affix a note or list to the refrigerator door. The field set up by these magnets consists primarily of fringe flux; that is, there is normally no attempt to concentrate the flux density in the area of the conductors through iron magnetic return paths.

Such systems as these can be made in individual sections for HF, MF, and LF coverage in order to achieve good horizontal dispersion. They operate as dipoles at very low frequencies, and in this connection the relatively high resonant Q (low damping) of these systems at LF helps maintain fairly flat response down to the 40 or 50 Hz range. The large expanse of the printed coil may result in a nominal dc resistance in the range of 5 or 6 ohms; thus, there is no need for an additional transformer to match the system with an amplifier. Some units employ a degree of horn loading on one side for increased efficiency.

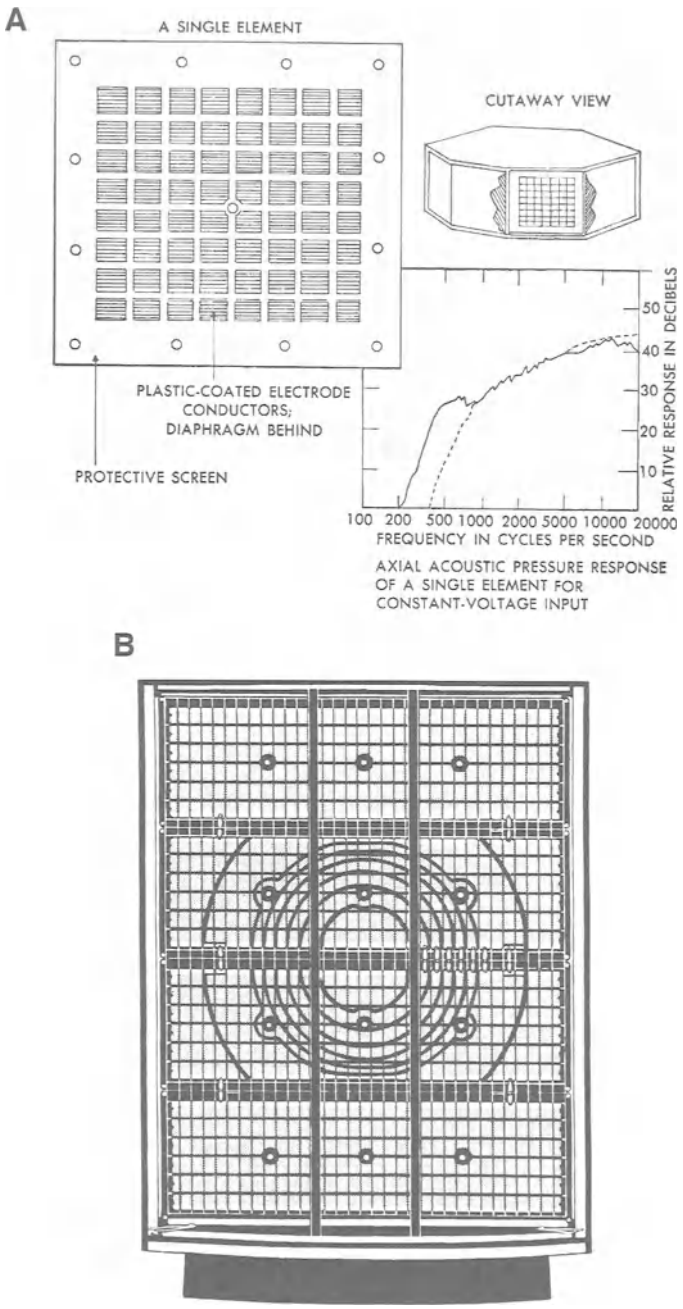

Figure 6-5. Commercial ESL systems. Details of the Janszen panel (A); view of the Quad ESL-63 system (B). (Data at *A* from *The Sound of High Fidelity*, Jordan & Cunningham; data at *B* reproduced with the kind permission of Quad Electroacoustics Ltd.)

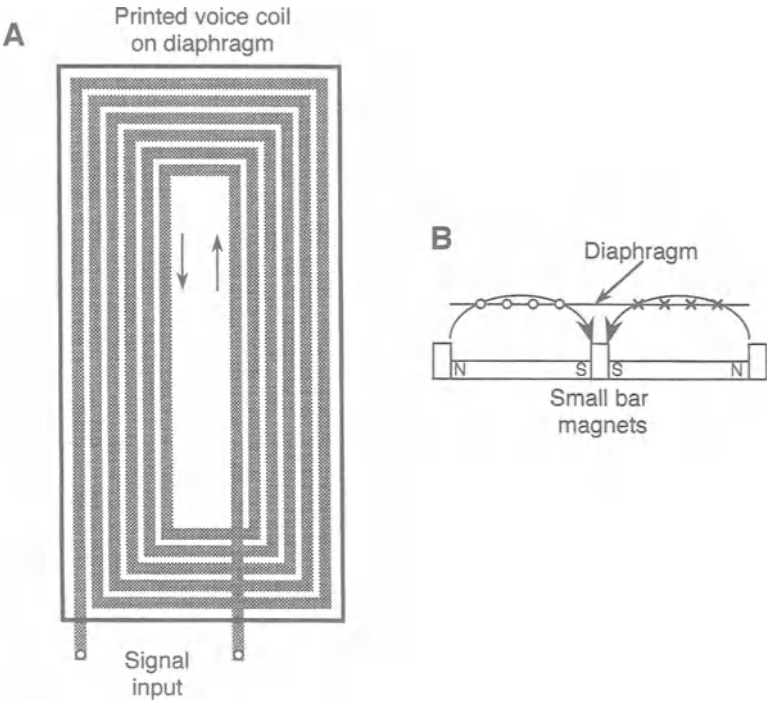

Figure 6-6. Details of a magnetic planar driver. Printed circuit voice coil (A); top view of voice coil and diaphragm relative to magnet structure (B).

Figure 6-7 shows details of a typical commercial loudspeaker based on these principles. The Magnepan model MG20.1 is shown at *A*, and driver details are shown in the cutaway sketches shown at *B* and *C*. The version shown at *B* consists of a large section of 0.0005 in (20 micron) thick Mylar plastic with a thin conductor printed on it in an alternating pattern. The magnets alternate as shown, providing a uniform force on the diaphragm. This configuration is used at MF and LF. The version shown at C consists of a single ribbon of plastic with a printed conductor. The single ribbon is used at HF.

Another approach to a consumer line array system is shown in Figure 6-8. The Infinity Reference Standard was a breakthrough system in its day and used printed conductor drivers for both MF and HF reproduction.

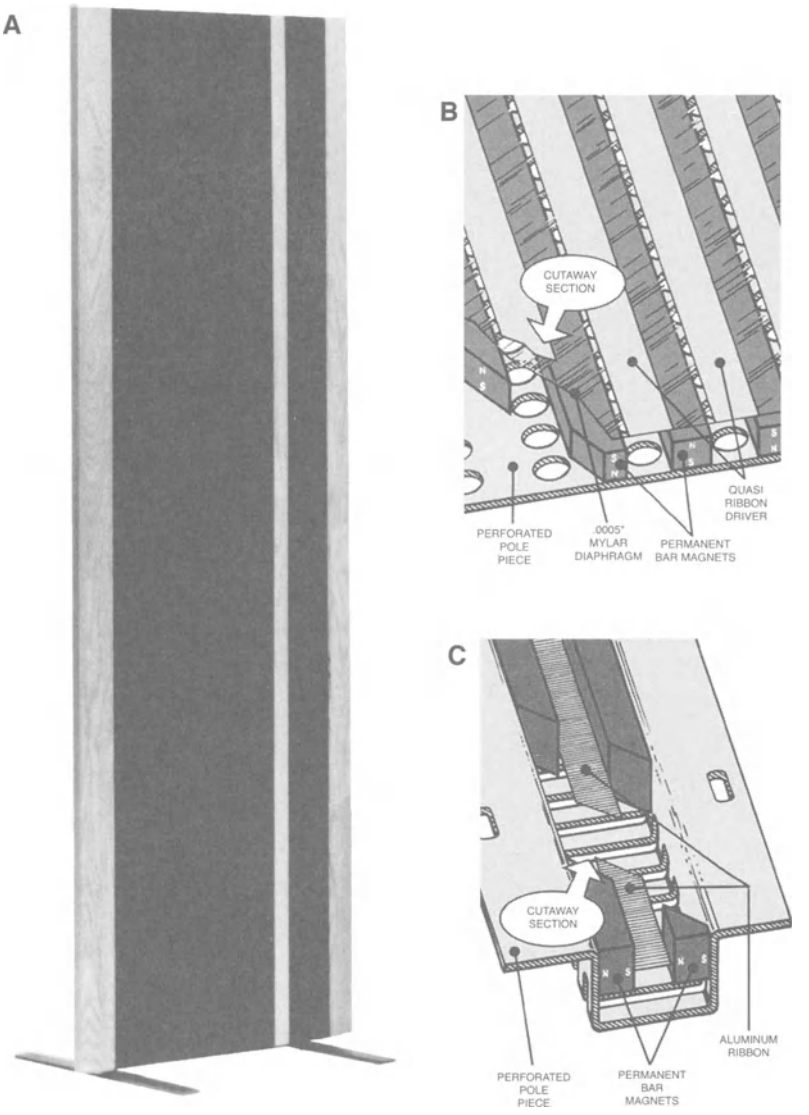

Figure 6-7. Details of the Magnepan MG20.1. Photo of system (A); detail of basic driving mechanism (B); detail of HF ribbon mechanism (C). (Data courtesy Magnepan Incorporated)

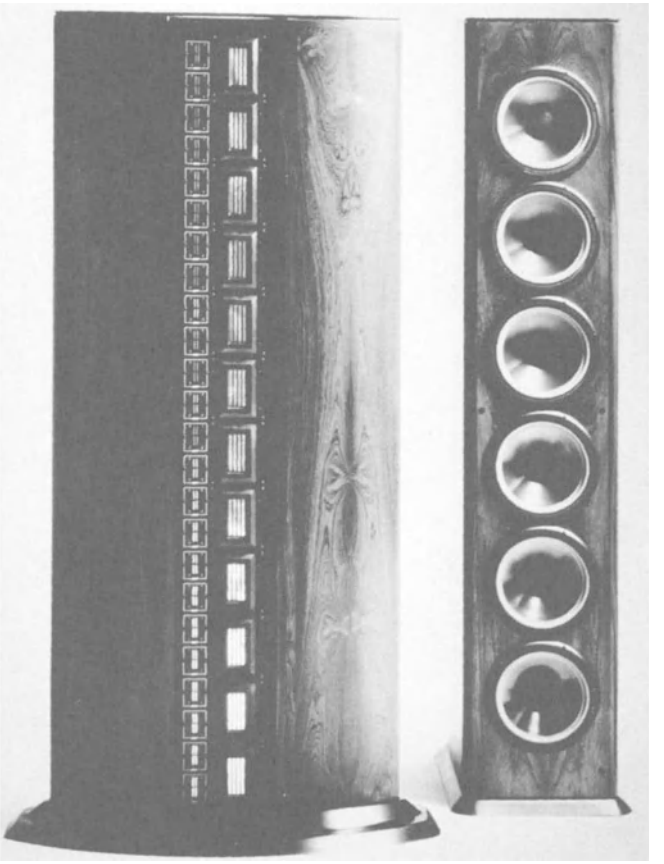

Figure 6-8. Photo of the Infinity Reference Standard system. (Data courtesy Infinity Systems)

6.3 Discrete line arrays

Most traditional line array systems are composed of a number of small cone drivers, making it possible to drive them at different levels and with different frequency response shaping. There is nothing simple about a "simple line array," as we will now observe. Figure 6-9 shows a perspective view of a vertical column composed of small cone drivers. With the dimensions given, the vertical polar response of this array is shown in Figure 6-10A through *D* for frequencies of 200, 350, 500, and 1000 Hz. For frequencies above 1 kHz, the vertical polar response becomes very sharp on-axis, with the development of many side lobes.

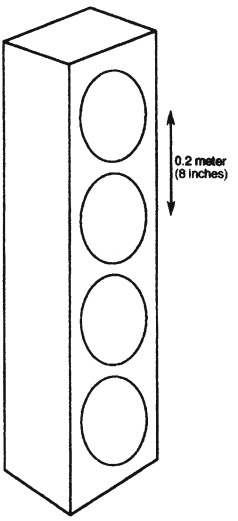

Figure 6-9. Perspective view of a 4-element column.

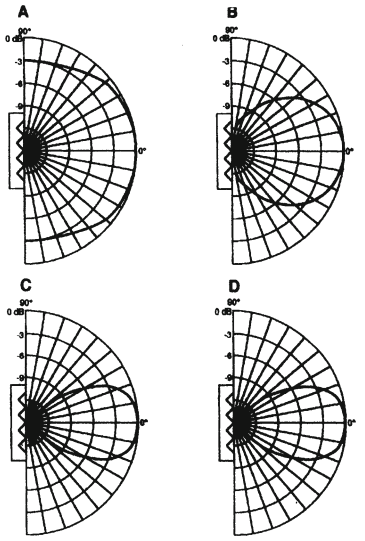

Figure 6-10. Polar response of 4-element column. 200 Hz (A); 350 Hz (B); 500 Hz (C); and 1 kHz (D).

The response for a general line array is given by:

$$R(\phi) = \sin [1/2\ Nkd \sin \phi]/[N \sin (1/2\ kd \sin \phi] \qquad 6.6$$

where N is the number of elements in the array, k is equal to $2\pi f/c$, d is the spacing of the elements in the array, and ϕ is the measurement angle in the plane of the array, relative to the normal to the array. The value c is the speed

of sound. All linear measurements are in meters, and the quantities in brackets are evaluated in radians.

Figure 6-11 shows the directivity factor for columns composed of more than four elements. Note that for driver separation/wavelength ratios greater than about unity, the on-axis directivity of the array drops as more of the acoustical power is radiated in side lobes.

The chief application of vertical arrays, or "sound columns," is in relatively low-cost speech reinforcement, but for these systems to be useful above the d/λ frequency limit, there must be some kind of frequency shaping, or "tapering," in order to allow the column to become effectively smaller at higher frequencies. Figure 6-12 shows some of the ways this has been done.

The arrangement shown at *A* may be thought of as a column within a column. The inner, HF, section is appropriately shorter than the LF section, and this will provide good coverage at high frequencies.

The arrangement shown at *B* uses identical drivers, but attains the necessary tapering of frequency response through variable HF damping via wedges of fiberglass (Klepper and Steele, 1963).

The "barber pole" arrangement shown at *C* takes advantage of the gradual off-axis fall-off of high frequencies in single cone drivers. Observing the column along a fixed horizontal axis, it can be seen that only the few elements in the center will be effective at high frequencies, while at middle and lower frequencies progressively more of the drivers will be effective.

6.3.1 Bessel arrays

Based on the work of Franssen at Philips, Kitzen (1983) discusses a family of loudspeaker arrays in which the far-field directional response of an entire line array is very nearly equal to the directional response of a *single driver* in the array. If the Bessel array consists of omnidirectional drivers, then the overall directivity in the far field will be omnidirectional. Alternatively, if the array element has some desirable directional characteristic, then the array will have basically that same directivity, with the added benefit of increased power handling.

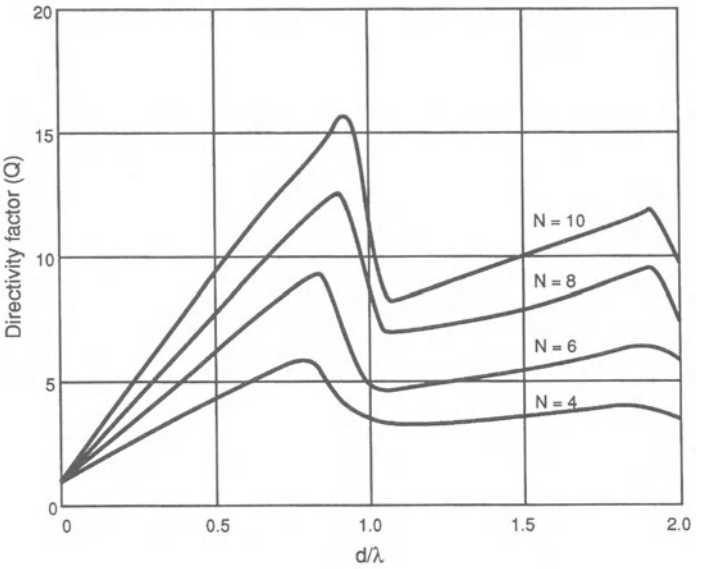

Figure 6-11. Directivity factor plots for simple columns of 4, 6, 8, and 10 elements.

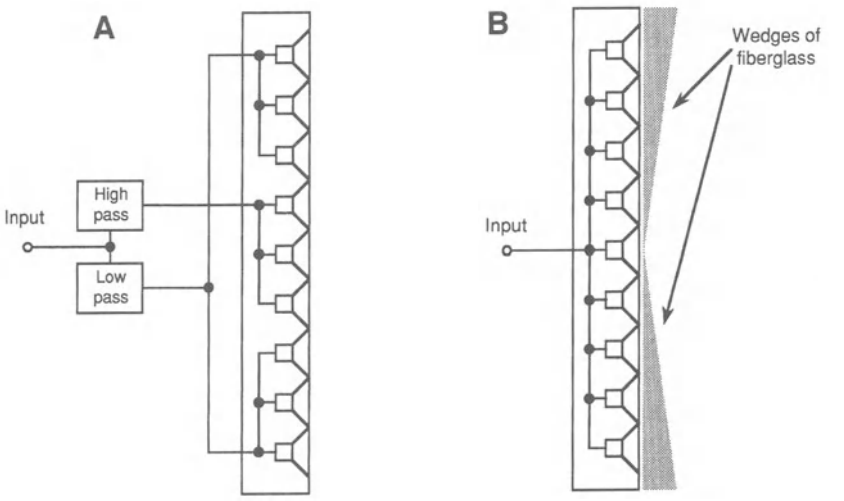

Figure 6-12. Tapered line arrays. Tapering via electrical frequency response (A); tapering via acoustical frequency response (B); tapering via positional relationships (C).

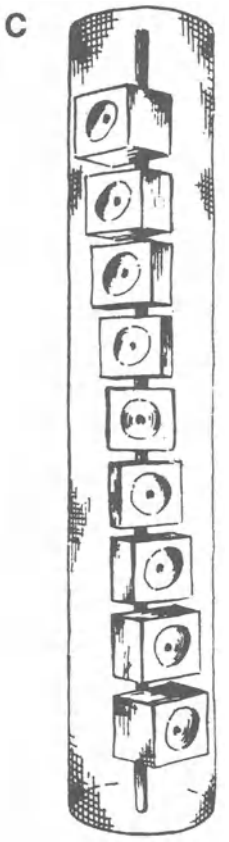

Figure 6-12. Continued.

The drive coefficients for the elements of the array, and the spacing between drivers, are determined by Bessel coefficients through a design procedure involving complex algebra. We will present here only two such realizations, leaving it to the interested reader to study the Kitzen reference, which is available as a Philips reprint. In the specific cases shown here, the necessary coefficients can be derived directly from series-parallel hookup of the drivers in the appropriate polarity. Two arrays are shown, one with 5 drivers (Figure 6-13) and the other with 7 drivers (Figure 6-14). The primary application of Bessel arrays is in speech reinforcement systems.

Keele (1990) has analyzed Bessel arrays in considerable detail. In order to show the performance advantages of the 5-element Bessel array, Keele presents synthesized polar data on both a 5- element standard parallel (non-

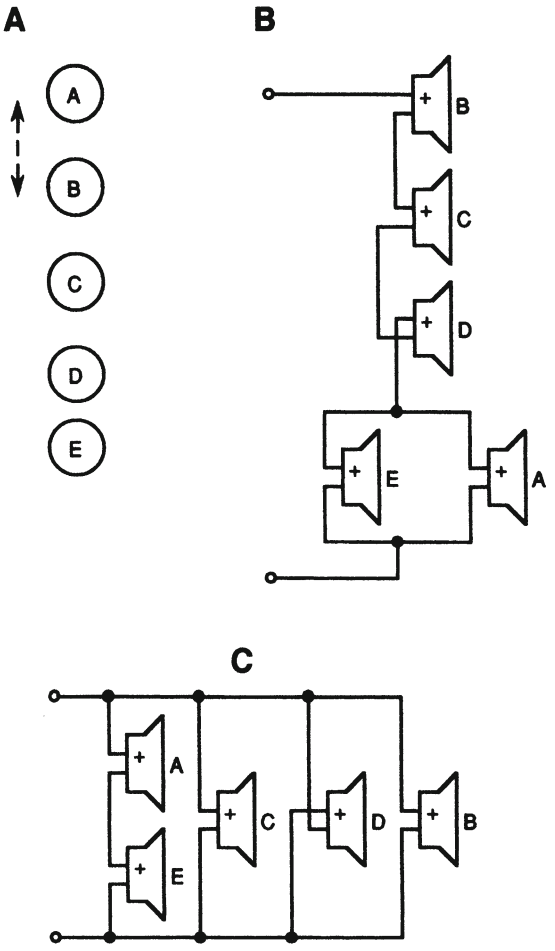

Figure 6-13. Details of a 5-element Bessel array. Array layout (A); possible wiring diagrams (B and C).

Bessel) array (Figure 6-15) and the corresponding Bessel array (Figure 6-16). Note the considerably extended frequency range over which the Bessel array provides reasonable omnidirectional response. (In these representations, the length of the array is equal to 1 wavelength at 1 Hertz, so that the data can be conveniently rescaled.)

Keele's analyses further show that the 5-element array is the best overall performer in the Bessel family. The price paid for the uniform polar response of the Bessel arrays is the diminished output power capability, as compared with the standard array. In particular, the 5-element Bessel is only 16% as

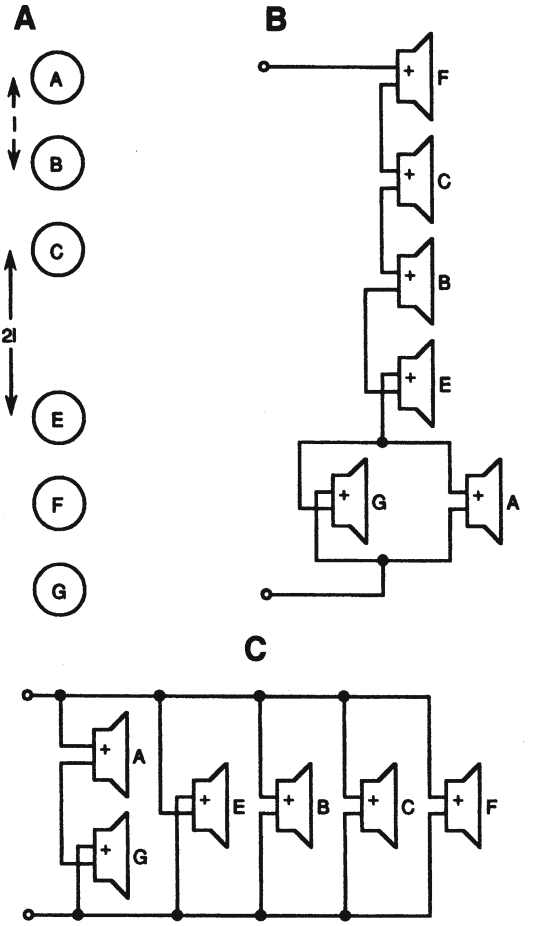

Figure 6-14. Details of a 7-element Bessel array. Array layout; since the driving coefficient for the center loudspeaker is zero, it can be omitted, but normal space for it must be allowed (A); possible wiring diagrams (B and C).

efficient as the standard array. However, the bandwidth-efficiency product of the 5-element Bessel array is excellent, exceeding that of the standard array by slightly more than a factor of 6.

For a 5-element Bessel array 1 meter in length, rescaling of the operating frequency indicates that excellent response can be maintained well out to 9 kHz.

Keele states that the only significant anomalies in Bessel response are its non-minimum phase performance, both as a function of frequency and

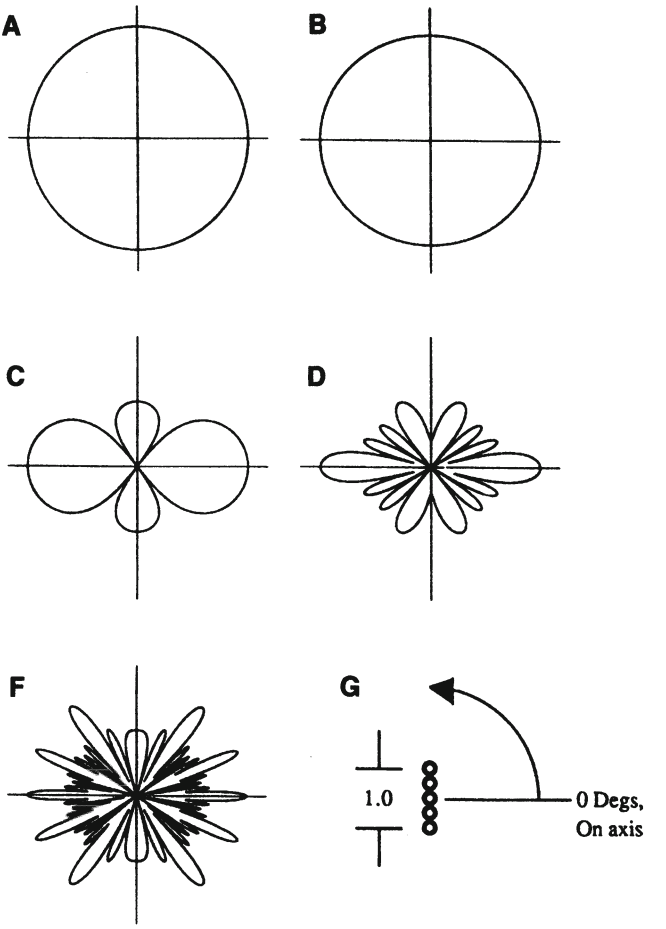

Figure 6-15. Polar response of a standard (non-Bessel) array (equal level, polarity, and spacing) when array length is one wavelength at 1 kHz. 0.1 Hz (A); 0.316 Hz (B); 1 Hz (C); 3.16 Hz (D); 10 Hz (E). Measurements simulated at a distance of 20 times array length; all polars are normaliz ed so that on-axis value is unity. (Data courtesy J. Audio Engineering Society and D. B. Keele)

measurement angle. These factors would severely limit the degree with which Bessel arrays could be combined with standard arrays.

6.4 Large-scale arrays for sound reinforcement

Figure 6-17 shows an array designed for speech reinforcement in large spaces. This is typical of what might have been designed in the 1960s. It is expensive,

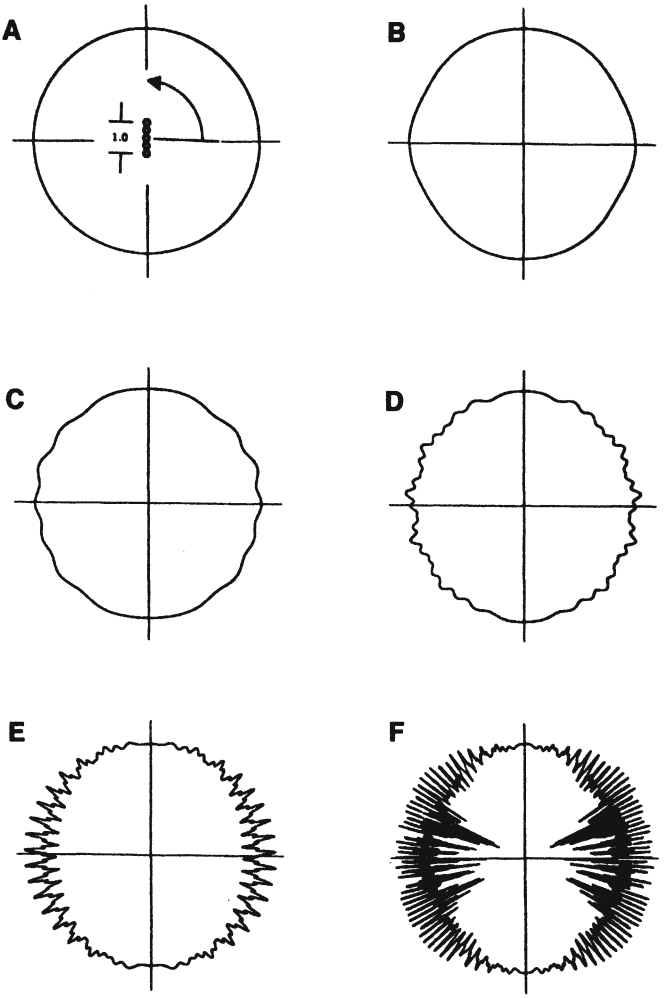

Figure 6-16. Polar response of a 5-element array (equal level, polarity, and spacing) when array length is 1 wavelength at 1 kHz. 0.316 Hz (A); 1 Hz (B); 3.16 Hz (C); 10 Hz (D); 31.6 Hz (E); 100 Hz (F). Measurements simulated at a distance of 20 times array length; all polars are normalized so that on-axis value is unity. (Data courtesy *J. Audio Engineering Society* and D. B. Keele)

occupies much space, and by today's standards is limited in power bandwidth at low and high frequencies. It met the requirements of its day, using transducers developed originally for motion picture work.

During the 1990s, "continuous" line arrays were introduced. These arrays use LF, MF, and HF elements incorporated in arrayable enclosures in such a

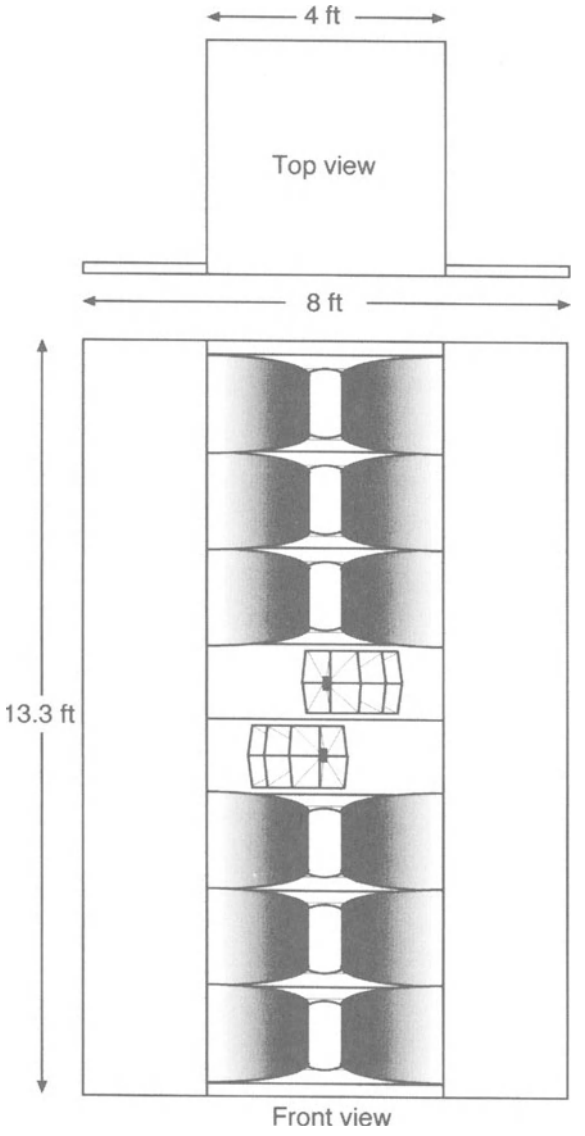

Figure 6-17. Early large 2-way array for speech and music reinforcement in large spaces.

manner that, over each portion of the frequency range, radiation takes place essentially from a contiguous line of drivers. Figure 6-18A shows a photo of a vertical array of 12 such elements, and views of a single array element are shown at *B*.

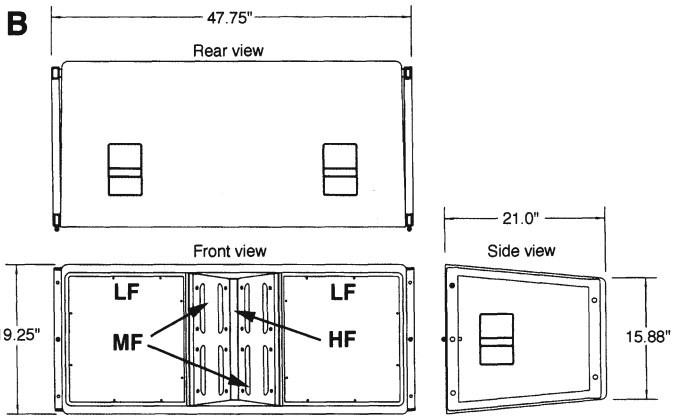

Figure 6-18. Modern 3-way line array. Photo (A); views of single element (B). (Data courtesy JBL)

If such arrays are straight, and if the drive signal is equal in all elements, then the response as a function of distance will be as shown in Figure 6-19A. You will note that the distance, *r*, at which the attenuation makes the transition from 3-dB to 6-dB per doubling of distance is given by:

$$r = l^2 f/690 \text{ meters} \qquad 6.7$$

where *r* is the distance in meters, *l* is the length of the array in meters, and *f* is the frequency.

The polar response, θ, in the far-field is shown in Figure 6-19B and is given by:

$$\theta_{\text{line array}} = 2 \sin^{-1}(0.6\lambda/l) \qquad 6.8$$

where λ is the radiated wavelength and *l* is the length of the array, both in meters.

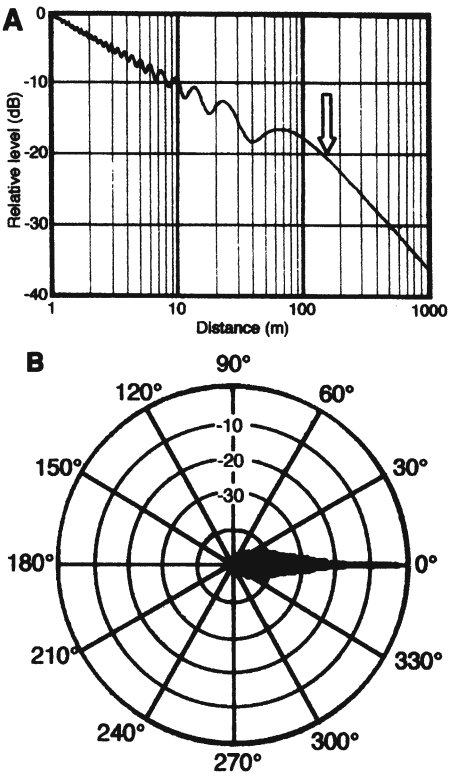

Figure 6-19. Response of a straight continuous line array. Level versus distance (A); far-field polar response (B).

Arrays such as these are normally curved or articulated in order to provide more uniform response over a wider vertical angle for both distant and close-in listeners. One of the most useful arraying methods is the *spiral array*, in which the incremental angle relationship between adjacent sections follows an arithmetic series (Ureda 2001). A side view of a spiral array is shown in Figure 6-20A. The directional response of this array is given by:

$$R_{spiral}(\alpha) = \frac{1}{m+1}\left|\sum_{s=0}^{m} e^{-jkr_s(s,\alpha)}\right| \qquad 6.9$$

where α is the vertical angle of the array and s is an index along the spiral indicating the incremental distance. The directivity response is remarkably uniform with frequency over about a decade, as shown in Figure 6-20B.

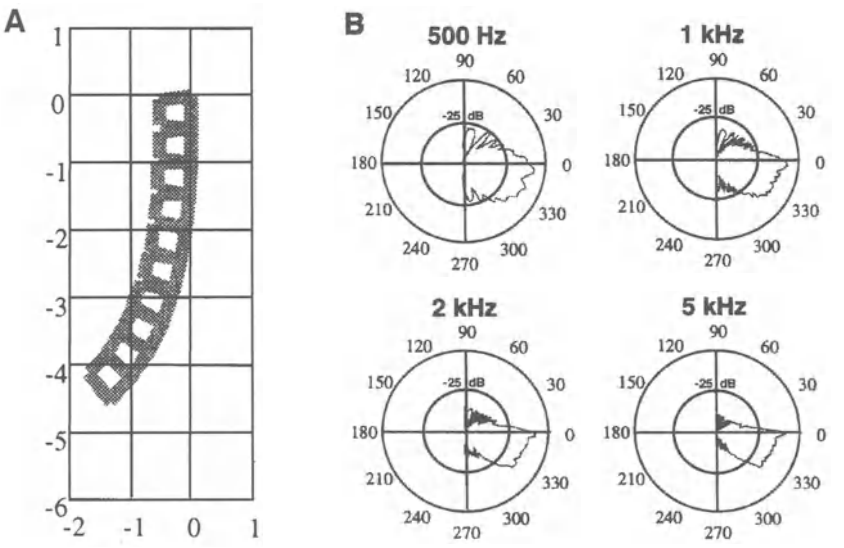

Figure 6-20. The spiral continuous array. Side profile of a 10 element array (A); polar response of the array (B).

6.5 Programmable arrays

Much of the early development work in programmable arrays was carried out by Duran Audio and other workers in the Netherlands, and with the rapid rise of digital signal processing during the 1990s, numerous other companies have made significant contributions.

The system shown in Figure 6-21A was developed by EAW and is typical of what can be done on a fairly small scale. Normally, these arrays are straight and consist of small drivers. Each driver has its own dedicated DSP section and power amplifier, and the system can be programmed remotely. For the most part, these systems are used in indoor spaces for speech reinforcement, and their straight configuration makes them easily adaptable to a wide variety of architectural settings.

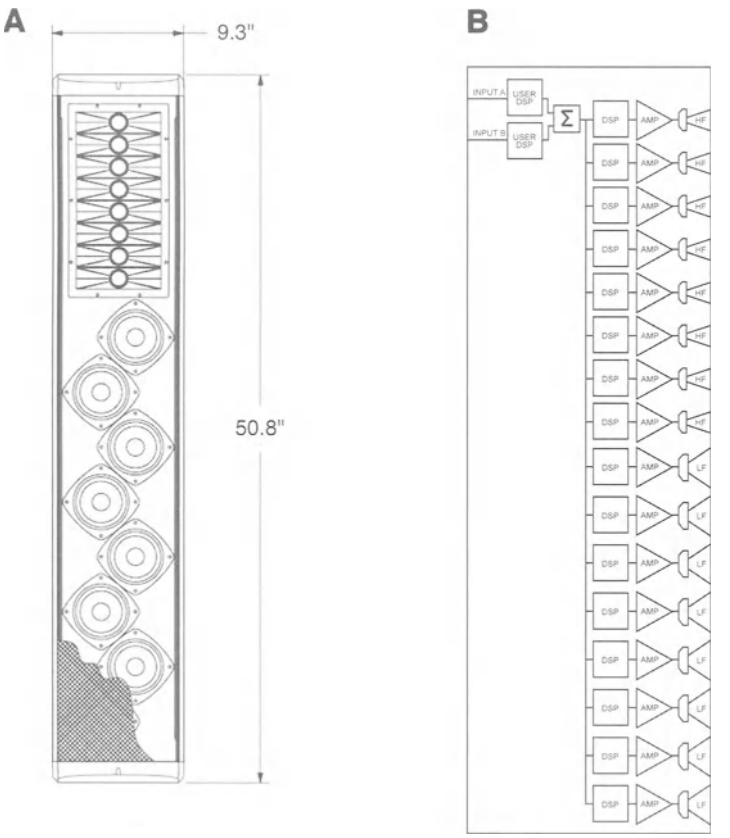

Figure 6-21. Views of the EAW Model DSA250 digitally programmable line array. Front view showing array elements (A); signal flow diagram (B). (Data courtesy Eastern Acoustics Works)

The signal flow diagram for the array is shown at *B*. Delay, equalization, and drive level for all drivers can be individually set to produce a given family of polar patterns and, in this system, the polar angle of maximum output can be steered as required. Since the array is vertical, these manipulations are effective only in the vertical plane, and the nominal horizontal coverage angle is 120°. Families of polar response curves on octave frequency centers are shown in Figure 6-22.

An important element in the operation of such system as these is a rational and intuitive PC program that allows the user to reconfigure the system as needed. Multiple units can be combined and jointly programmed.

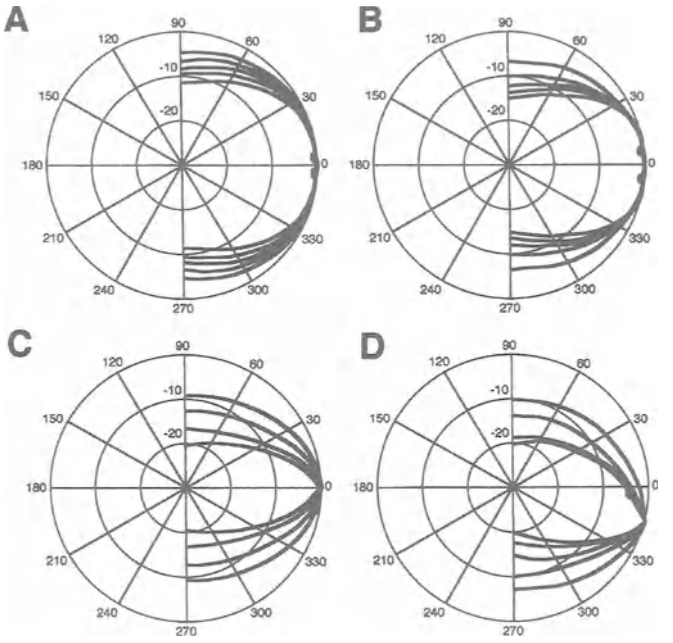

Figure 6-22. Examples of programmable polar response at 500 Hz, 1, 2, 4, and 8 kHz. 120° vertical beam (A); 75° vertical beam (B); 30° vertical beam (C); 30° beam steered downward 15° (D). (Data courtesy Eastern Acoustics Works)

The Hacousto Messenger XL line array system is shown in Figure 6-23A. It is a thin profile vertical array that is 2920 mm (9.6 ft) in length. It is designed for uniformly narrow coverage over considerable distances, indoors or out, and each of its equally spaced 27 transducers is individually addressed with DSP and power amplification. A typical set of polar diagrams is shown at *B*. An advantage of such an extensive array is its ability to suppress side lobes and to deliver a uniform signal both on-axis and off-axis as required in long-throw applications. Its characteristerics are remotely adjustable.

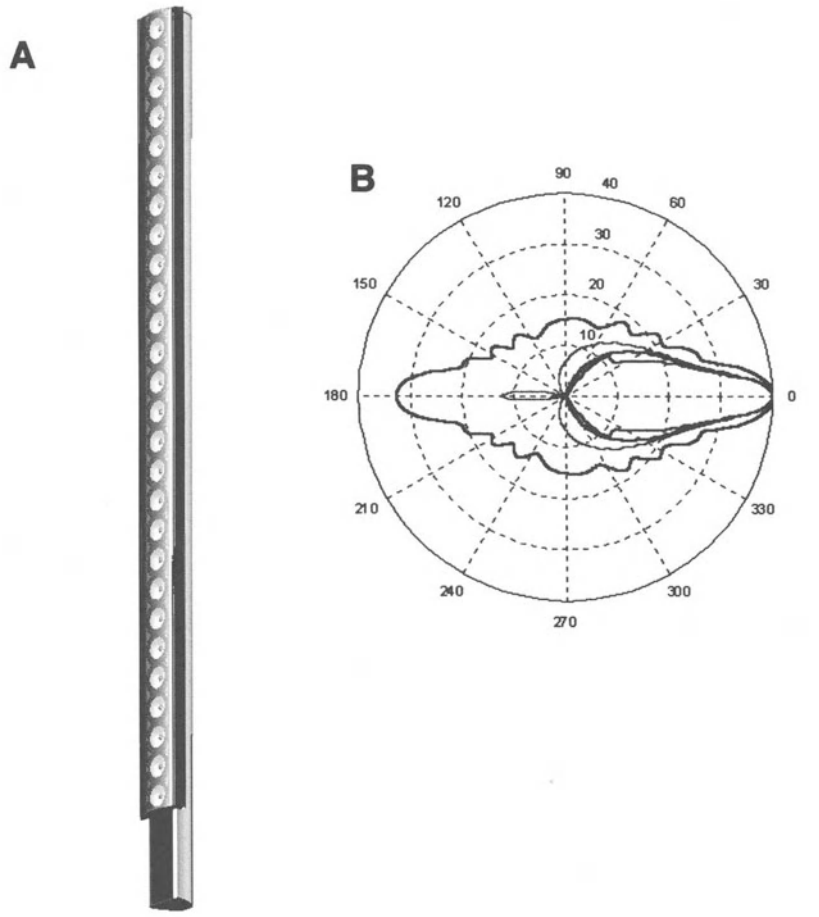

Figure 6-23. View of the Hacousto Messenger XL system (A); typical polar patterns at 500 Hz, 1, 2, and 4 kHz (B). (Data courtesy Hacousto International)

BIBLIOGRAPHY AND REFERENCES:

Baxandall, P., "Electrostatic Loudspeakers," Chapter 3 in *Loudspeaker and Headphone Handbook*, J. Borwick, ed., Butterworths, London (1988).

Eargle, J., *Electroacoustical Reference Data*, Kluwer Academic Press, Boston (1994).

Jordan, E., *Loudspeakers*, Focal Press, London (1963).

Jordan, R., & Cunningham, J., *The Sound of High Fidelity*, Windsor Press (Chicago 1958).

Keele, D., "Effective Performance of Bessel Arrays," *J. Audio Engineering Society*, volume 38, number 1 (1990).

Kitzen, J., "Multiple Loudspeaker Arrays Using Bessel Coefficients," *Electronic Components & Applications*, volume 5, number 4 (September 1983).

Klepper, D., and Steele, D., "Constant Directional Characteristics from a Line Source Array," *J. Audio Engineering Society*, volume 11, number 3 (1963).

Kuttruff, H., *Room Acoustics*, Applied Science Publishers, London (1979).

Rathe, E., "Notes on two common problems of sound propagation," *J. Sound and Vibration*, volume 10, pp. 472-479 (1969).

Ureda, M., "J" and "Spiral" Line Arrays," presented at the Audio Engineering Society 111th Convention, New York, 2001; preprint number 5485.

van der Wal, M., *et al.*, "Design of logarithmically spaced constant directivity transducer arrays," *J. Audio Engineering Society*, volume 44, number 6 (June 1996).

Chapter 7:
HORN SYSTEMS

7 Introduction

The history of the horn as an acoustic device dates to antiquity. Early man used hollowed animal horns for signaling over long distances, and in time the horn became the basis of a number of musical instruments.

Horn loudspeakers were developed fairly early in electroacoustics and were useful primarily because of their relatively high efficiencies and the ease with which their directivity patterns could be controlled. Important work was carried out by Wente and Thuras at Bell Laboratories in the mid 1920s, soon followed by RCA, Lansing, Altec, Jensen and Stephens.

For several decades, the development of horn systems was driven by the requirements of motion picture sound and the need for filling large spaces with fairly high sound pressure levels using power amplifiers of relatively modest output. Further refinements in horn systems during the sixties and seventies were driven by the demands of recording technology and high-level music reinforcement in outdoor venues.

Modern horn systems are characterized by high power handling capability, uniform directional control and low distortion at high output levels.

7.1 Horn flare profiles

In distinction to a direct radiator, whose moving system is mass controlled and looks into a radiation resistance that rises with frequency, the horn presents a load that is resistive over a large portion of its normal passband. Figure 7-1A shows the section profiles of two horns, exponential and hyperbolic, that have been widely used in electroacoustics. As shown at *B*, the hyperbolic (Hypex) horn (Salmon 1941) exhibits a slight rise in radiation resistance just above the nominal cutoff frequency, f_C, followed by a rapid drop. While it has

J. Eargle, *Loudspeaker Handbook*

been used in a number of high frequency devices, the hyperbolic horn is not normally used for midrange applications. Its application at LF has been limited, but its rise in radiation impedance could offer substantial advantages in acoustical loading at LF.

The profile of the exponential horn is shown in greater detail in Figure 7-1C. The equation for the horn's cross-sectional area, as a function of x, is given by:

$$S(x) = S_T e^{mx} \qquad 7.1$$

where: $S(x)$ = area at a distance, x, from the throat
S_T = area of the throat, meter^2
$e = 2.718$ (base of the natural logarithm system)
m = flare constant, meter^{-1}
x = distance from the throat along horn axis, meter

The flare constant is:

$$m = 4\pi f_C/c \qquad 7.2$$

where: f_C = cutoff frequency
c = velocity of sound, meter/sec

In terms of the horn's cutoff frequency, the approximate complex load at the throat of the horn is given by:

$$Z_{AT} = (\rho_0 c/S_T)\left[\sqrt{1 - (f_C/f)^2} + jf_C/f\right] = R_{AT} + jX_{AT} \qquad 7.3$$

where: f = driving frequency
$\rho_0 c$ = 406 mechanical ohms at standard temperature and pressure

The values of R_{AT} and X_{AT} for an infinite exponential horn are shown in Figure 7-1D. At frequencies lower than f_C, the impedance of the horn will be largely (but not entirely) reactive, and relatively little power will be transmitted. At frequencies much higher than f_C, the reactive term will become very small, and the resistive term will be dominant. For reasons having to do with size, many LF horns are used down to frequencies fairly close to cutoff.

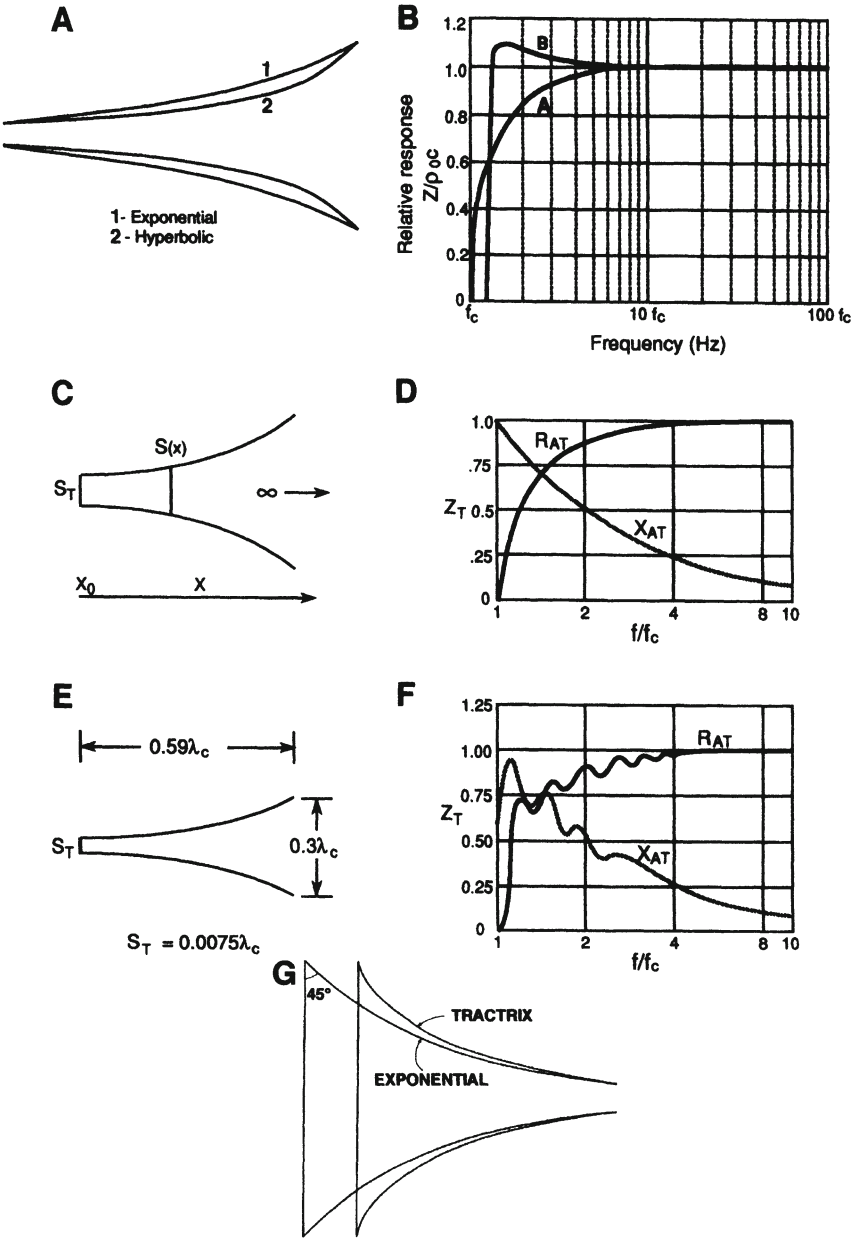

Figure 7-1. Horn profiles and impedances. Section views of exponential and hyperbolic horns (A); radiation resistance for exponential and hyperbolic horns (B); detail of an infinite exponential horn (C); approximate radiation resistance and reactance for an infinite exponential horn (D); detail of a finite exponential horn (E) radiation resistance and reactance for horn shown at *E* (F); tractrix and exponential profiles (G). (*A* through *F* after Beranek, 1954; *G* after Edgar, 1981)

HF horns, for reasons having to do with efficiency and proper driver loading, are designed to be used in the range where resistive loading is dominant.

If the circumference of the horn's mouth is greater than approximately three wavelengths of the lowest frequency to be reproduced, then the horn's impedance will behave very much like that shown in Figure 7-1D. The data shown at *E* and *F* are for a finite horn of the dimensions indicated. The ripple in the plotted curves is caused by reflections from the mouth of the horn back to the driver due to the acoustical impedance discontinuity the traveling wave sees as it passes the abrupt termination at the mouth. In these figures, λ_C is the wavelength of the cutoff frequency.

The normal passband of the horn is that region above which the resistive component of impedance has effectively reached its maximum value, which is equal to:

$$Z_{MT} = \rho_0 c S_T, \text{ mechanical ohms} \qquad 7.4$$

where: S_T = area of the throat, square meters

HF horns are often used as high as *8* to $10f_C$, and in the range above $4f_C$ the radiation resistance will be that of a piston, as shown in Figure 1-6. The response will thus show the characteristic ripples in the radiation resistance above ka = 2, even in the case of the so-called infinite horn (Keele 1973).

The *tractrix* horn, developed by Voigt (1927), has earned special status among horn-enthusiasts and audiophiles. Unlike the exponential horn, whose contour is normally generated outward from the throat, the tractrix horn is fundamentally generated from the mouth back to the throat. The mouth size is scaled according to the desired LF cutoff frequency, and the throat boundary is set by the initial expansion rate that is required for the chosen cutoff frequency. As can be seen in Figure 7-1G, the initial flare rates for both exponential and tractrix horns are quite similar, and the loading characteristics of the two are similar as well.

There are two slight advantages of the tractrix horn over the exponential: the throat resistive component of impedance of the tractrix horn maintains a higher value in the neighborhood of cutoff than the exponential horn, and the bell-like flaring at the mouth contributes to maintaining broader coverage at HF.

7.2 The driving transducer

The transducer normally used with a horn is called a *compression driver*, and several photos and cutaway views of modern compression drivers are shown in Figure 7-2. Drivers such as these provide response from 500-800 Hz to about 20 kHz when mounted on appropriate horns. Modern drivers which are used to cover the range from about 500 Hz to 20 kHz fall generally into three size categories:

Diaphragm diameter:	Driver exit diameter:	Peak power rating:
44.5 mm (1.75")	25.4 mm (1")	40 W
76 mm (3")	38 mm (1.5")	75 W
100 mm (4")	50 mm (2")	100 W

Figure 7-3 shows a labeled section and end view of a driver of the types illustrated in Figure 7-2.

The driver design shown here was pioneered by Bell Telephone Laboratories and its associated manufacturing division, Western Electric (WE). This driver design is characterized by its unique annular slit phasing plug, which provides the necessary compression ratio between the diaphragm and the driver's outlet. Also characteristic here is the position of the diaphragm at the rear of the driver, with the signal firing through the magnetic structure to its output at the front.

7.2.1 Other phasing plug designs

Alternate phasing plug profiles are shown in Figure 7-4 in both end and section views. The WE design is shown at *A*. The design shown at *B* was introduced by the Lansing Manufacturing Company in the late 1930s, ostensibly as a means of working around the basic WE patent on the annular slit design. The form shown at *C* was introduced during the 1940s by the British Tannoy company in their legendary "Dual-Concentric" coaxial monitor loudspeaker, and it continues to this day.

7.2.2 Other driver concepts

There have been variations on the basic driver concept, as shown in Figure 7-5. The "tear-drop" design shown at *A* has only one annular path between the diaphragm, and as such it has limited high frequency capability. The multiple tear-drop design, shown at *B*, is often used in high frequency radiators. Here,

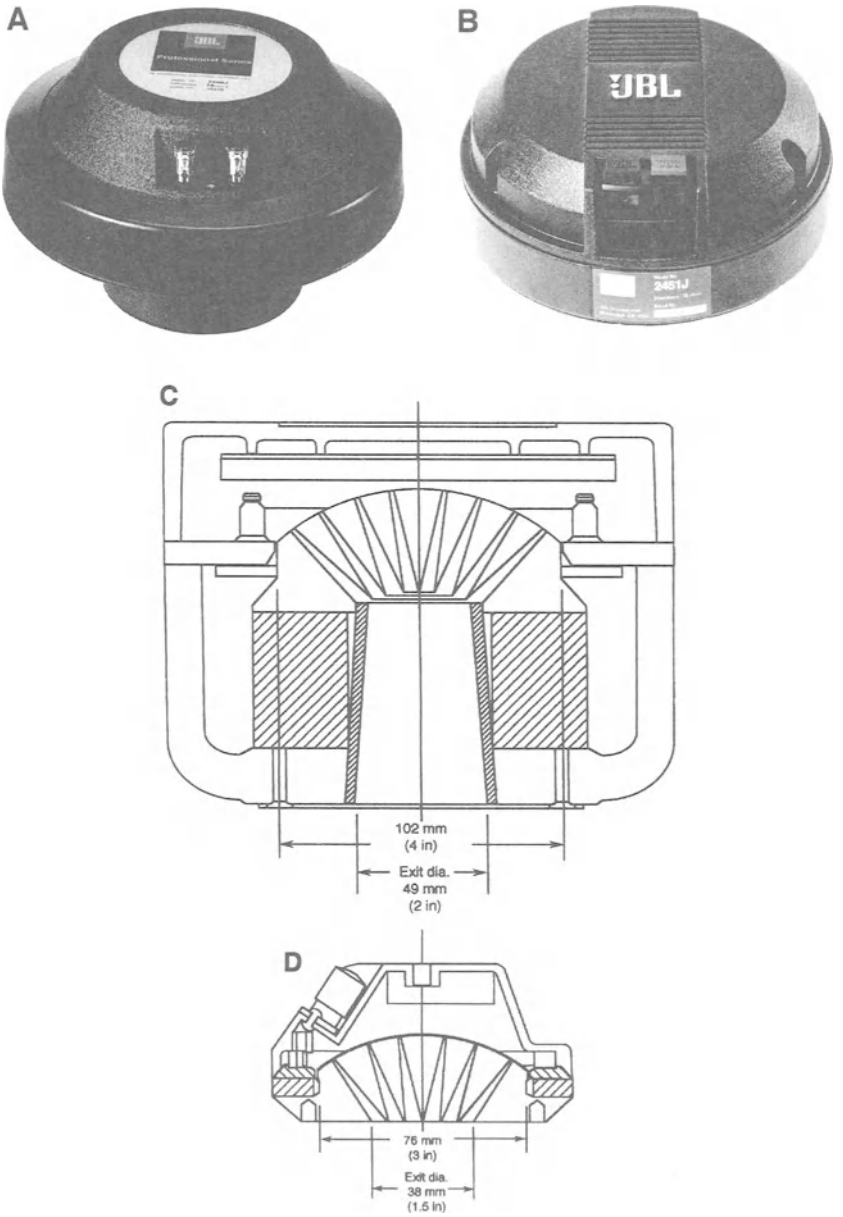

Figure 7-2. Photos and cutaway views of HF compression drivers. 100-mm diaphragm with ferrite magnet (A); 100-mm diaphragm with neodymium magnet (B); section view of 100-mm diaphragm driver with Alnico V magnet (C); section view of 76-mm diaphragm driver with neodymium magnet (D). (Data courtesy JBL)

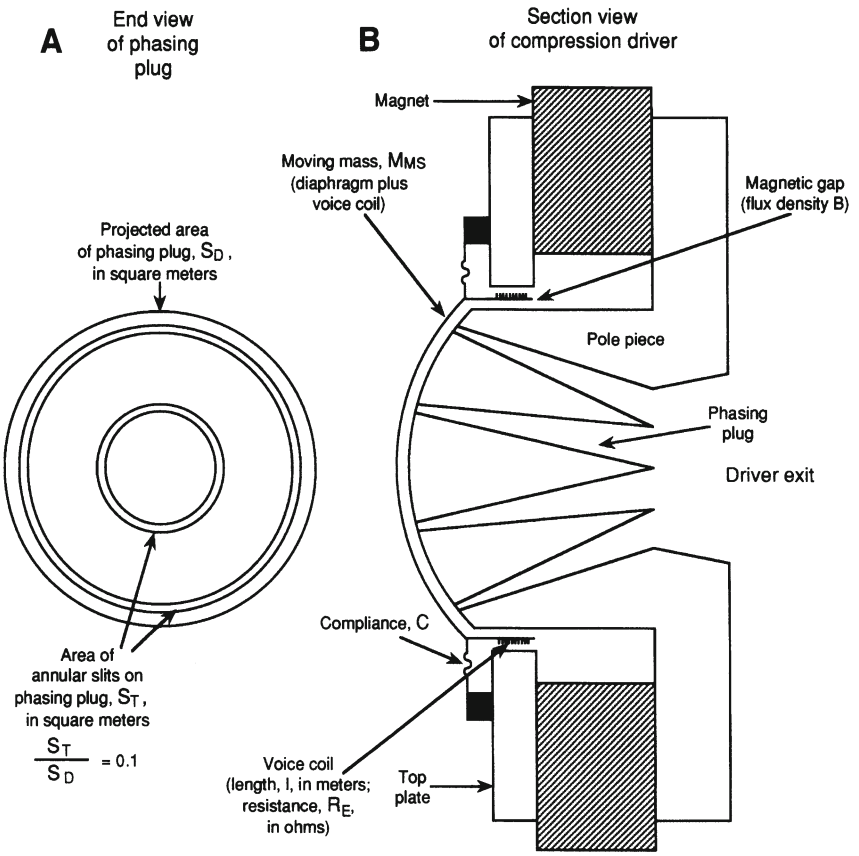

Figure 7-3. Views of a HF compression driver. Normal view of phasing plug as seen from diaphragm side (A); section view (B). (Data courtesy JBL)

the sections are circular, and the response is very much like that of the basic WE design. The design shown at *C* is basically a ring radiator in that its output originates from an annular diaphragm clamped on the inside and outside of the radiating surface. The design is normally limited to small drivers. The design shown at *D* (Voishvillo & Surupov, 1996) has a free-edged diaphragm and is clamped in the center. It is a close cousin to the Community VHF 100 design, which was introduced in the early 1990s.

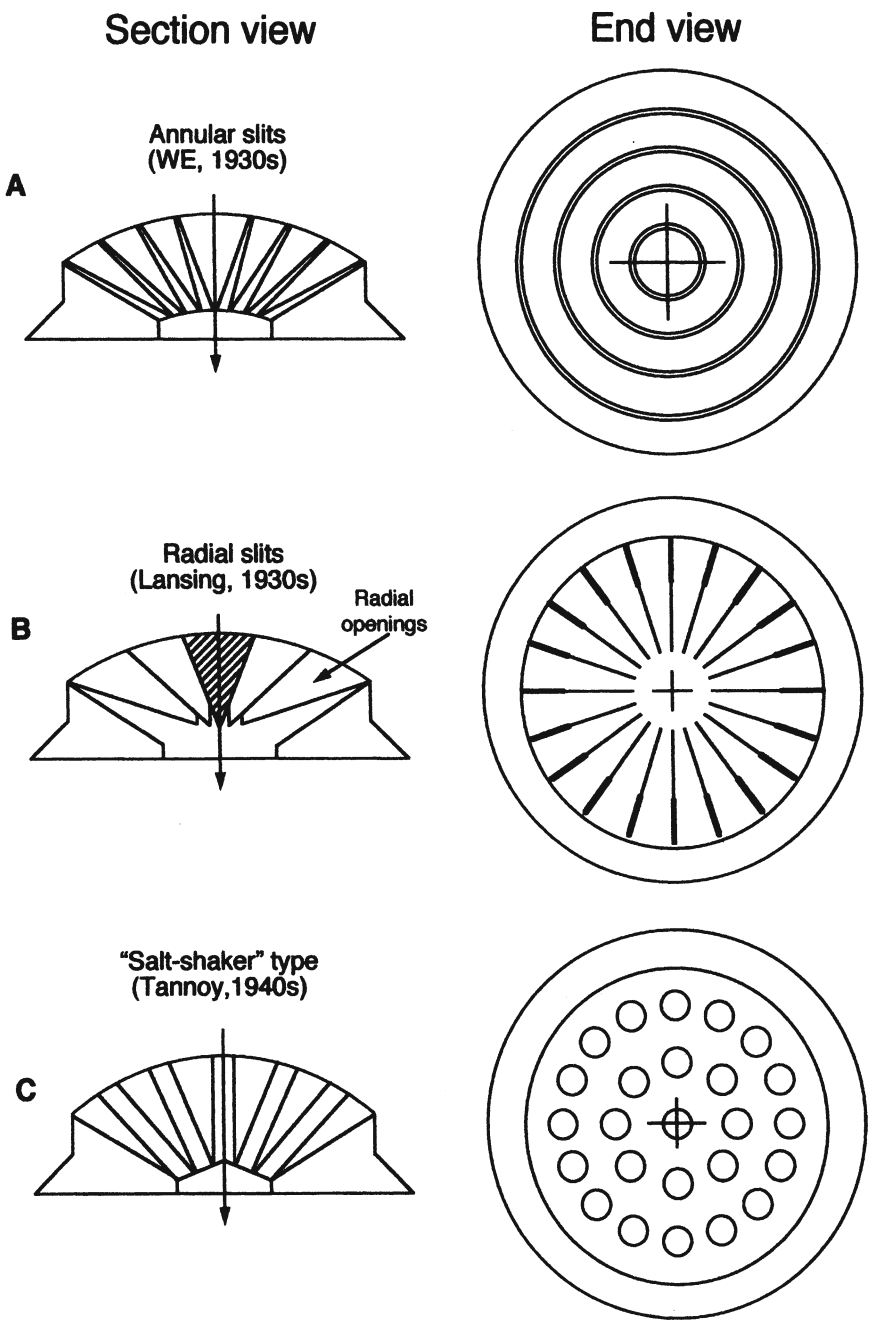

Figure 7-4. Section and end views of several types of phasing plugs.

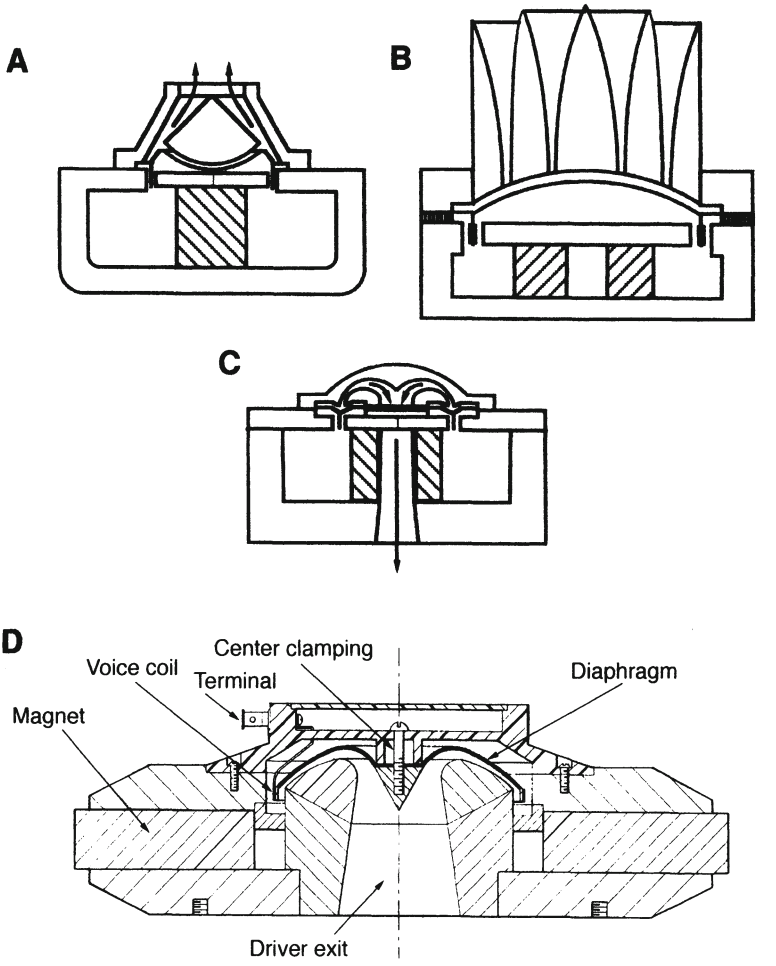

Figure 7-5. Views of other types of compression drivers. Teardrop type (A); multiple teardrop type (B); re-entrant type (C); center-clamped, free-edge type (D); two-way design (E). (Data at *D* courtesy A. Voishvillo; data at *E* courtesy BMS ElektronikGmbH)

The design shown at *E* is unique in that it contains both MF and HF sections in a two-way configuration. Both MF and HF transducers take the form of ring radiators, and an elaborate manifold (not shown in this figure) directs the two outputs to their respective channels, with no interaction beteween them. The frequency division between sections is at 7 kHz.

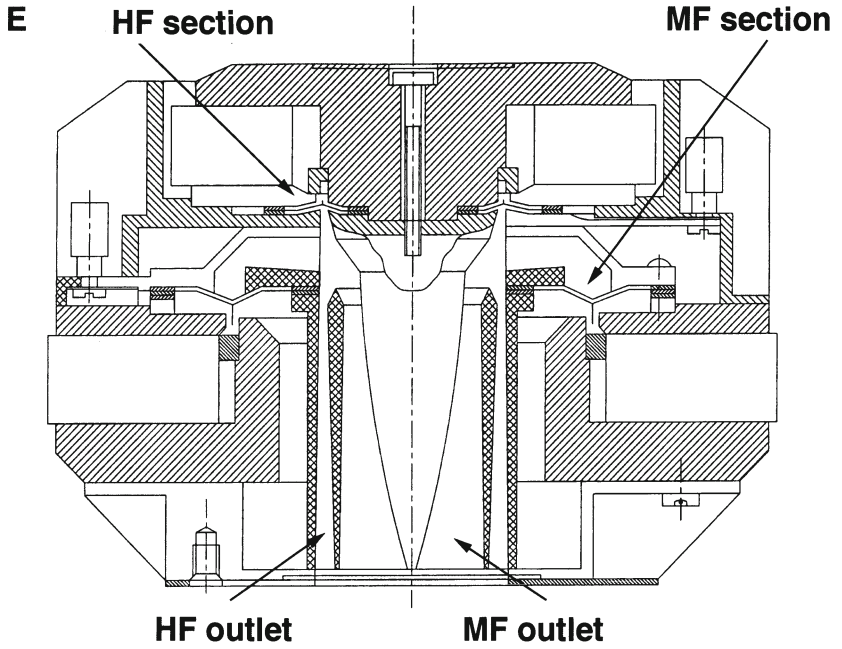

Figure 7-5. Continued.

7.2.3 Diaphragm compliance designs

The diaphragm designs shown in Figure 7-6A through *C* are normally formed from a single piece of metal by pneumatic or hydraulic drawing of the material. Aluminum, titanium, and some forms of beryllium can be shaped in this manner. In other designs, vacuum electro-deposition of beryllium is used.

The *tangential* compliance shown at *A* dates from the late 1920s and is still used today. Its main feature is that it provides a fairly high, well damped secondary resonance, which yields extended frequency response. The design works well with aluminum, due to the high ductility of that material.

The half-roll surround shown at *B* provides a rather abrupt mechanical termination at the edge of the diaphragm which results in a HF response rise followed by a sharp drop in response.

The so-called "diamond" surround shown at *C* consists of a number of diamond-shaped impressions pressed into the surround, resulting in a response similar to that of the tangential surround, but with less stress in the metal, and consequently greater reliability and ease of manufacture.

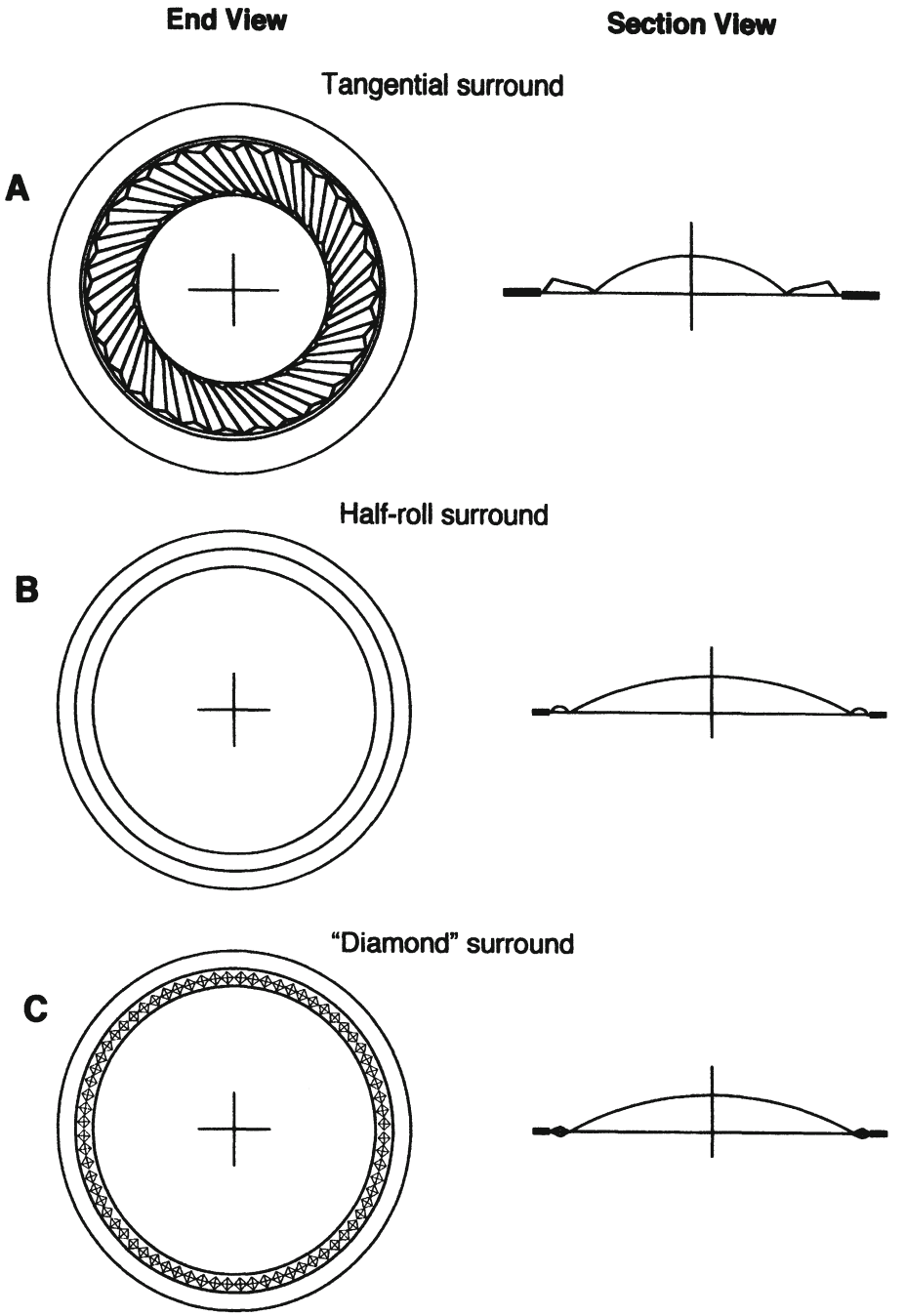

Figure 7-6. Diaphragm types. Tangential (A); half-roll (B); diamond (C); composite (D).

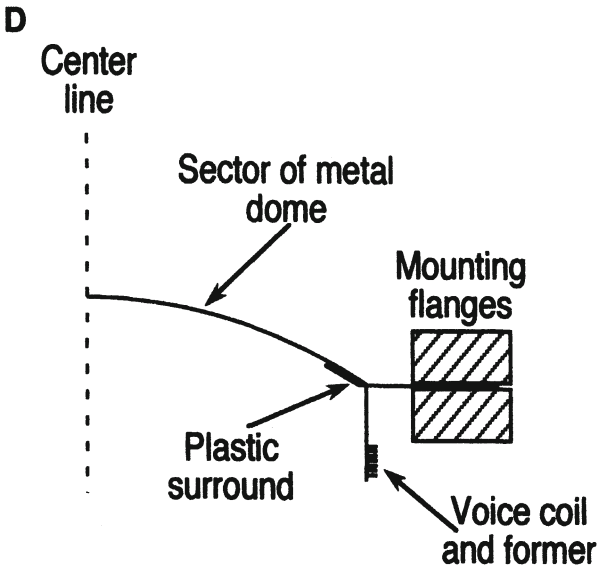

Figure 7-6. Continued.

Figure 7-6D shows a diaphragm-voice coil assembly composed of a metal diaphragm and a plastic surround structure. Designs such as these restrict the high bending motions to the plastic materials, which are far better equipped to handle them than is the metal dome itself. In construction, these designs are more difficult to make than single-piece structures, and there is likely to be more variation in unit-to-unit response. High temperature adhesives are used, along with robust plastic materials such as Kapton and various polyamids.

7.2.4 Construction details

The high frequency driver is a precision device with many design tolerances in the range of ±40 microns (± 0.001 in). The magnetic circuit normally operates with the top plate and pole piece at or near saturation, and gap flux densities in excess of 2.0 T can be attained.

Typical HF diaphragm diameters range from about 45 to 100 millimeters. Diaphragm materials have included phenolic impregnated linen, aluminum, titanium, and beryllium. The metal diaphragms have a thickness of about 40 to 80 microns. The ideal diaphragm material for extended high frequency response is one that is rigid, of low mass, and fatigue resistant. The search for better materials continues. Diaphragm moving mass is generally quite low, and a typical value for a 100-mm diameter diaphragm/voice coil assembly is about 3.5 grams.

The diaphragm is separated from the phasing plug by a space just large enough to ensure that it will not hit the phasing plug on large excursions at lower frequencies. The annular slits in the phasing plug have a collective area that is about one-tenth that of the diaphragm itself, resulting in a pressure-volume velocity transformation ratio of ten-to-one between the diaphragm and the exit of the phasing plug. It is this mechanical-to-acoustical transformation action that effectively matches the driver's diaphragm impedance to that at the throat of the horn.

7.3 Analysis of compression drivers

Figure 7-7A shows a simplified section view of a portion of a WE-type phasing plug with details of diaphragm spacing, slit spacing, and slit width. Using this representation as a starting point, Wente and Thuras (1934), described the acoustical impedance of the diaphragm as seen at the phasing plug. Using the terminology shown at *A*, *2W* is the slit width, *H* is the diaphram-to-phasing plug spacing, and *L* is the center-to-center spacing between adjacent annular slits. Figure 7-7B and *C* show the resulting diaphragm acoustical resistive and reactive impedance values corresponding to the *H/W* ratios shown at *A*.

The quantity *2L* in Figure 7-7A is the spacing between adjacent slits in the phasing plug, and it determines the reference frequency in the graphs. For example, if the spacing between adjacent slits in the phasing is 12 mm (a typical value), the corresponding frequency for the 0.1 marker along the horizontal axis is approximately 700 Hz, and the frequency corresponding to 1.0 is 7 kHz. It is clear from Figure 7-7B and C that optimum response is obtained at curve 2, where the *H/W* ratio is equal to 2/3. While curve 1 would seem a better choice for extended frequency response, note that it would lead to lower overall driver sensitivity and/or lower diaphragm excursion capability, due to the closer spacing of the diaphragm to the phasing plug.

Virtually all professional compression drivers built from the 1930s to the present time have made use of the basic diaphragm-phasing plug relationships developed by Wente and Thuras. Variations and improvements have been based largely on diaphragm construction, adhesives and magnet materials.

Working some 45 years later – and an octave higher in frequency response – Locanthi and Kinoshita (1978) essentially validated the earlier analysis. Using the equivalent circuit shown in Figure 7-8A, they produced families of response curves in which the exact roles of several design parameters were

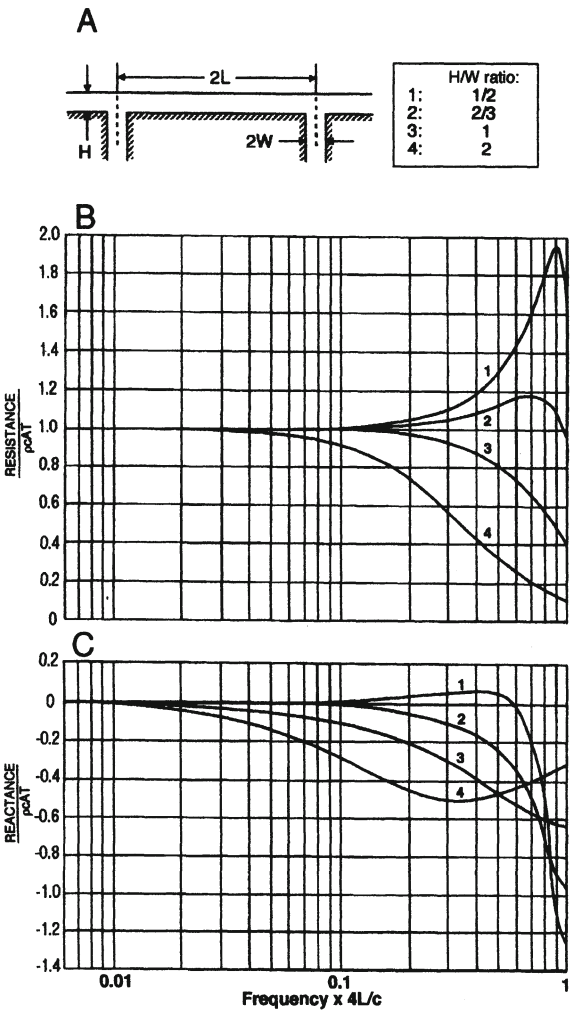

Figure 7-7. Wente's analysis of compression drivers. Basic model (A); response (B). (Data after Wente and Thuras, 1934)

individually optimized in producing highest efficiency. Their findings are summarized as follows:

1. The *Bl* product should be as large as practicable (see Figure 7-8B).
2. The diaphragm-to-phasing plug spacing should be as small as possible, consistent with excursion demands (see Figure 7-8C).
3. Diaphragm moving mass should be as small as possible (see Figure 7-8D).
4. The spacing between phasing plug slits should be as large as possible, consistent with maintaining the desired HF power response extension.

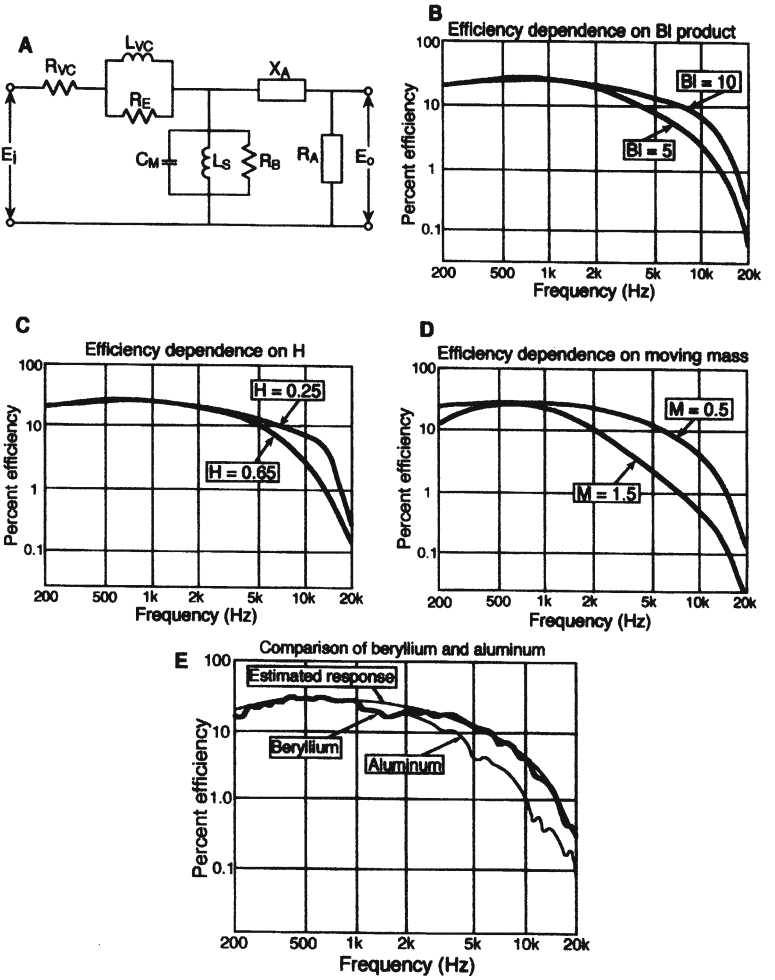

Figure 7-8. Compression driver analysis. Equivalent circuit (A); effects of parameter variations (*B* through *E*). (Data after Kinoshita and Locanthi, 1978)

5. The ratio of diaphragm area to slit area has little effect on efficiency, but a high ratio reduces peak excursion requirements for a given output, while increasing second harmonic distortion.

In summary, the authors state that the most important factors in obtaining the flattest and most extended HF response are low diaphragm mass and high *Bl* product. This quest for ultimate performance leads to beryllium as the material of choice for diaphragms (because of its high stiffness and low mass), and to high saturation alloys in magnet assemblies. Both of these options are expensive, but well worth the investment for ultimate performance. The

measured difference between beryllium and aluminum diaphragms is shown in Figure 7-8E.

During the same period, Murray and Keele at JBL arrived at a set of equations that defined the broad parameters of compression driver mid-band response. An analogous circuit for the driver, loaded by a horn, is shown in Figure 7-9A. On the mechanical and acoustical side, the circuit is of the mobility type, where M_{MS} is the mass of the moving system (diaphragm and voice coil). C_{MS} is the mechanical compliance and C_{MB} is the compliance of the air space behind the diaphragm; r_{MS} and r_{MB} are their associated values of mechanical responsiveness. C_{M1} is the compliance of the small (but by no means insignificant) air space between the diaphragm and the phasing plug.

In the normal passband of the driver we can simplify this equivalent circuit, reflecting it back to the electrical side as shown in Figure 7-9B. Here, R_E represents the electrical resistance in the amplifier-voice coil circuit and R_{ET} represents the effective radiation resistance in ohms reflected through the mechanical and acoustical systems:

$$R_{ET} = S_T(B1)^2/\rho_0 c S_D^2 \qquad 7.5$$

If a driver has been designed for flattest response, then R_E and R_{ET} will both be just about equal, and the efficiency will be:

$$\text{Efficiency (\%)} = [2\, R_E R_{ET}/(R_E + R_{ET})^2\,] \times 100 \qquad 7.6$$

This value will be 50% when R_E and R_{ET} are equal.

At high frequencies, the equivalent electrical circuit is as shown in Figure 7-9C. The additional reactive elements affect the frequency response by progressively rolling off high frequency response. L_E represents the inductance of the voice coil, and its effect can always be seen in the impedance curve of the driver as a rise in impedance at higher frequencies. Some driver manufacturers deposit a thin copper or silver ring on the polepiece, which minimizes the rise in impedance due to the coil's inductance by acting as a transformer with a shorted secondary turn.

C_{MES} is a shunt capacitance which causes the so-called *mass breakpoint* in the driver's frequency response. This is a 6 dB/octave roll-off in high frequency response commencing at f_{HM}:

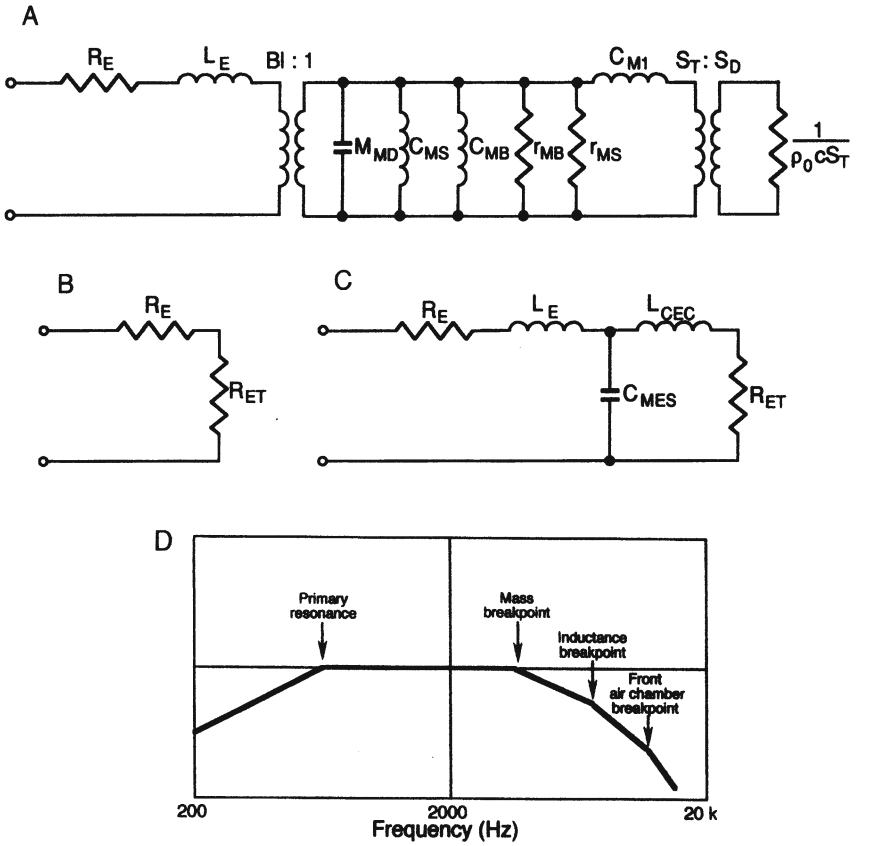

Figure 7-9. Equivalent circuit of a compression driver (A); simplified circuit for MF operation (B); simplified circuit for HF operation (C); response (D).

$$f_{HM} = (Bl)^2/\pi R_E M_{MS} \qquad 7.7$$

The mass breakpoint is significant in all traditional high frequency compression driver designs and normally falls in the range between 3 and 4 kHz.

Finally, L_{CEC} is a series inductance corresponding to the front air chamber between the diaphragm and phasing plug. In some drivers the effect of the front air chamber may be noticed as low as 8 kHz. For drivers optimized for high frequencies its effect may be negligible.

At low frequencies, the driver's response is limited by the primary diaphragm resonance, and in most high frequency drivers this usually takes

place in the range of 500 Hz. Although a given horn may provide extended resistive loading below the driver's resonance, operating the driver below resonance will call for careful monitoring of signal input. Most manufacturers will state a driver power derating value for such operation. The regimes of response of the compression driver are shown in Figure 7-9D.

We should note that the mid-band efficiency of a compression driver, when measured on a typical horn, may be 1 to 1.5 dB lower than that measured on a PWT. The insertion loss is due primarily to slight acoustical impedance differences between the two loading conditions.

7.3.1 Calculations of driver performance

As examples of performance calculations based on driver parameters, we will use the JBL 2441J compression driver:

Bl = 17 Tm (gap flux density times coil length)
M_{MS} = 3.3 g (mass of moving system)
f_S = 500 Hz (resonance frequency of moving system)
S = 32.5 x 10^3 N/m (restoring force of compliance, newtons per meter)
$\omega = (S/M)^{0.5}$ (2π times resonance frequency)
Force (f) = S x displacement (force on moving system)
Voice coil diameter = 4 in
Number of turns in voice coil = 30
B = 2.0 T
R_{DC} = 7.1 ohms (dc resistance of voice coil)

Maximum displacement:

Assume a spacing of 0.55 mm between voice coil and phasing plug. Then, the maximum possible force is:

$f = (32.5 \times 10^4)(5 \times 10^{-4}) = 16.25$ N

Now, force = Bli, so
i = 16.25/17 = 0.96 amperes, peak current
i = (0.96)(0.707) = 0.68 rms current.
Power = i^2R, and if
$R = Z_{min}$ = 12 ohms
then power = 5.5 watts

Note: This condition exists at very low frequencies and is an indication of how little power is required to reach mechanical limits in a compression driver in that frequency range.

Maximum diaphragm acceleration:

power rating of driver = 35 watts, continuous sine wave (with 3-dB crest factor)
therefore: peak power = 70 watts
Z = 16 ohms
$W = I^2R$, and
$I = (W/Z)^{0.5} = (70/16)^{0.5} = 2.1$ amperes peak current
Bl = 17 N/A
peak force = 17 x 2.1 = 35.7 newtons
moving mass of 2441 driver = 0.0033 kg, and 1 N = 1 kg-m/s^2
therefore: 35.7/0.0033 = 10,818 m/s^2 maximum acceleration
since 1 G = 9.8 m/s^2,
maximum acceleration = 10,818/9.8 = 1103 G's, or 1103 times the acceleration of gravity.

Peak acceleration at 2441 driver thermal limit:

rating of the driver: 75 watts, continuous sine wave
150 watts, continuous program
300 watts, program peak

With a pink noise input (6-dB crest factor), the diaphragm undergoes 600 watts of instantaneous power input:
(600/70)(1103) = 9454 G, or approximately 10,000 G's peak acceleration.

7.4 The plane wave tube (PWT)

In carrying out compression driver development, engineers normally measure the driver's response on a plane wave tube (PWT) rather than a horn. Figure 7-10 shows details of the PWT. The tube is normally of the same diameter as the exit of the driver, and a probe microphone is placed fairly close to the mounting flange for the driver. There is a loss of acoustical power as sound progresses down the tube which is caused by a tapered wedge of fiberglass or other suitable damping material. The tube may be 2 or 3 meters in length, and by the time sound has propagated over that distance, it has become attenuated

to such a point that there is little acoustical power to reflect back to the microphone. Acoustically, the tube presents a resistive load to the driver such as would be presented by an infinite horn with a cutoff frequency of zero Hz.

The upper useful frequency of a PWT is given as 1.22(c/d), where c is the speed of sound and d is the diameter of the tube, both given in the same units. Thus, for a PWT with a diameter of 25.4 mm (1 in), the upper frequency limit is 16.5 kHz. The lower frequency limit of a PWT is given as c/4l, where c is the speed of sound and l is the length of the tube, both given in the same units. Thus, a tube 2 meters long would provide reliable data down to about 43 Hz.

It is clear that measuring a 51-mm (2 in) exit driver on a matching PWT would only give reliable HF data up to about 8 kHz. However, many such drivers are are routinely capable of response well beyond that frequency, and tapered driver inserts are often used in order to measure the frequency response of larger drivers on smaller tubes.

However, when measuring at absolute midband sensitivity of the driver, a matching diameter PWT should be used. The reason for this is that the acoustical impedance seen by the driver is equal to ρc_0 times the PWT cross-section area, and the area difference between 25.4 and 51 mm diameter tubes is significant.

The sound pressure level in the PWT is uniform in the portion ahead of the damping material and is equal to:

$$L_P = 94 + 20 \log \sqrt{W_A (\rho_0 c)/S_T} \qquad 7.8$$

where W_A is the acoustical power in watts delivered by the driver and S_T is the cross-section area of the tube in square meters. Most manufacturers normalize their PWT data to a standard tube with a diameter of 25.4 mm (1 in). Let us now put one watt of acoustical power into such a tube and calculate the value of L_P:

$$L_p = 94 + 20 \log [(1)406/0.0005]^{0.5}$$

$$L_p = 94 + 20 \log (901) = 94 + 59 = 153 \text{ dB}$$

As a rule, a reference power of 1 milliwatt is used, producing a level of 123 dB in the tube.

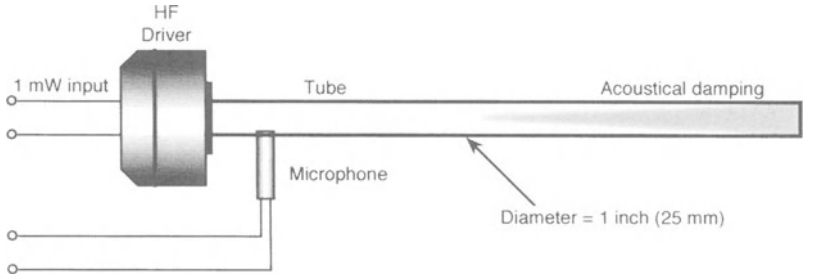

Figure 7-10. Section view of a plane wave tube (PWT).

Figure 7-11shows typical 1 milliwatt PWT response of a JBL 2446 compression driver. Note that the maximum level in the pass-band of the driver is 119 dB L_p. This value is 4 dB lower than the 1 mW reference level of 123 dB L_p, indicating that the driver's efficiency is 100 x $10^{-4/10}$, or 40%.

We can also see the effect of the mass breakpoint in the driver's response in the 3.5 kHz range. We can compare this with the value given by equation 7.7:

$Bl = 18$ Tm
$R_E = 8.5$ ohms
$M = 0.00346$ kg
$f_{HM} = (18)^2/\pi(8.5)(.00346) = 3507$ Hz

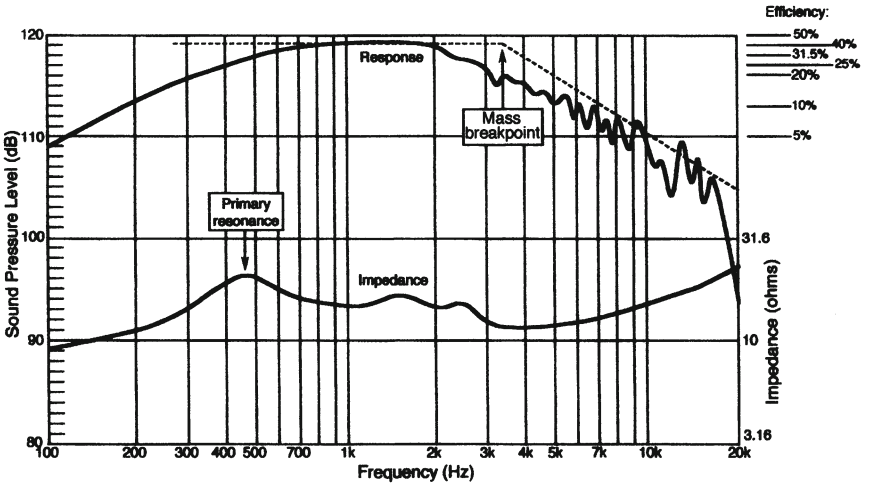

Figure 7-11. Plots of amplitude response and impedance for JBL 2445J driver on PWT. (Data courtesy JBL)

On the graph, a breakpoint at 3500 Hz has been superimposed by dotted lines over the response curve. Note that it effectively matches the transition point in the curve.

The modulus of impedance of the driver has been plotted below the response curve, and the driver's primary resonance at about 500 Hz is obvious.

7.5 Secondary resonances in the compression driver

Our analysis thus far has assumed that the driver's diaphragm moves as a unit. At high frequencies, more complex motion occurs and may have a profound effect on response. There is, in most drivers, a secondary resonance that occurs in the surround, or suspension, of the driver. When this resonance takes place, motion from the voice coil causes considerable motion in the surround itself and relatively little in the diaphragm.

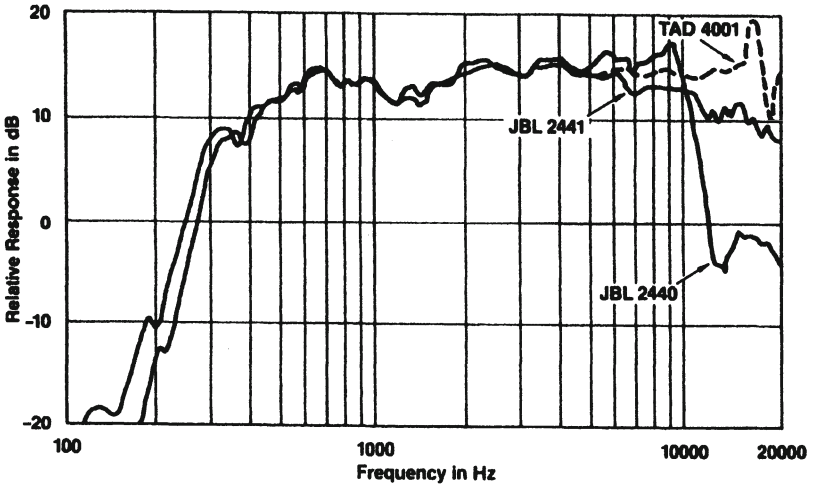

Figure 7-12. Response of three drivers mounted on JBL 2350 radial horn. (Data courtesy JBL)

Figure 7-12 shows superimposed response curves of three drivers mounted on a JBL 2350 radial horn. The curves are unequalized, and two of them (JBL 2440 and TAD 4001) show the effect of secondary resonances in their half-roll surrounds. The elevated response of the 2440 driver at 9 kHz and at 17 kHz in the 4001 driver are due to secondary resonances at those frequencies. The beryllium diaphragm in the 4001 driver is considerably stiffer than the aluminum diaphragm in the 2440, and this accounts for the shift of nearly an octave in its secondary resonance. By comparison, the 2441 diaphragm design has a *diamond* surround treatment (see Figure 7-6C) that distributes secondary

resonances, providing a smoother overall curve, but one that has more apparent roll-off than the other two in the range between 5 and 10 kHz. These response curves are typical of the many design factors and trade-offs that the transducer engineer must deal with.

7.6 Ring radiators and UHF drivers

Ring radiators are very high frequency devices operating normally in the range from about 4 kHz to 20 kHz. They embody the elements of a compression driver and horn in a single unit. Section and perspective views of the JBL 2402 ring radiator, often called the "bullet," are shown in Figure 7-13. The diaphragm is clamped at the outer edge as well as in the middle, effectively forming an annular, or ring shaped, radiating surface. The initial horn flare is annular in shape, eventually making a transition to a horn with a circular cross-section. Other models of the ring radiator have the same basic driving mechanism but with different horn configurations.

Over their operating range, ring radiators can exhibit efficiencies on the order of 6.3% and handle peak power inputs of up to 40 watts, yielding a power output, per device, of about 2.5 acoustic watts. They are often used in multiple arrays for greater output capability.

Figure 7-13B shows a section view of the JBL Be045 compression driver, which is designed to cover the frequency range from 10 kHz to 50 kHz. The driver has a 25-mm (1 in) diameter phasing plug and is used in monitoring high-resolution digital recordings. The driver is normally used above 10 kHz, and typical frequency response is shown at *C*.

7.7 Families of horns

In this section we will discuss various families of horns that have been developed over the last seventy-five years of loudspeaker evolution. The exponential horn basically has poor pattern control, narrowing progressively with rising frequency. The families of horns we will discuss here have attempted, each in its own way, to solve problems in pattern control, while maintaining some degree of exponential flare for good loading. We will discuss them in the approximate order in which they were developed.

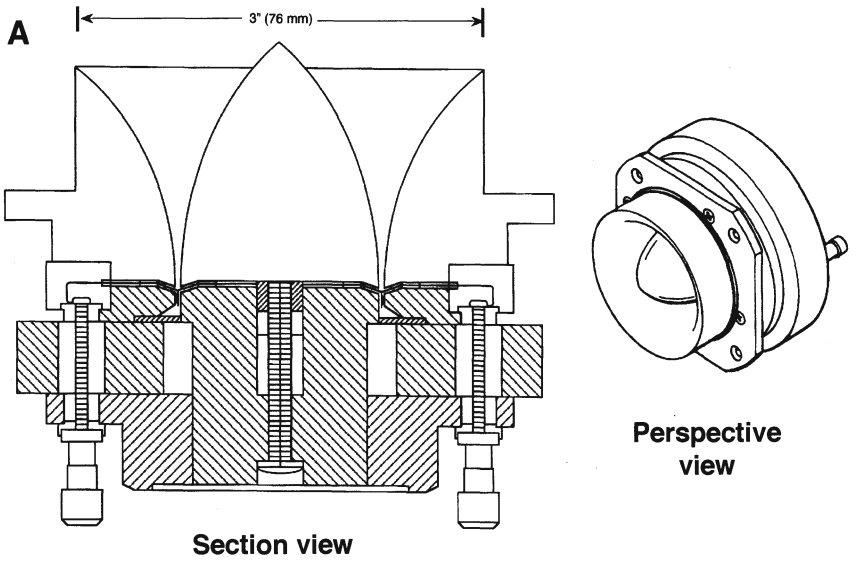

Figure 7-13. Section and perspective views of JBL 2402 ring radiator (A); section view (B) and 1-meter on-axis response (C) of JBL 045Be UHF driver. (Data courtesy JBL)

7.7.1 Multicellular horns

The multicellular horn was developed during the 1930s and found extensive application in motion picture theaters, where it was necessary to aim sound quite specifically at seating areas in large houses. It also became a staple in sound reinforcement applications during the 1950s, but was later generally replaced by the radial horn.

Figure 7-14A shows a group photograph of Altec multicellular horns. Individual cells were nominally 25 degrees wide and were of exponential flare. Models with 800 Hz and 500 Hz lower frequency limits were the most common. The theoretical pattern control of the multicellular horn is shown at *B*. Note that pattern control above about 1 kHz is determined by cell multiples; however, in the range between 500 Hz and 1 kHz, there is substantial narrowing of the pattern as the distance across the mouth of the assembled cells becomes equal to the radiated wavelength. At lower frequencies the cell array loses pattern control altogether.

Selected polar measurements are shown at *C*, *D*, and *E*. At 1 kHz (as seen at *C*) the patterns are well behaved and follow the data shown at *B*. At 2 kHz (shown at *D*) the polar response is still good, but a pattern of "fingering" can

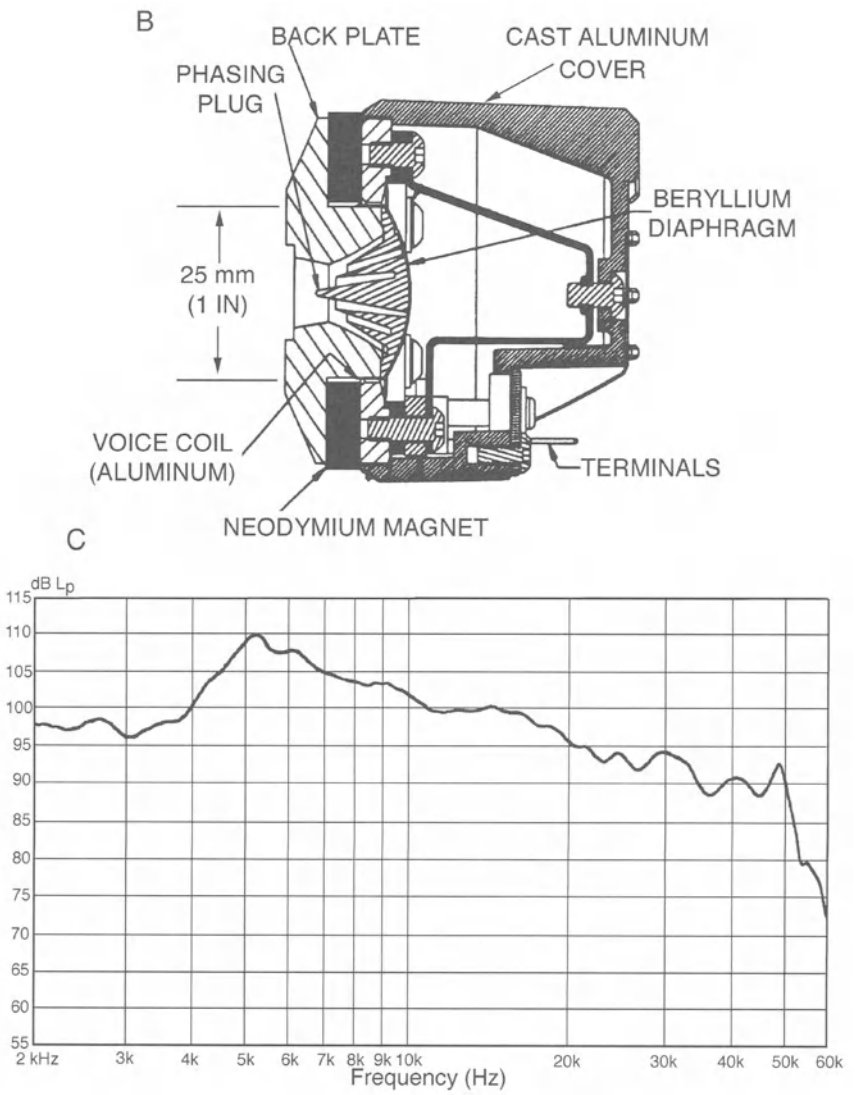

Figure 7-13. Continued.

be seen toward the edges of the patterns. At 10 kHz (shown at *E*) there is considerable fingering in the main coverage zones of the horn, even to the extent of 10 dB variations in the horizontal plane. Note that fingering is at a maximum along the septum dividing adjacent cells.

7.7.2 Radial horns

Figure 7-15A shows a photo of a family of radial horns. Top and side views of a typical design are shown at *B*. The radial horn is so named because its straight sides outline radii of a circular arc formed by the horn's mouth. They are also called *sectoral* horns. As seen in side view, the horn's flare is exponential; as seen in top view it is conical. In the vertical plane the exponential flare determines the pattern control, and at *C* we note that the pattern narrows progressively with rising frequency. However, in the horizontal plane, the pattern remains fairly constant, corresponding to the angle set by the straight sides. At frequencies above 8 or 10 kHz there may be horizontal pattern variations due to interference problems in the early flare development at the throat. The data shown at *C* is for the JBL 2345 radial horn.

The horizontal pattern loses control below the frequency whose wavelength is approximately equal to the mouth width. Often, there is a narrowing of the horizontal pattern in this range, just above the frequency where control is lost.

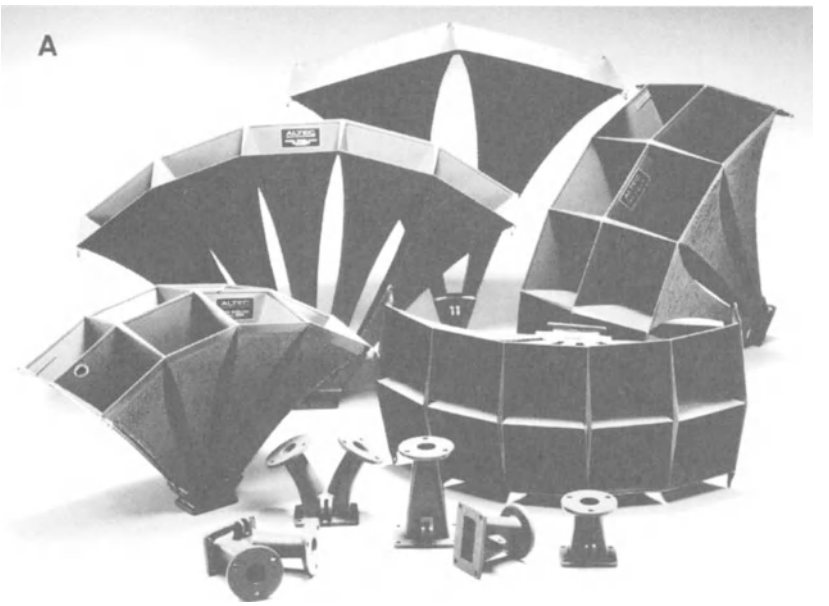

Figure 7-14. The multicellular horn. Photo of various multicellular horns (A); theoretical beamwidth data for multicellular horns (B); vertical and horizontal polar response of horn at 1 kHz (C); 2 kHz (D); 10 kHz (E). (Photo courtesy Altec; data at *B* after Beranek, 1954)

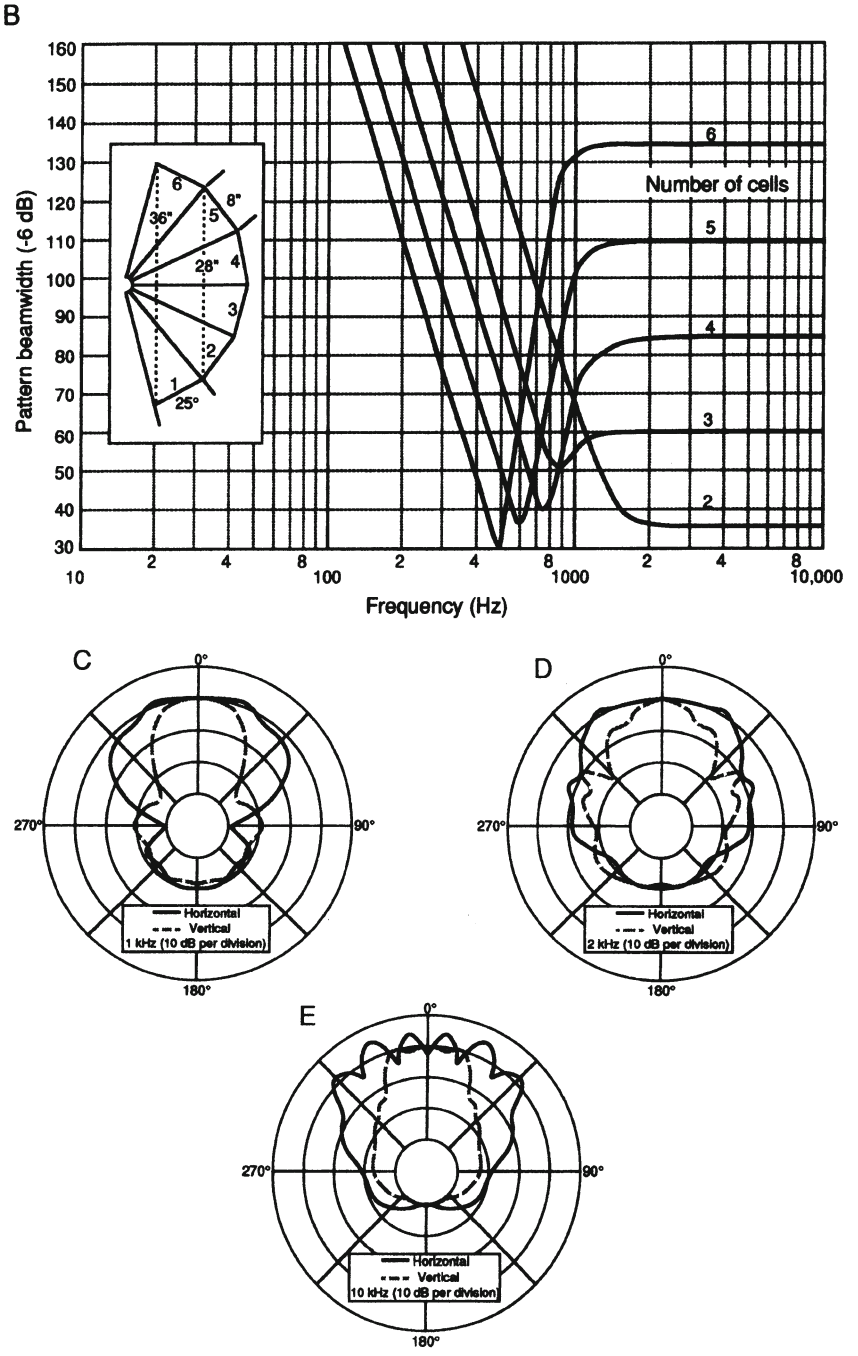

Figure 7-14. Continued.

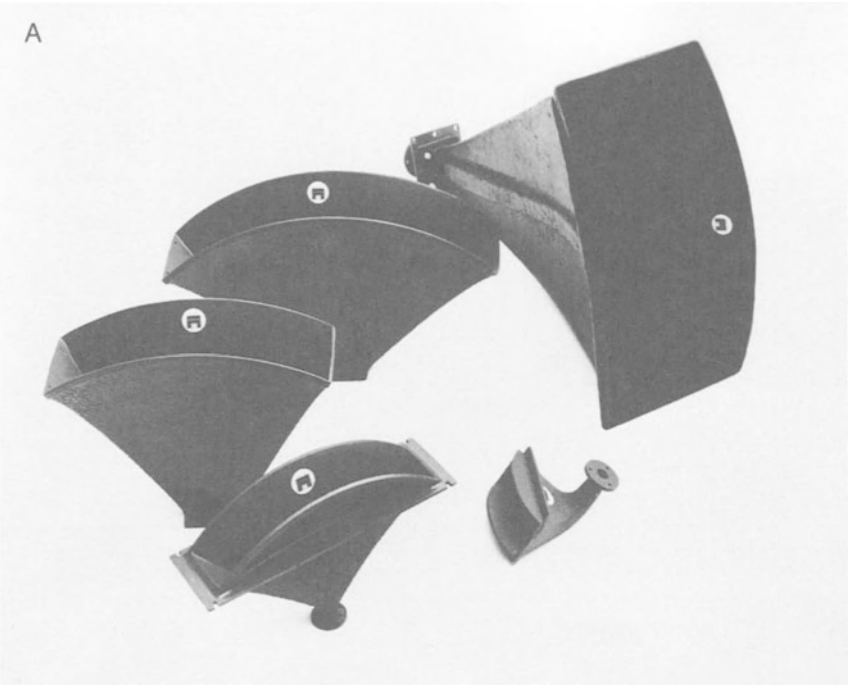

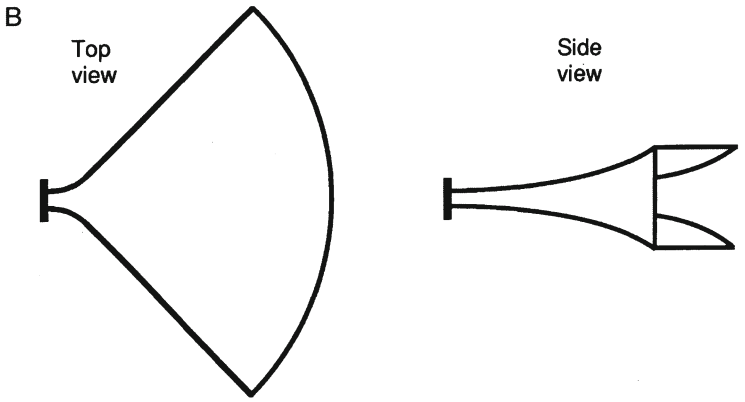

Figure 7-15. The radial horn. Photo of various radial horns (A); top and side views of a radial horn (B); directivity data for JBL model 2345 horn (C). (Data courtesy JBL)

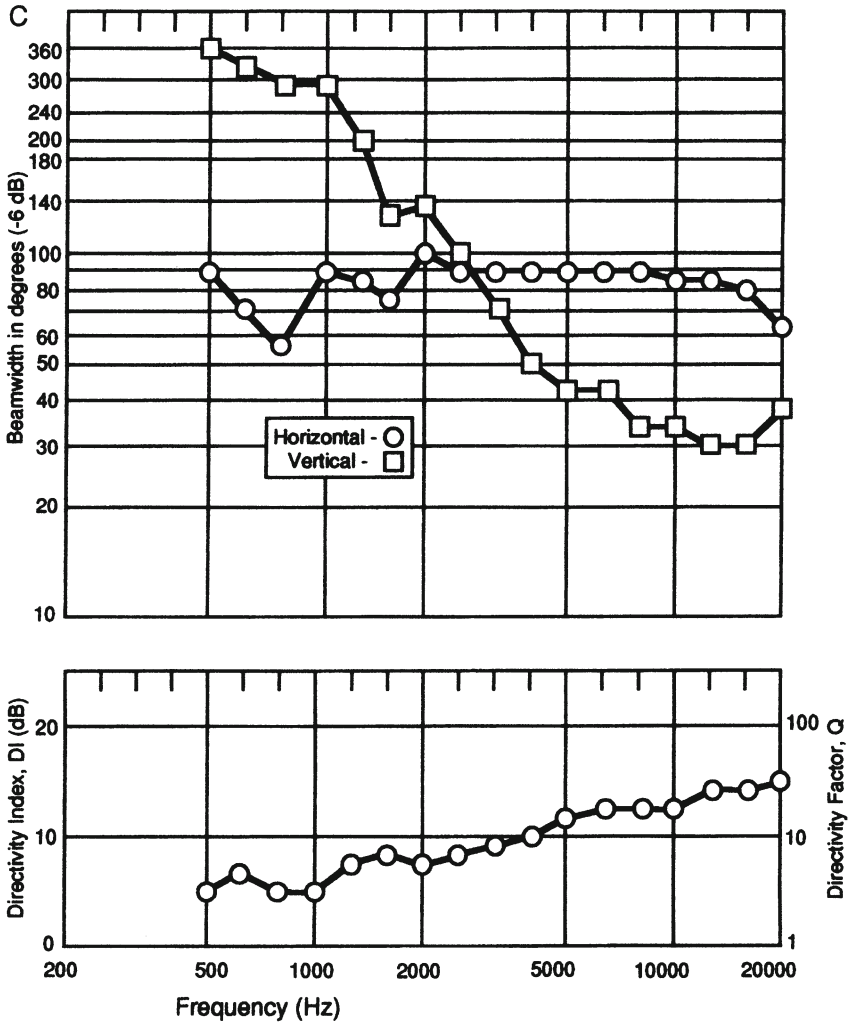

Figure 7-15. Continued.

For applications in which vertical pattern control may not be critical, the radial horn is an excellent choice, and many modern studio monitoring systems are designed with them. The rising directivity index acts as an acoustical equalizer, boosting the on-axis response and counteracting, to a large extent, the driver's roll-off above the mass breakpoint.

7.7.3 Acoustic lenses

Acoustic lenses came into prominence during the 1950s, when they were first used in motion picture systems. Like the multicellular horn, they were developed essentially to compensate for the high frequency beaming of exponential horns.

Figure 7-16A shows a photo of a family of horn-lens combinations. There are three basic lens types, *slant plate*, *perforated plate* and *folded plate*. These three types are shown at *A*. The action of the slant plate and folded plate lenses is shown at *B* and *C*, and the action of the perforated plate is shown at *D*. The folded plate lens is a variation of the slant plate type and functions in the same way.

The lens works by providing a shorter sound path through the middle than at the sides; thus, the wavefront exits the device with greater curvature and hence greater dispersion. The slant plate and folded plate lenses provide wide pattern control only in the horizontal plane, while the perforated plate lens spreads high frequencies in a conical pattern. These distinctions are shown in the figure. Directional properties of the JBL 2307/2308 slant plate lens are shown in Figure 7-16E.

The acoustic lens is rarely used today, but the concept and execution of these designs are held in high esteem by many engineers. They were the hallmark of many of the JBL studio monitors during the 1960s and 1970s.

7.7.4 Diffraction horns

A diffraction horn (Smith 1951) has a mouth that is quite narrow in one plane and fairly wide in the other, as shown in Figure 7-17A. Pattern control in the plane perpendicular to the narrow opening will be quite wide at middle and lower frequencies, since it is largely diffraction controlled. In the other plane pattern control is dictated by the mouth angle. In the case of the horn illustrated here, the mouth defines an angle of 120°, and it is necessary to incorporate a set of tapered vanes inside the horn to maintain wide angle response at high frequencies. The directional characteristics are shown in Figure 7-17B.

Diffraction horns have had considerable application in monitoring systems over the years, and variations of it are in use today.

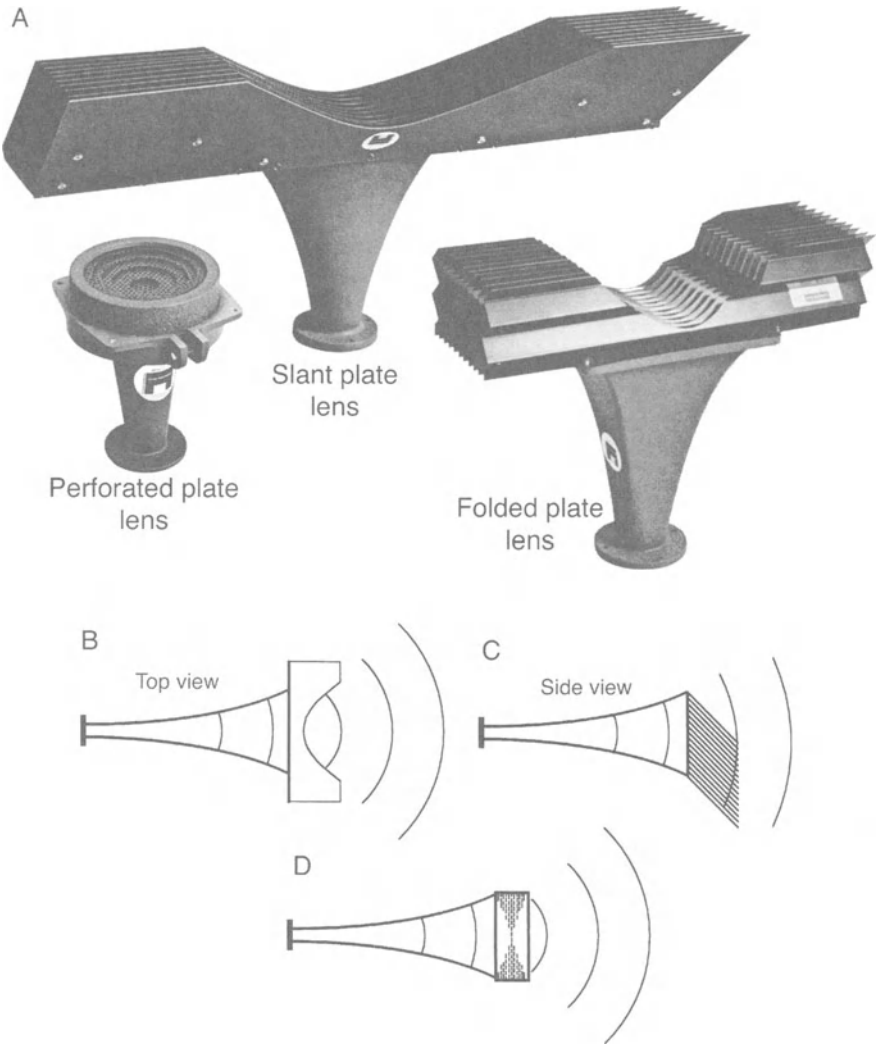

Figure 7-16. The acoustic lens. Photo of various horn-lens combinations (A); side and top views of a slant plate horn-lens (B and C); section view of a perforated plate horn-lens (D); directivity data for JBL 2307/2308 horn-lens combination (E). (Data courtesy JBL)

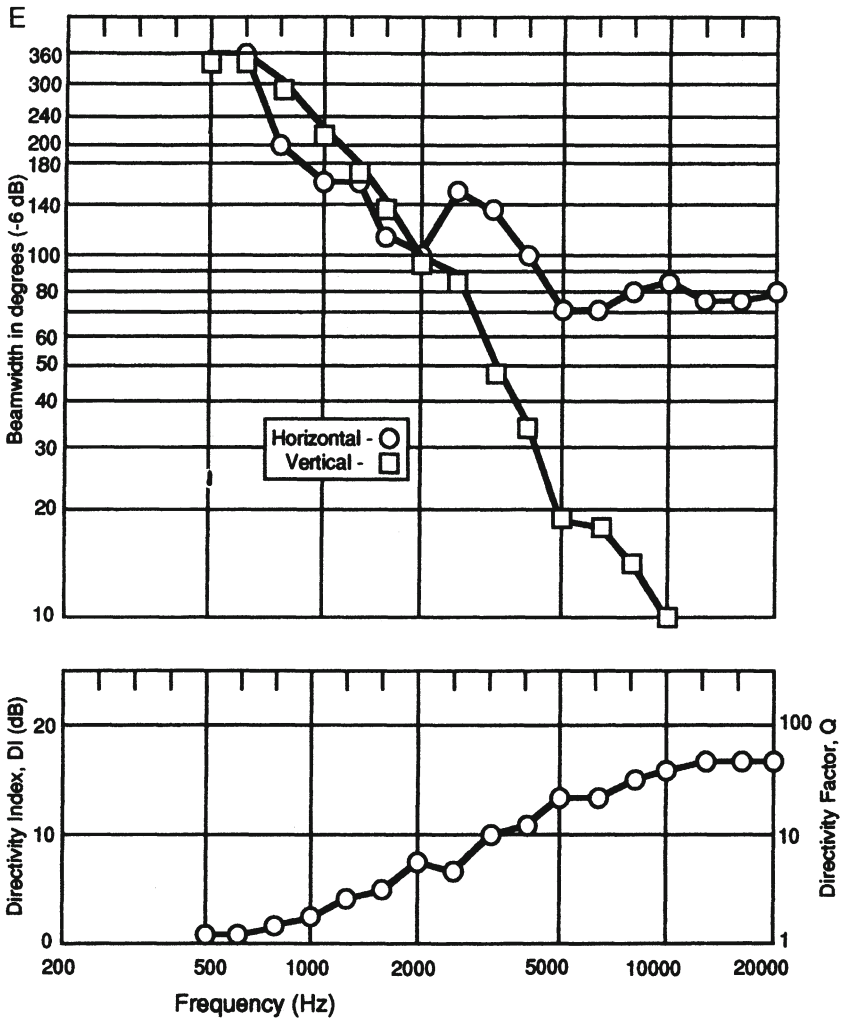

Figure 7-16. Continued.

7.7.5 Uniform coverage horns

In studying the directional data on the horns so far discussed, it is apparent that none of the horns exhibits uniform control in both horizontal and vertical planes. As a general rule, control in the vertical plane has been sacrificed for desired pattern control in the horizontal plane.

During the 1970s and early 1980s, considerable work was done by Henricksen and Ureda (1978) and Keele (1982) in designing horns that were able to maintain uniform pattern control in both planes. Such devices are

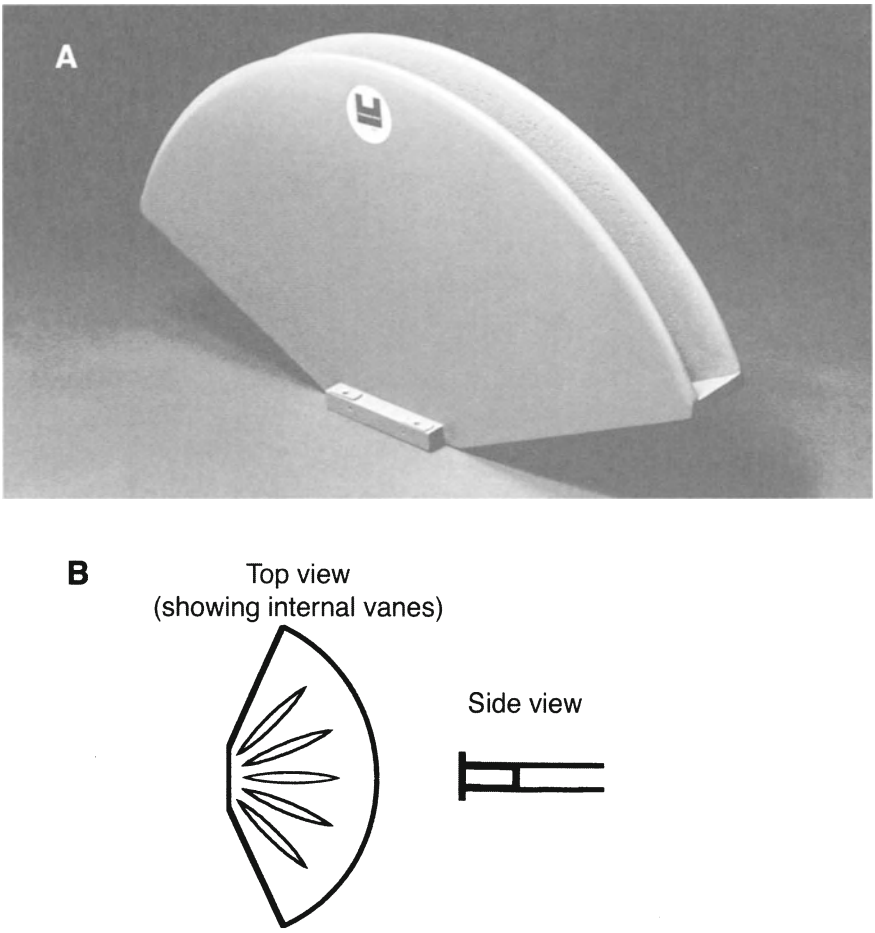

Figure 7-17. The diffraction horn. Photo of JBL 2397 horn (A); structural details of the horn (B); directivity data for 2397 horn (C). (Data courtesy JBL)

universally used today for general sound reinforcement and motion picture work. They are also referred to as *constant coverage* horns.

Figure 7-18A shows a photo of a group of uniform coverage horns. Detailed top and side views of a 90° by 40° uniform coverage horn are shown at *B* and *C*. In the horizontal plane (90° coverage), a curved diffraction slot feeds a large flared bell whose sides have been tapered to maintain the desired 90° coverage angle to 10 kHz and beyond. The initial section of the horn which feeds the diffraction slot is exponential, and the flare rate is determined by the requirement of attaining the desired vertical coverage angle.

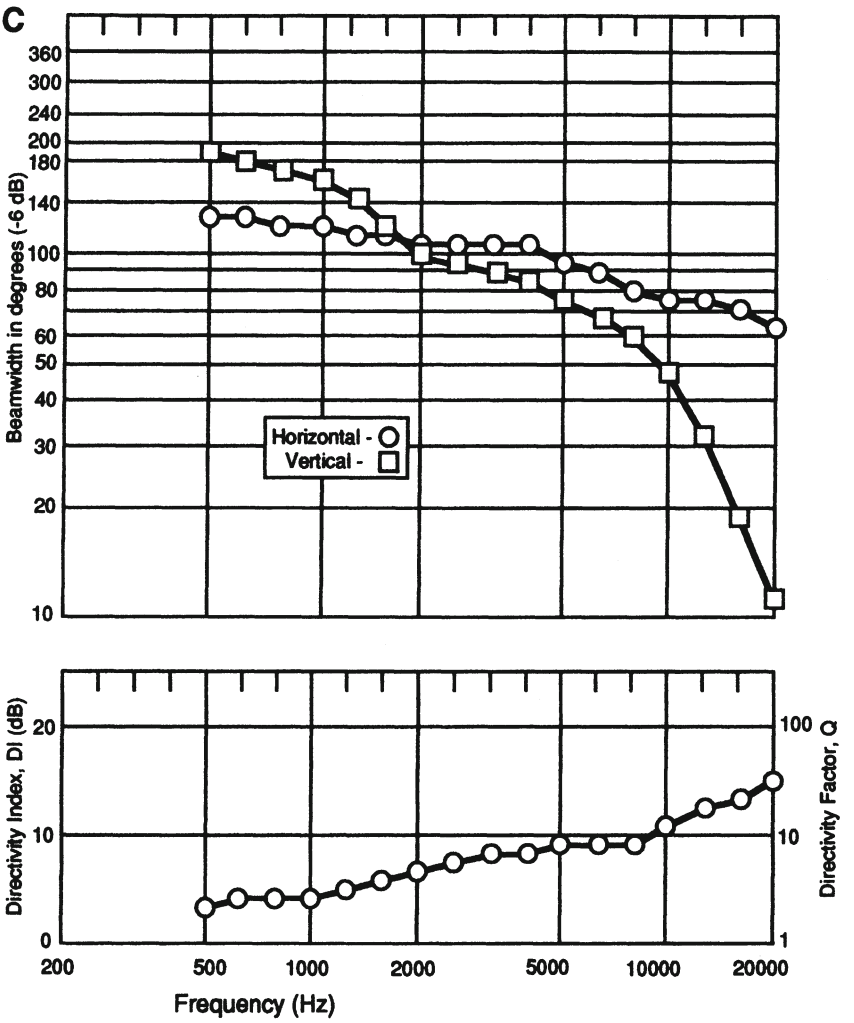

Figure 7-17. Continued.

In the vertical plane (40° coverage), the horn appears to be nearly straight sided, except for a slight flare at the mouth. Directional characteristics are shown in Figure 7-19A. Note that the pattern control in both vertical and horizontal planes is smooth over the frequency decade from 1 to 10 kHz. In both planes the pattern is maintained down to 500 Hz.

Uniform coverage horns have changed the way sound system engineers equalize their systems. Figure 7-19B shows families of on- and off-axis response curves for the JBL 2360 Bi-Radial® horn and the JBL 2350 radial horn. In the upper set of curves, the 2360 horn has been equalized for

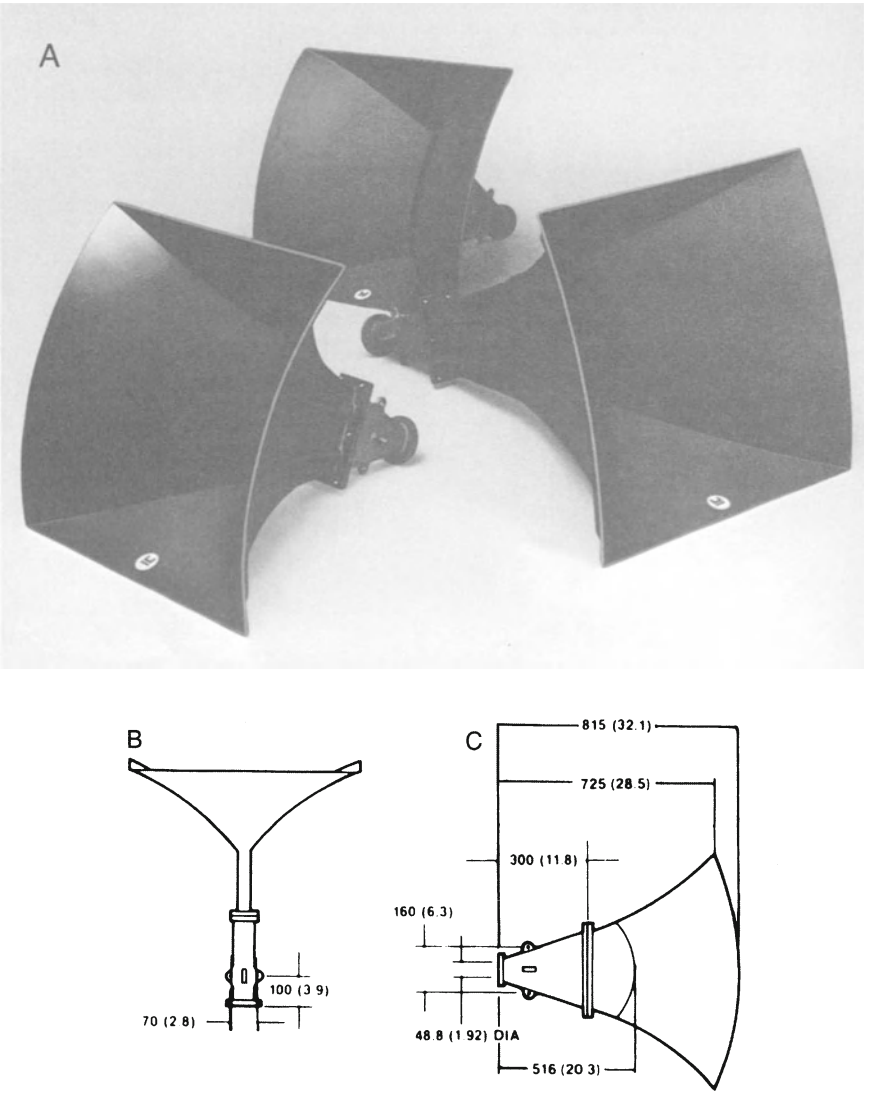

Figure 7-18. The uniform coverage horn. Photo of various uniform coverage horns (A); top view of JBL model 2360 horn (B); side view of 2360 horn (C). (Data courtesy JBL)

approximately flat on-axis response, and you will note that the response at off-axis angles of 15, 30, 45, and 60 degrees is quite uniform.

In the lower set of curves we see the corresponding on- and off-axis response for the 2350 radial horn. No on-axis equalization is needed, inasmuch as the horn's rising directivity index will maintain it fairly flat. However, the

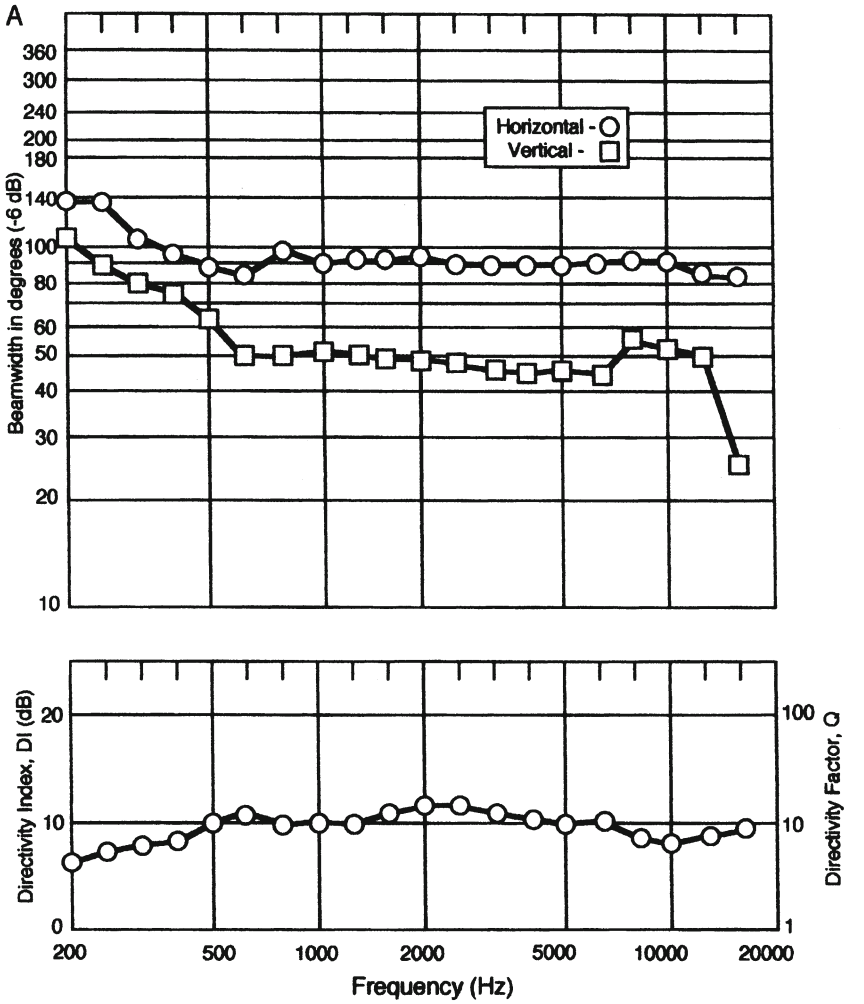

Figure 7-19. Directivity data for JBL 2360 Bi-Radial® horn (A); on- and off-axis data for uniform coverage and radial horns (B). (Data courtesy JBL)

loss of HF pattern control in the horn is obvious as we observe the response at angles of 15, 30, 45, and 60 degrees. There is in fact no way that the radial horn can be equalized to produce a family of off-axis curves similar to those of the uniform coverage horn.

7.7.6 Influence of mouth size on LF pattern control

If a horn is to maintain desired pattern control down to some given low frequency, the horn's cutoff frequency will have to be well below the desired

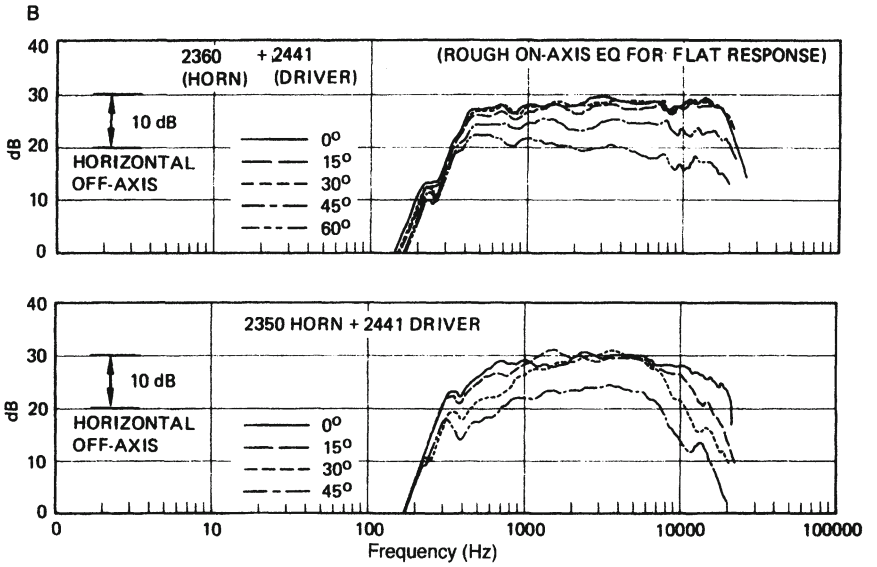

Figure 7-19. Continued.

coverage frequency, and the horn's mouth will have to be of a certain minimum dimension in order to maintain the pattern. A relatively small mouth dimension will be able to maintain, say, a 90° -6 dB beamwidth at a given frequency; however, in order to maintain a beamwidth of, say, 40° at the same frequency, a much larger mouth dimension will be required.

Figure 7-20A shows the approximate behavior of a generic uniform coverage device. The loss of pattern control at LF is a function of the horn mouth dimensions, and the loss at HF is a function of the horn throat dimensions.

The lowest pattern control frequency in each plane is given approximately by the following equation:

$$f = 10^6/h\theta \qquad 7.9$$

where h is the mouth dimension in inches and θ is the nominal –6-dB coverage angle. The corresponding equation in metric units is:

$f = 25 \times 10^6/h\theta$, where h is the mouth dimension in mm.

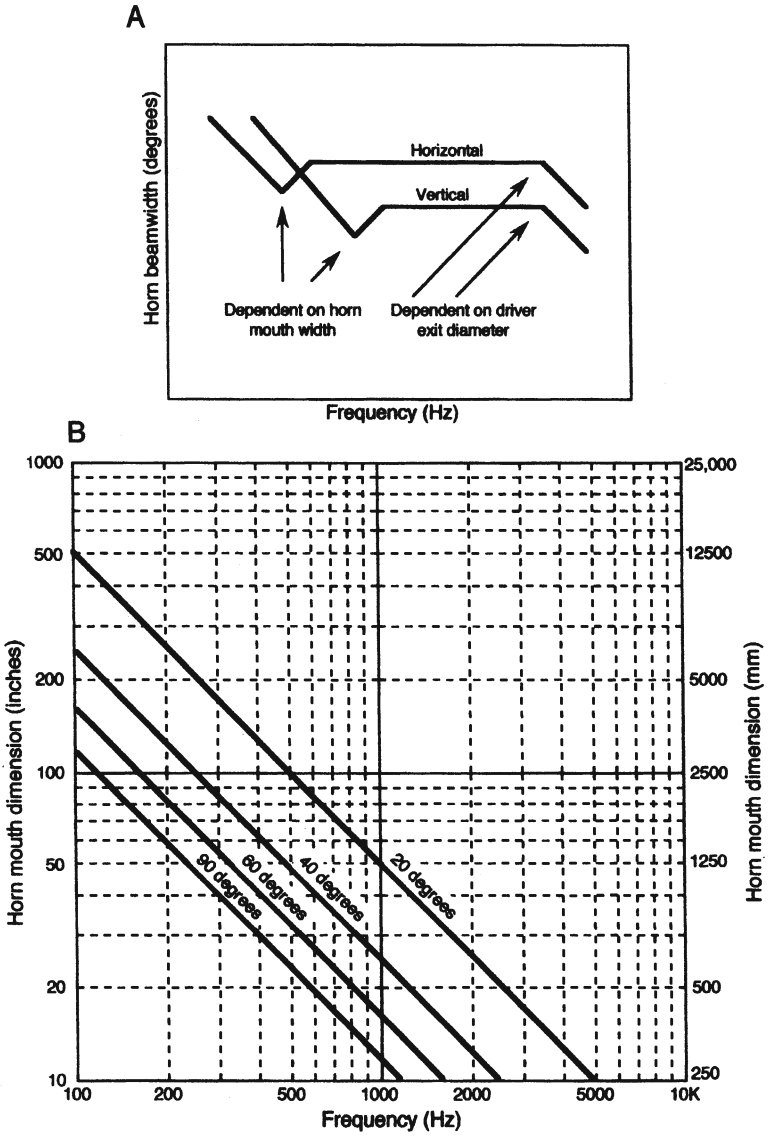

Figure 7-20. Uniform coverage horns. Basic pattern control regimes (A); coverage angle as a function of mouth dimensions and frequency (B).

As an example, the JBL 2360 Bi-Radial horn has a horizontal mouth dimension of 30 inches and a nominal coverage angle of 90°. Entering these values into equation 7.9:

$$f_H = 10^6/(90x30) = 1{,}000{,}000/2700 = 370 \text{ Hz}$$

The vertical coverage angle is 40°, and the mouth dimension in that plane is also 30 inches.

$$f_V = 10^6/(40x30) = 1{,}000{,}000/1200 = 833 \text{ Hz}$$

Figure 7-20B presents solutions to equation 7.9 for several coverage angles.

7.7.7 Horns, waveguides, and coverage

In modern horn design, the term *waveguide* is often encountered. Actually, the designation comes from microwave radio technology, in which RF signals are sent through carefully constructed tubes acting as virtually lossless transmission lines, eventually terminating in a feed to a dish reflector for long distance transmission.

As we have seen, the basic horn designs themselves do not have uniform radiation characteristics at HF. As a general rule in the newer horn designs, only the initial one-third or so of a horn's flare will be exponential, with the remainder of the horn consisting of a diffraction slot terminated with a large bell with rapidly flaring end sections.

These structural features may be seen in several families of horns, including those shown shown in Figure 7-18. The design methodology is discussed in detail in the following references: Henricksen and Ureda (1978), Keele (1982), and Smith, et al. (1983). Further directions are discussed in Geddes (2002).

7.8 Impedance measurements on horns

Figure 7-21 shows superimposed plots of the impedance modulus for the JBL 2445 driver mounted on a PWT and mounted on the JBL 2380 horn. Such variation in impedance is typical of finite length horns, and it is due to mouth reflections back toward the driver. The curve bears some resemblance to the data shown in Figure 7-1F. In general, a 3-to-1 variation in impedance value is acceptable over the passband of the driver-horn combination. Variations in excess of this usually indicate abrupt transitions in the horn flare itself and may become evident as variations in the system's amplitude response.

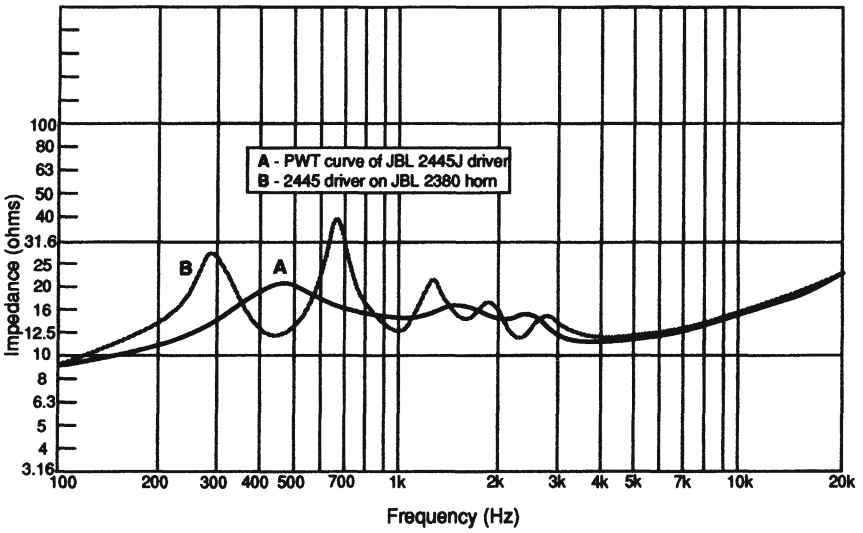

Figure 7-21. Driver impedance on a PWT and horn.

7.9 Distortion in horn systems

The predominant form of distortion in a well designed horn system is second harmonic distortion, which comes as a result of high pressures in the horn's throat. The effect is thermodynamic in origin and can only be reduced by increasing the flare rate so that pressures downstream in the horn are more quickly relieved. Figure 7-22A shows the nonlinearity in the volume-pressure relationship for air, which causes the distortion. The following equation (Thuras 1935) gives the value of 2nd harmonic distortion:

$$\text{Percent 2nd harmonic} = 1.73\ (f/f_C)(I_T)^{0.5} \times 10^{-2} \qquad 7.10$$

where f is the driving frequency, f_c is the horn cutoff frequency, and I_T is the intensity at the throat in watts per square meter. Figure 7-22B presents graphical solutions to this equation. In the figure, however, intensity is expressed as watts per square centimeter, which is 10^{-4} times the value in watts per square meter.

Figure 7-22C shows 2nd harmonic distortion for two driver-horn combinations. For these tests, the fundamental output was maintained flat from 1 kHz to 10 kHz, and the measured 2nd harmonic distortion was raised 20 dB for ease in reading.

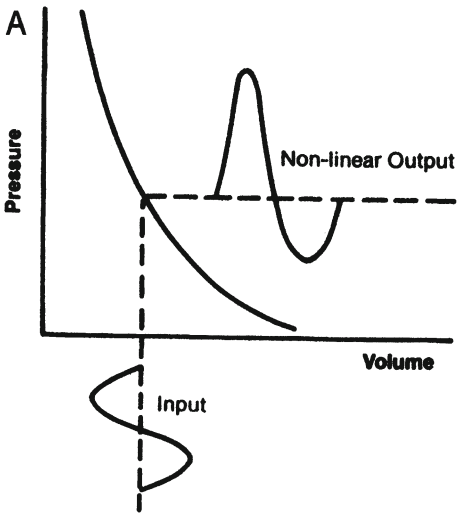

Figure 7-22. Basic thermodynamic distortion mechanism in horn systems (A).

We can compare these measurements with calculations using equation 7.9, as follows:

The JBL 2360/2446 horn/driver combination has a mid-band sensitivity of 113 dB L_p, 1 watt measured at 1 meter. In these tests, the level, referred to 1 meter, was set 6 dB lower to 107 dB at 1 meter for an electrical power input of 0.25 watt. As determined from the driver's PWT measurements, the driver has an efficiency of 40%, so we now know that the acoustical power generated by the driver is (.25)(.4) = 0.1 watt.

The exit diameter of the driver is 50 mm, which has an area of 1.96×10^{-3} m^2. The intensity is then $0.1/(1.96 \times 10^{-3}) = 51$ W/m^2. Thus, at 2 kHz:

$$\text{Percent 2nd harmonic} = 1.73\ (2000/70)(51)^{0.5} \times 0.01 = 3.52\%$$

Checking the data in the graph, we see that the measured distortion reads just below 3%, indicating excellent agreement between calculation and measurement (a difference of about 1.3 dB). The JBL 2352 horn has a much higher cutoff frequency in both driver and horn flare development, resulting in distortion 6 to 8 dB lower than the 2360 horn.

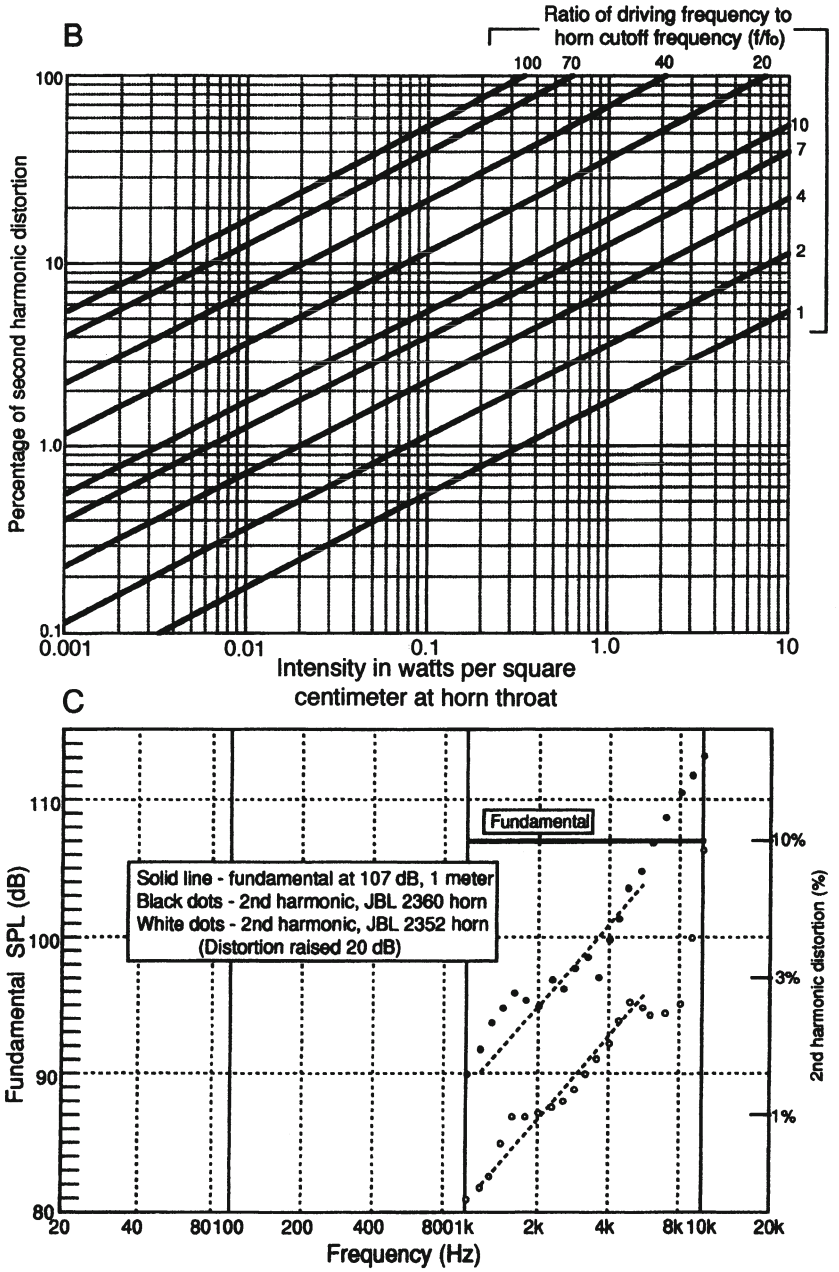

Figure 7-22. Continued. Graph for determining second harmonic distortion in horn systems (B); example of rapid and slow flare rate horn distortion (C). (Data at *C* courtesy JBL)

7.10 Horn driver protection

In many applications, high frequency horn systems carry a large portion of the acoustical load, with very high crest factors when HF power response equalization is added to the signal input. Also, in other applications, there may be low frequency surges when amplifiers are turned on. Either effect here can cause driver damage and care must be taken so that the devices are not unduly stressed.

Low frequency protection can be provided by placing a high quality capacitor in series with the driver using values taken from Table 7.1.

Table 7.1. Blocking capacitor values for horn driver protection

Capacitor value:	For protection below these frequencies:		
	16 ohms	8 ohms	4 ohms
72 μF	275 Hz	550 Hz	1000 Hz
52	400	750	1500
20	1000	2000	4000
16.5	1200	2500	5000
13.5	1500	3000	6000
12	1700	3500	7000
8	2500	5000	10,000
7	3000	6000	12,000
6	3500	7000	14,000
4	5000	10,000	—
3	7000	14,000	—

The values are selected to present a reactance at one-half of the crossover frequency equal to the nominal impedance of the driver.

HF limiting can be used for driver protection, and if properly applied its audible effects will be very slight, if noticeable at all. The methods shown in Figure 7-23 have been used for passive driver protection at high frequencies. The method shown at *A* and *B* uses back-to-back Zener diodes chosen to clamp the signal to the driver at the desired voltage maximum values. Consult the driver manufacturer for details before doing this. The effects may be quite audible if used in prolonged high-level application.

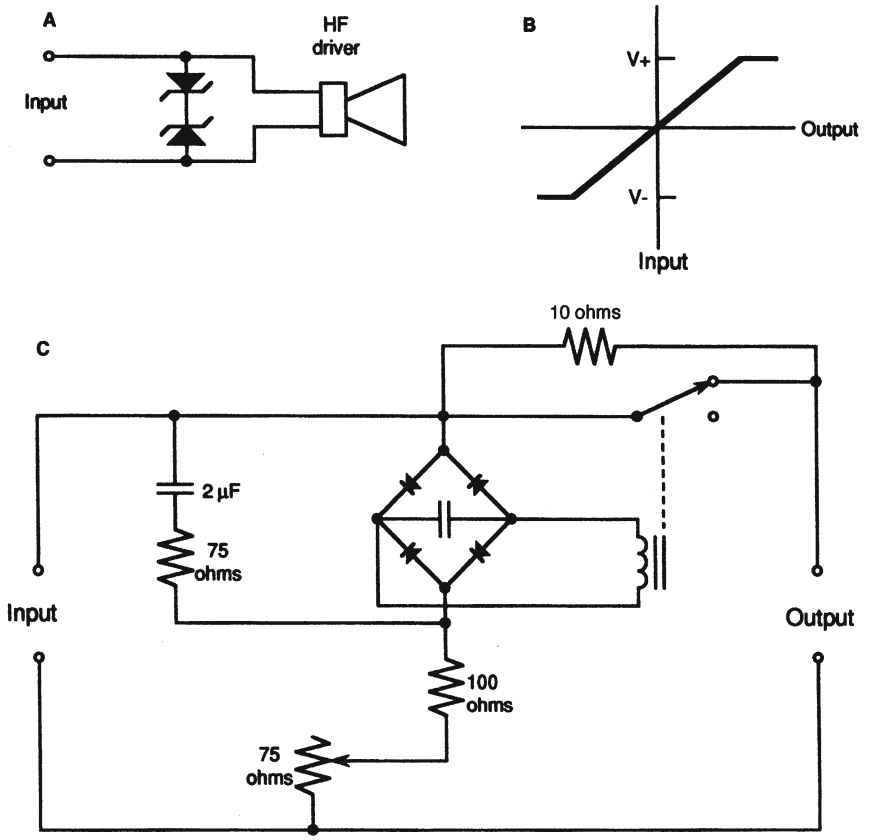

Figure 7-23. HF driver protection. Zener diodes (A) can be used to clamp the signal to a safe voltage (B); a relay can be used to reduce the level of HF signals fed to the driver (C).

The bridge circuit shown at *C* was developed by Electro-Voice and provides a rectified voltage for operating a relay in series with the HF driver. When the relay is actuated, a 10 ohm resistor is placed in series with the driver, reducing the signal to a safer level.

Many small systems include *varistors* in the design of dividing networks. Varistors are elements whose resistance at normal temperatures is quite low, rising significantly when their temperature increases. These elements can be placed in series with fixed resistors to limit the amount of high-level signal reaching HF drivers.

7.11 Lower midrange and LF horn drivers

During the 1980s a few manufacturers developed drivers and horns to cover the frequency range from approximately 250 Hz to 2500 Hz. Below 250 Hz, specially designed cone drivers are normally used, but in the critical frequency decade from 250 to 2500 Hz, a compression driver format is necessary. Figure 7-24 shows several solutions; the Community M-4 is shown at *A*, and the JBL 2490 is shown at *B*. The M-4 has an effective diaphragm diameter of 168 mm (6.65 in) and a voice coil diameter of 114 mm (4.5 in). The exit diameter is 102 mm (4 in). The 2490 has a voice coil diameter of 100 mm (4 in) and an exit diameter of 76 mm (3 in).

Figure 7-24C and *D* show solutions that use specially designed cone drivers with accompanying phasing plugs to provide the necessary transformation ratios. The JBL model shown at *C* uses an annular slit phasing plug, and the EAW model at *D* uses radial slits.

7.12 LF horns

In the early days of motion picture sound, screen loudspeaker systems made use of horn elements throughout because of their efficiency. A 10-watt amplifier was about the limit of what was available, and loudspeaker efficiencies in the 25 to 35% range were necessary to produce the desired volume of sound. Figure 7-25 shows details of what is probably the only LF compression driver ever designed. It was developed by Bell Telephone Laboratories for experimental long distance sound transmission in the early 1930s. At that time there were no LF cone devices with the necessary parameters for driving horns directly, so a compression driver with an 8 in (200 mm) dome was developed. It was used in the system shown in Figure 7-27.

Today, virtually all LF horns are driven by cone devices whose primary characteristics are low cone mass and high *Bl* product. Keele (1977) determined the cone driver parameters necessary for successful horn application, and the data shown in Figure 7-26 can be used for determining the various response breakpoints with a given set of Thiele-Small LF parameters.

As seen in the figure, there will be a region of flat power response bounded by f_{LC} at low frequencies and by f_{HM} at higher frequencies. Beyond f_{HM} there will be two additional breakpoints in the response envelope due to voice coil inductance and the effect of the air chamber directly in front of the transducer's

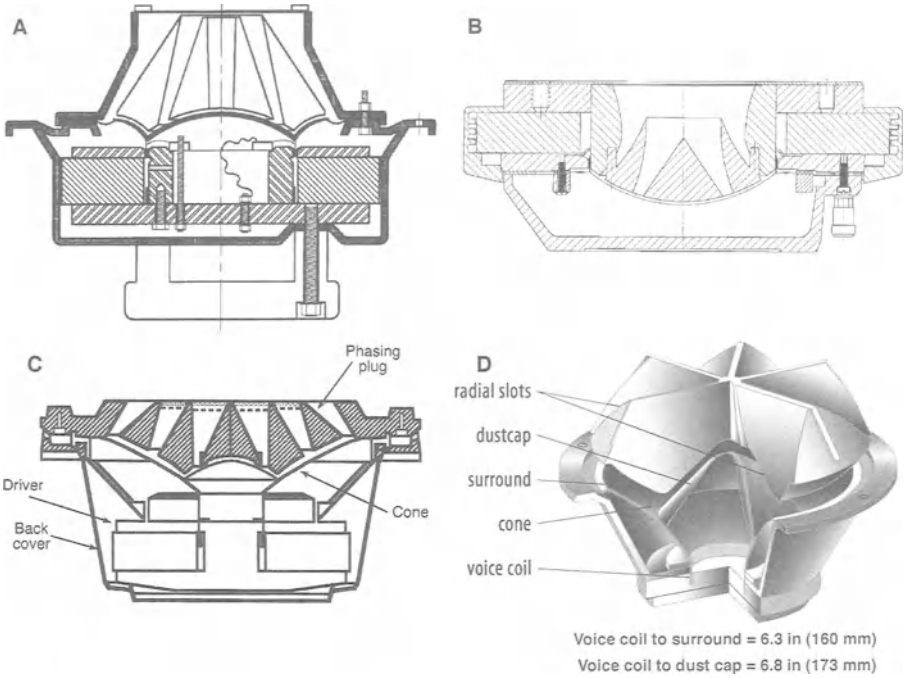

Figure 7-24. MF compression drivers. Community M-4 (A); JBL 2490 (B); cone driver mounted with annular slit phasing plug (C); cone driver mounted with radial slits (D). (Data at *A* courtesy Community; data at *B* and *C* courtesy JBL; data at *D* courtesy EAW)

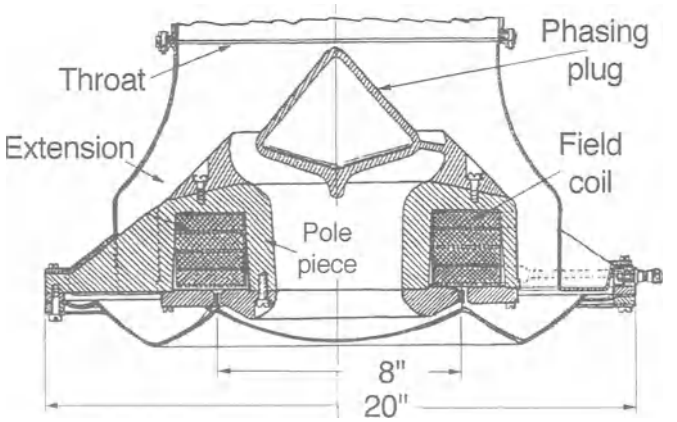

Figure 7-25. A low frequency compression driver designed by Bell Telephone Laboratories.

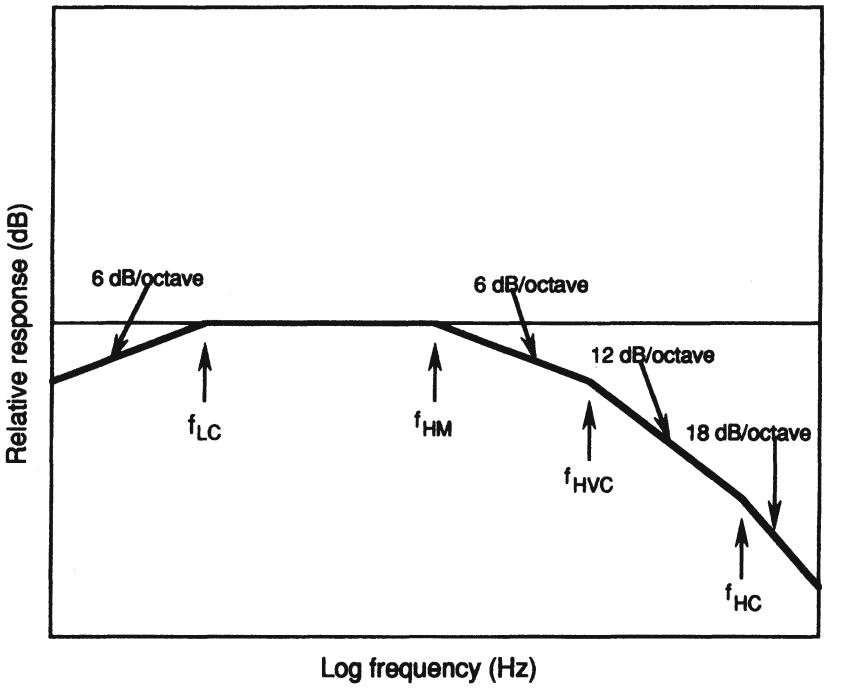

Figure 7-26. Selecting cone drivers for LF horn use.

diaphragm. Each of these will add a 6 dB/octave rolloff to the overall response curve. The various breakpoints are defined as follows:

$$f_{LC} = (Q_{TS})f_S/2 \qquad 7.10$$
$$f_{HM} = 2(f_S)Q_{TS} \qquad 7.11$$
$$f_{HVC} = R_E/\pi L_E \qquad 7.12$$
$$f_{HC} = (2Q_{TS})f_S(V_{AS}/V_{FC}) \qquad 7.13$$

where:

Q_{TS} = total Q of transducer
f_S = free-air resonance of the transducer
R_E = voice coil dc resistance (ohms)
L_E = voice coil inductance of the transducer (henrys)
V_{AS} = volume of air that provides a restoring force equal to that of the driver's mechanical compliance (liters)
V_{FC} = volume of front air chamber (liters)

These quantities are analogous to those studied earlier in the discussion of HF compression drivers.

7.12.1 Re-entrant horns

There have been very few LF re-entrant horns, and perhaps the best known example is that shown in Figure 7-27. The system was used in Bell Telephone Laboratories' experiments in long distance sound transmission and were never commercially available. With a path length approaching 9 feet and a mouth area of nearly 25 square feet, the system provided response down to 50 Hz.

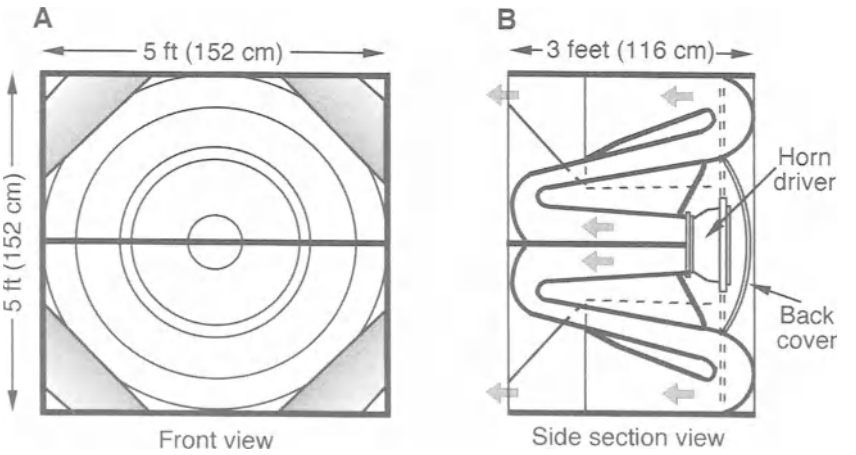

Figure 7-27. Bell Telephone Laboratories LF system. Front view (A); section view (B).

7.12.2 Folded horns

During the 1940s and 1950s a number of consumer folded LF horn systems were developed. The most notable here was the Klipschorn, and the LF section is shown in three views in Figure 7-28A. It was designed for corner placement, with the walls and floor of the room extending the horn outward. The system provided considerable low distortion output down to about 35 Hz. The JBL Hartsfield LF section is shown at B. It covered the same approximate range as the Klipschorn but never attained the general acceptance of the Klipsch model.

Both of these systems addressed a high-end market that barely exists today. The Hartsfield was discontinued three decades ago, and the Klipschorn was redesigned in a simpler form during the latter 1990s. Nevertheless, owners of these systems hold them in the highest esteem.

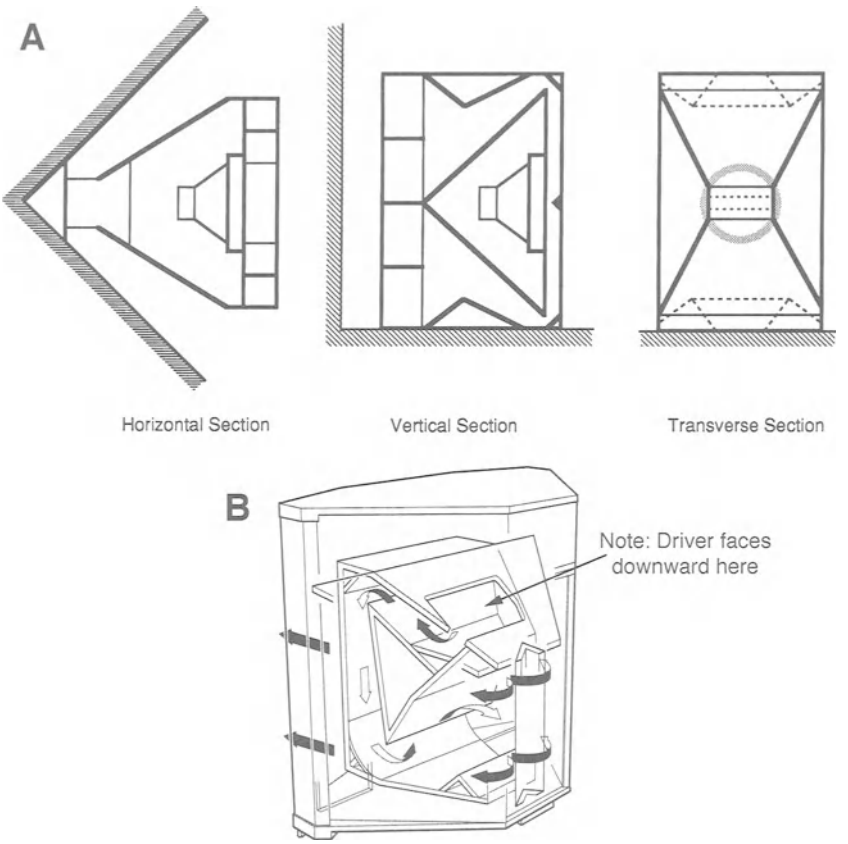

Figure 7-28. Folded LF horns. Klipschorn (A); JBL Hartsfield (B).

7.12.3 Hybrid LF horns

The sound and music reinforcement industries have over the years produced a wide variety of LF systems, many of them combining horn sections with ported direct radiating sections or with direct radiating cone drivers. The ported front-loaded horn system shown at *A* has on-axis response as shown at *B*. Note that there is a step-down in output as the horn portion of the system unloads and the ported section comes into play. These systems were used in both single an dual driver form, and the dual version had significant response down to about 40 Hz.

The rear-loaded horn shown at *C* exhibited rather choppy response, as shown at *D*, due to the partial cancellation between direct and horn outputs.

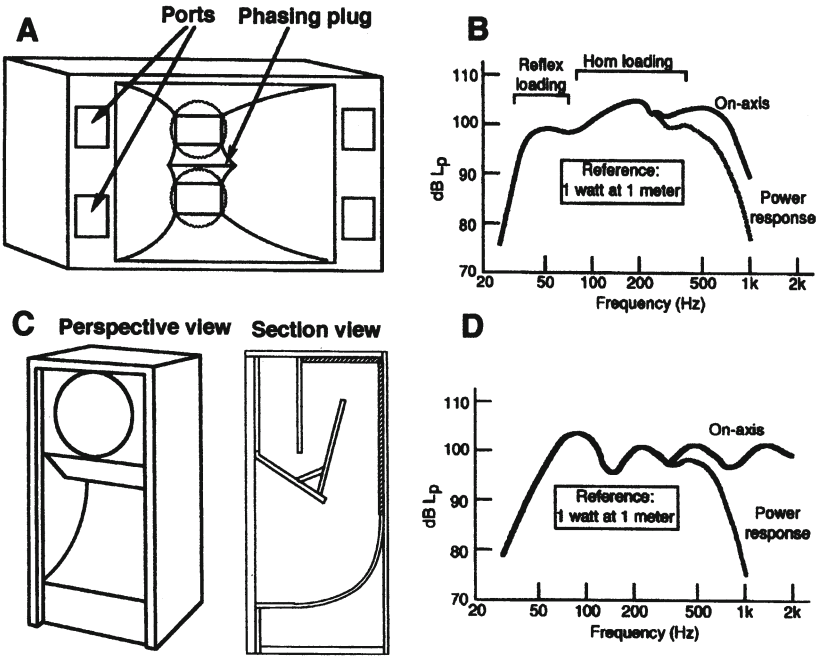

Figure 7-29.Hybrid LF horns. Front loading (A and B); back loading (C and D). (Data courtesy JBL)

7.12.4 Straight horns

Straight LF horns have generally been used in music reinforcement. Many of these are of moderate size and are used primarily for directional control in the mid-bass down to the 50 - 60 Hz range. Details are shown in Figure 7-30.

7.13 Horn arrays

Horns are very useful in many professional sound applications because precise directional properties can be designed into them. Furthermore, horn arrays can be assembled both to narrow their coverage angles as well as widen them. Some of the options here are shown in Figure 7-31, where vertical stacking of horns can be used to increase low and mid-frequency directivity in the vertical plane. If this technique is taken beyond three horns, then lobing in the vertical plane may defeat the advantages that have been gained (JBL 1984).

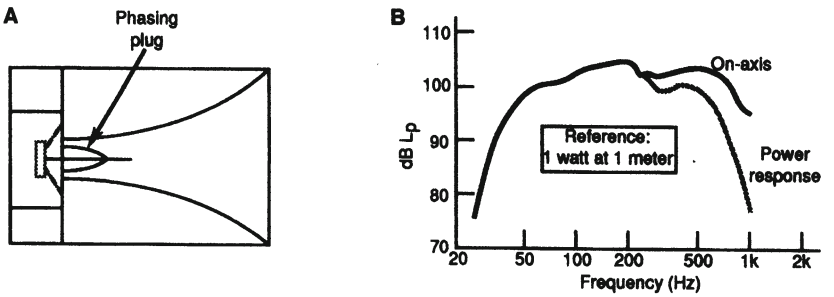

Figure 7-30. Front loading LF horns. Section view (A); typical response (B).

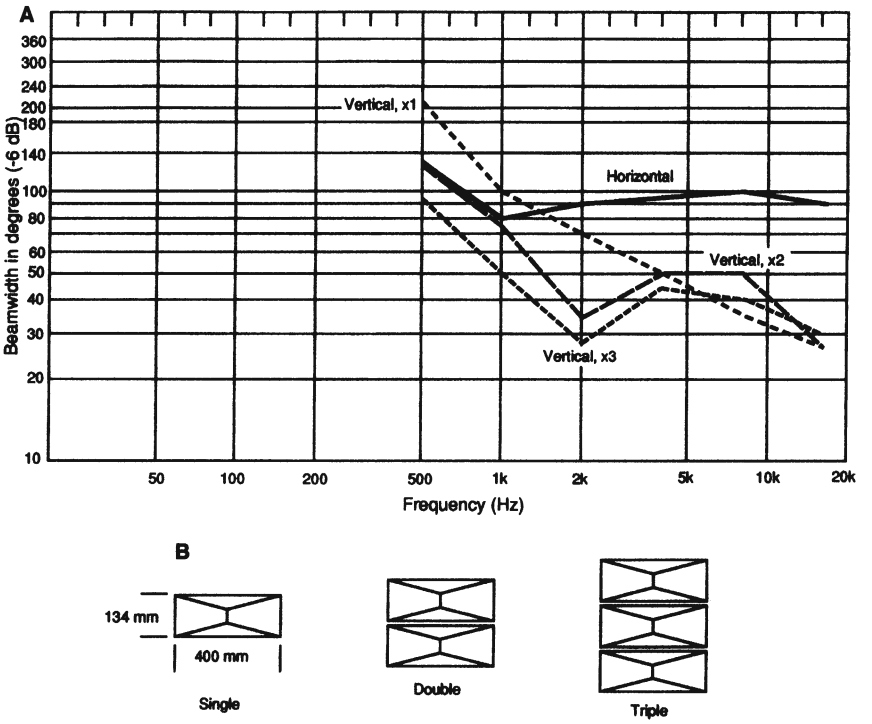

Figure 7-31. HF horn stacking to provide higher vertical directivity. Beamwidth data (A); stacking configurations (B).

The beamwidth data is shown at *A*, and the three stacking versions are shown at *B*. For speech reinforcement applications, the reduced beamwidth in the 2 kHz octave range will improve speech intelligibility because the horns may be stacked and splayed along their -6-dB coverage zones to increase the horizontal coverage, as shown in Figure 7-32. Beamwidth data is shown

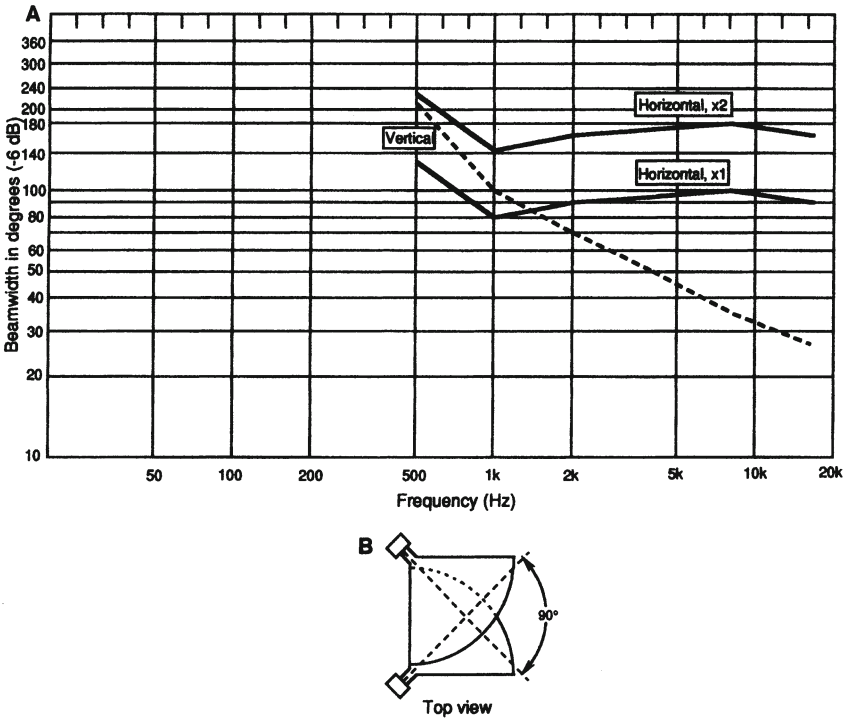

Figure 7-32. Stacking and splaying of horns to increase horizontal coverage. Beamwidth data at (A); stack-splay data at (B).

at *A*, and the stack-splay configuration is shown at *B*. Both horns individually have 90° horizontal coverage, so they have splayed by 90° for a total horizontal coverage angle of 180°.

BIBLIOGRAPHY AND REFERENCES:

Beranek, L, *Acoustics*, John Wiley & Son, New York (1954), reprinted by ASA 1993.

Eargle, J., *Electroacoustical Reference Data*, Kluwer Academic Publishers, Boston (1994).

Edgar, B., "The Tractrix Horn Contour," *Speaker Builder*, volume 2, 1981.

Frayne, J. and Locanthi, B., "Theater Loudspeaker System Incorporating an Acoustic Lens Radiator," *J. Society of Motion Picture and Television Engineers*, volume 63 (September 1954).

Geddes, E., *Audio Transducers*, ISBN 0-9722085-0-X (2002).

Henricksen, C. and Ureda, M., "The Manta-Ray Horns," *J. Audio Engineering Society*, volume 26, number 9 (Sept 1978).

Hilliard, J. and Clark, L "Headphones and Loudspeakers," Chapter VII in *Motion Picture Sound Engineering*, D. Van Nostrand, New York (1938).

JBL, Technical Note 1(7), Northridge, CA (1984).

JBL, Technical Notes 1(8), Northridge, CA (1985).

Johansen, T., "On the Directivity of Horn Loudspeakers," *J. Audio Engineering Society*, vol. 42, no. 12 (1994).

Keele, D., "What's so Sacred about Exponential Horns?" presented at the 51st Convention of the AES, *J. Audio Engineering Society* (abstracts) vol. 23, p. 492 (1975); convention preprint 1038.

Keele, D., "Low Frequency Horn Design Using Thiele-Small Driver Parameters," presented at AES Convention, Los Angeles, CA, May 1977. Preprint number 1250.

Keele, D. "Optimum Horn Mouth Sizes," presented at the 46th AES Convention, New York, September 1973; convention preprint 933.

Keele, D., U. S. Patent number 4,308,932 (1982).

Kinoshita, S., Locanthi, B., et al., "Design of a 48-mm Beryllium Diaphragm Compression Driver," presented at AES 60th Convention, 2-5 May 1978 (Preprint number 1364).

Kinoshita, S. and Locanthi, B., "The Influence of Parasitic Resonances on Compression Driver Loudspeaker Performance," Presented at AES 61st Convention, 3-6 November 1978 (Preprint number 1422).

Klipsch P., "A Low-frequency Horn of Small Dimensions," *J. Acoustical Society of America*, vol. 18, pp.137-144 (1941).

Kock, W., and Harvery, F., "Refracting Sound Waves," *J. Acoustical Society of America*, volume 21, number 5 (September 1949).

Lansing, J. and Hilliard, J., "An Improved Loudspeaker System for Theaters," *J. Society of Motion Picture Engineers*, vol. 45, pp.339-349 (1945).

Locanthi, B., "Application of Electric Circuit Analogs to Loudspeaker Design Problems," *J. Audio Engineering Society*, vol. 19, p.778-785 (1971).

Olson, H. Acoustical Engineering, D. Van Nostrand, New York (1957), reprinted by Professional Acoustical Journals, 1991.

Plach, D., "Design Factors in Horn-Type Speakers," *J. Audio Engineering Society*, volume 1, number 4 (1953).

Post, J. and Hixson, E., "A Modeling and Measurment Study of Acoustic Horns," dissertation, University of Texas at Austin, Department of Electrical and Computer Engineering , May 1994.

Salmon, V. "Hypex Horns," *Electronics*, volume 14, p. 39 (1941).

Smith, B. "A Distributed-Source Horn," *Audio Engineering*, (Jan 1951).

Smith, D., Keele, D., and Eargle, J., "Improvements in Monitor Loudspeaker Systems," *J. Audio Engineering Society*, volume 31, number 6 (June 1983).

Wente, E. and Thuras, A., "Auditory Perspective: Loudspeakers and Microphones," *Electrical Engineering*, January 1934.

Voishvillo, A., and Surupov, S., U. S. Patent 5,537,481 (1996)

Thuras, A. "Extraneous Frequencies Generated in Air Carrying Intense Sound Waves," *J. Acoustical Society of America*, volume 6, pp. 173-180 (1935).

Voigt, P., British Patent 278,098, "Improvements in Horns for Acoustic Instruments," 1927.

Chapter 8:
THE ELECTRONIC INTERFACE

8 Introduction

In this chapter we will deal with the interface between amplifier and loudspeaker. Subjects will include the detailed nature of the loudspeaker load, amplifier characteristics, line losses, parallel and series operation of both amplifiers and loudspeakers, and multi-amplification.

8.1 The power amplifier

The great majority of amplifiers used today are solid state, or transistor, designs. The art has progressed steadily over decades, and a very high order of performance is now available. Nevertheless, there are many audiophiles who still prefer vacuum tube designs, be they older models or newer ones.

Figure 8-1 shows a simplified signal flow diagram of one channel of a modern solid state stereo amplifier. In normal operation it is essential that both output voltage and current be constrained to certain limits. As opposed to tubes, transistors will fail catastrophically if certain limits are exceeded, even if only for very brief times.

An oscilloscope can be used to monitor both the input and output of an amplifier, as shown in Figure 8-2. Here, the input signal is fed to the horizontal (x-axis) deflection plates in the oscilloscope and the output signal is fed to the vertical (y-axis) deflection plates. The amplifier gain has been adjusted so that the voltages fed to the oscilloscope are the same. In this example, the output stages have been driven into clipping, and the ± output voltage limits are clearly shown.

We can also use the oscilloscope to observe output voltage and output current relationships, as shown in Figure 8-3. If the load on the amplifier is resistive, current and voltage will be in phase with each other, and a diagonal line will be traced on the face of the scope, as shown at *A*. If the load is both

J. Eargle, *Loudspeaker Handbook*

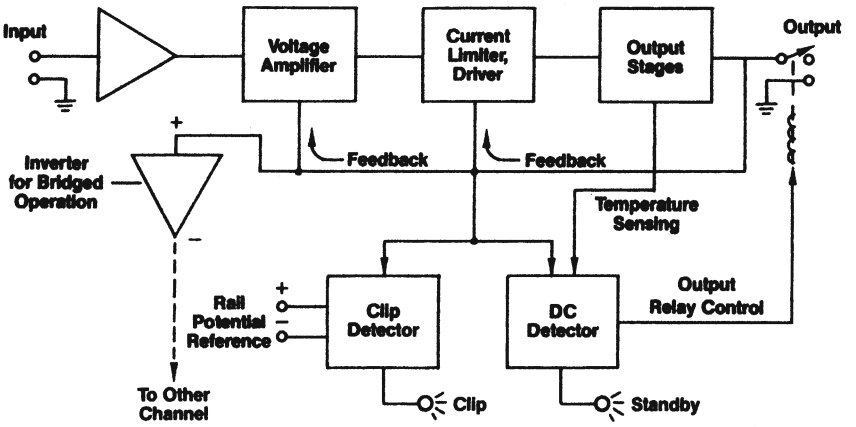

Figure 8-1. Simplified view of one half of a stereo solid state power amplifier. (Courtesy JBL)

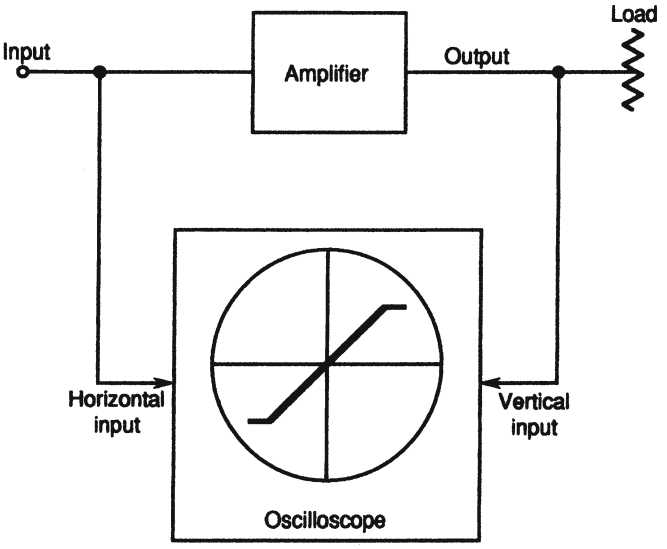

Figure 8-2. Monitoring input and output of an amplifier with an oscilloscope.

resistive and reactive, as many loudspeakers are, the current-voltage relationship will be elliptical, as shown at *B*. The actual phase angle may be computed from the ratio of height of the ellipse and the y-axis intercept as:

$$\text{Phase angle} = \cos^{-1}(a/b) \qquad 8.1$$

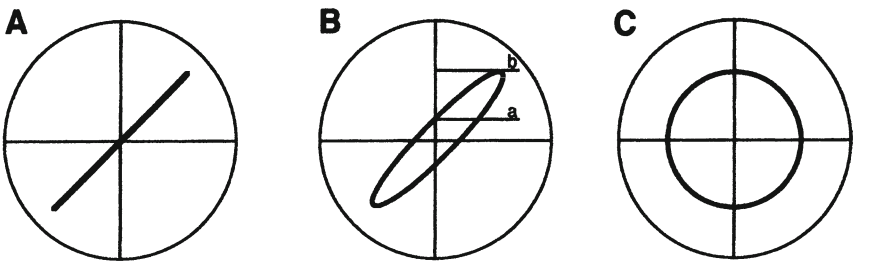

Figure 8-3. Scope figures. Current and voltage with a resistive load (A); a load with both resistive and reactive components (B); a load that is purely reactive (C).

If the load is purely reactive, such as a capacitor, the scope trace will be circular, indicating that voltage and current are 90° with respect to each other, or in *quadrature*. Under this condition, no net power is transferred to the load. Power fed to the load on one half-cycle is returned to the amplifier on the next half-cycle.

The signal returned to the amplifier from the reactive element on the negative half-cycle is referred to as back EMF (electromotive force), or back voltage. In the case of high efficiency loudspeaker systems, the back EMF may cause trouble, in that it may force the amplifier to pass current when the output voltage is zero. This is a problem that is usually discussed under the subject of safe operating conditions for the amplifier. Amplifier users manuals normally discuss the liabilities involved under all conditions of loading.

8.1.1 Amplifier current and voltage limits

An amplifier is designed with fixed output current and voltage limits, and there are additional limits based on the instantaneous relation between the two. Early solid state amplifiers often had little or no protection against short-circuited outputs, and transistor failure was common. Later amplifiers have solved these problems, often, some would say, at the expense of sonic integrity. The better engineered an amplifier is, the more tolerant it will be of adverse loading – going in and out of its protection modes, as needed, with little degradation of sound.

From a loudspeaker design viewpoint, every effort should be made to keep the load from becoming too reactive or too low in resistance. As a target, the phase angle of the load should never exceed ±60° and the lowest resistive load

value presented by the loudspeaker over its operating pass band should not be less than about 80% of the nominal load value.

8.1.2 The basic design impedance

We can define the impedance at which the amplifier can deliver its maximum amount of power:

$$Z = E_{max}/I_{max} \qquad 8.2$$

Most professional amplifiers today will have a design impedance in the range of four ohms or slightly less, inasmuch as this is normally about as low a value of impedance as engineers would choose to operate a system.

8.1.3 Damping factor

For most practical purposes we can assume that the source impedance of a modern power amplifier is virtually zero. That is, the output section behaves as a constant voltage source, regardless of variations in the load itself. Strictly speaking, there is a finite source impedance looking back into the amplifier; this is known as *damping factor* and is defined as:

$$\text{Damping factor} = R_L/R_g \qquad 8.3$$

where R_L is the nominal value of the load and R_g is the source resistance of the amplifier's output section. Details are shown in Figure 8-4. Values of damping factor in the range of 200 to 250 are common. Damping factor is measured by loading down the amplifier's output with increasingly low resistance until the output voltage has dropped to one-half of its open-circuit value. When this condition is reached, the value of the load equals that of the internal source impedance of the amplifier.

8.2 Line losses

Much more significant than amplifier source resistance is the effect of line resistance between the amplifier and load. Tables 8.1 and 8.2 show values for different gauges of copper wire, both solid and stranded. In most professional sound installations today, it is standard practice for power amplifiers to be located at or very near their respective loudspeakers, thus ensuring minimum line losses.

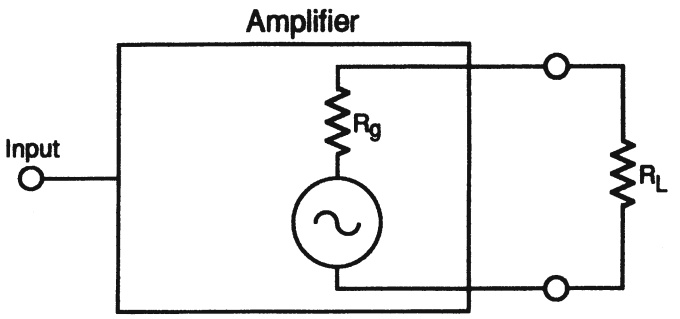

Figure 8-4. Measurement of amplifier-load damping factor.

Line losses may be calculated by the method shown in Figure 8-5. The equation to be solved here is:

$$\text{Loss in dB at the load} = 20 \log \{R_L/(R_L + 2R_l)\} \quad 8.4$$

Note that the loss at the load in dB as given here results from *two effects*; one is the actual loss in the line and the other is the loss due to the target impedance mismatch at the load itself.

A great deal of money can be spent on system wiring, perhaps more than really needs to be. One beneficial fallout of expensive cable is the generally high quality of the connectors themselves. In this regard, it is a good thing to periodically disconnect a system and reconnect it, making sure that all connections are positive and clean. Any signs of corrosion should be thoroughly cleaned.

The reader should also bear in mind that the loudspeaker itself has a dc resistance that may be in the range of 5 or 6 ohms. Common sense tells us that an additional series resistance of perhaps one-hundredth that value should have little if any audible effect on the loudspeaker's performance. However, if line losses are excessive, say, in the range of 1 or 2 ohms, the predominant audible effect may be a change in the frequency balance of the loudspeaker, due to the interaction of line resistance with the varying impedance of the loudspeaker with respect to frequency.

8.2.1 Series and parallel hookup of loudspeakers

Where many loudspeakers are to be operated by a single amplifier, as in paging or music distribution systems, it is customary to use a series-parallel

Table 8.1. Resistance for various gauges of solid copper wire

Conductor cross-sectional area (mm^2)	AWG* number	Resistance per 300 m (1000')
5.2	10	2.00 Ω
3.3	12	3.15
2.1	14	5.00
1.3	16	8.00
0.87	18	12.5
0.52	20	20.0

*American Wire Gauge

arrangement of loads so that the net impedance is in the proper operating range of the amplifier. While such practice may be acceptable for non-critical applications, it is not recommended for demanding applications. Each loudspeaker should ideally look back directly into the power amplifier for proper electromagnetic damping.

For professional distribution systems, the 70-volt line is often used. In this arrangement, the full output of the power amplifier is available at 70 volts rms. Individual distribution transformers are then used with each driver to tap a given amount of power from the line. The user does not have to keep

Table 8.2. Resistance of various gauges of stranded (tin-coated) copper wire

Diameter of stranded conductor (mm)	AWG number	Resistance per 300 m (1000')
3	10	2.54 ohms
2.6	12	4.16
1.9	14	6.0
1.5	16	9.5
1.3	18	12.1
1.0	20	18.1

American Wire Gauge (AWG #)	Resistance per single run 300 meters (1000 feet) of copper wire (ohms)
5	.3
6	.4
7	.5
8	.6
9	.8
10	1.0
11	1.2
12	1.6
13	2.0
14	2.5
15	3.2
16	4.0
17	5.0
18	6.3
19	8.0
20	10

Note: Paralleling two identical gauges reduces effective gauge by 3.

EXAMPLE: Find the power loss at an 8-ohm load due to a fifty meter run of AWG #14 wire

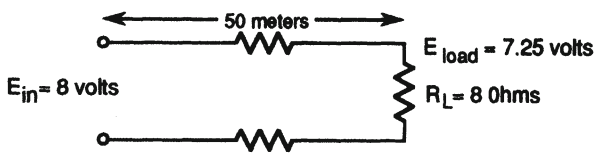

$$R = \frac{50}{300} \times 2.5 = 0.416 \text{ ohms}$$

$$E_{load} = \frac{8}{8 + (2 \times .416)} \times 8 = 7.25 \text{ volts}$$

$$\text{Power in load} = \frac{(7.25)^2}{8} = 6.56 \text{ watts}$$

$$\text{dB loss} = 10 \log (6.56/8) = .86 \text{ dB}$$

Figure 8-5. Calculation of loudspeaker line losses.

track of load impedances; rather, the total amount of power drawn from the line is totaled and of course must not exceed that available from the amplifier. For further discussion of this subject the reader is referred to Chapter 11.

8.3 Matching loudspeakers and amplifiers

An age-old question in audio engineering is what size power amplifier to use with a given loudspeaker. As we have seen earlier, the loudspeaker system carries a thermal power rating that is based on cumulative heating effects. The system may also carry a displacement power rating (more aptly, a derating) for very low frequency application.

Taking these ratings at their face value, we can come up with a rational approach to power amplifier selection based on the system applications. There are three general cases:

A. High level music reinforcement applications: The recommendation here is that an amplifier be used that has a continuous output power rating exactly equal to the thermal rating of the loudspeaker. This will ensure that normal, highly compressed musical program will drive the loudspeakers safely at all times.

B. Speech reinforcement applications: The recommendation here is that an amplifier be chosen that has a continuous power output rating equal to *twice* the thermal rating of the loudspeaker system. This will give an additional 3 dB of program headroom, which the loudspeakers can take in stride on a momentary basis.

C. Critical music monitoring applications: The recommendation here is that an amplifier be chosen that has a continuous power output rating equal to *four-times* the thermal rating of the loudspeaker system. This will give an additional 6 dB of program headroom, to be judiciously implemented by the supervising engineer only when peak program demands require it.

It is strongly recommended that amplifiers for professional use be chosen that have high current capability, inasmuch as certain dynamic program conditions can give rise to peak current values that are far greater than those that would be estimated from an examination of the loudspeaker's complex impedance curves based on the conventional continuous swept sine wave measurement signal (Otala and Huttunen, 1987).

8.3.1 Pertinent amplifier specifications

Outside of the nominal power rating of an amplifier and its damping factor, primary specifications are: voltage sensitivity, input impedance, distortion at

rated output (with all recommended loading options), and output noise. Secondary specifications may deal with dynamic headroom capability and matters of power bandwidth.

The voltage sensitivity of an amplifier is the input rms voltage that will produce rated output power into a stated load value. A typical value here would be 1 Vrms for maximum rated output into 8 ohms. Input impedances are normally resistive and values in the range of 20,000 ohms are common.

Distortion at rated output power is normally stated for the 20 Hz to 20 kHz range, as well as 1 kHz, for each recommended load impedance. Wide-range values of 0.15 to 0.2% are common, while values at 1 kHz may be as low as 0.015 to 0.02%. These measurements are normally made into a purely resistive load.

Output noise is normally a wide-band measurement, and values of 100 dB below rated output are common.

8.4 Amplifier bridging

Many stereo amplifiers today can routinely be set up for bridged operation. In this mode, the two amplifiers are effectively operated in series, and the output voltage capability is thus doubled. The basic hook-up is shown in Figure 8-6. The two output grounds are connected together, and the amplifiers are driven in antiphase. (Note the detail in Figure 8-1 showing an inverting amplifier stage for bridged operation.)

A very important point in bridged operation is that the load impedance must be *twice* that for the amplifiers when used in their normal mode. For instance, assume that a stereo amplifier is rated for continuous operation of 600 watts per channel into 4 ohms. In the bridged mode the new rating would be 1200 watts into 8 ohms.

Bridging is a convenient way of matching amplifiers with a 4-ohm design impedance to drive loads of 8 ohms or higher. The problem is that two stereo amplifiers will be needed for normal stereo operation.

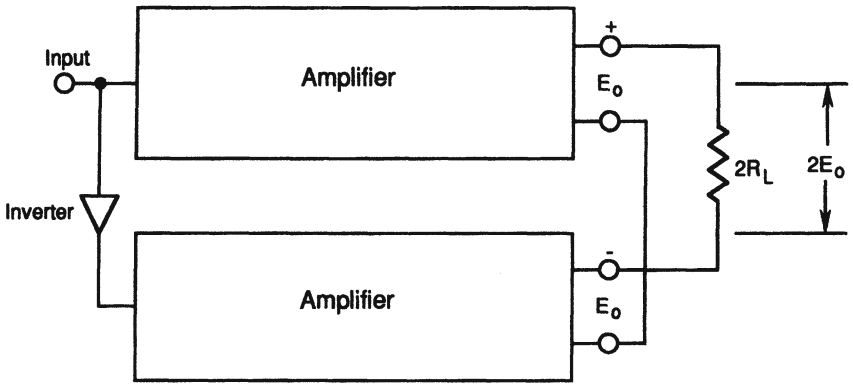

Figure 8-6. Example of amplifier bridging.

8.5 Amplifier paralleling

The technique shown in Figure 8-7 has been used in certain sound reinforcement applications where system reliability specifications demand amplifier backup at all times. In general, it is not possible to parallel two amplifiers directly. Any slight imbalance between them is apt to lead to failure of one or both amplifiers. The circuit shown provides isolation between the two amplifiers by means of two autoformers in a balanced bridge circuit and provides *twice* the power into *one-half* the normal load impedance. If one of the amplifiers fails, the output drops by 6 dB, and there will be a signal present at the balance check point, indicating that the system, while still functioning, needs maintenance. The technique is expensive if it is to be done correctly. Today, this kind of redundancy would be provided by automatic switching.

Some modern amplifiers are capable of operation with paralleled outputs on a continuous basis, thus affording the system designer with additional options in loudspeaker loading.

8.6 Biwiring

Many in the audiophile community use what is termed *biwiring* in connecting the amplifier and loudspeaker. Figure 8-8 shows the basic difference between a normal connection and biwiring. In normal connection, shown at *A*, a single pair of wires from the amplifier is connected to the two terminals of the loudspeaker, and frequency division takes place in the loudspeaker system. In biwiring, it is necessary for the HF and LF sections of the loudspeaker system

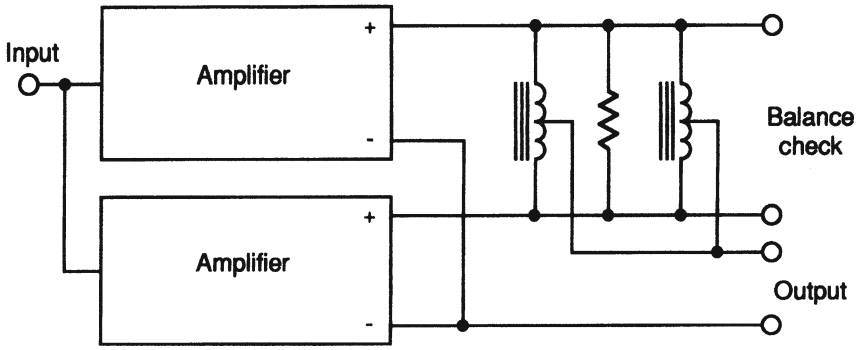

Figure 8-7. Example of amplifier paralleling.

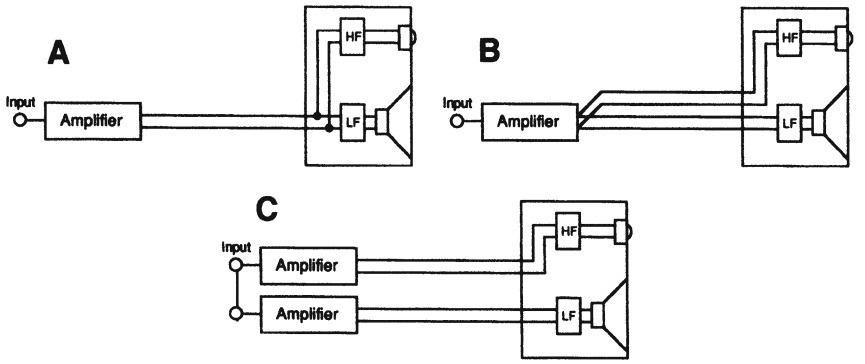

Figure 8-8. Amplifier-loudspeaker biwiring. Normal hookup (A); biwiring with a single amplifier (B); biwiring with a stereo pair of amplifiers (C).

to be separately available, each with its full dividing network complement. Each section is then fed from the amplifier through a separate pair of wires, as shown at *B*.

It is difficult to see what advantages, if any, this offers compared to a single pair of wires of equivalent gauge. However, a variant of biwiring, as shown at *C*, does offer substantial advantages. Here, the single amplifier has been replaced by two amplifiers, both fed exactly the same full-range program signal. One amplifier drives the LF section and the other drives the HF section. Since LF and HF drives are completely independent, there can be no intermodulation between the two sections of the loudspeaker, and improved performance will result.

8.5 Multi-amplifying

It is just a step away to full multi-amping of the system, as shown in Figure 8-9. Here, there is no need for passive crossover components since the necessary frequency shaping for the system has been carried out ahead of the power amplifiers. In this example it can be seen that a pair of 100-watt amplifiers can handle an input signal that could require 400-watt capability in a non-biamplified configuration. Biamplification is quite common, but triamplification and quadamplification have also been used in larger systems.

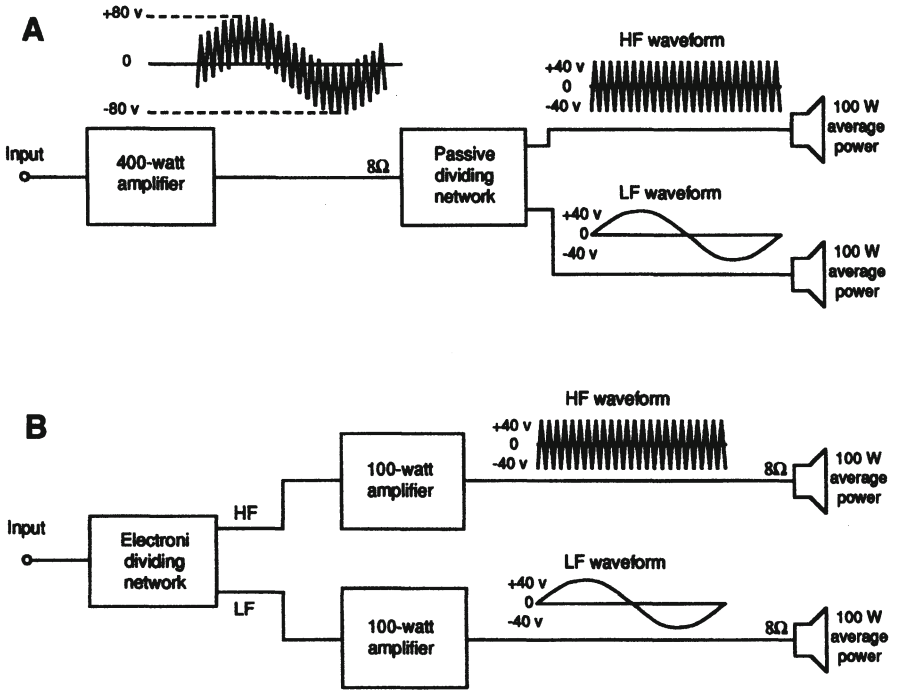

Figure 8-9. Principle of multiamplification. Normal operation (A); biamplification (B).

8.5.1 Details of electronic dividing networks

Figure 8-10 shows a signal flow diagram for one channel of a multi-amplification front end. Many such electronic dividing networks are commonly available. Until fairly recently, these have been analog designs. As generic devices, they have adjustable crossover frequencies and slopes, and of course individual output level controls. Many designs include some degree of loudspeaker power response equalization.

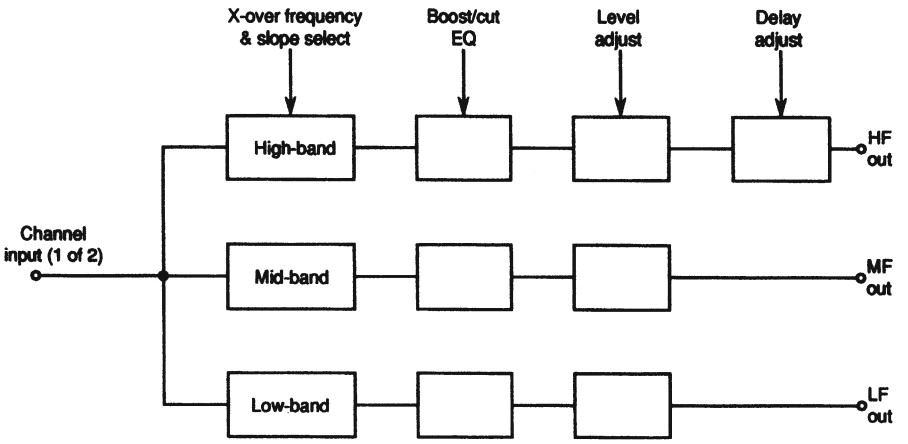

Figure 8-10. Electronic frequency division and basic signal processing.

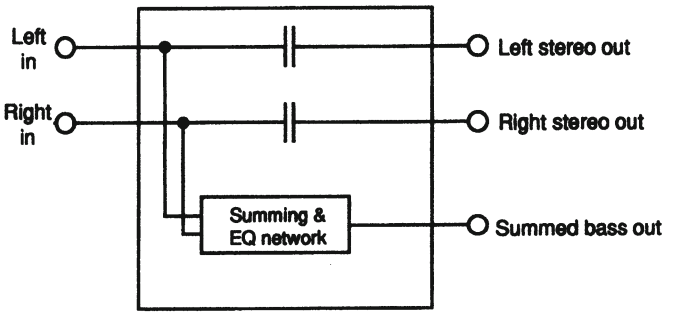

Figure 8-11. Electronic dividing network for subwoofer operation.

Figure 8-11 shows a simpler design for driving a single LF subwoofer in conjunction with a stereo pair of full-range loudspeakers. Here, the passive LF rolloff of the left and right channels feeds the stereo amplifier directly. The two channels are summed, low-passed, and equalized as required for proper LF system operation.

Today, there are many digital controllers for loudspeaker application. These provide the functions of frequency division, time correction, and additional equalization. Such a system is shown in Figure 8-12.

8.6 Electronic control of loudspeaker system dynamic performance

Traditionally, one of the great promises in audio engineering has been the prospect of improving loudspeaker performance through the analysis of distortion components and subsequently correcting them electrically. Negative

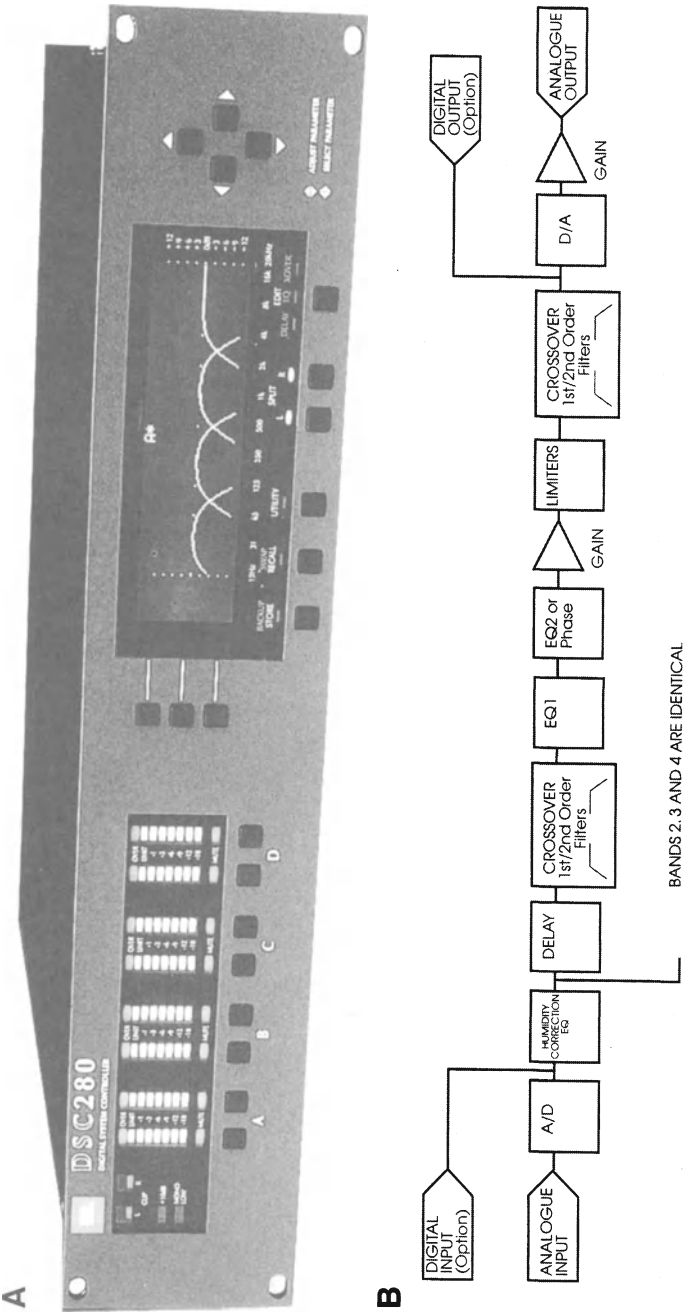

Figure 8-12. Details of a digital controller for loudspeaker application. Photo of a digital controller (A); signal flow for one frequency band of a single channel. (Data courtesy JBL)

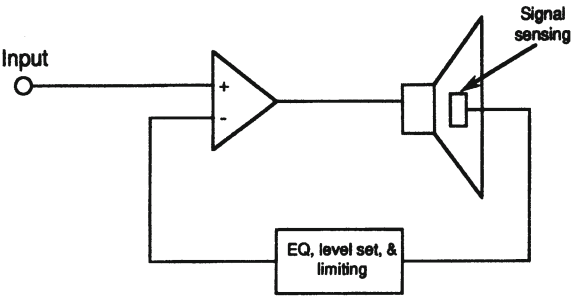

Figure 8-13. Principle of motional feedback applied to loudspeakers.

feedback is widely used in electronics for just this purpose, so its application to loudspeakers seems appropriate.

It is an idea whose time has never really come, perhaps because each step in implementation has been followed by substantial improvements in driver linearity and power handling capability. Most engineers would agree that there is little to be gained by electronically improving the linearity of an ensemble of mediocre drivers. The complexity of the solution might just as well be put into the engineering of better drivers in the first place, through attention to mechanical matters and magnetic circuit design.

Nevertheless, various feedback methods have been used, many to very good effect. Figure 8-13 shows the normal approach that is taken. Here, the *velocity* or *displacement* of the cone is monitored, and that signal is reintroduced into the amplifier input in antiphase. When this is carefully done, the system will be stable and performance will be improved. However, fundamental mechanical limits in the driver cannot be exceeded, so careful limiting of the output signal is called for.

In recent years, as digital processing has become more cost effective, methods of correcting the loudspeaker-room-listener interface have been developed. Here, the basic aim is to take the room "out of the picture" at lower frequencies and thus ridding the electroacoustical transmission path of much of its normal coloration. The technique shown in Figure 8-14.

Basically, the loudspeaker-listener paths are analyzed at the target listening position via impulse functions fed to the loudspeakers. The impulse response is measured; it is then inverted and used for pre-filtering the program material.

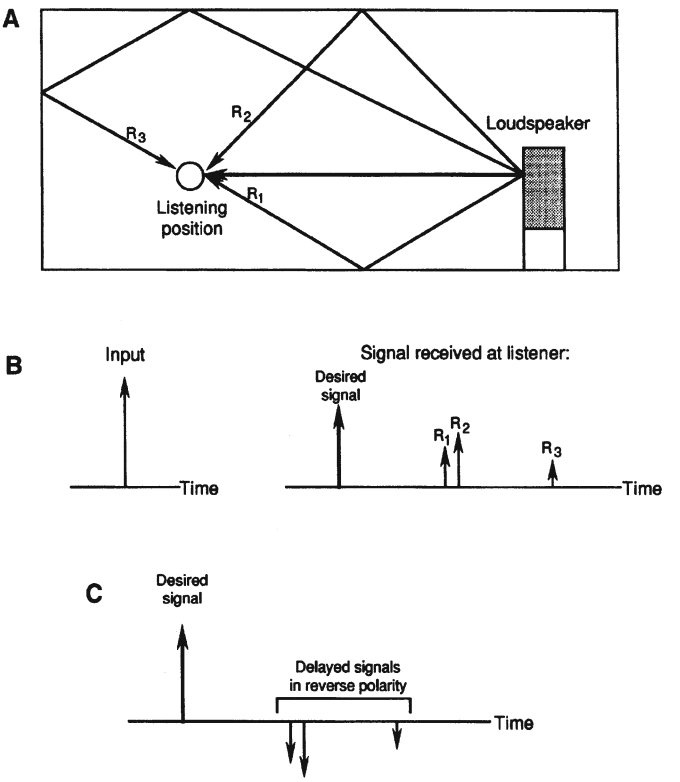

Figure 8-14. Application of digital signal processing for eliminating room reflections. Acoustical environment (A); signal input with reflections as perceived by listener (B); addition of delayed antiphase correction signals.

When carefully done, the performance improvements can be substantial. The listener, however, is fairly limited to a given seating position.

A number of manufacturers have addressed the problems of user interface in an age in which high-technology products often overwhelm the customer. The problem is one of simplifying system installation and installation, while at the same time ensuring that the customer benefits fully from the technology.

JBL's EVO product group consists of a controller and its associated loudspeaker. This combination interfaces with a conventional console which accommodates microphones and other program sources. The system is set up via a PC, and the following functions can be carried out:

1. Automatic equalization: A test signal is sent to the loudspeakers, and the signal sampled in the room is compared with a reference stored in the controller. The system is then equalized to match the standard.

2. Feedback control: Feedback modes are detected and dipped out via sharp filters.

3. Compression and limiting: These functions can be implemented for all operations, maximizing the system's overall output.

4. Diagnostic functions: Amplifier, power supply, and loudspeaker component thermal status can be identified and compensated for.

Figure 8-15 shows the basic signal flow of the system, and a typical setup is shown in Figure 8-16.

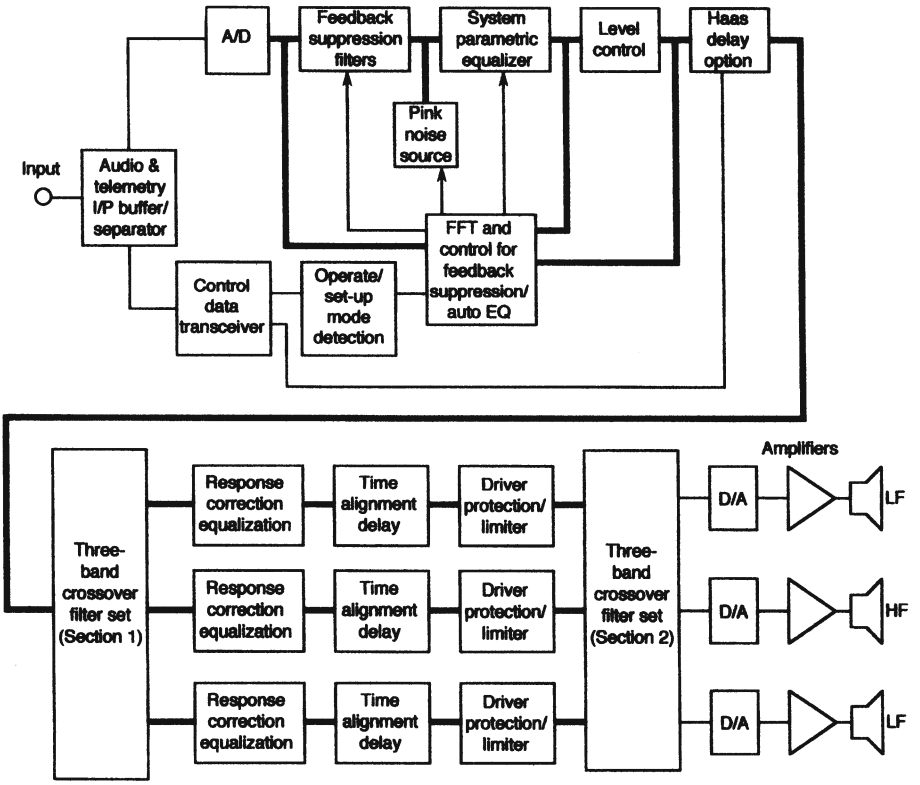

Figure 8-15. Operational diagram of the JBL EVO system. (Data after JBL)

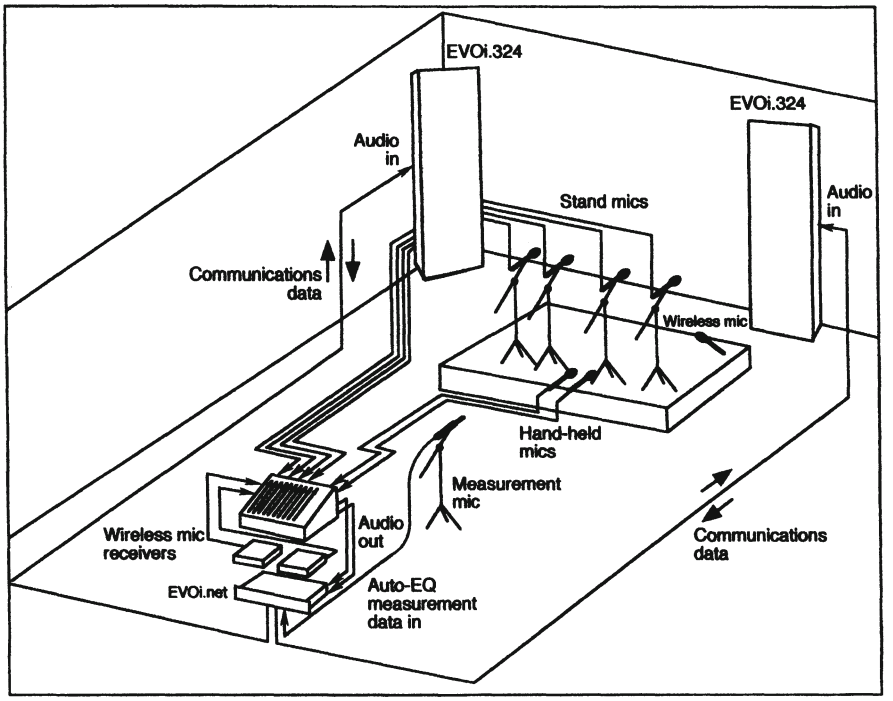

Figure 8-16. Sketch showing typical operation of the EVO system. (Data after JBL)

BIBLIOGRAPHY AND REFERENCES:

Borwick, J. (editor), *Loudspeaker and Headphone Handbook*, third edition, Focal Press, Boston (2001).

Collums, M., *High Performance Loudspeakers*, 4th edition, J. Wiley and Sons, New York (1991).

Giddings, P., *Audio Systems Design and Installation*, Sams, Indianapolis (1990).

Otala, M. and Huttunen, P., "Peak Current Requirements of Commercial Loudspeaker Systems," *J. Audio Engineering Society*, volume 35, number 6 (1987).

Chapter 9:
THERMAL FAILURE MODES OF LOUDSPEAKERS

9 Introduction

In professional applications such as sound reinforcement the dominant failure mode of a loudspeaker driver is due to excess heating of the voice coil. Often, there is a chain of events in which heating causes expansion of the voice coil, with subsequent rubbing of the voice coil against the top plate and electrical shorting of the voice coil windings.

When we realize that even the sturdiest LF drivers may be no more than 5 or 6% efficient, it is clear that the vast bulk of electrical energy delivered to the driver over time must be converted directly to heat. It is no wonder then that much transducer engineering deals with problems in heat transfer, as well as selection and development of materials and adhesives that are heat resistant.

In this chapter we will outline the basics of heat transfer as they apply to drivers and describe the numerous measures that have been taken to alleviate these problems. We will also examine the gradual change in driver performance parameters that take place during the heating process.

9.1 Basic heat transfer mechanisms

There are four dimensional quantities we must have an intuitive understanding of: temperature, thermal energy, thermal conduction, and specific heat. Superficially, temperature is the measure of how hot or cold something is; we can sense it by touch. We measure it in degrees Celsius or degrees Fahrenheit, and we can think of it as an *intensive* measure of heat. Thermal energy is the corresponding *extensive* quantity; we simply call it heat, and it is measured in *joules*. It is temperature which drives heat from one point to another in a thermodynamic system.

The basic notion is shown in Figure 9-1A. Here, we have a rectangular bar of material, and we are applying heat (Q) to one end of it. As the bar takes

J. Eargle, *Loudspeaker Handbook*

on heat its temperature rises, and heat energy begins to flow toward the other end of the bar, which is assumed to be at the ambient temperature of the space around the bar.

Let us assume further that heat is being added to the bar at a given rate of some fixed number of joules per second (watts). This of course is *power*, and is the quantity that we normally calculate from measurements of voltage and current. As the bar heats up it will begin to give off some of that heat to its surroundings by radiation, convection (cooling by the motion of air adjacent to the bar), or by direct conduction to some other object. Eventually the system will come to *thermal equilibrium*, in which the rate at which heat is applied will be equal to the rate at which it leaves the bar, as shown at *B*.

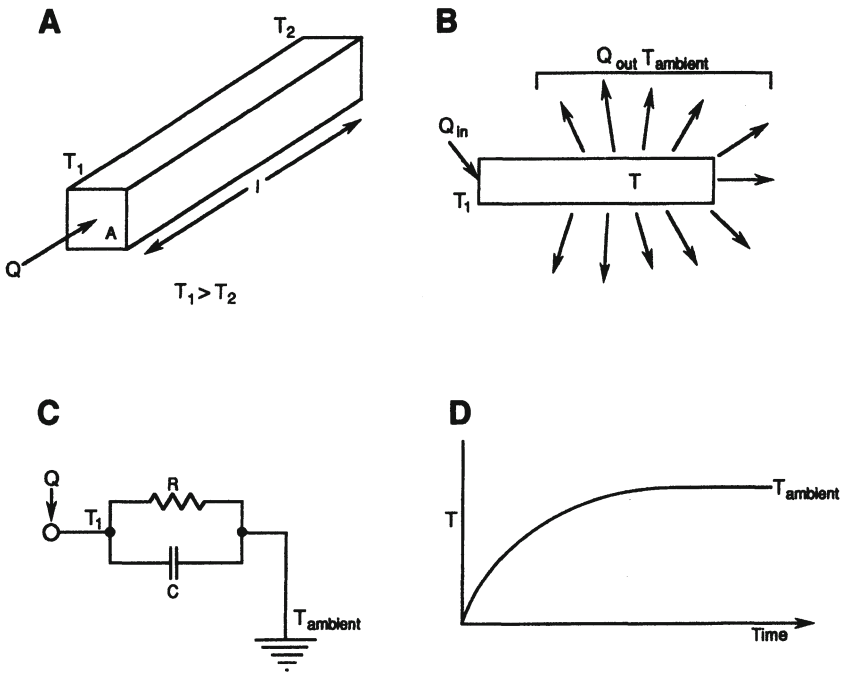

Figure 9-1. Basic heat transfer. Heat (Q) applied to the end of a rectangular bar (A); at equilibrium, heat introduced into bar equals heat emitted by bar (B); equivalent thermal circuit (C); temperature rise over time (D).

While this is in accordance with our everyday understanding of physics, it is a fairly complex phenomenon. First, there is the basic *thermal conduction* in the bar material itself. Such metals as aluminum and copper have relatively high coefficients of thermal conduction, while other materials such as brick, glass, or concrete have thermal conduction coefficients that are about one-hundredth that of most metals. Accordingly, they are known as good *thermal insulators*.

It may be more convenient to think in terms of thermal resistance than conductance, and the following equation applies to heat transfer along the bar shown in Figure 9-1:

$$R_{thermal} = l/AK \qquad 9.1$$

where R is the thermal resistance (°C/watt), l is the length of the bar (m), A is the cross-sectional area of the bar (m^2), and K is the thermal conductivity of the bar (°Cm/W).

There is another quantity, *specific heat*, or heat capacity, which we will now define. Materials vary in the amount of heat required to raise or lower their temperature by some given amount. Specific heat is measured in J°C/kg, the number of joules of energy, per kilogram of material, required to raise the temperature 1 degree Celsius. We may think of this as *thermal capacitance*, as given by the following equation:

$$C = mH_s \qquad 9.2$$

where C is the thermal capacitance (J°C), m is the mass (kg), and H_S is the specific heat (J°C/kg).

Over normal operating temperatures, aluminum has a high specific heat – about twenty times that of copper. That is, with equal sample masses, it takes twenty times the amount of heat to raise the temperature of aluminum a given amount, as compared with copper. It is no surprise then that aluminum, because of its high thermal conduction and high specific heat, is the material of choice for heat sinking in electronics manufacturing.

Considering the effects of thermal resistance and specific heat, we can now model the heat transfer process as shown in Figure 9-1C. A typical temperature versus time plot is shown at *D*. The equation that defines the rise in temperature is:

$$\Delta T = CR(1 - e^{t/mH_sR}) \qquad 9.3$$

The thermal time constant, τ, is the time interval during which the temperature has risen to 63% of its maximum value and is given by:

$$\tau = mH_sR \qquad 9.4$$

9.1.1 Heat transfer in the driver

The principles we have just discussed can be used to model the performance of a typical cone driver, as shown in the equivalent circuit of Figure 9-2A (Button, 1994). Here, we use two network sections, one representing the relatively short thermal time constant of the voice coil and the other representing the relatively long thermal time constant of the metal structure of the motor.

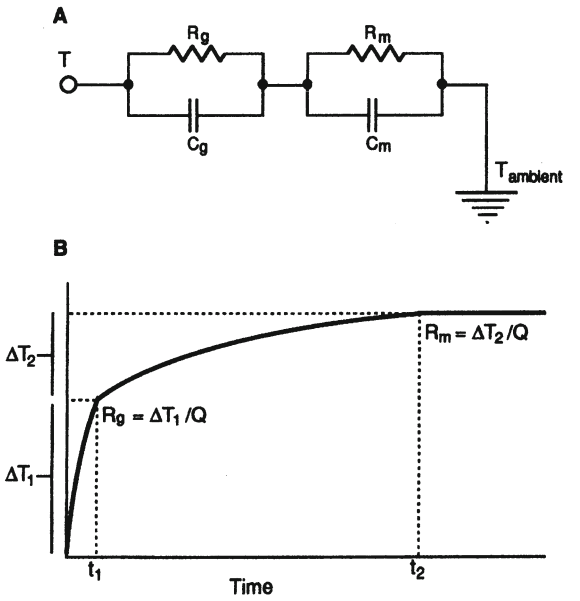

Figure 9-2. Heat transfer in a typical driver. Equivalent circuit for a voice coil and associated magnet structure (A); temperature rise over time (B).

When we apply a constant power signal to the driver, the voice coil heats up quite rapidly to the value ΔT_1 because of its low mass and low conduction path to the adjacent metal. After that state has been reached, we then observe a much longer time constant as the temperature further attains the added value

of ΔT_2 as heat is conducted away from the voice coil through the metal structure to the outside ambient temperature.

The total temperature rise will be $\Delta T_1 + \Delta T_2$, and the plot of overall temperature rise with time is shown in Figure 9-2B.

9.2 Estimating values of thermal resistance

There is no direct way to measure thermal resistances in a complex structure such as a dynamic transducer, and indirect methods are used. Button (1994) estimated values of R_g and R_m by applying signals to the driver and closely tracking the rise in voice coil resistance. Various voice coil diameters and lengths were measured, as were various magnetic structures. Two types of excitation signals were used, LF noise and a mid-frequency sine wave. Button's data can be summarized as follows:

1. With LF noise input, the value of R_g was reduced. This indicates that significant voice coil motion itself aids in heat removal, either through turbulence or through closer proximity of all parts of the voice coil to the top plate and pole piece.

2. Increasing input power reduces R_g. Increased turbulence is a factor here, as is the expansion of the voice coil, placing it closer to the top plate where heat conduction is increased.

3. All other factors remaining equal, larger voice coils run cooler than smaller ones, due to their increased surface area.

4. More massive voice coils exhibit slower heating and as such will have better thermal transient capability. This suggests possible design trade-offs in that lighter voice coils have lower mass and inductance, both of which improve transient response.

5. Since most drivers have roughly the same aluminum frame volume and surface areas, values of R_m were virtually the same. (One significant departure was observed with a driver configuration in which thermal short-circuiting of the voice coil to the frame was apparent.)

6. Excessive voice coil overhang may be detrimental. Even with high level noise signals, the outer portions of the voice coil remain far from the top

plate and pole piece and thus cannot take advantage of that low resistance thermal path.

9.3 Low frequency performance shifts

Figure 9-3 shows the on-axis response of a 380 mm driver with inputs varying from 0.8 watts to 100 watts in 3-dB increments, all with the same vertical scale. Examined casually, it appears that subsequent increments are in fact 3 dB. A clearer way to see what is really going on is to plot, say, 1-watt and 100-watt curves with a 20-dB offset between them, as shown in Figure 9-4. Here, we can clearly see that the 100-watt curve is compressed approximately 2 dB relative to the 1-watt curve. The effect is often referred to as *dynamic compression.*

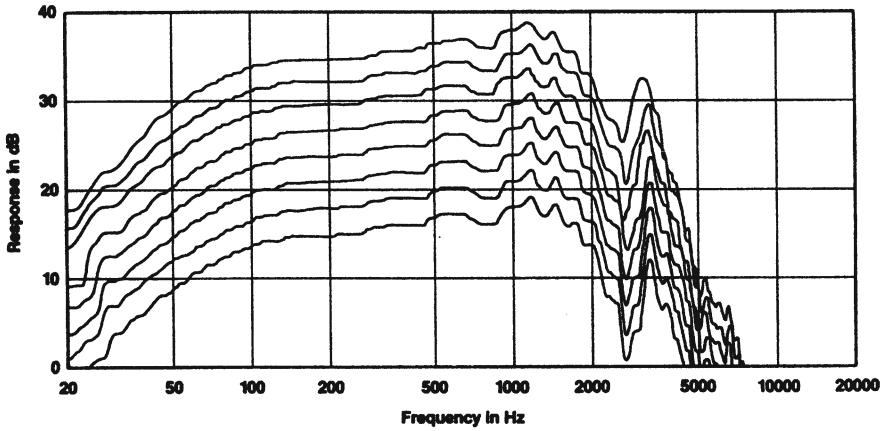

Figure 9-3. Axial response of a 380-mm LF driver at 1 meter driven at input powers of 0.8, 1.6, 3.15, 6.3, 12.5, 25, 50, and 100 watts. Bottom line is 80 dB L_P. (Data courtesy JBL)

One may question whether this degree of compression is audible as such. The answer to this question may be seen in the data shown in Figure 9-5. The frequency and impedance response of a 460 mm LF driver at normal temperature of 27 °C (80 °F) are shown at *A*. The response at an elevated temperature of 150 °C (300 °F) is shown at *B*. Note that the low frequency alignment has been shifted by a considerable amount that would be quite audible to experienced listeners.

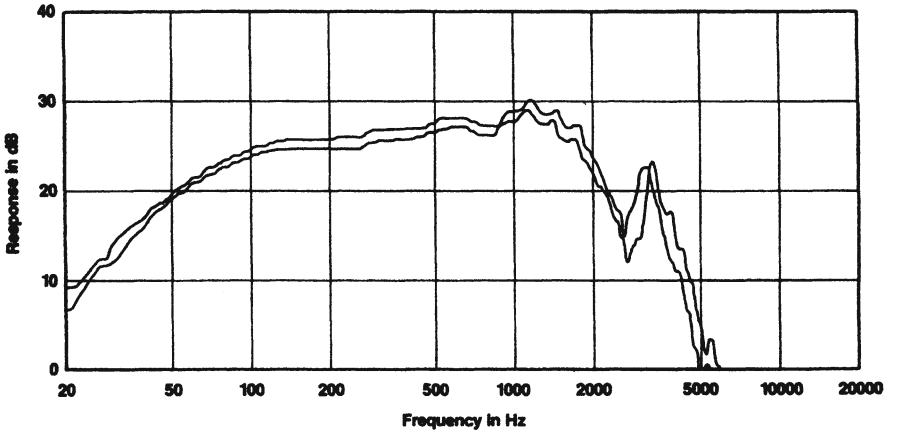

Figure 9-4. Curves of 1 and 100 watts, 1 meter on-axis, displaced 20 dB. Bottom line is 70 dB L_p for 1 watt and 90 dB L_p for 100 watts. (Data courtesy JBL)

9.4 Techniques for heat removal

Air convection and turbulence are very effective methods of removing heat from the magnetic gaps of large drivers. By directly opening up portions of the gap area to the outside of the driver, JBL's Vented Gap Cooling (VGC) provides a set of paths through which air can be pumped in and out at high excursions. Figure 9-6 shows details of the VGC design

The effectiveness of the heat removal is shown in Figure 9-7. Here, the on-axis output versus time is shown for three 380 mm LF drivers. The VGC design is compared with a standard design, as well as with a smaller voice coil diameter design.

9.4.1 Ferrofluids

Many smaller cone and dome drivers used for MF or HF applications are often designed with ferrofluid in their magnetic gaps. Ferrofluids consist of a suspension of extremely fine iron oxide particles in a liquid mixture that functions as a lubricant, damping substance, and a surface active agent that prevents the magnetic particles from clumping together. The material is applied to the magnetic gap with the voice coil in place.

Without such an agent, the voice coil of the typical 25 mm dome HF device will heat up very rapidly due to its very small size and the poor thermal

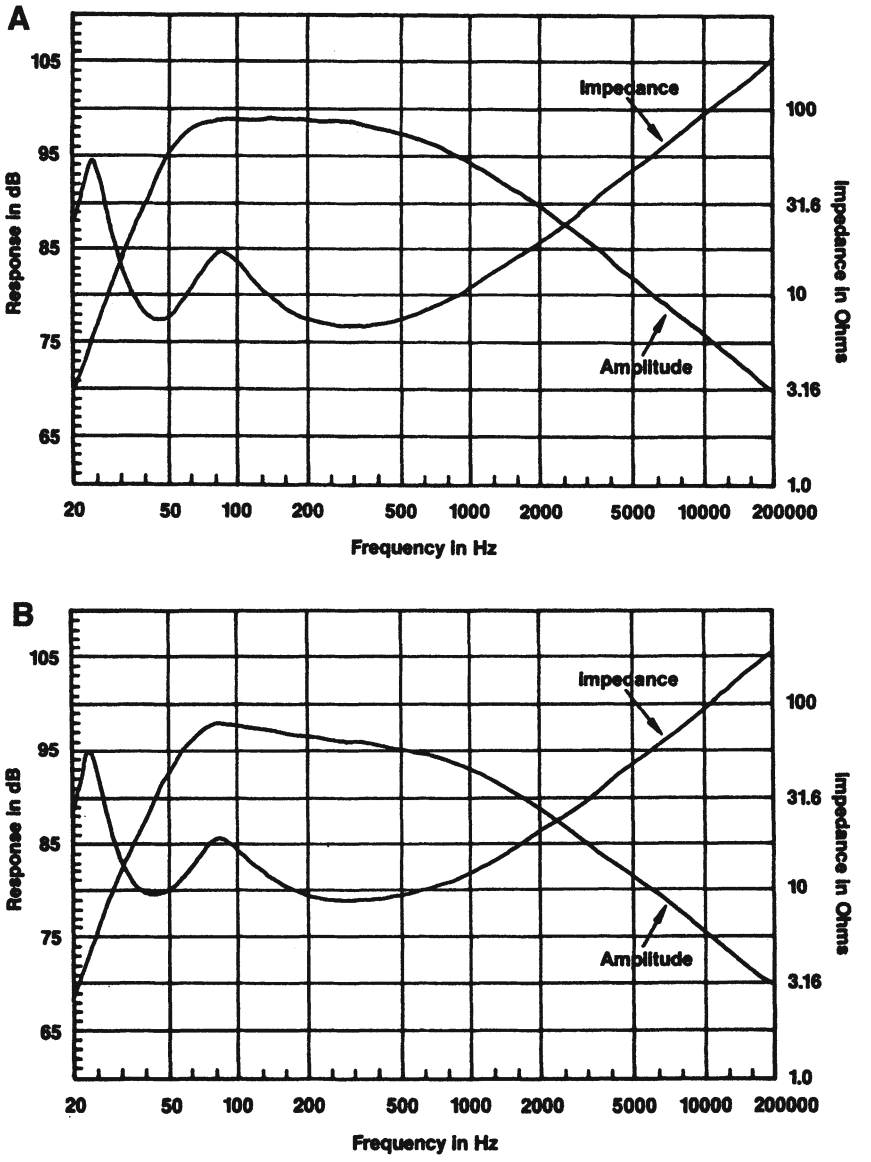

Figure 9-5. LF alignment shifts. Normal operation at 27 °C (A); elevated operation at 150 °C. Note: R_E doubles at 525 °F, relative to 70 °F. (Data courtesy JBL)

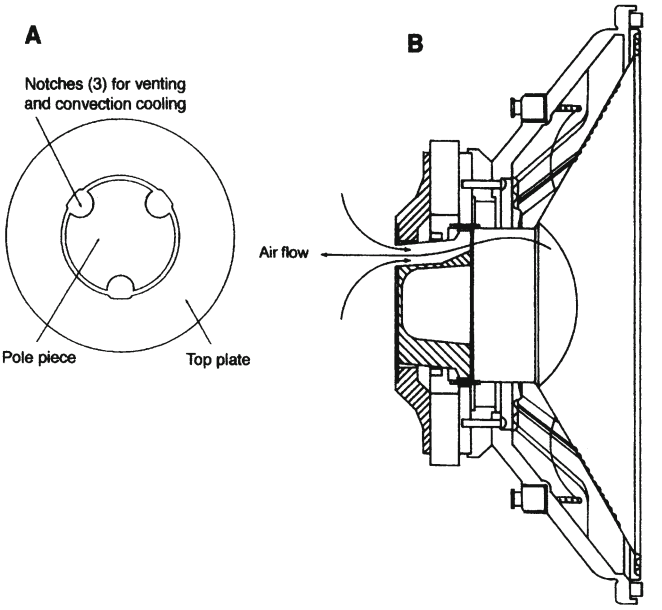

Figure 9-6. Details of the VGC structure. Back view (A); section view (B). (Data courtesy JBL)

conductivity provided by the air path to the metal portions of the driver. Ferrofluid can effectively short circuit the thermal path to the metal structure, giving the driver a much longer thermal time constant and allowing it to handle relatively high electrical transient input signals.

If the viscosity of the ferrofluid is properly chosen, then the HF sensitivity of the driver will be only slightly diminished. An added benefit in some designs is that ferrofluid can be used to damp the fundamental resonance of the driver. There may also be a slight advantage in reducing the reluctance of the magnetic path, resulting in an increase in output of perhaps 0.75 dB, depending on other driver parameters.

Ferrofluids may be used in LF drivers, but are generally not used in those drivers intended for large excursions, inasmuch as non-laminar flow may result, with consequent nonlinearities.

Early ferrofluids had problem s with aging and stability under high temperature drive conditions, but these problems have largely been solved in recent years.

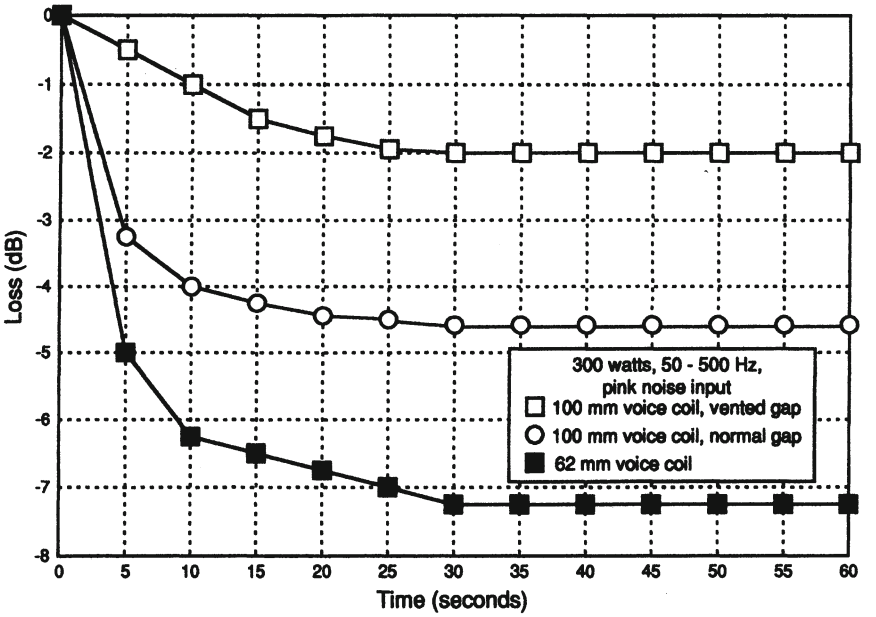

Figure 9-7. Output versus time for three 380-mm (15") LF drivers. (Data courtesy JBL)

BIBLIOGRAPHY AND REFERENCES:

Collums, M., *High Performance Loudspeakers*, John Wiley & Sons, New York (1991).

Button, D., "Heat Dissipation and Power Compression in Loudspeakers," *J. Audio Engineering Society*, volume 40, number 1/2 (1992).

Button, D., "Heat Dissipation and Power Compression in Low Frequency Transducers," *Sound & Video Contractor*, volume 12, number 2 (February 1994).

Henricksen, C., "Heat Transfer Mechanisms in Loudspeakers: Analysis, Measurement, and Design, "*J. Audio Engineering Society*, volume 35, number 10 (1987).

JBL Professional, Technical Note 1(18), "Vented Gap Cooling in Low Frequency Transducers," Northridge, CA (1991).

Mellilo, L. and Raj, K., "Ferro-fluid as a Means of Controlling Woofer Design Parameters," *J. Audio Engineering Society*, volume 29, number 3 (1981).

Chapter 10:
RECORDING MONITOR LOUDSPEAKERS

10 Introduction

The term "monitor loudspeaker" is loosely applied to almost any loudspeaker used for monitoring recorded product at any stage in sound production or postproduction. In a more restrictive sense the term applies to products that are widely accepted in monitoring operations and have to some extent been modified or designed to meet a list of performance attributes determined by recording and broadcast engineers. Broadly speaking, those attributes are:

1. Extended bandwidth. The range from 40 Hz to 16 kHz (± 3 dB) represents the minimum acceptable for a full-size monitor. Smaller monitors should be just as flat across their passband, but the allowable LF limit may be raised somewhat.

2. Uniform frontal angle response. The bandwidth stated in item 1 should be uniform over a horizontal beamwidth of ± 30° and a vertical beamwidth of ± 15°, both with respect to the forward axis.

3. Controlled power response. The DI of the system should be free of any deviations exceeding ±3 dB over the range from 250 Hz to 8 kHz.

4. Accurate time domain response. The group delay of the system should fall within the Blauert & Laws criteria.

5. Accurate stereophonic imaging. If the loudspeaker is not inherently of horizontal mirror image symmetry, it should be offered in separate left and right models so that symmetrical listening geometry can be achieved.

J. Eargle, *Loudspeaker Handbook*

6. Robust construction with high reliability. In the most general terms the system should be well constructed, road-worthy, and able to handle its share of inadvertent abuse.

7. Well behaved impedance characteristic. The dc resistance of the system should not drop below 80% of the nominal impedance value, and the phase angle should not exceed ±60°.

8. Low distortion at normally required operating levels. The system should be able to handle the levels expected of it with little, if any, audible distortion. In the rock studio, level requirements for a stereo pair of monitors at a distance of 3 meters, may be in the range of 115 dB L_p.

This is an imposing list, and few monitor loudspeakers earn outstanding marks in all areas. In many cases, the optimization of one attribute may work against another. Typically, a monitor system optimized for classical recording, with its demands of very low distortion and flat frequency response, may not be up to the high volume level demands of the modern pop/rock s tudio. And conversely, the typical HF horn system used in the pop/rock studio may have a much too aggressive sound for the classical engineer and producer.

In this chapter we will discuss monitor attributes in detail and present examples of well known designs that have met most of these requirement s.

10.1 A historical survey

As monitor systems developed during the thirties and forties, a premium was placed on efficiency, inasmuch as power amplifiers of that era generally offered no more than 20 to 40-watt output capability. The normal approach was to use a high efficiency LF driver, coupled with a HF horn/compression driver. The earliest such system is unquestionably the "Iconic," first manufactured in the thirties by the Lansing Manufacturing Company. The utility form of the product is shown in Figure 10-1. This was a 2-way system, as are many modern systems with HF horns. The LF driver had a rather high resonance frequency for increased efficiency, and the HF portion consisted of a compression driver/ multicellular horn combination, crossing over in the range of 800 to 1200 Hz. Because high energy magnets were not available at the time, dc field coils were used in both LF and HF transducers to generate the required magnetic flux densities. The field coil power supply (with vacuum tubes) can be seen on the top of the enclosure. By today' s standards, such a system had limited

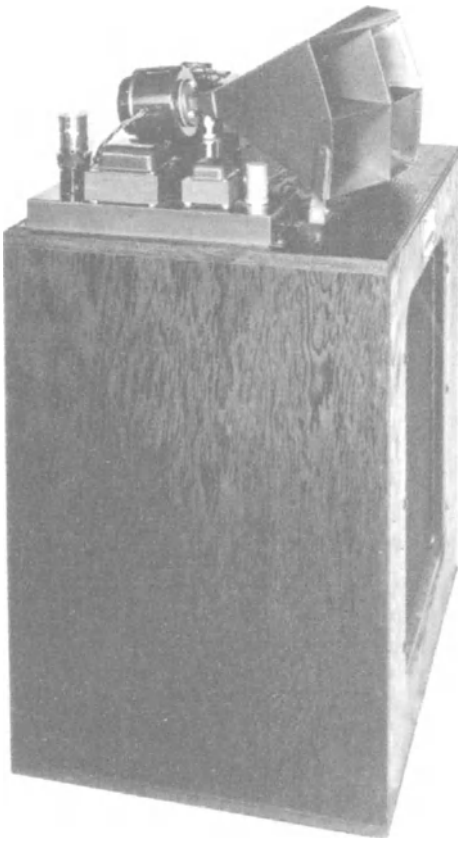

Figure 10-1. Photo of Lansing "Iconic" monitor system. (Data courtesy JBL)

bandwidth and irregular frequency response – but doubtless excelled in the areas of ruggedness and high output capability.

The forties saw the rise of several so-called coaxial two-way designs, in which the HF unit is located in the center of the LF cone. Most notable of the U. S. products was the 380 mm (15") Altec-Lansing 604. So widely has the 604 been used over the years that during the seventies several companies designed their own dividing networks for the basic unit.

Another noted U. S. loudspeaker was the RCA LC-1A coaxial model. This was a 380 mm (15") LF driver with a uniquely stiffened LF cone and a small HF cone located at its apex. It was widely used in broadcasting.

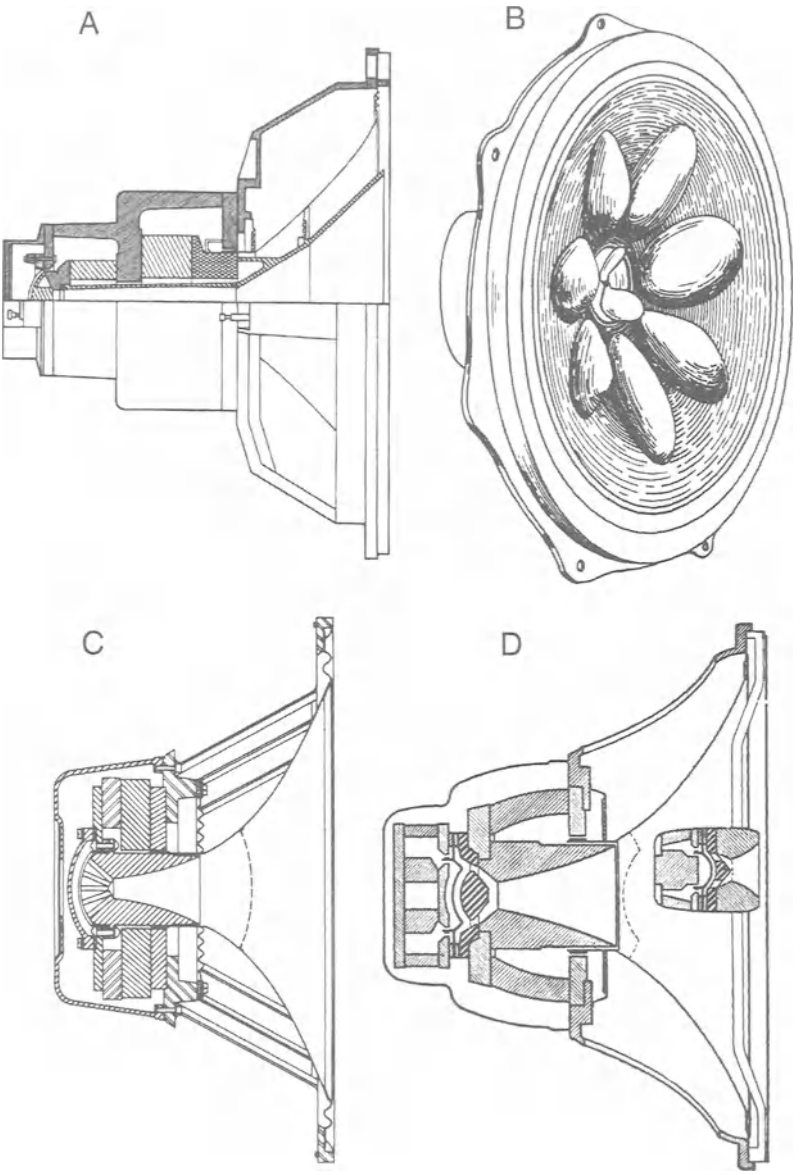

Figure 10-2. Views of coaxial and triaxial loudspeakers. Altec 604 (A); RCA LC-1A (B); Tannoy Dual-Concentric (C); Jensen G-610. Data courtesy: Altec (A); RCA (B); Tannoy (C); Jensen (D).

In England, the Tannoy Dual-Concentric design followed the general form and size of the 604, but with the unusual distinction of using its curvilinear LF cone as an extension of the HF horn.

While not designed specifically for the studio monitoring market, the Jensen G-610 triaxial loudspeaker extended the coaxial concept with the addition of a separate HF unit. Views of these designs are shown in Figure 10-2.

10.2 The modern era

Since the eighties, monitor loudspeakers have taken two distinct paths. There are those adherents of the traditional horn HF approach, with normally ported LF sections. But many engineers and producers are now finding that the newer cone/dome monitors, if outfitted with multi-amplification and judicious signal limiting, can easily handle high studio playback levels.

The primary differences between horn HF systems and cone/dome systems is that the former produce greater second harmonic distortion at high frequencies at normal operating levels (95 to 110 dB L_p at 1 meter) than do the cone/dome systems. On the other hand, the cone/dome system ordinarily has to be operated as a multi-way system, with its inevitable problems in lobing and driver interference. The horn HF system can easily be designed for 2-way operation, with minimal lobing problems. Finally, there is the ability of the horn to withstand all manner of assaults from the driving amplifier and still hold together, albeit with significant distortion.

The bottom line then is dependent on how loud the engineer and producer wish to monitor their activities. For moderate levels, there appears to be an advantage with cone/dome systems where distortion is concerned. For rock recording there will probably always be an advantage to the HF horn approach.

10.3 Evolution of modern horn HF systems

As rock music developed during the 1970s there was a need for relatively "bullet-proof" monitor systems that could produce high levels in the control room with few signs of distress. There was also a need for a flat output spectrum with *flat power bandwidth* – the capability of producing virtually identical peak levels uniformly over the frequency band.

For this need, JBL developed the 4-way 4350 monitor system shown in Figure 10-3. These systems were normally mounted in the soffit space above and to the sides of the control room window and were aimed toward the principal listening area just behind the console. Given the fairly close-in listening position, relative to the large baffle array, the response was not notably smooth; but this was a small price to pay for the advantages the system offered.

Another well known monitor system of the 1970s was the UREI 813, which is shown in Figure 10-4. Taking note that the Altec 604 had long been a studio favorite, UREI designed a dividing network for the 604 that included in the low-pass section a passive delay network that effectively aligned the LF section so that the two outputs were coherent. The term Time-Align™ was used to describe the design. In the 813 system, an additional 380 mm (15 in) LF driver is incorporated to increase the system's output capability.

During the early 1980's JBL introduced the dual-LF model 4435, shown in Figure 10-5. The system was the first monitor to exhibit uniform power response from about 500 Hz to 12 kHz. The system's directivity index is uniform at 9 dB (±2 dB) from 315 Hz to 12 kHz.

Westlake Audio has manufactured various size monitor systems since the 1970s, and the 3-way model TM-3 shown in Figure 10-6 is typical of their larger designs. The system can be passively driven, biamplified or triamplified as the user wishes.

Today, many large soffit-mount monitors are custom designed by consultants and architects who specialize in the layout of recording and postproduction spaces. These tend to be 2-way designs incorporating dual 380 mm (15 in) LF drivers, crossing over to a horn HF section at about 800 Hz. In most of these designs, a modified radial or diffraction horn is used to achieve uniform horizontal dispersion to beyond 12.5 kHz, while the vertical dispersion is allowed to become narrower with rising frequency. This approach maintains relatively flat on-axis response at HF without the need for significant electrical boost above 3 kHz.

10.4 Modern cone/dome systems

Beginning in the 1980s, cone/dome systems from the consumer sector began making appearances in recording studios. British companies such as KEF and B&W were significant here. In particular, the B&W model 801 was broadly

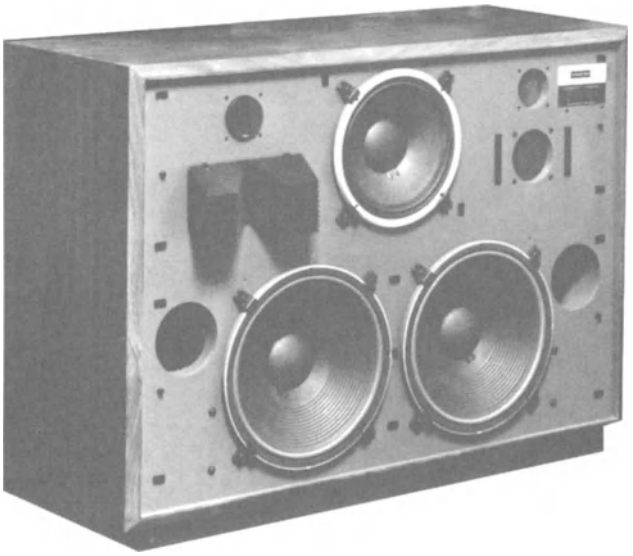

Figure 10-3. Photo of JBL 4350 4-way monitor loudspeaker. (Data courtesy JBL).

Figure 10-4. Photo of UREI 813-C monitor system. (Data courtesy UREI and JBL).

Figure 10-5. Photo of JBL 4435 2-way monitor. (Courtesy JBL)

Figure 10-6. Photo of Westlake Audio TM-3 three-way monitor. (Courtesy Westlake Audio)

adopted as the preferred monitor for classical recording, very nearly on a world-wide basis.

In the pop studio, British designs by Quested and Boxer led the movement, and in more recent years the contributions of ATC Loudspeaker Technology have been significant. Figure 10-7 shows a view of the ATC model SCM 300 three-way system.

Figure 10-7. Photo of the ATC model SCM 300 three-way system. (Courtesy ATC Loudspeaker Technology)

There are two key elements in the success of cone/dome systems: use of multi-amplification (with associated signal processing) and the availability of rugged MF dome drivers. The typical MF dome driver used in this application has a diameter of 75 mm (3 in), a sensitivity of 94 dB (1 watt at 1 meter), and an average power rating of 150 watts. As discussed in Section 2.5, this design can produce peak levels of 115 dB L_p at a reference distance of 1 meter – more than enough to satisfy all monitoring requirements except the loudest rock music. These systems are all multiamplified and have carefully designed circuitry to protect the drivers from excessive overload or burnout.

Cone/dome three- and two-way designs are also very popular. Figure 10-8A shows baffle details of a Genelec Model 1038A monitor system. The design is 3-way, triamplified, with each amplifier section providing the necessary frequency division and limiting. User adjustable equalization provides for various boundary effects and helps in interfacing the system with the listening environment. A signal flow diagram is shown at *B*, and system response is shown at *C*.

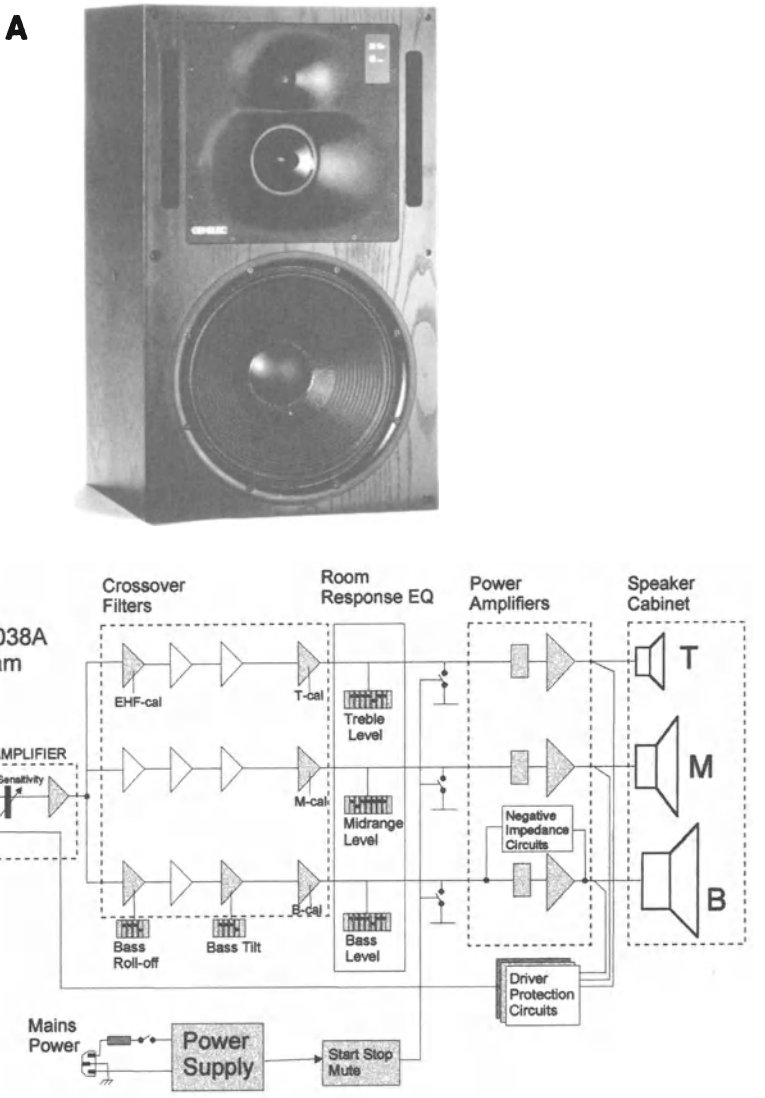

Figure 10-8. The Genelec 1038A monitor. Photo (A); Signal flow diagram (B); response curves (C). (Courtesy Genelec)

C

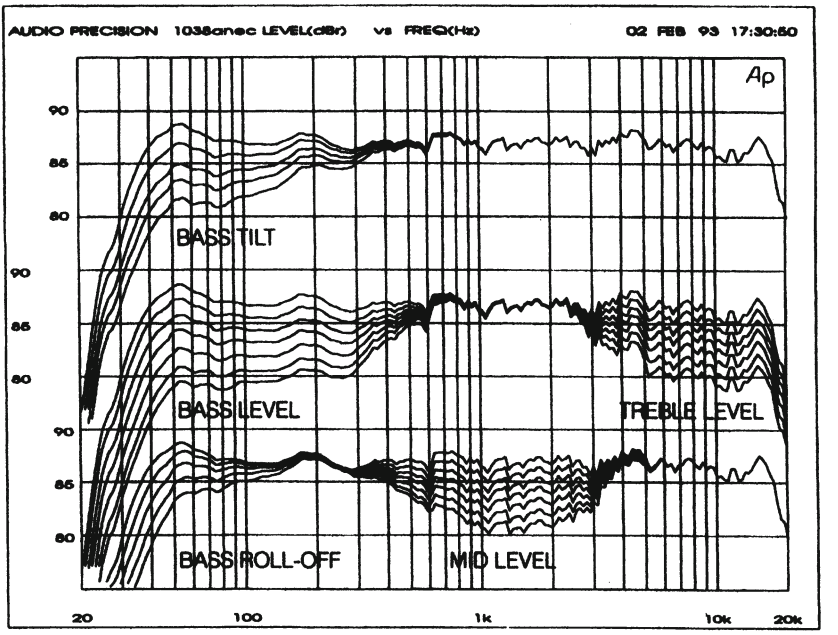

Figure 10-8. Continued.

Figure 10-9A shows a view of the JBL LSR28P 2-way design. A signal flow diagram is shown at *B*. Note that the electronic design provides equalization for several boundary mounting conditions, input sensitivity control, as well as HF trim.

A

Figure 10-9. The JBL LSR28P 2-way system. Photo (A); signal flow diagram for system (B). (Courtesy JBL)

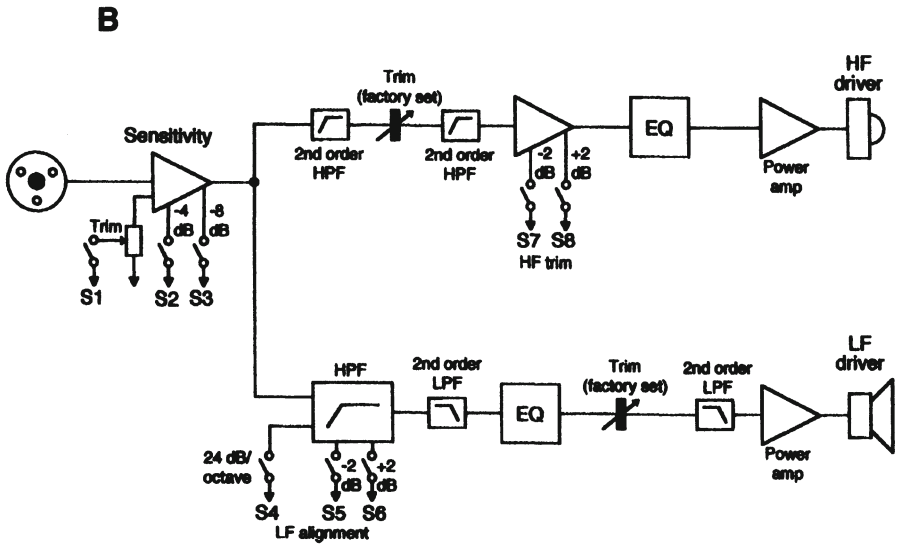

Figure 10-9. Continued,

10.5 Smaller monitor designs

For postproduction and near-field applications there are seemingly limitless products for the engineer to choose from, running the gamut from sturdy 3-way designs down to small 2-way designs. Many of these monitors are passive and of course will require external amplification.

The Westlake BBSM6 (Figure 10-10) is typical of the upper end of small monitor design and is shown here with recommended foam baffle for minimizing response problems when mounted under less than ideal conditions. The JBL 4400-Series monitors are shown in Figure 10-11 and are typical of monitor families provided by many companies.

10.6 Thermodynamic distortion in dome systems

Figure 10-12 shows the thermodynamically induced distortion produced by a 25 mm (1 inch) dome on sine wave input signals. As a general rule we can state that the maximum sine wave input to a 25 mm device is about 20 or 25 watts. The normal maximum sensitivity of these devices is limited to about 93 dB, one watt at one meter. Therefore, a single unit driven at 25 watts will produce a level of 107 dB at a distance of 1 meter. From the graph we can see

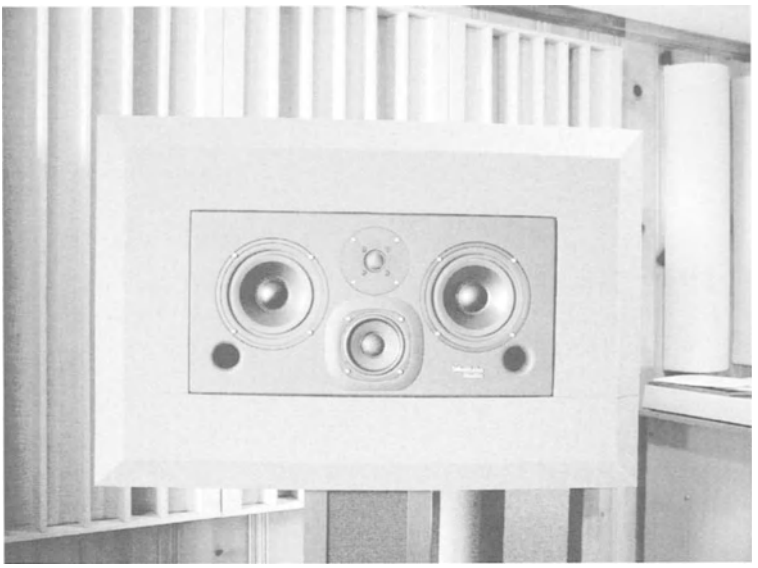

Figure 10-10. The Westlake Audio model BBSM-6 monitor with foam baffle. (Courtesy Westlake Audio)

Figure 10-11. Photo of a family of small monitor loudspeakers. (Courtesy JBL)

that the resulting thermodynamic distortion will be between 1 and 2%, a very low figure.

For comparison with horn HF systems you may wish to review the data in Figure 7-22C. For an output level of 107 dB L_p at a distance of 1 meter, a low distortion (rapid flare rate) horn design will produce second harmonic distortion in the range of about 5%. There is no question that, level for level, a dome system will produce somewhat less HF distortion than a good horn system. The lingering question in the minds of many recording engineers, however, may be the capability of the dome to reach the desired levels in the first place.

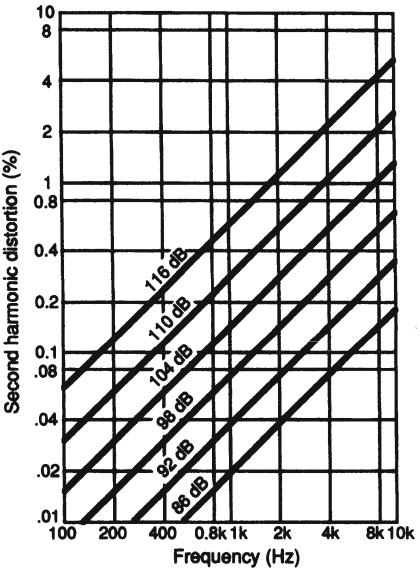

Figure 10-12. 25-mm (1 in) dome thermodynamic distortion as a function of frequency and level at a distance of 1 meter. (Data adapted from Thuras, *et al.*)

10.7 The monitoring environment

There is always a strong argument for monitoring recording activities in an environment that resembles a typical living room. Indeed, the IEC has proposed a "standard room" for making loudspeaker subjective listening tests that is in essence the average of a number of such listening spaces. While a classical engineer may prefer the comfort of a living room environment, the pop/rock recording engineer generally prefers the conditions that exist in a typical control

room. In the control room the primary monitor loudspeakers are usually soffit mounted. There are several reasons for this; primarily, it reduces discrete loudspeaker reflections from the large expanse of glass at the front of the control room. Secondly, it conserves space — which there is never enough of in a control room.

Augspurger (1990) points out that the average ratio of direct to reflected sound in a wide variety of monitoring environments is unity at the listening position. That is, there is as much direct sound as reflected sound. The job of the studio designer is to ensure that the direct sound in the control room is diffuse enough so that it does not interfere with the perception of direct sound. On the other hand, if the reflected sound is too low in level the listener will feel the oppressiveness of such a dead acoustical environment. One way of handling this problem is to make the front portion of the monitoring space fairly absorptive and the back portion fairly live, with good diffusion (Davis and Meeks 1982). Another concern in monitor space design is to minimize direct reflections from nearby surfaces. Figure 10-13 shows the normal arraying of surfaces for this purpose.

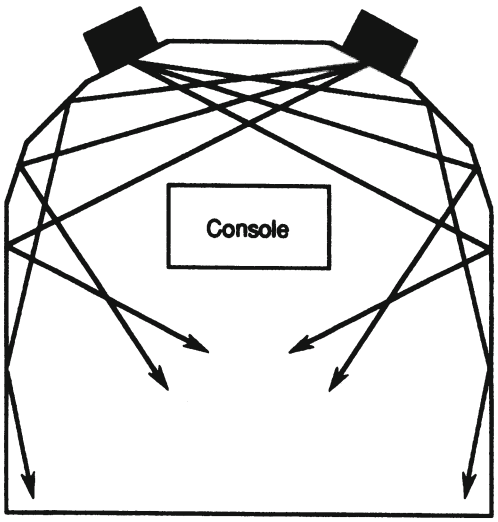

Figure 10-13. A reflection-free zone around a recording console.

Low frequencies present a problem in small monitoring spaces. If the room is not sufficiently damped, discrete room response modes will become apparent, adding mid-bass coloration to the sound. The easiest way around this problem is to damp all low frequencies by means of so-called bass traps. These are architectural elements that are fairly deep (often on the order of a

meter), filled with absorptive materials, and intended to minimize standing waves. Since bass traps absorb LF sound power, it is usually necessary to reinforce the LF capability of the primary monitoring system to restore the net LF capability of the system. Figure 10-14 shows details of a modern control room in which the principal monitors are soffit mounted. It is common in such spaces to provide a variety of smaller monitors, at the client's discretion, to be positioned on the console meter bridge or on stands in front of the console. These may be used for remix activities or as a "reality check" of how the recorded product will sound over small home loudspeakers.

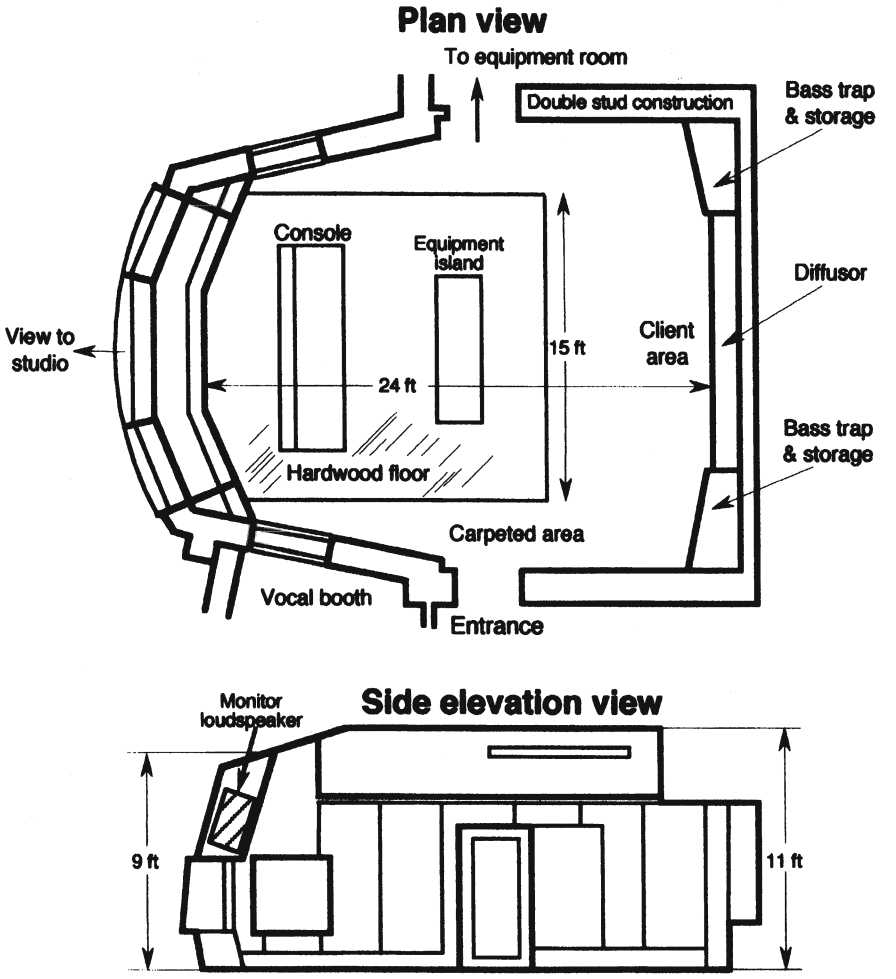

Figure 10-14. A modern control room. (Courtesy G. L. Augspurger and Perception Incorporated)

10.8 The home project studio

During the last two decades the lowly home studio has come of age, and many successful recordings are now made in these informal spaces. The driving force has been MIDI (Musical Instrument Digital Interface) control of electronic instruments and the rise of modular digital multitrack (MDM) and disc-based recorders.

In most cases there is little, if any, acoustical recording done in these spaces. If a vocal line needs to be added, a multi-track work tape or CD can be taken to a full-line studio and the new track added there. Monitoring in these project studios is relatively simple, and is often done entirely over headphones. Small monitors of the type shown in Figure 10-11 are the best choice in these applications.

10.9 Monitor system equalization

Where careful attention has been paid to architectural acoustical details and to monitor specification, response of the left and right loudspeakers may be virtually identical, with only slight differences between them. When channel balance is this close, it may be expedient to use a pair of high-quality one-third octave equalizers to fine tune the systems so that they have the same response at the prime listening position.

Figure 10-15A shows details of the instrumentation used in monitor system equalization. The output of a pink noise generator is fed to the equalizer-amplifier-loudspeaker chain, and the filter sections carefully adjusted so that the acoustical output, as measured on a real-time analyzer matches the desired contour. The filters used for the purpose are *minimum phase*, and their response usually provides a direct complement to that of the loudspeaker drivers themselves. The functioning of the real-time analyzer is shown in Figure 10-15B.

A typical application is shown in Figure 10-16A and *B*. Here, the unequalized left and right channels are reasonably balanced in the monitoring space. However, due to flexible wall structures, LF absorption is considerable, requiring a significant boost in both channels to maintain flat acoustical response down to the 40 Hz range. A 6 dB per octave rolloff above 8 kHz is evident. The amplitude and phase response of the adjusted equalizers are shown at *C* and *D*.

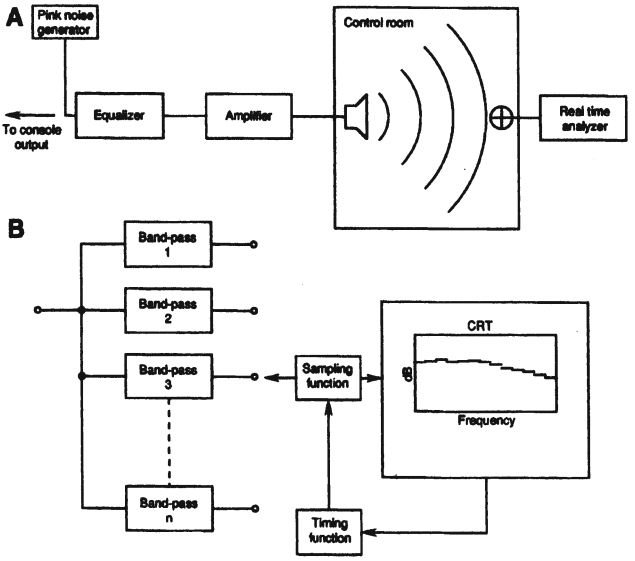

Figure 10-15. Monitor system equalization. A pink noise generator is inserted into the monitor chain just before the equalizer (A); details of the real-time analyzer (B).

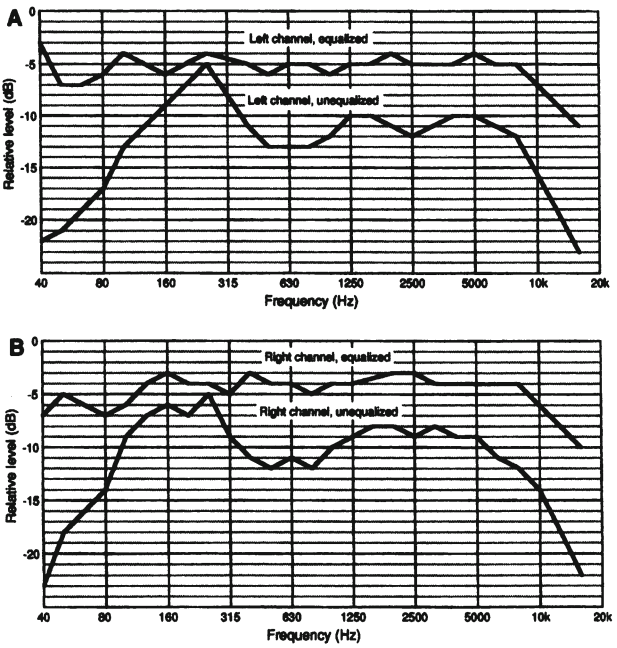

Figure 10-16. An example of monitor equalization. Left channel amplitude resonse before and after equalization (A); right channel response before and after equalization (B); equalizer amplitude response (c) and phase response (D).

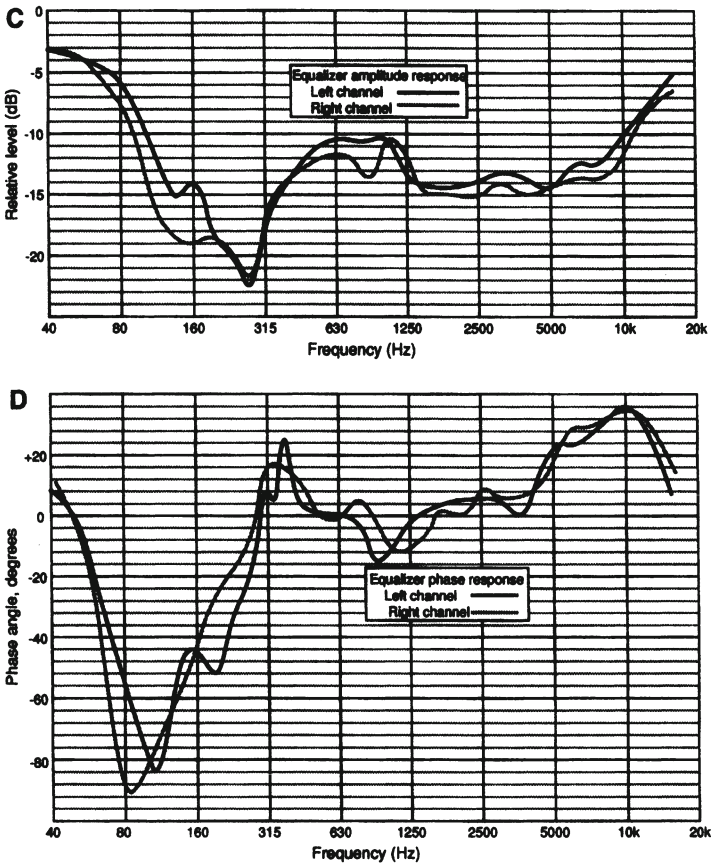

Figure 10-16. Continued.

Finally, we present a number of target monitor system equalization curves. While it may seem natural to equalize monitor system for flat response, a survey of home listening environments indicates that normal system response is rolled off at high frequencies, due primarily to the interaction of room acoustics with the axial and power response of typical home high fidelity loudspeakers. If the engineer and producer balance a recording over flat monitors that sounds correct to them, that recording may sound dull in some listening environments.

This leads, at least tentatively, to the conclusion that the final mastering/ mix-down environment for recordings should represent a center line value in terms of stereo system equalization in the average home and automobile environments. Accordingly, the curves shown in Figure 10-17 provide guidelines for what should be done.

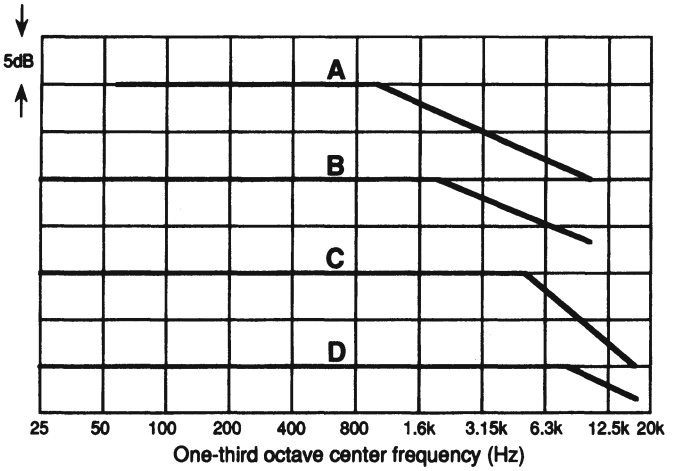

Figure 10-17. Target equalization curves for monitoring. Curve A is used widely in sound reinforcement; curve B is used in motion picture practice; curves C and D have been used in recording control room equalization, with a general preference for curve D. Tolerances of ±1.5 dB can be generally be met above 200 Hz in control rooms, while tolerances of +2, -4 dB can be met below 200 Hz. In well designed control room , smoother response can be expected below 200 Hz.

BIBLIOGRAPHY AND REFERENCES:

Augspurger, G., "The Importance of Speaker Efficiency," *Electronics World*, January 1962.

Augspurger, G., "Versatile Low-Level Crossover Networks, *db Magazine*, March 1975.

Augspurger, G., "Loudspeakers in Control Rooms and Living Rooms," *Proceedings of the AES 8th International Conference*, Washington, DC (1990).

Cooper, J., *Building a Recording Studio*, Synergy Group, Los Angeles (1996).

Davis, D., and Meeks, G., "History and Development of the LEDE Control Room Concept," Preprint number 1954, Audio Engineering Society Convention, Los Angeles (1982).

Eargle, J., "Equalizing the Monitoring Environment," *J. Audio Engineering Society*, volume 21, number 2 (1973).

Eargle, J., "Requirements for Studio Monitoring," *db Magazine*, February 1979.

Eargle, J., and Engebretson, M., "Survey of Recording Studio Monitoring Problems," *Recording Engineer/Producer*, volume 4, number 3 (1973).

Eargle, J., *Handbook of Recording Engineering*, 4th Ed., Kluwer Academic Publishers, Boston (2003).

Engebretson, M., "Low Frequency Sound Reproduction," *J. Audio Engineering Society*, volume 32, number 5 (1984).

Fink, D., "Time-Offset & Crossover Design," *J. Audio Engineering Society*, volume 28, pp. 601-611 (1980).

Gander, M., Chapter 11 in *Loudspeaker and Headphone Handbook* (J. Borwick, ed.), Focal Press, Boston (2001).

Lansing, J., "The Duplex Loudspeaker," *J. Society of Motion Picture Engineers*, volume 46, pp. 212-219 (1946).

Newell, P., *Studio Monitoring Design*, Focal Press, Boston (1995).

Smith, D., Keele, D., and Eargle, J., "Improvements in Monitor Loudspeaker Design," *J. Audio Engineering Society*, volume 31, number 6 (1983).

Thuras, et al., *J. Acoustical Society of America*, volume 6, number 3 (1935).

Chapter 11:
LOUDSPEAKERS IN SPEECH AND MUSIC REINFORCEMENT

11. Introduction

Reinforcement of speech and music has long been commonplace, and performance standards are continually on the rise. With care, the all-important aspects of naturalness and system stability can be maintained, and today many major musical events, indoors and out, are performed with reinforcement of both orchestra and vocalists.

One reason for this is the use of larger venues for performance. For reasons of return on investment, producers of music and stage events prefer to play to as large a house as possible. Outdoor music events are routinely reinforced. When the Hollywood Bowl was built in the twenties, there was no sound reinforcement. There were also no freeways and few if any overflights. Today, ambient noise levels everywhere are on the rise, and sound reinforcement is a way to compensate for it.

Modern pop music, wherever it is performed, is reinforced, primarily because it nearly always has its first existence over loudspeakers and is first distributed by recordings. Generally, young patrons prefer their music to be loud, often to the detriment of their long-term hearing acuity.

11.1 Systems for speech reinforcement

The general requirements for intelligible speech reinforcement are:

1. Good loudspeaker coverage of all patrons.
2. Absolute system stability (freedom from feedback).
3. Adequate signal level at each listener above the ambient noise level in the listening space.
4. Adequate signal to reverberant level at each listener.
5. Suitably short reverberation time in the listening space.

J. Eargle, *Loudspeaker Handbook*

6. Freedom from discrete reflections and echoes in the listetening space.

To these requirements we can add three more that will enhance the quality of listening:

7. Naturalness of sound; the spectrum of reinforced sound should reasonably match that of the talker.
8. The perceived direction of reinforced sound should correspond to that of the talker.
9. The reinforced sound should be substantially free of distortion and be able to reach realistic levels.

11.1.1 Central arrays versus distributed systems

Historically, there have been two approaches to speech reinforcement, the *central array* and the *distributed array*. Generally, the central array is preferred from the point of view of satisfying the nine requirements stated in the previous section. However, in very live spaces the distributed array is often more effective. The choice here can be seen from the decision flow diagram shown in Figure 11-1.

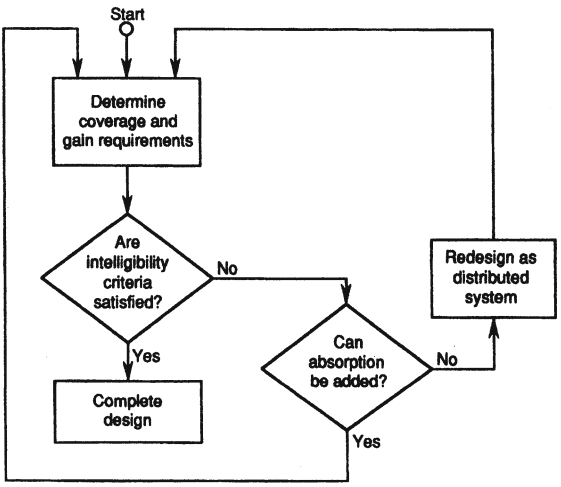

Figure 11-1. Speech reinforcement system design, a decision flow chart.

A central array will work if it can be located so that the longest "throw" of the system will be no more than about four times its height above the floor. There is the further assumption that reverberation time, direct-to-reverberant level, and the pattern of discrete reflections in the listening space satisfy items three to five in the foregoing list of requirements. In highly reverberant spaces it may be impossible to meet these requirements with a central array, and if sufficient absorption cannot be added to the space, the system designer will have to opt for a distributed system.

A distributed system is one in which there are many loudspeakers, each covering only a small portion of the listening area. Since these loudspeakers are located close to the listeners, they will provide a higher direct-to-reverberant ratio at the listener than will the central array, thereby satisfying requirements two and three. However, this is often done to the detriment of perceived naturalness of the reinforced sound.

11.2 The role of signal delay

Through the use of signal delay devices, the performance of distributed arrays can be much improved in terms of naturalness. Signal delay also facilitates the use of both central and distributed arrays in the same space. In general, the use of delay makes it possible to compensate electrically for the acoustical delay that occurs over distance. The principle is shown in Figure 11-2A. If a talker is directly amplified and fed to an overhead loudspeaker, the listener will localize the source of amplified sound directly above. If the signal is delayed by an amount equal to x/344 seconds, where x is the talker-listener distance in meters, then both direct and amplified sound will arrive at the listener at the same time. Because the overhead source will be louder, the listener will still localize the source directly above. However, if the signal is further delayed by a few milliseconds, the source of sound will then appear to be from the front.

The trading value between level and signal delay is indicated at *B*. For a given excess signal delay to the overhead loudspeaker, as indicated on the horizontal scale, the overhead loudspeaker can be driven at a higher level, as shown, with localization tending toward the front.

Another important point in system design is shown in Figure 11-3. Whatever the design approach, it is essential that reinforced sound be aimed where it will do the most good — at the listener. Acoustical power radiated

indiscriminately, as shown at *A*, will result in a greater reverberant level in the listening space than if that same power is radiated into the fairly absorptive audience area, as shown at *B*. The absorption coefficient of an audience at mid and high frequencies is in the range of 0.8, indicating that the initial reflected sound level will be only 20% of the impinging sound, or 7 dB lower.

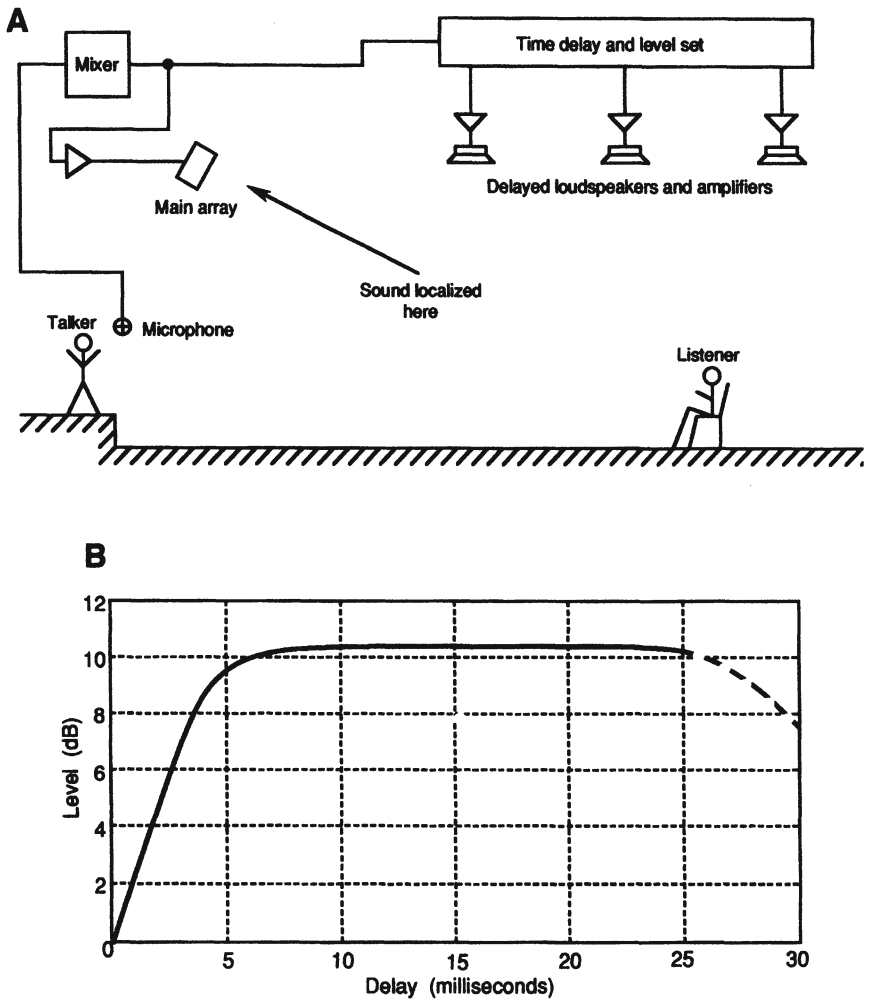

Figure 11-2. The Haas, or precedence, effect. The listener will localize the source of sound along the first arrival direction, even though a later arrival may be significantly louder (A); range of precedence effect; beyond about 25 msec, the listener begins to hear the delayed sound as a discrete echo (B).

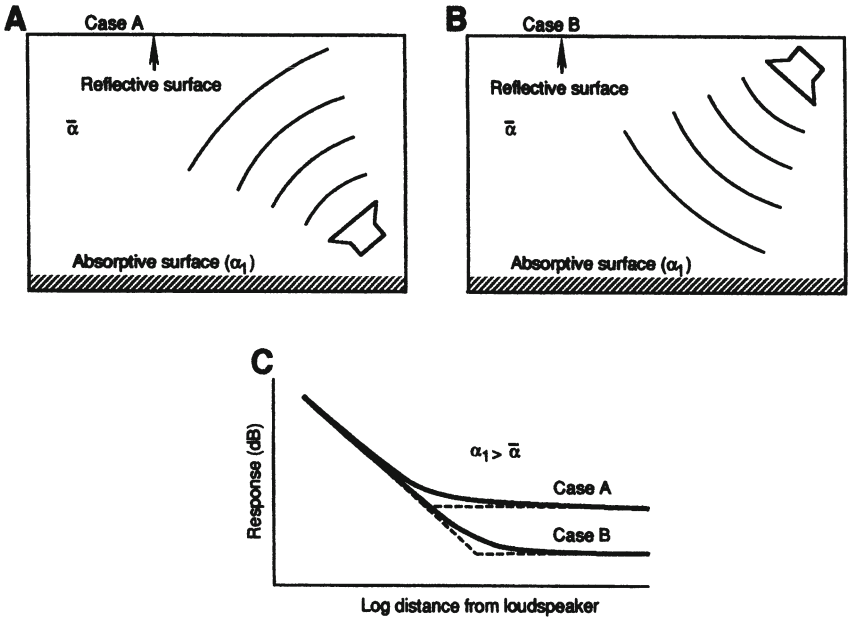

Figure 11-3. Controlling reflected sounds in a performance space. Loudspeakers aimed at reflective surfaces produce a relatively high reverberant field level (A); loudspeakers aimed at the highly absorptive audience area will reduce the reverberant field proportionally (B); attenuation of sound with distance under both conditions *A* and *B* (C).

11.3 Case studies

A few case studies will show how these techniques are normally integrated into sound systems.

11.3.1 Central array with delayed under-balcony loudspeakers

The system shown in Figure 11-4 is typical of many traditional auditoriums. The central array is located above the proscenium in the center of the house. Horns are chosen for their vertical and horizontal nominal coverage angles and splayed along their –6-dB zones in order to provide coverage at MF and HF for all parts of the seating area that are visible from the array. It is advantageous for the horn mouths to be adjacent to each other. If the horns are not of the same length, then the signal to the shorter horns should be delayed so that their electrical acoustic centers are substantially in alignment with the longer ones, as shown.

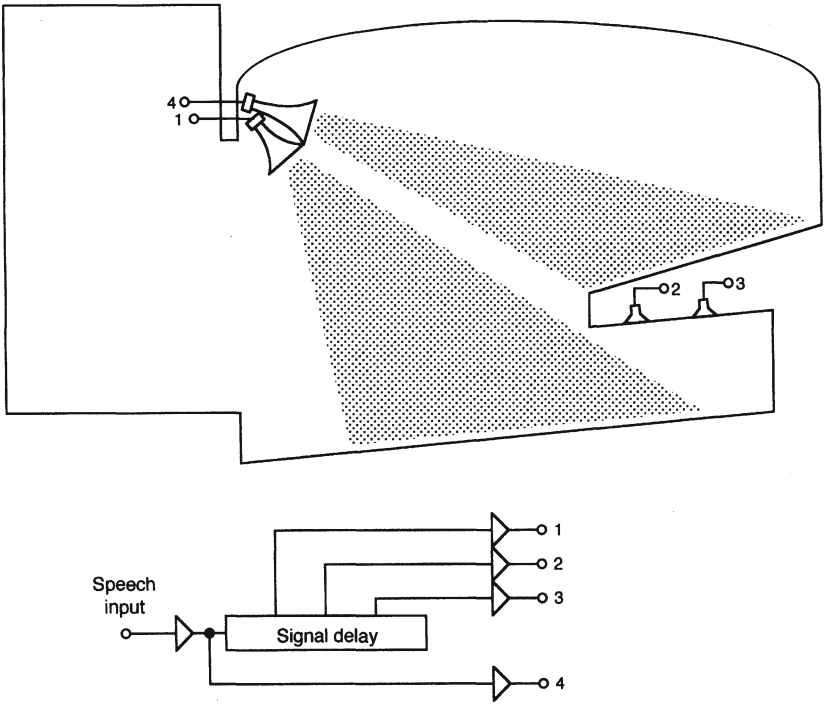

Figure 11-4. Use of signal delay in a large theater sound reinforcement system.

The under-balcony array of loudspeakers is then delayed so that the sound arriving at the listener is slightly delayed, relative to the spill-over sound from central array. In this manner, the listeners well under the balcony will be able to hear clearly, and those listeners in the transition zone at the front of the under-balcony area will not be bothered by disturbing echoes produced by the multiple sources.

The loudspeakers used in the design of the central array are chosen for their precise coverage angles (see Section 7.7). Those mounted in the balcony soffit are chosen for the broadest hemispherical coverage over the frequency range up to about 2 kHz. Nominally, the target angle for –6-dB coverage is 90°.

11.3.2 A pewback system

The pewback system is often used in large, reverberant worship spaces. Essentially, it is a way of reducing the loudspeaker-listener distance so that

the listener is clearly in the direct sound field of the nearest loudspeaker and thus isolated from the room reverberation. Details are shown in Figure 11-5.

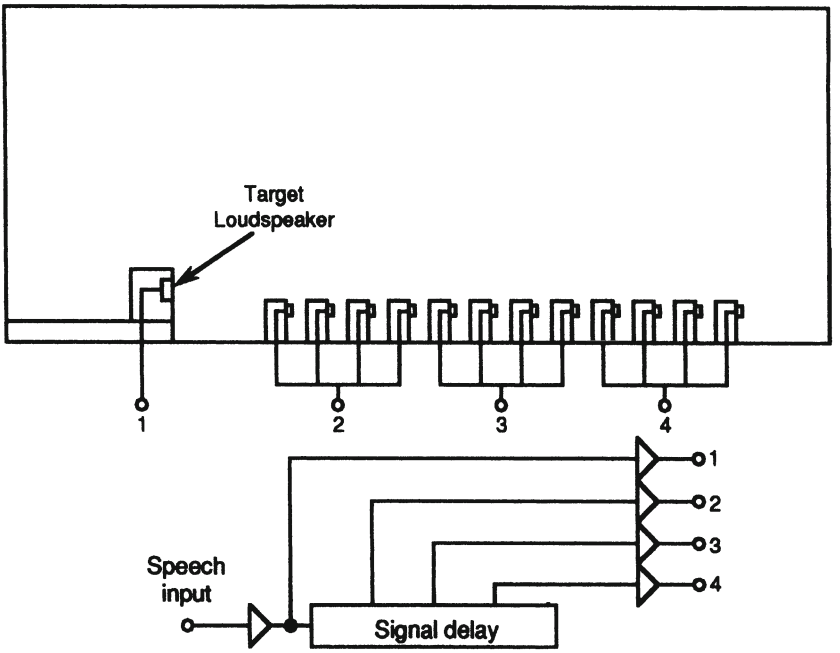

Figure 11-5. Details of a pewback speech reinforcement system in a worship space.

Normally, there is a target loudspeaker at the front of the space. The distributed loudspeakers are located every 1.5 meters or so on the backs of the pews and are zoned for signal delay every 7 meters (20 msec) as measured from the target loudspeaker at the front so that the first arrival sound at each listener will from the front of the room. The delay interval of 20 msec is chosen so as not to exceed the range over which the Haas effect will provide clear localization without echoes. In this way, the listener will tend to localize sound from the front of the space, even though the bulk of the sound heard by the listener is actually coming from the nearest pewback loudspeaker. The loudspeakers chosen for this purpose are small models of perhaps 75 mm diameter with fairly wide frequency range. Whizzer cones are commonly used for their good HF dispersion. The LF bandwidth may be limited to 125 Hz.

These systems are normally used only with speech. Music and other liturgical activities are not generally reinforced over these systems, relying on the natural acoustics of the space.

11.3.3 Speech reinforcement in large public spaces

Modern transportation terminals and convention facilities have large spaces of extended area with relatively low ceilings. Central arrays are normally out of the question here, and ceiling mounted loudspeakers are the usual choice, primarily for good coverage as well as the ease with which they can be zoned for local announcements. When these systems do not work well, it is normally due to insufficient loudspeaker density in the ceiling layout.

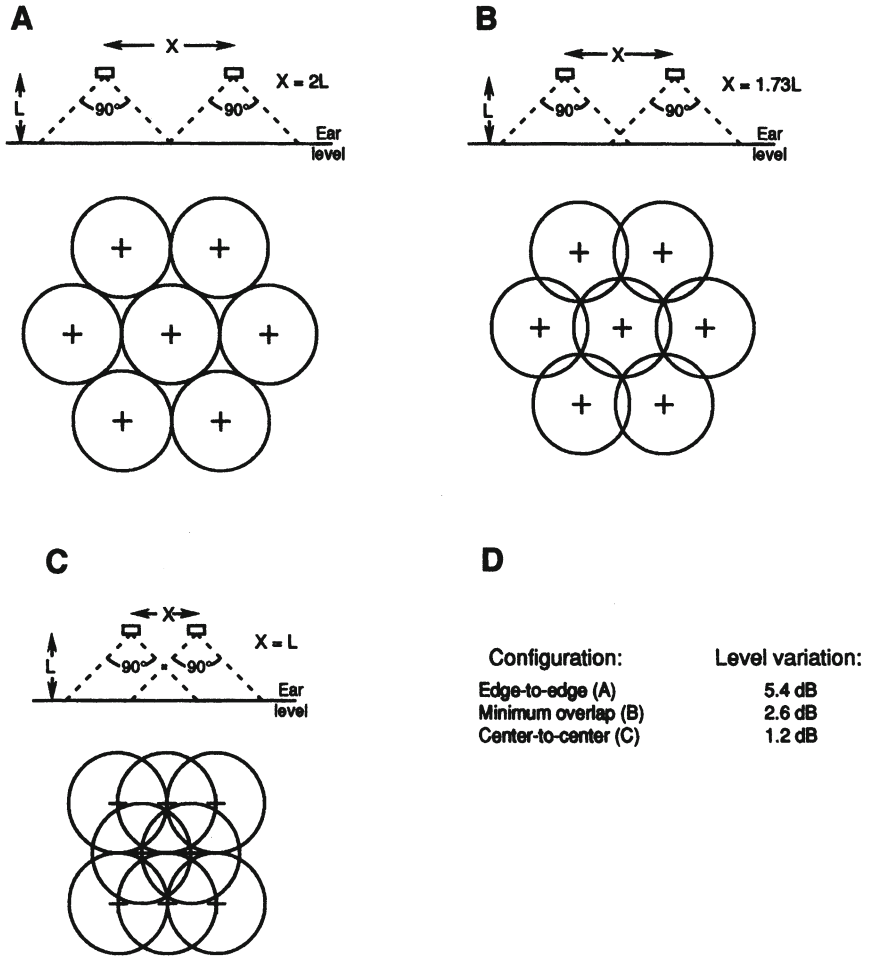

Figure 11-6. Details of triangular ceiling loudspeaker layout. Edge-to-edge layout (A); minimum overlap (B); 100% overlap (C); expected level variations at the ear plane (D).

The layout density determines the smoothness of coverage. No loudspeaker should be used in distributed systems if it does not have a nominal coverage angle of 90° (–6-dB) at 2 kHz. Two loudspeaker layout patterns are commonly used, triangular and square; these are shown respectively in Figures 11-6 and 11-7. Three versions of each layout are shown: edge-to-edge, minimum overlap, and 100% overlap. The recommended choices with either configuration are minimum or 100% overlap. The response variation for each configuration over the coverage area is indicated at *D* in each figure.

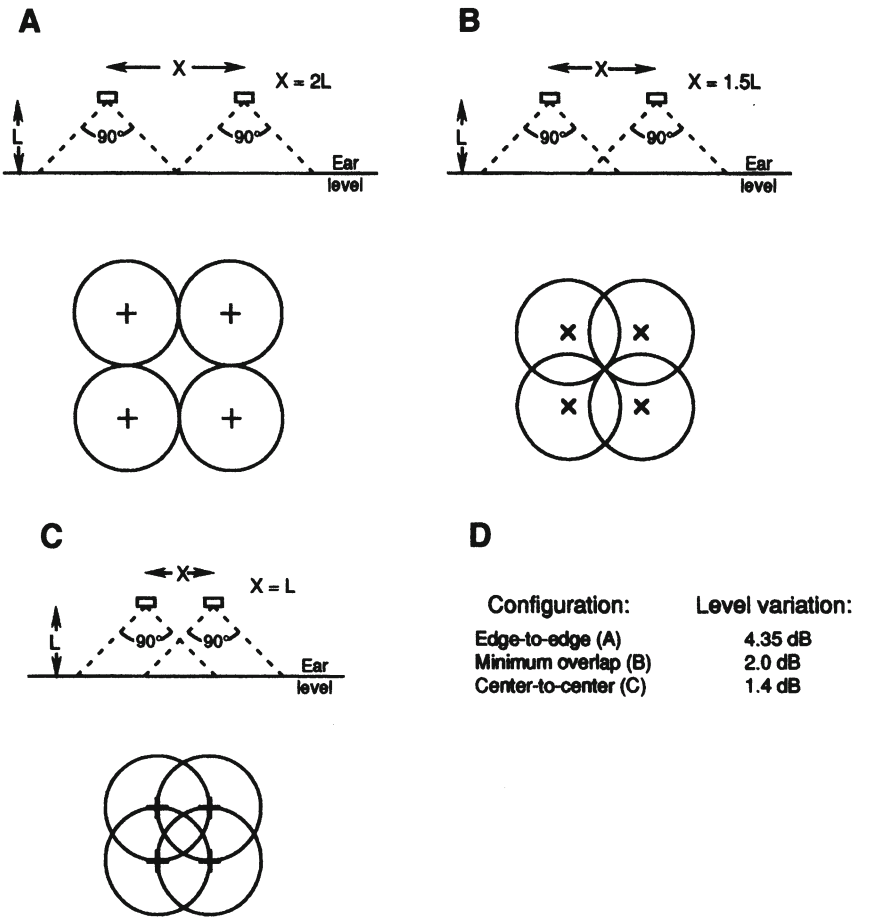

Figure 11-7. Details of square ceiling loudspeaker layout. Edge-to-edge layout (A); minimum overlap (B); 100% overlap (C); expected level variations at the ear plane (D).

Large ballrooms are often provided with distributed systems. In these cases there might be demands for fairly high music levels, and the ceiling requirement may call for a large number of 380 mm (15 in) diameter drivers mounted in suitable enclosures. A matter often forgotten here is the deflection of the driver's cone due to gravity when mounted vertically. This will result in nonlinear performance which may be aggravated over time. The amount of cone deflection is inversely proportional to the square of the free-air resonance frequency of the driver and is shown in Figure 11-8. A high driver resonance frequency, consistent with the required signal bandwidth, should be chosen for these applications.

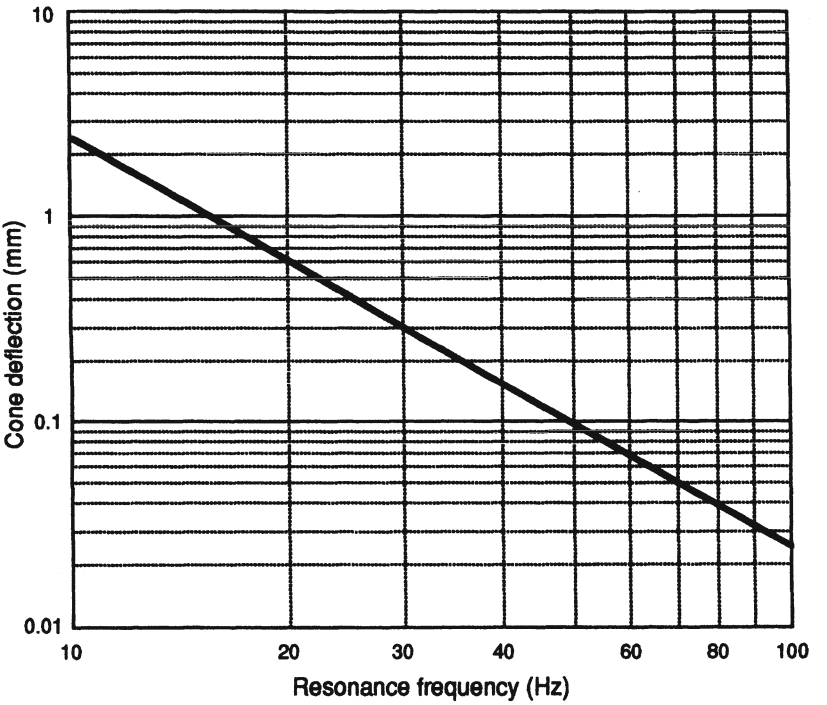

Figure 11-8. Cone displacement for horizontally mounted ceiling loudspeakers.

11.4 Computer simulation of loudspeaker coverage

There are several personal computer programs available for systems designers and consultants in laying out loudspeaker systems in large spaces. (the most popular of these programs is EASE.) The user first enters room boundary and other architectural data. Then, one or more loudspeakers are chosen, mounted,

and oriented in the space. The program then computes the values of direct field coverage and a variety of other readouts, including direct-to-reverberant ratio and an estimate of system intelligibility. Various loudspeaker pattern merging strategies may be used.

Another feature of some of these programs provides a level-versus-time display at any selected listening position. This shows the effects of reflections in the space and can be used to identify troublesome "clusters" of reflections. Some programs also support an auralization program module that will enable the user to actually audition the target system (normally via binaural listening) while it is still on the drawing board.

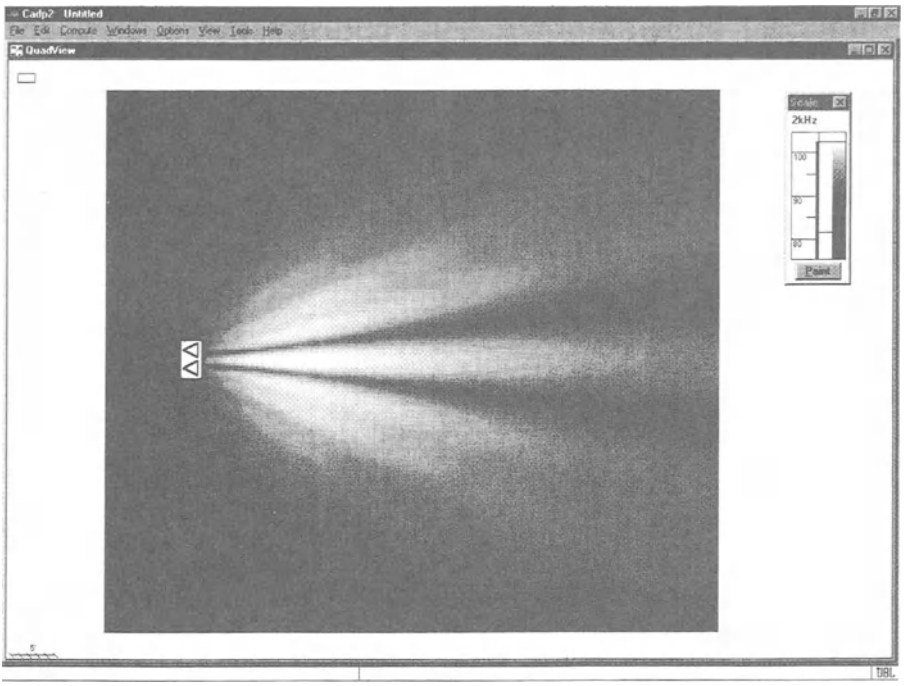

Figure 11-9. Computer estimated direct field coverage at 2 kHz for two HF horns splayed in the horizontal plane. Coverage is as seen from above.

Figure 11-9 shows an example of the coverage pattern of two 90° horns splayed horizontally. The gray scale at the right indicates the resulting levels at the listening plane at 2 kHz. Note that the interference patterns caused by

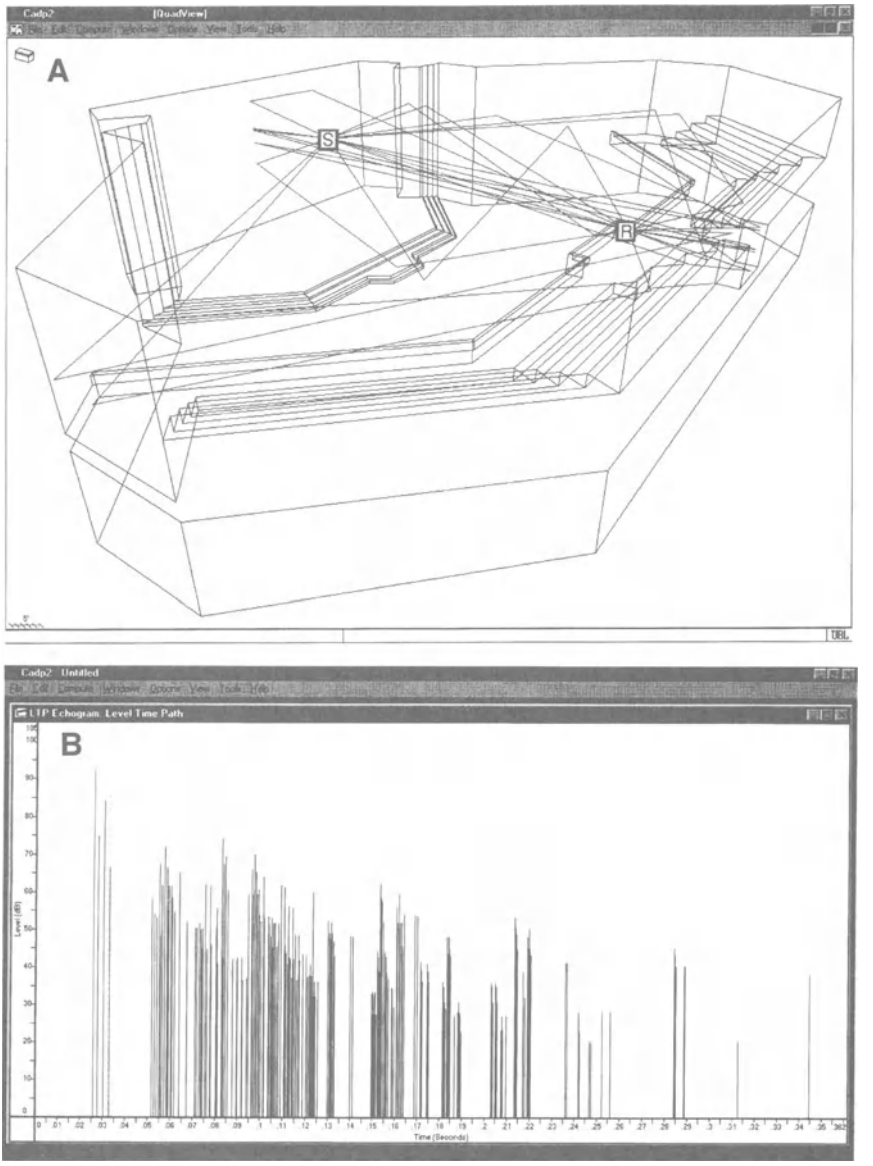

Figure 11-10. Ray tracing through the second order from a source to a receiver in enclosed space (A); impulse response at a typical listening position due to first and second order reflections (B).

reflections is shown at *A*, and the arrival times at a given listener location are shown at *B*. Reflections here are calculated through the second order. Higher order reflections may be examined as well, but the graphical plot showing sound rays tends to get very dense with succeeding orders of reflections.

11.5 System equalization

Even though every effort is usually made to design a reinforcement system that exhibits flat power output over the bulk of its range, some degree of one-third-octave band equalization is normally applied to tailor the system to its acoustical environment, or perhaps to "fine tune" it to the tastes of the user. The measurement technique is similar to that discussed in the previous chapter, and the typical target equalization curve for sound reinforcement systems is shown in Figure 11-11.

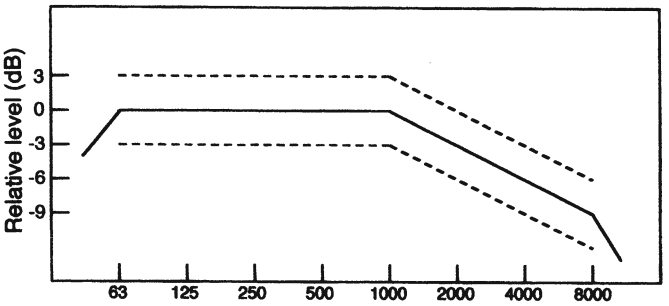

Notes:
1. A tolerance of ±3 dB is suggested.
2. Below 63 Hz and above 8 kHz, let the system roll off steeply.

Figure 11-11. Target equalized resonse of a speech reinforcement system when fed with a wide-band pink noise signal.

Some consultants additionally use a set of individually tuned narrow band dip (notch) filters as a hedge against acoustical feedback at high system operating levels. Normally, only a few of these initial feedback modes will be notched out. The curve shown in Figure 11-12A shows the response of both broad and narrow band equalization of a system. The resulting acoustical response of that system is shown at *B*.

11.6 Measurements and estimation of system intelligibility

There are high expectations of sound reinforcement systems today, and there is a vast body of excellent engineering practice that supports the art. One of the most difficult remaining jobs however is that of estimating speech intelligibility performance that may be expected for a system that is still on the drawing board.

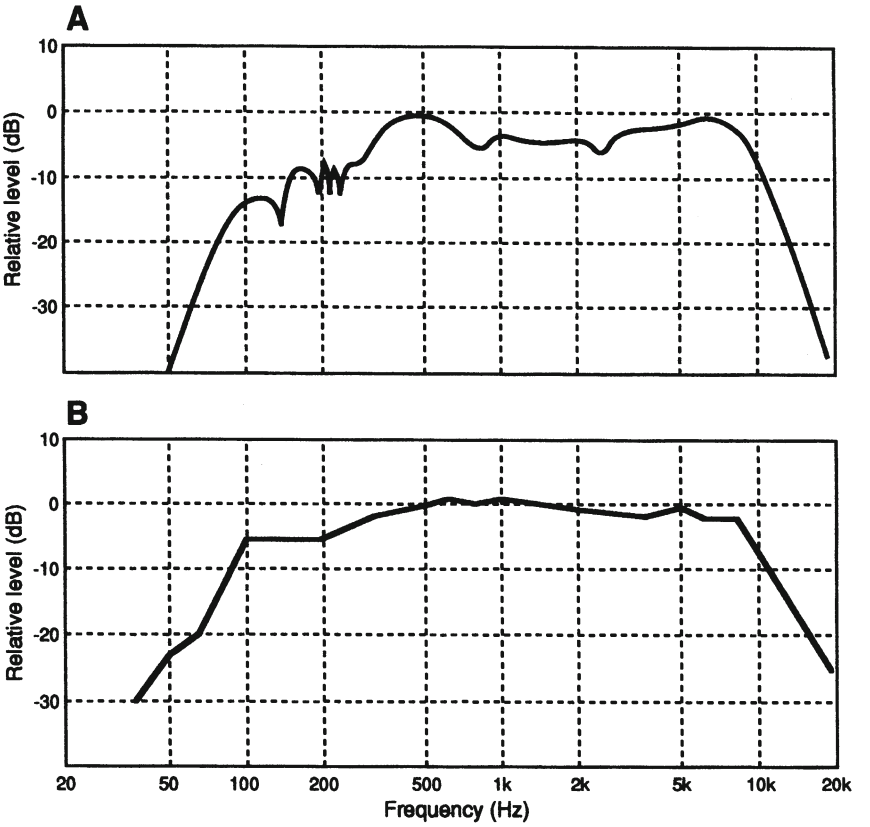

Figure 11-12. Broad band and narrow band system equalization. Electrical response of filters (A); net acoustical resonse, measured on 1/3-octave intervals (B).

There are number of on-site measurement methods for determining the effectiveness of installed systems:

1. *Actual syllabic testing:* Subjects are asked to write down test words as they hear them in various parts of the hall. The test words are imbedded in a "carrier sentence" so that the words to be identified are heard in the context of running speech. Many tests must be made with the same group of subjects in order to establish reasonable testing confidence limits. In general, if a subject identifies 85% of the random test words, then that subject would be able to identify about 97% of all words in the sentence context of normal speech.

2. *Modulation Transfer Function (MTF):* Houtgast and Steeneken (1972) developed a method for measuring the effects of noise and reverberation on the integrity of speech. Their method of measuring these effects is to play

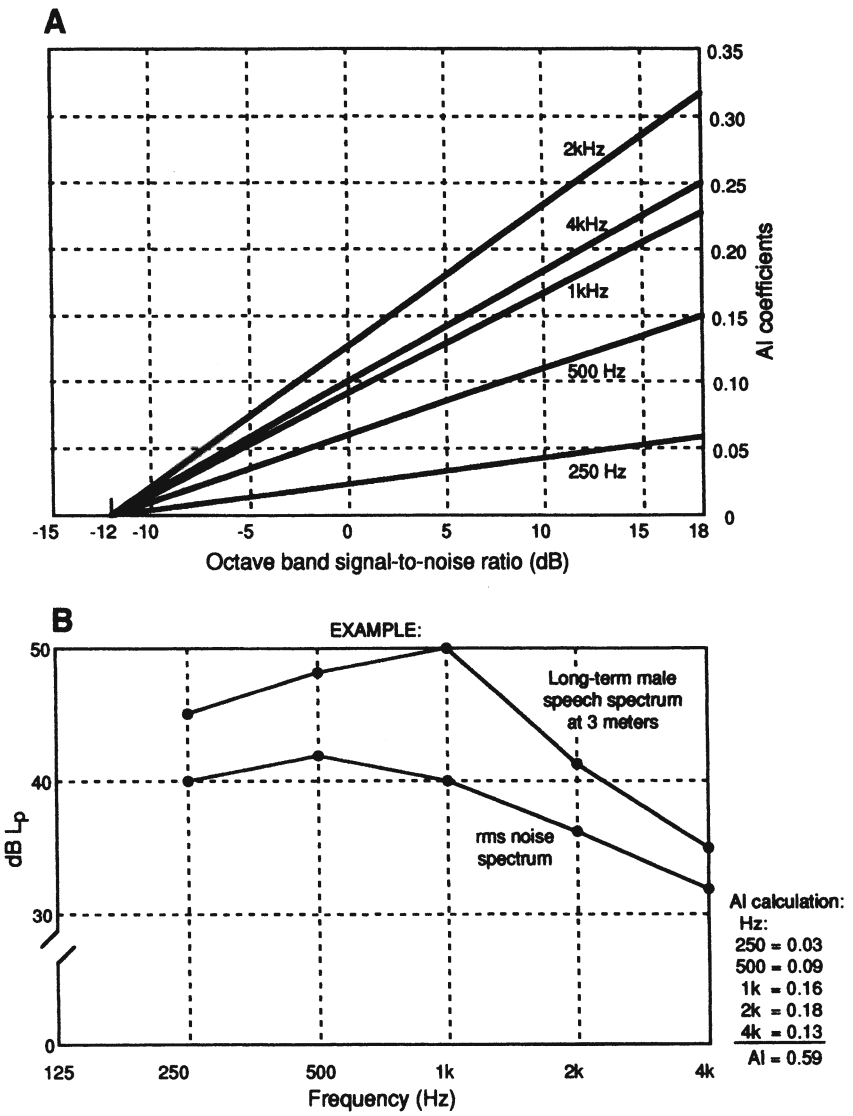

Figure 11-13. Calculation of Articulation Index (AI). Determination of weighting factors (A); example of a typical calculation (B).

a complex signal into the test space via loudspeaker and measure it at selected test points. The signal is then analyzed, noting the reduction in modulation index of the signal caused by noise and reverberation effects. These components are weighted and a numerical rating is given to the system.

A simplification of this procedure, known as RASTI (RApid Speech Transmission Index) has been implemented into a convenient measuring

system for on-site use. A small loudspeaker receives the test signal and is placed where the talker would ordinarily be. The receiving microphone is located at a target listening position and fed to the analyzer. The output is a numerical rating of the speech transmission index over that particular path.

3. *Clarity Index (Deutlichkeit):* Thiele (1953) proposed a measurement of speech clarity based on early-late ratios of reflections of an impulse function delivered to a room. His basic equation is:

Other workers in the field have devised methods for estimating intelligibility, without necessarily making measurements in the target space:

$$\text{Deutlichkeit} = \frac{\int_0^{50\text{ ms}} [g(t)]^2\,dt}{\int_0^{\infty} [g(t)]^2\,dt} \times 100\% \qquad 11.1$$

1. *Articulation Index (AI):* As developed by Bell Telephone Laboratories for use primarily in telephone research, AI evaluates intelligibility in terms of signal-to-noise ratios in five weighted octave bands. The method, as modified by Kryter (1962), is shown in Figure 11-13.

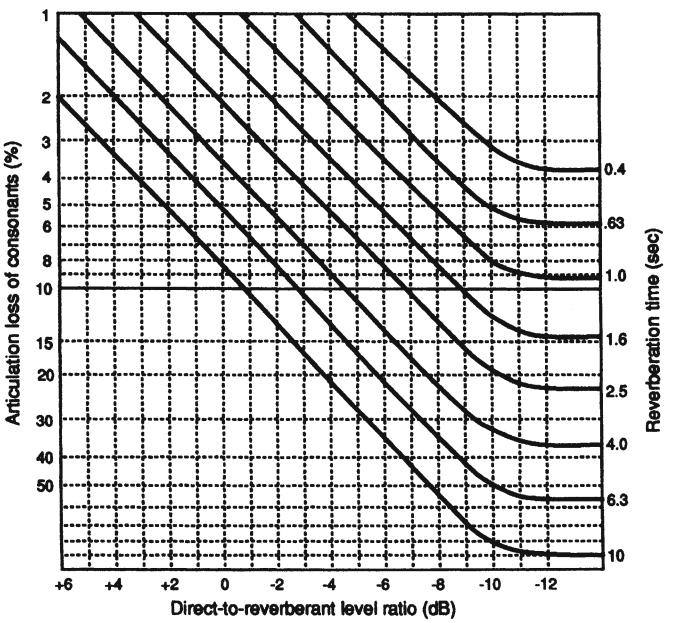

Figure 11-14. Calculation of Peutz' percentage articulation loss of consonants.

2. *Percentage Articulation Loss of Consonants (%Al_{cons})*: Peutz (1971) determined that, in spaces where the speech-to-noise ratio was high, articulation loss of consonants could be determined by noting the reverberation time and direct to reverberant ratio in the octave band centered on 2 kHz. The basic relationships are shown in Figure 11-14.

Al_{cons} calculations can be modified to include the effect of the A-weighted noise level in the space to be analyzed, as follows:

$$\%\text{Alcons} = 100 \times (10^{-2(A + BC - ABC)} + 0.015)$$

where:

$$A = -0.32 \log \left(\frac{E_R + E_N}{10E_D + E_R + E_N} \right)$$

$$B = -0.32 \log \left(\frac{E_N}{10E_R + E_N} \right)$$

$$C = -0.5 \log \left(\frac{T_{60}}{12} \right)$$

$$E_R = 10^{\frac{L_R}{10}}$$

$$E_D = 10^{\frac{L_D}{10}}$$

$$E_N = 10^{\frac{L_N}{10}}$$

In these equations, L_R, L_D, and L_N are, respectively, the A-weighted levels of reverberation, direct sound, and noise. See Eargle and Foreman (2002) for examples using this procedure.

The various methods of estimating intelligibility can be compared with each other, as shown in Figure 11-15. For example, the correlation between syllabic testing and AI is given at *A*. The correlation between clarity index and measured speech intelligibility is shown at *B*. While these figures show reasonable trends, the standard errors appear fairly large, often of the order of ±10%.

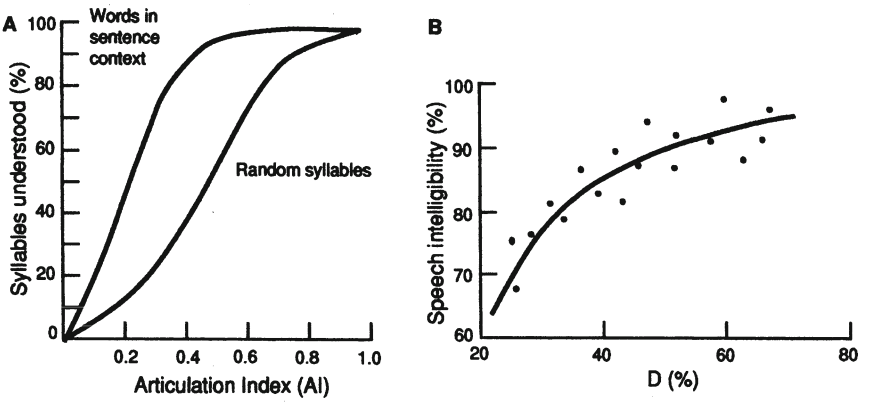

Figure 11-15. Correlation between intelligibility of random syllables and words in normal sentence context (A); correlation between clarity index and measured speech intelligibility (B).

If it is possible, within reasonable limits, to estimate noise levels, reverberation time, and direct to reverberant ratios that will exist in yet unbuilt spaces, that data may be entered into the AI and $\%Al_{cons}$ charts and a rough estimate of sound system intelligibility made. The charts may tell us that a system is going to be very good (or very bad), but confidence limits on marginal system performance may be rather wide.

11.7 Electronic halls

The term "electronic hall" refers to spaces whose acoustics have been enhanced via signal processing and loudspeakers. Many modern halls are multi-purpose designs, and as such must provide well damped acoustical properties for, say, lectures and motion pictures, as well as varying degrees of acoustical liveness for music performance. Electronic enhancement is one way of accomplishing this. Other halls may be acoustically deficient in one regard or another, and electronic enhancement may represent a more attractive economical alternative to actual acoustical redesign of the hall. In the future we may see halls in which simultaneous cultural and public events are presented, along with large-scale video projection – all at great remove from the actual event.

11.7.1 Assisted Resonance

One of the earliest successful applications of electronics in architecture was the Assisted Resonance system installed in Royal Festival Hall in London (Parkin 1975). As originally designed, the hall lacked sufficient volume for its

seating capacity and target reverberation time. The Assisted Resonance system was installed to increase reverberation time in the frequency range from 60 to 700 Hz.

As shown in Figure 11-16, a total of 172 individual microphone-amplifier-loudspeaker channels were installed in the ceiling of the hall. The microphones were mounted in Helmholtz resonators so that each channel responded to a single narrow band of frequencies. Tunings were spaced so that they effectively overlapped in the desired frequency band. The microphones are located well away from direct sound sources and pick up primarily reverberant cues in the space. Because of their narrow band response, the individual channels are quite stable, and the increase in apparent reverberation time results primarily from the high-Q tuning of each resonator.

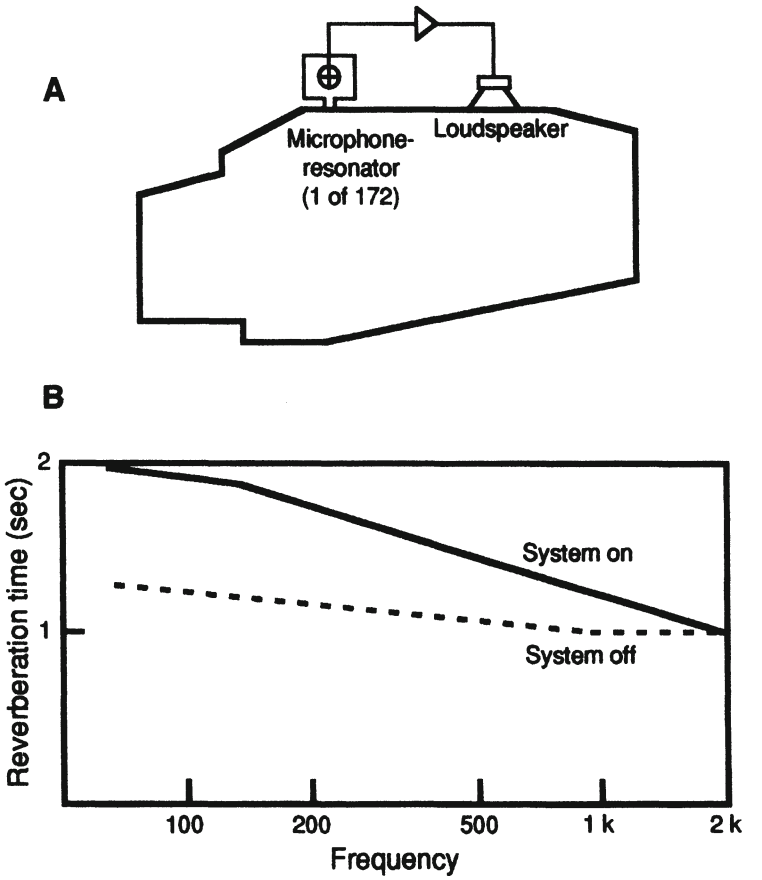

Figure 11-16. Assisted resonance. System layout (A); reverberation time with and without system functioning (B).

11.7.2 Sound field amplification

Sound field amplification was a later development, and there are a number of directions that have been pursued. In the method shown in Figure 11-17, many individual wide-band microphone-amplifier-loudspeaker channels are arrayed about a performance space, more or less randomly, and each is operated at a relatively low gain setting (usually in the range of –15 to –20 dB). Properly adjusted, the ensemble of these amplification channels can produce the effect of a more reverberant target space – one of the same dimensions as the actual space in which the system is operating. In other words, the system effectively decreases the natural boundary absorption, resulting in an increase in reverberation time as well as a decrease in direct to reverberant ratio.

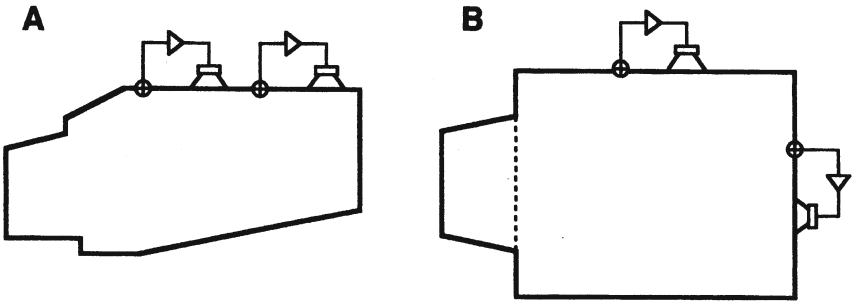

Figure 11-17. Sound field amplification. Section view (A); plan view (B).

11.7.3 Lexicon Acoustical Reverberance Enhancement System (LARES)

LARES is a relatively recent development consisting of a number of microphone-reverberator-loudspeaker chains distributed about a space. For a large installation there would typically be 2 microphone inputs channels, 16 reverberators, 8 amplifier channels, and upwards of 40 loudspeakers, as shown in Figure 11-18. LARES is basically configured as a large distributed sound reinforcement system with the inclusion of digital reverberation generators, and as such can be operated for purposes of sound reinforcement as well as reverberation enhancement.

An important element in the performance of LARES is the use of randomly varying delay parameters in the operation of the reverberation elements, making it difficult for acoustical feedback to occur at normal gain settings of the system. Since reverberation time can be set independently of system gain,

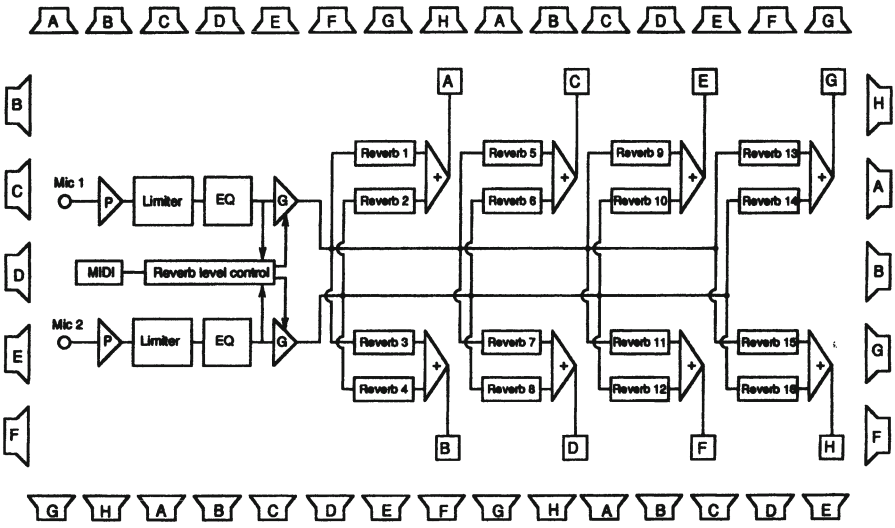

Figure 11-18. Details of LARES system.

LARES offers the user a degree of flexibility in meeting program demands that the other systems discussed here cannot match.

11.7.4 Acoustical Control System (ACS)

As described by Berkhout (1988), ACS, a horizontal line of microphones in front and over a performance stage is connected with a line of house loudspeakers through a control matrix, as shown in Figure 11-19. This portion of the system amplifies the direct sound from the stage, and the subsequent wavefront reconstruction by the line of loudspeakers gives an accurate mapping of the stage sound sources for all listeners. An additional part of the system provides a number of microphone-delay-amplifier-loudspeaker loops located in the performance space to increase reverberation.

11.7.5 Delta Stereophony

Delta Stereophony is a system that is used to increase loudness in large performance spaces without compromising the natural directional cues that come from the stage. Details of the system are shown in Figure 11-20. The system includes loudspeakers positioned at stage level as well as overhead. The number of delay channels can depend on the venue size, but does not normally exceed 6 to 8.

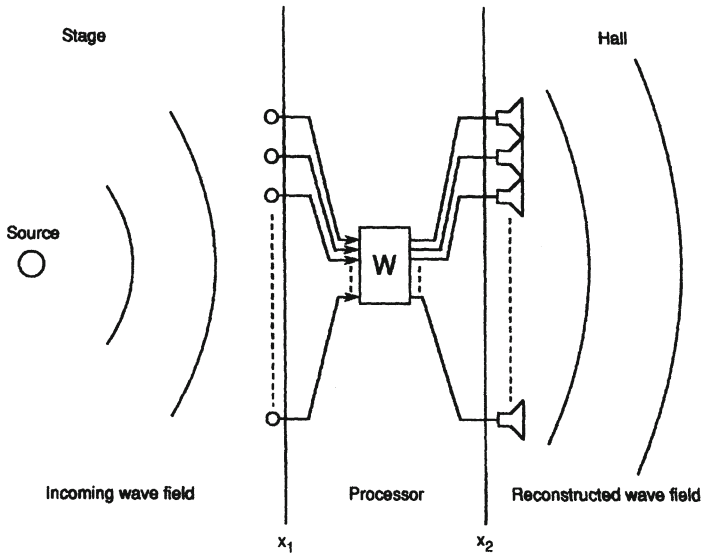

Figure 11-19. Details of ACS system.

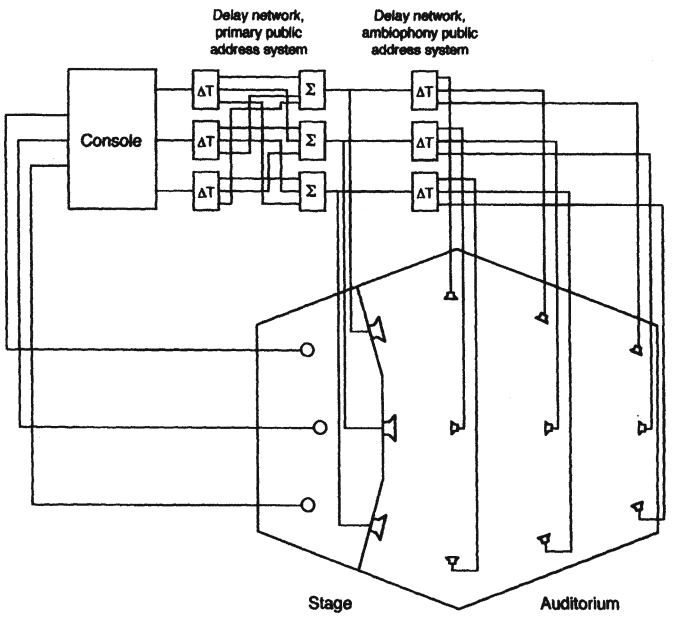

Figure 11-20. Details of Delta Stereophony system.

11.8 Environmental effects on sound propagation

The propagation of sound can be profoundly influenced by wind, temperature, and humidity. These are are aggravated all the more by gradient effects that often exist out of doors.

11.8.1 Effects of wind

The velocity of sound in air is the sum of its velocity in still air and the velocity of wind in a given direction. Moderate winds will have little effect, but pronounced wind velocity gradients, especially over large distances, affect the distribution of sound, as shown in Figure 11-21. The effect on the direction of sound in a strong cross breeze is shown in Figure 11-22.

11.8.2 Effects of temperature

Sound travels faster in warm air than it does in cool air, and the gradient effects shown in Figure 11-23 are commonly observed in early morning and evening hours as the sun rises or sets. Over very large distances, sound may be observed to skip, creating quiet zones.

11.8.3 Effects of humidity

Humidity effects can easily be noticed indoors. and typical examples are shown in Figure 11-24. As seen at *A*, the frequency spectrum of a sound reinforcement system will vary significantly over distance, especially if the relative humidity is fairly low.

The data shown at *B* indicates the excess attenuation with distance as a function of frequency and relative humidity.

It is also worth noting that reverberation time will be shortened at high frequencies when the relative humidity is quite low.

11.9 Systems for high-level music performance

Traditionally, music amplification in large venues has made use of multiple arrays of full-range systems, assembled on-site. These systems are rigged so that they flank the performance stage, providing multichannel reinforcement. Subwoofers are normally placed at gound level.

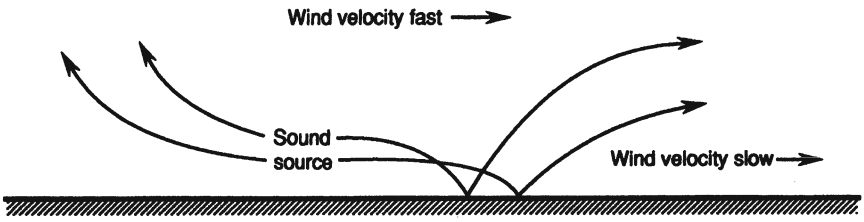

Figure 11-21. Effects of wind velocity gradient on sound propagation.

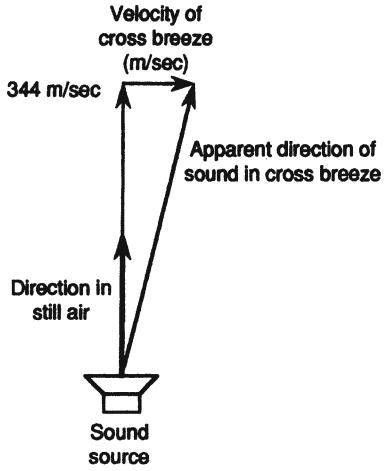

Figure 11-22. Effect of cross breeze on sound propagation.

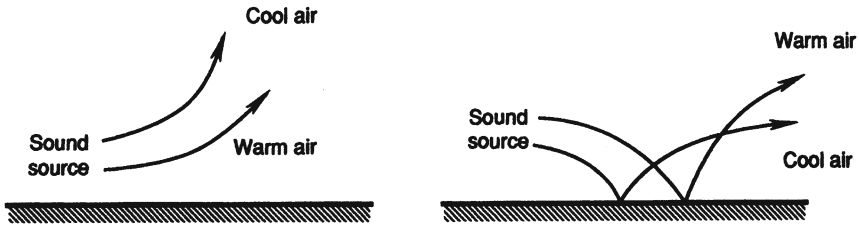

Figure 11-23. Effect of temperature gradients on sound propagation.

A typical ground level "stack" is shown in Figure 11-25A. Ground plane measurements made at a distance of 10 meters (33 feet) of this system over several horizontal angles are shown at *B*. At LF, where the signals are relatively coherent, the response is very strong. At MF and HF the response shows the progressive effects of cancellations and reinforcement among the ensemble of elements. Severe comb filtering is basically inherent at MF and HF in systems of this design, and this requires extensive equalization of the system

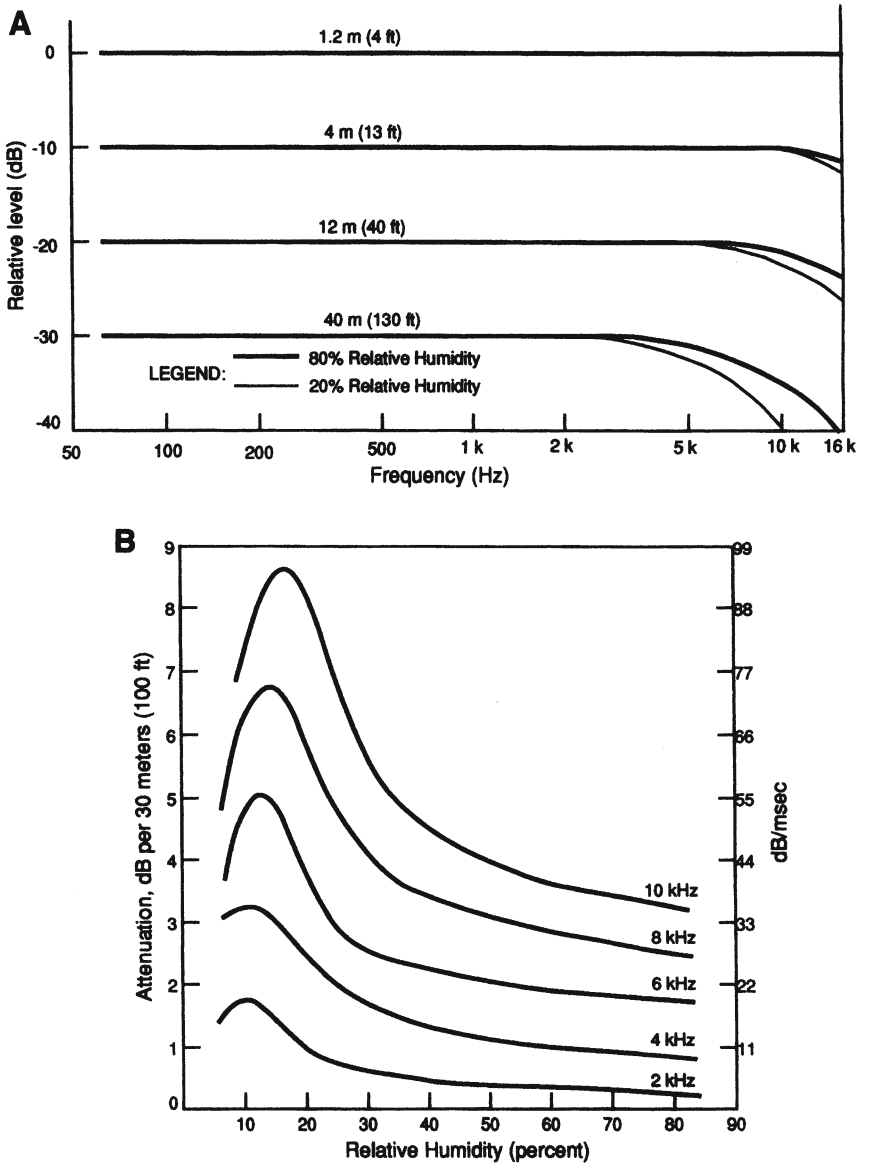

Figure 11-24. Atmospheric losses: due to both inverse square relationships and humidity (A); relative attenuation versus distance and signal transit time as a function of relative humidity and frequency (B).

to provide a more uniform spectrum over the listening area. While systems such as these have served the music reinforcement industry well over three decades, newer trends in large scale music reinforcement favor the use of high performance line arrays, as discussed in Chapter 6.

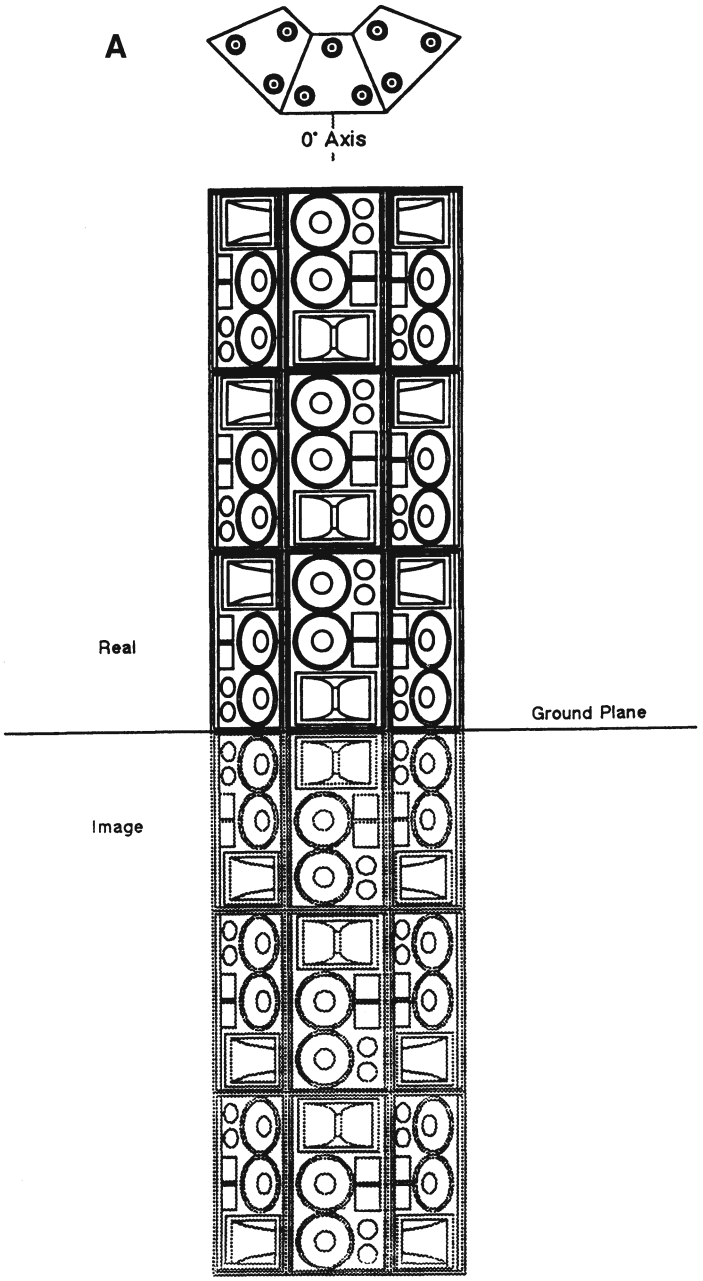

Figure 11-25. Response of a large loudspeaker array for music reinforcement. View of array (A); ground plane frequency response measurements of array in the horizontal plane (B).

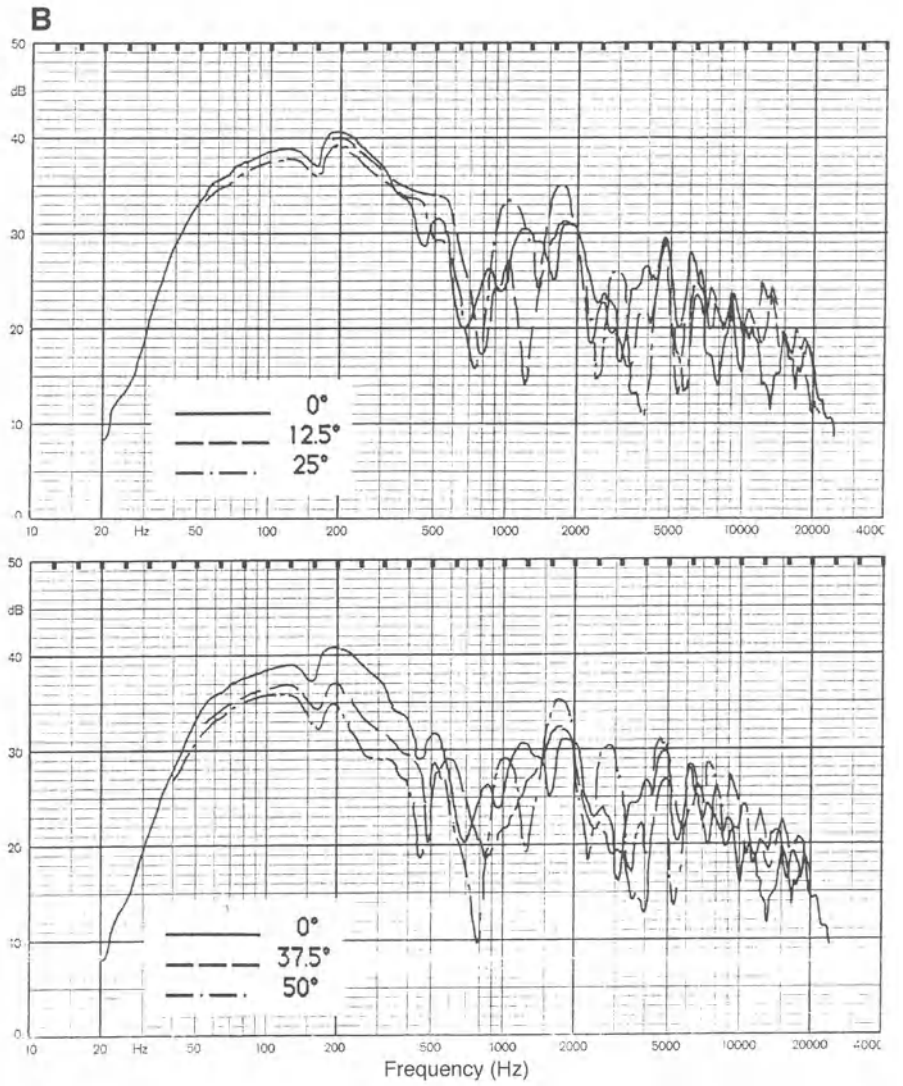

Figure 11-25. Continued.

11.10 System stability

Throughout this chapter we have emphasized the importance of stability in sound reinforcement systems without defining the factors that govern it. Stability is defined here as the absence of electroacoustical feedback, a condition in which sound from the loudspeakers finds itself recirculating

through the system microphones and back again through the loudspeakers. There are several factors that can minimize the problem:

1. Use of close operating distances between microphone and talker/performer.
2. Locating microphones well outside the direct field coverage of loudspeakers.
3. Gating off any unused microphones.
4. Using well-behaved microphones, those whose pickup patterns are uniform over a wide frequency range and whose response is peak free.
5. Skillful employment of signal processing.

For example, the LARES system discussed in section 11.7.3 permits relatively high reinforcement system gain through the use of random delay parameters that "spoil" the normal tendency of the system to go into electroacoustical feedback at high gain settings.

REFERENCES AND BIBLIOGRAPHY:

Ballou, G., *Handbook for Sound Engineers*, Focal Press, Boston (1987).

Boner, P. and R., "The Gain of a Sound System," *J. Audio Engineering Society*, volume 17, number 2 (April 1969).

Borwick, J., (ed.), *Loudspeaker and Headphone Handbook*, Butterworths, London (1988).

Davis, D. and C., *Sound System Engineering*, Focal Press, Boston (1987).

Eargle, J., *Electroacoustical Reference Data*, Kluwer Academic Publishers, Boston (1994).

Eargle, J. and Foreman, C., *Audio Engineering for Sound Reinforcement*, Hal Leonard, Milwaukee, WI (2002)

French, N., and Steinberg, J., "Factors Governing the Intelligibility of Speech Sounds," *J. Acoustical Society of America*, volume 19, pp. 90-119 (1947).

Houtgast, T. and Steeneken, H., "Envelope Spectrum and Intelligibility of Speech in Enclosures," Presented at IEE-AFCRL Speech Conference (1972).

Kryter, K., "Methods for the Calculation and Use of Articulation Index," *J. Acoustical Society of America*, volume 34, p. 1689 (1962).

Parkin, P., "Assisted Resonance," *Auditorium Acoustics*, pp. 169-179, Applied Science Publishers, London (1975).

Peutz, V., "Articulation Loss of Consonants as a Criterion for Speech Transmission in a Room," *J. Audio Engineering Society*, volume 19, number 11 (1971).

Thiele, R., *Acustica*, volume 3, page 291 (1953).

Chapter 12:
MULTICHANNEL SYSTEMS FOR FILM, VIDEO, AND MUSIC

12 Introduction

In a commercial sense, film and video entertainment dominate the world of audio, and yet are completely dependent on it. While motion picture sound has made steady strides over the decades, the relatively recent home theater phenomenon, driven in recent years by videotape, Laserdiscs, and the DVD, has literally redefined how most people spend their leisure time at home and, by extension, how they listen to music.

For music-only presentation, the familiar stereo system, which has delivered music to us for more than four decades, is slowly being replaced by digital five-channel systems. This new technology is capable not only of delivering convincing multichannel sound for video, but also music in a format known generally as *surround sound*. The loudspeakers have not changed significantly, but the playback environment has.

In this chapter we will examine the requirements for sound reproduction at the film production end, as well as observe how these techniques are brought into the home with maximum effectiveness.

12.1 Evolution of theater loudspeaker systems

When sound was introduced into the motion picture in the late twenties, the requirement of filling a large room with adequate sound levels was hard to meet. Amplifiers of the day were usually in the 10-watt range, and loudspeakers had to be as efficient as possible. No wonder then that the early art depended almost entirely on the development of horn systems. Figure 12-1 shows significant stages in the early art. The Western Electric model 15A horn and 555 driver are shown at *A*. This one-way system had a frequency response of 100 Hz to 3 kHz. A subsequent version added a HF element along with a

J. Eargle, *Loudspeaker Handbook*

group of 460 mm (18 in) diameter subwoofers in open back enclosures, as shown at *B*.

The first promising step in the art occurred in the mid-thirties with the introduction of the Shearer-Lansing two-way system, shown in Figure 12-2. The on-axis bandwidth of this system was fairly smooth from 50 Hz to 8 kHz, and the output capability was sufficient for the largest houses of the day.

A

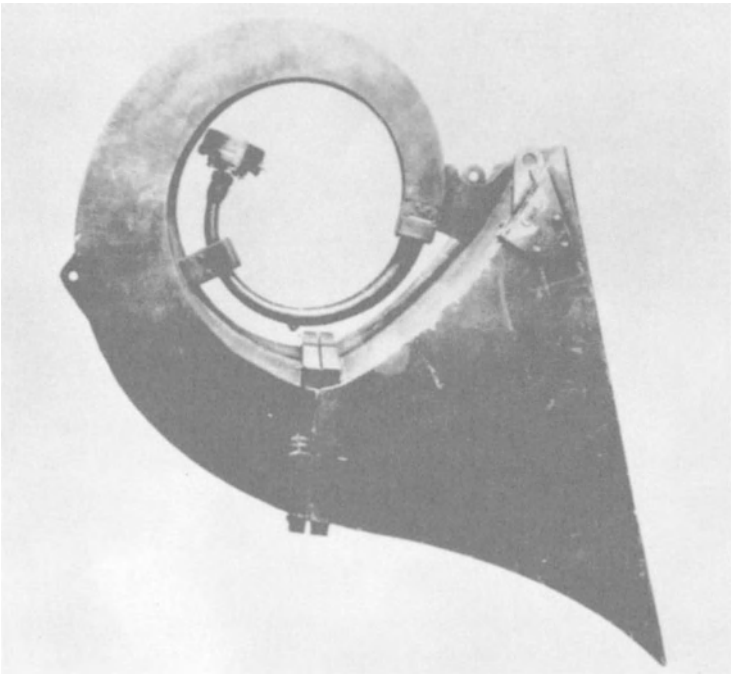

Figure 12-1. Western Electric 15A horn with 555 driver (A); an early three-way system (B). (Bell Telephone Laboratories data)

During the forties, the LF portion of this design gave way to a hybrid ported horn system, similar to that shown in Figure 12-3. The HF portion of the system remained as a multicellular horn-driver combination, crossing over from the LF section in the range of 500 Hz. This system approach, with minor variations, served the industry until the mid-1970s.

During the 1970s, Dolby Laboratories introduced noise reduction systems to the film industry; as a result, a new look was taken at both theater acoustics and existing loudspeaker hardware. It was soon discovered that biggest obstacle

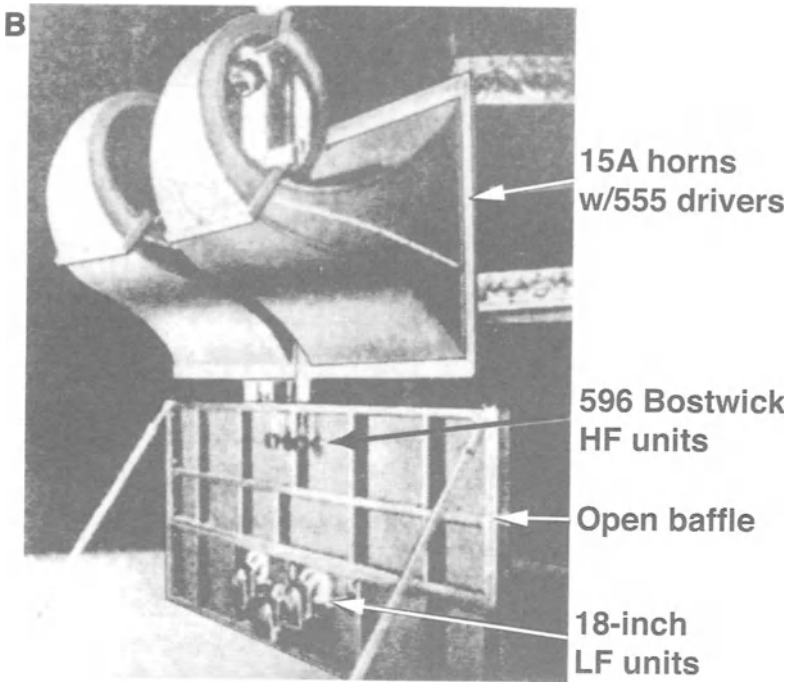

Figure 12-1. Continued.

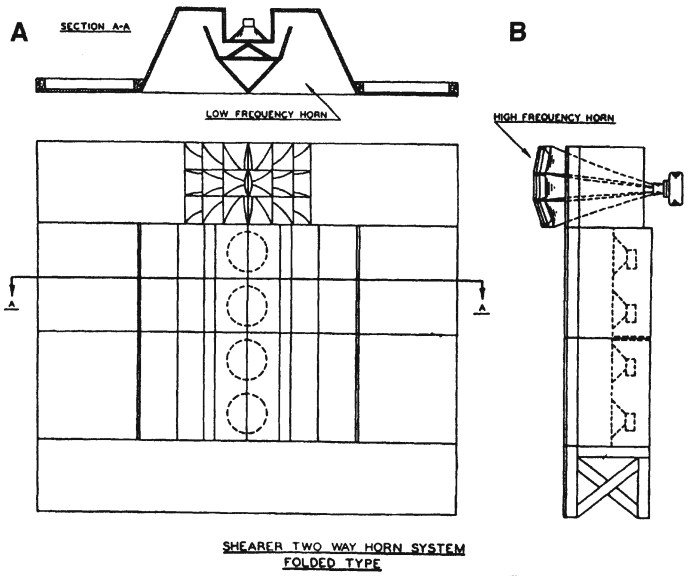

Figure 12-2. The Shearer-Lansing (MGM) system. Front view (A); side view (B). (From *Motion Picture Sound Engineering*, Van Nostrand, 1938)

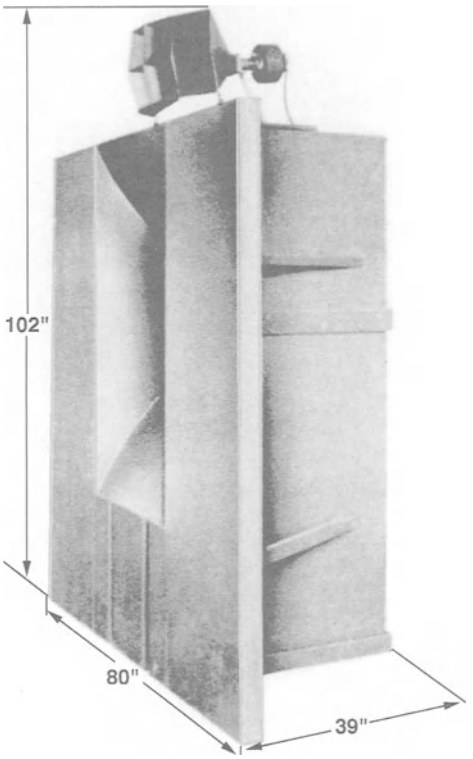

Figure 12-3. The Altec Voice of the Theatre A-4 system. (Data courtesy Altec)

to good sound coverage in the theater was the disparity between the on-axis response of existing systems and their power response. While the existing systems could be coaxed into producing reasonable on-axis response, the power response of the systems was far from ideal, often exhibiting large "lumps" in response in the mid-bass and lower treble ranges.

Figure 12-4 makes this clear. Off-axis response of a typical ported horn system is shown at *A*. The disparity between on- and off-axis response above 200 Hz indicates uneven audience coverage in a very critical portion of the frequency range. At HF, the standard multicellular horn was generating its own patterns of response irregularities (see Section 7.7.1). The one-third octave measurements shown at *B* indicate the range of variation in power response encountered in theaters of the day.

Responding to these difficulties, a number of loudspeaker companies undertook new designs, and the 2-way art reached its culmination in systems

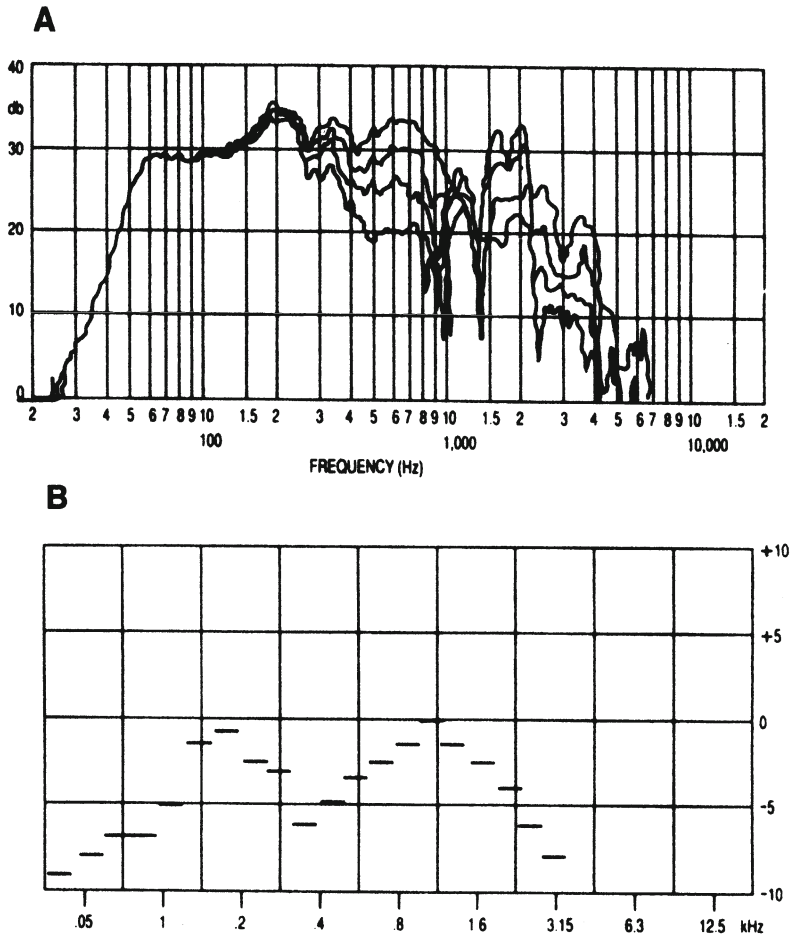

Figure 12-4. Response of ported LF horn systems. On- and off-axis response (A); reverberant field response in the theater (B). (Data at *B* courtesy Dolby Laboratories)

designed in the early 1980s. The JBL model 4675, shown in Figure 12-5A, is typical of a new engineering approach that stressed:

1. Use of simple ported LF enclosures instead of hybrid systems. This was made possible largely through the development of LF drivers with high power handling capability and modern amplifier designs capable of delivering peak power per-driver in the range of 600 watts. Stated differently, efficiency was traded for added bandwidth and lower distortion. Off-axis measurements on the new LF systems are shown at *B*.

2. Use of uniform coverage HF horns instead of multicellular horns, resulting in far smoother response at the highest frequencies.

A very important aspect of these new power-flat systems is that the directional properties of both LF and HF sections are nearly the same at the crossover frequency of 500 Hz. The horizontal beamwidth is nominally 90 degrees, providing wide coverage in the theater, and the vertical beamwidth is nominally 40 degrees, providing controlled coverage over the entire audience area, front to back as seen from the screen. Such systems can be equalized for a desired overall response, and that response will be relatively uniform throughout the house. The importance of narrow vertical pattern control is to minimize the amount of sound that impinges directly on the walls and ceiling of the theater, which would generate needless reverberant effects.

Figure 12-5. Photo of JBL 4675 two-way theater system (A). Horizontal and vertical dispersion for 4675 LF section. (Data courtesy JBL)

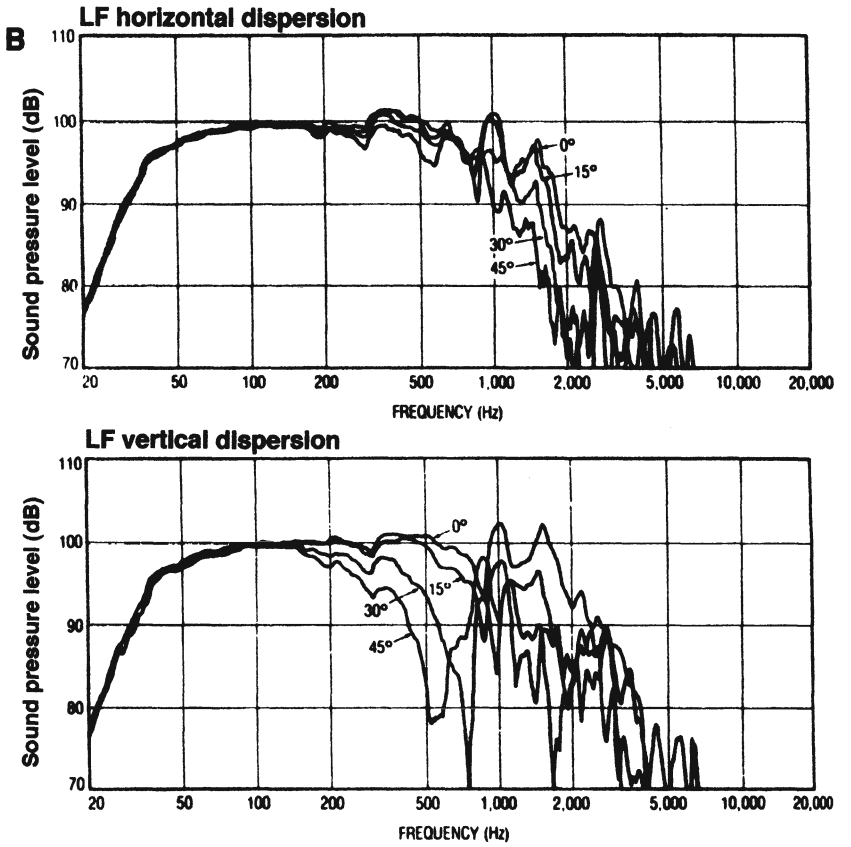

Figure 12-5. Continued.

12.2 Evolution of theater architecture and acoustics

Early motion picture houses were often converted Vaudeville houses, and as such had deep stages, large orchestra pits, and steep balconies. These large rooms often seated 1000 to 1500 or more patrons and were acoustically fairly live in order to support unamplified music and speech. From the viewpoint of acoustics for sound motion pictures, there was much left to be desired. In time, the balcony went away, and capacity was generally restricted to no more than 800 to 1000 patrons. Better structural isolation and use of architectural damping made for quieter spaces, and the sound tracks could thus convey a wider range of music, dialog, and effects for the sake of the picture itself.

The modern motion picture theater is usually designed for reverberation times in the range as shown in Figure 12-6. The average house volume is about 5 cubic meters (190 cubic feet) per patron, so it can be seen that a house seating 1000 patrons will have a relatively short reverberation time, certainly

as compared with a music performance venue of the same seating capacity. The back wall of the theater is normally made very absorptive in order to reduce the level of reflections back toward the screen.

Care should be taken in the theater architectural design to avoid discrete reflections, especially from the side walls, that would tend to interfere with dialog intelligibility. In general, the pattern of reflections in the theater should be quite neutral, not in any way suggesting a sense of large space. If called for, such effects are picture dependent and would be conveyed through the surround loudspeaker systems in the house.

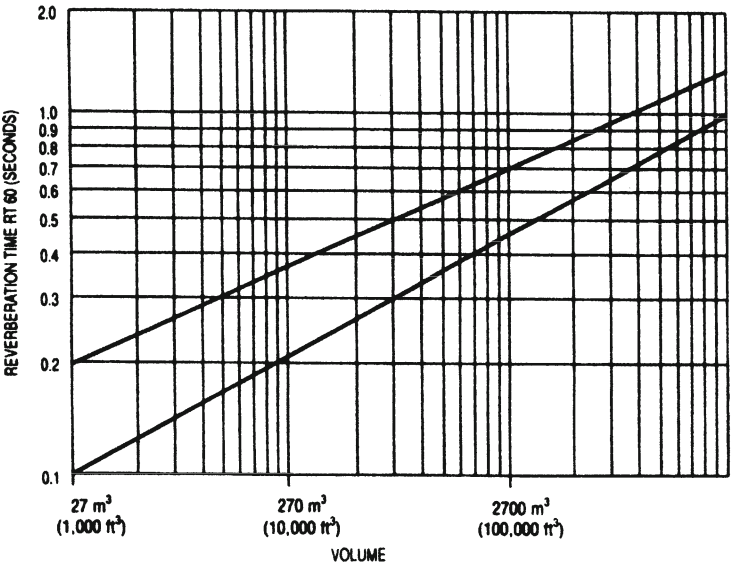

Figure 12-6. Optimum reverberation time in a motion picture theater as a function of room volume.

12.3 A professional theater

By the mid-1990s, digital sound tracks had become commonplace, and this focused renewed attention on all aspects of the audio chain. Three-way loudspeaker designs were gradually replacing those 2-way models that had been updated in the early 1980s. Subwoofers, which had been introduced for special effects in the 1970s, became commonplace in virtually all theaters. Stereo surround channels were also introduced.

Figure 12-7A shows a photograph of the 3-way screen loudspeakers in a large professional theater seating about 1000 persons before installation of the perforated screen. Note that the loudspeakers are mounted in a large wall that extends from floor to ceiling and from side to side in the space. The five screen channels shown here are primarily for exhibiting the 70-mm 6-track magnetic format, which is not used for new releases at the present time. Today, the normal format used in the theater consists of three screen channels, two surround channels, and a special effects LF channel.

The loudspeaker layout for this theater is shown in plan view in Figure 12-7B, with the corresponding electrical flow diagram shown at *C*. The 5 screen loudspeaker are used to accommodate multichannel films made in all formats introduced since the 1950s. Virtually all commercial theaters today have only three screen channels, left, center, and right.

The very low frequency (VLF) requirements are taken care of by a set of subwoofers, each driven by a separate amplifier from a common LF program source. This channel is used for the normal LF extension of program, as well as for special effects, with response that can be maintained flat down to 25 Hz.

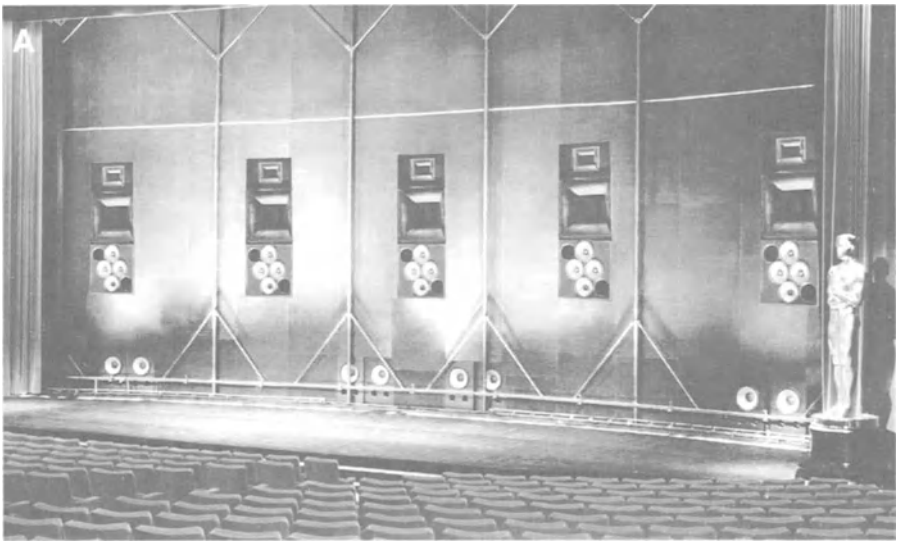

Figure 12-7. A modern professional theater with screen removed. Photo of interior of Goldwyn Theater, Academy of Motion Picture Arts and Sciences (A); loudspeaker layout (B); signal flow diagram (C). ("Academy Award" and "Oscar" image © AMPAS®)

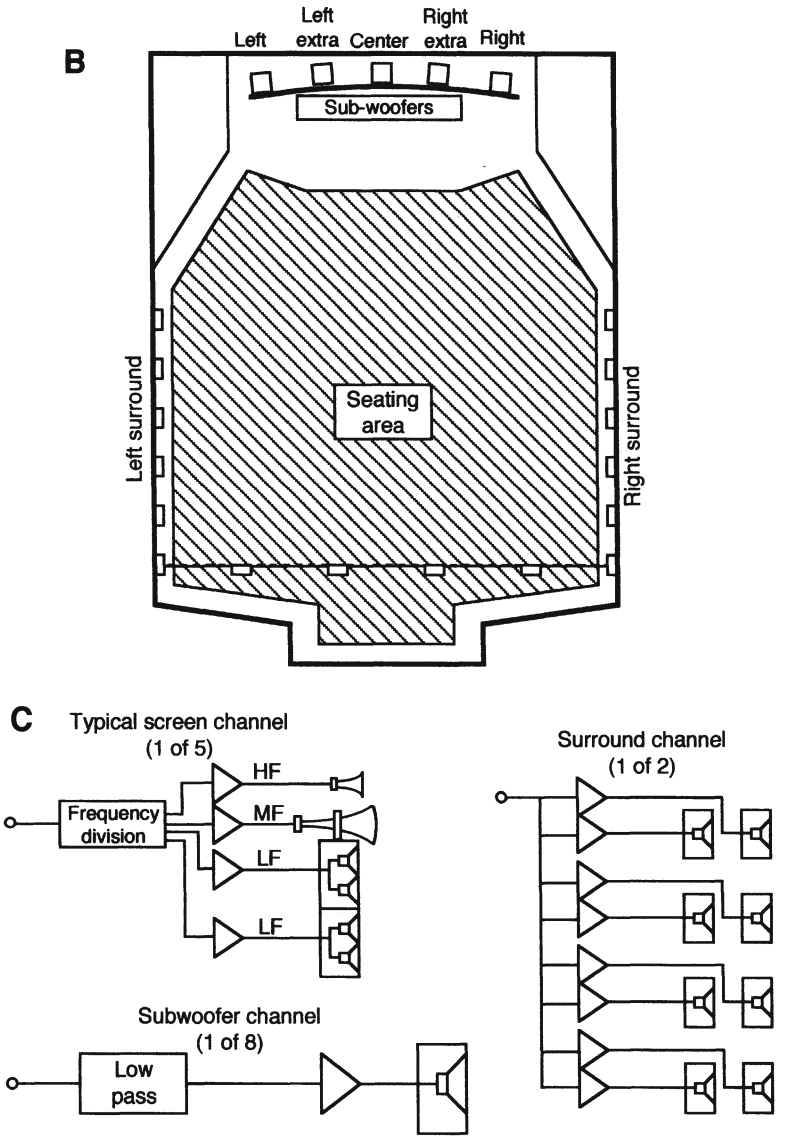

Figure 12-7. Continued.

12.4 Theater audio chain calibration

Equalization: The screen and surround systems are equalized using an averaged multiple microphone pickup in the house. The standard curve to which each loudspeaker is equalized is as shown in Figure 12-8; it is standardized as ISO (International Standards Organization) Bulletin 2969. It is familiarly known as the "x-curve" and was introduced in the 1970s. Equalization takes place

through the screen, thus taking into account the screen losses at HF. The degree of loss depends on screen material, percentage perforation, and the specific angle of transmission through the screen. Typical on-axis loss for 8% perforation through a 0.3 millimeter thick screen is shown in Figure 12-9.

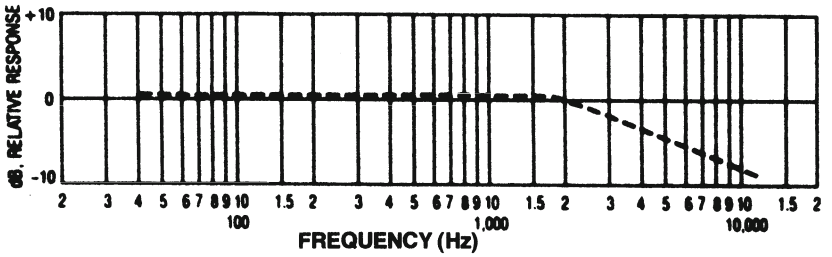

Figure 12-8. ISO Bulletin 2969 recommended response curve for motion picture loudspeaker systems.

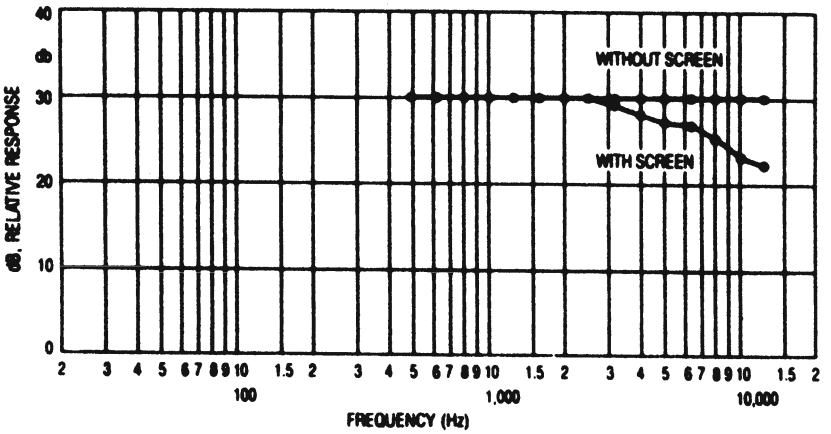

Figure 12-9. Typical on-axis screen losses.

It is customary practice today to equalize the screen systems out to 16 kHz in accordance with the standard curve, and this may require considerable boosting of the HF signal to the compression drivers, often on the order of 10 dB at the highest frequencies. You will note that the general shape of the x-curve and the screen loss curve are quite similar. This is not by accident, and it indicates that a properly equalized theater screen channel is fundamentally delivering a flat power response signal – before it encounters the screen.

Playback level: Throughout the professional motion picture industry, both at the studio and public exhibition stages of the process, playback levels are fairly well controlled. Considering digital sound tracks, each screen channel

is set so that a nominal digital signal level of -20 dBFS (dB relative to digital maximum modulation, or full scale) will produce an average level in the house of 85 dB L_p. Dialog is normally reproduced at peak levels of 85 dB, while the remainder of the 20 dB headroom is in reserve for music and sound effects. Each screen channel is specified to handle broadband signal levels of 0 dBFS, thus producing peaks in the range of 105 dB. An ensemble of three screen channels can thus produce a level about 5 dB higher. Through careful aiming of the HF horns, HF level variations in the seating area from front to back in the theater can be kept within a range of ±3.5 dB.

Subwoofers: The subwoofer channel is normally capable of greater sound pressure levels, due primarily to the equal loudness contours at low frequencies, as shown in Figure 12-10. As an example, for a 1 kHz level of 85 dB L_p, a signal at a frequency of 25 Hz will have to be about 112 dB L_p in order to sound as loud as the 1 kHz signal. At a mid-band reference level of 105 dB, the 25 Hz signal will have to be presented at a level of about 125 dB for equal loudness!

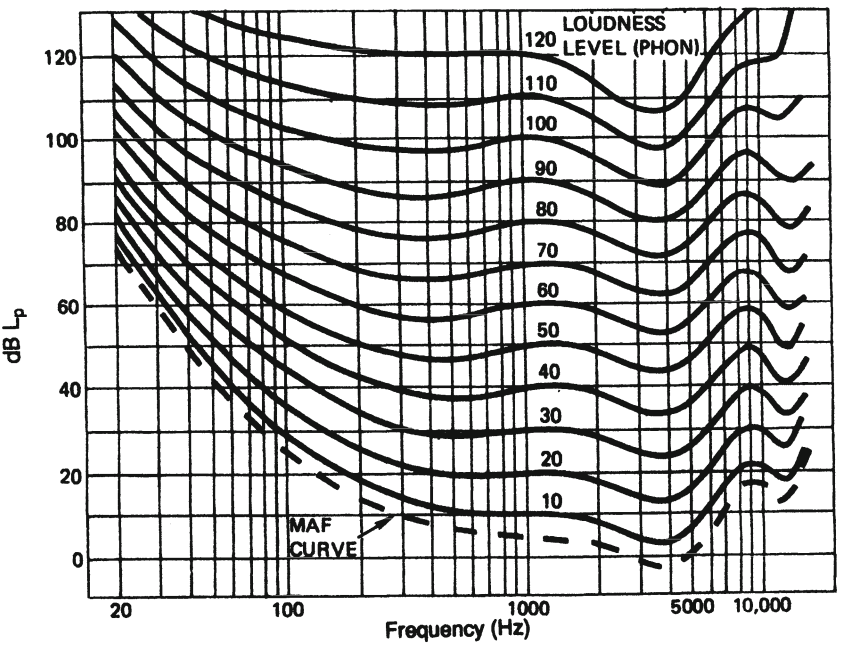

Figure 12-10. Robinson-Dadson equal loudness contours.

Obviously such levels are very difficult to generate in a large theater, and there is no attempt to do so. However, the situation does point out the necessity of some degree of elevated peak level capability for the sub-channel relative to the screen channels. In general, if the subwoofer channel can deliver levels of 115 dB at 25 Hz, it is considered excellent indeed.

12.5 Power bandwidth of audio formats for film

Numerous formats have been used in motion pictures over the years, including monophonic optical and matrixed stereo optical tracks as well as four and six channels of magnetic tracks. Since the mid-nineties, digital formats have become the norm, providing up to 5 screen channels (3 is most common), along with two surround channels and a special effects LF channel.

From the point of view of loudspeaker design and choice, the digital formats have brought very stringent requirements, inasmuch as these formats all exhibit flat power bandwidth at the highest frequencies. This capability can clearly be seen in Figure 12-11.

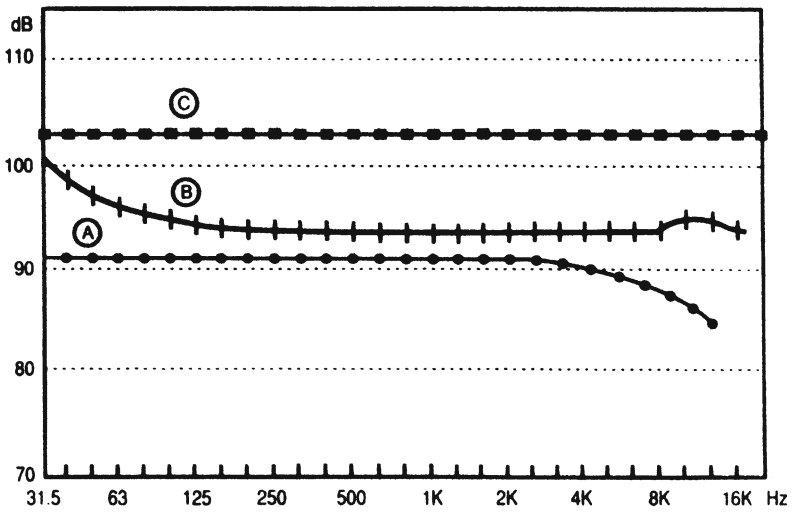

Figure 12-11. Relative electrical headroom in Dolby motion picture recording systems. Dolby A-Type noise reduction (A); Dolby SR spectral recording (B); Dolby Digital recording (C). (Data courtesy Dolby Laboratories)

12.6 Current state-of-the-art in theater loudspeakers

The mid-1990s saw a number of significant changes in motion picture exhibition. Traditional architecture gave way to so-called stadium seating, which resulted in a steeply raked floor. This created a sense of greater immediacy for the patron and complemented the trend toward heavy action and special effects in film content. Further, theaters were constructed in mulplex form, with upwards of 16 to 20 theaters in a single large complex. Depth behind the screen was necessarily limited.

Systems for such spaces had to conserve depth and offer very uniform off-axis response in order to cover the stadium seating area uniformly. We now describe in detail one of the new designs, the JBL 4632 ScreenArray™ system:

Figure 12-12A shows a photo of the system. Note that the traditional midrange horn has been replaced by a manifold arrangement of four cone drivers feeding waveguides. The on-axis frequency response is shown at *B*, and the –6 dB beamwidth is shown at *C*.

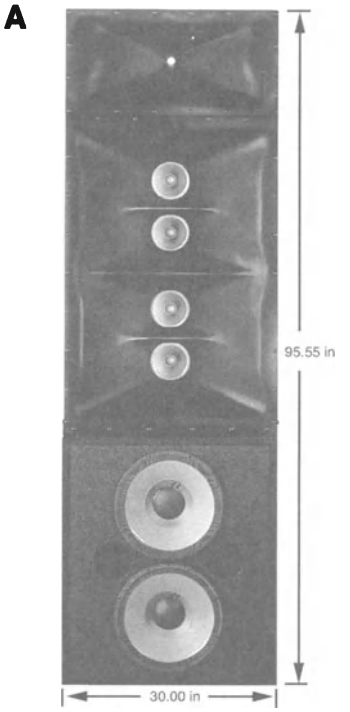

Figure 12-12. The JBL 4632 screen system. View of system (A); typical response (B) and beamwidth (C) of system. (Data courtesy JBL)

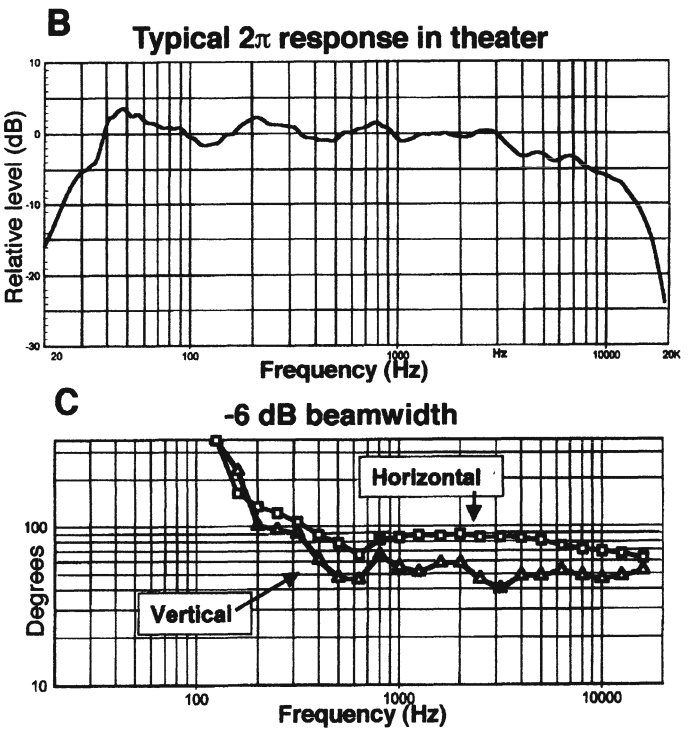

Figure 12-12. Continued.

The entire MF and HF portion of the system relies on the detailed design of passive network components to "fine-tune" the system's response in terms of both frequency response and pattern control, as shown in Figure 12-13. Here, the system's three passbands are shown in detail:

Lower MF Section: These drivers operate in series through a third-order low-pass section followed by an impedance correcting shunt path.

Upper MF Section: This network branch is fairly complex, with a third-order low-pass section followed by two sections of similar topology. One of these controls impedance, while the other provides response shaping. The final section in the upper MF network consists of an all-pass bridge network which maintains proper phase relationships between the upper and lower MF sections. This section also corrects a response dip and an undesirable "tilt" in the MF polar repsonse.

HF Section: This network branch consists of a fourth-order high-pass section, along with impedance correction.

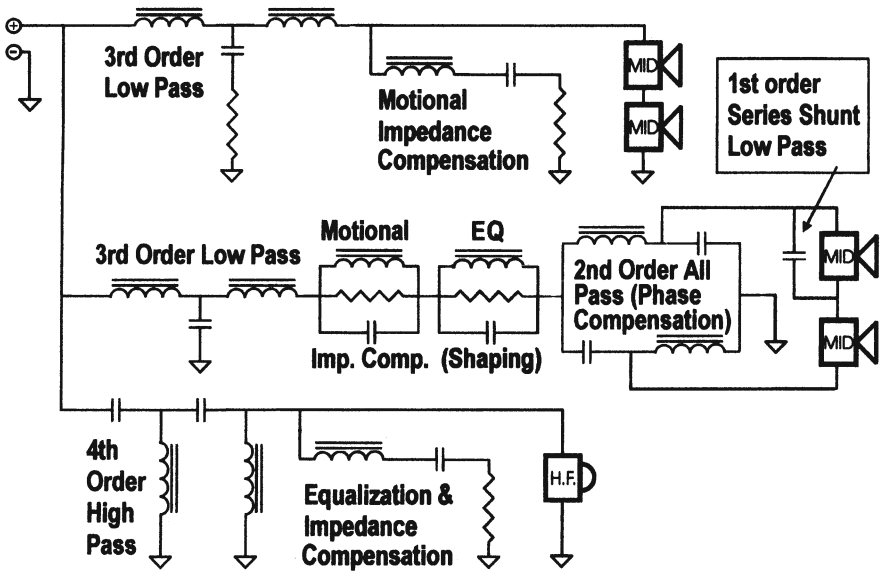

Figure 12-13. Details of dividing network for upper three sections of JBL 4632 screen channel system (Data courtesy JBL)

Figure 12-14A shows the raw response of each passband. Response through the network is shown at *B*, along with each of the three components.

The author wishes to thank Bernard Werner of JBL Professional for the data presented in this section.

12.7 Multichannel video in the home

The home theater revolution of the early nineties was based largely on the wide availability of Dolby Stereo encoded analog tracks on both Laserdiscs and VHS videotapes of current motion pictures. At first a handful of hardware manufacturers began making AV (audio-video) receivers, which provided five channels of amplification along with front-end processing using an integrated circuit Dolby matrix decoder. This produced left, center, right, and surround outputs derived from the basic stereo signal.

The Dolby stereo matrix had earlier made its entry into the motion picture world as Dolby Stereo Optical, an economical alternative to magnetic tracks on 35 and 70-mm film. It is this same stereo pair of tracks that subsequently drove the home market for surround sound video.

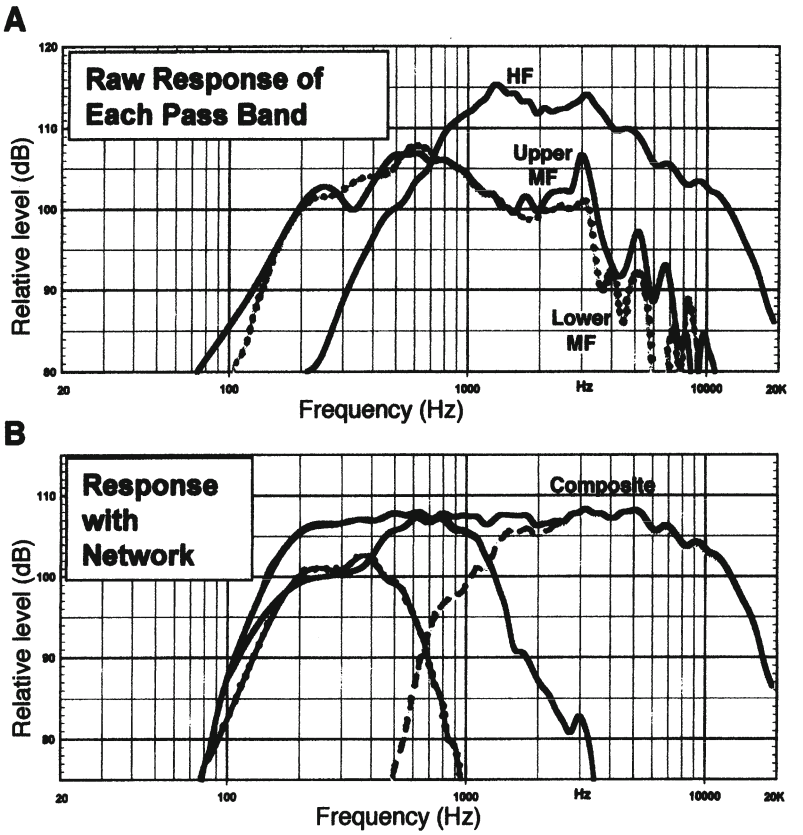

Figure 12-14. Network response for 4632 system. Raw response of components (A); final bandpass responses of network and overall system (B). (Data courtesy JBL)

The translation of the theater experience into the home began in a rather casual way. Manufacturers at first provided small loudspeaker models for the purpose so as not to upset traditional notions of home decor, but these did not necessarily do justice to modern action films.

12.7.1 Frontal loudspeakers

Much of the early guidance for consumer manufacturers in this area was provided as a licensing service by the THX division of Lucasfilm, a major producer of films. THX had earlier promulgated audio and optical performance standards for commercial motion picture theaters and was now turning that expertise toward the home market. From the loudspeaker point of view, THX proposed that the accurate translation of the motion picture experience into

the home called for frontal loudspeakers with essentially the same wide horizontal pattern control and relatively narrow vertical mid-range control characteristic of motion picture theater systems. In the theater the directional control is normally provided by a horn, which can control horizontal and vertical radiation patterns independently of each other over a large frequency range. By comparison, consumer loudspeaker systems are generally composed of cone and dome drivers, and as such are subject to the diameter dependent radiation patterns of those devices as described in an Chapter 1.

In order to meet the narrow vertical coverage requirement, THX specifies MF transducers as vertically arrayed pairs. A frontal view of a typical wide range frontal loudspeaker array might be as shown in Figure 12-15A. Note that the center loudspeaker, since it must be placed above or below a TV screen, has a relatively low vertical profile.

12.7.2 Surround loudspeakers

Surround channel requirements are a bit more difficult to define. In the theater a large number of surround loudspeakers are used; for a typical listener the surround impression is the result of many loudspeakers, whose individual sounds arrive at the listener's ears with different levels, directions, and delay times. The result of this is a degree of sound diffusion whose timbre and general spatial impression may be difficult to duplicate in the typical living room. The THX proposal here is to use single dipole loudspeakers on each side of the listening room with their null axes aimed at the primary listening position, as shown in Figure 12-15B. Under this condition, the major contribution of the surround channels at the listener comes by way of first-order room reflections, not directly from the surround loudspeakers themselves. While this may not be an exact translation of the theater experience into the home listening environment, it does provide a good approximation. For direct-ambient music reproduction, the dipole arrangement provides an adequate timbral match with the front channels if the listening space is acoustically well damped.

12.7.3 Low frequency requirements

The attractiveness of subwoofers in the home is that a single subwoofer can often deliver the LF output necessary to complement a 5-channel full-range loudspeaker array. This can substantially reduce the size requirement of the individual 5-channel array, since the directionality of frequencies below about 100 Hz is difficult to assess. Subwoofers are most easily integrated into home

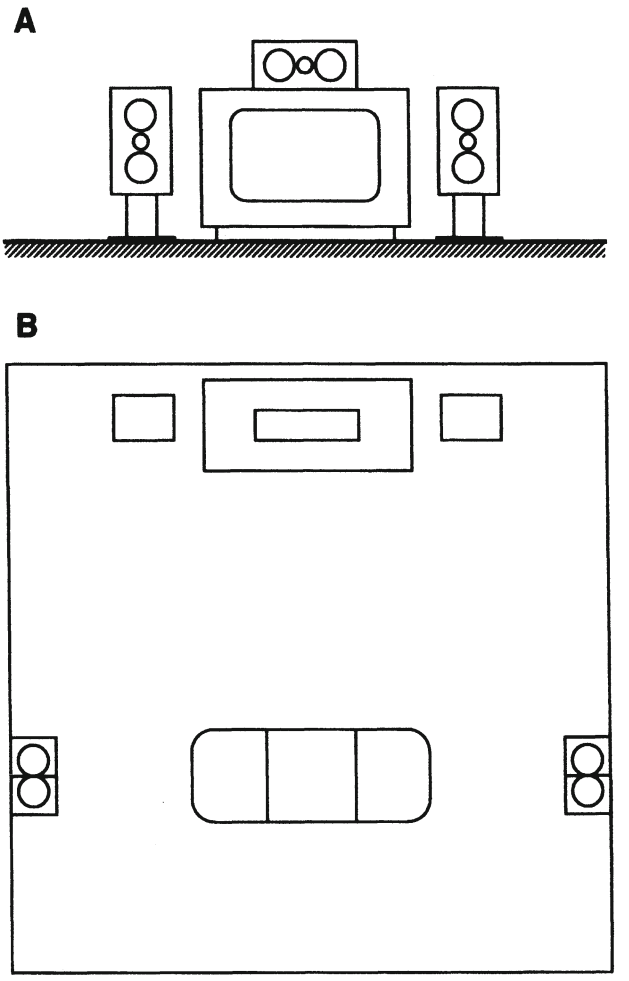

Figure 12-15. Typical baffle layouts for front channels in a home theater system (A); plan view of a home theater setup using dipole loudspeakers for surround channels.

environments if they are self powered and fed from a dedicated output on the basic AV receiver.

12.7.4 General comments on home theater

Not all manufacturers are in agreement that home theater loudspeakers should necessarily emulate the character of theater loudspeaker systems. Strong voices of dissent state that what has traditionally been good for music should be good for home video as well, so there is ample room for individual taste.

Figure 12-16 shows a typical family of loudspeakers intended for home video reproduction.

Figure 12-16. Photo of a typical group of home loudspeakers for video and surround sound application as viewed from the position of the left-rear loudspeaker. (Data courtesy Infinity Systems)

12.6 Overview of music in surround sound

The first attempt to bring multichannel music without a picture into the home was *quadraphonic sound* during the mid 1970s. This effort failed, due primarily to conflicting software standards, as well as technical shortcomings in all of the proposed systems.

When home video and its accompanying surround sound became wildly successful during the mid-1990s, the question of surround sound for music-only applications was naturally raised. On the surface of it, it seems perfectly logical that, having made the investment in a surround sound system for video, the consumer would naturally want to hear music over the same system – and would gladly buy new software (DVD Audio and SACD discs) in order to support it.

Again, there are conflicting software standards; and, perhaps more important, the general business recession of the late 1990s and early 2000s has given the record companies more important matters to attend to. In any

event, there is a body of technology and practice waiting in the wings, so to speak, to be implemented when the record industry decides to move forward. Hardly an audio technical conference passes without important contributions to the art and science of recording music for surround sound and its allied technologies.

The ITU (International Telecommunications Union), in its document ITU-R BS 775-1, suggests the loudspeaker layout shown in Figure 12-17 as a basic platform for establishing musical balances in the mastering of surround sound music. Experience has shown that music mixed in the ITU environment does in fact translate well into a wide variety of home loudspeaker setups. There are no constraints on the loudspeakers used, except that they all be of the traditional forward-firing type.

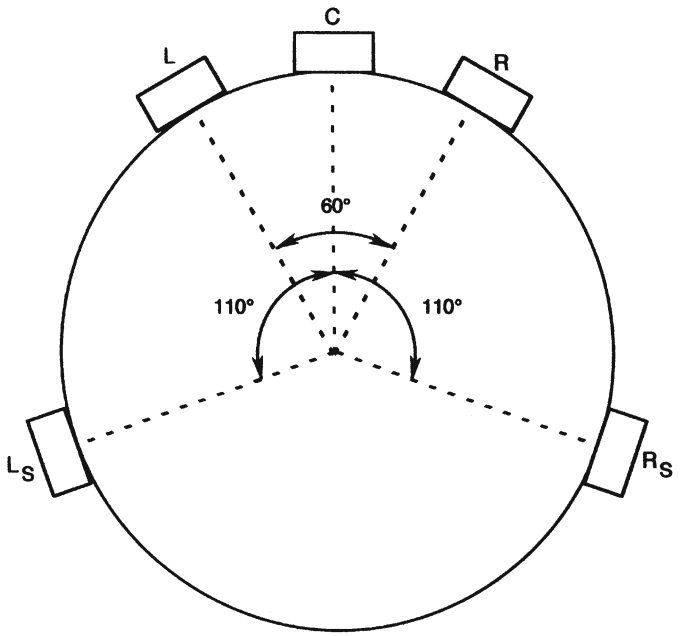

Figure 12-17. Diagram of the ITU recommended setup for mixing audio program for surround sound presentation.

Looking into the future of both home and special venue applications, TMH Corporation has demonstrated what they call a *10.2* playback configuration, as shown in Figure 12-18 (Holman, 2000). While traditional surround sound is active only in the horizontal listening plane, the 10.2 array specifies height channels precisely positioned to enhance the envelopmental aspects of performance of music and other stage events in typical venues. The principal components are described as follows:

Left, Center, and Right Channels: These function largely as do the corresponding channels in a 5.1 system, conveying the primary on-stage images.

Left and Right Wide Channels: These deliver early side reflections which convey an impression of the size and liveness of the actual recording space.

Left and Right Height Channels: These frontal overhead channels deliver early reflections from the proscenium, further strengthening the sense of envelopment and height of the recording space.

Left and Right Rear Channels: These channels function largely as do the corresponding channels in a 5.1 system. These loudspeakers may be of the dipole type in order to enhance the diffuseness of reverberant signals.

Back Center Channel: This channel anchors the back axis of the listening space.

Two Subwoofer (point-one) Channels: These operate in stereo, conveying subtle spatial cues below 100 Hz.

TMH states that the spatial densities of the channel layouts are based on the relative acuity of human hearing in a normal setting. For example, seven of the ten channels are located in the front half of the listening hemisphere – because the ear's ability to discern source localization is greatest in these directions. Three channels are sufficient in the back half of the hemisphere, since localization is not nearly as precise in those directions.

TMH also points out that the system provides great leeway in both recording and playback processes. Nothing in the system is so prescribed that it cannot be altered for artistic or other production reasons.

12.9 Holographic techniques in surround sound reproduction

A holographic audio system would allow the listener to move about in the listening space while still being able to identify the directions of specific sources and discernining near-distant relationships with accurate parallax. The sheer density of raw recorded data required for such presentation would virtually rule it out, were it not for the appropriate techniques of data minimization that can be applied. Horbach (2000) describes one approach to this.

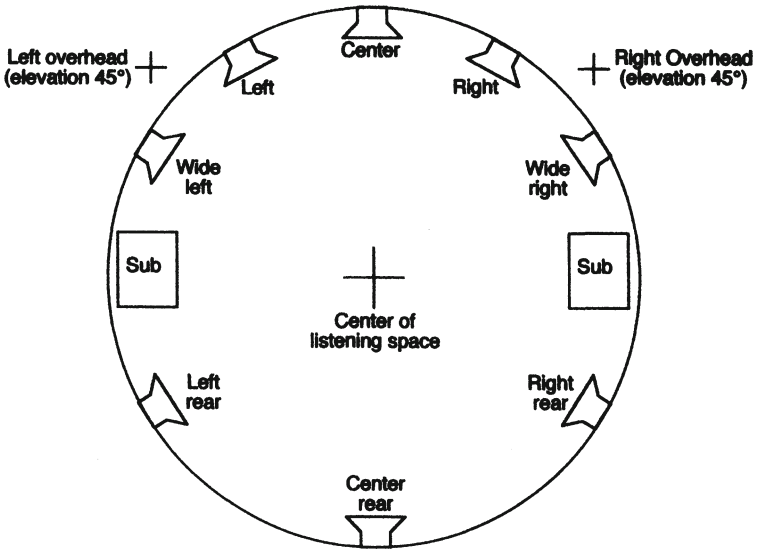

Figure 12-18. Plan view of TMH 10.2 surround setup. "Plus" signs indicate the positions of the 45-degree overhead loudspeaker pair.

A playback environment is visualized as shown in Figure 12-19. A large number of small loudspeakers are placed across the front of the listening space, with additional linear arrays across portions of the sides and rear of the space.

The actual data recorded consists only of the relatively dry tracks of instruments, instrumental sections, or other specific events in the presentation, be it audio-only or a video presentation. Other necessary data relating to the acoustics of the recording space will have been previously gather via impulse measurements, and this data will be transmitted along with the raw audio data. In addition, large-room cues can be captured via impulse response measurements and reconstructed later for presentation over the back and side loudspeakers.

One way this can be done is shown in Figure 12-20. The large outline of the space shows individual locations of sound sources, and the boundaries of a target listening area are superimposed on this overall space. Within that smaller space, numerous two-dimensional microphone positions are identified, and individual impulse response data is taken at all microphone locations for

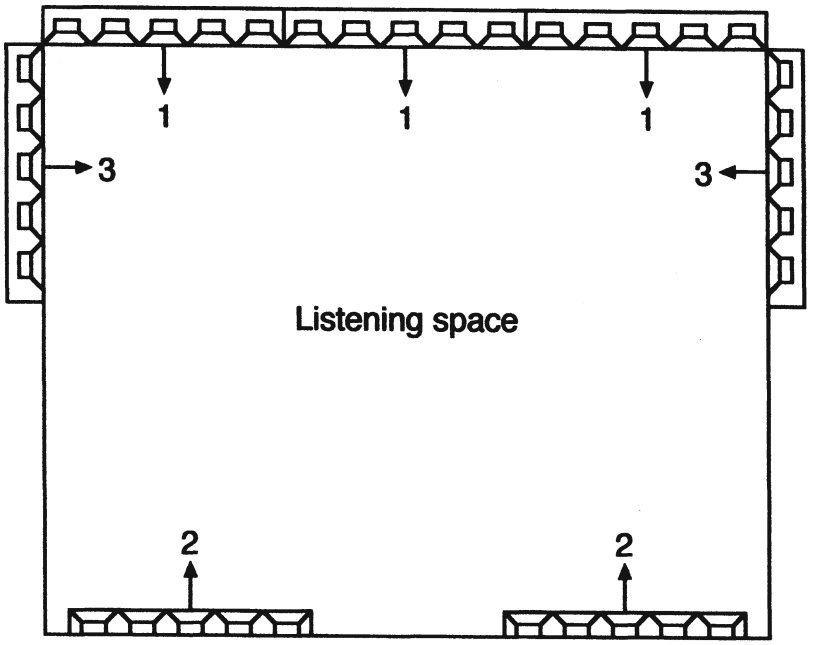

Figure 12-19. Playback environment for holographic sound presentation. (Data after Harbach)

each instrumental source. The collective impulse data is stored and later transmitted along with the raw audio data for accurately positioning of each instrument or section in the virtual space of the playback room. On playback, each audio source is convolved with the impulse data to create the ensemble of loudspeaker outputs for that particular source.

For example, distance cues depend largely on the curvature of the wavefront at the listener, and listeners at different positions in the playback environment will both be able to "point" accurately at a given source, as shown in Figure 12-21.

12.10 Positioning sound sources via reflections and focusing

Using a large array of small transducers, the British 1Limited company proposes a method of three-dimensional wave construction at the listener via multiple reflections at room boundaries. The array is shown in Figure 12-22.

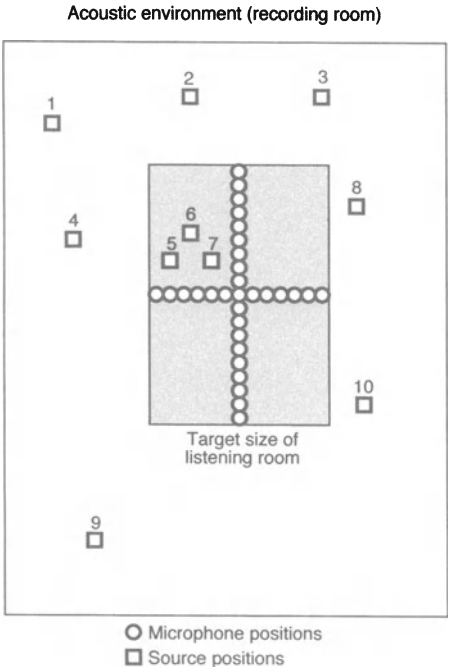

Figure 12-20. Recording environment for holographic sound pickup. (Data after Harbach)

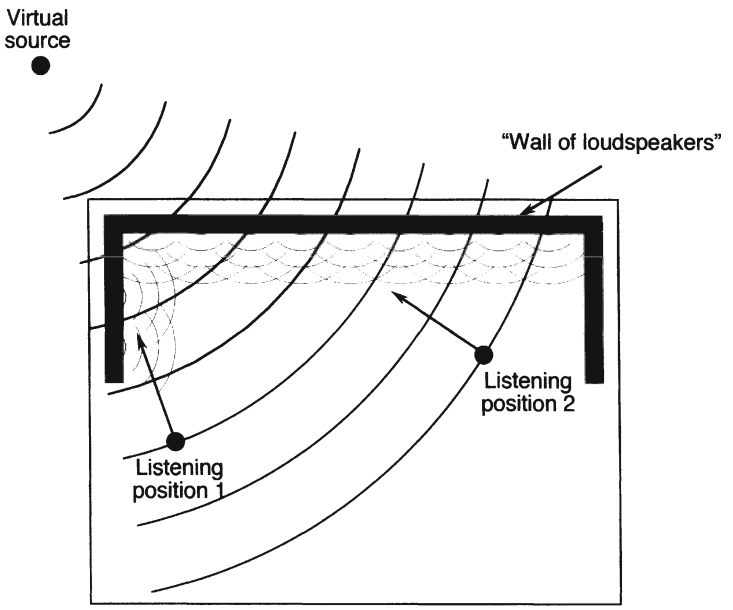

Figure 12-21. Playback of a virtual source and the directions perceived by two listeners. (Data after Harbach)

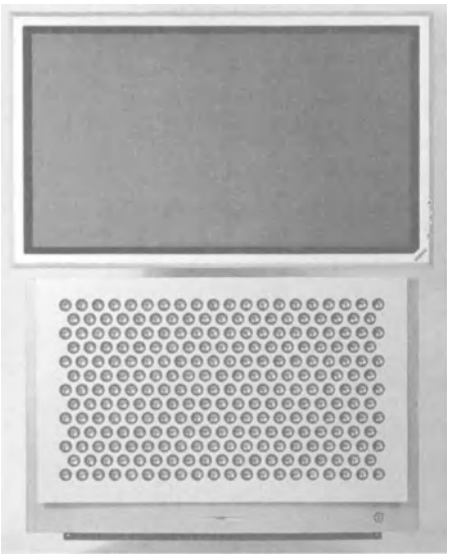

Figure 12-22. Photo of 1Limited system for projecting sound images. (Data courtesy 1Limited)

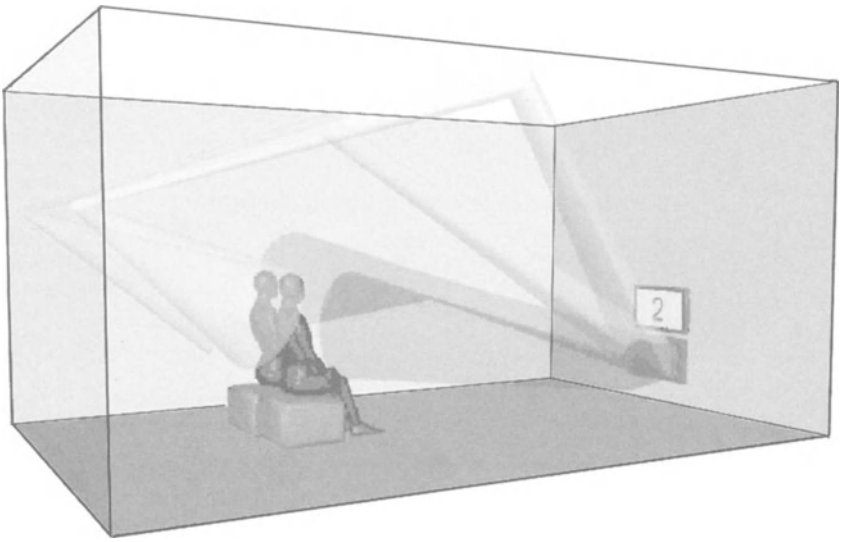

Figure 12-23. Representation of images via multiple reflections. (Data courtesy 1Limited)

In application, the user enters room boundary and seating coordinates; the system then generates the 254 individual signals required to produce a cone of actual reflections focusing at the listening position as shown in Figure 12-23. The difficulties that must be overcome have to do with masking by direct sound from the source directly to the listener, relative to the time delay of reflected signals and their net levels at the listener. If the masking thresholds of the direct sound can be kept low enough through the use of compensating delays, then the listener will localize sources via the reflections.

BIBLIOGRAPHY AND REFERENCES:

Allen, I., *Technical Guidelines for Dolby Stereo Theatres*, Dolby Laboratories, San Francisco (1993).

Berkhout, A., "A Holographic Approach to Acoustic Control,""*J. Audio Engineering Society*, volume 36, number 12 (1988).

Eargle, J., *Handbook of Recording Engineering*, Kluwer Academic Publishers, Boston (2002).

Eargle, J., *Electroacoustical Reference Data*, Kluwer Academic Publishers (1994).

Eargle, J., Bonner, J., and Ross, D., "The Academy's New State-of-the Art Loudspeaker System," *J. Society of Motion Picture and Television Engineers*, volume 94, number 6 (1985).

Eargle, J., and Means, R., "A Microcomputer Program for Determining Loudspeaker Coverage in Motion Picture Theaters." *J. Society of Motion Picture and Television Engineers*, volume 93, number 8 (1984).

Engebretson, M., and Eargle, J., "Cinema Sound Reproduction Systems," *J. Society of Motion Picture and Television Engineers*, volume 91, number 11 (1982).

Harbach, U., "Practical Implementation of a Data-Based Wave field Reproduction System," Presented at 108th AES Convention, Paris (2000).

Holman, T., *5.1 Surround Sound - Up and Running*, Focal Press, Boston (2000).

International Organization for Standardization (ISO) Bulletin No. 2969.

Cinema Sound System Manual, JBL Incorporatded, Northridge, CA (2001).

Various, *Motion Picture Sound Engineering*, D. Van Nostrand Company, New York (1938).

Chapter 13:
LOUDSPEAKER MEASUREMENTS AND MODELING

13 Introduction

Loudspeaker measurement technology has grown significantly in the last two decades as digital signal processing has come on the scene. In earlier days, the industry relied on mechanically driven sine wave oscillators operating in synchronism with moving paper chart recorders, many of which are just now winding down their useful existence. More to the point of loudspeakers, we are still learning which performance attributes need to be measured, and to what degree of detail.

At the transducer design stage, there are matters of basic mechanical system linearity and integrity, which are often preceded with detailed modeling by the design engineer. Here, it may be helpful to examine cone and diaphragm movements via stroboscopic and laser methods so that higher order performance anomalies can be analyzed. Later, when drivers are assembled into systems, acoustical measurements will dominate the design process.

Many acoustical measurements take place in the loudspeaker's operating environment. These are discussed in those chapters that deal with loudspeaker applications. We will begin with a discussion of analog frequency based measurements.

13.1 Frequency response measurements

Figure 13-1 shows details of a common method of running frequency response curves. A beat frequency oscillator (BFO) is motor driven and puts out a constant level sine wave signal that normally covers the frequency range from 20 Hz to 20 kHz. The sweep is logarithmic, so that that the sweep time is constant per-octave or other bandwidth percentage. The BFO signal is fed to the device under test (DUT), and a measurement microphone is placed at a fixed reference distance. The signal from the microphone is fed to a graphic

J. Eargle, *Loudspeaker Handbook*

level recorder where it is converted to level in dB and plotted via a vertically moving pen on a horizontally moving strip of paper. The paper movement is in exact synchronism with the signal generator through either electrical or mechanical interlocking.

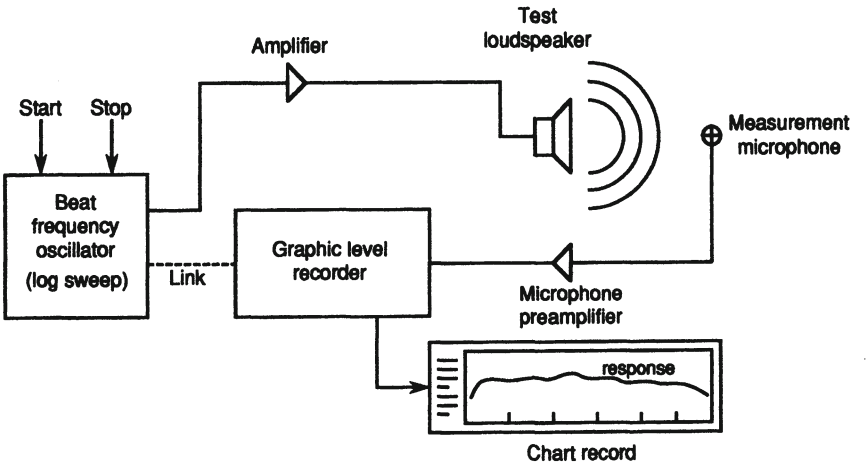

Figure 13-1. Block diagram for analog measurement of frequency response using a beat frequency oscillator (BFO).

The important variables in operating the system are setting the paper speed and the pen writing speed to ensure good data. Examples are shown in Figure 13-2A and *B*. At *A*, the paper speed is slow and the writing speed fast, producing the greatest detail; at *B*, the paper speed is fast and the writing speed slow, producing highly averaged data. The data at *A* may be valuable to the transducer designer, while the data at *B* may be more representative of subjective effects as perceived by the listener. Most analog measurement systems have a range of 40 to 50 dB, depending on the chart paper that is used and the range built into the recorder. You must remember that the only record of the measurement is the piece of paper itself – there is no "data file" as such.

The system can be varied slightly to produce averaged data. Figure 13-3 shows a configuration for driving a tracking band-pass filter, with a constant *pink noise* (equal power per-fraction of an octave) signal fed to the loudspeaker. The method can be varied further so that consecutive 1/3-octave noise bands, or other ratios, are delivered sequentially to the loudspeaker under test.

The magnitude (or modulus) of a loudspeaker's impedance can be plotted by measuring the voltage drop across the loudspeaker when the loudspeaker

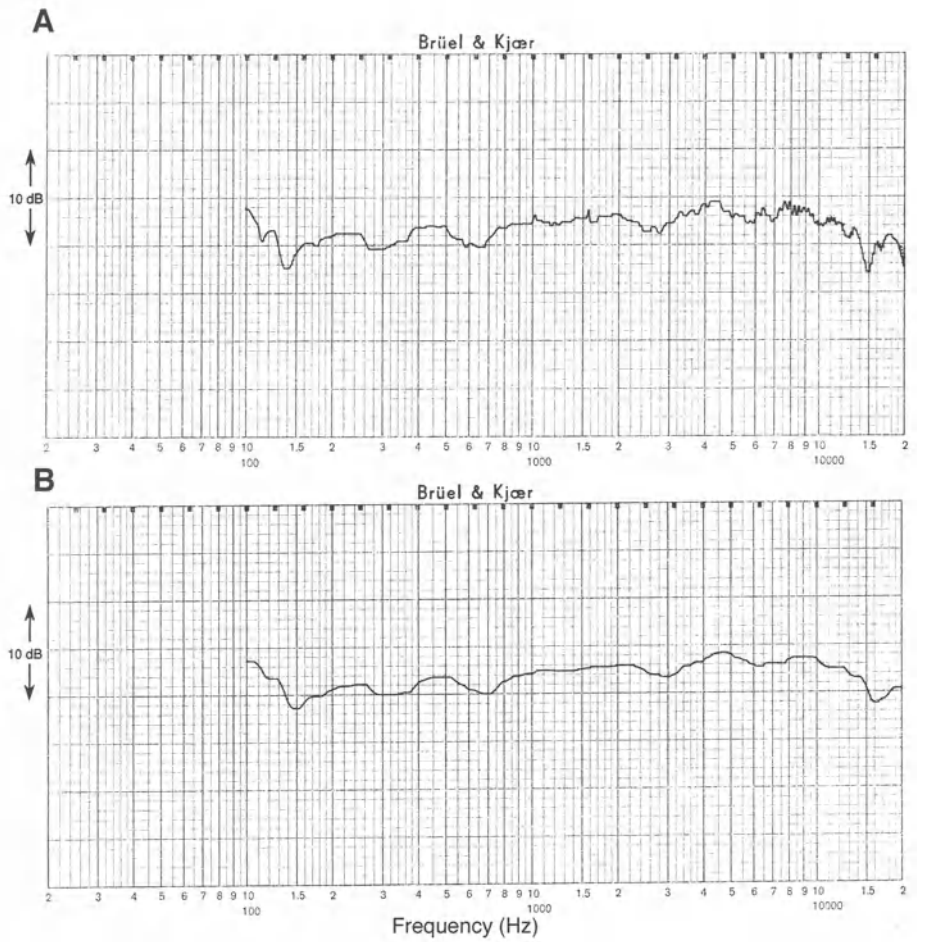

Figure 13-2. Effects of writing and paper speeds on data resolution. Fast writing speed and slow paper speed (A); slow writing speed and fast paper speed (B).

is driven with a *constant current* source. In the circuit shown in Figure 13-4, the system is calibrated by inserting a 10-ohm resistor and adjusting the gain of the graphic level recorder so that its pen indicates the 10-ohm marker on the chart paper. When the proper gain has been set, the calibration resistor is switched out and the loudspeaker load inserted in its place. The impedance plot generated in this manner is a plot of *log impedance*, rather than a linear representation. This convention is used throughout the book.

When making measurements in an anechoic environment, small diameter (12 mm or less) test microphones exhibiting flat response on-axis are normally used, with the source positioned along the primary axis of the microphone.

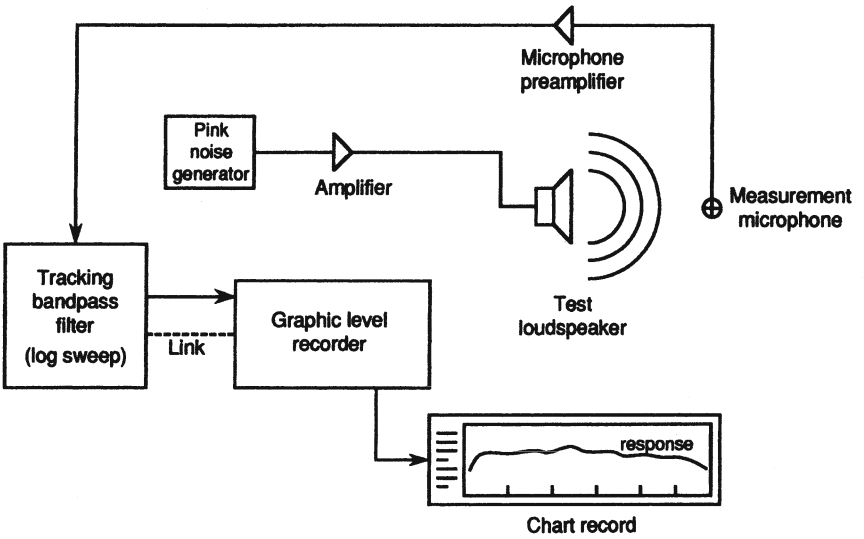

Figure 13-3. Block diagram for analog measurement of frequency response using a pink noise source and variable bandpass analyzer.

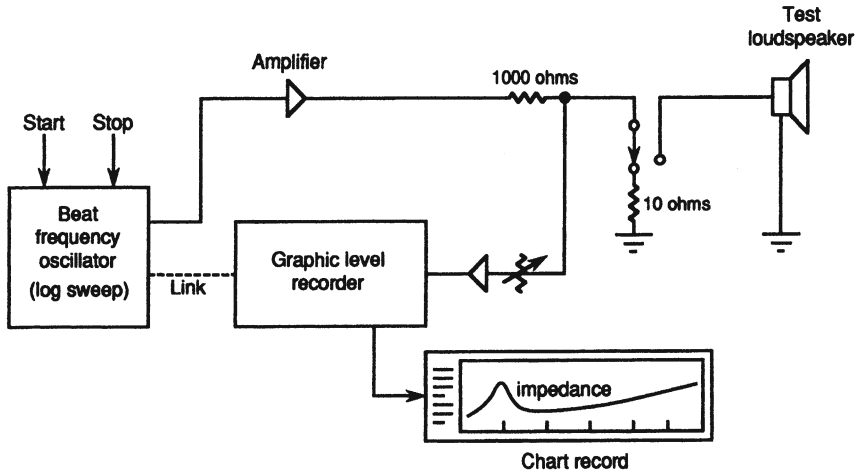

Figure 13-4. Measurement of loudspeaker modulus of impedance.

13.2 Distortion measurements

There are a number of relevant distortion measurements that may be made on loudspeakers. The most common is to drive the loudspeaker with a swept sine wave at various nominal power inputs and measure the relative amounts of second and third harmonic distortion components which the DUT produces, relative to the fundamental component. The setup for this is shown in Figure 13-5.

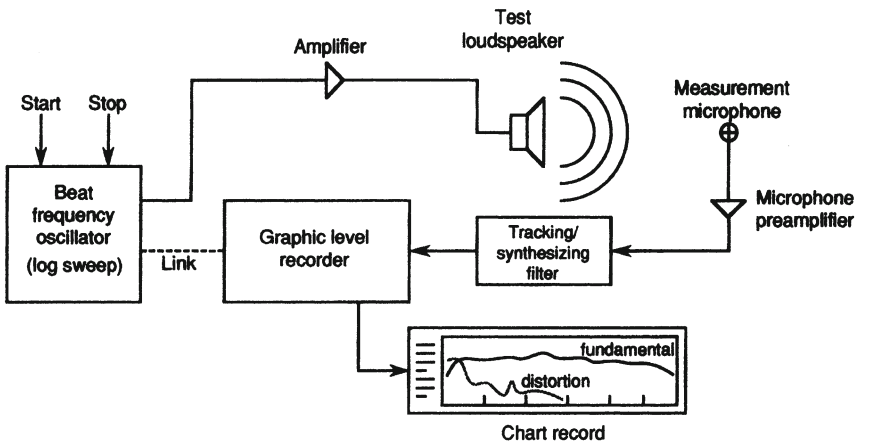

Figure 13-5. Measurement of harmonic distortion.

In normal practice, a frequency plot of the fundamental is first made. Then the chart paper is rewound, and a tracking-synthesizing filter is used to generate the second harmonic passband; that signal is then plotted. The paper is once again rewound, and the third harmonic is plotted. In normal practice, the gain of the recorder is increased 20 dB when plotting the distortion components, so that they may be clearly seen on the rather narrow (40 or 50 dB) vertical window of the display.

When using chart paper with an upper frequency limit of 20 kHz, it should be clear that second harmonic components cannot be plotted for fundamentals higher than 10 kHz, or third harmonic components higher than about 6700 Hz.

Another way of looking at distortion is the THD + N (total harmonic distortion plus noise) method. Here, a tracking band rejection filter is used to notch out the fundamental frequency, leaving only the power summation of harmonics and of course any noise that may be present. This method is generally more applicable to electronic systems than to loudspeakers.

Most harmonic distortion in loudspeakers is related to mechanical or magnetic nonlinearities, and these produce amplitude distortion. In some systems, where cone displacement is excessive, there may be frequency modulation (FM) effects as the cone's velocity becomes a significant fraction of the speed of sound. The measurement methods discussed here do not

distinguish between the two, and a frequency modulation discriminator is necessary to directly isolate the FM components. In general, amplitude modulation effects predominate in normal cone driver performance. Horn systems, as we discussed in Chapter 7, are prone to thermodynamic distortion when driven at high levels.

13.2.1 Use of compressed fundamental

Some measurement systems have a compressor circuit that can be used to keep the fundamental signal from the loudspeaker flat at the measurement microphone. This feature is of considerable use when comparing different transducers under identical output conditions. An example is shown in Figure 13-6, where the fundamental level for a compression driver-horn combination has been maintained at 105 dB at a distance of 1 meter. We can clearly see the steady increase in 2nd harmonic distortion at a rate of 6 dB per octave. Above about 7 kHz, the distortion rises rapidly as air motion in the compression driver reaches overload values.

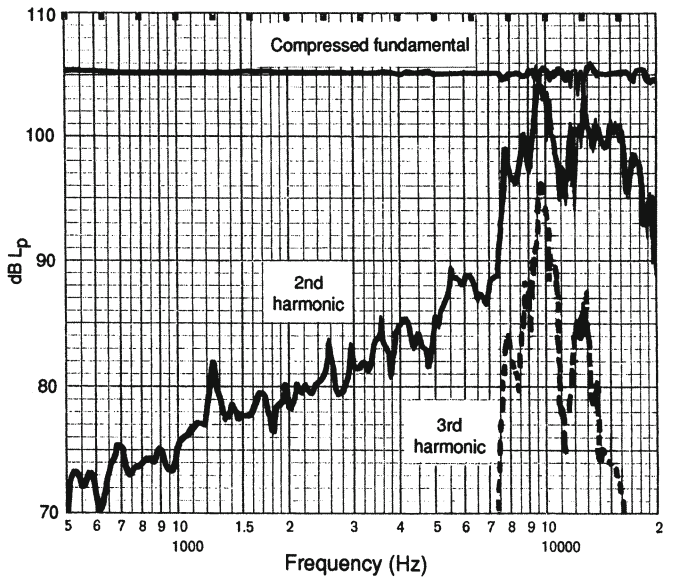

Figure 13-6. Illustration of the use of compressed fundamental in distortion measurements.

13.2.2 Intermodulation distortion measurements

Intermodulation (IM) distortion results from the interaction between two or more signals and is normally simulated by a combination of two sine waves. The sum and difference combination tones that are generated by system nonlinearities are plotted. Many of the various combination tones can be analyzed by available tracking filter-analyzer systems. Figure 13-7A shows the basic measurement setup.

The attractiveness of IM distortion measurement is that it relates, at least in part, to the way systems behave on actual program material. As such, it may be a good indicator of when problems will occur, but it may not identify the specific cause of the problem as easily as single frequency measurements will. Today, IM distortion is normally carried out by establishing a fixed frequency difference between two sine waves, and then sweeping the pair of tones over the entire frequency band. If f_1 is one of the tones and f_2 the other, then $f_1 - f_2$ will be a constant value; it is normally set in the range from 200 Hz to 1 kHz.

Due to nonlinearities in the system, several combinations of tones will be generated; the most significant are: $f_1 - f_2$ and the second-order tones $2f_1 - f_2$ and $2f_2 - f_1$. Figure 13-7B shows the output of the $2f_2 - f_1$ difference tone under the same drive conditions as the data in Figure 13-6. In the data shown here, there is very little distortion until just above 7 kHz, where it rises rapidly.

13.3 Phase and group delay response of loudspeakers

Traditionally, these have been difficult measurements to make, but the newer transform based digital systems have made the process much easier. The older method of making phase measurements is shown in Figure 13-8. Because of the acoustical delay path between the loudspeaker and microphone, the oscillator output to the phase meter must be delayed by the same amount. If this is not done, the phase meter will register multiple phase rotations, especially at high frequencies, and the data will be very difficult to interpret. With digital delay this adjustment can be made easily and good data taken. The reader can readily understand that such measurements as these were rarely undertaken in the pre-digital era.

Group delay is the derivative of the phase response with respect to frequency, $-d\phi/d\omega$, and in the early days was usually calculated by inspection

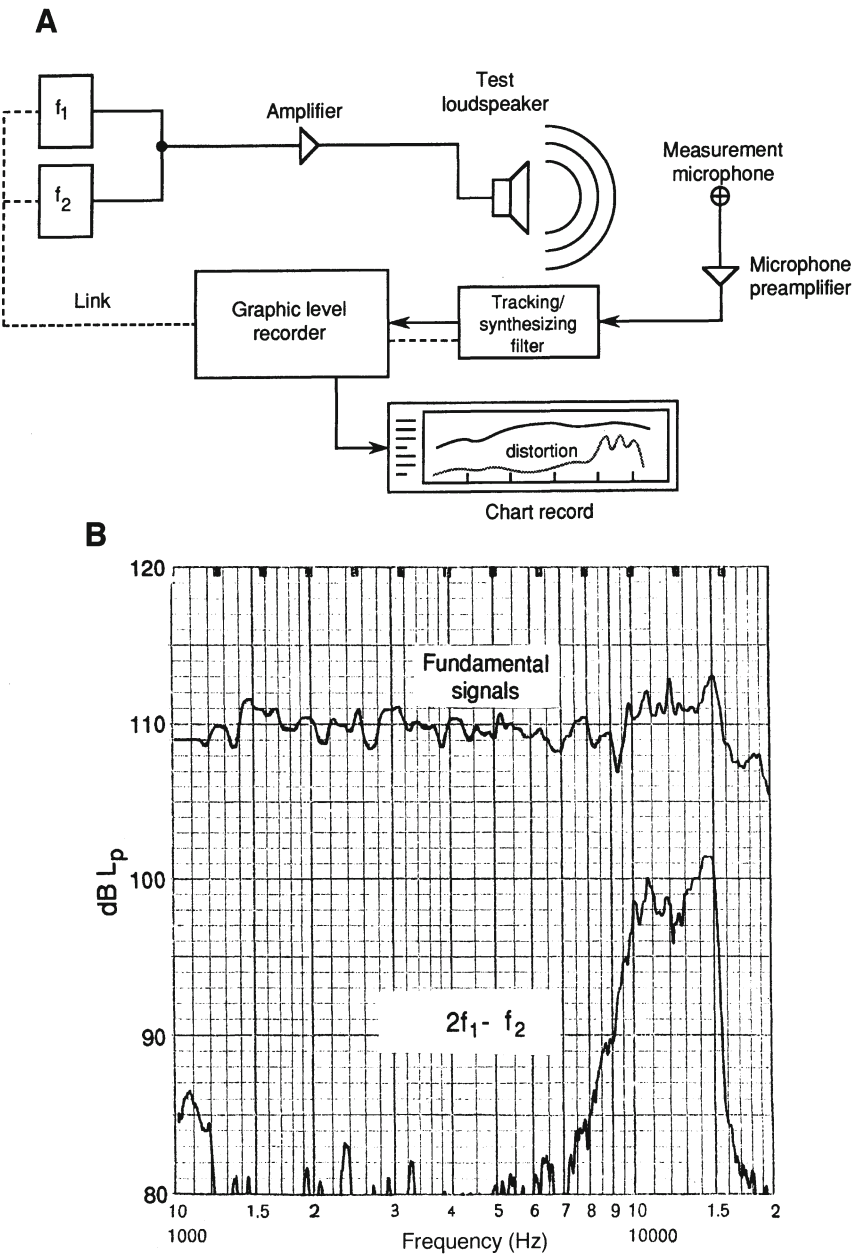

Figure 13-7. Twin-tone intermodulation measurements. Block diagram (A); typical data presentation (B). Distortion raised 20 dB.

and graphical differentiation of the phase plot. Today's instrumentation presents delay data directly.

13.4 Measurement of directional data

Although we are primarily interested in the directional response of a loudspeaker system over its nominal frontal radiation angle, there are several applications of system modeling that require a complete spherical description of the loudspeaker's directional response – and this at many different frequencies. The traditional way of showing directional data is by way of the *polar graph*. The Brüel and Kjaer standard chart recorder, long the mainstay of the electroacoustics industry, can accommodate a circular piece of sprocketed graph paper, driving it 360 degrees in synchronism with a turntable that carries the loudspeaker. The basic setup is shown in Figure 13-9A. A typical polar graph of a loudspeaker is shown at *B*. The system of polar coordinates is normally used in polar measurements, with the amplitude, ρ, plotted in terms of the rotational angle θ.

There are a number of derived methods for presenting directional data for a loudspeaker, as shown in Figure 13-10.

Frontal isobars: This method, shown at *A*, gives a quick picture of the three-dimensional frontal characteristics of a device and is very handy in the specification of sound reinforcement components. A separate isobar plot is necessary for each frequency band.

Family of off-axis curves: These curves, shown at *B*, are often presented with the on-axis curve normalized, as shown here, and are generally given only in horizontal and vertical planes.

Horizontal and Vertical Beamwidth (–6 dB) plots: These curves, shown at *C*, are useful in sound reinforcement applications where they clearly indicate to the specifying engineer regions of loss of pattern control or excessive narrowing of pattern control.

Plots of Directivity Index and Directivity Factor: This plot, shown at *D*, gives a single value at each frequency which enable certain rapid calculations to be made in many aspects of sound reinforcement.

Spherical data file: A complete data file, shown at *E*, for an arbitrary device will consist of 180 degrees of front-to-back information for the entire 360

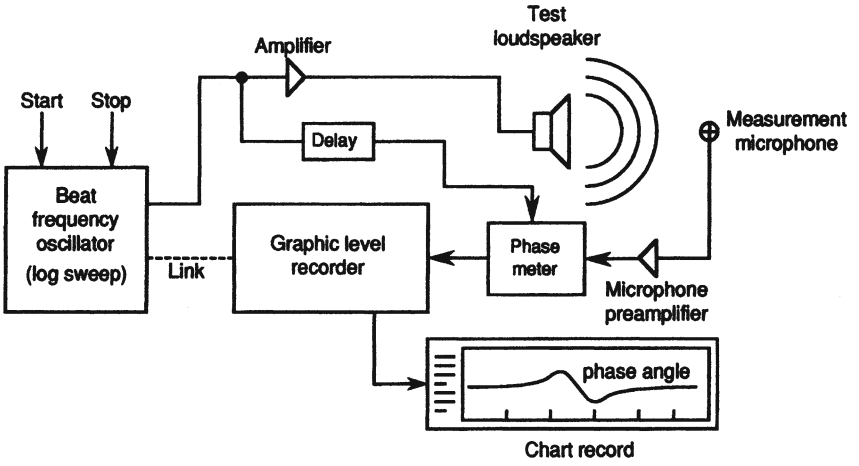

Figure 13-8. Analog measurement of phase response.

degrees of rotation about the frontal axis. The data is normally measured at 5 or 10 degree increments and stored in tabular form on spherical coordinates. A separate file is needed for each frequency, or frequency band, of interest. In many cases, data "packing" reduces the space actually occupied by one of these files. For example, device symmetry about one or two axes can considerably reduce these requirements.

The amassing of this degree of data used to be a laborious process. Today, there are computerized methods of mechanically indexing large devices, along with multi-microphone arrays, for gathering much data through parallel processing. A typical tabular file is shown in Figure 13-10. Here, ϕ (phi) represents the off-axis rotation from front to back of the device, while θ (theta) represents rotation about the frontal axis of the device from horizontal to vertical.

13.5 The measuring environment

The traditional measurement environments are anechoic chambers, open fields, and reverberant rooms. A section view of an anechoic chamber is shown in Figure 13-11. The wedges are made of medium density fiber glass and form a gradual "lossy" path from the interior of the chamber to the outer walls of the chamber. The wedges should be about one-quarter wavelength deep at the lowest frequency at which the chamber is intended to operate. Furthermore, there must be adequate working space in the chamber so that low frequency measurements can take place at least a quarter-wavelength away from the wedge tips.

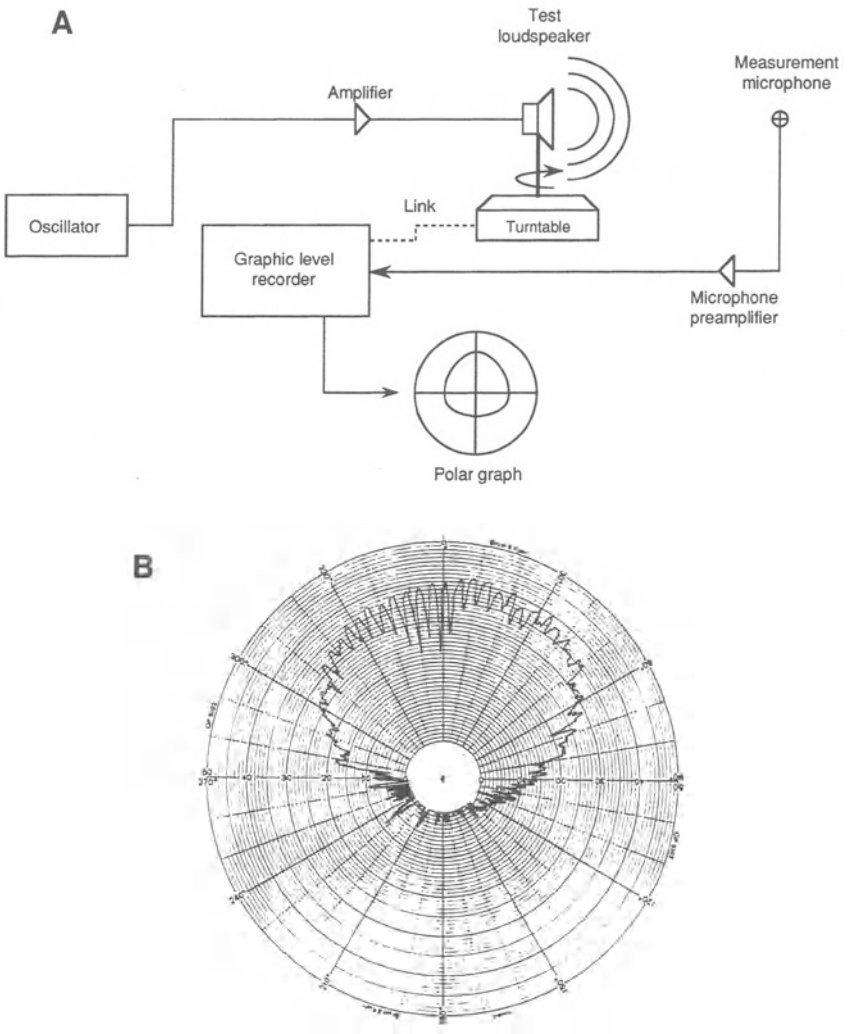

Figure 13-9. Polar graphs. Block diagram (A); typical data presentation (B).

Anechoic chambers are very expensive, and many tens of thousands of dollars may be involved, even in a modest one. A chamber that works well down to 100 Hz is adequate, since performance below that frequency can usually be accurately estimated. The anechoic chamber is often referred to as a 4π, or full-space, measuring environment.

The *open field* is shown in Figure 13-12. It is often built on a roof top, where there are few space limitations. Surfaces ten meters on a side are quite

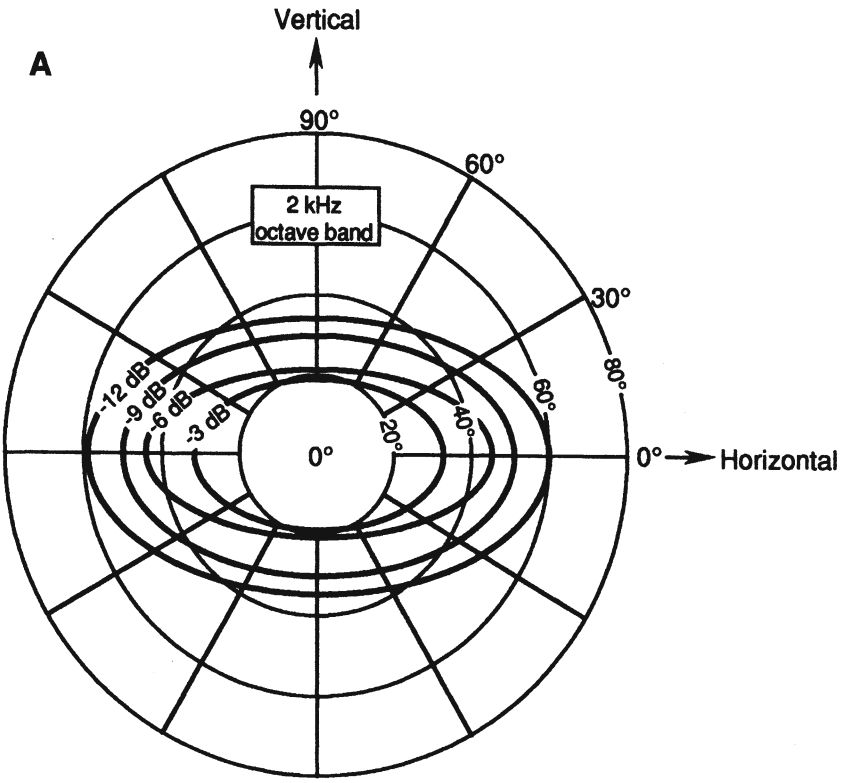

Figure 13-10. Derived methods of directional data presentation. Frontal isobars (A); off-axis curves (B); beamwidth (-6 dB) versus frequency (C); DI (directivity index) (D); spherical data file, front hemisphere only; octave band on 10° intervals (E).

common and permit excellent low frequency measurements to be made. On the debit side, there are weather and noise problems to contend with. Tracking filters can help under noisy conditions, but bad weather puts these facilities out of business. The open field is often referred to as a 2π, or half-space, measuring environment.

A *reverberant environment* can be used for making measurements of loudspeaker power output integrated over all directions. Figure 13-13 shows a space in which boundary absorption is kept low so that the reverberant field predominates over the direct field at the measurement microphone. Normally, a small diameter test microphone with a flat random incidence response is used for these measurements. The test environment must be calibrated throughout its intended frequency range (Eargle and Larson 1963), taking into account both room boundary absorption and air absorption at HF.

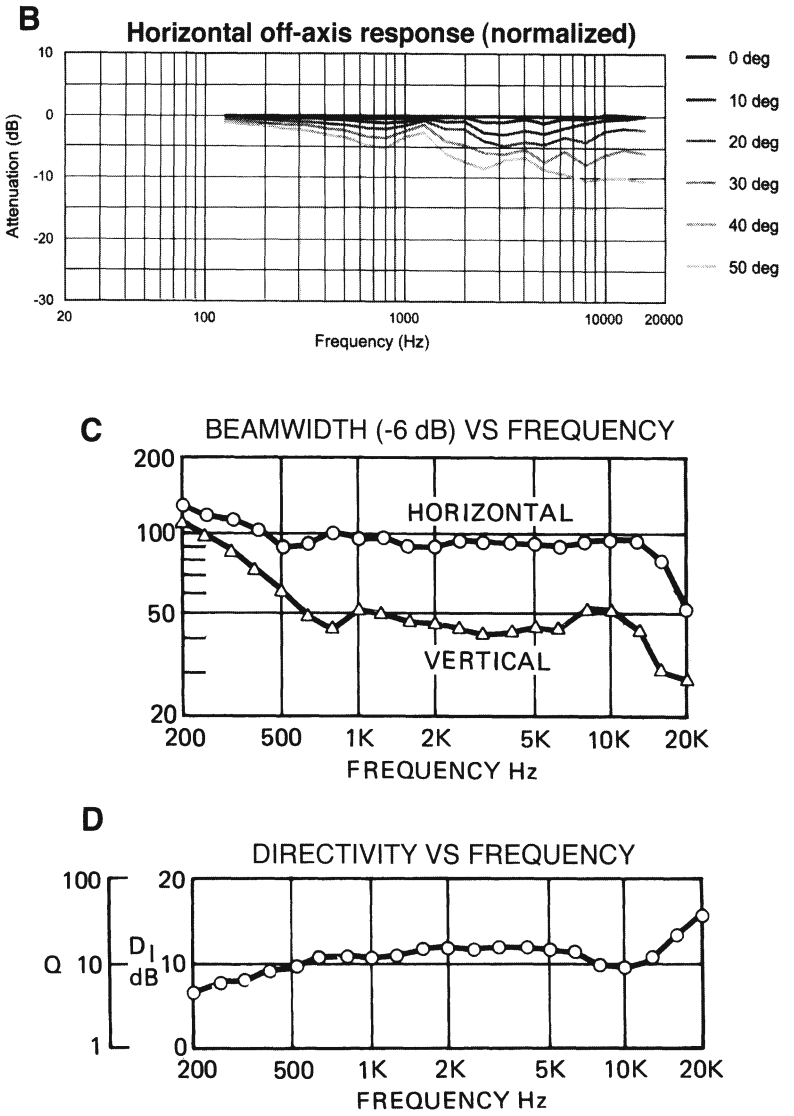

Figure 13-10. Continued.

The reverberant level in the space is given by:

$$L_{REV} = 126 + 10 \log W_A - 10 \log A \qquad 13.1$$

where W_A is the acoustic power (watts) fed into the space and A is the total absorption (m^2) in the space. L_{REV} is the reverberant sound pressure level in the space.

E

LOUDSPEAKER FILE: jbl2360
FREQUENCY BAND: 0-5 kHz
DIRECTIVITY INDEX: 9
SENSITIVITY: 112
MAXIMUM POWER: 50

UPPER HEMISPHERE DB(THETA,PHI)

PHI / THETA	0o	10o	20o	30o	40o	50o	60o	70o	80o	90o
0o	0	0	-2	-3	-5	-6	-8	-10	-13	-14
10o	0	0	-1	-2	-5	-6	-8	-11	-13	-15
20o	0	0	-2	-3	-5	-7	-10	-12	-14	-17
30o	0	-1	-2	-3	-6	-9	-11	-13	-17	-19
40o	0	-1	-2	-4	-6	-9	-12	-14	-17	-20
50o	0	-1	-2	-4	-7	-10	-12	-15	-18	-21
60o	0	-1	-2	-4	-8	-12	-13	-14	-18	-20
70o	0	-1	-2	-5	-8	-11	-13	-15	-17	-19
80o	0	-1	-2	-5	-9	-11	-13	-15	-17	-20
90o	0	-1	-3	-5	-9	-12	-13	-15	-17	-19
100o	0	-1	-2	-5	-9	-11	-13	-15	-17	-20
110o	0	-1	-2	-5	-8	-11	-13	-15	-17	-19
120o	0	-1	-2	-4	-8	-12	-13	-14	-18	-20
130o	0	-1	-2	-4	-7	-10	-12	-15	-18	-21
140o	0	-1	-2	-4	-6	-9	-12	-14	-17	-20
150o	0	-1	-2	-3	-6	-9	-11	-13	-17	-19
160o	0	0	-2	-3	-5	-7	-10	-12	-14	-17
170o	0	0	-1	-2	-5	-6	-8	-11	-13	-15
180o	0	0	-2	-3	-5	-6	-8	-10	-13	-14
190o	0	0	-1	-2	-5	-6	-8	-11	-13	-15
200o	0	0	-2	-3	-5	-7	-10	-12	-14	-17
210o	0	-1	-2	-3	-6	-9	-11	-13	-17	-19
220o	0	-1	-2	-4	-6	-9	-12	-14	-17	-20
230o	0	-1	-2	-4	-7	-10	-12	-15	-18	-21
240o	0	-1	-2	-4	-8	-12	-13	-14	-18	-20
250o	0	-1	-2	-5	-8	-11	-13	-15	-17	-19
260o	0	-1	-2	-5	-9	-11	-13	-15	-17	-20
270o	0	-1	-3	-5	-9	-12	-13	-15	-17	-19
280o	0	-1	-2	-5	-9	-11	-13	-15	-17	-20
290o	0	-1	-2	-5	-8	-11	-13	-15	-17	-19
300o	0	-1	-2	-4	-8	-12	-13	-14	-18	-20
310o	0	-1	-2	-4	-7	-10	-12	-15	-18	-21
320o	0	-1	-2	-4	-6	-9	-12	-14	-17	-20
330o	0	-1	-2	-3	-6	-9	-11	-13	-17	-19
340o	0	0	-2	-3	-5	-7	-10	-12	-14	-17
350o	0	0	-1	-2	-5	-6	-8	-11	-13	-15

Figure 13-10. Continued.

The total absorption can be derived from the reverberation time equation:

$$T_{60} = 0.16V/A \qquad 13.2$$

where V is the room volume in m^3.

The room calibration procedure is fairly straightforward and should be carried out on one-third octave center frequencies. If the room is subject to changing values of relative humidity (RH), the calibration will vary at HF. If the RH can be controlled, then the calibration should be fairly stable.

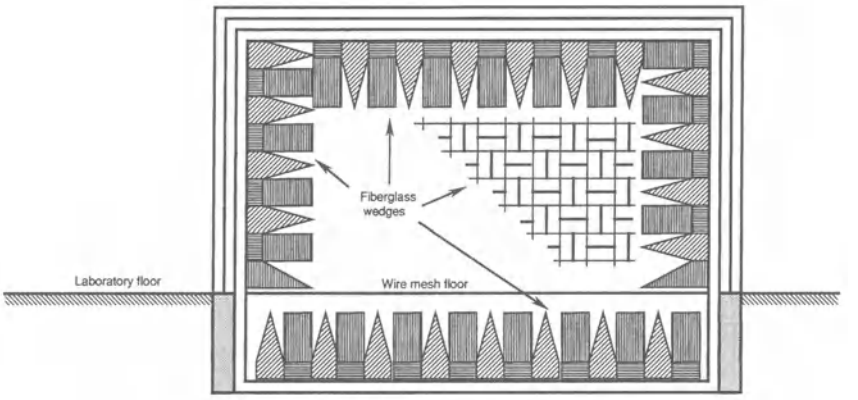

Figure 13-11. Section view of an anechoic chamber.

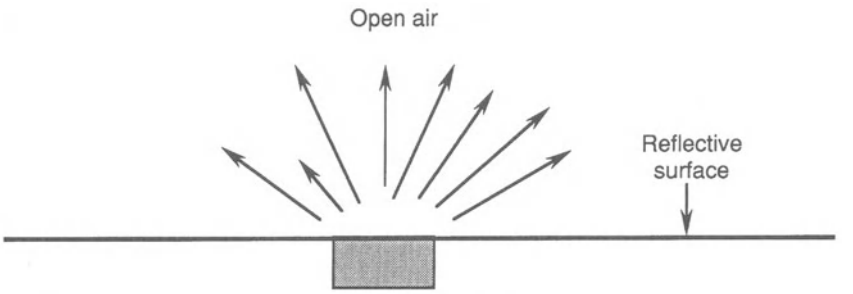

Figure 13-12. Section view of an open field.

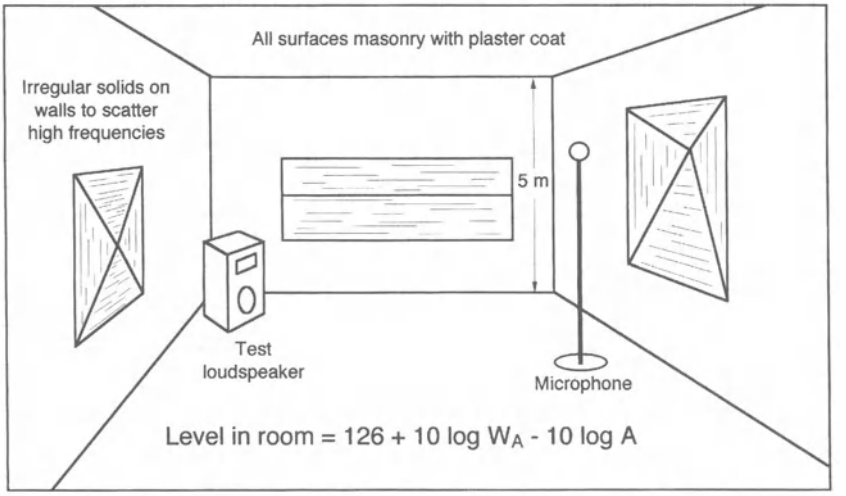

Figure 13-13. View of a reverberation room.

Outside of large research facilities, reverberant chambers are rarely found these days. They may have outlived their usefulness in loudspeaker work, with the many improved methods of data gathering that are common today. The virtue of the reverberant space is that it provides a "real time" spatial integration of the signal, facilitating power response and efficiency measurements.

Today, the listening room itself has become a measuring environment. Many modern techniques provide for signal gating and can result in useful signal reception before the onset of the earliest room reflections. We will discuss this in a later section.

13.6 Ground plane measurements

Using the technique shown in Figure 13-14, ground plane measurements can be used to approximate anechoic measurements normally made in full-space. The representation at *A* shows a loudspeaker placed on a large plane surface with a microphone at some distance. Because there is a reflected image of the loudspeaker due to the plane surface, the equivalent free-space condition is shown at *B*, where a pair of loudspeakers are placed side by side.

The presence of the reflected image will cause a doubling of pressure at the microphone, and this additional 6 dB can be compensated for by positioning the microphone at 2 meters rather than the normal 1 meter distance. When this is done, the measurement will show the normal 1-meter sensitivity of the loudspeaker.

The virtual presence of two loudspeakers rather than one will produce a slight difference, as compared with a single loudspeaker in anechoic free-space, as shown at *C*. There will some degree of mutual coupling at LF, and the effective baffle size will of course be larger. You can see that there is only a small difference in LF response between the ground plane and anechoic measurements. See Gander (1982) and D'Appolito (1998) for added details of this measurement method.

13.7 Near-field measurements

Keele (1974) describes a method of making precise LF measurements very close to a LF driver so that room effects can be swamped out. These measurements can then be calibrated so that they can be accurately combined

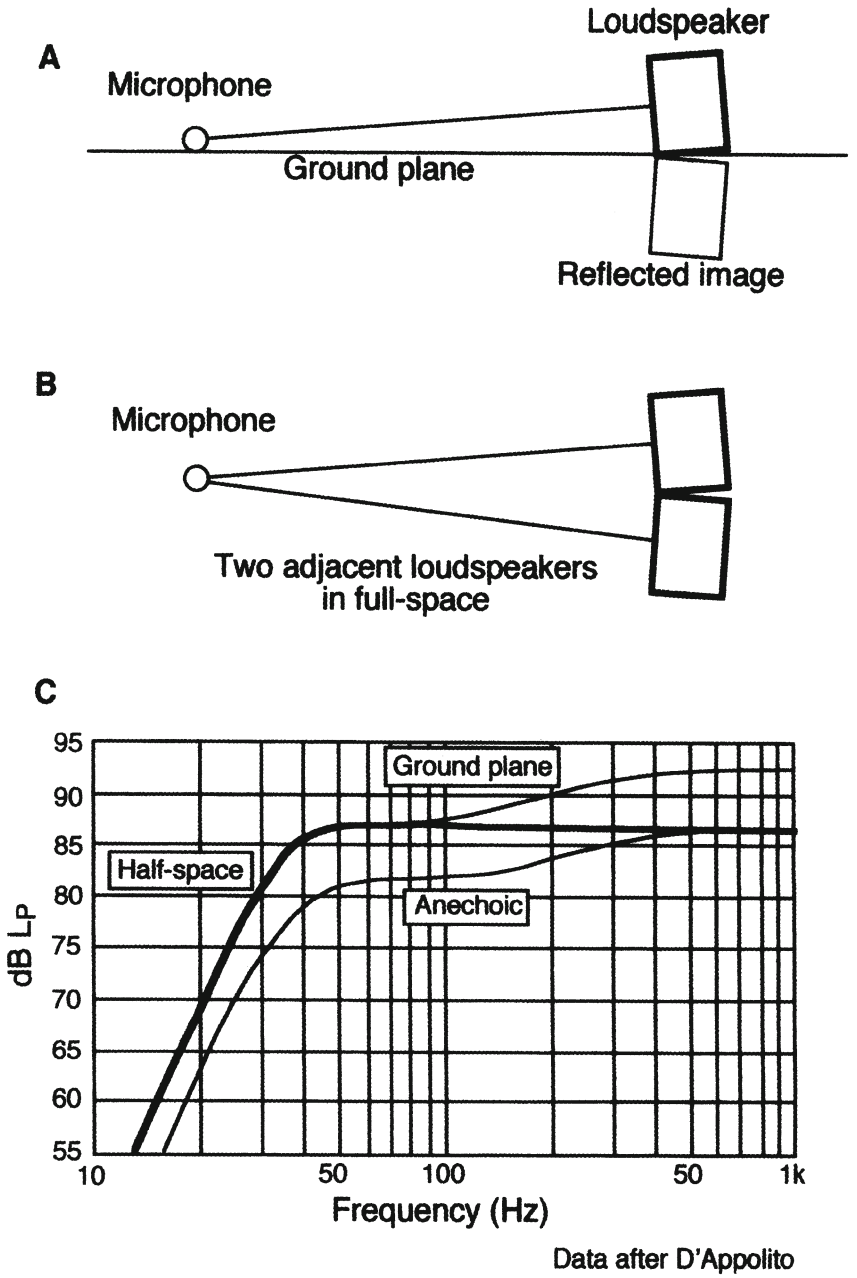

Figure 13-14. Ground plane measurements. Basic setup (A); equivalent setup (B); typical curves (C).

with measurements made at other distances. The basic technique is shown in Figure 13-15.

The microphone is placed within 0.11 the radius of the cone. The measurements will be accurate up to a frequency given by:

$$f_{lim} = 4300/D_{inches} = 10{,}922/D_{cm} \qquad 13.3$$

where D is the cone diameter.

The conversion of the near-field measurement to a 2π far-field measurement is given by:

$$L_{far\text{-}field} = L_{near\text{-}field} - 20 \log(2r/a) \qquad 13.4$$

where r is the far-field measurement distance and a is the cone radius. In practice, the near-field measurement is adjusted to match the normal 1-watt, 1-meter measurement at the frequency of interest.

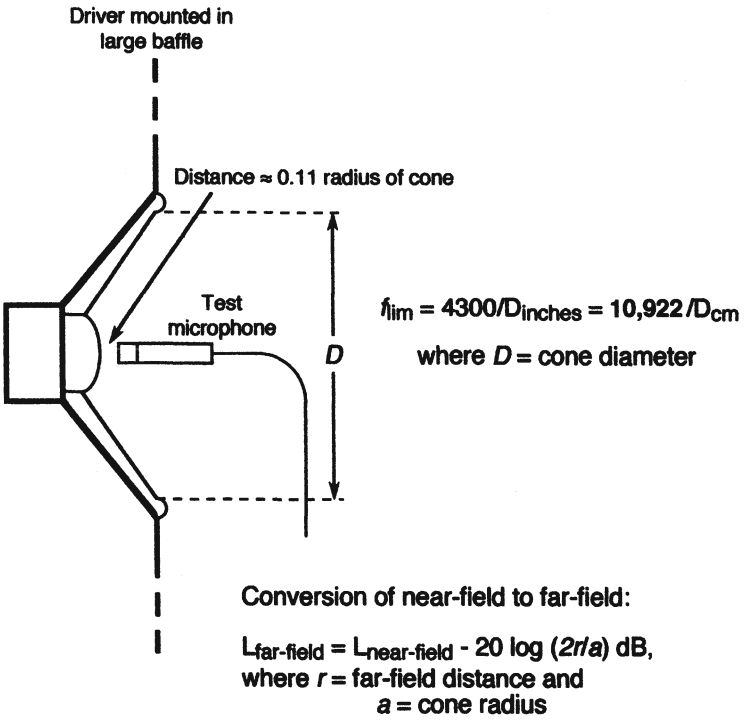

Figure 13-15. Near-field measurement setup.

13.8 An overview of transform measurement methods

The modern personal computer (PC) is the heart of most of the transform testing methods used today. As opposed to the analog techniques we have discussed so far, the PC stores the results of the measurements, allowing them to be processed later and graphically reformatted as desired. By comparison, the output of the earlier analog testing methods was a piece of paper – a graph. If other formatting was desired, the measurement had to be re-run or manually redrawn.

The Fourier transform is the basis of these new methods, and it provides a mathematical connection between time and frequency domains. Facilitated by the Fast Fourier Transform (FFT) algorithm, the modern PC can process the data very nearly on a real-time basis. Figure 13-16 shows the basic outline of the transform process.

Fundamentally, transform systems use a deterministic test signal that is specific in both amplitude and phase over the relevant bandwidth. For example, the unit impulse function at some reference t = 0 seconds is equivalent to an unbounded number of individual sine wave signals whose signal values are all maximum at t = 0, so both amplitude and time (phase) relationships are known for every component.

The unit impulse function sounds like a very sharp "snap." Such a signal can be used to drive a system, and the measurement of that system directly compared with the driving signal. From this data, the transfer characteristics of the device under test can be calculated and displayed in a variety of ways. The major drawback with the impulse test signal is that it has a very high peak to rms ratio (crest factor) and may cause system overload if any attempt is made to secure a good signal-to-noise ratio.

Some systems use a linear frequency sweep as the test signal. The relation between the linear sweep and the impulse function is a fundamental one; if the impulse function is passed through an all-pass network that linearly shifts phase from high frequency to low, the resulting output will in fact be a downward gliding linear frequency sweep. The swept frequency has an advantage in that it can be fed to the system under test at a fairly high level, with little tendency for overload and thus ensuring a very high signal-to-noise ratio. Obviously, a certain amount of time is required to make the frequency sweep.

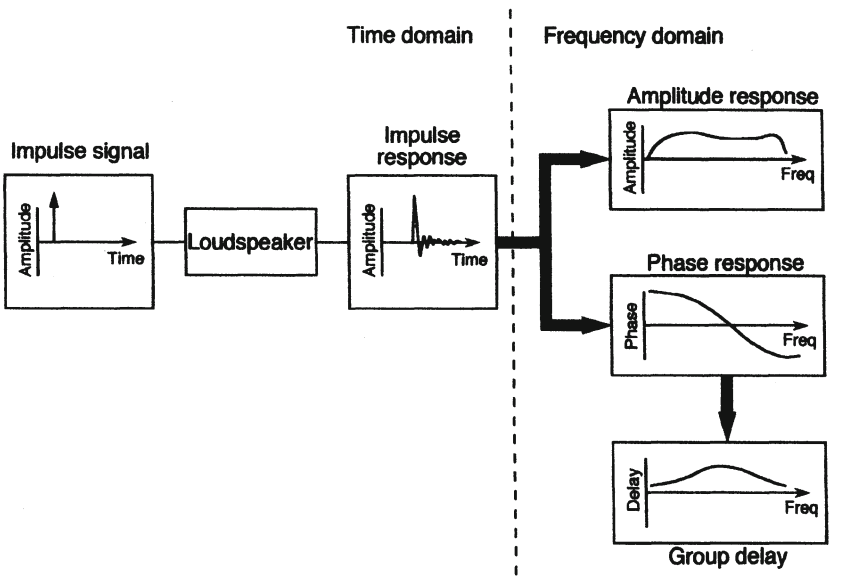

Figure 13-16. Symbolic view of Fourier transform measurement techniques.

Maximum Length Sequence (MLS) systems use a test signal that is a pseudorandom sequence of on-off pulses that repeat at fixed intervals, with a sequence length defined by the relationship $2^N - 1$, where N is any integer. The autocorrelation of the signal will be unity at the sequence length, but when compared with the return signal via the measurement microphone, the autocorrelation, as a complex value, will contain data that describes the transfer function of the system under test. Without going into further nature of the signal, we will say only that it provides an excellent signal-to-noise ratio and sounds very much to the ear like a continuous white noise signal.

All of the transform systems require high signal-to-noise ratios and low nonlinear distortion in the device under test if the resulting frequency response data is to be useful.

13.8.1 Examples of transform measurements

Traditional frequency response measurements can be easily duplicated by transform methods. Figure 13-17 shows a measurement of a HF compression driver made on a PWT using the Techron TEF® system. When all parameters are matched, the curve virtually overlays similar measurements made on analog chart recorders.

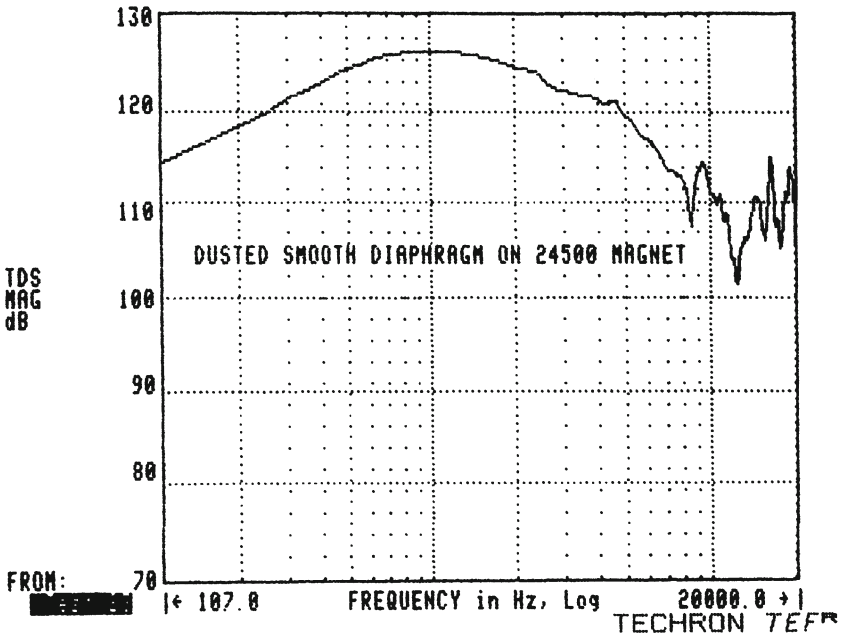

Figure 13-17. Response of a HF compression driver made on a PWT using the TEF measuring system.

The curves showing horn-driver complex impedance data, both modulus and phase angle, shown in Figure 13-18, were made using the MLSSA maximum length sequence system, with driver voltage and current values being fed to the analyzer.

13.8.2 Time and frequency trade-offs

Transform methods come into their own when used to generate a family of time-frequency curves on a single graph. Hidden lines in the display make it possible to present realistic and intuitively obvious three-dimensional displays.

For example, the data shown in Figure 13-19 shows successive level versus frequency plots over discrete time intervals. In this set of graphs level is measured along the vertical scale, frequency along the left-to-right scale, and time along the back-to-front scale. This family of curves is normally known as a TEF (time-energy-frequency), or "waterfall," display. This display shows details of stored energy and transient overhang in acoustical systems, and as such the displays may be valuable in both loudspeaker and room analysis.

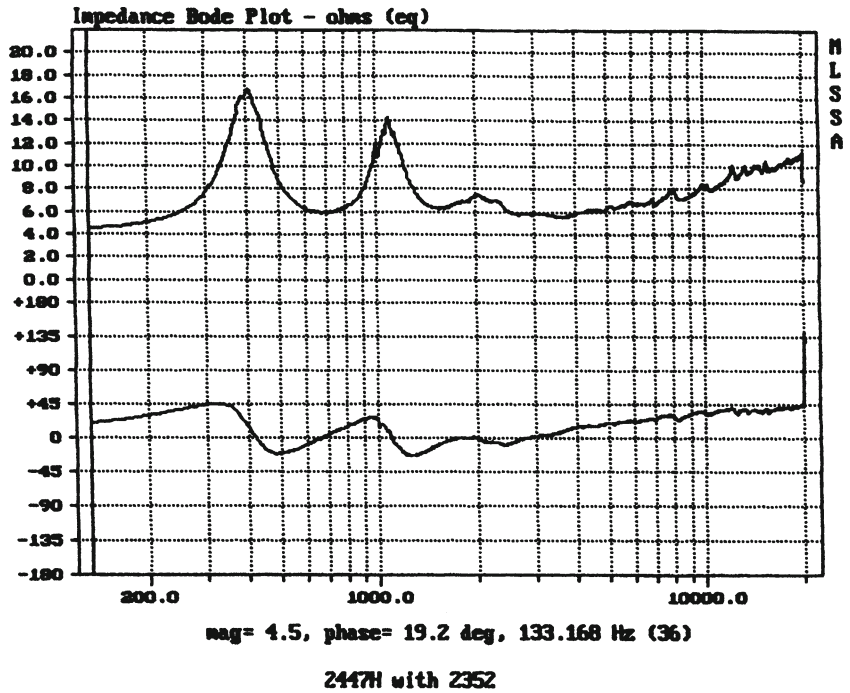

Figure 13-18. Loudspeaker modulus and phase of impedance made in free space using the MLSSA method.

There is however a pitfall associated with these measurements which has to do with joint *period-frequency resolution*. The relation between period and frequency is given by:

$$\text{Period} = 1/\text{frequency} \qquad 13.5$$

which implies that the product of period and frequency is always unity.

If it is desired to observe frequency details as low as, say, 100 Hz, then successive "time frames" must be spaced by 1/100 seconds (10 msec) if the lowest frequency is to be accurately observed. Figure 13-20 shows two sets of measurements of the same driver. At *A*, the time intervals are spaced so that considerable LF detail is seen; at *B* the time interval has been decreased, resulting in less LF detail. Engineers must know what they are looking for in order to make the right decision here. A great deal of excess and confusing data has been published in recent years through ignorance of this fundamental relationship.

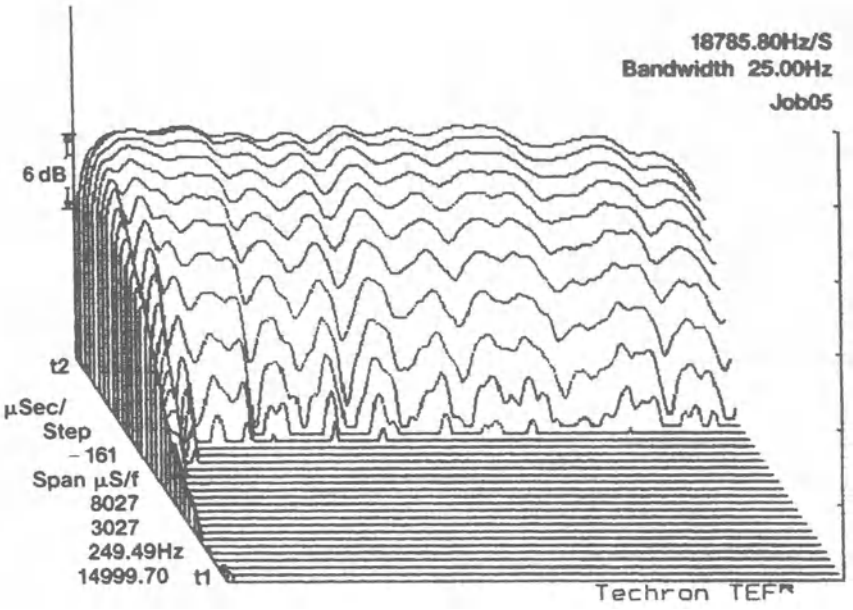

Figure 13-19. A "waterfall" display showing successive relationships among time, frequency, and level in the decay pattern of a loudspeaker, using the TEF measuring method.

13.8.3 Gating techniques

Frequency response measurements can be made in normal acoustical spaces if the signal reception can be gated off before the first room reflections arrive at the measurement microphones. It is of great benefit to be able to make *in situ* frequency response measurements, but LF resolution is dependent on the time interval between reception of direct sound and that of the first reflection. Considering the details of Figure 13-21, the distance between the loudspeaker and microphone is 5 meters, and the total distance traveled by the first reflection is 8 meters. The difference here is 3 meters, representing a delay of 3/344 seconds. This is the period corresponding of a frequency of 344/3, or 115 Hz, which may or may not be adequate for the measurement purpose. Typically, in large spaces, the cutoff frequency due to gating will be considerably lower, rendering the measurements useful.

13.9 Optical measurement techniques

The transducer design engineer always has a need for direct visual examination of cone and diaphragm motions. The simplest method here is the stroboscope. The best analogy to suggest here is watching a western movie and seeing the

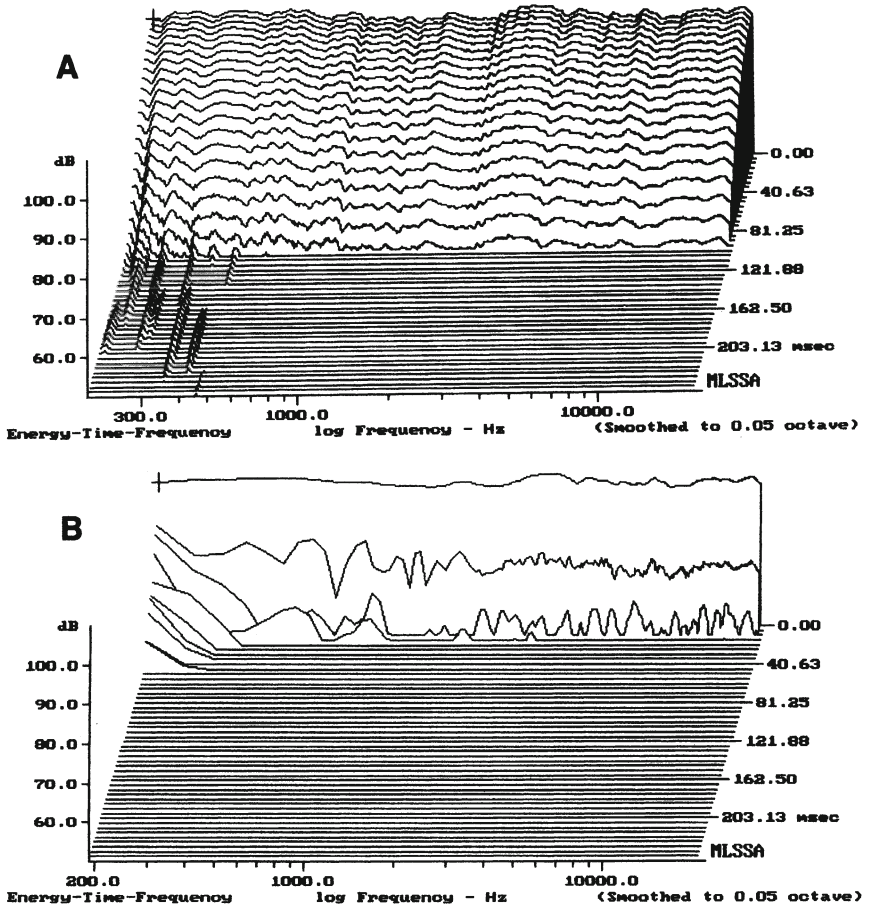

Figure 13-20, Illustration of time-frequency trade-off. Time intervals spaced so that considerable LF detail can be seen (A); increasing time resolution diminishes the LF detail but presents more accurate time information (B).

stagecoach wheels come to a halt, and slowly start to spin backwards, even as the stagecoach actually increases in speed.

The rotation of the wheel spokes is cyclic and is sampled by the motion picture camera at a rate of 24 frames per second. When the successive "spoke rate" corresponds to the frame rate, the spokes appear stationary.

The same principle can be applied to a loudspeaker as it is observed under a strobe light, as shown in Figure 13-22. The strobe light is a gas discharge device and as such can generate a very short pulse of light at rapid rates. In

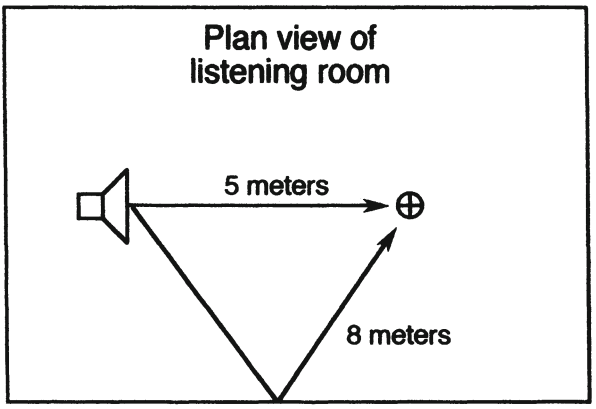

Figure 13-21. Frequency reponse made in a room using gating techniques. Return signal gated off at 3/344 seconds, corresponding to one period for 115 Hz.

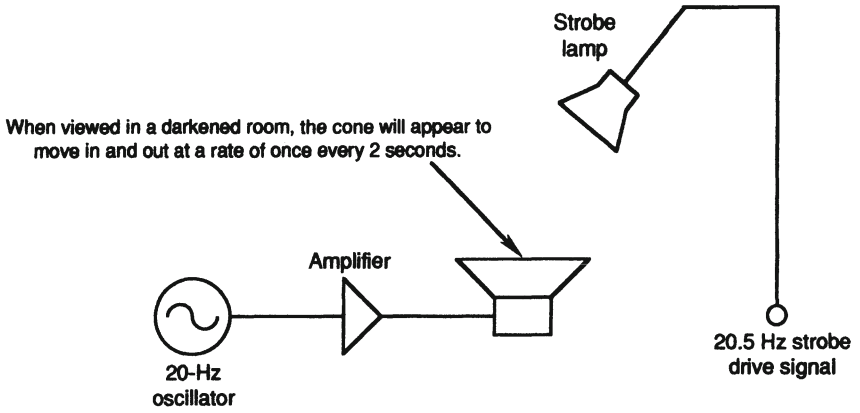

Figure 13-22. Principle of stroboscope testing of large cone motion of the driver.

the example shown here, the driver is operated at 20 Hz, and the strobe light is flashed at a rate of 20.5 Hz. When examined in a darkened room, the cone will appear to move in and out at a frequency of 0.5 seconds, or once each 2 seconds. Any gross departures from normal linearity will be visible to the naked eye.

Various kinds of laser measurements can be applied to loudspeaker analysis, when the cone is moving at microscopic displacements. Here, a laser beam is scanned over the cone or diaphragm and the reflections measured, stored, and displayed in a variety of ways. Wavelength interferometry can be used, or Doppler shifts in the laser wavelength can be measured. As with the

stroboscopic method, time varying behavior can be displayed with considerable amplification. A "snapshot" example of this technique is shown in Figure 13-23 for a 100-mm compression driver dome radiator operating successively at low, mid, and high frequencies. Note the clear departure from linear motion of the dome at mid and high frequencies.

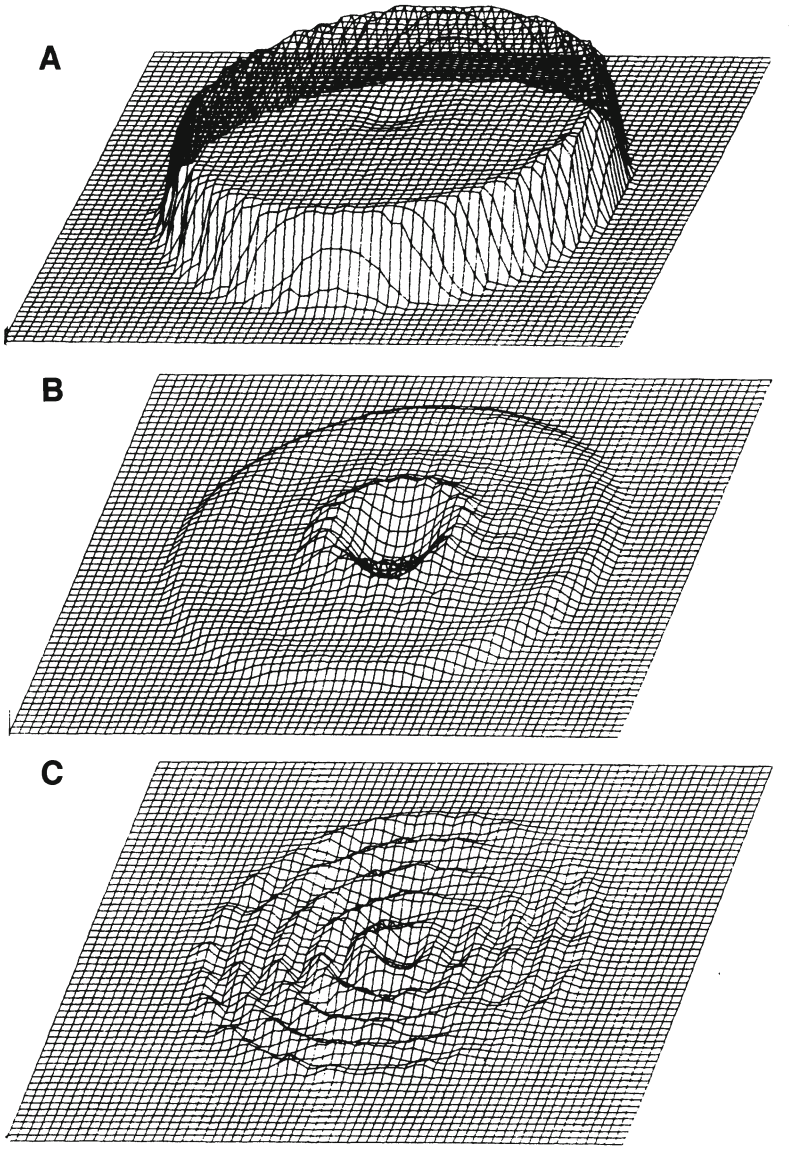

Figure 13-23. Laser techniques showing diaphragm motion at frequencies of 1 kHz (A); 4 kHz (B); and 8 kHz (C). (Data courtesy JBL and Fancher Murray).

13.10 Modeling techniques

If sufficient performance data on a physical system can be measured and analyzed, it is possible to model the physical process for estimating actual performance. As we saw earlier, the nonlinearities of magnetic circuits can be modeled by *finite elements analysis* (FEA). These techniques can be extended to cones and domes. An example is shown in Figure 13-24 of a 100-mm diaphragm used in a compression driver. The various circumferential modes

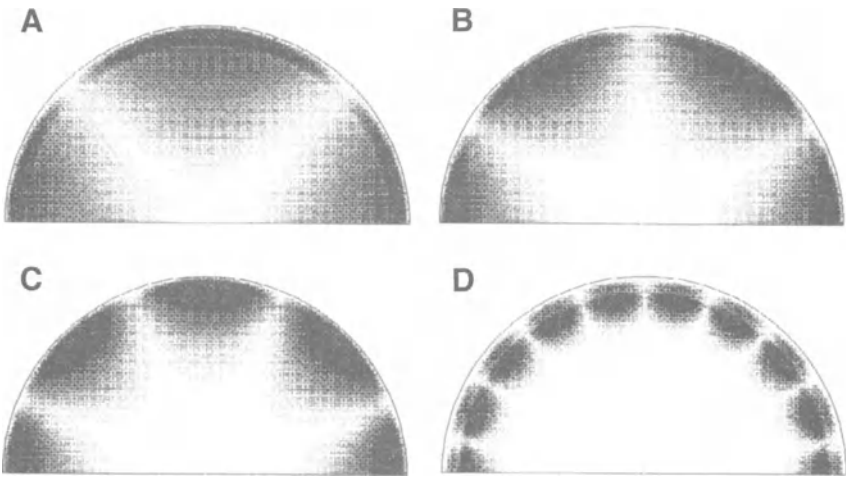

Figure 13-24. Finite element analysis. Modeling of the performance of a 100-mm diaphragm at several high frequencies. (Data courtesy JBL)

are clearly seen and are of much help to the transducer design engineer in further stages of product refinement.

13.11 Destructive testing

While we normally think of destructive testing in terms of automobiles, housing structures, and the like, having to do with life and limb, the techniques are very useful in loudspeaker assessment. Loudspeaker drivers are routinely tested to the breaking point, primarily as a means of quality assurance and manufacturing control of all processes. This concern also extends to the design

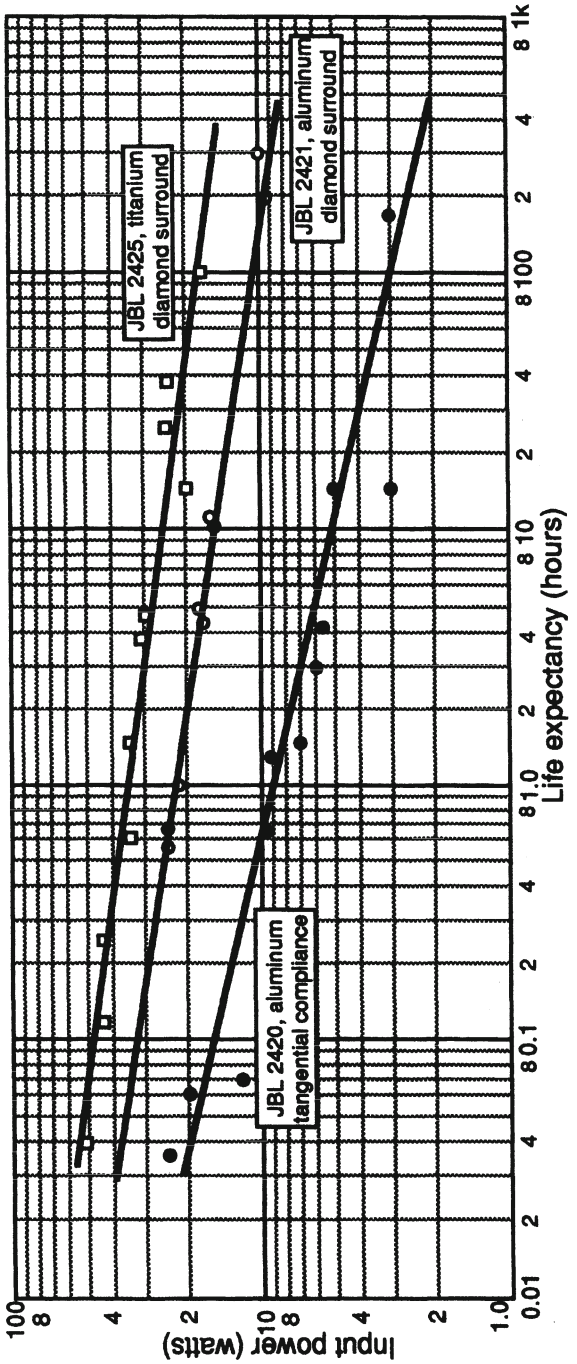

Figure 13-25. Failure modes. Cumulative failure data for samples of aluminum and titanium diaphragms driven at various powers. (Data courtesy JBL and Fancher Murray)

stages of HF compression drivers where the moving systems are normally made of materials that exhibit stress related failure modes.

Under typical stress-strain (force-displacement) conditions, aluminum, for example, will exhibit a unique failure history over long operating periods. For small diaphragm excursions, many flexures may be endured before weakness, and eventual failure, sets in. For larger excursions, the failure point will be reached with fewer flexures, or at an earlier time in the driver's history.

Many plastics do not exhibit such a "bend and break" behavior, and beryllium, specifically, does not exhibit a cumulative failure history. Rather, it may shatter suddenly, at any time, when a specific physical displacement limit is exceeded. Titanium is less prone to cumulative fatigue history than aluminum, but it is not as good in this respect as beryllium. The failure rate of any material can only be inferred from statistical observation of many samples, and three examples of aluminum and titanium behavior are shown in Figure 13-25.

BIBLIOGRAPHY AND REFERENCES:

Collums, M., *High Performance Loudspeakers*, John Wiley & Sons, New York (1991).

D'Appolito, J., *Testing Loudspeakers*, Audio Amateur Press, (Peterborough, NH, 1998).

Davis, D. and C., *Sound System Engineering*, Sams, Indianapolis (1987).

Eargle, J. and Larson, R., "Loudspeaker Testing in Reverberant Rooms," *IEEE Transactions on Audio*, Volume AU-11 (March/April 1963).

Gander, M., "Ground-Plane Measurement of Loudspeaker Systems," *J. Audio Engineering Society*, volume 30, number 10 (October 1982).

Heyser, R., "Acoustical Measurements by Time Delay Spectrometry," *J. Audio Engineering Society*, volume 15, number 10 (1967).

Murray, F., "MTF (modulation transfer function) as a Tool in Transducer Selection," Proceedings of the AES 6th International Conference, May 1988.

Rife, D. and Vanderkooy, J., "Transfer-Function Measurements with Maximum-Length-Sequences, *J. Audio Engineering Society*, volume 37, number 6 (1989).

Vanderkooy, J., "Aspects of MLS Measuring Systems," *J. Audio Engineering Society*, volume 42, number 4 (1994).

Chapter 14:
LOUDSPEAKER SPECIFICATIONS FOR PROFESSIONAL APPLICATIONS

14 Introduction

In this chapter we will discuss the principal specifications of loudspeaker components used in professional sound design. These include:

1. On-axis frequency response
2. Impedance
3. Sensitivity
4. Electrical power input ratings (thermal and displacement)
5. Power compression
6. Distortion (discrete harmonics)
7. Directional characteristics
8. Thiele-Small parameters

The topics covered here are central to specification writing and proper system layout, and it is essential that they be clearly understood.

14.1 On-axis frequency response

The familiar on-axis frequency response curve of a transducer or system is normally referred to a distance of one meter with a stated input power or voltage. Most commonly used is an input of 1 watt or an applied voltage of 2.83 volts rms. Often, the curve is run at a distance greater than 1 meter, and the results adjusted for an equivalent 1 meter distance using inverse square relationships. A quick examination of a variety of specification sheets will disclose the wide variety with which such basic, and fundamentally simple, data is given. There are two major areas of divergence: the ratio of frequency and level (decibels per octave of frequency) and the degree of data smoothing introduced by the manufacturer. The general recommendation for the presentation ratio is 25 or 50 dB for each frequency decade.

J. Eargle, *Loudspeaker Handbook*

In the listing of specifications for a device or a system, tolerances on the response may be stated. For example, the usable frequency range of a device may be given as the nominal the range over which the response is no lower than −10 dB, relative to the mid-band rated sensitivity, but engineers would probably be more interested in the range over which the response is ± 3 dB The primary data is shown in graphical form as a function of level versus frequency. For systems, the range of any of the system's level controls are normally indicated on the on-axis response graph. An example of this is shown in Figure 10-6C.

14.2 Impedance

A plot of the impedance modulus may be presented on the same graph as the on-axis frequency response. The modulus varies with frequency, and it is of special importance to the system designer to know the lowest value of impedance that a device will present to an amplifier. Care should be taken by the specifying engineer to consider the effects of paralleling of loads. Figure 14-1 shows both amplitude (modulus) and phase components of impedance for a typical bookshelf loudspeaker system. As a rule, a plot of the impedance phase response is not presented in specification sheets; rather, it is more useful to state at what frequencies the phase angle may be in excess of ± 60 degrees, or some other specified amount.

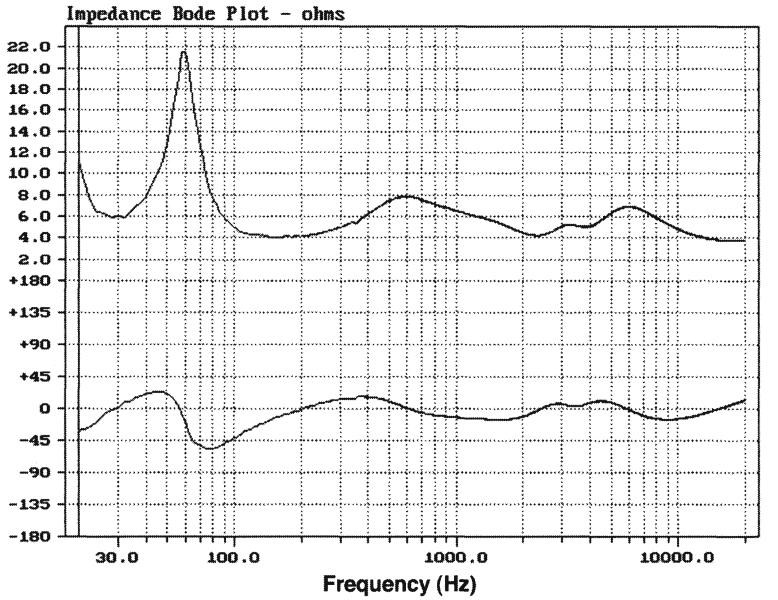

Figure 14-1. Complex impedance plots for a loudspeaker system.

14.3 Reference sensitivity ratings

A loudspeaker system or driver is normally given a sensitivity rating based on a band limited pink noise power input of 1 watt and measuring the L_p at some distance along the principal axis of the device. Today, the reference distance for the measurement is always one meter.

The voltage, *E*, required to produce a 1-watt input signal is derived from the nominal impedance, *Z*, of the device by the following equation:

$$E = \sqrt{Z} \qquad 14.1$$

Thus:	Nominal impedance	Applied voltage
	16 ohms	4 Vrms
	8 ohms	2.83 Vrms
	4 ohms	2 Vrms

As we have noted, the impedance of a system or a transducer is not uniform across the frequency band, and the term *nominal impedance* describes an average value which is approximately 15% greater than the *minimum* value of impedance the device exhibits. Most drivers and systems are conveniently designed around nominal impedances of 4, 8, and 16 ohms.

The signal bandwidth used for sensitivity measurements on systems is normally 500 Hz to 2.5 kHz. For LF drivers and systems, the noise bandwidth is usually 200 Hz to 500 Hz, and for HF systems it is usually from 1 to 4 kHz.

In older specification data we may find references to one-watt sensitivity measured at a distance of 4 feet. This measurement will be 1.7 dB *lower* than the corresponding one-meter measurement.

Another rarely encountered standard is the old EIA (Electronic Industries Association) sensitivity rating of 1 milliwatt sensitivity at a reference distance of 30 feet. This value will be 49.2 dB *lower* than the one-meter, one-watt rating.

For professional system design it is vital that the sensitivity data be accurate, since a small error, in a large sound system installation, can add up to many dollars spent unnecessarily on amplifiers – or worse, an inadequate specification of required power. Another potential problem is the increasing

tendency of some manufacturers to use voltage sensitivity measurements. Here, a 2.83 Vrms signal is used to make the sensitivity measurement. If the device under test has a nominal impedance of 8 ohms, then the measurement is equivalent to an input of one watt. However, if the device has an impedance of 4 ohms, it will receive 2 watts from the source and generate an output 3 dB greater than for one watt input. The matter can get very confusing, and users are urged to make careful measurements of their own. If the impedance of the device is not stated, and a voltage sensitivity is given, then power sensitivity cannot be calculated – it must be measured.

The *boundary conditions* adjacent to transducers or systems will play an important role in their LF measured frequency response and directivity properties. For example, most HF devices are measured in a *free field*; that is, the horn is free-standing in space, and there are no nearby surfaces that could influence sound propagation from the mouth of the horn. By comparison, LF systems are normally measured mounted in a large, solid boundary out of doors. We refer to the former as full-space mounting, or 4π; the latter is called half-space, or 2π mounting. In 2π mounting, the adjacent surface provides a mirror image of the transducer that will reinforce its LF output by 3 dB, while providing a minimum DI of 3 dB. This results in a net increase of 6 dB at low frequencies, as compared to free-field mounting of LF systems.

14.3.1 Sensitivity data for compression drivers

There are no rigorous standards for compression driver sensitivity measurements, and the reader of specifications will have to look closely if driver comparisons between manufacturers are to be made. However, for drivers mounted on horns, the same one-watt, one-meter method we have discussed will apply.

For making direct driver-to-driver comparisons, response is customarily measured on a plane wave tube (PWT) with a modest power input of 1 milliwatt. The cross-sectional area of the tube will then be a factor in the measured pressure level in the tube. For many years it was more or less standard practice to adjust the pressure level reading to match that of a 25 mm (1 inch) diameter PWT, whether or not the driver under test had a 25 mm exit diameter. As driver manufacturers proliferated, and models of different exit diameters were introduced, a certain amount of confusion was bound to set in.

The data shown in Figure 14-2 will enable the reader to determine the efficiency of a given driver, based on the diameter of the PWT and the resulting pressure level for an input of 1 mW. It is of course the efficiency that will facilitate the driver-to-driver comparisons. In virtually all cases, professional driver PWT measurements are normalized so that 1 mW of acoustical power will produce a PWT reading of 123 dB L_p. Thus, a mid-band reading of 119dB L_p for a compression driver with 1 mW input would indicate a nominal efficiency of 40%, a typical value. Remember that the 1 mW reference PWT diameter is 1 inch; using a 2-inch PWT will require scaling the level readings and efficiency upward by 6 dB, as indicated in Figure 14-2, for direct comparisons with data taken on 1-inch PWTs.

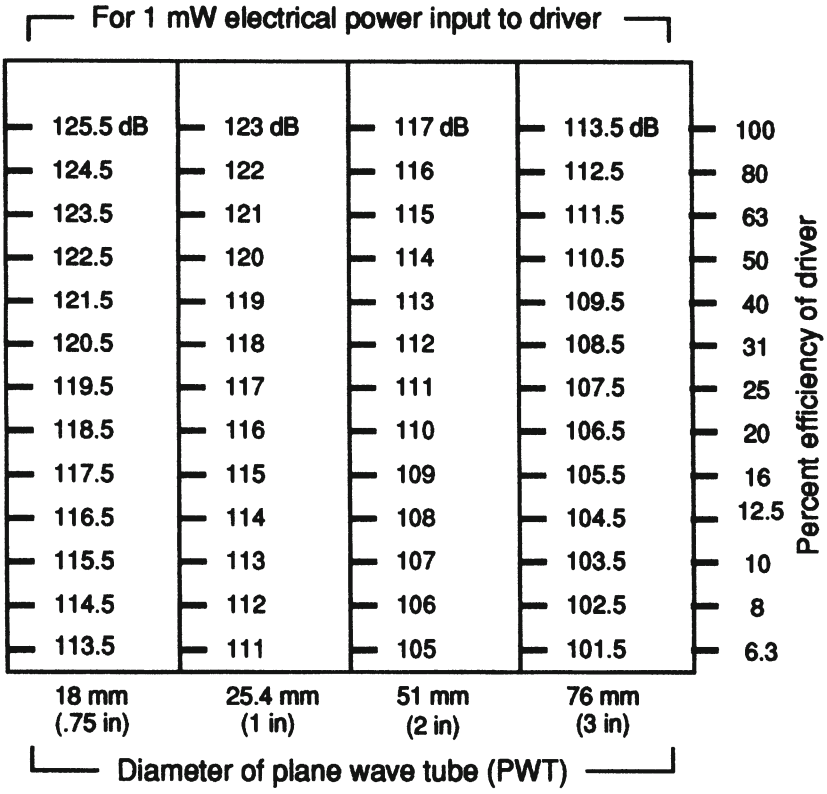

Figure 14-2. Compression driver sensitivity with constant 1 milliwatt signal input.

14.4. Power ratings of drivers and systems

Assigning power ratings to transducers and systems is a complicated matter. What we are attempting to do is give the user a proper guideline for choosing a power amplifier that is large enough so that its output signal will not clip during normal use – but not so large that we run the risk of burning out the loudspeaker or causing mechanical damage.

These two requirements are not always easy to sort out. For example, a typical three-way cone-dome monitor loudspeaker may carry a nominal input power rating of 150 watts, using a pink noise signal. Examining this specification closely, we note that the noise signal generally has a specified crest factor of 6 dB. This means that the average power delivered to the loudspeaker will be 150 watts, but instantaneous peak power values of *four-times* (+ 6 dB) that amount, or 600 watts, will be delivered to the system.

For this system, let us assume that single frequency signals in the 300 to 800 Hz range of 1200 watts can be safely delivered to the system – if they are short enough in duration and with a duty cycle (the time ratio of power-on to power-off) that allows the voice coil to cool down before the next burst of input power. Also, let us assume that sustained operation at 10 Hz at a power input of only 75 watts can mechanically harm the LF driver, due to excessive displacement of the cone.

Obviously, the manufacturer cannot consider all of these extreme contingencies in the matter of setting power ratings, so practical ratings must be based on normal operation of systems according to good engineering practice. There is the further assumption that the user will not intentionally abuse the systems.

For full-range loudspeaker systems, most professional manufacturers use a shaped pink noise (6 dB crest factor) spectrum established by the IEC (International Electrotechnical Commission). This spectrum fairly well approximates modern music and speech spectra, and the 6 dB crest factor implies that signal peaks 6 dB higher can be safely handled if they are within the operating bandwidth of the system. The stated rating is the highest average power input that the system can sustain for a long period of time over the specified bandwidth without any sign of permanent damage. This is essentially a *thermal rating*; that is, if the loudspeaker system fails in this test, it is normally as a result of overheating, with consequent burnout of the voice coil.

Figure 14-3 shows weighting curves that are used in loudspeaker system evaluation. Curve 1 shown at *A* has been suggested by the EIA (Electrical Industries Association) for loudspeaker system measurement, with white noise as the input. Curve 2 is an updated curve as suggested by the EIA for modern program material.

The curve shown at *B* is suggested by the IEC for loudspeaker system measurements, with a signal input of pink noise with a 6 dB crest factor.

The curve shown at *C* is recommended by the AES (Audio Engineering Society) for individual LF component rating. LF drivers are normally power rated according to the AES method. In this measurement, a one-decade (10-to-1) frequency range of band limited pink noise (6 dB crest factor) is applied to the device under test. The manufacturer states the particular frequency decade over which the tests have been run, and the test is run with the transducer placed in free space (not in an enclosure). This is an attempt to qualify a given driver by itself, with no necessary relationship to the enclosure it will be mounted in.

If the frequency decade is chosen at higher frequencies, then the rating will primarily reflect the thermal limit of the device. If the decade extends low enough in frequency, it will reflect, to a greater or lesser extent, the displacement limits of the device.

HF drivers are similarly rated by choosing a particular frequency decade with a given horn load on the driver.

It is up to each manufacturer to select and state the appropriate frequency decade for a given transducer, and it is not uncommon for a transducer to carry more than one AES rating, depending on the frequency decades that have been chosen.

14.5. Power (dynamic) compression

When high powers are delivered to a transducer over relatively long periods of time, the voice coil will heat up and its resistance will rise. As a result of this, the loudspeaker will draw less power from the amplifier, and its sensitivity

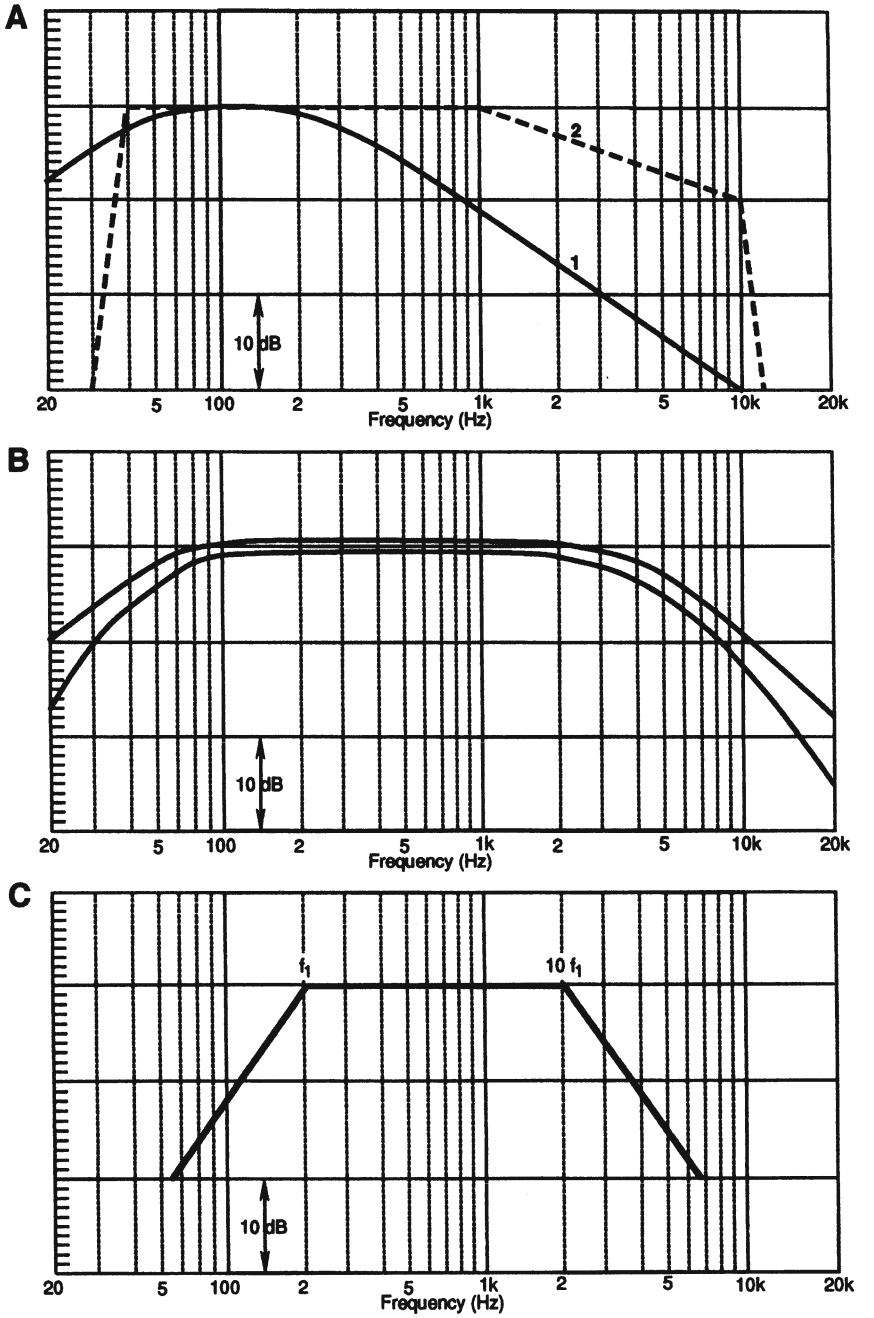

Figure 14-3. Weighting curves for loudspeaker system power testing. EIA data (A); IEC data (B); AES data (C).

will decrease. Typical data presentation is shown here for a professional 380 mm diameter driver with a 100 mm voice coil:

At -10 dB power (60 watts):	0.7 dB
At -3 dB power (300 watts):	2.5 dB
At rated power (600 watts):	4.0 dB

These values assume that the driver under test has reached thermal equilibrium at each of the power values listed. Additional data on power compression is presented in Chapter 9. Not all manufacturers routinely present compression data in their specification sheets, and there are no generally agreed upon value limits.

14.6 Distortion

The standard method for showing distortion is to plot 2nd and 3rd harmonic components on the same graph with the fundamental. The distortion curves may be raised 20 dB for ease in reading, and the normal power input for the measurements is usually one-tenth (–10 dB) rated power. An example of this is shown in Figure 2-26.

At any point on the graph where the fundamental and distortion curves intersect, the value of distortion is 10%. Because of the 20-dB offset of the distortion curves, the actual value of distortion is 20 dB lower than the fundamental, corresponding to 10%. In this figure, the value of third harmonic distortion at 40 Hz is 10%.

14.7 Directivity characteristics of systems and components

As discussed in several preceding chapters, directional data on loudspeakers covers much ground, and Figure 13-10 summarizes the chief graphical methods of display. It is appropriate in this chapter to suggest data presentation methods and performance guidelines for various areas of professional sound work.

14.7.1 Speech reinforcement

The major problem in selecting components for speech reinforcement in reverberant spaces is that of ensuring proper directivity control throughout the speech range. Traditionally, this range of interest has been assumed to be from 500 Hz to about 4 kHz, but many workers in the field feel that systems

sound far more natural when good pattern control is maintained down to 200 Hz and up to 8 kHz.

Most high frequency horns, large or small, will provide good loading at least an octave below the point at which pattern control in the narrow plane starts to widen. Assuming that the HF driver can handle the anticipated load, many designers may opt for a lower crossover frequency in an effort to carrying the LF portion of the system too far beyond its range of flat power output capability. Good engineering calls for an innovative approach in the upper bass region, for example, the use of a vertical array of relatively small LF drivers to fill in that portion of the spectrum with good forward directivity.

While not actually a driver design problem, the vast majority of ceiling distributed arrays in public places suffer from insufficient coverage at frequencies up to 2 kHz. The present state of the art in small ceiling drivers that are economical to build permits a nominal radiation cone of about 90 degrees (–6 dB) at 2 kHz. The data presented in Figures 11-6 and 7 demonstrates the need for a fairly dense array. If this is not possible, for whatever reason, the system may probably be better off with a small number of wide-angle radiating devices hanging from the ceiling at calculated locations.

14.7.2 Music applications

In the recording studio it is essential to achieve good horizontal coverage for both seated and standing personnel. The vertical coverage at high frequencies may be allowed to vary from relatively wide in the mid-range to about 45 degrees at the highest frequencies. The relatively dry acoustic environment will minimized the broad shift in actual power response of the system. HF elements exhibiting wide variations in directional response should be avoided.

14.8 Thiele-Small parameters

The T-S parameters have become an important specification for any professional LF driver. They should be accurately determined from an adequate sampling of actual production units. Particular attention should be paid to X_{MAX} and P_E, since these parameters determine the large-signal performance of the driver. Normal production variations in cone mass should be negligible, and incoming inspection procedures should pick up any shift here.

The stiffness of surrounds and spiders may tend to vary to some degree, causing the V_{AS} and Q_{TS} parameters to shift. The main question here may not be the variation itself, but the effect that the variation may have on system performance. In most ported systems, the LF alignment is dominated by enclosure volume and tuning parameters, and slight shifts in these parameters may have little practical effect. Nevertheless, the quality assurance activity in the manufacturing plant should be aware of them.

14.9 Powered loudspeaker systems

For many smaller monitoring applications, especially in surround sound formats, relative small powered systems have become very popular. A typical design is built around a 200 mm (8 inch) LF unit and a dome HF, and the ensemble, whether stereo or surround, is normally supplemented with one or more dedicated subwoofers.

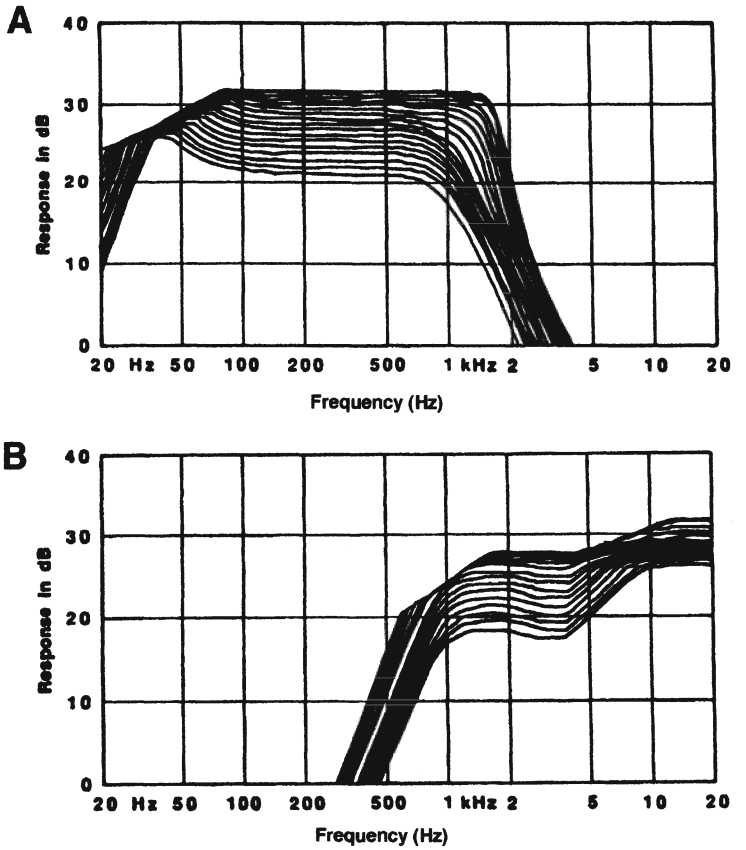

Figure 14-4. Electronic compression curves for a 2-way biamplified system.

The user of these systems can only assume that they have been engineered to be virtually indestructable in normal usage, and this implies some degree of electronic signal limiting and compression when these small systems are driven to their maximum performance levels. An important specification for such a system would be a set of curves showing the progressive onset of output signal limiting.

Figure 14-4 shows a set of curves run individually on LF and HF sections of a powered loudspeaker system. You can see that the spectral modification of the overall spectrum is quite pronounced, although many users would be unable to identify this extent of signal manipulation. Very few manufacturers present data of this sort. Actually, nobody wants to be the first to present such data. However, once introduced to the marketplace, all manufacturers would have to follow suit.

BIBLIOGRAPHY AND REFERENCES:

Recommended Practices for Specifications of Loudspeaker Components Used in Professional Audio and Sound Reinforcement (AES 2-1984; ANSI S4.26-1984). Printed in *J. Audio Engineering Society*, volume 32, number 10 (October 1984).

IEC 60268, Sound System Equipment, Part 5. "Loudspeakers," 2nd edition, International Electrotechnical Commission, Geneva (1989).

AES Information Document – Plane-Wave Tubes: Design and Practice, New York (1991).

Chapter 15:
STEREO AND THE LISTENING ENVIRONMENT

15 Introduction

While the professional sound world relies heavily on loudspeaker specifications in systems design and layout, the choice of loudspeakers for home listening is likely to be the result of a far more personal set of experiences and associations. This can be inferred from a casual reading of high fidelity manufacturers' literature and advertisements.

But there is nothing casual about a truly first-rate home audio system. When care has been given to the choice of loudspeakers, room treatment, and electronic componentry, a consumer playback system can outperform a more perfunctorily designed professional system – and often for a lesser price.

A big obstacle to putting together a truly fine home system is the dedication of space required for it. In a family setting this may be difficult to justify, and perhaps as a result, many high fidelity loudspeaker companies have put significant efforts into the conceptual design and engineering of smaller systems capable of excellent performance in the modern home environment.

In this chapter we will examine many of these concerns, stressing the nature of the listening room as a very complex transmission path between loudspeaker and listener.

15.1 Listening room boundary conditions: the laboratory meets the real world

Virtually all loudspeaker design is carried out in simulated open space (4π) or ground plane half-space (2π) environments. The professional designer can infer much from this data, but the consumer, and the consumer dealer, are often left in the dark. The actual home loudspeaker environment is apt to be somewhere between a 4π and 2π condition, and some loudspeakers, notably corner horns, are intended to be operated virtually in a $\pi/2$ (one-eighth space) environment. Roy Allison (1974) is one of only a handful of loudspeaker

J. Eargle, *Loudspeaker Handbook*

designer-manufacturers who have tackled this problem headlong in making specific loudspeaker placement recommendations for the consumer.

As discussed in Chapter 4, halving the solid angle into which an omnidirectional device radiates will double its LF efficiency. Additional power doublings take place at adjacent pairs of surfaces (dihedral corners) and at adjacent trios of surfaces (trihedral corners). The precise nature of this effect is wavelength dependent and Allison shows this in Figure 15-1. The curves show the normalized power output of an omnidirectional source as a function of distance (x, y, or z) and signal wavelength (λ), at a single wall (A), a wall-floor boundary (B) and a corner-floor boundary (C).

Considering only curve A, for a loudspeaker in the far field (beyond $x/\lambda = 2$), the output has been assigned an arbitrary reference level of zero dB. As the loudspeaker is moved closer to the boundary, there will be a slight ripple in the response due to reflections from the boundary. This is wavelength dependent, and at very long wavelengths ($x/\lambda = 0.02$ or less) the reflection will be virtually in-phase with the primary source.

Curves B and C show similar data for sources of a given distance and wavelength from a pair of perpendicular surfaces and a trio of perpendicular surfaces. In these cases the response irregularities are more pronounced, due to the multiple anti-phase reflected images.

The picture is a complex one, and Allison has worked out several examples, as shown in Figure 15-2. In general, the closer a low frequency driver can be brought to a boundary, or set of boundaries, the smoother the response will be. If the driver cannot be operated in this position, it may be better overall if it can be placed well out into the listening space on a stand. In this case the reflected images will be farther removed from the listener and the response thus made smoother.

15.2 Room modes

The foregoing analysis assumed that the boundaries adjacent to the loudspeaker were quite large. In typical rooms, the conditions discussed by Allison will be modified by discrete frequencies, or room modes, at which the room will become very responsive. Extending the analysis of boundary conditions to an arbitrary space is complicated, but if we can limit the discussion to a rectangular space the analysis will be much simpler.

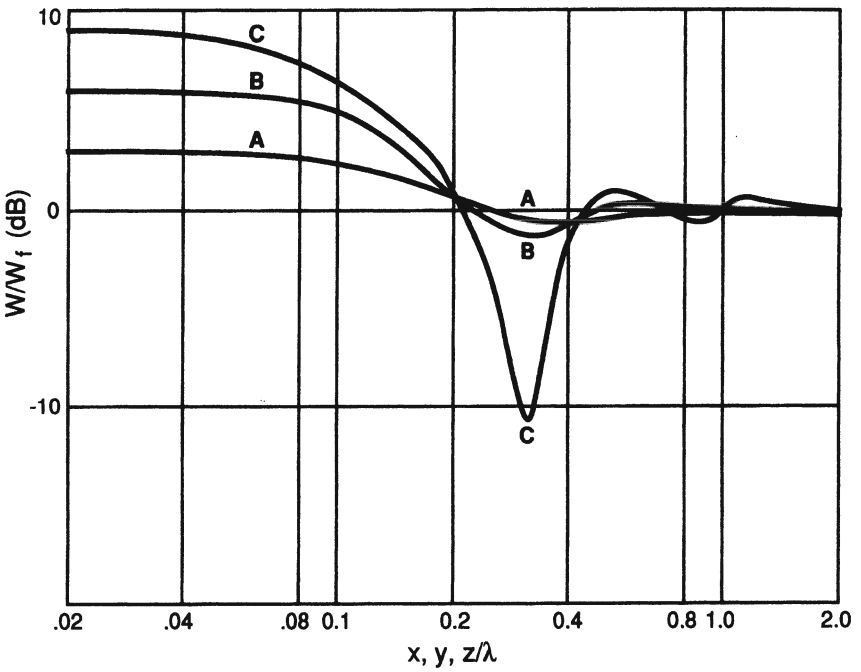

Figure 15-1. Acoustical power output for a source relative to its free-field output when located next to a single wall (A); two right angle walls (B); two right angle walls and floor (C). Horizontal scale shows the source location in terms of wavfelength (x/λ, y/λ, and z/λ). For two- and three-boundary cases, the curves apply only on lines of symmetry. (Data after Allison 1974)

The normal modes of a rectangular room are given by the following equation:

$$f = \left(\frac{c}{2}\right)\sqrt{(n_l / l)^2 + (n_w/w)^2 + (n_h/h)^2} \qquad 15.1$$

where c is the speed of sound, l, w, and h the length, width, and height of the room; n_l, n_w, and n_h are taken separately as integer values.

At middle and high frequencies in all but the smallest spaces, room modes will overlap, and the room will respond to a loudspeaker more less uniformly with a pattern of discrete reflections that are normally described statistically, leading to a definition of reverberation, or "ring-out," in the space.

At lower frequencies the modes are not so closely spaced and the acoustical description of the room changes significantly; the natural modes of the room

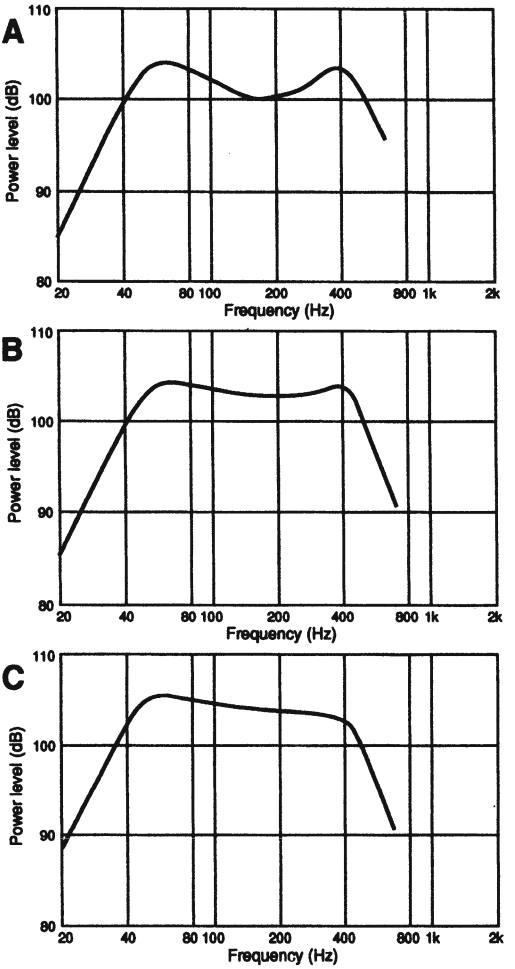

Figure 15-2. Location for a single LF radiator. Back of enclosure 1 inch from wall (A); LF driver one-half inch from wall (B); LF driver one-half inch from wall and floor (C).

set up a variation in level over space that profoundly affects the transmission of sound from loudspeaker to listener. While there is certainly sound propagation directly from source to listener at frequencies other than the natural modes, such propagation will be relatively low in level, as compared with the effect of room modes.

In many underdamped rooms, certain modes may be prominent enough in the 100 to 250 Hz range to cause audible coloration of normal speech sounds produced in the space. If this situation exists, it is a clear indication that sound reproduction in the space will suffer, and every effort should be

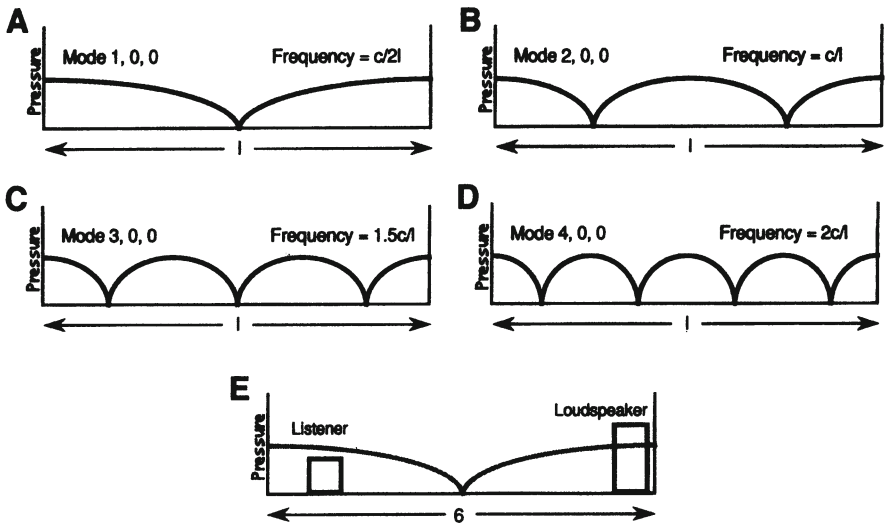

Figure 15-3. Pressure distribution for first four axial modes in a rectangular space along the largest dimension (A through D). Adjusting loudspeaker and listening positions for correct spectral balance of the lowest axial mode at 28.7 Hz (E).

made to correct it before attempting to install a stereophonic listening system. This problem is most often found in smallish rooms with hard structural surfaces, such as concrete floor slabs, cinder block walls, and the like. Flexible surfaces, such as dry-wall construction and large expanses of glass, will alleviate this specific problem – but will usually require drapery or other wall treatment to minimize mid and high frequency reflections.

In most rooms, the low frequency modes along the front-back listening axis will predominate, and their pressure distribution will be as shown in Figure 15-3A through *D*. Only the first four or so modes may be significant in determining the relative levels at the listener. Where both source and listener are high on a given modal response curve, as shown at *E*, the coupling between the two will be strong for that mode. When a loudspeaker is placed at a null point for a particular mode, the coupling will be weak. However, if a dipole loudspeaker is placed at a null point along the curve and oriented along the direction of the mode, the coupling will again be strong.

As an example, consider a listening room that has floor dimensions of 4 and 6 meters. Let the listening axis be along the 6 meter dimension of the room. Accordingly, we will use n_l values of 1, 2, 3, and 4, setting all n_w and n_h

values to zero. These values are individually entered into equation 15.1, giving frequency values of: 28.7, 57.3, 86, and 115 Hz.

The nature of room modes is that they are the preferred modes of the room itself, and the response of a loudspeaker, if appropriately positioned, will excite room resonances at those frequencies. Those frequencies will generally be louder to the listener than non-modal frequencies, but the distribution will vary considerably throughout the room.

As a practical matter, it would be desirable to excite the room at the lowest room mode (28.7 Hz) in order achieve added room support at that low frequency. Examining Figure 15-3A and looking at the pressure distribution for n = 1, we see that both listener and loudspeaker should be placed so that each is fairly close to the ends of the room. Moving the listening and loudspeaker positions farther from or closer to the walls will determine the spectral balance balance precisely, as shown in Figure 15-3E. As a practical matter it would be best to move both loudspeaker and listening position slightly into the room in order to reduce the coupling between the two in order to achieve the best overall acoustical balance. However, we should not forget Allison's recommendations regarding the spacing of the LF driver and its closest room boundaries.

15.3 Room treatments at mid and high frequencies

In general, a home listening space is governed by boundary reflections and mode structure below about 250 Hz. Above that frequency the mode structure gradually becomes fairly dense, and the response at the listener for frequencies higher than about 500 Hz is dominated by the specific directional properties of the loudspeaker and the mid and high frequency reverberant nature of the room. The range between these two frequencies is a transition zone between the two modes of operation.

In summary, at low frequencies the response is room dominated, while at high frequencies it is loudspeaker dominated. For a given direct field level, a more highly directional loudspeaker will produce less reflected acoustical power in the listening space; however, care should be taken that the room is not so heavily damped that its acoustic character seems oppressive to the listener. Discrete reflections, especially from the sides, should be minimized, and wall surfaces that provide diffusion may be better than those that absorb sound power. Irregular and reticulated surfaces are excellent in this regard, and the surface details shown in Figure 15-4 are useful in listening room

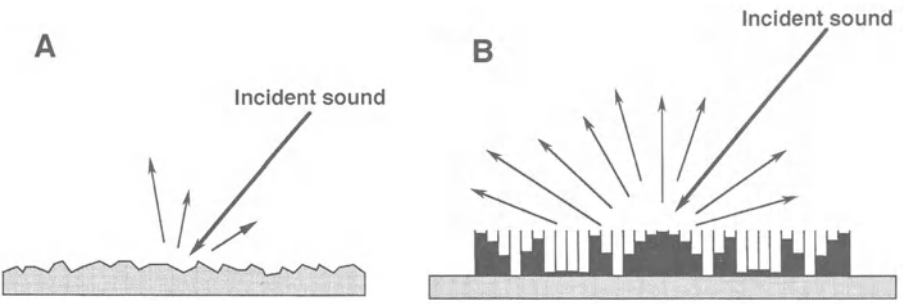

Figure 15-4. Sound diffusion from random reticulated surface (A); from quadratic residue diffusing surface (B).

treatment. The quadratic residue diffuser in particular affords uniform diffusion over a relatively wide frequency range (Schroeder 1984).

Large exposed areas of floor, wall, and glass surfaces should be covered at least in part by carpet, adjustable drapery, and absorptive or diffusive wall treatments. The option of wall-to-wall carpeting should be considered with caution, inasmuch as it may not actually be necessary for the control of room reflections.

Examples of location and room treatment for two kinds of loudspeakers are shown in Figure 15-5. The system shown at *A* is a traditional four-way cone-dome design with a characteristic DI plot that varies from 0 dB at low frequencies to about 14 dB at the highest frequencies.

The first consideration is to locate the loudspeakers so that LF response is smooth and free of peaks. If the room is well damped, with generous amounts of LF absorption, the job may be fairly easy. While the recommendations of Allison are always appropriate, they are specific to loudspeaker systems whose LF drivers can be positioned as required without compromising midrange and HF projection into the room. In the room plan view shown at the left, dimensions A and B should be experimented with at some length. If both A and B are reduced to small values, then there will be a considerable LF rise, as is seen in Figure 15-1. If A and B are increased so that the loudspeakers are well out from the walls, then there may be a smooth LF rolloff below, say, 125 Hz. Distances A and B can be experimented with individually, and the ideal (or acceptable) balance determined by ear. A final adjustment of the seating position should then be made, primarily in order to

adjust the stereo listening angle. Once this has been accomplished it is a relatively easy matter to finish the room in terms of midrange and HF absorption, largely to the taste of the user.

Some users may prefer the room plan view shown at the right. Here, the loudspeakers have been placed along the longer wall and as such will be well inboard of the adjacent corners. In this case, loudspeaker positioning fairly close to the wall may be best, with distances C adjusted for best listening angle.

The system shown in Figure 15-5*B* is of the dipole type. Many readers may assume that a dipole loudspeaker, because it radiates as much sound power from the back as it does from the front, unnecessarily contributes to the reverberant field in the listening room. This is not the case, inasmuch as the DI of the dipole never drops below a value of 4.8 dB. (Recall that the dipole has minimal radiation at off-axis angles of ±90°.)

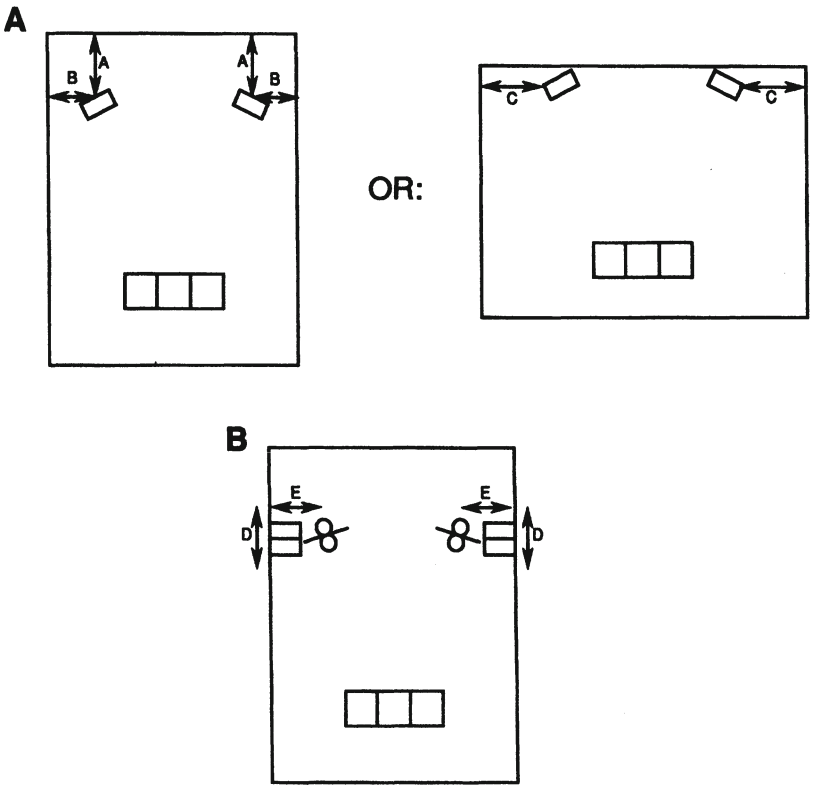

Figure 15-5. Suggested guidelines for room placement of a cone-dome system (A); for a dipole system (B).

The chief problem in interfacing the dipoles in a typical listening space is to ensure that there will be adequate LF response. It will be useful to identify those room modes of second and higher order along the listening axis of the room and experiment with placing the loudspeakers at nodal points, perhaps with the loudspeakers located fairly closely to the side walls to increase LF response. The difficulty here is that the room may be too wide for the normal stereo stage width of 45° to 60°.

Some listeners prefer to augment dipole loudspeakerswith sealed cone LF systems – so-called monopole systems – in order to satisfy their LF requirements. Most devotees of dipoles however refuse to do this, preferring the natural bass rolloff as a simple price to pay for the special listening experience that these loudspeakers generally provide. Other designers have experimented with large area LF dipole arrays to augment the bass portion of the listening spectrum. If these devices are used, they should be placed against the long side walls of the room, with the full-range units inboard. Values of D and E may be experimented with for the best overall LF and MF balance, and the seating position adjusted for best listening angle.

In any event, once the LF coupling via room to listener has been satisfactorily made, the details of room treatment at mid and high frequencies should not be materially different from the approach used with traditional cone-dome loudspeakers.

15.4 Optimizing stereophonic localization

In most listening environments there are a number of things the listener can do improve the quality of stereophonic imaging. If care has been taken in the basic setup, and if the room is acoustically balanced with regard to mid-low and low-frequency coloration, then the imaging should be reasonably good to begin with. A good way to check for this is to set the system mode switch to mono, and then to play a pink noise signal over the system. There are a number of test discs for this purpose, and the proper signal to use here would be either a full range pink noise signal or one limited to the midrange portion of the spectrum. The listener should carefully assess the nature of the perceived signal while seated directly on the center line of the setup, equidistant from both loudspeakers.

The signal source should appear directly in front of the listener, located precisely on a line connecting the two loudspeakers. If all previous

recommendations regarding electrical and acoustical balance have been made, then there should be no problems here. If the image appears to be vague or diffuse, the listener should recheck all matters of balance. If the problem persists it is likely a sign that the room is too live at mid and low frequencies.

Considerable time should be spent in checking and refining image stability. If slight left-right nodding of the head causes the image to wander widely from side to side, it is probably a sign that the loudspeakers are too widely placed. The normal stereo listening angle may range from 45 to 60 degrees, depending on taste. When the subtended angle is in this range, then normal side-to-side head movements should have little deleterious effect.

Increasing the seating range over which stereo imaging will be effective depends on the "cross firing" of the loudspeaker's primary axes. If it is desired to widen this area somewhat, then the listener should experiment with toe-in of the loudspeakers so that their major axes cross slightly *in front* of the center listening position. It would be wise to position the loudspeakers rather precisely in doing this, since the trade-off between amplitude and time cues for off-axis listening is critical.

The best signal to use for making this assessment is the spoken voice, again with the system in monophonic mode. Finally, when the monophonic, or phantom center, image is well behaved, the listener can switch to the stereo mode and probably be delighted with the results.

15.5 Loudspeaker arrangements for extended stereo imaging

Extending the notion of crossfiring stereo loudspeakers, several designers have come up with interesting systems concepts using asymmetrical radiation patterns or other patterns that exhibited a rapid falloff in response with respect to listening angle. Bauer (1960) examines the application of dipole loudspeakers crossfired in front of the listening position. Since the dipole pattern is maintained well over the mid and low frequency ranges, a satisfactory tradeoff between level and delay can be produced in the listening zone. Figure 15-6 shows the basic setup, in which balance lies within 3 dB. The requirement of all these systems is to produce smooth off-axis response in addition to smooth on-axis response, something the dipole does naturally.

Data regarding the quantitative aspects of time-amplitude tradeoff is spotty, and the effect is quite program dependent. As a starting point for discussions,

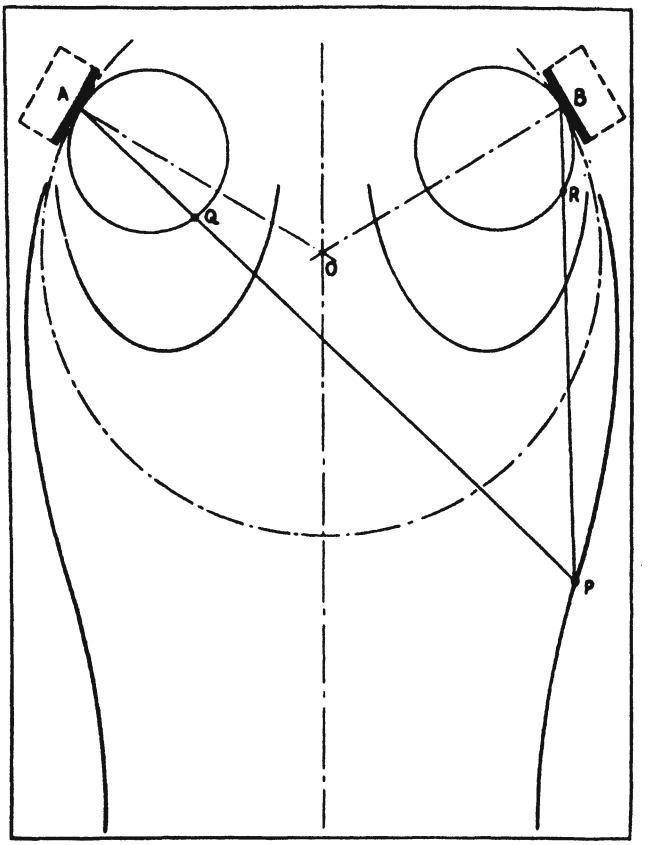

Figure 15-6. Bauer's dipole loudspeaker arrangement for extended stereo imaging. (Data courtesy JAES)

we present Franssen's data in Figure 15-7. Although this data was generated for description of recording systems, it does enable the loudspeaker designer to target a range of operation for off-axis maintenance of a center image. The off-axis position is determined in milliseconds, and that value is entered into the graph. Then, the required amplitude imbalance that will produce a center event is noted. See Rodenas et al. (2003) for recent work in this field.

Davis (1987) described a rather complex cone-dome system that produced a consistent off-axis response that steered the center image appropriately. The principal lobes were aimed side-to-side, as shown in Figure 15-8, and normal center listening took place along some off-axis angle. A listener to the right or left of that position moved into a range that was closer to the principal axis, and the increase in level provided a trade-off with the time cues.

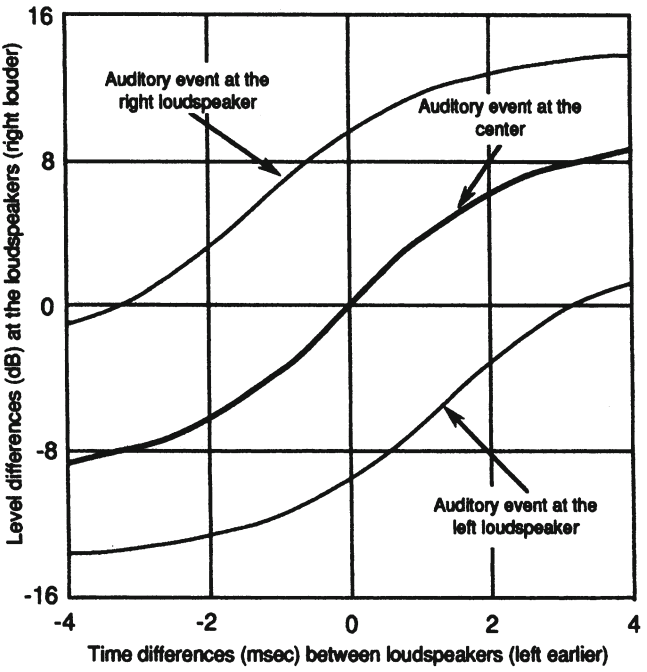

Figure 15-7. Franssen's data on center stereo event localization.

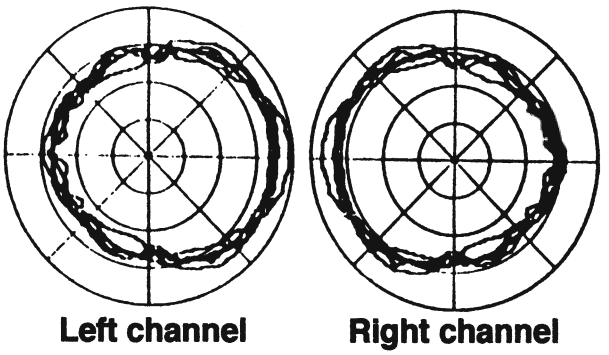

Figure 15-8 Details of Davis' extended imaging loudspeaker design. (Data after Davis)

Because asymmetrical horn radiation patterns are relatively easy to produce, they have also been used to produce systems for extended imaging. Eargle and Timbers (1986) describe a system using an asymmetrical HF horn to provide the necessary skewed response. Figure 15-9 shows the polar response of the system on several octave centers.

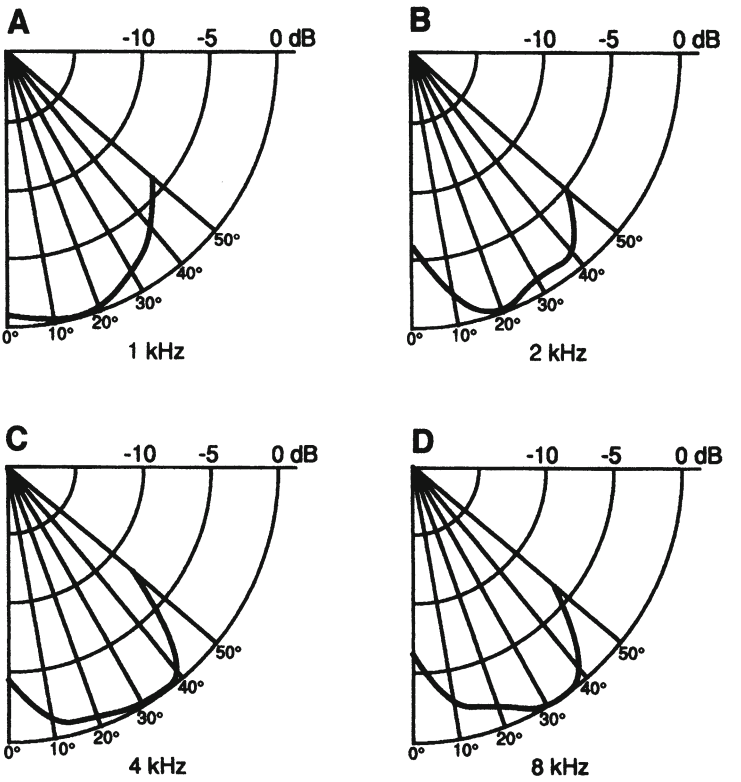

Figure 15-9. Use of asymmetrical horn patterns in extended stereo imaging. Polar graphs shown here are for the left channel; polars for the right channel are mirror images of those shown here. (Data courtesy JBL)

15.6 Stereo performance from a single unit

In the early days of stereo, considerable effort was expended in developing stereo loudspeaker systems that occupied no more floor space than a single monophonic loudspeaker. The aim here was to convince the neophyte stereophile that the transition from mono to stereo was perhaps not so difficult, afterall.

Figure 15-10 shows some of the early experiments of the 1950s in reproducing stereo from a single large enclosure (Levy, 1959). The system shown at *A* provides forward reflections from side panels which have been opened up to expose a stereo pair of loudspeakers. The approach shown at *B* uses the side walls of the listening room to reflect images from side-firing systems.

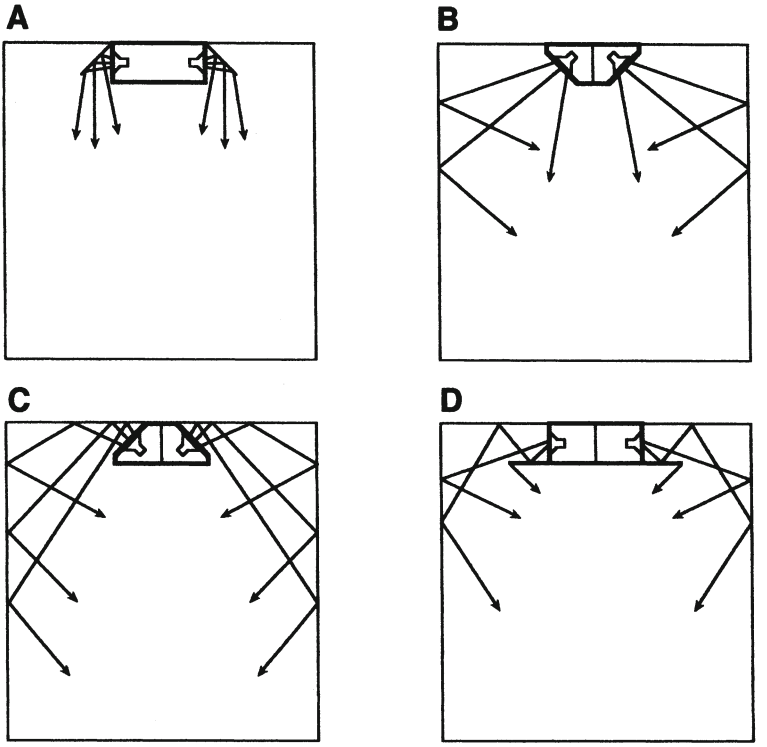

Figure 15-10. Attempts to achieve stereo performance from a single enclosure.

Extending the approach, the method shown at *C* uses double reflections from both back and side walls, and the approach shown at *D* uses a combination of the two.

The question is: do these systems work as shown? The general answer is *no*. The ray tracing shown here is applicable only to very high frequencies – perhaps only above about 4 of 5 kHz. These delayed reflections are apt to be swamped out by MF and LF signals that reach the listener via paths that wrap directly around the panels, reaching the listener ten or more milliseconds before the already attenuated late reflected signals. At best, these systems could convey to the listener a fairly vague impression of space, due not to the recording itself but rather to the effects of the playback environment. This is hardly the definition of stereo that we accept today.

Another approach is taken in the JBL Paragon system, introduced in 1958. Figure 15-11A shows a horizontal section view of this all-horn system three-way system; a photo of the system as seen from obliquely from one

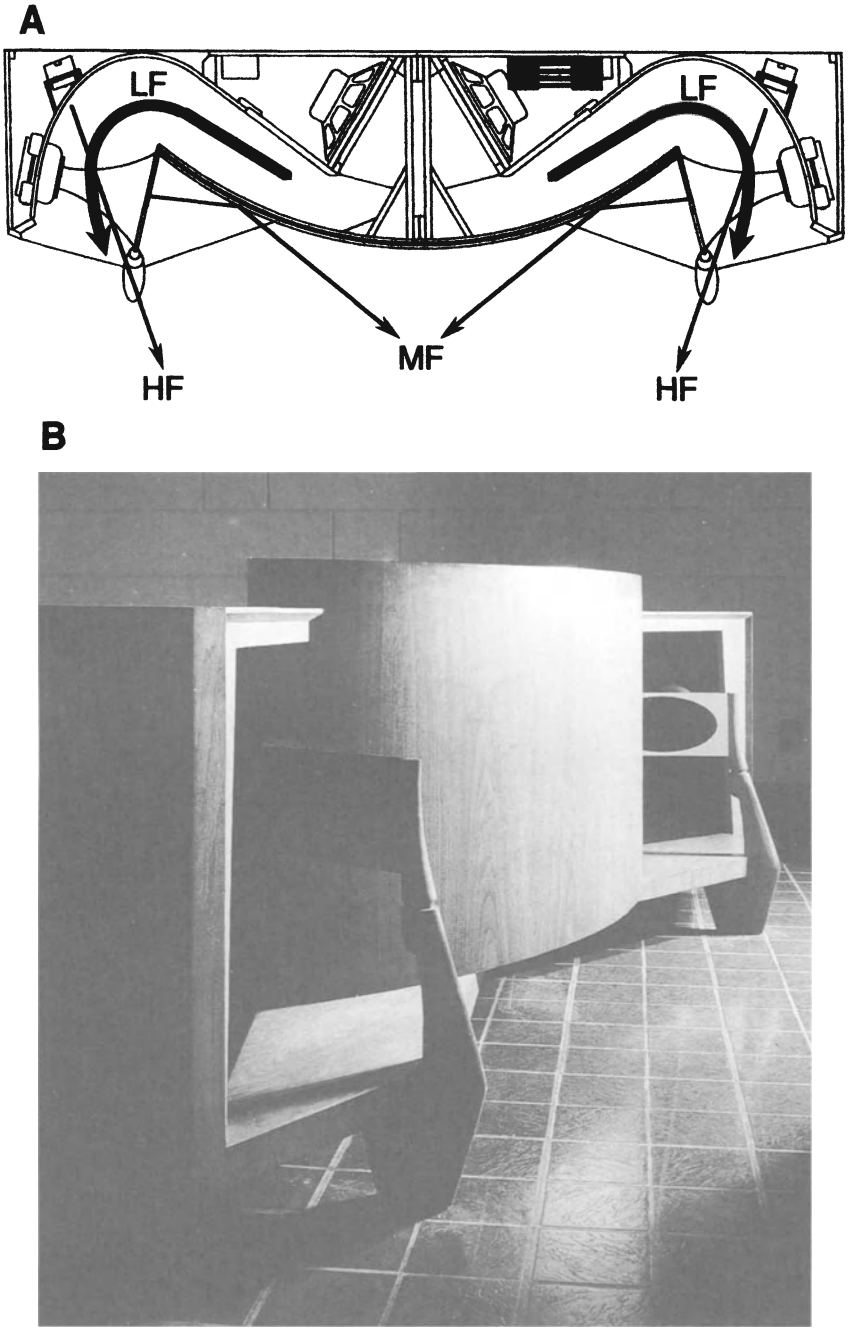

Figure 15-11. The JBL Paragon. Horizontal section view (A); oblique photo view. (Data courtesy JBL and Stereo Sound)

side is shown at *B*. Note that a large cylindrical section panel is used to reflect signals from the MF elements toward the listening area, with the beams crossing well in front of the nominal listening position. This may well be the first application of such cross-firing in commercial stereo history. The designer of the concept was Richard Ranger, who intended it as a center channel for behind-the-screen application in the early years of cinema multichannel sound.

The OWL system, shown in Figure 15-12A, is based on patents developed by Embracing Sound Experience (Embracing Sound™) and manufactured by EMES. The derivation of its name is obvious. The system consists of two independent two-way biamplified loudspeakers whose input signals are processed by means of the circuit shown at *B*. The L and R stereo inputs are converted by means of a matrix to equivalent sum (*S*) and difference (*D*) signals. While in the S/D domain the common mode information in the sum signal is reduced by an amount, α, calculated to compensate for the normal increase of in-phase signals at LF and MF due to mutual coupling. When this adjustment is carefully made, left and right channels will be radiated diagonally outward toward each side of the listening room. (You may think of this as an M/S microphone pair operating in reverse.)

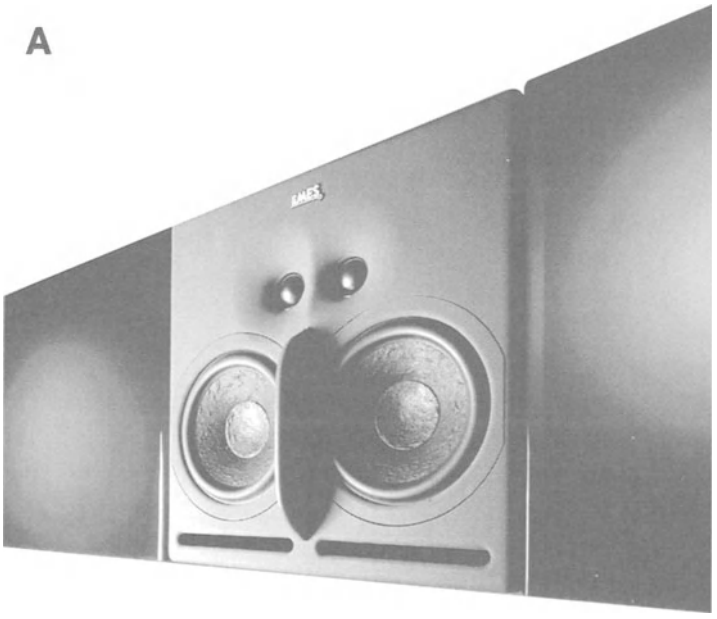

Figure 15-12. The EMES OWL loudspeaker system. Oblique view of system (A); circuit diagram for stereo processing (B). (Courtesy EMES Studio Monitor Systems)

B

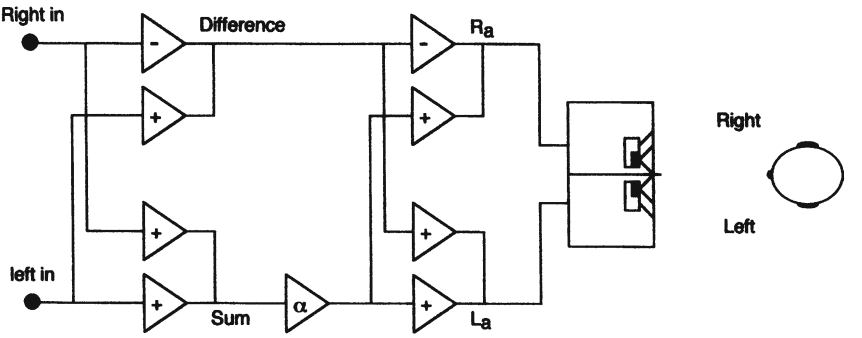

Figure 15-12. Continued.

In addition, a listener located on the primary axis of the system will localize left and right image sources slightly out-board of the loudspeakers, due to phasors created at the ears by the slight spacing between loudspeakers (Bauer 1956). As a result, the localization comes from two sets of complementary cues, resulting in a fairly large listening "sweet spot."

The OWL loudspeakers are primarily intended for use in postproduction spaces where the listening position of the remix engineer remains fairly consistent.

BIBLIOGRAPHY AND REFERENCES:

Allison, R., "The Influence of Room Boundaries on Loudspeaker Power Output," *J. Audio Engineering Society,* volume 22, number 5, June 1974.

Bauer, B., "Phasor Analysis of Some Stereophonic Phenomena." *J. Acoustical Society of America,* volume 33, number 11 (1956).

Bauer, B., "Broadening the Area of Stereophonic Perception," *J. Audio Engineering Society,* volume 8, number 2 (1960).

Blauert, J., *Spatial Hearing*, MIT Press (Cambridge 1997).

Collums, M., *High Performance Loudspeakers*, J. Wiley & Sons, New York (1991).

Davis, M.,"Loudspeaker Systems with Optimized Wide Listening Area Imaging," *J. Audio Engineering Society*, volume 35, number 11 (1987).

Eargle, J. and Timbers, G., "An Analysis of Some Off-Axis Stereo Localization Problems," Preprint number 2390; presented at the 81st Audio Engineering Society Convention, Los Angeles (1986).

Franssen, N., *Stereophony*, Philips Technical Bibliography (Eindhoven, Holland 1963).

Levy, S., et al., "A Compact, Single-Cabinet, Stereophonic Speaker System," *J. Audio Engineering Society*, volume 7, number 4 (1959).

Rodenas, J., *et al.*, "Derivation of an Optimal Directivity Pattern for Sweet Spot Widening in Stereo Sound Reproduction," *J. Acoustical Society of America*, volume 113, number 1 (January 2003).

Schroeder, M., "Progress in Architectural Acoustics and Artificial Reverberation: Concert Hall Acoustics and Number Theory," *J. Audio Engineering Society*, volume 32, number 4 (1984).

Toole, F.,"Loudspeaker Measurements and Their Relationship to Listener Preferences: Part 2," *J. Audio Engineering Society*, volume 34, number 5 (1986).

Chapter 16:
A SURVEY OF UNUSUAL TRANSDUCERS

16 Introduction

Standard dynamic transducers form the basis of mainstream loudspeaker system design. Indeed, there are few other principles of transduction that exhibit either the linearity or the acoustical output capability to form a basis for general loudspeaker design. Nonetheless, there is continuing interest in transducers based on other physical principles, or unusual variations of conventional technology. There are a number of reasons why a manufacturer might want to develop a new transducer, among them:

1. An exotic driver, purely for its own sake, may have possible marketplace appeal and other advantages.

2. Many exotic drivers are designed for 360° radiation in the horizontal plane, and this is considered an advantage by some systems designers.

3. In a few cases, an exotic driver has provided the basis for an entirely new extended range systems approach, thus enabling the manufacturer to make a major design-performance statement.

Some of the attendant problems are:

1. Difficulties in construction, which can lead to high manufacturing costs and production variations.

2. Some design components wear out in normal use and require periodic replacement of critical parts.

J. Eargle, *Loudspeaker Handbook*

3. Many designs are inherently low in sensitivity and output capability, limiting the appeal of the products to a dedicated but small clientele.

In many cases, the technical and patent history of these devices is not clear, and detailed technical descriptions may not be easy to come by. Accordingly, our coverage here will be broad and general.

16.1 Variations on a magnetic theme

All dynamic devices work on the principle of current flowing through an electrical conductor that is positioned perpendicular to a magnetic flux field. The resultant force produced on the conductor is mutually perpendicular to both the current flow and the magnetic flux. This relationship is fundamental to all dynamic transducers, and the useful acoustical output radiation from such device is normally along the same axis as the force that is produced by the driving mechanism.

16.1.1 The Heil air motion transformer (AMT)

The AMT, developed by Oskar Heil, represents a significant departure from the normal geometry of the dynamic driver. A perspective view of the original design is shown in Figure 16-1A. The vane-like elements in this view are projections from the magnetic structure and serve to route magnetic flux into the center region occupied by the pleated ribbon diaphragm. The open spaces between the vanes allow the egress of sound.

A top view of the pleated ribbon under a no-signal condition is shown at *B*. The magnetic flux path is from left to right, and current flows through a flat conductor bonded to the pleated diaphragm. By means of the top-to-bottom folds of the diaphragm, the current flows vertically in and out of the page, as represented here.

For positive current flow the diaphragm takes the position shown at *C*, which produces positive pressure to the left. For negative current flow the

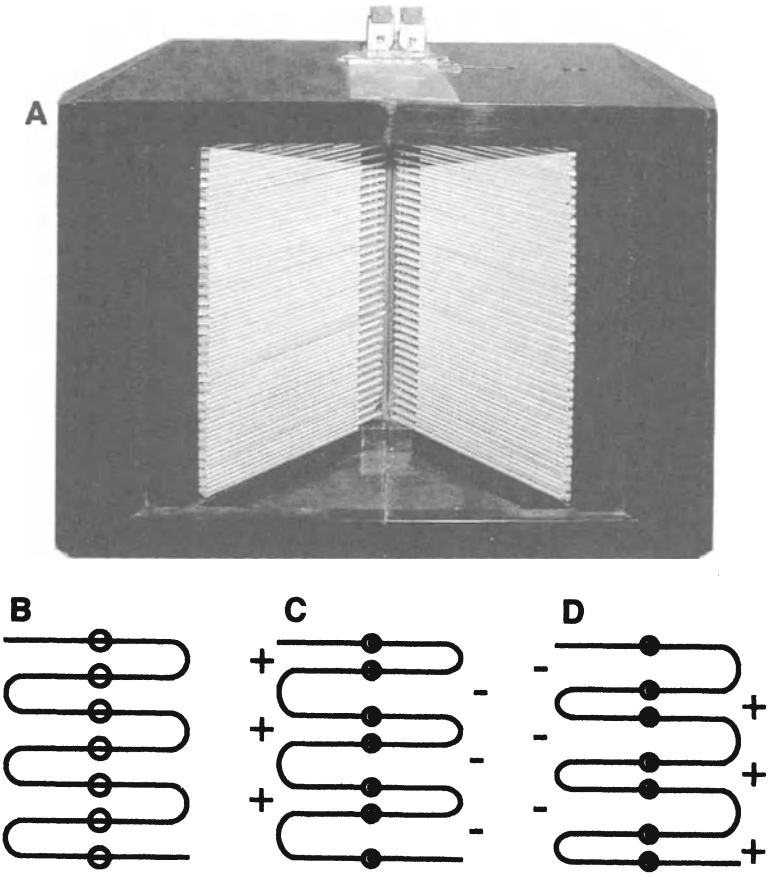

Figure 16-1. Photo of early Heil AMT (A); top views of diaphragm: at rest (B); positive to left (C); positive to right (D).

diaphragm folds take the position shown at *D*, with positive pressure to the right.

The notion of air motion transformation is an accurate one in that the air particle velocity outward from the folds is several times the velocity of the folds themselves.

The driver is normally used in the frequency range above 1 kHz. The efficiency of the driver is moderate, and the output can be raised to significant levels by placing a horn on one side of the diaphragm. A wide-range system based on AMT topology was developed in the 1970s by the ESS Corporation.

In more recent times the German company ADAM Audio GmbH has become the standard bearer for the technology. The devices have been radically redesigned using modern magnet materials and are both more sensitive and smoother in overall response. Figure 16-2A shows a front view of a HF transducer, and the pleated diaphragm is clearly visible through the grids, which are part of the magnetic structure. A larger MF transducer of similar design is also available. A perspective view of the inner structure, including pleats, printed circuit voice coil, and magnetic structure, is shown at *B*. A family of on- and off-axis response curves is shown at *C*.

The company builds loudspeaker systems intended primarily for recording and postproduction activities.

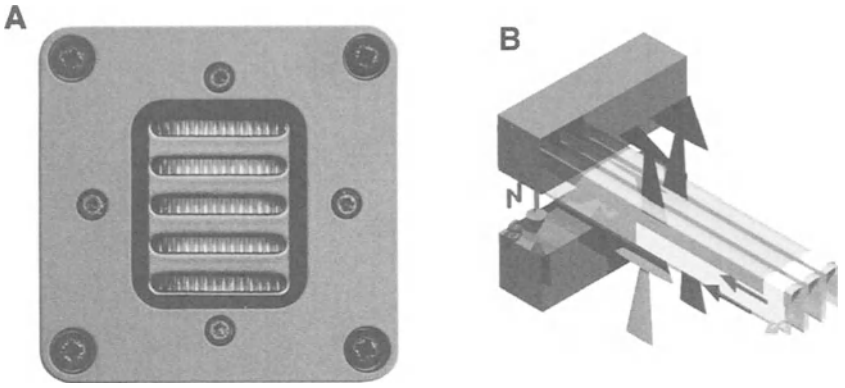

Figure 16-2. The ADAM Audio Advanced Ribbon Technology HF transducer (A); structural details of transducer (B); on- and off-axis response of transducer (C). (Data courtesy ADAM Audio GmbH)

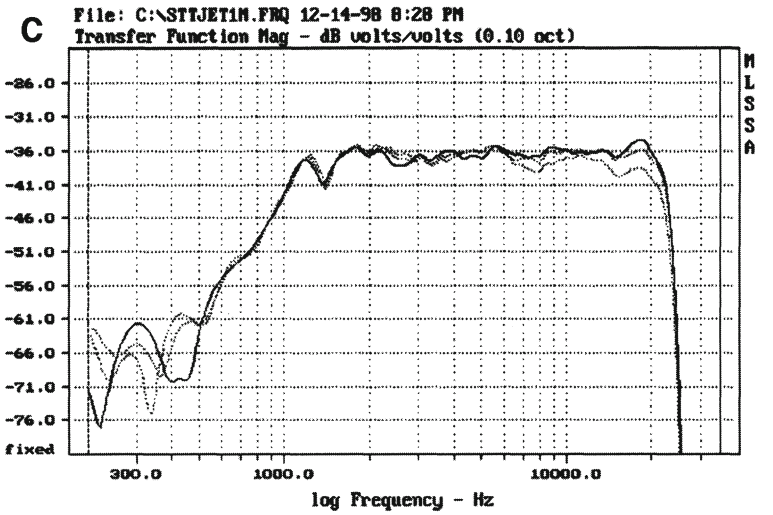

Figure 16-2. Continued.

16.1.2 Traveling (bending) wave radiators

In most dynamic transducers, pistonic action is considered ideal. Traveling waves in the diaphragm are generally regarded as detrimental, since the result is usually response irregularities. However, advantage may be taken of traveling waves if they can effectively be damped at the fixed outer termination of the diaphragm.

Figure 16-3 shows a section view of a transducer developed by Lincoln Walsh and commercialized by the Ohm company during the 1970s. The voice coil is attached to the apex of a deep cone which has been positioned vertically and is unimpeded on all sides.

MF and LF radiation from the cone will produce essentially omnidirectional radiation, operating in traditional fashion. At progressively higher frequencies, traveling wave motion in the cone will result in a gradual shift in radiation outward from the cone, and ultimately, at the highest frequencies, the radiation will be solely from a relatively small portion of the cone adjacent to the voice coil horizontally over 360 degrees. The device thus operates as a full-range radiator, as the voice coil effectively becomes decoupled from the mass of the cone.

There is nothing trivial about the design of the moving system, and it normally consists of several distinct sections, each optimized for a specific portion of the frequency spectrum. When well executed the Walsh driver can produce excellent response with moderate efficiency.

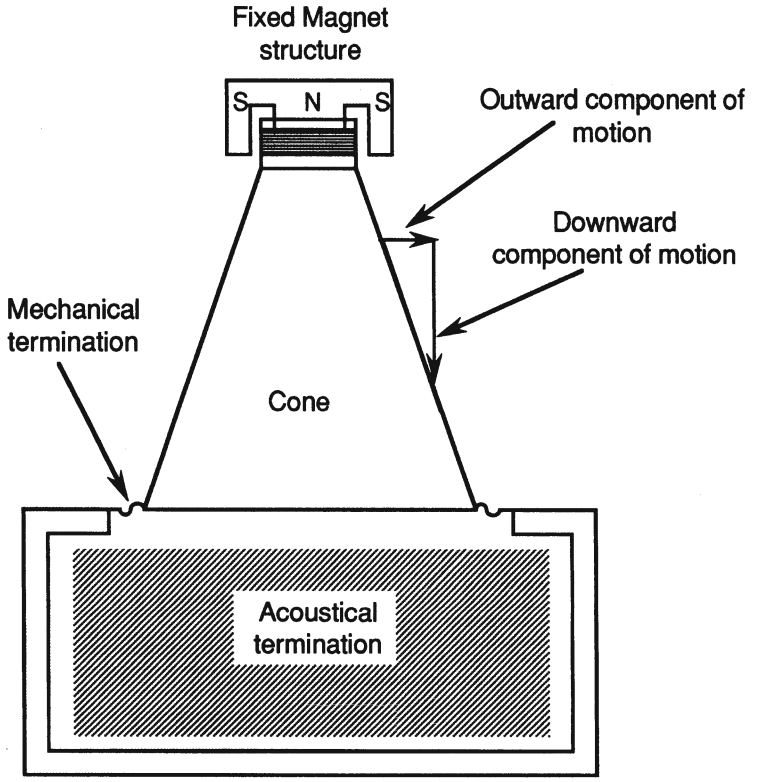

Figure 16-3. The Walsh radiator shown in section view.

Another traveling wave design is shown in Figure 16-4. The driver, made by Manger Products in Germany, is shown in section view at *A*. The driver is very shallow, and HF radiation is primarily from the center. MF and LF radiation take place from transverse bending wave motion, and the lowest frequencies are smoothly terminated by the serrated damping layer located around the edge of the driver. A photo of the driver is shown at *B*; the device is 210 mm (8.25") in diameter and 24 mm (0.95") thick.

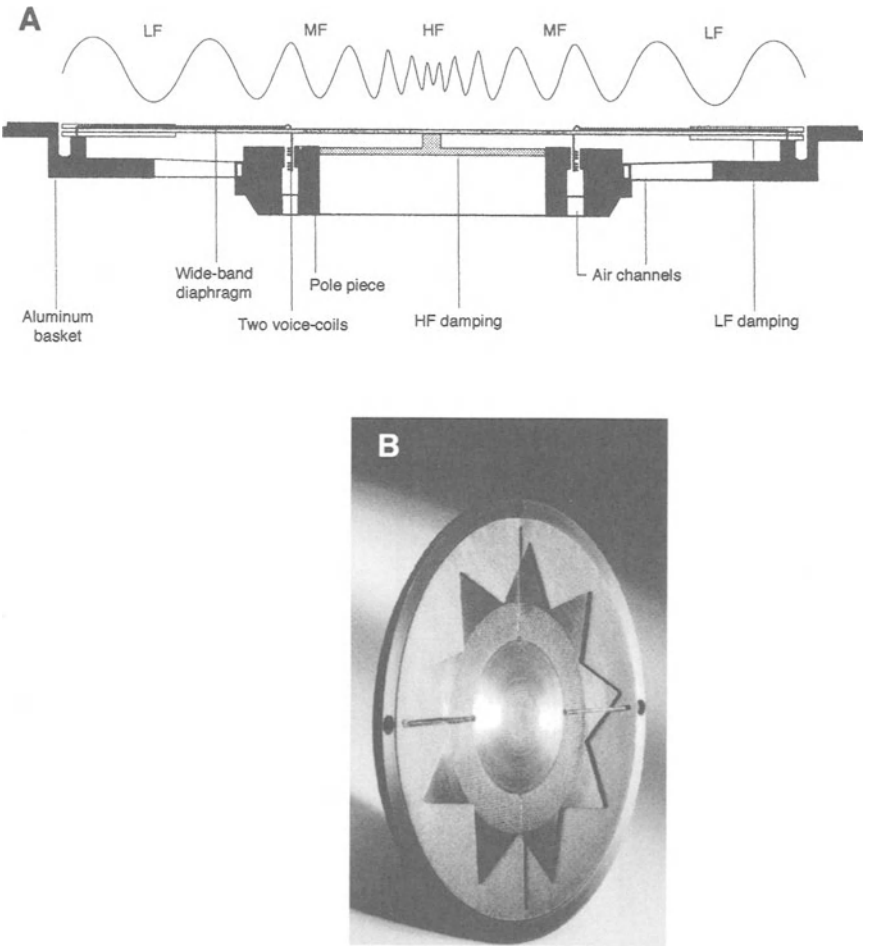

Figure 16-4. The Manger transducer. Section view (A); photo (B); impulse response (C); amplitude response (D); phase response (E). (Data courtesy Joseph W. Manger, Manger Products, Germany, www.manger-msw.com)

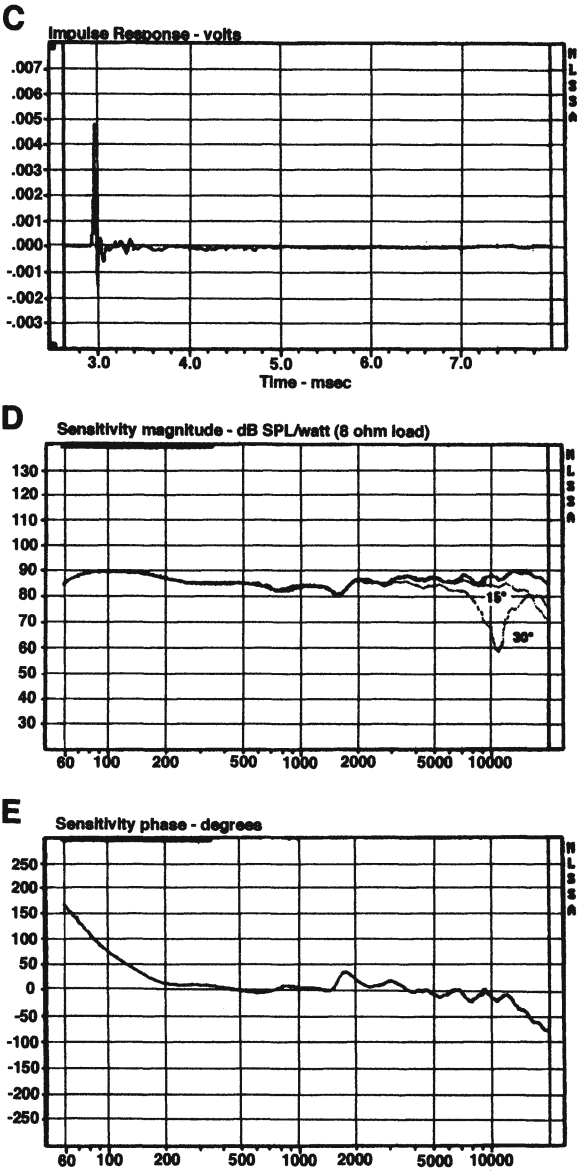

Figure 16-4. Continued.

Response graphs are shown at *C*, *D*, and *E*, and it is clear that the performance of the Manger driver closely approaches that of the ideal full-range driver. The fact that this response is produced virtually at a point source indicates that a very high order of performance will be evident over a wide listening area. The frequency range is nominally from 80 Hz to 33 kHz, and a subwoofer complements the system in normal application.

Another approach to traveling waves is shown in front view in Figure 16-5A. This design consists of a voice coil attached to a large area of plastic under tension which has a damped termination at its edges. Motion of the voice coil is translated into outwardly radiating rings, or ripples, as shown at *B*. HF signals are attenuated fairly quickly due to the mass of the diaphragm and are thus radiated from a small area around the voice coil. Successively longer wavelengths are radiated from larger portions of the diaphragm, and the dipole pattern of the system is consistent over a wide frequency range. The system is of moderate efficiency, and the chief problem in manufacture is maintaining consistent and uniform tension in the diaphragm.

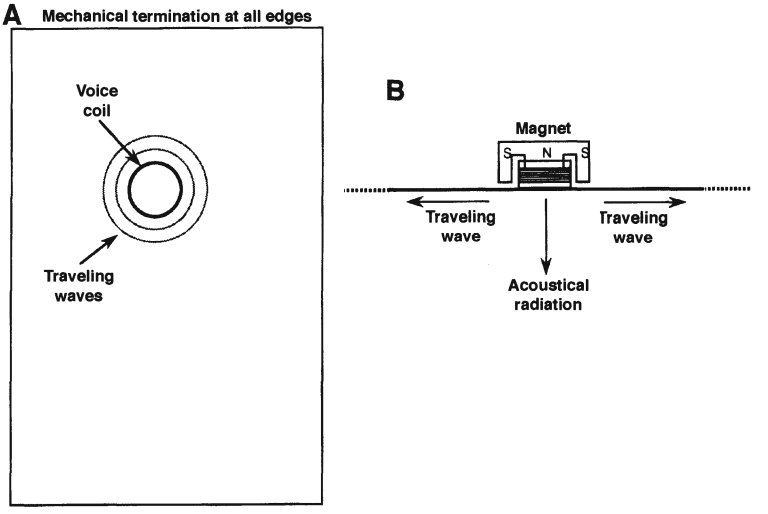

Figure 16-5. Traveling wave radiator. Front view (A); horizontal section view (B).

16.1.3 Systems using compound radiating surfaces

The three transducers discussed here exhibit complex motion with more than one degree of freedom and as such exhibit radiation patterns that may be unlike the ideal single degree of freedom radiators that acoustical engineers hold in esteem. While these devices may fall short of "ideal" pulsating spherical or cylindrical response, they may exhibit more uniform pattern control than typical cones and domes over fairly large portions of the frequency range.

The Linaeum driver is shown in front view in Figure 16-6A. The half-cylinder sections are fixed at their outside edges and driven along the other (middle) edges. The nature of the compound motion of the cylinder is shown at *B*. It is important in this design, as in all others with fixed terminations, that reflections from the termination back toward the driving point be properly damped.

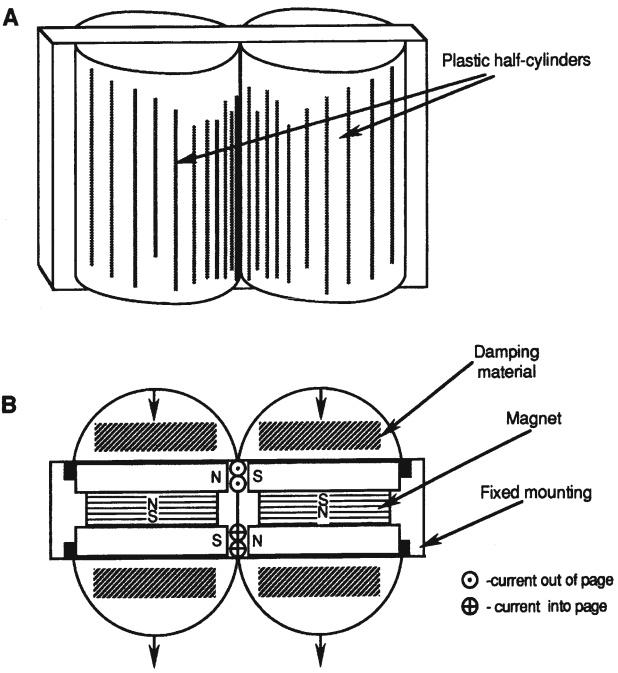

Figure 16-6. The Linaeum driver. Perspective view (A); horizontal section view (B).

Allison (1995) describes a HF dome radiator with an inverted outer section that exhibits radial components of movement, and as such does not exhibit the typical narrowing of HF pattern control of a single degree of freedom dome. A section view of the driver is shown in Figure 16-7A, and the normalized off-axis HF response is shown at *B*. The hoop stresses associated with warped surface motions (see Chapter 4) are minimized, inasmuch as the displacement of the diaphragm at high frequencies is extremely small. For comparison purposes the normalized off-axis response of a conventional 25 mm (1 inch) HF driver is shown at *C*.

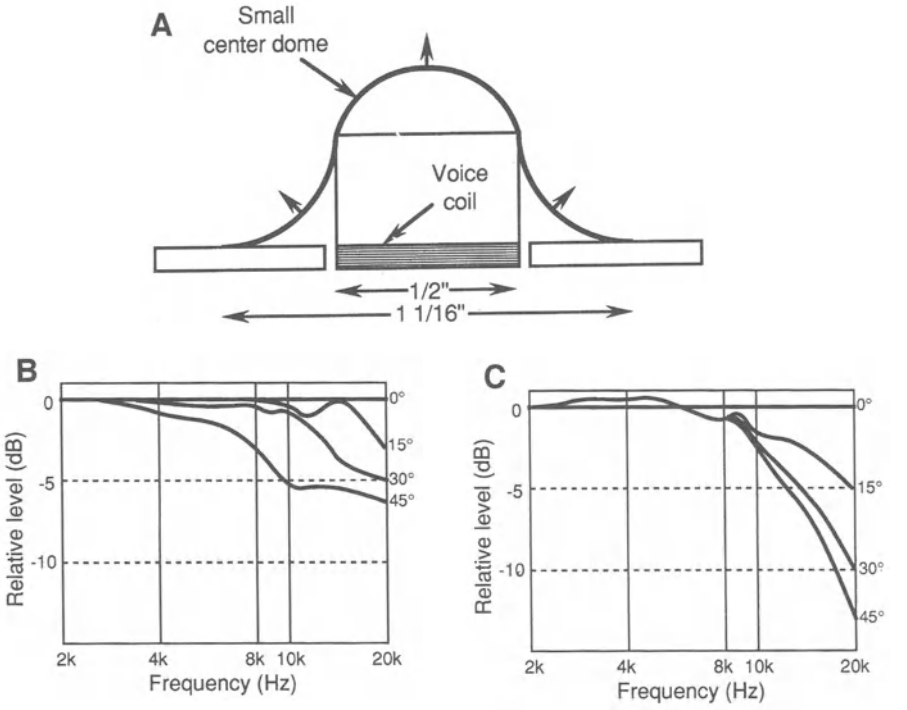

Figure 16-7. Section view of the Allison HF driver (A); normalized off-axis response curves (B); normalized off-axis response curves for a typical 25 mm dome (C). (Data after Allison)

The complex radiator shown in Figure 16-8 is made by the MBL company of Germany. Shaped like a seamed football set on end, it is fixed at one end and driven at the other along its vertical axis. The seams are flexible and allow the structure to pulsate in and out when excited by the voice coil. Drivers of this type are limited in their frequency range, and a three-way system with graduated components stacked vertically has been commercialized. Obviously, the radiation pattern is uniform in the horizontal plane.

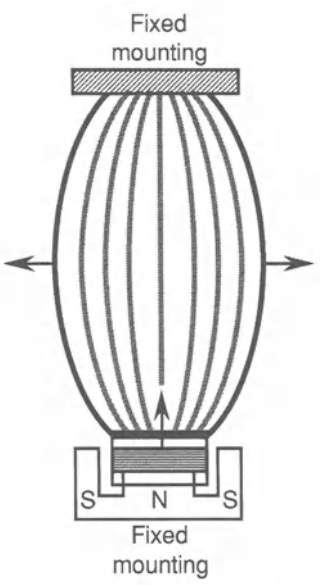

Figure 16-8. Section view of the MBL 360° compound radiator.

16.2 Piezo-electric and related devices

Certain crystal materials will bend, twist, or warp slightly if electrical signals are applied to opposite surfaces on them. In general, displacement is proportional to the applied voltage. The principle has been used for decades in low-cost microphones, mechanical sensors, and HF loudspeakers. Details of a piezo-electric HF driver are shown in section view in Figure 16-9. Here, a small bending element is attached to a stiff diaphragm that resonates in the HF range. The driving force is the result of the effective mass of the bending

element times the acceleration imparted by the driving signal. The range of flat power output may extend approximately one octave above the diaphragm resonance frequency, although the on-axis output can be extended to a somewhat higher frequency. These devices are not very smooth in their response, due to multiple HF modes as shown. This is a matter of secondary concern however in many applications. When used in multiples, and with horn loading, the output capability is fairly high.

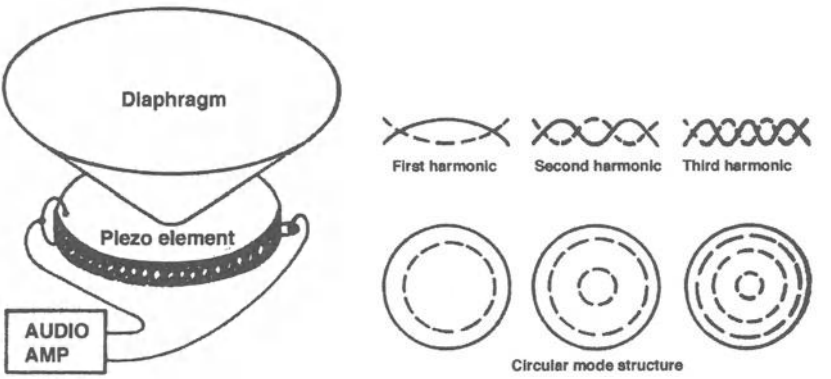

Figure 16-9. Views of a piezo-electric driver and associated higher modes of vibration. (Data courtesy CTS Wireless Components)

The HPM (High Polymer Material) HF unit is shown in Figure 16-10. As developed by Pioneer (Tamura, et al., 1975), this high frequency transducer consists of a sheet of polyvinylidene fluoride curved into a cylinder. The signal is applied to the two sides of the material, and the plastic effectively stretches and contracts under the electrical excitation, producing 360° radiation. The device is very uniform in response from 2 kHz to 20 kHz.

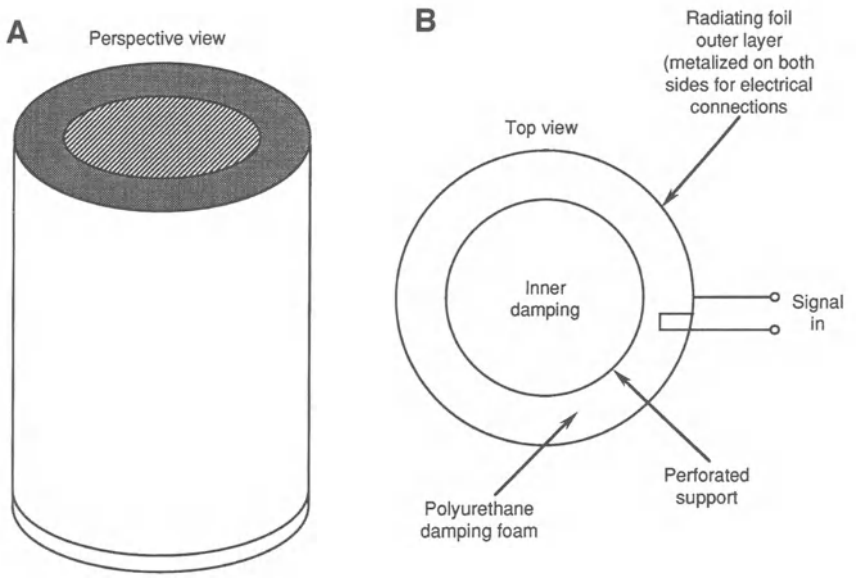

Figure 16-10. Views of the Pioneer HPM driver.

16.3 Ionized air devices

A view of the Klein (1952) Ionovac is shown, along with pertinent electronics, in Figure 16-11A. In this complex device, a high frequency-high voltage signal is fed to inner and outer electrodes separated by a quartz cell. The ionized air in the cell glows with a blue light as a result of what is called *corona discharge*, and this feature alone is sufficient to entice anyone attracted to the exotic. If the HF signal is amplitude modulated, then the volume of ionized air will vary accordingly, creating instantaneous pressure variations. The acoustical output is relatively low, and a horn is normally used to increase the acoustical signal. The curves shown at *B* were made some years ago on the Ionovac HF system manufactured by the DuKane Corporation. While fairly uniform above 3 kHz, the maximum output capability was limited at high frequencies, exhibiting noticeable signal compression.

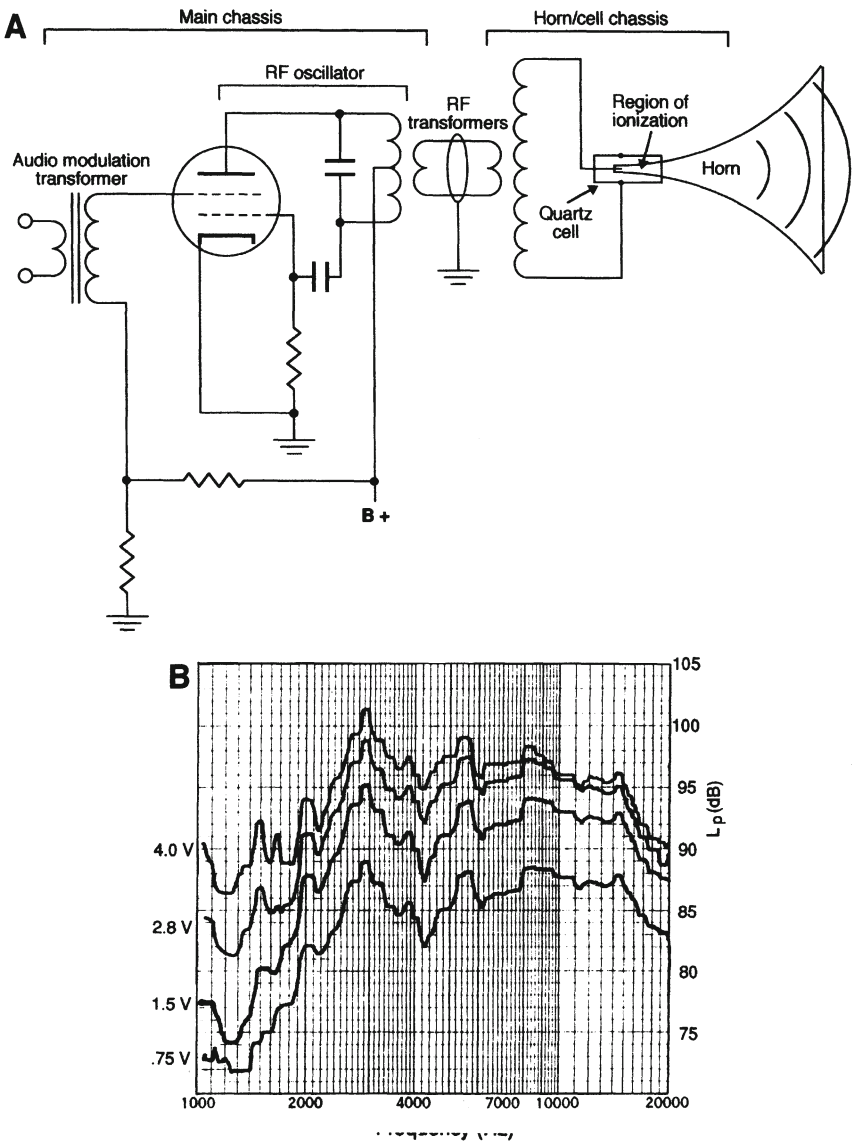

Figure 16-11. Design details of the DuKane Ionovac HF system (A); response curves of the system measured at 1.2 meters; scale at left indicates the signal input to the system's modulation transformer (B).

Over time, the quartz cell and inner electrode will erode and must be replaced; and in general the complexity of the system far outweighs its advantages. However, during the decades of the fifties and sixties, the Ionovac represented the leading edge in HF performance.

The so-called *corona wind* loudspeaker (Shirley 1957) operates with high voltage dc bias across which is impressed a high voltage audio signal. When the positive electrode is sharply pointed, and the negative electrode is blunt, as shown at Figure 16-12A, there will be a small but steady flow of air from positive to negative, hence the term corona wind. The air flow can be modulated by an audio signal, as shown.

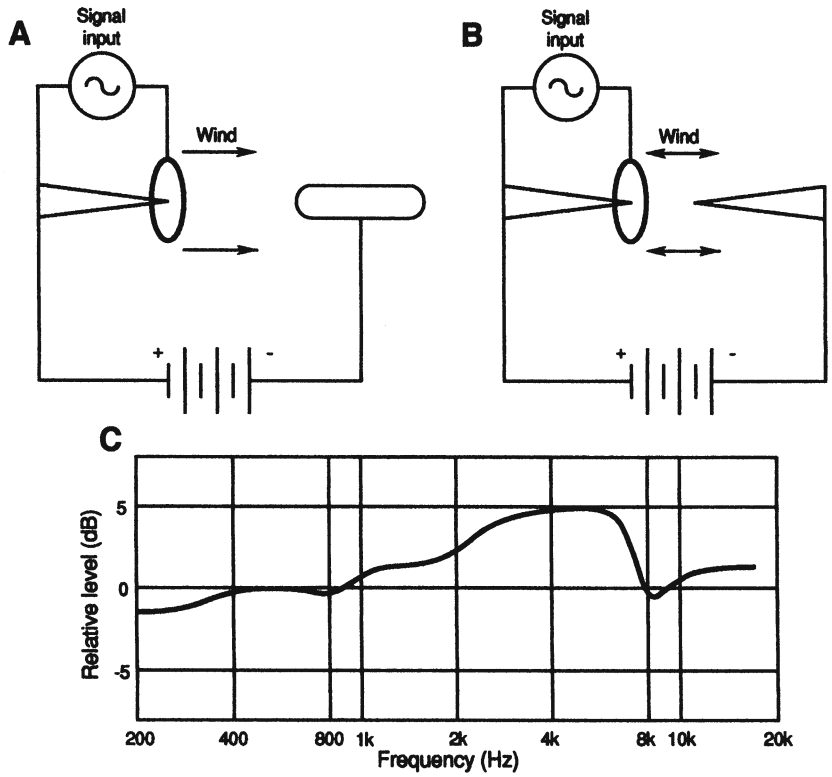

Figure 16-12. The corona wind loudspeaker. Embodiments of the concept (*A* and *B*); typical response (C)

If both electrodes are sharply pointed, as shown at *B*, there will be no wind under no-signal conditions. The corona action requires a dc polarizing voltage of 10 to 20 kV, while the audio signal usually varies over a range from 1 to 2 kV.

A typical system will be made up of many individual cells located on a plane. Typical response of a prototype system is shown at *C*. The dip in response at 8 kHz occurs when the spacing between the pointed electrodes is equal to $\lambda/2$. The dc operation of the form shown at *A* is used in the manufacture of room air filtration devices, due to its effectiveness in removing fine particles of dust through electrostatic attraction.

A word of caution: the various ionized air systems generate ozone and as such may constitute an environmental hazard.

16.4 The air modulator

The air modulator is a very practical device, but not for general high fidelity use. Essentially, it is a means of using a relatively low power dynamically driven valve to control the flow of a relatively high power source of compressed air (Hilliard 1965). One of the first embodiments of this principle was the Auxetophone, as developed by Parson during the early acoustical phonograph era (Read, 1952). The device used mechanical power from acoustical recordings to drive an air valve, which in turn was fed compressed air for greater acoustical output. Stability was a problem with this early pneumatic system; particles of dust could get into the delicate valve, resulting in hisses and other noises.

One form of the modern day version the air modulator is shown in Figure 16-13. A movable sleeve with multiple openings fits smoothly inside an outer fixed casing. In the rest position, there is a portion of overlap between the two sets of openings, and a steady stream of air is emitted through the system. When the inner sleeve is moved back and forth by a dynamic assembly, or other linear actuator, there will be an instantaneous change in the volume velocity of air through the valve, and hence a corresponding change in pressure

at the output. A major design challenge in such systems is to shape the various internal passages to minimize turbulence and air noise, while optimizing the system's linearity over the desired output range.

The air modulator is routinely used today for high pressure acoustical output of noise signals for environmental testing, where tens of thousands of acoustical watts are necessary to simulate the low frequency sound intensities developed by modern aircraft and space rocketry. In these applications the air overload can be excessive, as pressures are developed in the range of 150 to 160 dB and beyond. In such applications, signal linearity is not a primary concern; rather, a particular noise power spectrum at some target acoustic level and distance may be the primary concern.

There are distinct opportunities for the air modulator in producing very high pressure, very low frequency acoustical signals in special venues such as theaters, stadiums, and theme parks. In these cases the cost of maintaining a continuous source of compressed air is negligible, and a value analysis of the system, as compared with standard technology, might favor its use. Much work remains to be done in this area.

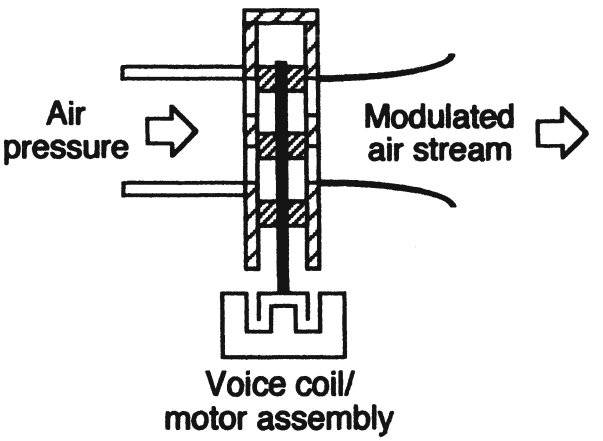

Figure 16-13. Section view of an air modulator

16.5 Rotary actuators

The rotary actuator is extensively used in mechanical indexing and control systems, and its application to acoustical systems follows as a natural consequence of this. The basic approach is shown in Figure 16-14, in which the rotary actuator converts normal alternating signals into corresponding rotary ones. The back-and-forth rotary action is mechanically converted into linear action required to move cone radiating surfaces. Depending on the mechanical transformation ratio between angular and linear motion, quite large excursions can be achieved, limited only by the mechanical suspensions used in restraining the radiating cones. The bandwidth limitations of the method normally restrict its application to LF operation. The earliest reference to rotary actuated loudspeakers is given by McLachlan (1934). In recent years, systems using this principle have been refined by Thomas Danley of Quantum Sound, Inc.

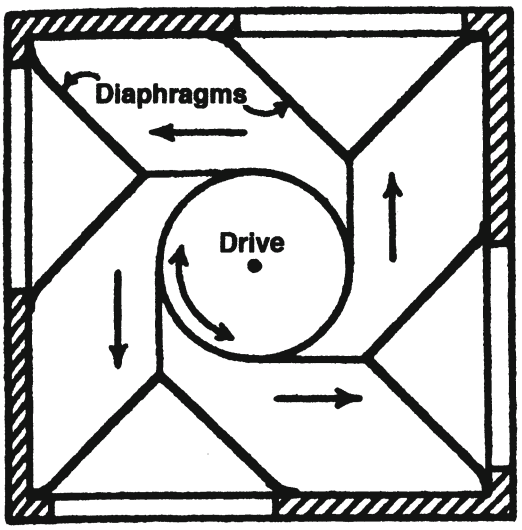

Figure 16-14. Section view of an array of cones driven by a rotary actuator. (Data after McLachlan, 1934)

16.6 Digital loudspeakers

In concept, a digital loudspeaker converts a parallel digital signal directly into pressure output pulses, each bit physically scaled according to its position from least to most significant bit. For a 16-bit system, the required scaling range is 65,536-to-1. Covering this range with concentric, or otherwise acoustically aligned radiating elements hardly seems possible or practical. However, a lesser-bit approach might work well enough to enable a hybrid system to be designed.

The method shown in Figure 16-15 shows an array of four electrostatic elements with areas scaled by powers of 2, each driven by a parallel digital signal. The least significant bit drives the center element, while the outermost element is driven by the most significant bit. The composite element can be used as a headset driver, with the acoustical output summation taking place directly at the listener's ear. This device works for some types of headphone communication, where the low dynamic range associated with it may be tolerated.

An additional approach is shown in Figure 16-16. The similarities with the previous example are evident, and the same problems of scaling and summing of the individual acoustical output "bits" remain. In this model, the

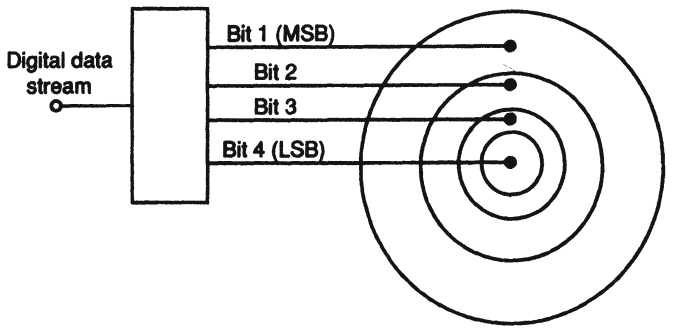

Figure 16-15. View of a 4-bit digital transducer.

direct digital-to-analog conversion is used only for the 8 most significant bits; the lower value bits are converted in the normal manner and fed to the 9th coil. This hybrid system thus is "acoustically digital" only for the upper 48 dB of its level range.

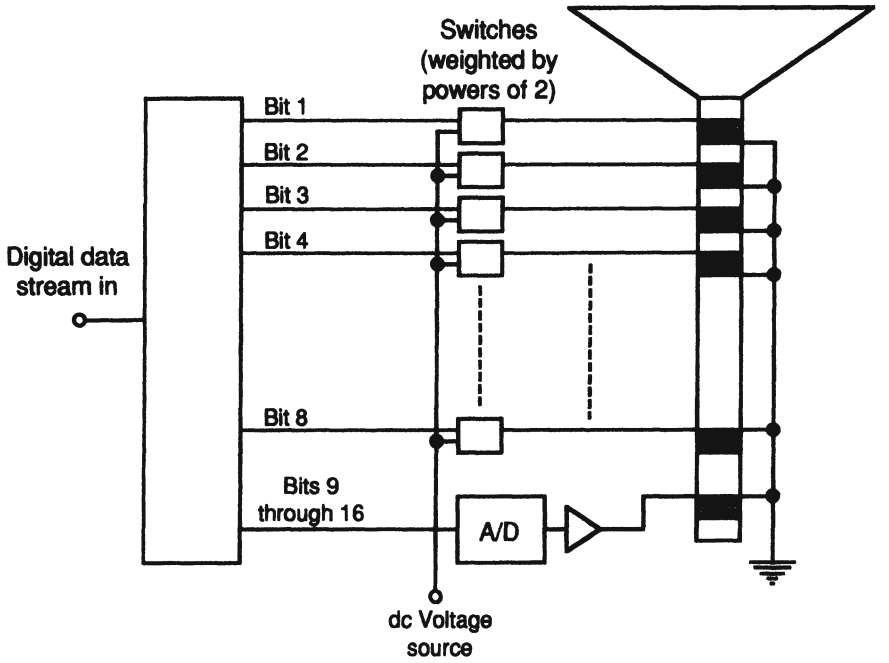

Figure 16-16. View of a hybrid digital loudspeaker.

16.7 Distributed mode loudspeakers (DML)

For more than 20 years, manufacturers have attached dynamic driving elements to a variety of Styrofoam panels in an effort to produce low cost loudspeaker elements that could easily fit into ceiling tile spaces. For the most part these systems were haphazardly engineered, and the resulting devices had pronounced resonances and highly variable radiation patterns. You might think of these devices as distant relatives of the whizzer cone.

The DML is a "high-tech" version of this in which good engineering has solved most of the fundamental problems. The DML is normally composed of a light composite material that is loosely suspended and driven with a dynamic actuator, as shown in Figure 16-17A. The system is suspended slightly inward of the edges of the panel, and, in most designs, motion is imparted by a driving transducer placed off-center and working against its own mass reactance.

The representation at *B* shows magnified views of the random motion of a typical DML panel. As a result of such motion, the directional characteristics of the panel tend to be fairly broad over a large frequency range. The diffuse response from the panels results in a relatively long impulse response (upwards of 25 msec); this in turn results in a frequency response characterized by a multiplicity of fine peaks and dips in response – but with no discernable coloration due to ringing at any one frequency.

The materials used for panels are stiff, light, have low internal mechanical loss, and operate over a frequency range dominated by higher order 2-dimensional bending modes in the panels themselves. The thickness of the panel is a crucial element in positioning these parameters relative to the desired operating spectrum. The system can operate uniformly over a fairly wide bandwidth with very wide dispersion and flat electrical impedance. Harris and Hawksford (1997) discuss the technology in detail and establish the approximate upper and lower bounds of uniform power response by the following equations:

$$\text{Upper frequency limit, } f_{max} = R_p/2\pi M_c \qquad 16.1$$

$$\text{Lower frequency limit, } f_{min} = R_p/2\pi M_m \qquad 16.2$$

where R_p is the radiation resistance of the panel and M_c and M_m are, respectively, the driven mass and the mass of the magnet structure. Thus, the system bandwidth can be scaled as desired through the control of only the two mass variables.

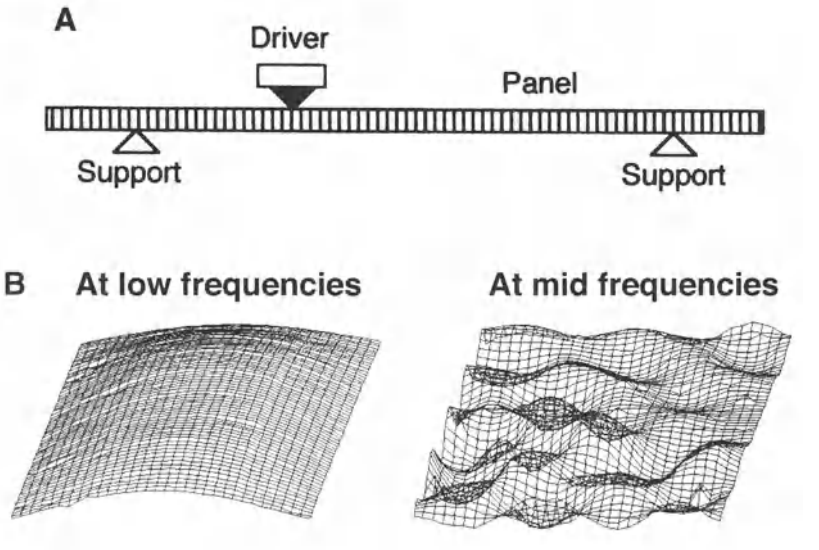

Figure 16-17. The DML loudspeaker. Driver and suspension of the system (A); magnified views of actual panel motion under typical drive conditions (B). (Data at *B* courtesy NXT Technology)

DML panels have many commercial applications where front-back depth limitations exist. When fairly large panels are used, they take advantage of the relatively low falloff of level with distance from the source, as discussed in Chapter 6. Their generally smooth response is an advantage in all aspects of speech reinforcement, including system feedback immunity. Other obvious applications are in conjunction with video technology, where their flat panel design complements the video elements.

The NXT company has been in the vanguard of DML development. Those interested in the technology are referred to the excellent chapter on DML systems by G. Bank in Borwick (2001.)

16.8 Overview of ultrasonic systems

Sometimes referred to as parametric loudspeaker systems, this technology is based on the signal demodulation capabilities of air when ultrasonic signals at levels approaching 130 dB L_p and higher undergo thermodynamic overload. One form of this technology is shown in Figure 16-18A, where a UHF carrier frequency of approximately 60 kHz is amplitude modulated by an audio signal.

If the radiating surface is, say, 350 mm (14 in) in diameter, and the radiated signal is at 60 kHz, the directivity of the signal will have a –6-dB beamwidth of about 3 degrees (Pompei, 1999). If this signal is audio modulated and radiated, the nonlinearity of the air will in effect demodulate the carrier signal, and the audio signal will be reproduced with the directional characteristics associated with the 60 kHz carrier frequency. Thus, a listener who intercepts this narrow beam of ultrasound will hear the audio signal in a very narrow beam, as shown at *B*. The radiating elements are normally small piezo-electric sections sized so that their efficiencies are fairly high at the system's carrier frequency.

The inherent problems with the technology are:

1. High carrier levels require considerable electrical power to the piezo-electric elements.

2. The useful level of the demodulated signal at the listener is fairly low, normally in the 60 to 70 dB L_p range.

3. The spectrum of the demodulated audio signal rolls off at LF by 12 dB per octave.

4. High carrier levels may be harmful to the hearing of any persons located close to the radiating surfaces.

The primary commercial advantage of the technology are:

1. Sound can be selectively aimed at the listener via overhead arrays at a given vantage point, unheard by someone standing fairly close by. This is a boon for museums and other exhibition venues, which currently must rely on local infrared transmission via headphones to patrons for narrative program material.

2. Workers in open-plan office spaces can be individually paged – if they are seated at their desks.

3. Commercial announcements in public spaces can be aimed specifically at those patrons located immediately in front of the display cases.

Presently, there are many workers in the field addressing the remaining problems with the technology, offering alternative modulation methods and means of increasing the effective level of the signal at the listener. Current development efforts in the art are led by American Technology Corporation, who have produced a detailed technical monograph covering developments over the years (Croft & Norris, 2001-2002).

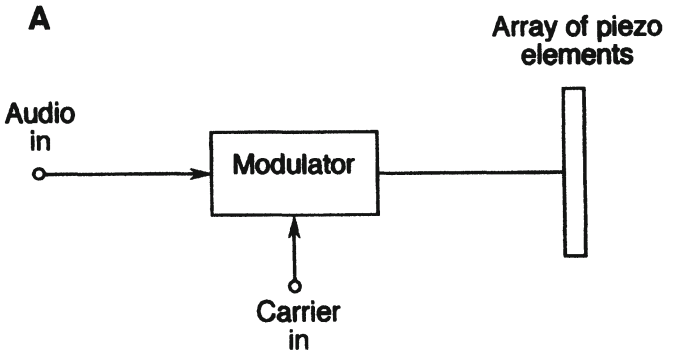

Figure 16-18. Details of ultrasonic systems. A simple modulation system (A); a typical application (B).

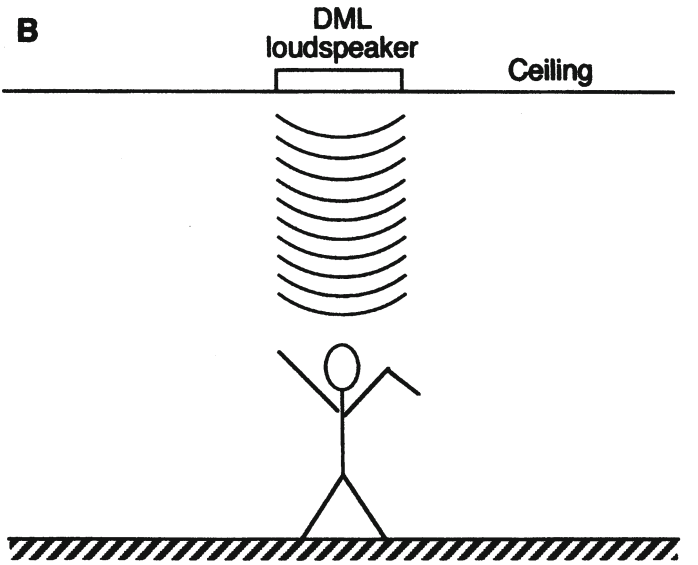

Figure 16-18. Continued.

BIBLIOGRAPHY AND REFERENCES:

Allison, R., "Imaging and Loudspeaker Directivity: To Beam or Not to Beam," Preprint number 4095; presented at the 99th AES Convention, New York, October 6-9, 1995.

Augspurger, G., "Theory, Ingenuity, and Wishful Wizardry in Loudspeaker Design — A Half-Century of Progress?" *J. Acoustical Society of America*, volume 77, number 4 (1985).

Borwick, J., editor, *Loudspeaker and Headphone Handbook*, third edition, Focal Press (Boston 2001).

Bost, J., "A New Type of Tweeter Horn Employing a Piezoelectric Driver." *J. Audio Engineering Society*, volume 23, number 10 (1975).

Collums, M., *High Performance Loudspeakers*, J. Wiley & Sons, New York (1991).

Croft, J., and Norris, J., "Theory, History, and the Advancement of Parametric Loudspeakers," Company monograph 98-10006-1100 Rev. D (www.atcsd.com).

Harris, N., and Hawksford, O., "The Distributed Mode Loudspeaker as a Broad-Band Acoustic Radiator," presented at the AES 103rd Convention, New York, September 1997, preprint 4526.

Hilliard, J., "High-Power, Low-Frequency Loudspeakers," *J. Audio Engineering Society*, volume 13, number 3 (1965).

Klein, S., *L'onde Electrique*, volume 32, page 314 (1952).

McLachlan, N., *Loudspeakers*, Oxford (London 1936). Second edition, Dover Publications (New York 1960).

Pompei, F., "The Use of Airborne Ultrasonics for Generating Audible Sound Beams," *J. Audio Engineering Society*, volume 47, number 9 (1999).

Read, O., *Recording and Reproduction of Sound*, Sams & Co, (Indianapolis 1952).

Shirley, G., "The Corona Wind Loudspeaker," *J. Audio Engineering Society*, volume 5, number 1 (1957).

Tamura, M., et al., "Electrostatic Transducers with Piezoelectric High Polymer Films," J. Audio Engineering Society, volume 23, number 1 (1975).

Yoneyama, M., and Fujimoto, J., "The Audio Spotlight," *J. Acoustical Society of America*, volume 75, number 5 (1983).

INDEX: